

*This information is distributed solely for the purpose of pre-dissemination peer review under applicable information quality guidelines. It has not been formally disseminated by the National Institute for Occupational Safety and Health. It does not represent and should not be construed to represent any agency determination or policy.*

## ***Revised External Review Draft***

# **Current Intelligence Bulletin: Health Effects of Occupational Exposure to Silver Nanomaterials**



**Centers for Disease Control  
and Prevention**  
National Institute for Occupational  
Safety and Health

*This information is distributed solely for the purpose of pre-dissemination peer review under applicable information quality guidelines. It has not been formally disseminated by the National Institute for Occupational Safety and Health. It does not represent and should not be construed to represent any agency determination or policy.*

## 1 **Disclaimer**

2 Mention of any company or product does not constitute endorsement by the National  
3 Institute for Occupational Safety and Health (NIOSH), Centers for Disease Control and  
4 Prevention (CDC). In addition, citations to websites external to CDC/CDC/NIOSH do not  
5 constitute CDC/NIOSH endorsement of the sponsoring organizations or their programs  
6 or products. Furthermore, CDC/NIOSH is not responsible for the content of these  
7 websites. All Web addresses referenced in this document were accessible as of the  
8 publication date.

## 9 **Ordering Information**

10 To receive documents or other information about occupational safety and health topics,  
11 contact NIOSH at

12 Telephone: **1-800-CDC-INFO** (1-800-232-4636)

13 TTY: 1-888-232-6348

14 E-mail: [cdcinfo@cdc.gov](mailto:cdcinfo@cdc.gov)

15 or visit the NIOSH website at **[www.cdc.gov/niosh](http://www.cdc.gov/niosh)**.

16 For a monthly update on news at NIOSH, subscribe to *NIOSH eNews* by visiting  
17 **[www.cdc.gov/niosh/eNews](http://www.cdc.gov/niosh/eNews)**.

## 18 **Suggested Citation**

19 NIOSH [2018]. Revised External Review Draft - Current Intelligence Bulletin: Health  
20 Effects of Occupational Exposure to Silver Nanomaterials. By Kuempel ED, Roberts JR,  
21 Roth G, Zumwalde RD, Drew N, Hubbs A, Dunn KL, Trout D, Holdsworth G. Cincinnati,  
22 OH: U.S. Department of Health and Human Services, Centers for Disease Control and  
23 Prevention, National Institute for Occupational Safety and Health.

24 August 24, 2018 Draft

25

26

27

On the Cover: Image to be provided.

28

## 1 **Abstract**

2 As more consumer and medical products use engineered silver nanomaterials, the need  
3 has grown for further health evaluations. Previous assessments of the adverse effects  
4 of occupational exposure to silver did not account for particle size. The National Institute  
5 for Occupational Safety and Health (NIOSH) assessed potential health risks by  
6 evaluating more than 50 silver nanoparticle studies in animals or cells. Researchers  
7 found no studies that reported health effects in workers exposed to silver nanomaterials.  
8 In studies that involved human cells, silver nanomaterials were associated with toxicity  
9 (cell death and DNA damage) that varied according to the size of the particles. Many  
10 studies showed that silver nanomaterials had greater harmful effects than larger particle  
11 sizes of silver. In animals exposed to silver nanomaterials, silver tissue concentrations  
12 were elevated in all organs tested. Exposure to silver nanomaterials decreased lung  
13 function, caused inflamed lung tissue, and produced histopathological (microscopic  
14 tissue) changes in the liver and kidney.

15 NIOSH evaluated the potential occupational health risk of silver nanomaterials using  
16 data from two published subchronic (intermediate duration) inhalation studies in rats.  
17 These studies reported lung and liver effects that included early-stage lung inflammation  
18 and liver bile duct hyperplasia. NIOSH researchers used these data to estimate the  
19 dose of silver nanoparticles that caused these effects in rats. They also calculated the  
20 corresponding dose that would be expected to cause a similar response in humans and  
21 considered the uncertainties in those estimates. Based on this evaluation, NIOSH  
22 derived a recommended exposure limit (REL) for silver nanoparticles ( $\leq 100$  nm primary  
23 particle size) of 0.9 micrograms per cubic meter ( $\mu\text{g}/\text{m}^3$ ) as an airborne respirable 8-  
24 hour time-weighted average concentration. In addition, NIOSH continues to  
25 recommend a REL of  $10 \mu\text{g}/\text{m}^3$  for total silver (metal dust, fume, and soluble  
26 compounds, as Ag). NIOSH further recommends the use of workplace exposure  
27 assessments, engineering controls, safe work procedures, training and education, and  
28 established medical surveillance approaches.

## 1 **Executive Summary**

### 2 **Introduction**

3 Nanotechnology is an enabling technology involving structures generally defined as  
4 having one, two, or three external dimensions in the range of approximately 1 to 100  
5 nanometers (nm) [ISO/TS 2008]. Nanoscale substances may have physical-chemical  
6 properties that differ from those of the same substances as larger particles or in bulk  
7 [Wijnhoven et al. 2009]; such useful properties may be exploited by manufacturers. One  
8 prominent example of these substances is silver nanomaterials, which are used in the  
9 manufacture of electronics and textiles, and which have been used as pigments,  
10 catalysts, and antimicrobials [Wijnhoven et al. 2009; Nowack et al. 2011]. The United  
11 States produced an estimated 20 tons of silver nanomaterials in 2010 [Hendren et al.  
12 2011], and an estimated 450–542 tons were produced worldwide in 2014 [Future  
13 Markets 2013].

14 The current Occupational Safety and Health Administration (OSHA) permissible  
15 exposure limit (PEL) and the National Institute for Occupational Safety and Health  
16 (NIOSH) recommended exposure limit (REL) are both 10 micrograms per cubic meter  
17 ( $\mu\text{g}/\text{m}^3$ ) as an 8-hour time-weighted average (TWA) concentration (total mass sample)  
18 of silver (metal dust, fume, and soluble compounds, as Ag) [NIOSH 1988, 2007; OSHA  
19 1988, 2012a]. The PEL and REL are based on preventing workers from developing  
20 argyria, which is bluish-gray pigmentation to the skin and mucous membranes, and  
21 argyrosis, which is bluish-gray pigmentation to the eyes (see Terminology/Glossary and  
22 Section 1.4 Human Health Basis for the NIOSH REL).

23 However, the REL has not been evaluated specifically for silver nanomaterials. Studies  
24 in animals and cells have shown that the fate and biologic activity of silver is affected by  
25 its physical-chemical characteristics, such as solubility and surface properties [Johnston  
26 et al. 2010; Foldbjerg et al. 2011; Beer et al. 2012], particle size [Park et al. 2011c; Kim  
27 et al. 2012; Gliga et al. 2014; Braakhuis et al. 2014], and particle shape [Stoehr et al.

1 2011]. Studies in rats exposed by subchronic inhalation to silver nanoparticles (AgNPs)  
2 of 15–20 nm in diameter showed exposure-related adverse lung and liver effects [Sung  
3 et al. 2009, Song et al. 2013].

#### 4 **Occupational Exposure and Human Evidence**

5 Workers can be exposed to silver throughout its lifecycle, including ore extraction,  
6 melting/refining, product fabrication, use, disposal, and recycling. Workplace exposures  
7 to silver have been reported to occur during brazing and soldering operations ( $\leq 6.0$   
8  $\mu\text{g}/\text{m}^3$  TWA) [NIOSH 1973, 1981, 1998]; during manufacturing of silver nitrate and silver  
9 oxide (39–378  $\mu\text{g}/\text{m}^3$  TWA) [Rosenman et al. 1979, 1987]; during smelting and refining  
10 of silver (1–100  $\mu\text{g}/\text{m}^3$  TWA) [DiVincenzo et al. 1985]; and during reclamation of silver  
11 from photographic film (5–240  $\mu\text{g}/\text{m}^3$  TWA) [Pifer et al. 1989; Williams and Gardner  
12 1995; NIOSH 2000]. These earlier studies provide little information on airborne-particle  
13 characteristics, and it is likely that the fumes generated while melting silver or during  
14 brazing and soldering contained AgNPs and/or agglomerates of AgNPs. More recent  
15 studies have shown exposures to AgNPs in the workplace [Park et al. 2009; Lee et al.  
16 2011b; Lee et al. 2012a,b; Miller et al. 2010; Lewis et al 2012; Lee et al. 2013b]. Worker  
17 exposures to airborne concentrations of silver nanoparticles were reported to range  
18 from 0.02 to 2.43  $\mu\text{g}/\text{m}^3$  TWA during their production [Lee et al. 2011b; Lee et al.  
19 2012a,b], whereas airborne concentrations were found to range from 13 to 94  $\mu\text{g}/\text{m}^3$   
20 TWA at a precious metal processing facility where melting and electro refining of silver  
21 occurred [Miller et al. 2010].

22 Published reports of adverse health effects on workers occupationally exposed to silver  
23 are limited, but they indicate that long-term exposure to silver can cause localized (in  
24 dermal and mucous membranes) and generalized (systemic) argyria [ATSDR 1990;  
25 Drake and Hazelwood 2005; Wijnhoven et al. 2009; Johnston et al. 2010; Lansdown  
26 2012]. Ocular argyrosis has been observed in workers exposed to either soluble or  
27 insoluble silver, but no deficits in visual performance could be attributed to the silver  
28 deposits [Rosenman et al. 1979; Pifer et al. 1989]. Other studies have revealed cases of  
29 abnormal kidney function or acute respiratory stress [Parikh et al. 2014; Rosenman et

1 al. 1987] in silver workers compared with unexposed workers, but frequently such  
2 exposure occurred concurrently with cadmium and solvents. Relatively few studies have  
3 been published on worker exposures to silver nanomaterials [Lee et al. 2011b, 2012a,b;  
4 Park et al. 2009; Miller et al. 2011]. These studies did not report adverse health effects,  
5 and also did not provide detailed characterization of the nanomaterial exposures.

## 6 Cellular studies

7 In vitro studies provide information on the cellular toxicological mechanisms associated  
8 with AgNPs and the effect of physicochemical properties. These findings may be  
9 relevant to potential in vivo mechanisms (at least qualitatively, as equivalent doses may  
10 not be estimable). Key findings from in vitro studies of exposure to either AgNPs or ionic  
11 silver include increased levels of reactive oxygen species [Hussain et al. 2005a; Carlson  
12 et al. 2008; Foldbjerg et al. 2009; Kim et al. 2009c], induction of oxidative stress  
13 management genes [Kim et al. 2009c; Miura and Shinohara 2009], and increased  
14 percentages of apoptotic cells [Hsin et al. 2008; Foldbjerg et al. 2009; Miura and  
15 Shinohara 2009]. Results of some cellular assay studies indicate that ionic silver can be  
16 more potent than AgNPs in causing apoptosis [Foldbjerg et al. 2009] and reducing cell  
17 viability [Carlson et al. 2008; Greulich et al. 2009; Kim et al. 2009c; Miura and  
18 Shinohara 2009], whereas results of other studies provide evidence of a relationship  
19 between the increase in intracellular reactive oxygen species generation and increasing  
20 particle size.

21 Reactive oxygen species generation was significantly elevated after exposure of rat  
22 alveolar macrophages to 15-nm-diameter AgNPs, but not after exposure to 30- or 55-  
23 nm-diameter AgNPs [Carlson et al. 2008]. DNA damage and high levels of apoptosis  
24 and necrosis were associated with exposure to either AgNPs or ionic silver [Foldbjerg et  
25 al. 2009, 2011]. Statistically significant increases in bulky DNA adducts were observed  
26 at doses from 2.5 µg/ml of AgNPs; however, pretreatment with the antioxidant N-acetyl-  
27 L-cysteine (NAC) (10 mM; 1 hr prior to Ag exposure) inhibited the formation of bulky  
28 adducts [Foldbjerg et al. 2009, 2011]. Silver AgNP surface chemistry and activity affects

1 the kinetics of ion release, and AgNP dissolution processes generate additional reactive  
2 oxygen species as a byproduct [Liu et al. 2010b]. These in vitro studies suggest  
3 nanoscale silver particles may be more toxic than microscale silver particles in both the  
4 lungs and extrapulmonary organs; however, results were more variable in rodent  
5 studies that compared the toxicity of nanoscale and microscale silver particles. Although  
6 several studies showed greater effects following exposure to smaller particles [Park et  
7 al. 2010b, Philbrook et al. 2011, Silva et al. 2016; Sieffert et al., 2015], some studies  
8 found that the larger particles were more toxic [Silva et al. 2015; Botelho et al. 2016].  
9 The differences of effect in the in vivo studies could be due to variations in route of  
10 exposure, form of silver, dose, and the target tissue. The in vitro findings also indicate  
11 that dissolution of AgNPs accounts for some degree of the observed toxicity, although  
12 the effects cannot be fully apportioned to the measured dissolved fraction of silver.

### 13 **Animal studies**

14 The most comprehensive data set on the potential toxicity of AgNPs comes from  
15 experimental animal studies. In vivo studies of rats exposed to AgNPs by subchronic  
16 inhalation provide evidence of (1) the uptake of silver ions or nanoparticles in the blood  
17 and subsequent distribution to all major organs and tissues [Sung et al. 2008, 2009;  
18 Song et al. 2014]; (2) perturbation of lung function and induction of inflammatory  
19 responses [Sung et al. 2008, 2009; Song et al. 2013]; and (3) histopathologic changes  
20 in the kidney and especially in the liver, in which bile duct hyperplasia and necrosis  
21 were identified [Sung et al. 2009]. These effects were reported at airborne  
22 concentrations of 49 or 133  $\mu\text{g}/\text{m}^3$ . Following exposure to AgNPs by various routes  
23 (inhalation, oral, intravenous), significant increases in the amount of silver have been  
24 observed in major organs and tissues, including the lungs, liver, spleen, kidneys,  
25 olfactory bulb, brain, and blood in both male and female rats [Ji et al. 2007b; Kim et al.  
26 2008; Sung et al. 2009; Kim et al. 2010a; Lankveld et al. 2010; Lee et al. 2013d], and  
27 these increases appear to be sex-specific [Sung et al. 2009; Kim et al. 2010a, 2011;  
28 Song et al. 2013; Dong et al. 2013].

1 In a 13-week (90-day) inhalation study by Sung et al. [2008, 2009], lung function deficits  
2 (decreased tidal volume, minute volume, and peak inspiration flow), inflammation  
3 responses, and alveolar accumulation of macrophages were observed [Sung et al.  
4 2008]. In a subsequent 12-week inhalation (and 12-week recovery) study from the same  
5 laboratory [Song et al. 2013], the alveolar inflammation had resolved in the female rats  
6 and had resolved in all but one of the male rats at the high dose 12 weeks after  
7 cessation of exposure. Acute and shorter subacute exposure studies have ranged in  
8 degree of pulmonary inflammation and lung injury but have a commonality in the trend  
9 of responses that resolve over time after the end of exposure [Kwon et al. 2012;  
10 Roberts et al. 2013; Seiffert et al. 2016; Silva et al. 2016; Stebounova et al. 2011].

11 Although the biological interactions with inhaled AgNPs are not fully understood, the  
12 possible mechanisms include dissolution and release of soluble silver species, and  
13 particle transformation through sulfidation (binding with sulfur) or opsonization (binding  
14 with protein), which can stabilize the silver [Liu et al. 2011; Loeschner et al. 2011;  
15 Bachler et al. 2013]. AgNPs are considered to have a greater potential for dissolution  
16 and release of ions than microscale particles, because of the increased surface area  
17 per unit mass of nanoparticles [Wijnhoven et al. 2009]. In vivo studies in rodents that  
18 compare effects of exposure to different particle sizes of silver (micro- and nano-  
19 diameter) are limited, although these studies show that nanoscale silver exposure  
20 resulted in greater retained mass dose [Braakhuis et al. 2014], alveolar macrophage  
21 uptake [Anderson et al. 2015], acute pulmonary inflammation [Anderson et al. 2015;  
22 Braakhuis et al. 2014], and cytotoxicity (both severity and duration) [Anderson et al.  
23 2015], as well as increased nasal cavity deposition, transport to the olfactory bulb, and  
24 microglial cell activation [Patchin et al. 2016].

## 25 **Published Occupational Exposure Limits (OELs) for Silver** 26 **Nanoparticles**

27 Christensen et al. [2010] derived OELs of 0.1–0.67  $\mu\text{g}/\text{m}^3$  as an 8-hr TWA for AgNPs,  
28 based on the rat subchronic inhalation data reported in Sung et al. [2008, 2009]. In their

1 assessment, Christensen et al. [2010] followed the ECHA [2008] guidelines (currently  
2 ECHA [2010]), starting with the rat no observed adverse effect level (NOAEL) for lung or  
3 liver effects, or the lowest observed adverse effect level (LOAEL) for lung function  
4 deficits. The rat NOAEL and LOAEL were adjusted by differences in rat and human  
5 exposure conditions and by uncertainty factors (UFs). The OEL estimates depended on  
6 the animal effect level and UFs used in the assessment.

7 Weldon et al. [2016] estimated an OEL of 0.19  $\mu\text{g}/\text{m}^3$  for AgNPs, based on the silver  
8 tissue dose and liver bile duct hyperplasia response in female rats [Sung et al. 2009].  
9 Liver bile duct hyperplasia was considered to be the critical effect (i.e., most sensitive),  
10 which was specific and quantifiable. The human-equivalent concentration (HEC) was  
11 estimated by applying dosimetric adjustment factors (DAFs) [U.S. EPA 1994] to the rat  
12 benchmark dose or concentration (BMD or BMC) estimates. The OEL was derived by  
13 applying UFs to the HEC. Further details are reported in Appendix G.

## 14 **NIOSH Quantitative Risk Assessment**

15 In the absence of data on human exposure to AgNPs, NIOSH considered the  
16 subchronic inhalation data in rats [Sung et al. 2008, 2009; Song et al. 2013] to be the  
17 best available data to evaluate the potential occupational health hazards of AgNPs. The  
18 airborne exposure concentrations in these rat studies ranged from 49 to 515  $\mu\text{g}/\text{m}^3$ ,  
19 which spans the 100  $\mu\text{g}/\text{m}^3$  OEL for inhalable silver (Table 1-2). No significant dose-  
20 related changes in rat body weight or organ weight were observed, and no toxicity that  
21 interfered with the study interpretation [Bucher et al. 1996; Oberdörster 1997] was  
22 reported [Sung et al. 2009; Song et al. 2013]. The pulmonary clearance rates of silver  
23 were similar to the normal rates for alveolar macrophage-mediated clearance (i.e., no  
24 evidence of overloading) (Section 6.2.1). Thus, the adverse lung and liver effects  
25 associated with exposure to AgNPs in these rat studies were considered to be relevant  
26 to humans.

27 Lung inflammation and lung function deficits occurred in both male and female Sprague-  
28 Dawley rats following inhalation of AgNPs for 13 and 12 weeks, respectively, as

1 reported by Sung et al. [2008, 2009] and Song et al. [2013]. The inflammation (chronic,  
2 alveolar) was reported to be of minimal severity on the basis of histopathologic  
3 evaluation [Sung et al. 2009; Song et al. 2013], and the inflammation had resolved by  
4 12 weeks post-exposure in 8 of the 9 rats in the high-exposure group (381  $\mu\text{g}/\text{m}^3$ ) [Song  
5 et al. 2013]. Pulmonary fibrosis was not reported as having been observed in either  
6 study at the AgNP inhaled doses in these studies [Sung et al. 2009; Song et al. 2013].  
7 These findings indicate that the rat pulmonary inflammation response to AgNPs  
8 following subchronic inhalation is an early-stage effect of minimal severity. However,  
9 long-term studies are not available on potential pulmonary effects following chronic  
10 exposure to AgNPs. Persistent inflammation in animals or humans can result in  
11 disease. Pulmonary inflammation and other adverse effects have been associated with  
12 some occupational exposures to hazardous airborne particles [NIOSH 2011, 2013].  
13 NIOSH considers the response of pulmonary inflammation to be relevant to workers.

14 Adverse effects in the liver were also associated with exposure to AgNPs in rats. The  
15 finding of liver bile duct hyperplasia in rats [Sung et al. 2009, Kim et al. 2010a] from  
16 exposure to AgNPs is consistent with the pathway in which silver is eliminated from the  
17 blood via biliary excretion and eventually from the body in the feces [DiVincenzo et al.  
18 1985; Wölbling et al. 1988]. The clinical significance of bile duct hyperplasia as an  
19 isolated lesion is not well known, but some evidence suggests that cholangiocellular  
20 carcinoma can develop from bile duct hyperplasia [Kurashina et al. 2006]. Hyperplasia  
21 is one of several factors believed to be involved in the development of  
22 cholangiocarcinoma, the biliary tract cancer of the liver [Rizvie and Gores 2014; Rizvi et  
23 al. 2014]. In rats exposed to AgNPs, the bile duct hyperplasia was accompanied by  
24 additional evidence of liver abnormalities, which includes liver necrosis at the higher  
25 exposures [Sung et al. 2009; Kim et al. 2010a]. On the basis of these findings, NIOSH  
26 considers the response of bile duct hyperplasia in a subchronic inhalation study in rats  
27 [Sung et al. 2009] to be a potential adverse effect of relevance to workers.

28 The risk assessment methods applied to the rat subchronic inhalation data included  
29 benchmark dose (BMD) modeling to estimate the doses associated with early-stage

1 adverse lung and liver responses. Human-equivalent exposure concentrations were  
2 estimated as described below.

### 3 **PBPK Modeling**

4 NIOSH used the results from a physiologically based pharmacokinetic (PBPK) model for  
5 AgNPs [Bachler et al. 2013] to estimate the 45-year working lifetime exposure  
6 concentrations associated with argyria at the lowest reported silver skin-tissue dose in  
7 humans (Section A.5.3). These estimates were 47, 78, and 253  $\mu\text{g}/\text{m}^3$ , respectively, for  
8 ionic, 15-nm-, and 100-nm-diameter silver (Table A-7). These estimates are  
9 approximately 5 to 25 times greater than the existing NIOSH REL of 10  $\mu\text{g}/\text{m}^3$  (8-hour  
10 TWA, total mass sample) of soluble or insoluble silver [NIOSH 2007], which suggests a  
11 relatively low risk of argyria at the REL, assuming equal response at equivalent mass  
12 tissue dose of silver.

13 The PBPK model of Bachler et al. [2013] was also used to estimate the 45-year working  
14 lifetime AgNP exposure concentrations that would result in tissue doses equivalent to  
15 those associated with the NOAEL or benchmark dose estimates for pulmonary  
16 inflammation or liver bile duct hyperplasia in the rat subchronic inhalation studies [Sung  
17 et al. 2009; Song et al. 2013]. The estimated HECs to the rat NOAELs for lung and liver  
18 effects were 0.19 to 3.8  $\mu\text{g}/\text{m}^3$  for total silver, and 6.2 to 195  $\mu\text{g}/\text{m}^3$  for soluble/active  
19 tissue doses, depending on particle size (15-nm- or 100-nm-diameter AgNPs) (Table A-  
20 9).

### 21 **DAF Method**

22 NIOSH used dosimetric adjustments to estimate the HECs to the rat doses associated  
23 with early-stage lung and liver effects in the subchronic inhalation studies [Sung et al.  
24 2009; Song et al. 2013]. DAF methods have been used for many years in the risk  
25 assessment of inhaled particles [U.S. EPA 1994], including for AgNPs [Weldon et al.  
26 2016]. The first step was to model the rat exposure-response data to estimate the  
27 benchmark concentration associated with a 10% increase in either liver bile duct  
28 hyperplasia or pulmonary inflammation, 95% lower confidence limit estimate (BMCL<sub>10</sub>).

1 DAFs were applied to the rat BMCL<sub>10</sub> estimates to derive the HEC estimates. The total  
2 DAF included individual factors based on the following data from animals and humans:  
3 ventilation rates (volume of air inhaled per day); respiratory tract deposition fractions of  
4 inhaled particles; and respiratory tract surface area or body weight. A DAF was not used  
5 to adjust for interspecies differences in clearance of AgNPs, because of uncertainty  
6 about the dissolution and clearance rates of AgNPs in animals and humans; instead, an  
7 UF was applied. The lowest HEC was 23.1 µg/m<sup>3</sup>, based on the pulmonary  
8 inflammation data from male and female rats in both subchronic inhalation studies  
9 [Sung et al. 2009; Song et al. 2013] (Section 6.2.3).

## 10 **NIOSH REL Derivation**

11 NIOSH applied well-established risk assessment methods [ICRP 1994; U.S. EPA 1994,  
12 2002, 2012b, 2015] to derive a REL for silver nanomaterials based on on rat data of  
13 lung and liver effects following subchronic (13-week) inhalation exposure to AgNPs.  
14 Dosimetric adjustments were used to estimate equivalent concentrations in humans,  
15 and UFs were applied to the lowest HEC estimate to derive a REL for silver  
16 nanomaterials. In applying these methods, NIOSH shows where scientific data are  
17 available; and where data are not available, UFs are used. A sensitivity analysis  
18 examining the influence of the various risk assessment methods and assumptions was  
19 performed (Section 6.4.6). This analysis showed that over the range of assumptions  
20 and uncertainties considered in the risk assessment methods for AgNPs, the OEL  
21 estimates derived by NIOSH and others are all relatively low airborne mass  
22 concentrations (0.1 to 2 µg/m<sup>3</sup>) compared to the current NIOSH REL of 10 µg/m<sup>3</sup> for  
23 total silver (metal dust, fume, and soluble compounds, as Ag) and to the other OELs for  
24 silver (up to 100 µg/m<sup>3</sup>) (Table 1-2).

25 The lowest HEC estimate of 23 µg/m<sup>3</sup> was used as the point of departure (PoD) to  
26 derive an REL for silver nanomaterials. A total UF of 25 (Table 6-7) was applied to the  
27 PoD estimate (i.e., 23 µg/m<sup>3</sup> / 25 = 0.9 µg/m<sup>3</sup>) (Table 6-8). Thus, the NIOSH REL for  
28 silver nanomaterials (≤100 nm primary particle size) is 0.9 µg/m<sup>3</sup> as an airborne  
29 respirable 8-hour time-weighted average (TWA) concentration.

1 The NIOSH REL is a health-based REL. Findings from the literature indicate that  
2 workplace exposures can in some situations be controlled at or below the REL.

### 3 **Recommendations**

4 Silver is produced and used in the workplace in varying particle size fractions including  
5 fine (which is defined as all particle sizes collected by respirable particle sampling) and  
6 ultrafine or nanoscale (defined as the fraction of respirable particles with a primary  
7 particle diameter of  $\leq 100$  nm) [NIOSH 2011]. NIOSH recommends that effective risk  
8 management practices be implemented for all processes that produce or use silver  
9 nanomaterials so that worker exposures do not exceed the NIOSH REL for either silver  
10 nanomaterials or total silver. The NIOSH REL for total silver (metal dust, fume, and  
11 soluble compounds, as Ag) is  $10 \mu\text{g}/\text{m}^3$  (8-hour TWA), measured as a total airborne  
12 mass concentration [NIOSH 1988, 2003; 2007]. The NIOSH REL for silver  
13 nanomaterials (primary particle diameter of  $\leq 100$  nm) is  $0.9 \mu\text{g}/\text{m}^3$  (8-hour TWA),  
14 measured as a respirable airborne mass concentration. Additional sample analysis is  
15 needed to determine if an airborne respirable particle sample includes silver  
16 nanomaterials (Chapter 7). Should the samples indicate airborne concentrations of  
17 silver exceeding the NIOSH RELs for total silver or nanoscale silver, then appropriate  
18 respiratory protection (Section 7.6) should be worn for those work tasks until control  
19 technologies (Section 7.2) are implemented to reduce airborne levels of silver below the  
20 RELs.

21  
22 NIOSH further recommends that employers who formulate, use, or otherwise handle  
23 silver nanomaterials or products containing silver nanomaterials develop a risk  
24 management program (see Chapter 7), with worker input, including these components:

- 25  
26
- Identification of processes and job tasks where there is potential for exposure to  
27 silver nanomaterials. Comprehensive assessment of exposures (including  
28 exposures to other potential hazards) should be performed as part of job hazard

1 analysis, and a hazard communication program should be developed following  
2 the OSHA Hazard Communication Standard (HCS) [CFR 1910.1200(h)].

- 3 • Development of criteria and guidelines for selecting, installing, and evaluating  
4 engineering controls (such as LEV, dust collection systems), with the objective of  
5 controlling worker airborne exposure to total silver (metal dust, fume, and soluble  
6 compounds, as Ag) below the NIOSH REL of 10  $\mu\text{g}/\text{m}^3$  (8-hour TWA) and to  
7 silver nanomaterials (primary particle size  $\leq 100$  nm) below the NIOSH REL of 0.9  
8  $\mu\text{g}/\text{m}^3$  (8-hour TWA).
  
- 9 • Routine systematic evaluation of worker exposure to silver nanomaterials at least  
10 annually, and/or whenever there is a change in a process or task associated with  
11 potential exposure to silver nanomaterials. Changes could include frequency,  
12 volume, duration, equipment, and procedures/processes.
  
- 13 • An education and training program for recognizing potential exposures and using  
14 good work practices to prevent exposure to silver, including the safe handling of  
15 silver nanomaterials.
  
- 16 • Development of procedures for selecting and using personal protective  
17 equipment (PPE; clothing, gloves, respirators). Development of a respiratory  
18 protection program following the OSHA respiratory protection standard (29 CFR  
19 1910.134) if respiratory protection is used.
  
- 20 • Development of spill control plans and routine cleaning procedures for work  
21 areas with a HEPA-filtered vacuum or wet-wipes. Do not use dry sweeping or air  
22 hoses. Avoid using or handling silver nanomaterials in powder form, where  
23 possible, and ensure silver nanomaterials are stored in tightly sealed containers  
24 and labeled in accordance with the HCS.

*This information is distributed solely for the purpose of pre-dissemination peer review under applicable information quality guidelines. It has not been formally disseminated by the National Institute for Occupational Safety and Health. It does not represent and should not be construed to represent any agency determination or policy.*

- 1       • Provision of facilities for hand washing to reduce the potential for dermal and oral  
2           exposures, and encouragement of workers to use these facilities before eating or  
3           leaving the worksite.
  
- 4       • Use of established medical surveillance approaches for workers potentially  
5           exposed to silver including silver nanomaterials.

## 6       **Future Research Needs**

7       Uncertainties in evaluating the health risks of silver nanomaterials may be reduced as  
8       new information becomes available from currently ongoing research studies, such as  
9       the National Institute of Environmental Health Sciences nanoGo consortium research  
10      [Schug et al. 2013] and the National Toxicology Program (NTP). As new data become  
11      available, NIOSH may assess the results and determine whether additional  
12      recommendations are needed to protect workers' health.

*This information is distributed solely for the purpose of pre-dissemination peer review under applicable information quality guidelines. It has not been formally disseminated by the National Institute for Occupational Safety and Health. It does not represent and should not be construed to represent any agency determination or policy.*

# 1 Contents

2	Disclaimer .....	2
3	Ordering Information .....	2
4	Suggested Citation .....	2
5	Abstract .....	3
6	Executive Summary .....	4
7	Introduction .....	4
8	Occupational Exposure and Human Evidence .....	5
9	Cellular studies .....	6
10	Animal studies .....	7
11	Published Occupational Exposure Limits (OELs) for Silver Nanoparticles.....	8
12	NIOSH Quantitative Risk Assessment.....	9
13	PBPK Modeling .....	11
14	DAF Method .....	11
15	NIOSH REL Derivation.....	12
16	Recommendations .....	13
17	Future Research Needs.....	15
18	Contents .....	16
19	Abbreviations and Definitions .....	21
20	Terminology/Glossary .....	27
21	Terms related to silver and silver nanomaterials.....	27
22	Terms used in risk assessment .....	29
23	Acknowledgments.....	34
24	Invited Expert Peer Reviewers of Previous Draft (January 7, 2016).....	35
25	1 Introduction.....	36
26	1.1 Background .....	36
27	1.2 Bases for Current Occupational Exposure Limits.....	40
28	1.3 Scientific Literature Review .....	42
29	1.4 Human Health Basis for the Current NIOSH REL .....	43
30	2 Occupational Exposures to Silver.....	48
31	3 Human Evidence of Internal Dose and Potential Adverse Health Effects.....	59
32	3.1 Background .....	59
33	3.2 Human Studies of Lung Deposition of Airborne Silver Nanoparticles .....	60
34	3.3 Biomonitoring Studies in Humans .....	61
35	3.4 Health Effects in Workers with Exposure to Silver.....	63
36	3.5 Health Effects in Humans with Nonoccupational Exposure to Silver .....	69
37	4 Cellular and Mechanistic Studies Overview.....	71
38	4.1 Overview of Cell-based AgNP Studies.....	71
39	4.2 AgNP Exposure Increases Cytotoxicity and Oxidative Stress.....	72
40	4.3 AgNP Exposure Induces Genotoxicity .....	73
41	4.4 Other Cellular Effects of AgNP Exposure .....	74
42	4.5 Effects of AgNP Size, Functionalization, and Ion Release.....	74
43	5 Animal Studies Overview .....	77
44	5.1 Toxicokinetic Findings .....	77

*This information is distributed solely for the purpose of pre-dissemination peer review under applicable information quality guidelines. It has not been formally disseminated by the National Institute for Occupational Safety and Health. It does not represent and should not be construed to represent any agency determination or policy.*

1	5.1.1 Pulmonary exposure—inhalation .....	77
2	5.1.2 Nonpulmonary routes of exposure .....	79
3	5.1.3 Sex differences .....	79
4	5.1.4 Physicochemical properties affecting kinetics .....	80
5	5.2 Toxicological Effects .....	83
6	5.2.1 Pulmonary exposure .....	83
7	5.2.2 Dermal, oral, and parenteral exposure.....	84
8	5.2.3 Sex differences .....	86
9	5.2.4 Potential mechanisms of toxicity .....	87
10	5.2.5 Physicochemical properties .....	88
11	5.3 General Conclusions .....	89
12	6 Hazard and Risk Evaluation of Silver Nanoparticles and OEL Derivation.....	91
13	6.1 Hazard Identification.....	91
14	6.1.1 Lung effects .....	91
15	6.1.2 Liver effects.....	93
16	6.1.3 Biological mode of action and physical-chemical properties.....	95
17	6.2 Quantitative Risk Assessment for Silver Nanoparticles .....	99
18	6.2.1 Animal studies .....	99
19	6.2.2 Basis for conducting a quantitative risk assessment .....	101
20	6.2.3 Point of departure from animal data (PoD <sub>animal</sub> ).....	101
21	6.2.4 Human-equivalent concentration estimates.....	102
22	6.2.4.1 Dosimetric Adjustment Factor (DAF) method.....	103
23	6.2.4.2 Selection of DAF values.....	105
24	6.2.4.3 Uncertainty Factor method and selection .....	109
25	6.3 Derivation of NIOSH REL for Silver Nanomaterials .....	110
26	6.4 Risk Characterization .....	112
27	6.4.1 Relevance of animal responses to humans .....	112
28	6.4.2 Biologically active dose metric .....	114
29	6.4.3 Human-equivalent tissue dose.....	114
30	6.4.4 Working lifetime equivalent concentration.....	116
31	6.4.5 Areas of uncertainty .....	116
32	6.4.6 Sensitivity analysis .....	118
33	6.5 Summary .....	119
34	7 Recommendations.....	132
35	7.1 Exposure Assessment for Silver Nanomaterials .....	134
36	7.2 Engineering Controls .....	139
37	7.3 Worker Education and Training.....	146
38	7.4 Cleanup and Disposal.....	147
39	7.5 Dermal Protection .....	148
40	7.6 Respiratory Protection.....	150
41	7.7 Occupational Health Surveillance.....	154
42	7.7.1 Hazard surveillance .....	154
43	7.7.2 Medical screening and surveillance .....	154
44	8 Research Needs .....	157
45	9 References.....	160
46	APPENDIX A.....	211

*This information is distributed solely for the purpose of pre-dissemination peer review under applicable information quality guidelines. It has not been formally disseminated by the National Institute for Occupational Safety and Health. It does not represent and should not be construed to represent any agency determination or policy.*

1	Physiologically Based Pharmacokinetic (PBPK) Modeling.....	211
2	A.1 Background .....	211
3	A.2 Silver Tissue Doses in Rats.....	215
4	A.2.1 Lungs .....	216
5	A.2.2 Liver .....	216
6	A.3 Effect Level Estimates in Rats and Humans .....	217
7	A.4 PBPK Model Estimates.....	218
8	A.4.1 Overview of PBPK modeling runs .....	218
9	A.4.2 Comparison of model-predicted and measured lung and liver tissue burdens in rats	
10	.....	220
11	A.4.3 Human-equivalent working lifetime exposure concentrations.....	223
12	A.4.4 Worker body burden estimates of silver from diet and occupational exposures..	224
13	A.4.5 Estimated working lifetime exposure concentrations associated with argyria.....	226
14	A.4.6 Estimated silver tissue burdens in workers with inhalation exposure to 10 µg/m <sup>3</sup> of	
15	AgNP .....	227
16	A.4.6.1 Lungs .....	228
17	A.4.6.2 Liver.....	229
18	A.4.7 Estimated 45-year working lifetime airborne exposure concentrations equivalent to	
19	rat effect levels .....	230
20	A.5 Evaluation of PBPK Modeling Results.....	231
21	A.5.1 Utility of PBPK modeling estimates .....	231
22	A.5.2 Comparison of human data to rat-based estimates .....	232
23	A.5.3 Argyria risk.....	233
24	A.5.4 Lung inflammation risk .....	234
25	A.5.5 Bile dust hyperplasia risk .....	235
26	A.5.6 Silver nanoparticle form .....	237
27	APPENDIX B .....	250
28	Statistical Analyses Supplement.....	250
29	B.1 Benchmark Dose Modeling of Rat Subchronic Inhalation Studies.....	250
30	B.2 No Observed Adverse Effect Level (NOAEL) Estimation of Rat Liver Bile Duct	
31	Hyperplasia .....	262
32	B.2.1 Background.....	262
33	B.2.2 Data.....	262
34	B.2.3 Analysis .....	263
35	B.2.3.1 Male rats.....	263
36	B.2.3.2 Female rats .....	264
37	B.2.4 Conclusion .....	264
38	B.3 Pooled Data Analysis of Rat Subchronic Pulmonary Inflammation .....	265
39	B.3.1 Background.....	265
40	B.3.2 Analyses.....	266
41	B.3.2.1 Phase 1: Pool all data (both labs, both sexes) .....	266
42	B.3.2.2 Phase 2: Pool all male data (both labs, only males).....	269
43	B.3.2.3 Phase 3: Pool all female data (both labs, only females) .....	271
44	B.3.2.4 Phase 4: Pool all Sung [2009] data (one lab, both sexes) .....	273
45	B.3.2.5 Phase 5: Pool all Song [2013] data (one lab, both sexes) .....	275
46	B.3.3 Conclusions.....	277

*This information is distributed solely for the purpose of pre-dissemination peer review under applicable information quality guidelines. It has not been formally disseminated by the National Institute for Occupational Safety and Health. It does not represent and should not be construed to represent any agency determination or policy.*

1	B.4 Exploration of Pooling Rat Subchronic Liver Effects Data .....	279
2	B.4.1 Background.....	279
3	B.4.2 Analysis .....	279
4	B.4.2.1 Liver Duct Hyperplasia.....	279
5	B.4.2.3.1 Male Liver Abnormality .....	284
6	B.4.2.3.2 Female Liver Abnormality.....	285
7	B.4.3 Conclusion .....	286
8	B.5 Evaluation of Biomarker Findings in Silver Jewelry Workers .....	287
9	B.5.1 Summary of findings .....	287
10	B.5.2 Statistical evaluation of findings .....	288
11	B.6 Conclusions .....	291
12	B.7 References .....	292
13	APPENDIX C .....	293
14	Literature Search Strategy.....	293
15	APPENDIX D.....	296
16	In Vitro/Mechanistic Studies .....	296
17	D.1 Oxidative Stress/Induction of Apoptosis .....	296
18	D.2 DNA Damage/Genotoxicity.....	314
19	D.3 Changes in Gene Expression/Regulation .....	325
20	D.4 Modeling the Perturbation of the Blood–Brain Barrier .....	328
21	D.5 Impact of Silver Nanoparticles on Keratinocytes .....	329
22	D.6 Effect of Silver Nanoparticles on Platelet Activation .....	330
23	D.7 Antitumor and Antimicrobial Activity of Silver Nanoparticles.....	330
24	D.8 Dermal Absorption (in Vitro).....	355
25	APPENDIX E .....	356
26	Toxicological and Toxicokinetic Effects of Silver Nanoparticles in Experimental Animal Studies	
27	.....	356
28	E.1 Inhalation Exposure.....	356
29	E.1.1 Toxicokinetics.....	356
30	E.1.2 Toxicological effects.....	357
31	E.2 Oral Exposure .....	374
32	E.2.1 Toxicokinetics.....	374
33	E.2.1 Toxicological effects.....	379
34	E.3 Exposure via Other Routes .....	403
35	E.3.1 Dermal.....	403
36	E.3.2 Intratracheal instillation, oropharyngeal aspiration, or intranasal instillation .....	407
37	E.3.2.1 Silver nanoparticles.....	407
38	E.3.2.2 Silver nanowires.....	418
39	E.3.3 Subcutaneous, intravenous, or intraperitoneal injection .....	420
40	E.3.3.1 Kinetics following subcutaneous injection .....	420
41	E.3.3.2 Kinetics following intravenous injection .....	422
42	E.3.3.3 Toxicological effects following intravenous or intraperitoneal injection.....	430
43	APPENDIX F.....	485
44	Rat Tissue Concentrations and Respiratory Parameters .....	485
45	F.1 Estimating Lung Tissue Concentration of Silver Relative to Steady-State Tissue	
46	Concentration in Rats.....	485

*This information is distributed solely for the purpose of pre-dissemination peer review under applicable information quality guidelines. It has not been formally disseminated by the National Institute for Occupational Safety and Health. It does not represent and should not be construed to represent any agency determination or policy.*

1	F.2 Rat Respiratory Parameters .....	487
2	F.3 Rat Measured and MPPD Model–Predicted Lung Burdens .....	488
3	APPENDIX G.....	493
4	Other Quantitative Risk Assessments for Silver Nanoparticles .....	493
5	G.1 Christensen et al. [2010].....	493
6	G.2 Weldon et al. [2016].....	494
7	G.3 Acute Inhalation Exposure to Silver .....	498
8		

## 1 **Abbreviations and Definitions**

2	AB	Alamar Blue
3	ACGIH	American Conference of Governmental Industrial Hygienists
4	Ag	silver
5	Ag <sup>+</sup>	ionic silver
6	AgCl	silver chloride
7	Ag <sub>2</sub> CO <sub>3</sub>	silver carbonate
8	Ag/Cu	silver copper
9	AgNO <sub>3</sub>	silver nitrate
10	Ag <sub>2</sub> O	silver oxide
11	Ag <sub>3</sub> PO <sub>4</sub>	silver phosphate
12	Ag <sub>2</sub> S	silver sulfide
13	Ag <sub>2</sub> SO <sub>4</sub>	silver sulfate
14	AgNP	silver nanoparticle
15	AgNW	silver nanowire
16	AIC	Akaike information criterion
17	Al <sub>2</sub> O <sub>3</sub>	aluminum oxide
18	ALT	alanine aminotransferase
19	AMG	auto-metallography
20	AP	alkaline phosphatase
21	ATSDR	Agency for Toxic Substances and Disease Registry
22	BAL	broncho alveolar fluid
23	BMC	benchmark concentration
24	BMCL	95% lower confidence limit estimate of BMC
25	BMCL <sub>10</sub>	95% lower confidence limit estimate of the BMC which is associated with a
26		10% increase over background in the proportion of animals with an adverse
27		response
28	BMD	benchmark dose
29	BMDL	95% lower confidence limit estimate of BMD
30	BMDL <sub>10</sub>	95% lower confidence limit estimate of the BMD which is associated with a
31		10% increase over background in the proportion of animals with an adverse
32		response
33	BMR	benchmark response

*This information is distributed solely for the purpose of pre-dissemination peer review under applicable information quality guidelines. It has not been formally disseminated by the National Institute for Occupational Safety and Health. It does not represent and should not be construed to represent any agency determination or policy.*

1	BW	body weight
2	°C	degrees Celsius
3	C <sub>6</sub> H <sub>5</sub> Ag <sub>3</sub> O <sub>7</sub>	silver citrate
4	CIB	Current Intelligence Bulletin
5	CKAP4	cytoskeleton-associated protein 4
6	cm	centimeter
7	cm <sup>2</sup>	centimeter squared
8	CMAD	count median aerodynamic diameter
9	CMC	carboxymethyl cellulose
10	CPC	condensation particle counter
11	DAF	dosimetric adjustment factor
12	DCF	dichlorofluorescein
13	DNA	deoxyribonucleic acid
14	EC50	median effective concentration
15	ECHA	EU European Chemicals Agency
16	EDS	energy dispersive X-ray spectroscopy
17	EPA	U.S. Environmental Protection Agency
18	ESP	electrostatic precipitator
19	EU	European Union
20	°F	degrees Fahrenheit
21	FAAS	Fame atomic absorption spectrometry
22	FITC	fluorescein isothiocyanate
23	FMPS	fast mobility particle sizer
24	FSH	follicle stimulation hormone
25	g	gram
26	GD	gestation day
27	GJIC	gap-junction intercellular communication
28	GM	geometric mean
29	GP	glutathione peroxidase
30	GSD	geometric standard deviation
31	GSH	glutathione
32	HEC	human equivalent concentration
33	HED	human equivalent dose

*This information is distributed solely for the purpose of pre-dissemination peer review under applicable information quality guidelines. It has not been formally disseminated by the National Institute for Occupational Safety and Health. It does not represent and should not be construed to represent any agency determination or policy.*

1	HEPA	high-efficiency particulate air
2	hMSC	human mesenchymal stem cell
3	hr	hour
4	HT	hydroxytryptamine
5	IC50	median inhibitory concentration
6	ICP-MS	inductively coupled plasma-mass spectroscopy
7	Ig	immunoglobulin
8	INEL	indicative no-effect level
9	ISO	International Organization for Standardization
10	JNK	c-Jun NH2-terminal kinase
11	kg	kilogram
12	L	liter
13	L/min	liters per minute
14	LC <sub>50</sub>	concentration resulting in a mortality of 50%
15	LCL	lower confidence limit
16	LD <sub>50</sub>	median lethal dose
17	LDH	lactate dehydrogenase
18	LEV	local exhaust ventilation
19	LFA	long amosite fibers
20	LH	luteinizing hormone
21	lpm	liters per minute
22	LOAEL	lowest observed adverse effect level
23	MALDI-TOFMS	matrix-assisted laser desorption/ionization–time-of-flight mass spectrometry
24	MEF	mouse embryonic fibroblasts
25	MES	mouse embryonic stem
26	mg/L	milligram per liter
27	mg/m <sup>3</sup>	milligram per cubic meter
28	min	minute
29	ml	milliliter
30	MMAD	mass median aerodynamic diameter
31	MN	marrow micronucleus
32	MNPCE	micronucleated polychromatic erythrocytes
33	MoA	mode of action

*This information is distributed solely for the purpose of pre-dissemination peer review under applicable information quality guidelines. It has not been formally disseminated by the National Institute for Occupational Safety and Health. It does not represent and should not be construed to represent any agency determination or policy.*

1	MOE	margin of exposure
2	MPPD	multiple-path particle dosimetry
3	MTD	maximum tolerated dose; or, minimally toxic dose
4	mRNA	messenger ribonucleic acid
5	MWM	Morris water maze
6	NA	not applicable
7	NaBH <sub>4</sub>	sodium borohydride
8	NAC	N-acetyl cysteine
9	NAG	N-acetyl-B-D glucosaminidase
10	ND	nondetectable
11	ng/cm <sup>2</sup>	nanograms per square centimeter
12	ng/g	nanograms per gram
13	NIEHS	National Institute of Environmental Health Sciences
14	NIOSH	National Institute for Occupational Safety and Health
15	NIST	National Institute of Standards and Technology
16	nm	nanometer
17	nm <sup>2</sup> /cm <sup>3</sup>	square nanometer per cubic centimeter
18	NOAEL	no observed adverse effect level
19	NTRC	Nanotechnology Research Center
20	OEB	occupational exposure band
21	OECD	Organisation for Economic Cooperation and Development
22	OEL	occupational exposure limit
23	OSHA	Occupational Safety and Health Administration
24	PBPK	physiologically-based pharmacokinetic [model]
25	PBS	phosphate buffered saline
26	PBZ	personal breathing zone
27	PCR	polymerase chain reaction
28	PI	propidium iodide
29	PKC	protein kinase C
30	PoD	point of departure used in quantitative risk assessment
31	PPE	personal protective equipment
32	PSM	process safety management
33	PtD	prevention through design

*This information is distributed solely for the purpose of pre-dissemination peer review under applicable information quality guidelines. It has not been formally disseminated by the National Institute for Occupational Safety and Health. It does not represent and should not be construed to represent any agency determination or policy.*

1	PVP	polyvinylpyrrolidone
2	PVR	poliovirus receptor
3	QRA	quantitative risk assessment
4	RBC	red blood cell
5	RCC	relative cell count
6	REL	recommended exposure limit
7	RNA	ribonucleic acid
8	ROS	reactive oxygen species
9	RT-PCR	reverse transcription polymerase chain reaction
10	SD	standard deviation
11	SEGs	similarly exposed groups
12	SEM	scanning electron microscope
13	SFA	short amosite fibers
14	SLC7A13	solute carrier family 7, member 13
15	SOD	superoxide dismutase
16	SOP	standard operating procedures
17	SPECT	single-photon emission computerized tomography
18	SPMS	scanning mobility particle sizer
19	STEM	scanning transmission electron microscopy
20	TEM	transmission electron microscope
21	TGF- $\beta$	transforming growth factor-beta
22	THF	tetrahydrofuran
23	TiO <sub>2</sub>	titanium dioxide
24	TLV®	threshold limit value
25	TWA	time-weighted average
26	UF	uncertainty factor
27	$\mu\text{g}$	microgram
28	$\mu\text{g}/\text{dL}$	microgram per deciliter
29	$\mu\text{g}/\text{g}$	microgram per gram
30	$\mu\text{g}/\text{kg}$	microgram per kilogram
31	$\mu\text{g}/\text{L}$	microgram per liter
32	$\mu\text{g}/\text{m}^3$	microgram per cubic meter
33	$\mu\text{g}/\text{mL}$	microgram per milliliter

*This information is distributed solely for the purpose of pre-dissemination peer review under applicable information quality guidelines. It has not been formally disseminated by the National Institute for Occupational Safety and Health. It does not represent and should not be construed to represent any agency determination or policy.*

1	μL	microliter
2	μm	micrometer
3	U/L	units per liter
4	UCL	upper confidence limit
5	WBC	white blood cell
6	WHO	World Health Organization
7	wk	week
8	wt	weight
9	yr	year
10	%	percent
11		

## 1 **Terminology/Glossary**

2 A number of terms used in the field of nanotechnology have specialized meanings, and  
3 definitions of certain terms have important biologic, legal, regulatory, and policy  
4 implications. Experimental animal and in vitro studies cited in this report frequently  
5 describe exposures to ‘silver,’ ‘nanosilver,’ ‘nanoscale silver,’ ‘silver nanoparticles  
6 (AgNPs),’ or ‘silver nanowires (AgNWs)’ without always providing complete information  
7 on particle dimension, species, and other physical-chemical properties. The absence of  
8 such information, especially from some in vitro studies, limits the ability to compare the  
9 toxicological outcomes reported in the in vitro studies with the exposure concentrations  
10 and doses that brought about AgNP-related effects observed in the in vivo studies.

11 Terms used in the risk assessment of silver nanomaterials are also defined in this  
12 section.

### 13 **Terms related to silver and silver nanomaterials**

14  
15 **Nanomaterials:** The International Organization for Standardization (ISO) has  
16 developed nomenclature and terminology for nanomaterials [ISO/TS 2008]. According  
17 to ISO 27687:2008, a *nano-object* is material with one, two, or three external  
18 dimensions in the size range of approximately 1–100 nanometers (nm). Subcategories  
19 of a nano-object are (1) *nanoplate*, a nano-object with one external dimension at the  
20 nanoscale (1–100 nm); (2) *nanofiber*, a nano-object with two external dimensions at the  
21 nanoscale (a nanotube is defined as a *hollow nanofiber*, and a nanorod is defined as a  
22 *solid nanofiber*); and (3) *nanoparticle*, a nano-object with all three external dimensions  
23 at the nanoscale. Nano-objects are commonly incorporated in a larger matrix or  
24 substrate called a *nanomaterial*. The term ‘silver nanomaterial’ used by NIOSH in this  
25 *Current Intelligence Bulletin* includes engineered AgNPs and AgNWs.

26 **Silver nanoparticles (AgNPs):** This document focuses primarily on exposure to  
27 engineered AgNPs. Several methods of AgNPs synthesis exist, including: the Lee-

1 Meisel or Creighton methods (involving silver salts and reducing agents), high-  
2 temperature reduction in porous solid matrices, vapor-phase condensation of a metal  
3 onto a solid support, laser ablation of a metal target into a suspending liquid, photo-  
4 reduction of silver ions, chemical vaporization, dry powder dispersion, and electrolysis  
5 of a silver salt solution. Most reports of the in vitro and in vivo studies described in this  
6 document do not note the source of exposure to AgNPs. Workers employed in  
7 industries using silver were assumed to have been exposed to AgNPs generated as a  
8 fume during the melting and electro-refining of silver or during brazing/soldering  
9 operations.

10 **Aggregate and agglomerate:** In many circumstances, primary AgNPs can aggregate  
11 or agglomerate into secondary particles with dimensions greater than 100 nm. These  
12 two terms have specific meanings [ISO 2006]: an *aggregate* is a heterogeneous group  
13 of nanoparticles held together by relatively strong forces (for example, covalent bonds)  
14 and thus are not easily broken apart. An *agglomerate* is a group of nanoparticles held  
15 together by relatively weak forces, including van der Waals forces, electrostatic forces,  
16 and surface tension. Aggregates and agglomerates of silver particles can occur in work  
17 environments where engineered AgNPs are synthesized and handled (such as during  
18 removal from the reactor or handling of “free” powder forms of AgNPs) and where  
19 fumes are generated during the melting of silver and silver alloys and during silver  
20 brazing/soldering. The extent to which AgNPs occurred as an aggregate or agglomerate  
21 in the cited studies with workers and in the in vitro and in vivo studies was often not  
22 described by the authors. Whether the constituent primary particles remained  
23 agglomerated or aggregated during the entire study period is also unknown.

24 **Colloid:** The term ‘colloid’ used in the cited studies refers to an assemblage of AgNPs  
25 suspended within a given medium that are smaller than microscale (less than  $10^{-6}$  m).  
26 For example, Wijnhoven et al. [2009] refers to colloidal silver as comprising silver  
27 particles primarily in the range of 250–400 nm, thereby distinguishing nanoscale silver  
28 from colloidal silver.

*This information is distributed solely for the purpose of pre-dissemination peer review under applicable information quality guidelines. It has not been formally disseminated by the National Institute for Occupational Safety and Health. It does not represent and should not be construed to represent any agency determination or policy.*

1 **Argyria:** Argyria is frequently described as a gray-blue discoloration of the skin, mucous  
2 membranes, and/or internal organs as a result of exposure to silver. Argyria may occur  
3 in an area of repeated or abrasive dermal contact with silver or silver compounds, or it  
4 may occur more extensively over widespread areas of skin after long-term oral or  
5 inhalation exposure. Localized argyria can occur in the eyes (argyrosis), where gray-  
6 blue patches of pigmentation are formed without evidence of tissue reaction.  
7 Generalized argyria is recognized by widespread pigmentation of the skin due to the  
8 deposition of silver complexes and by a silver-induced increase in melanin [Hathaway  
9 and Proctor 2004].

## 10 **Terms used in risk assessment**

11 These definitions are based on or adapted from those in the NIOSH document  
12 “Practices in Occupational Risk Assessment” [Nov. 2017 draft], unless otherwise cited.

13 **Acute Exposure:** A one-time or short-term exposure with a duration of less than or  
14 equal to 24 h [U.S. EPA 1994].

15 **Adverse Effect:** Change in the morphology, physiology, growth, development,  
16 reproduction, or life span of an organism, system, or population that results in an  
17 impairment of functional capacity, an impairment of the capacity to compensate for  
18 additional stress, or an increase in susceptibility to other influences.

19 **Aerosol:** All-inclusive term. A suspension of liquid or solid particles in air [U.S. EPA  
20 1994].

21 **Benchmark dose (BMD):** A dose that produces a predetermined change in the  
22 response rate of an adverse effect relative to the background response rate of this  
23 effect. The dose may be as administered or as measured in biological tissues or fluids.

*This information is distributed solely for the purpose of pre-dissemination peer review under applicable information quality guidelines. It has not been formally disseminated by the National Institute for Occupational Safety and Health. It does not represent and should not be construed to represent any agency determination or policy.*

- 1    **Benchmark concentration (BMC):** An exposure concentration of a substance (e.g., in  
2    air) that produces a predetermined change in the response rate of an adverse effect  
3    relative to the background response rate of this effect.
- 4    **Benchmark response (BMR):** A predetermined change in the response rate of an  
5    adverse effect relative to the background response rate of this effect. A BMR is typically  
6    in the low dose region of the data (e.g., 10% increase over background response).
- 7    **Critical Effect:** The first adverse effect, or its known precursor, that occurs as the dose  
8    rate increases; designation is based on evaluation of overall data base [U.S. EPA  
9    1994].
- 10   **Chronic Exposure:** Multiple exposures occurring over an extended period of time, or a  
11   significant fraction of the animal's or the individual's lifetime [U.S. EPA 1994].
- 12   **Dose:** Total amount of an agent administered to, taken up by, or absorbed by an  
13   organism, system, or (sub) population.
- 14   **Dose-response:** The relationship between the amount of an agent administered to,  
15   taken up by, or absorbed by an organism, system, or population and the change  
16   developed in that organism, system, or population in reaction to the agent.
- 17   **Dosimetric adjustment factor (DAF):** A multiplicative factor used to adjust observed  
18   animal or epidemiological data to estimate a human equivalent concentration (HEC) for  
19   an exposure scenario of interest. For inhaled particles, DAFs include factors to account  
20   for interspecies differences in ventilation rate, particle deposition fraction, and surface  
21   area of the respiratory tract region(s) of interest [adapted from U.S. EPA 1994].
- 22   **Exposure:** Contact between an agent and a target. Contact takes place at an exposure  
23   surface over an exposure period.

*This information is distributed solely for the purpose of pre-dissemination peer review under applicable information quality guidelines. It has not been formally disseminated by the National Institute for Occupational Safety and Health. It does not represent and should not be construed to represent any agency determination or policy.*

1    **Exposure assessment:** The process of estimating or measuring the distribution of the  
2    magnitude, frequency, and duration of exposure to an agent, along with the number and  
3    characteristics of the population exposed. Ideally, it describes the sources, pathways,  
4    routes, and the uncertainties in the assessment.

5    **Exposure duration:** The length of time over which continuous or intermittent contacts  
6    occur between an agent and a target.

7    **Exposure route:** The way in which an agent enters a target after contact (e.g., by  
8    ingestion, inhalation, or dermal absorption).

9    **Hazard:** The inherent property of an agent (or situation) having the potential to cause  
10   an adverse effect when an organism, system, or population is exposed to that agent.

11   **Hazard assessment:** The process of identifying the type and nature of adverse effects  
12   that an agent has an inherent capacity to cause in an organism, system, or population.  
13   Hazard assessment is the first of the four main steps of a risk assessment.

14   **Human-equivalent concentration:** The airborne concentration of a substance at the  
15   animal point of departure (PoD), which has been estimated by application of dosimetric  
16   adjustment factors (DAFs) for the respiratory tract region(s) of interest [adapted from  
17   U.S. EPA 1994].

18   **Lowest observed adverse effect level (LOAEL):** The lowest dose or concentration at  
19   which there are statistically significant increases in the frequency or severity of  
20   biologically significant adverse effects between the exposed population and its  
21   appropriate control group [adapted from U.S. EPA 1994].

22   **Mechanism of action:** A more detailed understanding and description of events, often  
23   at the molecular level, than is meant by mode of action.

*This information is distributed solely for the purpose of pre-dissemination peer review under applicable information quality guidelines. It has not been formally disseminated by the National Institute for Occupational Safety and Health. It does not represent and should not be construed to represent any agency determination or policy.*

1 **Mode of action (MoA):** A sequence of key events and processes, starting with  
2 interaction of an agent with a cell, proceeding through operational and anatomical  
3 changes, and resulting in disease such as cancer.

4 **No observed adverse effect level (NOAEL):** The highest dose or concentration at  
5 which there are no statistically significant increases in the frequency or severity of  
6 biologically significant adverse effects between the exposed population and its  
7 appropriate control group; some effects may be produced at this dose level, but they are  
8 not considered adverse or precursors of adverse effects observed [adapted from U.S.  
9 EPA 1994].

10 **Occupational exposure limit (OEL):** The allowable concentration or intensity of a  
11 hazardous agent in the worker's work environment over a period of time. Generally  
12 expressed as an 8-hour time weighted average or as a short-term exposure limit of 15  
13 or 30 minutes.

14 **Point of departure (PoD):** A point on the dose-response curve from experimental or  
15 observational data, which is a dose associated with a level of no or low effect, and  
16 which is estimated without significant extrapolation beyond the data. A PoD is often a  
17 NOAEL, LOAEL, or BMD estimate from an animal study.

18 **Risk assessment:** The determination of the relationship between the predicted  
19 exposure and adverse effects in four major steps: hazard identification, dose-response  
20 assessment, exposure assessment and risk characterization.

21 **Risk characterization:** The qualitative and, wherever possible, quantitative  
22 determination, including attendant uncertainties, of the probability of occurrence of  
23 known and potential adverse effects of an agent in workers under defined exposure  
24 conditions.

*This information is distributed solely for the purpose of pre-dissemination peer review under applicable information quality guidelines. It has not been formally disseminated by the National Institute for Occupational Safety and Health. It does not represent and should not be construed to represent any agency determination or policy.*

1 **Physiologically based pharmacokinetic (PBPK) modeling:** A mathematical  
2 modeling technique to predict the absorption, distribution, metabolism, and/or  
3 elimination of exogenous substances in animals or humans.

4 **Subchronic exposure:** Multiple or continuous exposures occurring for approximately  
5 10% of an experimental species lifetime, usually over 3 months [U.S. EPA 1994].

6 **Target:** Any biological entity that receives an exposure or a dose (e.g., an organ, an  
7 individual, or a population).

8 **Validity:** The quality of being logically or factually sound; the extent to which the  
9 measure describes that which is being measured.

10 **Uncertainty factor (UF):** One of several factors, generally 3- to 10-fold, used in  
11 deriving the recommended exposure limit (REL) from experimental data. UFs are  
12 intended to account for (1) the variation in sensitivity among the members of the human  
13 population, (2) the uncertainty in extrapolating laboratory animal data to humans, (3) the  
14 uncertainty in extrapolating from data obtained in a study that is of less-than-lifetime  
15 exposure, (4) the uncertainty in using LOAEL data rather than an NOAEL data, and (5) the  
16 inability of any single study to adequately address all possible adverse outcomes in  
17 humans [U.S. EPA 1994].

18 **Uptake:** The process by which an agent crosses an absorption barrier.

19

20

## 1 **Acknowledgments**

2 This Current Intelligence Bulletin (CIB) was developed by the scientists and staff of the  
3 National Institute for Occupational Safety and Health (NIOSH), Education and  
4 Information Division (EID), Nanotechnology Research Center (NTRC), with  
5 contributions by external collaborators. Paul Schulte is the Director of EID and Co-  
6 Manager of the NTRC; Charles Geraci is the NIOSH Associate Director for  
7 Nanotechnology and Co-Manager of the NTRC; and Laura Hodson is the Coordinator of  
8 the NTRC.

9 This document was authored by Eileen Kuempel, Gary Roth, and Nathan Drew,  
10 EID/NTRC; by Ralph Zumwalde (formerly in NIOSH/EID), by Jenny Roberts and Ann  
11 Hubbs, Health Effects Laboratory Division (HELD); by Kevin L. Dunn and Douglas  
12 Trout, Division of Surveillance, Hazard Evaluation, and Field Studies (DSHEFS); and by  
13 George Holdsworth, formerly with Oak Ridge Institute for Science and Education  
14 (ORISE), who provided an initial hazard review of the toxicology studies.

15 The data analyses were performed by Eileen Kuempel and Nathan Drew, EID/NTRC,  
16 and by Gerald Bachler, formerly with Institute for Chemical and Bioengineering, Zurich,  
17 Switzerland, who provided the PBPK modeling estimates used in the risk assessment.  
18 Responses to the external review comments were prepared by Gary Roth, Eileen  
19 Kuempel, Jenny Roberts, Nathan Drew, and Kevin L. Dunn. Sherri Fendinger,  
20 Document Development Branch (DDB)/EID, performed the scientific literature searches  
21 for this revised document. Paul Schulte, Kathleen MacMahon (EID), Paul Middendorf  
22 and Gerald Joy, NIOSH Office of the Director, and John A. Decker, formerly in the  
23 NIOSH Office of the Director, provided scientific and policy reviews of the external  
24 review draft documents.

25 The following NIOSH researchers provided scientific and technical input during the  
26 internal review of this document:

*This information is distributed solely for the purpose of pre-dissemination peer review under applicable information quality guidelines. It has not been formally disseminated by the National Institute for Occupational Safety and Health. It does not represent and should not be construed to represent any agency determination or policy.*

1 Kathleen MacMahon, Christine Whittaker, Randall Smith (EID), and David Dankovic  
2 (formerly in NIOSH/EID)

3 Aleksandr Stefaniak, Respiratory Health Division (RHD)

4 Bean Chen, HELD

5 Lee Portnoff, National Personal Protective Technology Laboratory (NPPTL) and Pengfei  
6 Gao (formerly in NIOSH/NPPTL)

7 Kevin H. Dunn, Division of Applied Research and Technology (DART), and Steven M.  
8 Schrader (formerly in NIOSH/DART)

9 Matthew Dahm, DSHEFS

10 External peer reviewers of specific sections of the updated document included Michael  
11 (Andy) Maier, University of Cincinnati; Lisa M. Sweeney, Naval Medical Research Unit  
12 Dayton; and David Malarkey, National Institutes of Health/National Institute of  
13 Environmental Health Sciences.

14 Editorial assistance on this document was provided by Seleen Collins, Ellen Galloway,  
15 and John Lechliter, EID.

16 **Invited Expert Peer Reviewers of Previous Draft (January 7, 2016)**

17 Karin Aschberger, European Commission, Joint Research Centre, Institute for Health  
18 and Consumer Protection; Terry Gordon, New York University, School of Medicine;  
19 Thomas Peters, University of Iowa; and Q. Jay Zhao, U.S. Environmental Protection  
20 Agency

21 **Invited Expert Reviewer of Previous Draft (January 7, 2016)**

22 Günter Oberdörster, University of Rochester Medical College

1  
2  
3  
4  
5  
6  
7  
8  
9  
10  
11  
12  
13

## 1 Introduction

This *Current Intelligence Bulletin* (CIB) presents an assessment of the potential health risks to workers occupationally exposed to silver, with emphasis on workers' exposure to silver nanomaterials. First, the CIB presents (1) workplace exposure data for silver; (2) information on the absorption, systematic distribution, metabolism, and excretion of silver; (3) an assessment of toxicological data from experimental animal studies; and (4) an analysis of in vitro and mechanistic studies. Based upon these data, the CIB next presents, (5) an assessment of the health risk to workers exposed to silver and silver nanomaterials; and (6) a recommended exposure limit (REL) for silver and silver nanomaterials. Finally, the CIB provides recommendations for (7) assessing exposure to silver nanomaterials, (8) managing associated risks, and (9) recommendations for future research related to silver nanomaterials.

### 1.1 Background

Silver (Ag) is a rare, naturally occurring element. It is often found as a mineral ore deposit—in association with copper, lead-zinc, and gold—from which it is extracted [USGS 2014]. In 2012, the United States produced approximately 1,050 metric tons of silver. Chemically, silver is the most reactive of the noble metals, but it does not oxidize readily; rather, it tarnishes by combining at ordinary temperatures with sulfur (H<sub>2</sub>S). Silver is slightly harder than gold and is very ductile and malleable. Silver can form many different inorganic and organic complexes, and its most stable oxidation states are elemental (+0) and monovalent silver ion (Ag<sup>+</sup>), although other cationic states (Ag<sup>+2</sup>, Ag<sup>+3</sup>) exist as well [USGS 2014]. The most abundant silver compounds are silver sulfide (Ag<sub>2</sub>S), silver nitrate (AgNO<sub>3</sub>), and silver chloride (AgCl).

Elemental silver has been commercially available for decades and used in applications as diverse as coins and medals, electrical components and electronics, jewelry and silverware, dental alloy, explosives, and biocides [Wijnhoven et al. 2009; Nowack et al. 2011; USGS 2014]. For centuries the antimicrobial potential of silver (medicinal silver colloids) for healing wounds and preserving materials [Nowack et al. 2011] has been

1 recognized, and within the last century silver has been used in antimicrobial tonics, in  
2 bandages for wound care, and in the processing of radiographic and photographic  
3 materials [Quadros and Marr 2010; Hendren et al. 2011]. The industrial demand for  
4 silver has declined for photographic applications, jewelry, electronic applications, and  
5 coins, but it has increased for brazing alloys and solders, as a replacement metal for  
6 platinum in automobile catalytic converters, and as a catalyst in numerous chemical  
7 reactions [USGS 2014].

8 Within the past decade, the demand has increased for production of silver  
9 nanomaterials to create different nanostructures such as spheres and wires [Wijnhoven  
10 et al. 2009]. These nanostructures of silver are typically commercialized as powders,  
11 flakes, and grains, and are sold in suspensions (such as in water, alcohol, or  
12 surfactant), colloidal preparations, and dry powders [Future Markets, 2013]. These  
13 various silver compounds have differing physical-chemical properties, such as solubility  
14 and surface charge, which all may affect their fate and biologic activity. Silver  
15 nanomaterials are increasingly being used in consumer and medical products, mainly to  
16 take advantage of their high antimicrobial activity. The consumer products and  
17 applications include coatings, paints, conductive inks, soaps and laundry detergents,  
18 refrigerator and laundry machine components, cooking utensils, medical instruments  
19 (dressings, catheters, pacemakers), drug delivery devices, water purifiers, textiles,  
20 antibacterial sprays, personal care products (toothpaste, shampoo, cosmetics), air  
21 filters, and humidifiers [Quadros and Marr 2010]. Additionally, different nano-forms of  
22 silver can be used in the field of electronics (e.g., transparent conducting films,  
23 transparent electrodes for flexible devices, flexible thin-film tandem solar cells) [Reidy et  
24 al. 2013]. These applications exploit their conductivity and electrical properties rather  
25 than antimicrobial properties. The Woodrow Wilson International Center for Scholars  
26 “Project on Emerging Nanotechnologies” (<http://www.nanotechproject.org/>) lists over  
27 100 consumer products containing silver nanomaterials, although the nanomaterial  
28 content of many of these products could not be verified [Vance et al. 2015]. It was  
29 estimated that 20 tons of silver nanomaterials were produced in the United States in  
30 2010 [Hendren et al. 2011], and an estimated worldwide production of 450–542 tons/yr

1 was projected for 2014 [Future Markets 2013]. As new products utilizing silver  
2 nanomaterials are produced and applications expanded, the potential for worker and  
3 consumer exposure to airborne silver nanomaterials (such as AgNPs) is expected to  
4 escalate throughout the materials' life cycle (that is, their synthesis, use, disposal, and  
5 recycling).

6 Numerous methods have been used to synthesize silver nanomaterials, which can be  
7 arbitrarily divided into traditional and nontraditional categories [Evanoff and Chumanov  
8 2005; Chen and Schluesener 2008; Quadros and Marr 2010]. Traditional methods  
9 include solution-phase synthesis techniques that are based on various modifications of  
10 the Lee-Meisel or Creighton methods, in which different silver salts and reducing agents  
11 are used. The most common traditional method for the synthesis of AgNPs is the  
12 reduction of  $\text{AgNO}_3$  with  $\text{NaBH}_4$ . The nontraditional methods include silver particle  
13 synthesis through high-temperature reduction in porous solid matrices, vapor-phase  
14 condensation of a metal onto a solid support, laser ablation of a metal target into a  
15 suspending liquid, photo-reduction of silver ions, chemical vaporization, dry powder  
16 dispersion, and electrolysis of a silver salt solution. Although each method has certain  
17 advantages and disadvantages, the selection of a method typically depends on the  
18 nature of the nanomaterial application. After synthesis, AgNPs can be coated with  
19 oxides or coated/embedded into organic polymeric matrices such as poly-  
20 (dimethylsiloxane), poly-(4-vinylpyridine), polystyrene, polymethacrylate, and Teflon.  
21 These coatings are used to tailor the surface chemical properties of the AgNP to  
22 particular applications and to protect them from chemically aggressive environments.

23 The metallic forms of silver nanomaterials can form stable suspensions in which the  
24 AgNPs slowly dissolve into silver ions [U.S. EPA 2012a]. Silver nanomaterials may also  
25 include other insoluble particulate forms, such as silver carbonate ( $\text{Ag}_2\text{CO}_3$ ), silver  
26 citrate ( $\text{C}_6\text{H}_5\text{Ag}_3\text{O}_7$ ), silver phosphate ( $\text{AgPO}_4$ ), silver oxide ( $\text{Ag}_2\text{O}$ ), silver sulfate  
27 ( $\text{Ag}_2\text{SO}_4$ ), and silver sulfide ( $\text{Ag}_2\text{S}$ ). However, the metallic salts of silver including nitrate  
28 ( $\text{AgNO}_3$ ) and silver chloride ( $\text{AgCl}$ ) are soluble in water [WHO 2005b]. The highly  
29 insoluble forms of silver typically have a low dissolution rate for releasing silver ions,

1 whereas the completely soluble forms of silver (such as AgNO<sub>3</sub>) have a high ion  
2 dissolution release potential in water. Factors that can affect the dissolution of AgNPs in  
3 water include size [Ma et al. 2012], surface coatings [Zook et al. 2011; Li et al. 2012a;  
4 Tejamaya et al. 2012], pH [Elzey and Grassain 2010;], and the solution concentration of  
5 sulfur or sodium chloride [Kent and Vikesland 2012]. Also, as the particle size of silver  
6 decreases, the potential for releasing silver ions via dissolution increases because of  
7 rising surface availability per mass of silver [Wijnhoven et al. 2009].

8 Although the overall amount of animal toxicological information is small and the studies  
9 have been comparatively short, the knowledge base includes these findings: (1) AgNPs  
10 in the body by various routes of exposure can be absorbed and become transported to  
11 target tissues; (2) lung inflammation and lung function decrements have been observed  
12 at certain exposure concentrations of AgNPs following subchronic inhalation in rats,  
13 suggesting the potential for chronic adverse health effects; and (3) the liver and (to a  
14 lesser extent) the kidney represent the primary target organs for systemic accumulation  
15 of silver and adverse effects associated with exposure to AgNPs. The studies also  
16 indicate that the higher surface volume ratio of AgNPs, compared with larger respirable-  
17 size silver particles, is a cause of concern because it makes AgNPs potentially more  
18 reactive than larger silver particles and makes it more difficult to predict how they will  
19 interact with biological systems (Table 1-1).

20

1 **Table 1-1. Differences between ionic, nanoparticulate, and bulk silver.**

Ions	Nanoparticles	Bulk (microscale) particles
<ul style="list-style-type: none"> <li>• Highly reactive</li> <li>• Condenses</li> <li>• Easily get inside cells</li> <li>• Form complexes with inorganic and organic compounds</li> </ul>	<ul style="list-style-type: none"> <li>• Greater surface area per unit mass, increasing dissolution and ionization rates on a mass basis</li> <li>• Highly reactive</li> <li>• Greater oxidative capacity</li> <li>• Increased ability for cellular uptake via active processes</li> <li>• Bind biomolecules</li> </ul>	<ul style="list-style-type: none"> <li>• Smaller particle surface area per unit mass, reducing dissolution and ionization rates on a mass basis</li> <li>• Lower reactivity</li> <li>• Lower oxidative capacity</li> <li>• Lower uptake by some cells (although not applicable to alveolar macrophages)</li> <li>• Limited binding of biomolecules</li> </ul>

2 Adapted from Reidy et al. [2013].

### 3 **1.2 Bases for Current Occupational Exposure Limits**

4 The accumulation of silver over time (body burden) has been shown to result in a  
5 condition known as argyria. This condition, a pathologic consequence of prolonged  
6 silver exposure, has been described as a blue-grey discoloration of the skin and  
7 mucous membranes (argyria) or as a localized condition of the eyes (argyrosis) [Harker  
8 and Hunter 1935; Hill and Pillsbury 1939]. Exposure to the soluble forms of silver has  
9 frequently been associated with the development of argyria [ATSDR 1990; Drake and  
10 Hazelwood 2005; Wijnhoven et al. 2009; Johnston et al. 2010; Lansdown AB 2012].

*This information is distributed solely for the purpose of pre-dissemination peer review under applicable information quality guidelines. It has not been formally disseminated by the National Institute for Occupational Safety and Health. It does not represent and should not be construed to represent any agency determination or policy.*

1 Generalized occupational argyria in exposed workers can occur as a result of the  
2 absorption of silver through the lungs, the digestive tract, or wounds in the skin.

3 Prevention of argyria is the basis for the current occupational exposure limits (OELs) in  
4 the United States and other countries. The Occupational Safety and Health  
5 Administration (OSHA) permissible exposure limit (PEL) and the National Institute for  
6 Occupational Safety and Health (NIOSH) recommended exposure limit (REL) are both  
7  $10 \mu\text{g}/\text{m}^3$  (total dust) for silver (metal dust, fume, and soluble compounds, as Ag) as an  
8 8-hour time-weighted average (TWA) concentration [OSHA 1988, 2012a; NIOSH 1988,  
9 2007]. The term “fume” is not included in the NIOSH Pocket Guide [NIOSH 2007]  
10 definition of the NIOSH REL and OSHA PEL for silver (total dust). However, fume is  
11 included in the other references for the NIOSH REL and OSHA PEL for silver, i.e.,  
12 “metal dust, fume, and soluble compounds, as Ag” [NIOSH 1988; OSHA 1988, 2012a].  
13 The American Conference of Governmental Industrial Hygienists (ACGIH) threshold  
14 limit values (TLVs<sup>®</sup>) [ACGIH 2001; TLV<sup>®</sup> updated in 1992] and the German MAK  
15 Commission MAK (Maximum Workplace Concentration) values are also  $10 \mu\text{g}/\text{m}^3$  for  
16 soluble silver but are higher, at  $100 \mu\text{g}/\text{m}^3$ , for insoluble silver compounds (Table 1-2).  
17 The evidence basis and derivation of the NIOSH REL are discussed in Section 1.4.

18 There is a growing body of toxicological evidence indicating that exposure to some  
19 forms and particle sizes of silver may pose a greater health risk to workers than other  
20 forms and sizes. Experimental animal studies with rats (for up to 3 months) exposed to  
21 AgNP concentrations of approximately  $100 \mu\text{g}/\text{m}^3$  (10 times the current OSHA PEL and  
22 NIOSH REL) showed mild adverse lung effects, including pulmonary inflammation and  
23 lung function deficits that persisted after the end of exposure. Bile duct hyperplasia has  
24 also been observed in rats after the inhalation of relatively low-mass concentrations of  
25 silver and AgNPs (Appendix E, Table E-5). It is not known how universal these adverse  
26 effects are, that is, whether they occur in animals exposed to all forms and particle sizes  
27 of silver. However, hyperplasia is believe to be one of several factors involved in the  
28 development of cholangiocarcinoma, the biliary tract cancer of the liver [Rizvie and  
29 Gores 2014; Rizvi et al. 2014]. Most important, it is not known whether similar adverse

1 health effects occur in humans following exposure to AgNPs. The extent to which  
2 workers are exposed to silver in the workplace, including exposure to silver  
3 nanomaterials, is also unclear because of limited published exposure data.

### 4 **1.3 Scientific Literature Review**

5 NIOSH conducted a comprehensive review of the literature to identify the scientific  
6 information available on occupational exposure to silver nanomaterials and potential  
7 adverse health effects associated with exposure. The scientific data and information  
8 includes published journal articles on exposure measurement in the workplace, medical  
9 monitoring in workers, and toxicology studies in animals and cell systems. These  
10 literature searches were conducted in several phases during the period from 2012 to  
11 2017. Initial searches were conducted by the Oak Ridge Institute for Science and  
12 Education (ORISE). Subsequent literature searches were conducted by NIOSH using  
13 the online databases and specific search terms described in Appendix C.

14 The initial literature searches were performed by ORISE through 2012 using several  
15 online databases (Appendix C). Search terms included silver nanoparticles and other  
16 relevant key words (e.g., toxicology, physical and chemical properties, dosimetry).  
17 NIOSH conducted literature searches in 2013 and 2014 to identify additional studies  
18 with information on exposure and response to silver and/or silver nanoparticles. Search  
19 terms were selected to ensure that all in vivo (animal) and in vitro (cellular) toxicology  
20 studies with silver and/or silver nanomaterials were identified, and all studies describing  
21 workplace exposures to silver and/or silver nanomaterials (Appendix C).

22 In response to external review comments of the 2016 draft CIB on the need to further  
23 update of the scientific literature review, NIOSH conducted an updated and expanded  
24 literature search to identify scientific studies published during the period of January 1,  
25 2011, to June 30, 2016. Several relevant subject areas were identified, including studies  
26 of exposure to AgNPs in humans, animals (including lung, oral, or dermal routes of  
27 exposure), in vitro (cellular), cell-free, and zebrafish. Two additional searches in October  
28 2016 focused on the kinetics of silver nanoparticles in biological systems, and on

1 reproductive studies that had been published since January 2011. A focused literature  
2 search on the biological significance of the rat biliary hyperplasia response to silver  
3 nanoparticles was performed in January 2017.

4 NIOSH evaluated the relevance of these search results by examination of the titles and  
5 abstracts. The publications selected for full review included all studies of occupational  
6 exposure to silver or silver nanomaterials, all in vivo studies on silver nanoscale or  
7 microscale particles, and any in vitro studies that provided information on the role of  
8 particle size and/or solubility on the toxicological effects. NIOSH obtained all relevant  
9 publications available in full English text. These publications were individually reviewed  
10 and considered for inclusion based on study design, relevance to workers, and study  
11 quality. Selected publications were categorized by their overall topics, such as worker  
12 exposure case studies, human health effects studies, cell culture-based studies, and  
13 animal studies. The publications in these categories were then analyzed, tabulated, and  
14 summarized as reflected in this document. All of the occupational exposure studies and  
15 in vivo and in vitro studies on silver nanoscale or microscale particles meeting the  
16 search and selection criteria were included in this document.

#### 17 **1.4 Human Health Basis for the Current NIOSH REL**

18 The NIOSH REL of  $10 \mu\text{g}/\text{m}^3$  (total dust) for silver (metal dust, fume, and soluble  
19 compounds, as Ag) [NIOSH 1988, 2003, 2007] was set to prevent argyria and was  
20 based on findings in workers exposed to airborne silver. The NIOSH REL is the same  
21 as the OSHA PEL and uses the same evidence basis [OSHA 1988, 2012a]. The  
22 derivation of the REL and PEL [OSHA 1988] are based on an earlier ACGIH TLV, as  
23 described below.

24 These OELs in the United States are based on early case reports of argyria in humans  
25 ingesting silver [Hill and Pillsbury 1939]. A total mass body burden of approximately 3.8  
26 g (1 to 5 g) of silver was associated with argyria [OSHA 1988]. The occupational  
27 airborne exposure concentration that would result in an equivalent body burden of silver  
28 was calculated. Assuming a worker air intake of  $10 \text{ m}^3/\text{day}$  and 25% deposition and

1 retention of inhaled silver in the body, ACGIH estimated a total deposition of  
2 approximately 1.5 g if a worker were exposed at the TLV of 100 µg/m<sup>3</sup> for 25 years  
3 [ACGIH 2001]. That is,

$$4 \quad 1.5 \text{ g} = 0.1 \text{ mg/m}^3 \times 10 \text{ m}^3/8\text{-hr d} \times 5 \text{ d/wk} \times 50 \text{ wk/yr} \times 25 \text{ yr} \times 0.25 \text{ [RF]}$$
$$5 \quad \quad \quad \times (1\text{g}/1,000 \text{ mg})$$

6 Although it is not stated explicitly in the documentation of the PEL and REL, the "body  
7 retention fraction" (RF) is a constant factor that represents the assumed total fraction of  
8 the inhaled dose of silver that is retained in the body (e.g., 0.25), which includes the  
9 fraction deposited in any region of the respiratory tract and also retained in the lungs or  
10 other tissues (i.e., following absorption into the blood or lymph and transported and  
11 retained in other organs). Likewise, 0.75 of the inhaled dose is assumed to be either not  
12 deposited or cleared from the body after deposition in the respiratory tract. The use of  
13 the factor in the total dose estimate means that a constant proportion of the Ag is  
14 retained, regardless of the inhaled dose. No uncertainty factors (UFs) appear to have  
15 been used in deriving this TLV. Over a full working lifetime of 45 years, the body burden  
16 of silver would be estimated to be higher (i.e., ~2.8 g, assuming 45 years worked at 8  
17 hours/day, 40 hours/week, 50 weeks/year, as well as the same volume of air inhaled  
18 per day [10 m<sup>3</sup>] and total RF). If a higher RF of 0.50 is assumed (as discussed below),  
19 the 45-year body burden would be estimated to be ~5.6 g, which exceeds the average  
20 (3.8 g) and minimum (1 g) body burdens associated with argyria in humans [OSHA  
21 1988; ACGIH 2001].

22 The OSHA PEL [OSHA 1988] and NIOSH REL [NIOSH 1988] are based on an earlier  
23 ACGIH TLV of 10 µg/m<sup>3</sup> for silver, which was derived from the same human data [Hill  
24 and Pillsbury 1939] but assumed an estimated fraction of 0.5 of inhaled silver was  
25 retained in the body (i.e., deposited and not cleared). The PEL of 10 µg/m<sup>3</sup> was based  
26 on the following estimates [OSHA 1988]. The retained body burden of silver associated  
27 with argyria in humans was estimated to be 1 to 5 g (from Hill and Pillsbury [1939]).  
28 Based on the assumption of the lower value of 1 g silver body burden, an 8-hour TWA

*This information is distributed solely for the purpose of pre-dissemination peer review under applicable information quality guidelines. It has not been formally disseminated by the National Institute for Occupational Safety and Health. It does not represent and should not be construed to represent any agency determination or policy.*

1 concentration of 50 µg/m<sup>3</sup> was estimated for a 20-year exposure duration [NIOSH 1988;  
2 OSHA 1988]. The PEL of 10 µg/m<sup>3</sup> provides a “safety factor” or “safety margin” of five  
3 [OSHA 1988] (assuming a 20-year exposure duration).

4 These calculations of the airborne exposure concentration (X mg/m<sup>3</sup>) associated with  
5 the target human body burden (as reported above) can be calculated as follows:

$$6 \quad X \text{ mg/m}^3 = \text{Body burden (mg)} / [\text{Exposure duration (d)} \times \text{Air intake per work day} \\ 7 \quad (\text{m}^3/\text{d}) \times \text{Body retention fraction, RF}]$$

8 An example calculation based on the equation above and using the information  
9 provided [NIOSH 1988; OSHA 1988] suggests a slightly lower 8-hour TWA  
10 concentration associated with a lower body burden estimate for argyria:

$$11 \quad 0.042 \text{ mg/m}^3 = 1,000 / (5,000 \times 9.6 \times 0.5)$$

12 where 1 g (or 1,000 mg) is the minimum estimated body burden associated with argyria  
13 [NIOSH 1988; OSHA 1988]; 5,000 is the number of exposure days in 20 years (5  
14 d/wk\*50 wk/yr\*20 yr); 9.6 m<sup>3</sup>/d is the volume of air inhaled per workday (light activity,  
15 reference worker value); and 0.5 is the RF (unitless). Based on this example calculation,  
16 the original “safety factor” of five is closer to four (0.042 mg/m<sup>3</sup> effect level for argyria in  
17 humans vs. 0.01 mg/m<sup>3</sup> PEL).

18 Using the same target human body burden (1 g) of silver, retention fraction, and air  
19 intake but assuming 45 years of exposure (5 days/week, 50 weeks/year) would result in  
20 an estimated airborne concentration of 18 µg/m<sup>3</sup> (8-hour TWA). Thus, assuming a 45-  
21 year working lifetime exposure, instead of a 20-year exposure duration, would result in a  
22 lower safety factor of <2 from the human argyria effect level and the current NIOSH REL  
23 and OSHA PEL of 10 µg/m<sup>3</sup> (8-hour TWA).

24 Airborne sampling for silver according to the NIOSH REL and other OELs (Table 1-2) is  
25 based on the total airborne mass concentration, as Ag (NIOSH Methods 7300, 7301,

*This information is distributed solely for the purpose of pre-dissemination peer review under applicable information quality guidelines. It has not been formally disseminated by the National Institute for Occupational Safety and Health. It does not represent and should not be construed to represent any agency determination or policy.*

1 and 7306) [NIOSH 2017]. These sampling criteria include collection of all particle sizes  
2 that can be inhaled in the human respiratory tract (approximately 1 nm to 100 µm in  
3 diameter). Inhaled particles depositing anywhere in the respiratory tract could potentially  
4 contribute to the body burden of silver either at the site of deposition (if retained) or at  
5 distal sites (if absorbed).

6

*This information is distributed solely for the purpose of pre-dissemination peer review under applicable information quality guidelines. It has not been formally disseminated by the National Institute for Occupational Safety and Health. It does not represent and should not be construed to represent any agency determination or policy.*

1 **Table 1-2. Current OELs for silver in the United States and other countries.**

Authority	Particle Size	Form	OEL ( $\mu\text{g}/\text{m}^3$ )	Reference
OSHA PEL <sup>a</sup>	Metal dust, fume, and soluble compounds, as Ag; total mass fraction	Soluble or insoluble	10	OSHA [1988, 2012a]
NIOSH REL	Metal dust, fume, and soluble compounds, as Ag; total mass fraction	Soluble or insoluble	10	NIOSH [1988, 2003, 2007]
ACGIH TLV <sup>®</sup>	Metal dust and fume; inhalable fraction	Soluble	10	ACGIH [2001; TLV <sup>®</sup> updated in 1992]
		Insoluble	100	
MAK <sup>b</sup>	Inhalable fraction	Silver salts (as Ag)	10	DFG [2013]
		Silver (Ag)	100	

2 <sup>a</sup> Current regulatory limit in the United States.

3 <sup>b</sup> Maximum Workplace Concentration (Germany).

4

## **2 Occupational Exposures to Silver**

Worker exposure to silver can occur throughout the life cycle of the metal (ore extraction, melting/refining, product fabrication, use, disposal, recycling) [Maynard and Kuempel 2005]. Inhalation and dermal contact with silver are considered to be the main exposure routes [ATSDR 1990; Wijnhoven et al. 2009]. Published information on worker exposure to silver is limited to study findings of airborne silver during brazing and soldering operations [NIOSH 1973, 1981, 1998]; fabrication of silver jewelry [NIOSH 1992; Armitage et al. 1996]; recovery of silver from photographic fixer solutions [Williams and Gardner 1995; NIOSH 2000]; production of silver oxide and silver nitrate [Rosenman et al. 1979, 1987; Moss et al. 1979]; refinement of silver [Williams and Gardner 1995]; reclamation of silver [Pifer et al. 1989; Armitage et al. 1996]; and handling of insoluble silver compounds [DiVincenzo et al. 1985; Wölbling et al. 1988]. The reports of these studies lack information on the physical-chemical characteristics (such as particle size or species) of the aerosol to which workers were exposed, although it's likely that aerosols/fumes generated during brazing/soldering [NIOSH 1973, 1981, 1998], the melting of silver alloys [NIOSH 1992], the refinement of silver [Williams and Gardner 1995], and the recovery of silver from photographic-fixer solutions [Williams and Gardner 1995; NIOSH 2000] contained nanometer-size silver particles and/or agglomerates of silver particles. In several workplace studies, airborne exposure to AgNPs was measured during the synthesis of engineered AgNPs [Park et al. 2009; Lee et al. 2011b; Lee et al. 2012a,b] and during the electro-refining of silver [Miller et al. 2010]. Workplace findings of the potential for dermal absorption of silver during handling of colloidal suspension (gel form) and liquid AgNPs also have been reported [Ling et al. 2012]. Table 2-1 summarizes reported workplace exposures to silver.

NIOSH has reported on several workplace studies in which workers were found to be exposed to silver and other airborne contaminants during brazing/soldering and milling operations at an air conditioning equipment company [NIOSH 1973], a metal fabrication facility [NIOSH 1981], and a manufacturer of construction equipment [NIOSH 1998].

*This information is distributed solely for the purpose of pre-dissemination peer review under applicable information quality guidelines. It has not been formally disseminated by the National Institute for Occupational Safety and Health. It does not represent and should not be construed to represent any agency determination or policy.*

1 Workers were found to be exposed to airborne silver concentrations that ranged from  
2 nondetectable to 6  $\mu\text{g}/\text{m}^3$  during brazing and soldering operations while they assembled  
3 air conditioning equipment [NIOSH 1973], in which the use of exposure controls was  
4 minimal. At the other two manufacturing facilities, workers performing brazing and  
5 soldering were exposed to airborne silver concentrations that were below the OSHA  
6 PEL and NIOSH REL of 10  $\mu\text{g}/\text{m}^3$  [NIOSH 1981] or ranged from nondetectable to 0.015  
7  $\mu\text{g}/\text{m}^3$  [NIOSH 1998]. In both facilities, controls were used to minimize worker exposure.

8 NIOSH also reported on a survey at a manufacturer of silver jewelry [NIOSH 1992], in  
9 which workers were potentially exposed to silver, copper, lead, and cadmium fume as  
10 well as to carbon monoxide and nitrogen dioxide. Exposure to silver was detected  
11 during the metal casting operation, in which 100 ounces of an Ag/Cu alloy was melted  
12 with an air-acetylene and oxy–natural gas torch. The operation took approximately 84  
13 minutes, and the airborne silver concentration to which the worker was exposed during  
14 this time was 54  $\mu\text{g}/\text{m}^3$ . Local exhaust ventilation (LEV) was used during the casting  
15 operation.

16 The highest airborne silver concentrations found in NIOSH workplace studies were at a  
17 precious metal recycling facility [NIOSH 2000] during the recovery of silver from  
18 photographic fixer solutions. Silver was recovered by the “metallic replacement  
19 method,” in which steel wool and fiberglass were used within a recovery cartridge to  
20 extract the dissolved silver ions from the fixer solution. The cartridges were then placed  
21 into silicon carbide or clay graphite crucibles and heated at a temperature of 2200–  
22 2300°F to separate silver from the impurities. A personal sample collected on a worker  
23 during the silver recovery process revealed an airborne TWA silver concentration of 140  
24  $\mu\text{g}/\text{m}^3$ . Area airborne samples collected over the full work shift at this facility revealed  
25 silver concentrations that ranged from 9 to 190  $\mu\text{g}/\text{m}^3$ .

26 Airborne exposure to engineered AgNPs has been documented during their synthesis in  
27 a liquid-phase production process [Park et al. 2009]. The airborne release of AgNPs  
28 was evaluated at the reactor (wet chemical method), dryer, and grinding processes with

1 use of a scanning mobility particle sizer (SMPS), to determine the size and particle  
2 number concentration, and with an electrostatic precipitator (ESP) to collect samples for  
3 particle characterization by transmission electron microscopy (TEM). Exposure  
4 measurements of AgNPs taken at the opening of the reactor showed the release of  
5 particles with diameters of 50–60 nm, which agglomerated into 100-nm particles shortly  
6 after their release. Particle measurements taken before the reactor door was opened  
7 ( $6.1 \times 10^4$  particles/cm<sup>3</sup>) increased to  $9.2 \times 10^4$  particles/cm<sup>3</sup> when it was opened. After  
8 a 24-hour aging process, the silver colloidal suspension was transferred from the  
9 reactor, filtered, and deposited in a dryer to remove volatile organic materials and water.  
10 Airborne particle concentrations determined after the drying of the silver suspension  
11 indicated a doubling in the number of AgNPs that were 60–100 nm in diameter,  
12 compared with background particle number measurements. Prior to packaging, the  
13 dried AgNPs were ground to reduce agglomeration; measurements taken at the  
14 opening of the grinder detected the release of airborne AgNPs 30–40 nm in diameter.

15 Lee et al. [2011b, 2012a] reported on the airborne release of engineered AgNPs during  
16 the synthesis of AgNPs <100 nm at two different facilities. Facility A used a large-scale  
17 pilot reactor operated at negative pressure in which various silver-containing precursors  
18 (wire, powder, liquid) were fed through an inductively coupled argon plasma (ICP) torch,  
19 where they were vaporized in argon plasma. Silver atoms were condensed to  
20 predominantly 20–30-nm particles in a temperature gradient and then amassed in a  
21 collector. Facility B synthesized silver nanoparticles (1 kg/day) by mixing sodium citrate  
22 with silver nitrate and pumping the solution into a reactor that was housed in a  
23 ventilated fume hood. Worker and area exposure measurements detected airborne  
24 silver concentrations up to 0.1 µg/m in Facility A and 0.4 µg/m<sup>3</sup> in Facility B [Lee et al.  
25 2011b]. Two of five workers who were involved in AgNP manufacturing at Facility A also  
26 participated in a health surveillance study [Lee et al. 2012a]. The two had been  
27 employed at the facility for 7 years. One worker was reported to have been exposed to  
28 an airborne silver concentration of ~0.3 µg/m<sup>3</sup> and the other worker to a concentration of  
29 ~1.35 µg/m<sup>3</sup>. Levels of silver in the blood of the two workers were 0.0135 and 0.034  
30 micrograms per deciliter (µg/dL), and those in the urine were 0.043 µg/dL and

1 nondetectable. All clinical chemistry and hematologic parameters were found to fall  
2 within the normal range, and the workers reported no adverse health effects. A follow-  
3 up study was conducted to evaluate workplace exposures over 3 days [Lee et al.  
4 2012b]. Personal and area samples were collected for silver determination and for  
5 particle characterization by means of scanning transmission electron microscopy  
6 (STEM) and energy-dispersive X-ray spectroscopy (EDS). Real-time airborne particle  
7 size and count concentrations were also determined, with an SMPS and a condensation  
8 particle counter (CPC). The highest airborne concentrations for silver were detected in  
9 the injection room, where silver powder along with acetylene and oxygen gas were  
10 introduced into the reactor to manufacture AgNPs. The personal samples of workers  
11 who spent a total of 10–20 minutes per day in the injection room had TWA silver  
12 concentrations that ranged from 0.04 to 2.43  $\mu\text{g}/\text{m}^3$  during those time periods. The use  
13 of exposure controls was not reported, but workers were required to wear half-facepiece  
14 respirators. TWA silver concentrations determined from area samples collected in the  
15 injection room ranged from 5 to 288.7  $\mu\text{g}/\text{m}^3$ , whereas area samples collected for silver  
16 at other locations in the facility had concentrations  $\leq 1.3 \mu\text{g}/\text{m}^3$  (sampling durations  
17 ranged from 159 to 350 minutes). Analysis of area and personal airborne samples by  
18 STEM showed the preponderance of AgNPs as agglomerates. Real-time aerosol  
19 monitoring with the SMPS revealed particle number concentrations that ranged from  
20 224,622 to 2,328,608 particles/ $\text{cm}^3$ , and measurements by CPC revealed  
21 concentrations of 533 to 7,770 particles/ $\text{cm}^3$ .

22 Lee et al. [2013b] also reported on total airborne particulate, silver, carbon, and volatile  
23 organic compounds at a printed electronics facility. Personal and area samples were  
24 taken in the proximity of the three roll-to-roll or roll-to-plate presses at the facility during  
25 operation and cleaning. Analysis was conducted by ICP-MS and STEM. Particulate  
26 number and size were assessed by SMPS-CPC and a dust monitor. TWA silver  
27 concentrations were 2–3  $\mu\text{g}/\text{m}^3$  during cleaning and 3–24  $\mu\text{g}/\text{m}^3$  during operation.  
28 Particle concentrations and sizes were measured, but were not quantitatively  
29 attributable to the silver fraction. Use of PPE at the facility was minimal and incorrect  
30 (workers did not use it or used it for insufficient periods of time, without proper storage);

1 ventilation systems and fume hoods were often not functioning or were set up  
2 incorrectly (such as by using unconventional fittings and repair materials) ; and waste  
3 disposal was handled in ways that would not protect workers from spills or evolved  
4 gases.

5 Airborne exposure to AgNPs was also reported to occur during the melting and electro-  
6 refining of silver feedstock [Miller et al. 2010]. A survey of worker exposures at a  
7 precious metals refinery yielded results from personal and area samples collected for  
8 metal determination as well as airborne particle number concentrations via a Fast  
9 Mobility Particle Sizer (FMPS). A handheld ESP was also used to collect airborne  
10 aerosols for TEM characterization. Concentrations in personal airborne samples for total  
11 silver (from use of NIOSH Method 7303) ranged from 13 to 94  $\mu\text{g}/\text{m}^3$ , whereas those in  
12 area samples ranged from 4 to 39  $\mu\text{g}/\text{m}^3$ . Concentrations in all area samples analyzed  
13 for soluble silver compounds (with use of ISO Method 15202) were  $<2 \mu\text{g}/\text{m}^3$ . TEM and  
14 EDS analysis of ESP samples indicated the presence of silver, lead, selenium,  
15 antimony, and zinc, with all metals in the nanometer size range. AgNPs were the  
16 primary aerosol, with a mean diameter of  $\sim 10 \text{ nm}$ , in samples collected near the  
17 furnace; samples collected at other worksites contained agglomerated AgNPs with  
18 diameters of  $\sim 100 \text{ nm}$ . Airborne particle number measurements made with an FMPS in  
19 work areas on the electro-refining floor and around the furnaces during mold pours were  
20  $>10^6/\text{cm}^3$ , representing up to a 1,000-fold increase in particle number concentration  
21 over baseline background particle concentrations.

22 Lewis et al. reported on an exposure to various metals (including silver) associated with  
23 loading and unloading catalysts for petroleum refining [Lewis 2012]. Depending on the  
24 particular process, loading and unloading can take multiple shifts (up to 96 hours). Area  
25 and personal samples were analyzed by ICP-atomic emission spectroscopy. In all  
26 cases, TWA silver concentration was  $<6 \mu\text{g}/\text{cm}^3$ . Workers used PPE such as goggles,  
27 full-body coveralls, impervious gloves and boots, and either a half-mask air-purifying  
28 respirator or a supplied-air respirator for certain operations.

*This information is distributed solely for the purpose of pre-dissemination peer review under applicable information quality guidelines. It has not been formally disseminated by the National Institute for Occupational Safety and Health. It does not represent and should not be construed to represent any agency determination or policy.*

1 **Table 2-1. Summary of occupational exposures to silver.**

2

Source of Exposure	Exposure Details and Airborne Silver Concentrations	Comments	Reference
Brazing, silver soldering, and milling at an air conditioning equipment facility	Personal samples (7): ND–6.0 µg/m <sup>3</sup> TWA Area samples (4): ND–6.0 µg/m <sup>3</sup> TWA	<ul style="list-style-type: none"> <li>➤ No clinical signs of argyria</li> <li>➤ No local exhaust ventilation (LEV) used</li> </ul>	NIOSH [1973]
Brazing, milling, and sanding at a metal fabrication facility	Personal samples (20): 0.001–0.01 µg/m <sup>3</sup> TWA	<ul style="list-style-type: none"> <li>➤ No clinical signs of argyria</li> <li>➤ LEV used</li> </ul>	NIOSH [1981]
Brazing at a manufacturer of construction equipment	Personal samples (99): ND–15 µg/m <sup>3</sup> TWA	<ul style="list-style-type: none"> <li>➤ No clinical signs of argyria</li> <li>➤ LEV used</li> </ul>	NIOSH [1998]
Casting of a silver alloy at a silver jewelry manufacturing facility	Personal sample (1): 54 µg/m <sup>3</sup> (84 min)	<ul style="list-style-type: none"> <li>➤ No medical assessment performed</li> <li>➤ LEV used</li> </ul>	NIOSH [1992]
Silver recovery from photographic fixer solutions	Personal sample (1): 140 µg/m <sup>3</sup> TWA Area samples (5): 9–190 µg/m <sup>3</sup> TWA	<ul style="list-style-type: none"> <li>➤ No medical assessment performed</li> <li>➤ Local exhaust in furnace room not operating correctly</li> </ul>	NIOSH [2000]
Manufacturing of silver nitrate and silver oxide	Personal samples (6): 39–378 µg/m <sup>3</sup> TWA	<ul style="list-style-type: none"> <li>➤ No mention of exposure controls</li> <li>➤ Medical assessment of 30 workers found               <ul style="list-style-type: none"> <li>• 6 workers with generalized argyria</li> <li>• 20 workers with argyrosis</li> </ul> </li> </ul>	Rosenman et al. [1979]

*This information is distributed solely for the purpose of pre-dissemination peer review under applicable information quality guidelines. It has not been formally disseminated by the National Institute for Occupational Safety and Health. It does not represent and should not be construed to represent any agency determination or policy.*

		<ul style="list-style-type: none"> <li>• 10 workers with decreased vision</li> </ul>	
Silver processing facility (silver salts and metallic silver)	Area samples: 1–310 µg/m <sup>3</sup> TWA (soluble silver compounds), 3–540 µg/m <sup>3</sup> TWA (insoluble silver compounds)	<ul style="list-style-type: none"> <li>➤ No mention of exposure controls</li> <li>➤ Medical assessment of 50 workers found <ul style="list-style-type: none"> <li>• 9 workers with argyrosis (soluble silver exposure)</li> <li>• No symptoms of argyrosis in workers exposed to insoluble silver</li> </ul> </li> </ul>	Wölbling et al. [1988]
Reclamation of silver from photographic film, paper, and liquid wastes (insoluble silver halides)	Personal and area samples (>100) over a 30-yr period: 5–240 µg/m <sup>3</sup> TWA	<ul style="list-style-type: none"> <li>➤ No mention of exposure controls</li> <li>➤ Medical assessment of 27 workers found <ul style="list-style-type: none"> <li>• No cases of argyria</li> <li>• 7 workers with some form of ocular argyrosis</li> </ul> </li> </ul>	Pifer et al. [1989]
Smelting and refining of silver and the preparation of silver salts for photosensitized products	Personal and area samples (62) over a 2-month period: 1–100 µg/m <sup>3</sup> TWA	<ul style="list-style-type: none"> <li>➤ No mention of exposure controls</li> <li>➤ Biologic samples for silver in blood, urine, and feces measured for 37 workers <ul style="list-style-type: none"> <li>• Low levels of silver in blood in 80% of workers; none detected in controls</li> </ul> </li> </ul>	DiVincenzo et al. [1985]
Manufacturing precious metal powder (silver nitrate, silver oxide, silver)	Personal samples (OSHA inspection): 40–350 µg/m <sup>3</sup> TWA	<ul style="list-style-type: none"> <li>➤ No mention of exposure controls; some workers reported to wear respirators</li> </ul>	Rosenman et al. [1987]

*This information is distributed solely for the purpose of pre-dissemination peer review under applicable information quality guidelines. It has not been formally disseminated by the National Institute for Occupational Safety and Health. It does not represent and should not be construed to represent any agency determination or policy.*

chloride, silver cadmium oxide)		<ul style="list-style-type: none"> <li>➤ Biologic samples for blood and urine silver showed raised levels in &gt;90% of studied workers</li> <li>➤ Acute irritation found for eyes and kidney</li> </ul>	
Six worksites: Silver reclamation, bullion production, jewelry manufacture, bullion/coin/tableware production, and chemical production (two factories)	No assessment of airborne silver concentrations reported	<ul style="list-style-type: none"> <li>➤ No mention of exposure controls</li> <li>➤ Blood silver levels measured for workers at all six worksites               <ul style="list-style-type: none"> <li>• Reclamation workers: 1.3–20 µg/L</li> <li>• Workers from the other 5 worksites: 0.1–16 µg/L</li> <li>• Jewelry workers had lowest levels: 0.2–2.8 µg/L</li> </ul> </li> </ul>	Armitage et al. [1996]
Two worksites: silver reclamation from X-rays and photographic film, and silver refinery	<p>Samples taken during silver reclamation (3): Area, 85 µg/m<sup>3</sup> (3 hrs) at incinerator; Personal, 1030 and 1360 µg/m<sup>3</sup> (&lt;15 min) at pulverizing area</p> <p>Samples taken during silver refining: Area, 110–170 µg/m<sup>3</sup> (229 min) at silver refining casting area; Personal, 100 µg/m<sup>3</sup> (224 min) and 59–96 µg/m<sup>3</sup> (28 min) at silver refining casting area</p>	<ul style="list-style-type: none"> <li>➤ Improvements in exposure control instituted</li> <li>➤ Medical assessment of a worker at each site for argyrosis and argyria:               <ul style="list-style-type: none"> <li>• Worker involved in silver reclamation (silver halides and oxide): no argyrosis</li> <li>• Worker involved in silver refining (soluble compounds; silver nitrate): argyrosis</li> </ul> </li> </ul>	Williams and Gardner [1995]

*This information is distributed solely for the purpose of pre-dissemination peer review under applicable information quality guidelines. It has not been formally disseminated by the National Institute for Occupational Safety and Health. It does not represent and should not be construed to represent any agency determination or policy.*

Production of nanoscale silver (liquid-phase production process; silver nitrate with nitric acid)	No quantitative silver exposure measurements; only particle count concentrations	➤ Improvements in exposure control instituted	Park et al. [2009]
Production of nanoscale silver at two facilities: Facility C used inductively coupled plasma torch with electric atomizer; Facility D used sodium citrate and silver nitrate	Personal breathing zone samples (2) at Facility C: 0.12–1.02 µg/m <sup>3</sup> (TWA) Area samples (8) at Facility C: 0.02–0.34 µg/m <sup>3</sup> (TWA) Personal breathing zone samples (2) at Facility D: 0.38–0.43 µg/m <sup>3</sup> (TWA) Area samples (8) at Facility D: 0.03–1.18 µg/m <sup>3</sup> (TWA)	➤ Facility C: The reactor and collector process was performed under vacuum to control release of airborne silver ➤ Facility D: The wet process reacting silver nitrates with citrate prevented release of airborne silver particles	Lee et al. [2011b]
Production of nanoscale silver at Facility C, as described in Lee et al. [2011b]	Personal samples (2): Worker 1, 0.35 µg/m <sup>3</sup> (TWA) Worker 2, 1.35 µg/m <sup>3</sup> (TWA)	➤ Biologic samples for silver <ul style="list-style-type: none"> <li>• Worker 1: blood (0.034 µg/dl); urine (0.043 µg/dl)</li> <li>• Worker 2: blood (0.030 µg/dl); urine (ND)</li> </ul> Some engineering controls used as well as PPE	Lee et al. [2012a]
Production of nanoscale silver at Facility C, as described in Lee et al. [2011b]	Samples were collected over 3 days. Personal samples (6):	➤ Highest silver concentrations found in the injection room, in which silver powder and acetylene/oxygen gas	Lee et al. [2012b]

*This information is distributed solely for the purpose of pre-dissemination peer review under applicable information quality guidelines. It has not been formally disseminated by the National Institute for Occupational Safety and Health. It does not represent and should not be construed to represent any agency determination or policy.*

	<p>Worker 1, 1.55–4.99 <math>\mu\text{g}/\text{m}^3</math> (2.43 <math>\mu\text{g}/\text{m}^3</math> TWA)</p> <p>Worker 2, 0.09–1.35 <math>\mu\text{g}/\text{m}^3</math> (0.04 <math>\mu\text{g}/\text{m}^3</math> TWA)</p> <p>Area samples (28): 0.02–426.43 <math>\mu\text{g}/\text{m}^3</math> (0.01–288.73 <math>\mu\text{g}/\text{m}^3</math> TWA)</p>	<p>were injected into the reactor</p> <ul style="list-style-type: none"> <li>➤ Particle number concentration ranged from 911,170 to 1,631,230 <math>\text{cm}^3</math> during reactor operation</li> <li>➤ Particle size: 15–710 nm during reactor operation</li> <li>➤ Natural ventilation used; workers wore half-mask respirators</li> </ul>	
Precious metal processing facility; melting and electro-refining of silver	<p>Total silver</p> <p>Personal, full-shift samples (6): 13–94 <math>\mu\text{g}/\text{m}^3</math></p> <p>Area samples (14): 4–39 <math>\mu\text{g}/\text{m}^3</math></p>	<ul style="list-style-type: none"> <li>➤ Highest personal exposures to silver found on electro-refining floor</li> <li>➤ Particle number concentrations <math>&gt;10^6</math>, with highest at furnaces/pouring</li> <li>➤ ~10-nm-diameter particles</li> <li>➤ Ventilation controls during pouring of molten metal</li> </ul>	Miller et al. [2010]
Petroleum refinery; Loading and unloading solid catalysts	<p>Total silver</p> <p>Personal, 54- to 543-min samples (13): <math>&lt;3 \mu\text{g}/\text{m}^3</math></p> <p>Area, 54- to 1505-min samples (54): <math>&lt;6 \mu\text{g}/\text{m}^3</math></p>	<ul style="list-style-type: none"> <li>➤ Catalysts can take 8–72 h to load and 8–96 h to unload</li> <li>➤ PPE includes respirator, goggles, full-body coveralls, gloves, and boots</li> <li>➤ Other metallic co-contaminants and dust detected and assayed</li> </ul>	Lewis et al. [2012]

*This information is distributed solely for the purpose of pre-dissemination peer review under applicable information quality guidelines. It has not been formally disseminated by the National Institute for Occupational Safety and Health. It does not represent and should not be construed to represent any agency determination or policy.*

<p>Electronic printing facilities; Roll-to-roll and roll-to-plate printing operation and cleaning</p>	<p>Total silver</p> <p>Operating press, 93- to 158-min samples: 4–24 µg/m<sup>3</sup></p> <p>Cleaning, 128- to 157-min samples: 2–3 µg/m<sup>3</sup></p>	<ul style="list-style-type: none"> <li>➤ “Conductive nano-ink, mostly silver nanoparticles or carbon nanotubes” used</li> <li>➤ Local exhaust ventilation and fume hoods</li> <li>➤ Minimal PPE usage, improper PPE filter storage, fume hoods and local exhaust ventilation systems defeated; authors recommended resolutions to these issues</li> <li>➤ Significant risks of organic solvent exposure noted</li> </ul>	<p>Lee et al. [2013]</p>
---	--	--	--------------------------

1

2 ND = nondetectable.

## **3 Human Evidence of Internal Dose and Potential Adverse Health Effects**

### **3.1 Background**

The majority of reports on workplace and health assessments of workers exposed to silver lack sufficient detail to adequately determine the physical-chemical characteristics (such as particle size and silver species) of the aerosol to which workers were exposed. However, it's reasonable to infer that some workers had exposure to nanometer-sized particles, on the basis of known characteristics of particles that are typically present (1) in fumes generated during brazing and soldering or the melting of silver alloys or silver recycled materials, (2) during the recovery of silver from photographic fixer solutions, and (3) during the handling of colloidal silver. Because of silver's many potential uses, workers can be exposed to a range of particle sizes and forms of silver that have the potential for entry into the body by different routes [Drake and Hazelwood 2005]. Ingestion can be a significant route of entry for silver compounds and colloidal silver [Silver 2003], whereas the inhalation of dusts or fumes containing silver occurs primarily in occupational settings [ATSDR 1990]. Skin contact can also occur in occupational settings from the handling of silver and silver-containing materials [ATSDR 1990].

Several factors are known to influence the ability of a metal to produce toxic effects on the body; these include the solubility of the metal at the biologic site (affected by particle size and pH of the surrounding media), the nature of any surface coating or binding material, the surface activity of the metal, the ability of the metal to bind to biologic sites, and the degree to which metal complexes are formed and sequestered or metabolized and excreted. Published studies appear to indicate that some forms of silver may be more toxic than others. The majority of health data from workers exposed to silver indicate that long-term inhalation or ingestion of silver compounds (especially soluble forms of silver) can cause irreversible pigmentation of the skin and mucus membranes (argyria) and/or the eyes (argyrosis), in which the affected area becomes bluish-gray or

1 ash gray [ATSDR 1990; Drake and Hazelwood 2005; Wijnhoven et al. 2009; Johnston  
2 et al. 2010; Lansdown 2012]. Generalized argyria has often been reported to occur in  
3 individuals following the ingestion or application of silver-containing medicines, but it  
4 has also been observed to varying degrees in workers exposed to silver compounds  
5 during the production, use, and handling of silver nitrate and silver oxide [Moss et al.  
6 1979; Rosenman et al. 1979; Williams 1999] and silver salts (nitrate and chloride)  
7 [Wölbling et al. 1988]; during the reclamation of silver from photographic film [Buckley  
8 1963; Pifer et al. 1989; Williams and Gardner 1995]; and during the handling of silver in  
9 photosensitized products [DiVincenzo et al. 1985]. Localized argyria has also been  
10 reported to be due to the following: application of burn creams containing silver [Wan et  
11 al. 1991]; silver soldering [Scrogges et al. 1992]; contact with silver jewelry [Catsakis  
12 and Sulica 1978; Murdaca et al. 2014]; use of silver acupuncture needles [Tanita et al.  
13 1985; Sato et al. 1999], catheters [Saint et al. 2000], or dental amalgams [Catsakis and  
14 Sulica 1978; Piña et al. 2012]; and accidental puncture wounds [Rongioletti et al. 1992].

### 15 **3.2 Human Studies of Lung Deposition of Airborne Silver** 16 **Nanoparticles**

17 Limited data are available on the deposition of inhaled AgNPs in humans and  
18 absorption from the lungs (i.e., transport across epithelial cell membranes and entry into  
19 the lymph or blood circulatory system) [Muir and Cena 1987; Cheng et al. 1996]. Muir  
20 and Cena [1987] exposed three male volunteers to air containing AgNPs with a mean  
21 count diameter of 9 nm (geometric standard deviation [GSD] = 2.0) and at a  
22 concentration of  $2 \times 10^5$  particles/cm<sup>3</sup>. Airborne particles were size-separated by a  
23 parallel-plate diffusing battery and counted with a nucleus particle counter. The particle  
24 size distribution of the aerosol was obtained before and after each inhalation experiment  
25 and the mean (or g.m.?) differed only slightly from 9 nm. The sampling of inhaled and  
26 exhaled air was undertaken at a fixed flow rate of 2 L/min. Particle deposition in the  
27 respiratory tract was determined by relating the concentrations of particles inhaled to  
28 the concentrations of particles exhaled by the subjects. The subjects breathed at a  
29 normal resting lung volume. Particle deposition was found to increase from 20% to 90%  
30 as the breathing cycle (duration of breath, including both inspiration and expiration)

1 increased from 2 to 10 seconds, but it was not affected by tidal volume (volume of air  
2 inhaled and exhaled at each breath; 0.5–3 L tested).

3  
4 In another lung deposition study with AgNPs, 10 male human subjects were exposed to  
5 four different particle sizes (4, 8, 20, and 150 nm in diameter) of silver wool (99.9%  
6 pure) via an evaporation–condensation method at two constant flow rates of 167 and  
7 333 cm<sup>3</sup> per second [Cheng et al. 1996]. Airborne concentrations of AgNPs were  
8 measured with a CPC. Each subject was repeatedly measured for aerosol deposition  
9 during 32 combinations of experimental conditions. Lung deposition efficiencies for 4-  
10 nm particles ranged from about 25% to 65% with nose-in/mouth-out breathing and 25%  
11 to 62% with mouth-in/nose-out breathing. For 8-nm particles, respective deposition  
12 efficiencies were 14% to 49% and 14% to 45%. The respective ranges for 20-nm  
13 particles were 2% to 35% and 3% to 28%. Although the values of deposition efficiencies  
14 varied among the 10 subjects, particle deposition in the lung appeared to result from  
15 diffusion, with AgNP deposition observed to increase as the particle diameter and flow  
16 rate decreased. The inter-individual variability of particle deposition efficiencies was  
17 correlated with the inter-subject variations in nasal dimensions (as measured by total  
18 surface area), smaller cross-sectional area, and complexity of the airway shape.

### 19 **3.3 Biomonitoring Studies in Humans**

20 Although no data are available on the body burdens in workers resulting from inhaled  
21 silver nanoparticles, some biomonitoring data are available on workers exposed to  
22 airborne silver (particle size not specified). Such information provides the best available  
23 data on internal doses, for comparison to the animal study data.

24 Following a study of 35 to 37 male silver-production workers (most with 5 or more years  
25 of experience in production areas), DiVincenzo et al. [1985] reported workplace airborne  
26 exposure measurements of 1 to 100 µg/m<sup>3</sup>. These researchers compared the estimated  
27 total silver dose in workers to the estimated dose associated with argyria (that is,  
28 approximately 2.3 g by intravenous injection [Hill and Pillsbury 1939, cited in DiVincenzo  
29 et al. 1985], or 23–115 mg, on the assumption of 1%–5% silver retention in the body

1 [Scott and Hamilton 1948, 1950; Fruchner et al. 1968, cited in DiVincenzo et al. 1985]).  
2 They estimated an annual dose of 14  $\mu\text{g}/\text{kg}$  in workers, by assuming 1% retention of  
3 silver that was absorbed in the body by diet (oral) or workplace (inhalation) exposure  
4 [DiVincenzo et al. 1985]. They then estimated a worker airborne exposure concentration  
5 of 30  $\mu\text{g}/\text{m}^3$  from fecal excretion data, which is within the measured air concentration  
6 range. The estimated annual dose of retained silver in a 70-kg worker was  
7 approximately 1 mg. Given the 23 to 115 mg retained dose estimated to be associated  
8 with argyria, DiVincenzo et al. [1985] estimated that at least 22 years of workplace  
9 exposure would be required for development of argyria. Although different assumptions  
10 were used in deriving these estimates, the results are similar to the estimates used as  
11 the basis for the NIOSH REL (Section 6.1).

12 A study of 50 workers in the silver processing industry (44 males, 6 females)  
13 investigated associations between the airborne exposure concentration and duration  
14 and the clinical symptoms or silver concentrations in skin samples [Wölbling et al.  
15 1988]. About half of the workers (52%) handled only metallic silver and 46% were  
16 exposed to silver salts (silver nitrate or silver chloride); one worker was exposed to both  
17 forms of silver. No cases of generalized argyria were observed, although 8 of the 23  
18 silver salt workers had localized argyria (especially in mucous membranes of the eyes,  
19 mouth, and nose). No cases of localized argyria were observed among the metallic  
20 silver workers. Airborne concentrations ranged from 1 to 310  $\mu\text{g}/\text{m}^3$  in the “salts” group  
21 and from 3 to 540  $\mu\text{g}/\text{m}^3$  in the “metal” group. Worker exposure durations were 3 to 20  
22 years. The lowest concentration associated with localized argyria (ocular) was 2 to 4  
23  $\mu\text{g}/\text{m}^3$ , although no relationship was observed between the exposure concentration or  
24 duration and the signs of argyrosis. The silver concentrations in skin (0.01–0.11  $\mu\text{g}/\text{g}$ )  
25 were within the range of previously reported values and were not associated with  
26 argyria. In another study, argyria was observed in a worker (silver polisher) with 3.7  
27  $\mu\text{g}/\text{g}$  silver in skin [Treibig and Valentin 1982, cited in Wölbling et al. 1988].

28

### 1 **3.4 Health Effects in Workers with Exposure to Silver**

2 Rosenman et al. [1979] reported findings of respiratory symptoms and argyria in  
3 workers ( $n = 30$ ) involved with the manufacturing of silver nitrate and silver oxide.  
4 Sixteen of the 30 had worked for 5 or more years. All the workers were white males,  
5 and the average age was 34.6 years. Chest radiographic findings and results of clinical  
6 examination of respiratory function were predominantly normal. Two workers were  
7 found to have small, irregular opacities on chest x-rays; one of the workers was  
8 reported to have had previous exposure to asbestos. None of the workers had evidence  
9 of restrictive pulmonary disease, and obstructive changes in pulmonary function were  
10 attributed to smoking. Ten of the 30 workers complained of abdominal pain, which  
11 appeared to be associated ( $p < 0.25$ ) with silver found in the blood. There was a history  
12 of x-ray-documented ulcers in six of these workers and a history of upper  
13 gastrointestinal bleeding in two others. Decreased vision at night was also reported by  
14 10 workers and was associated with the length of employment; however, no changes in  
15 visual performance could be attributed to silver deposits. The cross-sectional study did  
16 identify six workers with generalized argyria and 20 with argyrosis. At the time of the  
17 study, no exposure measurements were taken; however, personal airborne  
18 measurements made 4 months before the study revealed 8-hour TWA silver  
19 concentrations ranging from 39 to 378  $\mu\text{g}/\text{m}^3$  (total mass). A follow-up study of these 30  
20 workers [Moss et al. 1979] also revealed evidence of argyrosis and burns of the skin  
21 from contact with silver nitrate in 27 and a history of ocular burns in 11. An in-depth  
22 ophthalmic examination was conducted to determine if workers suffered from any visual  
23 deficits from their exposure. A direct relationship was shown between the amount of  
24 discoloration of the cornea and the length of time worked. Although some workers  
25 complained of decreased night vision, no functional deficits were found.

26  
27 Wölbling et al. [1988] reported on a cross-sectional study of 50 workers (44 males and 6  
28 females employed  $\geq 1$  year) at a silver processing plant to determine if symptoms of  
29 exposure differed between those exposed predominantly to insoluble silver ( $n = 26$ ) and  
30 those exposed exclusively to soluble silver compounds of silver nitrate and silver

1 chloride ( $n = 23$ ). Ten subjects, not occupationally exposed to silver, were used as a  
2 control group. Length of exposure ranged from 3 to 20 years. Exposure concentrations  
3 ranged from 1 to  $310 \mu\text{g}/\text{m}^3$  for workers exposed to soluble silver compounds and from  
4 3 to  $540 \mu\text{g}/\text{m}^3$  for those exposed to insoluble silver compounds. Among workers in the  
5 soluble exposure group, discoloration (argyrosis) was observed in the eyes of 5, the  
6 mouths of 2, the nose of 1, and the nape of the neck of 1. No symptoms of argyria or  
7 argyrosis were seen in workers in the insoluble exposure group. Skin biopsies analyzed  
8 for silver revealed a concentration of 0.03 to 13.5 ppm for the soluble group (median of  
9 0.115 ppm), 0.03 to 0.77 ppm for the insoluble group (median of 0.085 ppm), and 0.01  
10 to 0.11 ppm for the control group (median of 0.02 ppm). Silver concentrations found in  
11 the skin biopsies and air did not correlate with either ocular deposits or duration of  
12 exposure. The authors concluded that the occurrence of argyria and argyrosis is  
13 dependent upon individual susceptibility.

14  
15 Pifer et al. [1989] reported on a clinical assessment of 27 silver reclamation workers  
16 exposed primarily to insoluble silver halides. An equal number of workers not  
17 occupationally exposed were selected as a control group. Airborne silver concentrations  
18 ranged from 5 to  $240 \mu\text{g}/\text{m}^3$  (total mass). Silver was found in the blood of 21 silver  
19 reclamation workers, with a mean concentration of  $0.01 \mu\text{g}/\text{mL}$ . Only one worker had a  
20 detectable level of urinary silver; silver was not detected in the blood or the urine of the  
21 control group. Silver was measured in all fecal samples collected, with a mean  
22 concentration of  $16.8 \mu\text{g}/\text{g}$  for exposed workers ( $n = 18$ ) and  $1.5 \mu\text{g}/\text{g}$  for unexposed  
23 workers ( $n = 22$ ). Clinical examinations and skin biopsies revealed no cases of  
24 generalized argyria. Twenty of the 27 reclamation workers exhibited some degree of  
25 internal nasal septal pigmentation, and 7 of 24 workers were found to have ocular silver  
26 deposits in the conjunctiva and/or cornea. Optometric and contrast sensitivity test  
27 results revealed no significant deficits in visual performance. No abnormalities were  
28 revealed during tests of renal and pulmonary function or on chest radiographs. The  
29 researchers concluded there was no evidence that chronic exposure to insoluble silver  
30 halides had detrimental health effects on exposed workers at the concentrations  
31 measured.

1 DiVincenzo et al. [1985] reported on workers exposed to different species of silver  
2 during the smelting and refining of silver and preparation of silver salts for use in  
3 photosensitized products. The absorption and excretion of silver were monitored by  
4 measuring blood, urine, fecal, and hair concentrations in 37 male workers  
5 occupationally exposed primarily to insoluble silver compounds; a group of 35  
6 unexposed workers served as a control population. Personal and area airborne samples  
7 were collected for silver. The 8-hour TWA exposure to silver over a 2-month monitoring  
8 period (62 samples) ranged from about 1 to 100  $\mu\text{g}/\text{m}^3$  (total mass). Measured  
9 concentrations of silver in the blood, urine, and feces were 0.011  $\mu\text{g}/\text{mL}$ , <0.005  $\mu\text{g}/\text{mL}$ ,  
10 and 15  $\mu\text{g}/\text{mL}$ , respectively. The concentration of silver in the hair was higher for the  
11 silver workers than for controls ( $130 \pm 160$  vs.  $0.57 \pm 0.56$   $\mu\text{g}/\text{g}$ ). Using fecal excretion  
12 as an index of exposure for calculating body burden of silver and assuming that 1% to  
13 5% of the silver was retained in the body, the authors concluded that a minimum of 24  
14 years of continuous workplace exposure would be necessary for workers to retain  
15 enough silver to develop argyria.

16  
17 Williams and Gardner [1995] reported on the medical evaluation of two workers who  
18 were employed by a company involved in the reclamation of silver from old X-rays and  
19 photographic film. The reclamation and refining process required incineration of the film,  
20 pulverization of the ash, and extraction of the silver, followed by an electrolytic process  
21 involving nitric acid to obtain the desired purity prior to casting of the silver. The two  
22 workers had been employed for less than 7 years and were reported to be  
23 asymptomatic, with no evidence of argyria. A personal exposure measurement for one  
24 of the workers (Case 1) during the incineration of films was 85  $\mu\text{g}/\text{m}^3$  (180 minutes), and  
25 airborne concentrations of 1030 and 1360  $\mu\text{g}/\text{m}^3$  (<115 minutes) were measured in the  
26 pulverizing area. A blood silver determination for this worker at the time of  
27 environmental exposure assessments was 49  $\mu\text{g}/\text{L}$ . The second worker (Case 2) was  
28 mainly involved in silver refinement and was reported to have airborne concentrations of  
29 110 to 170  $\mu\text{g}/\text{m}^3$  (229 minutes) and 100  $\mu\text{g}/\text{m}^3$  (224 minutes) during the casting of  
30 silver. Short-term personal samples indicated exposure concentrations of 59 to 96  
31  $\mu\text{g}/\text{m}^3$  (28 minutes), and background airborne concentrations in the electrolytic area of

1 the refinery were 30 to 70  $\mu\text{g}/\text{m}^3$ . The background concentrations of silver were  
2 attributed to the presence of silver compounds from the electrolytic tanks rather than  
3 from the casting process. Follow-up visits to the plant revealed no change in the clinical  
4 outcome of the first worker (Case 1) exposed to silver halides and silver oxide. This was  
5 consistent with the report of Pifer et al. [1989] that exposure to insoluble silver  
6 compounds appeared to be relatively benign in causing argyria. Follow-up clinical  
7 assessment of the second worker (Case 2) revealed the onset of argyria, attributed to  
8 exposure to soluble silver compounds (silver nitrate) and metallic silver. Subsequent  
9 follow-up of this worker over a 5-year period [Williams 1999] indicated an average blood  
10 silver concentration of 11.2  $\mu\text{g}/\text{L}$  (range, 6–19  $\mu\text{g}/\text{L}$ ). During this period, no progression  
11 of argyria was noted.

12  
13 In a cross-sectional study of workers manufacturing silver (silver nitrate, silver oxide,  
14 silver chloride, silver cadmium oxide) and other metal powders, Rosenman et al. [1987]  
15 observed upper respiratory irritation, such as sneezing, stuffy or runny nose, and chest  
16 tightness, in 15 of 27 workers (56%). The average age of the 27 workers was 41, and  
17 they had worked at the plant for an average of 8.1 years. Kidney function was also  
18 evaluated, and the level of urinary enzyme N-acetyl-B-D glucosaminidase (NAG) was  
19 found to be significantly raised in four workers. The increase in NAG levels was  
20 correlated with blood silver concentrations and age, suggesting a possible toxic effect of  
21 silver on the kidney. In addition, the group's average NAG concentration was  
22 significantly higher ( $p < 0.01$ ) than that found in the control population. Because of  
23 concurrent exposure to known nephrotoxins, such as cadmium and solvents, the  
24 authors could not definitively determine if exposure to silver was responsible. Also, 96%  
25 of the workers had elevated urine silver concentrations (0.5–52.0  $\mu\text{g}/\text{L}$ ), and 92% had  
26 elevated blood silver concentrations (0.05–6.2  $\mu\text{g}/100\text{ ml}$ ). No correlation was found  
27 between raised blood and urine silver concentrations and the work area. However, this  
28 lack of an association may have been due to the workers' use of respiratory protection.  
29 An OSHA health inspection conducted at the plant revealed 8-hour TWA silver  
30 concentrations ranging from 40 to 350  $\mu\text{g}/\text{m}^3$  (total mass).

31

1 Although it is unclear whether there is a relationship between airborne exposure to  
2 silver and blood silver concentrations, Armitage et al. [1996] suggested that blood silver  
3 concentrations determined on a group level could be used to evaluate the overall  
4 effectiveness of workplace control measures. A total of 98 blood samples from  
5 occupationally exposed workers and 15 control blood samples from agricultural workers  
6 were analyzed for silver. Samples were collected from workers at factories involved in  
7 silver reclamation, jewelry manufacture, bullion production, silver chemical manufacture,  
8 and tableware production. A normal range of blood silver concentrations was found for  
9 the agricultural workers, with a mean of  $<0.1$   $\mu\text{g/L}$ . Reclamation workers were found to  
10 have some of the highest silver concentrations in the blood, ranging from 1.3 to 20  $\mu\text{g/L}$   
11 (average, 6.8  $\mu\text{g/L}$ ), whereas workers involved in refining silver to produce bullion,  
12 coins, and chemicals had blood silver concentrations that ranged from 0.1 to 16  $\mu\text{g/L}$   
13 (average, 2.5  $\mu\text{g/L}$ ). Workers employed in industries as silver refiners and those  
14 involved in the production of silver nitrate had the highest blood silver concentrations,  
15 whereas workers in jewelry production had the lowest, ranging from 0.2 to 2.8  $\mu\text{g/L}$ . No  
16 evidence of argyria was found in any of these workers. Murdaca et al. [2014] found  
17 evidence of argyria in a case study of a jewelry worker, but the exposure was not  
18 quantified. Aktepe et al. [2015] reported significantly increased DNA damage and  
19 oxidative stress among silver jewelry workers. DNA damage was quantified by alkaline  
20 comet assay of endogenous mononuclear leukocytes, while oxidative stress was  
21 assayed by quantitation of thiols and by oxidation and antioxidation potential of plasma.  
22 An exposure assessment was not conducted. The effects of silver exposure in jewelers  
23 may also be confounded by the presence of cadmium [Parikh et al. 2014]. A statistical  
24 evaluation of the results reported in the Aktepe et al. [2015] paper is provided in Section  
25 B.4.

26  
27 Likewise, Cho et al. [2008] reported normal hematology and clinical chemistry values for  
28 a subject whose serum silver level reached 15.44  $\mu\text{g/dL}$  (normal range, 1.1–2.5  $\mu\text{g/dL}$ )  
29 and urinary silver level reached 243.2  $\mu\text{g/L}$  (normal range, 0.4–1.4  $\mu\text{g/L}$ ) after exposure  
30 to aerosolized silver at a mobile telephone subunit facility. The aerosolized silver, which  
31 was reported to contain alcohol, acetone, and silver, was used for plating metal parts.

*This information is distributed solely for the purpose of pre-dissemination peer review under applicable information quality guidelines. It has not been formally disseminated by the National Institute for Occupational Safety and Health. It does not represent and should not be construed to represent any agency determination or policy.*

1 Exposure controls were not used during the plating of silver, and the worker did not  
2 wear respiratory protection. No information was provided on silver species or particle  
3 size. The worker developed generalized argyria of the face, and a biopsy of the  
4 epidermal basal layer of the skin revealed the presence of silver granules.

5  
6 Two studies evaluated health effects in workers exposed to AgNPs [Lee et al. 2011b; Lee  
7 et al. 2012a]. Exposure information from that study is described in Section 2. Lee et al.  
8 [2011b, 2012a] reported that workers were exposed to airborne engineered AgNPs  
9 during particle synthesis (via an inductively coupled argon plasma process in Facility A  
10 and the mixing of sodium citrate/silver nitrate in Facility B). Although traces of silver  
11 were detected in their blood and urine, all clinical chemistry and hematologic  
12 parameters were within the normal ranges, and no adverse health effects were reported  
13 for these workers. Other recent studies reporting health effect in workers exposed to  
14 silver did not report particle sizes or exposure concentrations (Section 3.3).

15  
16 In summary, these studies of health effects in workers included those with exposures to  
17 silver particles of various types (soluble, insoluble) and from various processes  
18 (manufacturing, processing, reclamation). Some of the findings included lung, liver,  
19 and kidney adverse effects, although none of these were significantly associated with  
20 the airborne exposure concentrations or the blood or urine concentrations of silver.  
21 None of these studies reported the particle size. Argyria and argyrosis were the only  
22 effects clearly associated with silver exposure, and were not associated with functional  
23 effects. The sample sizes in these studies was relatively small (a few workers in case  
24 studies to a few dozen workers), which may have limited the power to detect significant  
25 effects related to exposure. The duration of exposure was generally short relative to a  
26 full working lifetime. Some of these studies reported confounding exposures to other  
27 toxic substances.

28

## 3.5 Health Effects in Humans with Nonoccupational Exposure to Silver

Trop et al. [2006] reported on a burn victim who had an argyria-like condition and elevated activities of liver-specific plasma enzymes when an Acticoat™ dressing (containing ionic AgNPs) was applied to his wound. No mention was made of silver being sequestered in the liver, although this was possible since levels of the metal were elevated in plasma and urine. As reported by the authors, local treatment with Acticoat™ dressings for 7 days caused the plasma activities of alanine aminotransferase (ALT) and aspartate aminotransferase (AST) to rise incrementally to 233 and 78 units per liter (U/L), respectively (upper limits of normal: 33 U/L for ALT and 37 U/L for AST). The concentration of silver in blood plasma was 107 micrograms per kilogram ( $\mu\text{g}/\text{kg}$ ); this value subsequently dropped toward normal levels ( $13.3 \mu\text{g}/\text{kg}$  after 97 days) when Acticoat™ dressings were changed on day 8 to dressings containing betadine ointment. C-reactive protein level was also elevated, in parallel with plasma silver levels, reaching a maximum concentration of 128 milligrams per liter (mg/L) after 4 days. The level of this liver-synthesized marker for acute inflammation was back to normal (5 mg/L) after 8 silver treatment-free days.

In a prospective study of 30 patients with graft-requiring burns, Vlachou et al. [2007] found increased concentrations of silver in serum (median, 56.8 micrograms per liter [ $\mu\text{g}/\text{L}$ ]; range, 4.8–230  $\mu\text{g}/\text{L}$ ) when Acticoat™ dressings were applied to the wounds. The authors found no changes in hematologic or clinical chemistry parameters indicative of toxicity associated with the silver absorption, and at the 6-month follow-up, the median serum level had declined to 0.8  $\mu\text{g}/\text{L}$ . However, the absence of any toxicological effects of silver deposition from Acticoat™ dressings reported by Vlachou et al. [2007] contrasts with the findings of Trop et al. [2006], who reported elevated silver levels in plasma and changes in liver-related clinical chemistry parameters when the wounds of a patient with 30% mixed-depth burns were treated with Acticoat™ dressings. The patient developed argyria-like symptoms, including a grayish discoloration of the face. Plasma silver levels, clinical chemistry results, and the

*This information is distributed solely for the purpose of pre-dissemination peer review under applicable information quality guidelines. It has not been formally disseminated by the National Institute for Occupational Safety and Health. It does not represent and should not be construed to represent any agency determination or policy.*

1 patient's appearance improved on cessation of treatment [Trop et al. 2006]. However, it  
2 is unclear whether the liver perturbations were caused by silver deposition or were a  
3 response to the burns themselves. Thus, a review by Jeschke [2009] drew attention to  
4 the profound structural and metabolic changes in the liver of burn victims. Hepatic  
5 responses to thermal injury such as the formation of edema, release of proinflammatory  
6 cytokines, and activity of AST, ALT, and alkaline phosphatase (AP) have been shown to  
7 increase by up to 200% in the rat burn model [Jeschke et al. 2009].

8

9 The findings from burn victims treated with Acticoat™ do not provide adequate data to  
10 determine a threshold level of plasma silver that might be associated with the elevation  
11 of AST and ALT. The fluctuation in these markers of liver function deficits in the worker  
12 described by Trop et al. [2006] might be a consequence of thermal injury rather than  
13 wound treatment with silver [Jeschke 2009; Jeschke et al. 2009].

## 4 Cellular and Mechanistic Studies Overview

### 4.1 Overview of Cell-based AgNP Studies

The effects of AgNP exposure have been studied extensively in mammalian cell models, especially murine or human derived lung or liver models [Hussain et al 2005a; Shannahan et al. 2015; Gliga et al. 2014; Nymark et al. 2013; Kawata et al. 2009; Kim et al 2009c]. AgNP exposure is reported to result in increased oxidative stress levels [Hussain et al. 2005a; Carlson et al. 2008; Foldbjerg et al. 2009; Kim et al. 2009c], the upregulation of pro-inflammatory cytokines [Carlson et al. 2008; Gaiser et al. 2013; Sarkar et al. 2015], and genotoxicity [Kermanizadeh et al. 2013; Piao et al. 2011; Gliga et al. 2014; Nymark et al. 2013] in several cell models. Other mechanisms of AgNP toxicity indicated in the literature include inhibited selenoprotein synthesis [Srivastava et al. 2012], induction of the unfolded protein response [Huo et al. 2015], cell cycle arrest [Beer et al. 2012; Chairuankitti et al. 2013; Foldbjerg et al 2012; Lee et al. 2011a], and disruption of the cytoskeleton [Guo et al. 2016; Ma et al. 2011]. Pretreatment with anti-oxidants mitigates many of the endpoints discussed above [Avalos et al. 2015; Chairuankitti et al. 2013; Hsin et al. 2008; Kawata et al. 2009; Kim et al. 2009c].

Studies have indicated that although many toxic effects of AgNP may be mediated through Ag ion release and that cells are often more sensitive to Ag ion than AgNP [Beer et al. 2012; Foldbjerg et al 2012], certain effects differ between AgNP- and ion-exposed samples [Liu et al. 2010b; Arai et al. 2015; Garcia-Reyero et al. 2014; Guo et al 2016]. There are also indications that particle shape may significantly affect inhaled toxicity [Schinwald et al. 2012; Schinwald and Donaldson 2012; Kenyon et al. 2012] and that smaller AgNPs have greater cytotoxic and genotoxic effects than larger AgNPs [Park et al. 2011c; Kim et al. 2012; Gliga et al. 2012, 2014; Sahu et al 2014a; 2014b; 2016a; 2016b]. There remain few comparisons between different types of AgNP functionalization in the literature, a deficiency which prevents assessing many specific functionalizations or drawing a conclusion on their effects.

## 1 **4.2 AgNP Exposure Increases Cytotoxicity and Oxidative Stress**

2 A wide range of cellular assays have also been used to examine the oxidative stress  
3 and apoptotic effects of AgNPs in vitro. Key findings following exposure to either AgNPs  
4 or ionic silver include increased levels of reactive oxygen species (ROS) [Hussain et al.  
5 2005a; Carlson et al. 2008; Foldbjerg et al. 2009; Kim et al. 2009c], induction of  
6 oxidative-stress-management genes [Kim et al. 2009c; Miura and Shinohara 2009],  
7 increased percentage of apoptotic cells [Hsin et al. 2008; Foldbjerg et al. 2009; Miura  
8 and Sinohara 2009], and attenuation of cytotoxic effects of silver by N-acetylcysteine (a  
9 glutathione precursor, ligand for ionic silver, and ROS scavenger) [Avalos et al. 2015;  
10 Chairuangkitti et al. 2013; Hsin et al. 2008; Kawata et al. 2009; Kim et al. 2009c]. A  
11 number of studies indicate that ionic silver can be more potent than AgNPs in some  
12 cellular assays for causing apoptosis [Foldbjerg et al. 2009] and reducing cell viability  
13 [Carlson et al. 2008; Greulich et al. 2009; Kim et al. 2009c; Miura and Shinohara 2009].  
14 However, other studies provide evidence of a correlation between the increase in  
15 intracellular ROS and decreasing particle size [Carlson et al. 2008], and high levels of  
16 apoptosis and necrosis for both AgNPs and ionic silver [Foldbjerg et al. 2009, 2011].  
17 Additionally, AgNP exposure has been linked to upregulation of pro-inflammatory  
18 mediators. Rat alveolar macrophages increased expression of tumor necrosis factor  
19 (TNF)- $\alpha$ , macrophage inflammatory protein (MIP)-2, and interleukin (IL)-1 $\beta$  after  
20 exposure to AgNP supernatant [Carlson et al. 2008], indicating these effects are likely a  
21 result of Ag ion release from AgNP. In human monocyte-derived macrophages  
22 responding to *Mycobacterium tuberculosis* infection, it was demonstrated that although  
23 AgNP increased expression of IL-1 $\beta$  and IL-8, AgNP also decreased expression of IL-10  
24 as well as nuclear factor (NF)- $\kappa$ B, potentially demonstrating compromise of immune  
25 responses [Sarkar et al. 2015]. Upregulation of IL-1 $\beta$ , IL-8, IL-10, TNF- $\alpha$ , monocyte  
26 chemoattractant protein (MCP)-1, and IL-1RI transcripts has been demonstrated in  
27 human hepatoblastoma cells, and a greater response was observed after exposure to  
28 10-nm AgNP than to 30- to 50-nm AgNP [Gaiser et al. 2013].

### 1 **4.3 AgNP Exposure Induces Genotoxicity**

2 AgNP exposure has also been linked to genotoxicity. DNA fragmentation as assayed by  
3 single-cell gel electrophoresis, or comet assay, has been detected in human liver [Paino  
4 et al. 2015; Kermanizadeh et al. 2013; Piao et al. 2011], lung [AshaRani et al. 2009;  
5 Gliga et al. 2014; Nymark et al. 2013], and mesenchymal stem cells [Hackenberg et al.  
6 2011]. Markers of DNA damage response activation have also been observed following  
7 AgNP exposure, specifically H2AX phosphorylation in human liver cells [Kim et al.  
8 2009c], lung cells [Gluga et al. 2014], and mouse embryonic stem cells and fibroblasts  
9 [Ahmed et al 2008], as well as upregulation of DNA damage response and repair  
10 proteins [Ahmed et al 2008]. AgNPs were also observed to induce micronucleus  
11 formation in Chinese hamster ovary cells [Kim et al. 2013a], human lymphoblastoid cells  
12 [Li et al. 2012b], and human liver and colorectal cancer cells [Sahu et al 2014a; 2014b;  
13 2016a; 2016b]. AgNP-induced oxidative stress and the resulting high level of ROS are  
14 potential reasons for the observed DNA perturbations causing DNA breaks and  
15 oxidative adducts. Both oxidative stress and genotoxicity were observed in the presence  
16 of Ag ions as well as AgNPs, and in each case these were mitigated by anti-oxidant  
17 pretreatment [Kim et al. 2009c; Foldbjerg et al. 2011]. It was also indicated that particle  
18 size had a significant effect on genotoxicity. In colorectal cancer cells, 20-nm and 50-nm  
19 AgNP induced micronuclei, but only 20-nm AgNP induced micronuclei in liver cells  
20 [Sahu et al 2014a; 2014b; 2016a; 2016b]. A similar size-dependent toxicity was  
21 observed in lung cells, where 10-nm AgNP induced DNA fragmentation but larger  
22 particles did not [Gluga et al. 2014]. Interpretation of these in vitro findings compared to  
23 those reported in in vivo studies (Sections 5.2.1, E.1.2, E.2.1) is challenging. For  
24 example, genotoxicity studies that are performed on transformed or cancer-derived cell  
25 lines may have limited relevance to predicting effects in vivo in animals and humans.

1 The doses in in vitro studies can be much higher than those in vivo, and thus the in vitro  
2 results may not be predictive of the outcomes at much lower doses in vivo.

#### 3 **4.4 Other Cellular Effects of AgNP Exposure**

4 Besides the cytotoxic, genotoxic, and ROS-generation-related effects, AgNP exposure  
5 has been linked to other endpoints. AgNP and Ag ions (from Ag<sub>2</sub>SO<sub>4</sub>) have been shown  
6 to interfere with selenoprotein synthesis in keratinocytes (HaCat) and pneumocytes  
7 (A549), specifically by preventing incorporation of selenium ions [Srivastava et al. 2012].  
8 In bronchial epithelial (16HBE), but not hepatoblastoma (HepG2) and human umbilical  
9 vein endothelial (HUVEC) cells, AgNP (20-nm) and Ag ions (from AgNO<sub>3</sub>) have been  
10 shown to trigger the unfolded protein response and upregulation of pro-apoptotic  
11 markers specific to that pathway, relative to the mitochondrial pathway [Huo et al. 2015].  
12 Several studies have indicated that AgNP exposure causes cell cycle arrest in  
13 fibroblasts (L929) [Wei et al. 2010] and pneumocytes (A549) [Beer et al. 2012;  
14 Chairuangkitti et al. 2013; Foldbjerg et al 2012; Lee et al. 2011a]. Further, it has been  
15 noted that this effect was not caused by Ag microparticles [Wei et al. 2010] and is linked  
16 to the dissolved ion concentration [Beer et al. 2012; Foldbjerg et al 2012] but is  
17 independent of ROS-dependent pathways [Chairuangkitti et al. 2013]. Alteration of cell  
18 cycle-related gene expression in fibroblasts [Ma et al. 2011] and hepatoblastoma  
19 (HepG2) cells [Kawata et al. 2009] was also documented. Cytoskeletal fiber length  
20 reduction was observed following AgNP exposure in umbilical vein endothelial cells  
21 [Guo et al. 2016], and this effect was reflected at the gene expression level in fibroblasts  
22 [Ma et al. 2011]. Increased sensitivity of cystic fibrotic bronchial epithelial cells to AgNP-  
23 induced cytotoxicity has been reported [Jeanett et al. 2016]. Finally, AgNP may have a  
24 radiosensitizing effect in breast cancer cells [Swanner et al. 2015].

#### 25 **4.5 Effects of AgNP Size, Functionalization, and Ion Release**

26 The comparative in vitro cytotoxicity of elemental AgNPs and ionic silver has been  
27 examined in studies with mammalian cells, including human mesenchymal stem cells  
28 [Greulich et al. 2009; 2011], human monocytic cells [Foldbjerg et al. 2009], human  
29 HEPG2 hepatoma cells [Kawata et al. 2009; Kim et al. 2009c], human HeLa S3 cells

1 [Miura and Shinohara 2009], human lung cells [Gliga et al. 2014], human umbilical vein  
2 endothelial cells [Guo et al 2016], Neuro-2A and HepG2 cells [Kennedy et al. 2014],  
3 mouse macrophages [Arai et al. 2015], rat alveolar macrophages [Hussain et al. 2005b;  
4 Carlson et al. 2008], and mouse spermatogonia stem cells [Braydich-Stolle et al. 2010].  
5 The results from these studies indicate that (1) the cellular uptake and toxicity can be  
6 modulated when AgNPs are functionalized with monosaccharides [Kennedy et al.  
7 2014], (2) the mammalian cytotoxic response to elemental AgNPs appears to be  
8 influenced by the particles' physical and chemical characteristics, and (3) the response  
9 is similar to that observed with ionic silver, especially for AgNPs with small diameters  
10 (less than ~30 nm) [Park et al. 2011c; Kim et al. 2012; Gliga et al. 2012, 2014; Sahu et  
11 al. 2014a; 2014b; 2016a; 2016b].

12 Comparatively few reports of in vivo studies of AgNPs in experimental animals are  
13 available, whereas information on in vitro (cellular) studies with AgNPs is extensive. The  
14 in vitro studies indicate that AgNP uptake and localization in the cell appear to be  
15 dependent on the cell type. The surface properties and size of AgNPs also appear to be  
16 important factors. In summary, adverse physiologic and biochemical responses have  
17 been observed with AgNPs in isolated cells, including (1) formation of ROS, (2) cellular  
18 disruption, (3) impairment of cellular respiration, (4) DNA perturbation, and (5)  
19 stimulation of apoptosis. Unfortunately, insufficient information is available to compare  
20 the effective concentrations for the toxicological effects of AgNPs in the in vitro studies  
21 with the exposure concentrations and doses that brought about the agent-related  
22 responses in the in vivo studies. One of the reasons for this is the lack of sufficient  
23 characterization of the AgNPs used in experiments under the exposure conditions  
24 utilized, which makes it difficult to correlate any observed effect to the AgNP properties  
25 and the available dose (which may be affected by media components). The studies do  
26 indicate, however, that the larger surface area per unit mass of AgNPs, compared with  
27 larger respirable-size silver particles, is a cause of concern because it makes AgNPs  
28 potentially more reactive than larger silver particles and makes it more difficult to predict  
29 how they will interact with biologic systems [Reidy et al. 2013].

1 Exposure to AgNPs has also been found to generate more ROS than silver ions,  
2 suggesting that the ROS production is due to specific characteristics of AgNPs and not  
3 only to ion release [Liu et al. 2010b]. Although the dissolution of AgNPs accounts for at  
4 least a degree of toxicity observed with AgNP exposure, the effects cannot always be  
5 fully apportioned to the measured dissolved fraction of silver. Although certain AgNPs  
6 may have low solubility in certain media and conditions, their contact with biologic  
7 receptors may cause the release of ions that could be sustained over a long period.  
8 Additionally, differences in AgNP and dissolved ions intracellular behavior have been  
9 observed, including activation of differing response pathways [Garcia-Reyero et al.  
10 2014] and binding to different types/weights of proteins [Arai et al. 2015]. Necrotic  
11 (rather than apoptotic) cell death may be more common after exposure to silver ions  
12 than after exposure to AgNPs [Guo et al 2016].

13 Information is limited on the role of particle shape on the capacity to induce toxicity, but  
14 Stoehr et al. [2011] found AgNWs (length, 1.5–25  $\mu\text{m}$ ; diameter, 100–160 nm) to be  
15 more toxic to alveolar epithelial A549 cells than AgNPs (30 nm) and silver microparticles  
16 (<45  $\mu\text{m}$ ) at concentrations that overlapped in both mass and surface area. No effects  
17 were observed with AgNPs and silver microparticles on A549 cells, whereas AgNWs  
18 induced strong cytotoxicity, loss in cell viability, and early calcium influx that appeared to  
19 be independent of the length of the AgNWs.

20 In vitro studies provide information on the influence of physicochemical properties on  
21 the toxicity of AgNPs. However, it is not clear to what extent the mechanism of action  
22 for AgNP toxicity is related to specific physical-chemical properties, including particle  
23 size and shape, surface area, and release rate of silver ions, and it may involve a  
24 combination of these properties. Exposure of cells to silver particles and/or silver ions  
25 may elicit toxicity by different modes of action. Although the specific mechanisms may  
26 not be fully understood, most in vitro studies have shown that nanoscale particles are  
27 more toxic than microscale particles. A more detailed description of the in vitro studies  
28 on silver is provided in Appendix D.

## 1 **5 Animal Studies Overview**

### 2 **5.1 Toxicokinetic Findings**

3 Available data suggest that AgNPs or silver ions eluted from AgNPs can be absorbed  
4 via the inhalation, oral, parenteral, or dermal routes in humans and experimental  
5 animals. Differences in rate and degree of absorption varied according to route of  
6 exposure, particle size, degree of aggregation, dissolution rate, and/or nature of any  
7 surface coating or binding material, properties which may also be important in terms of  
8 toxicity. Although the rate of absorption varies by route of exposure, cumulative  
9 evidence on the systemic distribution of silver (irrespective of route of exposure to  
10 AgNPs) has shown the liver, spleen, and kidneys to be the primary target organs  
11 [Takenaka et al. 2001; Kim et al. 2008; Sung et al. 2009; Song et al. 2013; Loeschner et  
12 al. 2011; Korani et al. 2011, 2013; Lankveld et al. 2010; Park et al. 2011a;  
13 Dziendzikowska et al. 2012; Lee et al. 2013a,d; Smulders et al. 2014; Huo et al. 2015;  
14 Bergin et al. 2016; Boudreau et al. 2016; Chen et al. 2016; Hendrickson et al. 2016;  
15 Recordati et al. 2016; Qin et al. 2016; Tiwari et al. 2107]. Silver has also been shown to  
16 distribute to the brain and ovaries/testes following pulmonary and non-pulmonary routes  
17 of exposure (Figure 5.1) [Ji et al. 2007; Kim et al. 2008; Kim et al. 2009b; Tang et al.  
18 2008, 2009; Takenaka et al. 2001; Sung et al. 2008; Lankveld et al. 2010; Kim et al.  
19 2010b; Park et al. 2010b; Park et al. 2011a; Dziendzikowska et al. 2012; van der Zande  
20 et al. 2012; Xue et al. 2012; Genter et al. 2012; Lee et al. 2013a,d; Braakhuis et al.  
21 2014; Wen et al. 2015; Fennell et al. 2016; Patchin et al. 2016; Wang et al. 2016].

#### 22 **5.1.1 Pulmonary exposure—inhalation**

23 Silver concentrations in lung tissue were observed following a subchronic (12-week)  
24 inhalation study in male and female rats [Song et al. 2013] in a dose-dependent  
25 manner. The silver concentrations following exposure to 49 or 117  $\mu\text{g}/\text{m}^3$  gradually  
26 cleared from the lung tissue during a 12-week post-exposure (recovery) period, but the  
27 silver did not completely clear from the lung tissue at the highest exposure  
28 concentration of 381  $\mu\text{g}/\text{m}^3$ . The clearance half-times ( $T_{1/2}$ ) ranged from 28.5 to 112.9

1 days across dose groups and sexes. Silver concentrations also increased in a dose-  
2 dependent manner in all nonpulmonary tissues examined in male and female rats  
3 (except for brain in females) [Song et al. 2013]. During the 12-week recovery period,  
4 silver gradually cleared from most nonpulmonary tissues but remained significantly  
5 elevated (relative to controls) in the liver and spleen at the high dose in male and female  
6 rats, as well as in the eyes in male rats at the medium and high doses.

7 The absorption and distribution of AgNPs via the inhalation route were studied in female  
8 F344 rats following a single 6-hour exposure to AgNPs at 133  $\mu\text{g}/\text{m}^3$ ; four animals per  
9 time point were killed and examined at 0, 1, 4, or 7 days post-exposure [Takenaka et al.  
10 2001]. Immediately after exposure, silver was detected at elevated concentrations in the  
11 lungs, nasal cavity, liver, and blood, but the concentrations declined over time. A total of  
12 1.7  $\mu\text{g}$  of silver was measured in the lungs immediately after exposure had ended,  
13 although only 4% of the initial pulmonary burden remained after 7 days. Nanoparticles  
14 were detected in the blood on the first day (8.9 ng Ag per g tissue wet weight). The level  
15 of silver in blood decreased to approximately 4% of the initial dose, as silver was  
16 distributed to secondary target tissues such as the liver, kidney, heart, and  
17 tracheobronchial lymph nodes.

18 Distribution to organs following inhalation exposure has also been demonstrated in  
19 studies aimed at assessing toxicity, including a subchronic exposure study by Sung et  
20 al. [2009], a 28-day inhalation study by Ji et al. [2007b], a 4-day inhalation study by  
21 Braakhuis et al. [2014], a 1-day exposure by Kwon et al. [2012], and an inhalation study  
22 by Patchin et al. [2016]. Depending on duration of exposure, dose, and possibly particle  
23 characteristics, silver was measured in varying degrees in liver, kidney, spleen, olfactory  
24 bulb, brain, heart, and whole blood. A more detailed description of these and other  
25 inhalation studies, as well as studies utilizing alternative pulmonary exposure methods  
26 (intranasal instillation, oropharyngeal aspiration, intratracheal instillation), is provided in  
27 Appendix E.

## 1 5.1.2 Nonpulmonary routes of exposure

2 Recent studies have demonstrated that the liver is also a major site of redistribution  
3 when silver nanoparticles are administered via gavage, intranasal instillation, or  
4 intravenous injection [Lankveld et al. 2010; De Jong et al. 2013; Davenport et al. 2015;  
5 Hendrickson et al. 2016; Recordati et al. 2016; Wang et al. 2016] (Section E.1). For  
6 example, when citrate- or polyvinylpyrrolidone (PVP)-coated silver nanoparticles were  
7 intravenously injected in mice, the spleen and liver had the highest silver  
8 concentrations at one day after exposure [Recordati et al. 2016]. In rats, intravenous  
9 exposure to 20-nm AgNPs showed redistribution preferentially to the liver, followed by  
10 kidneys and spleen, while larger nanoparticles in the vasculature were preferentially  
11 redistributed to the spleen, followed by liver and lung [Lankveld et al. 2010]. In a 13-  
12 week gavage study of AgNPs, silver accumulated in all major organs, including the liver;  
13 organs of female rats accumulated more silver than the organs of male rats; and more  
14 silver accumulated in organs of rats receiving 10-nm AgNPs than those receiving 75- or  
15 110-nm AgNPs [Boudreau et al. 2016]. Similarly, the liver is a major site of silver  
16 accumulation in AgNP inhalation studies [Takenaka et al. 2001; Song et al. 2013].

17 Within the liver of rats repeatedly injected intravenously with silver nanoparticles, silver  
18 has been reported to accumulate in Kupffer cells, in endothelial cells, and at sites of  
19 inflammation [De Jong et al. 2013]. In rats in a 13-week AgNP gavage study, silver  
20 granules were identified in liver portal triads by transmission electron microscopy  
21 [Boudreau et al. 2016]. In addition, in multiple tissues, AgNPs often accumulate within  
22 cells, while soluble silver tends to accumulate extracellularly, suggesting important  
23 differences in their biodistribution [Boudreau et al. 2016]. In the mouse injection study,  
24 silver accumulated in Kupffer cells, in portal and sinusoidal endothelial cells, and to a  
25 lesser extent in hepatocytes 1 day after a single injection [Recordati et al. 2016].

## 26 5.1.3 Sex differences

27 Sex differences in biodistribution have also been observed in rodents. Following oral  
28 exposure, Lee et al. [2013a] found that silver levels accumulated in Sprague Dawley

1 rats in the gonads of both sexes; however, the levels in the testes persisted longer than  
2 in the ovaries. Persistence of silver in the testes over time, as well as in the brain, was  
3 also observed in rats by Van der Zande et al [2012] following oral exposure. One  
4 commonality across studies examining sex differences in silver absorption and  
5 distribution, irrespective of route of exposure or species, was an increase in silver levels  
6 in the kidneys of females (Sung et al. 2008; Sung et al. 2009; Song et al. 2013; Dong et  
7 al. 2013; Xue et al. 2012; Kim et al. 2008; Park et al. 2010a; Lee et al. 2013a; Kim et al.  
8 2009a; Kim et al. 2010a; Boudreau et al. 2016]. The accumulation of silver in the  
9 kidneys appears to be sex-specific, on the basis of results from 28-day, 90-day, and 12-  
10 week inhalation studies [Sung et al. 2009; Kim et al. 2011; Song et al. 2013; Dong et al.  
11 2013] and 90-day oral studies [Kim et al. 2010a].

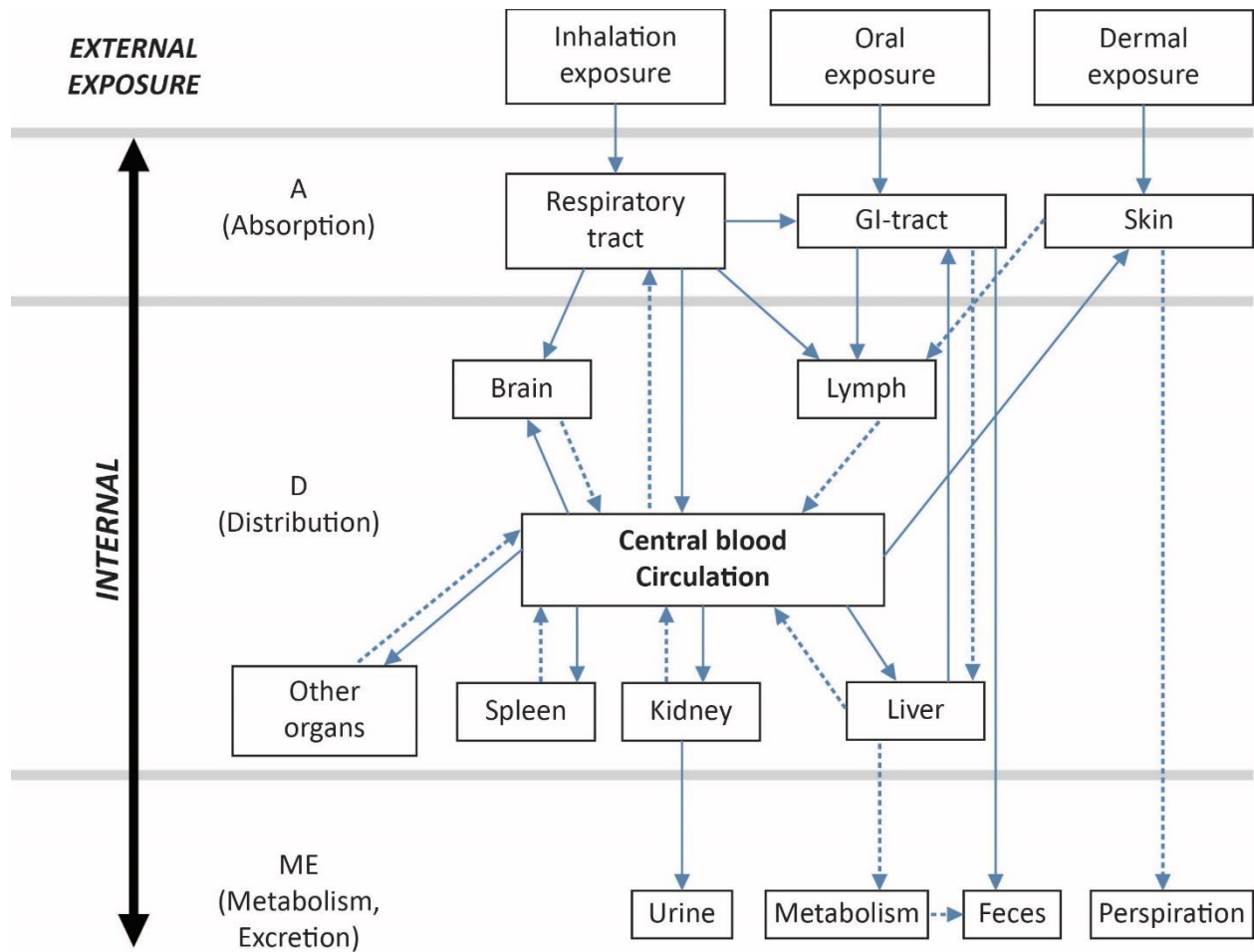
12 Both inhalation and oral exposure studies indicate that female rats have two to four  
13 times more silver accumulation than males in all kidney regions. In particular, the  
14 glomerulus in the kidney cortex of Fischer 344 rats was found to contain a higher  
15 accumulation in females than in males [Kim et al. 2009a]. The AgNPs were also  
16 preferentially accumulated in the basement membranes of the renal tubules in the  
17 cortex, in the medium and terminal parts of the inner and outer medulla of female rats;  
18 they also were detected in the cytoplasm and nuclei of the interstitial cells in the inner  
19 medulla of the kidneys [Kim et al. 2009a]. These sex differences have been suggested  
20 to be associated with metabolism and hormonal regulation, because the kidneys are a  
21 target organ for several hormones, such as thyroid hormones and testosterone [Kim et  
22 al. 2009a]. Increased level of silver in the spleens and gastrointestinal tract of female  
23 Sprague Dawley rats was reported following oral exposure [Boudreau et al. 2016].

#### 24 5.1.4 Physicochemical properties affecting kinetics

25 In terms of the physical and chemical properties of AgNP, studies indicate that solubility  
26 and size are critical factors in absorption and distribution of AgNP. In general, soluble or  
27 “ionic” silver was absorbed faster and in greater quantity than AgNP following  
28 pulmonary exposure [Arai et al. 2015; Wen et al. 2015] and oral exposure [Loeschner et

1 al. 2012; Park et al. 2013; Bergi et al. 2016; Qin et al. 2016; Boudreau et al. 2016].  
2 Smaller AgNPs were absorbed and distributed to a greater degree than larger silver  
3 particles following oral exposure [Boudreau et al. 2016], intravenous exposure  
4 [Lankveld et al. 2010; Dziendzikowska et al. 2012; Tang et al. 2008; Recordati et al.  
5 2016], and pulmonary exposure [Braakhius et al. 2014; Patchin et al. 2016]. The effect  
6 of particle size on the biodistribution of AgNPs remains largely unstudied for dermal  
7 exposure.  
8  
9 Few studies have directly compared the effects of surface coating of AgNPs on kinetics  
10 following pulmonary and oral exposure. In a study by Bergin et al. [2016], no differences  
11 were observed in biodistribution following oral exposure to PVP- or citrate-coated  
12 AgNPs. In a study of the pulmonary clearance of PVP and citrate-coated AgNPs,  
13 Anderson et al. [2015] found a greater rate of clearance for the 20 nm PVP-coated  
14 materials when compared to the 20 nm citrate-coated material. Systemic distribution  
15 was not examined by Anderson et al. [2015]. Following intravenous exposure of citrate-  
16 or PVP-coated nanoparticles, these nanoparticles showed a similar distribution pattern  
17 [Pang et al. 2016; Recordati et al. 2016]; however, polyethylene glycol (PEG)-coated  
18 materials (which are relatively neutral in charge and have a high affinity for binding  
19 protein) were more biopersistent, followed by branched polyethyleneimine (BPEI)-  
20 coated materials, compared to citrate- or PVP- coated materials [Pang et al., 2016].  
21 Regardless of coating, silver distributed primarily to the liver and spleen. Ashraf et al.  
22 [2015] demonstrated that both uncoated AgNPs and dextran-coated AgNPs also target  
23 the liver and spleen following intravenous exposure; however, recognition and uptake of  
24 dextran-coated AgNPs were slower. Further research is needed to more fully elucidate  
25 the effects of coating and particle shape on the absorption, distribution, metabolism, and  
26 excretion of AgNPs by various routes of exposure, including following long-term  
27 exposure.  
28  
29  
30  
31

1



2

3

4 **Figure 5.1. Systemic distribution of silver. The solid lines represent confirmed**  
5 **routes for silver (including AgNPs); the dashed lines represent possible routes**  
6 **and other organ sites (such as the heart and reproductive organs). Adapted from**  
7 **Hagens et al. [2007] and Oberdörster et al. [2005].**

8

## 1 **5.2 Toxicological Effects**

### 2 **5.2.1 Pulmonary exposure**

3 Inhalation studies provide the most physiologically relevant data for evaluating toxicity  
4 following respiratory exposure in mammalian models. The most comprehensive dataset  
5 on the potential toxicity of silver comes from studies of animals exposed by subchronic  
6 inhalation to silver nanoparticles [Sung et al. 2008, 2009; Kim et al. 2011a; Song et al.  
7 2013; Dong et al. 2013]. In these studies male and female rats were exposed to silver  
8 nanoparticles with diameters ranging from 2 to 65 nm (median of 16 nm) at three  
9 different doses for 12 to 13 weeks. There was a dose-dependent accumulation of silver  
10 in the lung, liver, kidneys, blood, and brain [Song et al. 2013; Sung et al. 2009], as well  
11 as in the spleen, eyes, testes, and ovaries, with a greater degree of silver accumulation  
12 in the kidneys of female rats [Song et al. 2013]. Lung function changes and  
13 histopathological lesions in the lung occurred at the highest dose (381  $\mu\text{g}/\text{m}^3$ ) [Song et  
14 al. 2013; Sung et al. 2008; 2009], with lung function deficits persisting up to 12 weeks  
15 post-exposure in male rats, while female rats showed gradual recovery in lung  
16 responses over time [Song et al. 2013]. Systemically, bile duct hyperplasia and  
17 hepatocellular necrosis were observed in both male and female rats following exposure  
18 [Sung et al. 2008, 2009]. Genotoxicity studies were performed in the same animals from  
19 the subchronic inhalation studies. Kim et al. [2011a] found no changes in micronucleus  
20 induction in bone marrow; however, Dong et al. [2013] did find variations in gene  
21 expression profiles when comparing the kidneys of male and female rats.

22 Following acute and subacute inhalation, lung inflammation ranged from nonexistent to  
23 minimal/moderate, with varying degrees of resolution over time [Stebounova et al. 2011;  
24 Kwon et al. 2012; Roberts et al. 2013; Braakhuis et al. 2014; Sieffert et al. 2016; Silva et  
25 al. 2016]. Lung function deficits, where present, were transient [Sieffert et al. 2016].  
26 Goblet cell hypertrophy and hyperplasia were noted in one study [Hyun et al. 2008].  
27 Systemic toxicity was also observed following acute or subacute inhalation exposure,

1 including effects in liver [Ji et al. 2007b] and in brain [Lee et al. 2010; Patchin et al.  
2 2016].

3 Pulmonary inflammation and lung function, with varying degrees of resolution over time,  
4 were also observed following acute or repeated aspiration, intranasal instillation, or  
5 intratracheal instillation [Park et al. 2011b; Roberts et al. 2012; Kaewamatawong et al.  
6 2014; Smulders et al. 2014; Seiffert et al. 2015; Silva et al. 2015; Botelho et al. 2016].  
7 Mucosal erosion in the nasal cavity was also noted by Genter et al. [2012]. As with  
8 inhalation studies, exposure by aspiration or instillation resulted in systemic effects in  
9 the liver [Gosens et al. 2015; Huo et al. 2015], spleen [Genter et al. 2012; Davenport et  
10 al. 2015], kidney [Huo et al. 2015], and brain [Liu et al. 2012; Davenport et al. 2015]. No  
11 chronic studies on carcinogenicity, reproductive toxicity, or developmental toxicity  
12 following pulmonary exposure have been reported.

13 A recent study may be the first report that inhaled silver nanoparticles in mice  
14 accumulated in placental and fetal tissues and was associated with an adverse  
15 pregnancy outcome [Campagnolo et al. 2017]. An increased number of resorbed  
16 fetuses was observed in female mice that had been exposed to 18-20 nm silver  
17 nanoparticles by nose-only inhalation at an airborne concentration of 640  $\mu\text{g}/\text{m}^3$ , for 4  
18 hr/d, each day during the first 15 days of gestation. The silver nanoparticles were freshly  
19 produced by a spark generator in an inert argon atmosphere. Estrogen plasma levels  
20 were reduced in the mothers, and inflammatory mediators were elevated in the lungs  
21 and placenta [Campagnolo et al. 2017].

## 22 5.2.2 Dermal, oral, and parenteral exposure

23 Dermal exposure represents another potential route of occupational exposure. Data  
24 specifically related to AgNP exposure are limited. Several studies show minimal to no  
25 effect following acute exposure [Kim et al. 2013b; Maneewattanapinyo et al. 2011]. In  
26 the acute and subacute studies where effects were observed, topical irritation at the  
27 contact site and focal inflammation/edema were observed [Korani et al. 2011, Samberg

1 et al. 2010], and in one subacute study epidermal hyperplasia and graying of the skin  
2 were noted [Samberg et al. 2010]. Only one set of studies examined subchronic  
3 exposure, which resulted in skin effects similar to acute exposure and also caused  
4 histopathological changes in the liver and spleen [Korani et al. 2011] and in kidney and  
5 bone [Korani et al. 2013].

6 Effects observed in the liver, either as histopathological changes in tissue or changes in  
7 blood chemistry indicative of liver injury/disease, have also been extensively reported in  
8 relation to oral and parenteral routes of exposure [Kim et al. 2009b; Kim et al. 2010b;  
9 Tiwari et al. 2011; Lee et al. 2013b; Kim et al. 2008; Park et al. 2010a; Kim et al. 2010a;  
10 Yun et al 2015; Elle et al. 2013; Katsnelson et al. 2013; Recordati et al. 2016; Qin et al.  
11 2016; Wang et al. 2013]. Kidney is also a likely target organ following exposure via oral  
12 and parenteral routes, with evidence of tissue and blood chemistry changes [Kim et al.  
13 2010b; Park et al. 2010a; Yun et al. 2015; Qin et al. 2016]. Both oral and parenteral  
14 exposure also result in changes to blood hemocytology, including red blood cells, white  
15 blood cells, platelets, and hemoglobin [Tiwari et al. 2011; Katsnelson et al. 2013; Park  
16 et al. 2013; Qin et al. 2016], which may suggest other potential target organs such as  
17 the spleen.

18 Results from studies focusing on neurological effects in response to oral or parenteral  
19 exposure to AgNP in terms of behavioral responses and biochemical changes in the  
20 brain have been variable; when effects have been noted, these have included changes  
21 in neurotransmitter levels and changes in gene expression [Rahman et al. 2009; Hadrup  
22 et al. 2012c; Dabrowska-Bouta et al. 2016]. Studies of intranasal instillation of AgNP in  
23 rodents have shown oxidative stress in the brain, but effects on learning and memory  
24 were mixed [Genter et al. 2012; Liu et al. 2012; Wen et al. 2015]. These studies  
25 suggest that the brain may be a target organ for AgNP, and that the ionic form of silver  
26 may translocate to the brain to a greater degree than the particle form. However, more  
27 research is needed on the potential for neurotoxicity following AgNP exposure.

1 Reproductive toxicity was evaluated following oral, intravenous, and intraperitoneal  
2 exposure to AgNP. In studies that observed toxicity, the most commonly observed  
3 effects in adult and pre-pubertal males included morphological abnormalities in the  
4 seminiferous tubules, reduction in spermatogenesis, and damage to and decreased  
5 viability of sperm [Gromadzka-Ostrowska et al. 2012; Sleiman et al. 2013; Miresmaeili  
6 et al. 2013; Mathiaas et al. 2014; Thakur et al. 2014; Lafuente et al. 2016]. Because  
7 effects in pregnant dams and in embryos/fetuses are highly variable, it is difficult to draw  
8 general conclusions related to pregnancy and embryo development [Philbrook et al.  
9 2011; Austin et al. 2012; Mahabady et al. 2012; Wang et al. 2013; Yu et al. 2014;  
10 Kovvuru et al. 2015].

11 Effects in the gastrointestinal tract specific to oral exposure included effects on  
12 microbiota populations after subchronic exposure [Williams et al. 2015], inflammation in  
13 the microvillus and damage to microvilli [Sharare et al. 2013], and increased goblet cells  
14 and secretions in mucins [Jeong et al. 2010], findings that are similar to those observed  
15 in respiratory mucosa [Hyun et al. 2008; Genter et al. 2012].

### 16 5.2.3 Sex differences

17 As discussed above, sex differences in rodents existed in absorption and biodistribution  
18 irrespective of the route of exposure, with the most prominent difference reported to be  
19 increased levels of Ag in the kidney of females. In vivo studies have also correlated this  
20 difference with toxicity in the kidney of females. Dong et al. [2013] demonstrated that  
21 gene expression was differentially regulated in males and females following inhalation  
22 of AgNP. Studies have shown increased kidney calcifications following oral exposure,  
23 which correlated with increased serum calcium [Yun et al. 2015], and have also shown  
24 increased allantoin in urine, indicative of oxidative stress [Hadrup et al. 2012a]. In  
25 addition to effects in kidneys, studies indicate oral exposure may also result in sex-  
26 related effects in the liver, although the findings vary in this regard. A number of studies  
27 have indicated increased serum liver enzymes in females [Kim et al. 2008; Park et al.  
28 2010a; Yun et al. 2015]; however, Qin et al. [2016] demonstrated a greater increase in

1 serum liver enzymes in males versus females. Blood cell profiles also differed between  
2 sexes following oral exposure, with increased white blood cells in females [Qin et al.  
3 2016; Yun et al. 2015] and increased platelets in males [Yun et al. 2015]. Williams et al.  
4 [2015] found differences between sexes in effects on the gut microbiota as well.

#### 5 **5.2.4 Potential mechanisms of toxicity**

6 Studies of AgNP-induced toxicity, irrespective of route of exposure, indicate oxidative  
7 stress as one of the primary mechanisms of toxicity in target organs. Following  
8 pulmonary exposure to AgNP, evidence of oxidative stress in the lung has been  
9 indicated in lavage fluid as increased malonaldehyde (MDA) [Liu et al. 2013a; Seiffert et  
10 al. 2015, 2016] and as alterations or increases in glutathione (GSH), super oxide  
11 dismutase (SOD), and nitric oxide (NO) [Liu et al. 2013a]. Changes in GSH and SOD  
12 have also been measured in lung tissue [Kaewamatawong et al. 2014; Gosens et al.  
13 2015] and the nasal cavity [Genter et al. 2012]. In addition, thiol-containing proteins,  
14 specifically metallothioneins, which are important in protecting against metal toxicity and  
15 oxidative stress, are increased in lung tissue [Kaewamatawong et al. 2014; Smulders et  
16 al. 2015a]. Increased GSH in spleen and Hmox1 expression in brain have also been  
17 measured after pulmonary exposure [Davenport et al. 2015]. Huo et al. [2015] found  
18 increased endoplasmic reticular stress in liver, kidney, and lung and increased  
19 apoptosis in lung and liver following pulmonary exposure; however, direct correlations of  
20 these parameters to oxidative stress were not delineated. Oxidative stress in target  
21 organs has also been evaluated following oral and parenteral routes of exposure. Oral  
22 exposure has resulted in increased MDA and NO in serum [Elle et al. 2013; Shrivastava  
23 et al. 2016] and superoxide anion in heart and liver [Elle et al. 2013], increased  
24 metallothionein in liver and kidney [Shrivastava et al. 2016], and increased markers of  
25 oxidative stress and DNA damage in urine [Hadrup et al. 2012b; Shrivastava et al.  
26 2016]. Following parenteral exposure, increased reactive oxygen species have been  
27 measured in blood, lung, liver, and kidney, along with apoptosis in lung liver and kidney  
28 [Tiwari et al. 2011; Kim et al. 2010b], and an increase in apoptosis and oxidative stress–  
29 related gene expression was detected in the brain [Rohman et al. 2009].

## 1 5.2.5 Physicochemical properties

2 As described earlier, a number of physical and chemical properties of nanomaterials  
3 have been considered to be important factors in toxicity, including shape, size, degree  
4 of agglomeration, surface area, chemical composition, surface charge, surface  
5 chemistry (coatings, capping agents, functional modifications), and dissolution rate. In  
6 turn, these factors, in combination with a specific route of exposure (different cell types,  
7 pH, surrounding physiologic fluids, etc.) influence the toxicokinetics of the materials  
8 (cellular uptake and tissue absorption, distribution, metabolism, and excretion of the  
9 material). The in vivo AgNP studies reviewed in detail in Appendix E for any given route  
10 of exposure are diverse in terms of species used, AgNP primary particle size and form,  
11 particle dose, use of reference materials/controls, and degree of characterization of  
12 particles as it relates to physical and chemical properties of the material. One of the  
13 more consistent findings across studies appears to indicate that more soluble forms and  
14 small particle sizes of silver may be more toxic than larger particles [Johnston et al.  
15 2010; Park et al. 2011a; Hadrup et al. 2012a,b; Gromadska-Ostrowska et al. 2012; Kim  
16 et al. 2012; Park et al. 2013; Gliga et al. 2014, Katsnelson et al. 2013; Arai et al. 2015;  
17 Qin et al. 2016; Silva et al. 2016]. These studies indicate that AgNPs, because of their  
18 small particle size and large surface area per unit mass, facilitate the more rapid  
19 dissolution of ions than the equivalent bulk material, potentially leading to increased  
20 toxicity. This, coupled with the particles' capacity to adsorb biomolecules and interact  
21 with biologic receptors, may mean that AgNPs can reach subcellular locations, leading  
22 to potentially higher localized concentrations of ions once those particles start to  
23 dissolve or degrade in situ. A small number of studies suggest larger particles may  
24 induce toxicity to a greater degree, depending on primary particle size and coating  
25 [Anderson et al. 2015b; Silva et al. 2015; Botelho et al 2016]; however, the majority of  
26 the data suggest that the smaller particles are associated with increased biodistribution  
27 and toxicity. Whether this is related to the material itself (coating, solubility,  
28 agglomeration) or the specific toxicological parameter being investigated is unclear.  
29 Studies also show that although toxicity may be increased with increasing solubility,  
30 solubility does not account entirely for toxicity, and particles contribute to toxicity as well

1 [Hadrup et al. 2012c; Holland et al. 2015; Qin et al. 2016]. Findings from studies that  
2 have compared surface coatings of the materials (primarily citrate or PVP) vary widely,  
3 and data available on AgNP are insufficient to draw general conclusions regarding  
4 coating and shape.

### 5 **5.3 General Conclusions**

6 As mentioned above, studies varied in species, strain, dose, size, form/coating of  
7 AgNPs (PVP, citrate, spark generated, CMC, colloidal), degree of characterization of  
8 the materials, and incorporation of controls or reference particles for different particle  
9 properties, making cross-study comparisons challenging. Despite these differences and  
10 with some exceptions, several broad conclusions can be drawn from the in vivo animal  
11 studies reviewed in this document.

- 12 • Particle size and degree of solubility likely affect distribution of silver and, in turn,  
13 toxicity, with greater distribution or a higher rate of distribution and increasing  
14 toxicity with decreasing size and increasing solubility, irrespective of the route of  
15 exposure.
- 16 • Sex differences in distribution and toxicity have been demonstrated, with the  
17 most common difference a greater accumulation of silver in the kidneys of  
18 females, irrespective of route of exposure (oral, intravenous, and pulmonary  
19 exposures).
- 20 • Dose-dependent effects are demonstrated in the primary organ systems related  
21 to the route of exposure (skin, lung, gastrointestinal tract); however, organ  
22 systems exposed to silver following absorption and distribution of AgNPs may be  
23 more sensitive to the toxic effects of silver. Liver is likely a target organ following  
24 AgNP exposure. In most studies, toxicological effects were demonstrated in liver,  
25 irrespective of the route of exposure or sex. Kidney and spleen are also likely  
26 target organs, depending on the route of exposure. Neurological and  
27 reproductive studies demonstrate long-term persistence of silver in the brain and  
28 testes; however, toxicological outcomes vary, and more studies are needed

*This information is distributed solely for the purpose of pre-dissemination peer review under applicable information quality guidelines. It has not been formally disseminated by the National Institute for Occupational Safety and Health. It does not represent and should not be construed to represent any agency determination or policy.*

- 1 across various routes of exposure in this area to correlate distribution with
- 2 toxicity.
- 3 • When toxicity is observed following exposure to AgNP, oxidative stress–induced
- 4 tissue injury is indicated as one of the primary mechanisms.
- 5 A more detailed description of the experimental animal studies of silver can be found in
- 6 Appendix E.

## 6 Hazard and Risk Evaluation of Silver

### Nanoparticles and OEL Derivation

#### 6.1 Hazard Identification

##### 6.1.1 Lung effects

In the absence of data on human exposure to AgNPs, the findings from subchronic inhalation studies in rats [Sung et al. 2008, 2009; Song et al. 2013] were determined to be the best available data to evaluate the potential occupational health hazard of AgNPs. Lung inflammation and lung function deficits occurred in both male and female Sprague-Dawley rats following inhalation of AgNPs for 13 and 12 weeks, respectively, as reported by Sung et al. [2008, 2009] and Song et al. [2013]. The inflammation (chronic, alveolar) was reported to be of minimal severity on the basis of histopathologic evaluation [Sung et al. 2009; Song et al. 2013]. Persistent pulmonary inflammation is relevant to the development of chronic respiratory disease in workers [NIOSH 2011; 2013]. Although the available AgNP inhalation studies have been limited in duration of exposure or dose, chronic pulmonary inflammation with epithelial injury and dysfunctional resolution is associated with pulmonary fibrosis attributable to nonoccupational as well as occupational causes [Cotton et al, 2017; Meyer, 2017; Oberdörster et al, 1994]. The pulmonary inflammation responses to silver nanoparticles observed in rats after subchronic inhalation are consistent with pulmonary responses to other respirable particles, including nanoparticles, following subchronic inhalation exposure [NIOSH 2011, 2013]. However, the pulmonary inflammation was not persistent in rats exposed to silver nanoparticles when the exposure was discontinued in a recovery study, resolving by 12 weeks post-exposure in all but one rat [Song et al. 2013]; in addition, pulmonary fibrosis was not documented in rats following subchronic inhalation of silver nanoparticles [Sung et al. 2009; Song et al. 2013]. These findings indicate that the rat pulmonary inflammation response to silver nanoparticles following subchronic inhalation is an early-stage effect of minimal severity. Exposures at which

1 this response is not observed therefore may be unlikely to be associated with adverse  
2 effects when chronically exposed.

3 Lung function deficits were reported in both of the subchronic inhalation studies in rats  
4 [Sung et al. 2008; Song et al. 2013], including decreases in tidal volume, minute  
5 volume, peak inspiration flow, and peak expiration flow. The 49- $\mu\text{g}/\text{m}^3$  exposure  
6 concentration was a LOAEL for lung function deficits in female rats in the study by Sung  
7 et al. [2008], but in the study by Song et al. [2013], 381  $\mu\text{g}/\text{m}^3$  was the NOAEL (that is,  
8 no lung function deficits were observed) in female rats. These results show large  
9 variability in the female lung function responses in the two studies. For male rats, 133  
10  $\mu\text{g}/\text{m}^3$  was the NOAEL for lung function deficits in Sung et al. [2008], and it was 49  
11  $\mu\text{g}/\text{m}^3$  in Song et al. [2013]. The difference in the number of rats in each exposure group  
12 ( $n = 10$  males and  $n = 10$  females in Sung et al. [2008];  $n = 5$  males and  $n = 4$  females  
13 in Song et al. [2013]) may have contributed to the variability in responses observed in  
14 the two studies. The lung function deficits were dose-related, although it is unclear  
15 whether the level of reduced lung function reported from these rat studies would be  
16 considered clinically significant in humans (as discussed in Christensen et al. [2010]). In  
17 addition to lung function deficits, pulmonary inflammation was observed in these rats, as  
18 discussed below.

19 The NOAEL for pulmonary inflammation was 133  $\mu\text{g}/\text{m}^3$  in male and female rats in a  
20 study by Sung et al. [2009]. Song et al. [2013] reported that 117  $\mu\text{g}/\text{m}^3$  was the LOAEL  
21 in male rats and a NOAEL in female rats. In male rats, lung inflammation was observed  
22 at 117  $\mu\text{g}/\text{m}^3$ , which had resolved by 12 weeks post-exposure (but was persistent in the  
23 381- $\mu\text{g}/\text{m}^3$  group). In female rats, lung inflammation was not observed at 117  $\mu\text{g}/\text{m}^3$ ,  
24 and the inflammation observed in the 381- $\mu\text{g}/\text{m}^3$  exposure group had resolved by 12  
25 weeks post-exposure. The rat lung inflammation data from the end of the subchronic  
26 inhalation (13 weeks [Sung et al. 2009] and 12 weeks [Song et al. [2013]]) were used for  
27 the quantitative risk assessment (Table 6-1) (Section 6.3). NIOSH considers persistent  
28 pulmonary inflammation to be a relevant potential adverse health effect in workers

1 because it has been associated with occupational exposures to some hazardous  
2 airborne particles [NIOSH 2011, 2013].

### 3 6.1.2 Liver effects

4 Silver in the blood is removed via biliary excretion and eliminated from the body  
5 primarily in the feces, as noted in studies of workers [DiVincenzo et al. 1985; Wölbling  
6 et al. 1988]. The finding of bile duct hyperplasia in rats [Sung et al. 2009, Kim et al.  
7 2010a] from exposure to AgNPs is consistent with this elimination pathway through the  
8 liver.

9 Bile duct hyperplasia is often associated with aging in rats (which is not the case in the  
10 subchronic studies) [Eustis et al. 1990]. When bile duct hyperplasia is accompanied by  
11 inflammatory cells and/or oval cell proliferation, it can be caused by exposure to a toxic  
12 substance [NTP 2014]. The clinical significance of bile duct hyperplasia is not clear,  
13 although some evidence suggests that cholangiocellular carcinoma can develop from  
14 bile duct hyperplasia [Kurashina et al. 2006]. Minimal biliary hyperplasia as an isolated  
15 finding in rats is sometimes considered non-adverse, particularly in the Sprague-Dawley  
16 rat, where the hyperplasia may be reversible after a recovery period [Hailey et al. 2013].  
17 However, the authors of the review reaching that conclusion also noted that “serum or  
18 tissue markers of hepatocellular injury may serve as a sentinel for potential untoward  
19 biliary epithelial proliferations” [Hailey et al, 2013]. On the basis of these findings,  
20 NIOSH considers the response of bile duct hyperplasia in a subchronic inhalation study  
21 in rats [Sung et al. 2009] to be a potential adverse effect. The rat liver bile duct  
22 hyperplasia response is evaluated in detail below to assess the scientific evidence  
23 regarding the relevance of this response to workers exposed to silver nanoparticles.

24 The liver effects in the subchronic (13-week) inhalation study in rats [Sung et al. 2009]  
25 was considered to be primarily relevant to estimating risk in workers. Bile duct  
26 hyperplasia of minimum or greater severity was reported in male and female rats  
27 exposed to silver nanoparticles at 515  $\mu\text{g}/\text{m}^3$ . The NOAEL for liver effects was 133

1  $\mu\text{g}/\text{m}^3$  (Section B.1). Silver was shown to accumulate in the liver in a dose-dependent  
2 manner [Song et al. 2013] (Section 5.1). In 3/10 female rats in the high-dose (515  
3  $\mu\text{g}/\text{m}^3$ ) group, the bile duct hyperplasia was accompanied by a pattern of individual  
4 hepatocellular necrosis, which was not seen in control rats. One of these female rats  
5 had bile duct hyperplasia of moderate severity with concurrent moderate centrilobular  
6 fibrosis, necrosis, and pigmentation [Sung et al. 2009]. One of the affected rats also had  
7 moderate multifocal hepatocellular necrosis [Sung et al, 2009]. The presence of foci of  
8 minimal necrosis in two control rats from the 13-week inhalation study, albeit with a  
9 different pattern, complicates the interpretation. The data on rat liver effects from the  
10 one subchronic inhalation study that reported liver effects [Sung et al. 2009] (Table 6-2)  
11 were used in the quantitative risk assessment (Section 6.3). No data were available on  
12 the persistence of the liver effects in the rats following subchronic inhalation.

13 In addition, oral studies that examined liver effects in rats are discussed below. These  
14 are considered to be relevant supporting data. A subchronic (13-week) oral exposure  
15 study did not show hepatocellular necrosis in any of the 20 control rats, but focal,  
16 multifocal, or lobular hepatocellular necrosis was seen in rats in each of the exposed  
17 groups (2/10, 2/10, and 2/10 affected females in the low-, medium-, and high-exposure  
18 groups; 4/10, 5/10, and 4/10 affected males in the low-, medium-, and high-exposure  
19 groups). In addition, clinical chemistry in the oral toxicity study supporting liver damage  
20 included elevation of serum cholesterol in male rats in the medium- and high-exposure  
21 groups and female rats in the high-exposure group, increased AP in female rats at the  
22 highest exposure, and increased total bilirubin in male rats in the medium-exposure  
23 group [Kim et al. 2010a]. Biliary hyperplasia, usually of minimal severity, was also  
24 higher after oral silver nanoparticle exposure. The concomitant presence of  
25 hepatocellular necrosis, biliary hyperplasia, and clinical pathology abnormalities in the  
26 oral toxicity studies indicate that the liver effects in male rats in the medium- and high-  
27 exposure groups and in female rats in the high-exposure group were adverse in this  
28 study [Kim et al, 2010a].

1 In a 28-day oral toxicity study of 42-nm-diameter silver nanoparticles in mice, AP and  
2 AST were increased in the serum of male and female mice at the highest exposure (1  
3 mg/kg), and alanine transaminase was also increased in the female mice in this  
4 exposure group [Park et al. 2010]. Similarly, serum AP was increased in male and  
5 female Sprague Dawley rats exposed to 1030.5 mg/kg AgNPs orally for 13 weeks [Yun  
6 et al. 2015].

7 Because of serum and/or histopathologic evidence of liver damage in rats or mice  
8 exposed to silver nanoparticles by the oral or intravascular routes, NIOSH considers the  
9 concomitant presence of bile duct hyperplasia and single-cell hepatocellular necrosis  
10 observed in the group of female rats exposed by inhalation (515  $\mu\text{g}/\text{m}^3$  for 13 weeks)  
11 [Sung et al. 2009] to be a potential adverse effect. The bile duct hyperplasia of minimum  
12 or greater severity in male and female rats exposed by inhalation to 515  $\mu\text{g}/\text{m}^3$  is  
13 interpreted as part of an apparent continuum of silver nanoparticle–induced  
14 hepatobiliary damage and is therefore also considered potentially adverse [Sung et al.  
15 2009]. In addition, the studies of silver nanoparticle biodistribution and acute  
16 hepatotoxicity from nonpulmonary routes of exposure (Section 5.1) provide additional  
17 relevant information to the interpretation of bile duct changes seen in subchronic toxicity  
18 studies. Based on the scientific findings described in this section, NIOSH considers the  
19 rat bile duct hyperplasia response to AgNPs to be a potential adverse health effect in  
20 workers.

### 21 **6.1.3 Biological mode of action and physical-chemical properties**

22 Based on the available toxicology data (reviewed in Section 5 and Appendix E),  
23 hypotheses related to the dose-response relationships and the potential adverse health  
24 risk of occupational exposure to silver nanoparticles include the following:

- 25 • The dissolution rate of silver particles in the lungs and other tissues is associated  
26 with particle size, and is faster for nanoscale than microscale particles;

- 1 • The binding of silver particles or ions to proteins and thiol groups in the body  
2 modifies the bioactivity of silver and increases silver uptake in liver and excretion;
- 3 • The toxicity of silver is related both to the release of ions (which occurs at a  
4 higher rate for nanoscale silver) and to the retention of silver particles in tissues.

5  
6 Current knowledge on these biochemical and biophysical processes is based primarily  
7 on acute or short-term studies of silver. The role of these processes on the toxicity of  
8 silver nanoparticles following repeated exposures is not well known. Both poorly  
9 soluble and soluble particles can potentially cause adverse effects when inhaled into the  
10 lungs. The silver ions are typically associated with acute effects, which may resolve if  
11 the exposure does not continue [Roberts et al. 2013], although repeated exposures  
12 could result in higher doses of both ions and particles (which may also release ions over  
13 time, depending on site of disposition in the body and reaction with cellular proteins and  
14 other compounds). Ions released from soluble particles (such as AgNO<sub>3</sub>) can react with  
15 cells and damage cell membranes, resulting in cell death [Cronholm et al. 2013; Zhang  
16 et al. 2014]. Smaller particles with greater surface area per unit mass would have a  
17 greater potential for ion release [Johnston et al. 2010]. One of the key complexities in  
18 hazard and risk assessment of silver particles, including nanoparticles, is uncertainty  
19 about the dissolution of various types of silver particles or silver compounds and the  
20 extent to which the tissue distribution and any potential adverse effects may be due to  
21 the ionic vs. particulate forms of silver.

22 Poorly soluble particles that are deposited in the pulmonary region of the lungs at doses  
23 that are not effectively cleared can trigger inflammatory responses, and particles that  
24 interact with epithelial cells lining the alveoli and translocate to the lung interstitial tissue  
25 can elicit fibrotic responses [NIOSH 2011, 2013]. Pulmonary fibrosis has not been found  
26 in the animal subchronic inhalation studies of inhaled AgNPs [Sung et al. 2008, 2009;  
27 Song et al. 2013] or in studies of workers in silver production or processing [DiVincenzo  
28 et al. 1985]. Inhalation is often the route associated with the highest potential for  
29 exposure in the workplace [Park et al. 2009; Miller 2010; Lee et al. 2011b; Lee et al.  
30 2012a]. In addition to inhalation, workers may be exposed to silver particles or ions

1 through dermal exposure or ingestion (for instance, as a result of mucociliary clearance  
2 of silver particles from the respiratory tract).

3 A study in rats showed that nanoscale (15-nm diameter) silver was more toxic than  
4 microscale (410-nm diameter) silver following subacute inhalation exposure (4 days, 6  
5 hours/day) to similar airborne particle concentrations (179 or 167 mg/m<sup>3</sup>, respectively);  
6 that is, pulmonary inflammation was observed in rats exposed to the nanoscale silver  
7 but not to microscale silver [Braakhuis et al. 2014]. The two different particle sizes were  
8 generated by different methods: the small NPs were made with a Palas spark  
9 generator, and the larger particles were purchased as PVP-coated NPs and generated  
10 by nebulization. The inflammation in the rats exposed to the 15-nm-diameter AgNPs  
11 resolved by 7 days post-exposure. The 15-nm particles were shown to have a higher  
12 alveolar (pulmonary) deposition fraction than the 410-nm particles, resulting in a 3.5  
13 times higher deposited mass dose (and 66,000 higher particle number dose). The 15-  
14 nm particles were observed in the rat lungs to have been reduced in size to <5 nm  
15 within 24 hours, suggesting relatively rapid dissolution in vivo of the nanoscale silver.

16 Acute inhalation studies in rodents suggest that soluble forms of silver are more  
17 biologically active and inflammogenic than poorly-soluble silver particles [Braakhuis et  
18 al. 2014; Roberts et al. 2013]. Decreased particle size has been associated with and  
19 increased rate of dissolution [Braakhuis et al. 2014], suggesting that the greater toxicity  
20 of nanoscale to microscale silver is due in part to the increased generation of ionic  
21 silver. Some in vitro studies found that soluble silver was more bioactive than AgNPs  
22 (including reduction in mitochondrial function and decreased cell viability) [Foldbjerg et  
23 al. 2011; van der Zande et al. 2012]. However, at least one in vitro study showed that  
24 AgNP was more damaging to cells than was silver in solution [Piao et al. 2011]. The  
25 mechanism of AgNP activity may be different from that of soluble silver.

26 The size and composition of silver to which workers may be exposed can vary,  
27 depending on the product being manufactured, production method, and job/task within  
28 the facility. Workers can be exposed to a mixture of silver particle sizes (nanoscale or

1 larger respirable or inhalable sizes) [Lee et al. 2011b]. In addition, workers can  
2 potentially be exposed to silver compounds (such as silver nitrate and silver acetate),  
3 which can exhibit different biologic availability and activity depending on the associated  
4 moieties. Potential worker exposure can occur during the use of silver in various  
5 applications and depends on the form of the silver or silver compound (such as dry  
6 powder or colloidal silver) [Drake et al. 2005]. In the case of colloidal silver compounds  
7 (such as used for disinfectant sprays), the ionic silver component can vary with the age  
8 of the product [Liu and Hurt 2010].

9 Studies in workers have shown that soluble forms of silver have been more frequently  
10 associated with the development of argyria than poorly soluble forms [as reviewed in  
11 ATSDR 1990; Drake and Hazelwood 2005; Wijnhoven et al. 2009] (Chapters 2 and 3). If  
12 the inflammation response is related to the release rate of ions during dissolution of the  
13 AgNP, then the soluble/active portion of the dose estimates from the PBPK model  
14 [Bachler et al. 2013] may be more closely associated with the inflammation responses  
15 in the lungs, including with repeated exposures (up to a 45-year working lifetime).

16 A primary goal of occupational health risk assessment is to evaluate exposure-related  
17 adverse effects in experimental animals that are relevant to humans and to estimate  
18 exposure levels that would not likely result in adverse health effects in workers, even if  
19 exposed for up to a 45-year working lifetime. Understanding the physico-chemical  
20 properties that influence their uptake and bioactivity is important to assessing the health  
21 risk of exposure to airborne particles. The inhalable and respirable mass fractions that  
22 deposit in the respiratory tract can be estimated with relatively low uncertainty, based on  
23 aerosol measurement data and deposition models (e.g., MPPD [ARA 2011]). In  
24 contrast, the fate of AgNPs after deposition in the respiratory tract is an area of higher  
25 uncertainty, which pertains to the potential adverse effects of exposure to silver dust or  
26 fumes (including nanoparticles), especially with chronic exposure.

27 Animal studies have measured silver in various organs in the body, including lungs,  
28 liver, kidneys, and brain. The adverse effects observed in rats following subchronic

1 inhalation exposures to AgNPs include persistent pulmonary inflammation and reduced  
2 lung function as well as biliary hyperplasia [Sung et al. 2008, 2009; Song et al. 2013],  
3 suggesting that effects occur at both the site of entry and systemically. The extent to  
4 which these effects were due to the AgNPs and/or ions cannot be determined from  
5 these studies.

## 6 **6.2 Quantitative Risk Assessment for Silver Nanoparticles**

### 7 **6.2.1 Animal studies**

8 The published rat subchronic inhalation data [Sung et al. 2008, 2009; Song et al. 2013]  
9 were used in this NIOSH risk assessment, as in other risk assessments for silver  
10 nanoparticles [Christensen et al. 2010; Weldon et al. 2016]. Lung and liver effects in  
11 male and female rats were observed to be associated with exposure concentration or  
12 tissue dose of silver nanoparticles (Section 6.1). These subchronic studies were  
13 conducted according to current OECD and GLP guidelines [OECD 1995; Sung et al.  
14 2009], and a standard subchronic inhalation exposure protocol was followed. Male and  
15 female rats were exposed by whole body inhalation to one of three exposure  
16 concentrations in each study, ranging from 49 to 515  $\mu\text{g}/\text{m}^3$  of airborne silver  
17 nanoparticles (18-20 nm diameter generated by a ceramic heater) or to air only  
18 (controls). The silver tissue doses were measured in the lungs, liver, and other organs.  
19 Exposure durations were 6 hr/d for 13 weeks in Sung et al. [2008, 2009]; and 6 hr/d for  
20 12 weeks in Song et al. [2013] following by 12 weeks of recovery.

21 The airborne exposure concentrations in these rat studies (49 to 515  $\mu\text{g}/\text{m}^3$ ) spans the  
22 concentration of 100  $\mu\text{g}/\text{m}^3$ , which is an OEL for inhalable silver (Table 1-2). These  
23 exposure concentrations are considerably below those associated with the highest  
24 recommended exposure concentration of 100,000  $\mu\text{g}/\text{m}^3$  (100  $\text{mg}/\text{m}^3$ ) in an experimental  
25 animal study according to standard toxicology methods for inhaled particles [Lewis et al.  
26 1989]. An exposure concentration of 100  $\text{mg}/\text{m}^3$  could also be considered the MTD  
27 (i.e., maximum tolerated dose [Oberdörster 1995, 1997] or minimally toxic dose [Bucher  
28 et al. 1996]) since the MTD is recommended as the highest exposure concentration to

1 be used in an experimental study [Bucher et al. 1996; Oberdörster 1997]. No evidence  
2 of toxicity that interferes with the study interpretation should be observed at the MTD  
3 [Bucher et al. 1996]. It is also recognized that the MTD would be lower for more toxic  
4 particles [Oberdörster 1997].

5 Following subchronic inhalation exposure to AgNPs, the clearance rates of silver from  
6 the rat lungs [Song et al. 2013] were generally within the normal range of 60-90 days for  
7 pulmonary clearance of poorly-soluble low toxicity particles in rats [Pauluhn 2014];  
8 these findings suggest that overloading of particle clearance had not occurred.  
9 However, for AgNPs, it is expected that the clearance rates may be faster than those for  
10 poorly-soluble particles given that dissolution as well as macrophage-mediated  
11 clearance would be expected to occur. The rat pulmonary clearance half-times ranged  
12 from 28 to 43 days at the lowest ( $49 \mu\text{g}/\text{m}^3$ ) and the highest ( $381 \mu\text{g}/\text{m}^3$ ) exposure  
13 concentrations of AgNPs. Higher clearance half times of 85 and  $113 \text{ d}^{-1}$  were reported  
14 at the medium ( $117 \mu\text{g}/\text{m}^3$ ) exposure concentration in male and female rats,  
15 respectively (Tables F-1 and F-2); however, these findings are not consistent with dose-  
16 dependent overloading of clearance and may instead reflect experimental measurement  
17 variability. The pulmonary inflammation that was observed in rats at the end of the 12-  
18 week inhalation exposure to AgNPs (medium and high dose groups) had resolved by  
19 the end of the 12-week recovery period in all but one rat (male, high dose group) [Song  
20 et al. 2013]; this finding is another indication that the inhalation MTD had not been  
21 exceeded [Oberdörster 1995], In addition, no dose-dependent changes in body weights  
22 or organ weights or “toxicity signs” were observed in these rat studies [Sung et al. 2009;  
23 Song et al. 2013]. No mortality was reported during or after exposure in Song et al.  
24 [2013], One rat died during an ophthalmological examination in Sung et al. [2009].  
25 Overall, these results suggest that pulmonary clearance was not overloaded and that  
26 the exposures did not exceed the MTD in these rat subchronic inhalation studies.

27 Subchronic studies in rodents are typically used in quantitative risk assessment (QRA)  
28 and OEL derivation in the absence of adequate data from humans or chronic studies in  
29 animals. Accordingly, NIOSH considers these studies to be of sufficient quality for

1 evaluation of the potential occupational health risks of inhaling silver nanoparticles. An  
2 updated literature search since that in the external review CIB [NIOSH 2016a] yielded  
3 no additional subchronic inhalation studies of nanoscale or microscale silver in the  
4 scientific literature.

### 5 6.2.2 Basis for conducting a quantitative risk assessment

6 Although there is a limited amount of information to assess the potential adverse health  
7 effects of occupational exposure to AgNPs, the following evidence provides the  
8 rationale for conducting a QRA and developing a REL. First, the effects in the lungs  
9 and liver of rats are significantly associated with airborne exposure to silver  
10 nanoparticles and to the retained target-tissue dose of silver. These effects which  
11 include early-stage pulmonary inflammation and bile duct hyperplasia (accompanied by  
12 liver necrosis at higher concentrations) are considered to be adverse and potentially  
13 clinically significant in humans. That is, if workers were exposed to equivalent airborne  
14 concentrations of silver over a period of time, it is assumed that they could also develop  
15 these effects. Second, silver is a high volume nanomaterial with an increasing number  
16 of workers potentially exposed. Under the existing REL for silver (total dust) of 10  
17  $\mu\text{g}/\text{m}^3$  (8-hr TWA concentration), workers would be at higher risk of developing these  
18 early-stage adverse lung and liver effects. For these reasons, NIOSH has concluded  
19 that there is a reasonable scientific basis for assessing the risk of adverse health effects  
20 in workers using the rat subchronic inhalation data and developing a REL for AgNPs.

### 21 6.2.3 Point of departure from animal data ( $\text{PoD}_{\text{animal}}$ )

22 A point of departure in the animal studies ( $\text{PoD}_{\text{animal}}$ ) is an estimate of the exposure or  
23 dose associated with a level of no or low effect, typically an adverse health effect to be  
24 prevented in humans. The  $\text{PoD}_{\text{animal}}$  in this risk assessment was estimated from the rat  
25 data on airborne exposure concentration and the rat lung or liver response data are  
26 modeled using the benchmark dose software (BMDS) [U.S. EPA 2012b]. The  $\text{PoD}_{\text{animal}}$   
27 in these analyses is the  $\text{BMCL}_{10}$ , which is the benchmark concentration, 95% lower  
28 confidence limit estimate, of the exposure concentration associated with an added 10%

1 response compared to the control (unexposed) rats. The dose associated with a small  
2 increase in response (e.g., 10% added to background) has long-standing use as a  
3 benchmark response [Crump 1984]. The exposure-response data and BMDS modeling  
4 results for liver or lung effects are shown in Figures 6-2 and 6-3, respectively.

5 The BMCL<sub>10</sub> estimates for liver bile duct hyperplasia were 50.5 and 92.5 µg/m<sup>3</sup> in  
6 female and male rats, respectively (Table B-5). These estimates are lower than the  
7 NOAEL of 133 µg/m<sup>3</sup> for the liver bile duct hyperplasia response in male and female  
8 rats in Sung et al. [2009] but higher than the estimate by Weldon et al. [2016] of 25.5  
9 µg/m<sup>3</sup> in female rats (based on a linear model of the relationship between the liver  
10 tissue dose and the airborne silver concentration). The BMCL<sub>10</sub> estimates for all liver  
11 abnormalities were lower than those for liver bile duct hyperplasia in both this analysis  
12 (Table B-12) and that of Weldon et al. [2016]; however, bile duct hyperplasia was  
13 selected as the liver endpoint for use in risk assessment in both analyses, since it is a  
14 specific, quantifiable endpoint in rats that is considered relevant to humans. The lower  
15 BMCL<sub>10</sub> estimate in female rats was selected as the PoD<sub>animal</sub> for bile duct hyperplasia.

16 The BMCL<sub>10</sub> estimate for pulmonary inflammation (minimum or higher severity) was  
17 62.8 µg/m<sup>3</sup>, based on the pooled male and female rat data from both subchronic  
18 inhalation studies [Sung et al. 2009; Song et al. 2013] (Table B-11). This endpoint was  
19 not used in the risk assessments of Christensen et al. [2010] or Weldon et al. [2016].

#### 20 6.2.4 Human-equivalent concentration estimates

21 Three methods have been used to estimate human-equivalent concentrations (HECs)  
22 from the rat subchronic inhalation effect levels: the uncertainty factor method; the  
23 dosimetric adjustment factor (DAF) method; and PBPK modeling (Appendix A). HECs  
24 have been estimated with each of these methods. Details of these analyses can be  
25 found in Appendixes A and B.

*This information is distributed solely for the purpose of pre-dissemination peer review under applicable information quality guidelines. It has not been formally disseminated by the National Institute for Occupational Safety and Health. It does not represent and should not be construed to represent any agency determination or policy.*

1 NIOSH evaluated all of these methods and determined that the best approach on which  
2 to base the REL is the DAF method. The analysis is described in Section 6.4 here. The  
3 DAF method has been used for many years in the risk assessment of inhaled particles  
4 [U.S. EPA 1994]. In applying this method, NIOSH shows where scientific data are  
5 available to derive the individual DAFs; and when data are not available, uncertainty  
6 factors (UFs) are used.

#### 7 **6.2.4.1 Dosimetric Adjustment Factor (DAF) method**

8 A DAF method applied to inhaled particles takes into account the factors that influence  
9 the internal dose in each species in order to extrapolate a dose estimate from animals  
10 to humans [ICRP 1994]. A benchmark dose is the preferred dose estimate when  
11 sufficient dose-response data are available; otherwise, a no observed adverse effect  
12 level (NOAEL) is used [U.S. EPA 2012b]. The basis for the DAF method has been  
13 described in U.S. EPA [1994] and Jarabek et al. [2005]. NIOSH and others used a DAF  
14 method in deriving OEL estimates for carbon nanotubes [NIOSH 2013a]. A recent  
15 application of these methods on silver nanoparticles has been reported by Weldon et al.  
16 [2016] (discussed further in Appendix G.2).

17 For inhaled particles, the key factors that influence the estimated particle dose in  
18 animals and humans include the following:

- 19 (a) Ventilation rates
- 20 (b) Deposition fraction of inhaled particles
- 21 (c) Exposure, clearance, and retention kinetics
- 22 (d) Interspecies dose normalization

23 Deposition fraction by respiratory tract region is based on the airborne particle size, the  
24 breathing pattern (nasal and/or oral), and the lung airway geometry. The respiratory  
25 tract region(s) of interest are where the adverse effects are observed in animal and/or  
26 human studies and represented in the dose-response data being analyzed.

1 Ventilation rate is the inhaled air volume per unit of time and depends on the basal  
2 metabolic rate in each species as well as breathing rate associated with activity level.  
3 The air intake per 8-hour workday (light exercise) [ICRP 1994] or the rat exposure (6-  
4 hour) day is used in this analysis.

5 Exposure duration and clearance kinetics determine the total deposited particle dose  
6 and the retained dose over time. Clearance or retention of inhaled particles depends on  
7 the biological clearance mechanisms in the respiratory tract region (e.g., alveolar  
8 macrophage-mediated clearance of particles in the pulmonary region; mucociliary  
9 clearance from the tracheobronchial region; expectoration or swallowing of particles in  
10 nasopharyngeal region). Clearance can also be influenced by dissolution, as evidence  
11 suggests for silver nanoparticles [Song et al. 2013; Braakhuis et al. 2014]. Dissolution  
12 depends on chemical composition, particle size, and the biological medium. To the  
13 extent that the dissolution and transfer rates of soluble particles into blood depend  
14 primarily on the physicochemical properties of the material, the biokinetics of soluble  
15 particles may be similar across species [Dahl et al. 1991].

16 Normalization of the delivered dose adjusts for the differences across species that  
17 determine the effective dose (e.g., particle mass dose per unit of tissue surface area).  
18 The dose normalization, and thus the effective dose metric, depends on the biological  
19 mode of action.

20 Estimates for each of these factors are included in the total DAF to the extent that data  
21 are available. The data values used for these individual DAFs in the NIOSH risk  
22 assessment are described in Section 6.2.3.1.

23 The human-equivalent concentration PoD (HEC\_PoD) is estimated by adjusting the  
24 animal PoD by the DAF as follows:

25 
$$\text{HEC\_PoD} = \text{PoD}_{\text{animal}} / \text{DAF} \text{ [Equation 6-1]}$$

*This information is distributed solely for the purpose of pre-dissemination peer review under applicable information quality guidelines. It has not been formally disseminated by the National Institute for Occupational Safety and Health. It does not represent and should not be construed to represent any agency determination or policy.*

1                    where  $PoD_{\text{animal}}$  is the animal effect level selected for the PoD; and DAF is  
2                    the dosimetric adjustment factor estimated, as shown below:

3                     $DAF = (VE_H/VE_A) \times (DF_H/DF_A) \times (RT_H/RT_A) \times (NF_A/NF_H)$  [Equation 6-2]

4                    where VE is the ventilation rate (e.g., as total volume of air inhaled per  
5                    exposure day,  $m^3/d$ ) in humans (H) or animals (A); DF is the deposition  
6                    fraction in the target respiratory tract region; RT is retention half-time of  
7                    particles in the lungs, and NF is the interspecies dose normalization factor  
8                    (e.g., by mass, surface area, or volume of target tissue).

9                    The version of the DAF shown in Equation 6-2 is from NIOSH [2013, in Section A.6.3.1  
10                    of that document], and it is similar to other versions reported in EPA [1994], Jarabek et  
11                    al. [2005], and Pauluhn [2010b]. The DAF version in Equation 6-2 was also used by  
12                    Weldon et al. [2016] for silver nanoparticles (discussed in Section G.2).

13                    An advantage of using a DAF method to estimate the HEC\_PoD is that it is a clear,  
14                    evidence-based method that can be systematically applied and evaluated for the  
15                    influence of alternative estimates. A disadvantage of this method is that it is not a  
16                    comprehensive, biologically based model and assumes linear (proportional)  
17                    relationships in the animal and human parameters that influence the inhaled dose.  
18                    Factors that are not accounted for in the DAF method are typically addressed with UFs  
19                    (Section 6.2.3.2). An example of the DAF and UF methods used by Weldon et al. [2013]  
20                    and Christensen et al. [2010] to derive an OEL for silver nanoparticles is provided in  
21                    Sections G.1 and G.2.

#### 22                    **6.2.4.2 Selection of DAF values**

23                    The individual parameter values to estimate the total DAF (Equation 6-2) are shown in  
24                    Tables 6-3 and 6-4. Table 6-3 shows the factors applied to the exposure concentration  
25                    associated with liver bile duct hyperplasia in female rats, and Table 6-4 shows the  
26                    factors applied to the exposure concentration associated with pulmonary inflammation  
27                    in male and female rats.

1 **DAF 1 - Ventilation rates:** Measured ventilation rates in humans are available, and  
2 thus the values used by NIOSH are nearly identical to those used by Weldon et al.  
3 [2016] (Equation G-1). However, DAF 1 values used for rats differ by a factor of two.  
4 The specific calculations and parameter values to estimate the rat DAF in this analysis  
5 are provided in Section F.2, and the basis for the values used by Weldon et al. [2016]  
6 are provided in that paper (and summarized in Section G.2). The NIOSH and Weldon et  
7 al. [2016] assessments accounted for the differences in exposure duration by  
8 considering the total volume of air inhaled in one day in workers or in rats. Christensen  
9 et al. [2010] adjusted the rat NOAEL for human ventilation rate for light work vs. resting  
10 (10 vs. 6.7 m<sup>3</sup>/d) (Section G.1).

11 **DAF 2 - Deposition fraction of inhaled particles:** Particle deposition fractions in this  
12 analysis were based on the total respiratory tract dose in humans and rats because  
13 NIOSH considered the total internal deposited dose of silver to be a relevant dose  
14 metric for the endpoint of liver bile duct hyperplasia. In Weldon et al. [2016], only the  
15 pulmonary deposition fraction was considered. In both cases, it is assumed that 100%  
16 of the deposited dose is available for uptake into the systemic circulation and transfer to  
17 the liver. Neither of these approaches would account for the unknown oral dose that the  
18 rats may have received from grooming and ingesting silver nanoparticles that deposited  
19 on the fur during the whole-body inhalation exposure.

20 The DAF 2 value in rats also differs from that used in Weldon et al. [2016] (Equation G-  
21 1) because the MPPD v. 3.04 model for Sprague-Dawley rats [ARA 2015; Miller et al.  
22 2014] was used in this analysis, rather than the Long-Evans rat model used in Weldon  
23 et al. [2016]. The Long-Evans rat model was the only rat model available in the earlier  
24 version of MPPD (v. 2.11). The total respiratory tract deposition fraction of 0.95 for 18  
25 nm silver nanoparticles in the Sprague-Dawley rat model (Table 6-3) is greater than the  
26 0.62 total respiratory tract deposition fraction in the Long-Evans rat model (MPPD v.  
27 3.04, default values for 300-g rat), apparently because of the greater deposition  
28 efficiency of the nanoparticles in the nasal-pharyngeal (head) region in the Sprague-  
29 Dawley rat. As a result, the estimated deposition fraction of particles in the pulmonary

1 region is substantially lower in Sprague-Dawley rats (0.064) than in Long-Evans rats  
2 (0.28; or 0.29 reported in Weldon et al. [2016]). Christensen et al. [2010] did not adjust  
3 for differences in particle deposition in the respiratory tract in rats and humans.

4 **DAF 3 - Exposure, clearance, and retention kinetics:** The data included in this factor  
5 varied across analyses. Christensen et al. [2010] adjusted for the rat vs. human  
6 exposure time (6 vs. 8 hour). Weldon et al. [2016] assumed a relationship based on  
7 first-order clearance of poorly soluble particles [Snipes 1989] that was used by Pauluhn  
8 [2010b] for carbon nanotubes, i.e., a human/rat ratio of 10. However, other information  
9 suggests that particle dissolution kinetics across species may be similar since the rates  
10 of dissolution and transfer of soluble particles into blood may depend primarily on the  
11 physicochemical properties of the material [Dahl et al. 1991]. To the extent that the  
12 retention kinetics depend on dissolution of the silver nanoparticles, the retention rates  
13 may be similar across species. However, the dissolution rates can also depend on  
14 particle size [Braakhuis et al. 2014].

15 In the NIOSH assessment, the uncertainty of the long-term clearance and retention of  
16 silver nanoparticles is addressed in the selection of UFs (Section 6.2.3.3) because of  
17 the lack of specific information for DAF3. This approach is consistent with the DAF  
18 approach reported in Jarabek et al. [2005], who suggest adjusting the HEC by a  
19 subchronic-to-chronic UF when the  $PoD_{animal}$  is based on subchronic rather than chronic  
20 data. The need to account for uncertainty in a possible chronic effect level based on the  
21 subchronic data is supported by an evaluation of the lung clearance kinetics data  
22 reported in Song et al. [2013] and estimation that a steady-state tissue concentration of  
23 silver was not reached by the end of the 12-wk exposure (Section F.1).

24 DAF 3 values are the major difference in the total DAF in the NIOSH analyses, in  
25 comparison with those of Weldon et al. [2013]. The limited information on DAF 3 is a  
26 large source of uncertainty in this assessment.

*This information is distributed solely for the purpose of pre-dissemination peer review under applicable information quality guidelines. It has not been formally disseminated by the National Institute for Occupational Safety and Health. It does not represent and should not be construed to represent any agency determination or policy.*

1 **DAF 4 - Interspecies dose normalization:** Interspecies dose normalization was based  
2 on the pulmonary (alveolar) surface area in the Weldon et al. [2016] analysis, although  
3 the critical effect used was the rat liver bile duct hyperplasia response. NIOSH also  
4 used the rat liver bile duct hyperplasia response as a critical effect but used either the  
5 total respiratory tract surface area or the body weight (Table 6-4; Table 6-5) to  
6 normalize the dose of silver nanoparticles across species.

7 For the rat pulmonary inflammation response, NIOSH used pulmonary surface area to  
8 normalize the rat dose to humans (Table 6-4). The rationale for interspecies dose  
9 normalization based on respiratory tract surface area is that silver nanoparticles  
10 depositing on the cell surfaces of the respiratory tract would represent either (1) the  
11 target tissue for stimulating pulmonary inflammation (alveolar epithelial cell surface  
12 area) or (2) the cell surface in the total respiratory tract, across which silver  
13 nanoparticles could be translocated to the blood circulation or cleared via the  
14 mucociliary clearance and swallowed. For adverse effects beyond the lungs, such as in  
15 the liver, body weight is often used to extrapolate the rodent effect levels to humans,  
16 especially for oral routes of exposure.

17 The human-to-rat ratio of either the total respiratory tract surface areas or the  
18 pulmonary region surface areas are similar within a given source (e.g., ~260 for either  
19 total or alveolar surface area ratios from Miller et al. [2010] or ~160 from U.S. EPA  
20 [1994]) (Table 6-5). The human-to-rat ratios based on the values reported in Stone et al.  
21 [1992] are also similar to those reported in Miller et al. [2010]. The differences in the  
22 reported values may relate to the degree of inflation of the lungs during the  
23 measurements. The human-to-rat ratio of body weights is also similar to the ratios  
24 based on total respiratory tract or pulmonary region surface area reported in Miller et al.  
25 [2010] or Stone et al. [1992]. Thus, the interspecies dose normalization factors (DAF 4)  
26 used in Weldon et al. [2016] (Equation G-1) and the current analysis (Tables 6-3 and 6-  
27 4) are all similar (i.e., a factor of approximately 260), regardless of whether body weight,  
28 total respiratory tract surface area, or pulmonary region surface area is used. [Note that

1 the interspecies dose normalization ratio is inverted (i.e., A/H vs. H/A) in the DAF, as  
2 described in this document (Equations 6-1, 6-2, and G-1)].

3 Alternative normalization metrics such as the total alveolar macrophage cell volume in  
4 humans or rats related to a pulmonary overload mechanism (e.g., as used by Pauluhn  
5 [2010b]) could result in a different ratio (e.g., differing by a factor of ~4.5 compared to  
6 pulmonary surface area [NIOSH 2013a]); however, the overload mechanism for poorly  
7 soluble particles has not been reported for silver nanoparticles. As shown in Song et al.  
8 [2013], the lung burdens declined at the end of exposure, consistent with normal first-  
9 order clearance; at 12-weeks post-exposure, the lung burdens in rats exposed at 49 or  
10 117  $\mu\text{g}/\text{m}^3$  were no longer significantly elevated (although the lung burden was still  
11 significantly elevated in rats exposed at 515  $\mu\text{g}/\text{m}^3$ ).

12 **Total DAF:** The HEC is estimated by dividing the  $\text{PoD}_{\text{animal}}$  by the total DAF (Equation  
13 6-1). The data-based HEC estimate is further divided by UFs to account for  
14 uncertainties in the data used to estimate the HEC (Section 6.3). A health-based default  
15 is proposed for the DAF to be no less than 1 (i.e., assuming HEC is not greater than the  
16  $\text{PoD}_{\text{animal}}$ ). This default is used for the liver bile duct hyperplasia response (shown in  
17 Table 6.3).

#### 18 **6.2.4.3 Uncertainty Factor method and selection**

19 UFs are used in the derivation of OELs from animal bioassay data to account for the  
20 uncertainty and variability in the scientific data available to extrapolate the animal dose  
21 to the human population (e.g., workers) [Dankovic et al. 2015]. When sufficient  
22 information is available, the HECs are first estimated by DAF adjustment of the  
23  $\text{PoD}_{\text{animal}}$ , and the UFs are applied to the HEC estimate to derive the OEL. This  
24 approach was used in the NIOSH risk assessment for silver nanoparticles (Sections  
25 6.2.3.1 and 6.2.3.2).

26 The values of UFs typically used in occupational health risk assessment are shown in  
27 Table 6-6. These UFs include the following factors: (1)  $\text{UF}_A$  to account for possible

*This information is distributed solely for the purpose of pre-dissemination peer review under applicable information quality guidelines. It has not been formally disseminated by the National Institute for Occupational Safety and Health. It does not represent and should not be construed to represent any agency determination or policy.*

1 interspecies differences in the toxicokinetics (influencing the internal dose) or  
2 toxicodynamics (influencing the biological response) in extrapolating the  $PoD_{\text{animal}}$  to the  
3 average human; (2)  $UF_H$  to account for human inter-individual variability; (3)  $UF_L$  to  
4 adjust for the use of a higher effect level than the NOAEL or  $BMDL_{10}$ ; (4)  $UF_s$  to account  
5 for the possibility that the critical effect that is the basis for the  $PoD_{\text{animal}}$  could develop at  
6 a lower dose or the incidence or severity of the effect could increase, with a longer  
7 exposure duration; and (5)  $UF_D$  to account for insufficient data or a severe endpoint.  
8 None of the available risk assessments on silver nanoparticles (as discussed in this  
9 section) included a value for  $UF_D$ ; therefore, the focus in this section is on the other four  
10 UFs. Because exposure-related effects were observed in two rat subchronic inhalation  
11 models, an  $UF_D$  was not considered to be needed.

12 Table 6-7 summarizes the scientific evidence related to each of the UFs for the silver  
13 nanoparticles data, as well as values deemed to be appropriate to apply to the HEC.  
14 NIOSH considered the available evidence to be insufficient to use in accounting for  
15 possible interspecies differences in the long-term retention kinetics of silver  
16 nanoparticles in estimating the HEC (Section 6.2.3.2). An  $UF_s$  of  $\sqrt{10}$  (3.16) was used to  
17 account for uncertainty in rat subchronic  $PoD$  and in whether a lower  $PoD$  or a more  
18 severe effect may be observed at the same airborne concentration over a longer  
19 exposure duration. That  $UF_s$  was based on the average findings from studies that  
20 examined the subchronic and chronic exposure-response data [Naumann and  
21 Weideman 1995; Kalberlah et al. 2002]. The need to adjust for uncertainty in the  
22 subchronic to chronic HEC based on the rat subchronic inhalation studies is evidenced  
23 in the finding that the rat lung tissue doses of silver had not yet reached steady-state (as  
24 estimated in Section F.1), suggesting that higher lung burdens (and hence higher  
25 response) could be observed with longer exposure.

### 26 **6.3 Derivation of NIOSH REL for Silver Nanomaterials**

27 A health-based REL is estimated by dividing the lowest HEC by a total UF (Equation 6-  
28 1) (Table 6-8). The HEC is a human-equivalent estimate of the rat effect level, based on

1 the pooled exposure-response data on pulmonary inflammation in male and female rats  
2 at the end of subchronic (12- or 13-wk) inhalation exposure to silver nanoparticles [Sung  
3 et al. 2009; Song et al. 2013]. The rat effect level estimate (BMCL<sub>10</sub>) is the benchmark  
4 exposure concentration, 95<sup>th</sup> percentile lower confidence limit estimate, of silver  
5 nanoparticles associated with an added 10% of rats developing pulmonary inflammation  
6 of minimal or higher severity, based on histopathological examination. The HEC  
7 estimate to the rat BMCL<sub>10</sub> of 23 µg/m<sup>3</sup> was derived from available data for dosimetric  
8 adjustment (Section 6.3).

9 The UFs used in occupational risk assessment (Table 6-6) were evaluated for  
10 application to the HEC estimates from the rat subchronic inhalation data. A total UF of  
11 25 is suggested for the HEC (Table 6-7). That is, HEC\_PoD / total UF = REL, or 23  
12 µg/m<sup>3</sup> / 25 = 0.9 µg/m<sup>3</sup>. Thus, the NIOSH recommended exposure limit (REL) for silver  
13 nanomaterials (≤100 nm primary particle size) is 0.9 µg/m<sup>3</sup>, as an airborne respirable 8-  
14 hour time-weighted average (TWA) concentration.

15 The NIOSH REL for silver nanomaterials is set to protect workers from developing  
16 pulmonary inflammation due to airborne exposure to silver nanoparticles (15–20 nm in  
17 diameter), and is established from rat subchronic inhalation data. In addition, the REL  
18 should protect workers from developing liver bile duct hyperplasia, since the lower HEC  
19 estimate was used to derive the REL (Table 6-8). Similarly, the NIOSH REL for silver  
20 nanomaterials should protect workers from developing argyria, since much higher  
21 exposure concentrations (47–253 µg/m<sup>3</sup>) over a 45-year working lifetime were  
22 estimated from the Bachler et al. [2013] PBPK model to be equivalent by mass to the  
23 human skin tissue doses associated with argyria (Table A-10). The REL for silver  
24 nanomaterials based on rat data of subchronic inhalation exposure to 15- to 20-nm-  
25 diameter silver nanomaterials should also protect workers exposed to larger silver  
26 nanomaterials (up to 100-nm diameter), since the toxicological evidence suggests that  
27 the smaller nanoparticles are more toxic (Chapters 4 and 5).

*This information is distributed solely for the purpose of pre-dissemination peer review under applicable information quality guidelines. It has not been formally disseminated by the National Institute for Occupational Safety and Health. It does not represent and should not be construed to represent any agency determination or policy.*

1 NIOSH recommends that effective risk management control practices be implemented  
2 so that worker exposures to silver nanomaterials do not exceed the NIOSH REL of 0.9  
3  $\mu\text{g}/\text{m}^3$  (8-hour TWA), measured as a respirable airborne mass concentration. As new  
4 data become available, NIOSH may reevaluate these recommendations to determine  
5 whether additional recommendations are needed to protect workers' health.

## 6 **6.4 Risk Characterization**

7 This risk characterization section includes an evaluation of the overall evidence and a  
8 discussion of uncertainties in the available data. The main areas of uncertainty include  
9 relatively limited available animal data (for one type of silver nanoparticles) and  
10 extrapolation of the rat subchronic early effect levels to workers with long-term  
11 exposures. These and related areas of uncertainty are discussed further below.

### 12 **6.4.1 Relevance of animal responses to humans**

13 Qualitatively, the lung and liver effects appear to be relevant to humans (Section 6.2).  
14 The pulmonary inflammation and liver bile duct hyperplasia responses were early stage  
15 and included minimal or more severe lesions [Sung et al. 2008, 2009; Song et al. 2013].  
16 As noted in Sections 1.2 and 6.1.2, hyperplasia is believed to be one of several factors  
17 involved in the development of cholangiocarcinoma, the biliary tract cancer of the liver  
18 [Rizvie and Gores 2014; Rizvi et al. 2014]. Minimal biliary hyperplasia as an isolated  
19 finding in rats is sometimes considered non-adverse and can occur in aged rats [Hailey  
20 et al. 2013; Eustis et al. 1990]. However, the rats in the subchronic study were not aged,  
21 and biliary hyperplasia was sometimes accompanied by evidence of hepatocellular  
22 injury, including necrosis [Sung et al. 2009]. The concomitant presence of both  
23 hepatocellular injury and biliary hyperplasia in rats is more frequently a concern than  
24 biliary hyperplasia alone [Hailey et al. 2013]. Thus, as noted in Section 6.1.2, biliary  
25 hyperplasia is considered to be potentially adverse. The lowest effect level estimates  
26 (as airborne concentration or tissue dose) associated with those responses were used  
27 to estimate human equivalent tissue doses and airborne concentration (as 8-hour TWA  
28 for up to a 45-year working lifetime).

1 Areas of uncertainty include the extrapolation of these subchronic effects in rats to  
2 workers who may be exposed for up to a 45-year working lifetime. One study  
3 investigated the biopersistence of the lung effects in rats and the retention of silver in  
4 tissues [Song et al. 2013]. The lung inflammatory effects had generally resolved 12  
5 weeks after the end of the 12-week inhalation exposure to 14-nm-diameter silver  
6 nanoparticles. Clearance of silver from the lung and other tissues was observed, and  
7 the lung tissue doses of silver were no longer significantly elevated at the 49- and 117-  
8  $\mu\text{g}/\text{m}^3$  exposure concentrations. These findings suggest silver was cleared by normal  
9 clearance processes and that overloading of lung clearance had not occurred at the  
10 animal doses used in the risk assessment (i.e., NOAEL or BMDL<sub>10</sub>). Pulmonary fibrosis  
11 was not reported as having been observed in rats exposed to silver nanoparticles [Sung  
12 et al. 2008, 2009; Song et al. 2013]. This finding is consistent with a biological mode of  
13 action of the silver ion release and/or the nanoparticles (prior to clearance) being related  
14 to the early lung effects, and with the observed recovery from those effects observed in  
15 the rats. However, the hematoxylin and eosin staining and examination by light  
16 microscopy conducted in these studies does not exclude the possibility that subtle  
17 fibrosis, if it occurred, may not have been visible. It is also relevant to consider that  
18 workers could potentially be exposed daily during a working lifetime and thus could  
19 potentially have a sustained pulmonary inflammation response to silver nanoparticles.  
20 Such sustained pulmonary inflammation is associated with the development of  
21 pulmonary interstitial fibrosis from some non-occupational as well as occupational  
22 causes [Cotton et al. 2017; Meyer 2017; Oberdörster et al. 1994].

23 A limitation in the available data is the absence of information on the persistence of the  
24 adverse effects observed in the liver, including liver bile duct hyperplasia and necrosis  
25 [Sung et al. 2009]. Another area of uncertainty is the potential for adverse effects in  
26 other organs, especially with chronic exposures.

## 1 6.4.2 Biologically active dose metric

2 The biologically active tissue dose causing the adverse lung and liver effects is not well  
3 understood. The most predictive dose metric could include the total particle mass  
4 (including silver that is biologically sequestered through binding with proteins and  
5 sulfhydryl groups) and/or the soluble/active silver particles (which are capable of  
6 releasing reactive ions). Only the PBPK model [Bachler et al. 2013] provides estimates  
7 of tissue doses (although Weldon et al. [2010] used a linear regression model to  
8 associate the airborne exposures and tissue concentrations). To date, no data are  
9 available to assess which of these dose metrics (total and/or soluble/active) is most  
10 closely associated with potential long-term effects in animals or humans. However,  
11 smaller particle size and ion release are associated with acute pulmonary effects  
12 [Roberts et al. 2013; Braakhuis et al. 2014]. Assumptions about the biologically active  
13 dose metric have a large influence on the estimates of the HECs in the PBPK modeling  
14 (Table A-9).

## 15 6.4.3 Human-equivalent tissue dose

16 Human data on silver tissue doses in the general population or in workers provide  
17 reference points from which to evaluate the findings from the rat studies (Sections  
18 A.5.2, A.5.4, and A.5.5). The finding that the rat effect levels (liver tissue doses of silver)  
19 associated with liver bile duct hyperplasia are similar to the “background” level of silver  
20 in liver tissue in the general human population [ICRP 1960] raises questions about the  
21 relevance of the finding to humans, since adverse liver effects have not been reported  
22 to be associated with silver exposure in workers or in the general population. A possible  
23 explanation is that the silver nanoparticles in the rat inhalation studies were more toxic  
24 than the silver to which the general population is exposed in the diet (by oral route of  
25 exposure) or the airborne silver to which workers were exposed. The worker studies  
26 revealed argyria and argyrosis associated with exposure to airborne silver particles (of  
27 various types and sizes) but did not reveal adverse liver effects in those workers  
28 (Section 3.3). Another possible explanation is that the earlier stage bile duct hyperplasia

1 (based on histopathology examination) reported to occur in the rat studies was not  
2 detected in the studies of workers in which less invasive tests were performed; the  
3 human studies were relatively small in terms of the number of workers examined and  
4 did not cover a full 45-year working lifetime. It is also possible that the rat liver doses  
5 included additional silver ingested from grooming fur with silver nanoparticles deposited  
6 during the whole-body inhalation. Analytical measurement error could have been  
7 another factor. If the silver tissue doses were underestimated because of analytical  
8 challenges (e.g., as reported in NIEHS studies, Society of Toxicology 2015 annual  
9 meeting), the actual silver tissue mass dose associated with the adverse effects might  
10 have been higher than measured (and thus, the human background tissue levels could  
11 be below the true rat effect level). However, no information is available to assess this  
12 question, and only the one rat subchronic inhalation study report [Sung et al. 2009] has  
13 noted liver effects. The persistence of those effects is unknown.

14 The lung tissue doses of silver (nanoparticles and/or ions) in the rat studies are higher  
15 than those reported to occur in lung tissues of smelter workers [Brune 1980]. No  
16 adverse pulmonary health effects have been associated with long-term occupational  
17 exposure to silver (Section 3.3). However, adverse acute lung effects were reported to  
18 occur in workers exposed to airborne concentrations of silver that were likely very high  
19 (although unmeasured), including silver nanoparticles emitted from heating silver  
20 [Forycki et al. 1983]. Qualitatively, the rat lung responses are considered relevant to  
21 workers, although the clinical significance of these early-stage effects is uncertain. The  
22 current evidence on the role of particle dissolution and ion release on the acute lung  
23 effects [Roberts et al. 2013; Braakhuis et al. 2014] suggests that the soluble/active  
24 particle dose may be the most biologically relevant dose metric for the pulmonary  
25 effects. Given that workers could be exposed daily over a working lifetime, the REL  
26 estimates based on the soluble/active dose metric (Table A-10) may be the most  
27 relevant estimates for prevention of lung inflammation. Much lower concentrations  
28 (0.19–0.83  $\mu\text{g}/\text{m}^3$ ) are estimated for the total silver dose metric. The biological mode of  
29 action and relevant dose metric for liver bile duct hyperplasia are also uncertain.

#### 1 6.4.4 Working lifetime equivalent concentration

2 The estimation of working lifetime equivalent concentration depends on the deposition  
3 fraction of silver nanoparticles in the respiratory tract and on the clearance or retention  
4 of silver after deposition. The deposited dose of silver nanoparticles in humans or rats  
5 can be estimated with low uncertainty because of the availability of respiratory tract  
6 deposition models, which have been validated in a number of studies for microscale  
7 particles (and less extensively for nanoscale particles). The deposition efficiency in the  
8 respiratory tract depends on the airborne particle size distribution (aerodynamic  
9 diameter for microscale particles and thermodynamic for nanoscale). However, the fate  
10 of inhaled silver nanoparticles after deposition is not well known. Some information on  
11 the biokinetics of silver uptake, retention, and clearance is available from earlier studies  
12 in workers [DiVincenzo et al. 1985]. The airborne particle size of silver in that study was  
13 not reported, although the smelting and refining processes described could have  
14 included exposure to nanoscale silver aerosols.

#### 15 6.4.5 Areas of uncertainty

16 Uncertainties in hazard and risk assessments based on the rat subchronic inhalation  
17 studies [Sung et al. 2011; Song et al. 2013] include the following:

- 18 • Clinical significance to humans of the early-stage lung and liver effects in the rat  
19 subchronic inhalation study.
- 20 • Quantification of the tissue doses associated with the adverse effects in rats, and  
21 extrapolation of those doses to humans for up to a working lifetime.
- 22 • Role of the soluble/active vs. total silver tissue burden on the dose-response  
23 relationships for lung or liver effects.
- 24 • Lack of chronic studies in rats and on the potential for other adverse effects (e.g.,  
25 neurotoxicity).

26

1 Information is lacking on whether the early-stage adverse lung and liver effects in the rat  
2 studies result in functional impairment. Inconsistent results were reported from the two  
3 studies within the same rat sex [Sung et al. 2008, 2009; Song et al. 2013]. For example,  
4 lung function deficits were measured in female rats at 49  $\mu\text{g}/\text{m}^3$  (LOAEL) [Sung et al.  
5 2008] but not at 381  $\mu\text{g}/\text{m}^3$  (NOAEL) [Song et al. 2013]. The variability in these and  
6 other lung responses results in uncertainty about the functional significance of the lung  
7 effects in rats or as extrapolated to humans. No data are available on whether bile duct  
8 hyperplasia would lead to a clinically adverse effect.

9 Data on the chemical composition and physical state of AgNPs are limited in the rat  
10 studies and in the human studies as well. Thus, there is uncertainty about the extent to  
11 which the total silver or the soluble silver portion contributed to the adverse lung and  
12 liver effects associated with inhalation exposure to silver nanoparticles in the rat studies.  
13 In addition, to the extent that differences in the physicochemical characteristics of the  
14 silver particles influence the kinetics and toxicity of silver, the findings from the two  
15 subchronic inhalation studies used to derive the REL [Sung et al. 2009; Song et al.  
16 2013] may differ from the findings of studies using other forms of silver. Despite the  
17 reported differences in the methods used to generate the silver nanoparticles and in the  
18 particle composition or coating, the general conclusions from the literature are that the  
19 small size and greater solubility of silver nanoparticles results in increased toxicity  
20 (Section 5.6).

21 Potential for adverse effects in organs other than the lungs and liver is unknown,  
22 especially with chronic exposure. For example, the potential for neurotoxic effects of  
23 inhalation of silver nanoparticles [Hubbs et al. 2011] is suggested from the exposure-  
24 related, statistically significant increase in silver in the brain tissue in one of the rat  
25 subchronic inhalation studies [Sung et al. 2009]. However, the lack of an exposure-  
26 related increase in the brain tissue dose in the other rat subchronic inhalation study  
27 [Song et al. 2013] raises uncertainty about the extent of translocation of silver to the  
28 brain following inhalation exposure to nanoparticles and/or the reliability of quantifying  
29 silver in tissue. In the latter study, the silver tissue concentration in the brain tissue of

1 unexposed (control) rats was four-fold higher (0.004 µg/g in females; not measured in  
2 males) than that in control rats in the Sung et al. [2009] study (0.001 µg/g in female or  
3 male rats). Those measurements were at the end of the inhalation exposure in both  
4 studies (week 12 or 13).

#### 5 6.4.6 Sensitivity analysis

6 Because of the limited available data for risk assessment of silver nanoparticles, a  
7 comprehensive sensitivity analysis was not feasible. However, the risk assessment  
8 included consideration of several alternative estimates. These include: (1) an array of  
9 estimates of the dose of silver associated with the adverse lung and liver effects  
10 observed in the rat studies (Section 6.2.3); and (2) alternative assumptions that were  
11 examined in the estimation of the human-equivalent dose (Section 6.2.4). In addition,  
12 several response endpoints were evaluated from the rat study for possible PoDs in  
13 estimating the human-equivalent concentrations (Section 6.1). A range of PoD  
14 estimates was evaluated, including NOAEL and LOAEL, as well as BMCL<sub>10</sub> or BMDL<sub>10</sub>  
15 estimates (based, respectively, on either airborne exposure concentrations or internal  
16 tissue doses of silver) (Table A-1). Alternative data and assumptions were evaluated in  
17 the application of the DAF and UF methods (Section 6.2.4). In the PBPK modeling  
18 method, alternative assumptions on particle size and solubility were considered in the  
19 PBPK model-based estimates of Ag tissue dose and equivalent airborne exposure  
20 concentrations (Tables A-7 through A-10); different durations of exposure (i.e., 15, 30,  
21 or 45 years) were evaluated (Table A-8); and comparisons were made of the PBPK  
22 model estimates to the limited available data on silver tissue doses in humans (Section  
23 A.5.2; Tables A-4 and A-5).

24 These findings showed that estimates of the animal effect levels and the HEC estimates  
25 varied by a factor of up to three orders of magnitude – depending on the animal effect  
26 level estimate (NOAEL, LOAEL, or BMCL<sub>10</sub>) (Tables A-1 and 6-8); the particle size and  
27 type (15 to 100 nm diameter particle or ionic Ag) (Tables A-7 and A-9); and the  
28 assumed biologically-relevant dose metric (soluble/active or total silver) (Table A-9).

1 Also evaluated was the influence of the different risk assessment methodologies on the  
2 OELs derived by NIOSH in this document (Section 6.3) and by others [Christensen et  
3 al. 2010; Weldon et al. 2016]. The data used to derive these OELs (Table 6-8) was  
4 from the same subchronic inhalation studies [Sung et al. 2008, 2009; Song et al. 2013].  
5 However, these risk assessments selected different rat responses as the critical effect  
6 (i.e., lung function deficits, lung inflammation, or liver bile duct hyperplasia); different  
7 PoD estimate types (NOAEL, LOAEL, or BMCL<sub>10</sub>); and different dose metrics (airborne  
8 exposure or tissue dose of silver). In addition, these risk assessments used different  
9 DAFs and UFs, which vary by up to an order of magnitude (Section 6.2.4). The HEC  
10 and OEL estimates also vary by about an order of magnitude (Table 6-8). However,  
11 each of these OEL estimates for silver nanomaterials, by NIOSH and others, are all  
12 relatively low airborne mass concentrations (0.1 to 2 µg/m<sup>3</sup>) compared to the current  
13 NIOSH REL of 10 µg/m<sup>3</sup> for total silver (metal dust, fume, and soluble compounds, as  
14 Ag) and to the other OELs for silver (up to 100 µg/m<sup>3</sup>) (Table 1-2).

15 The sources of uncertainty that could not be evaluated quantitatively were characterized  
16 with regard to the available scientific evidence and needs for future research (Sections  
17 6.4.5 and 8). These areas of uncertainty include: (1) the clinical significance to humans  
18 of the adverse effects observed in the rat studies (discussed in Section 6.4.1); (2) the  
19 role of particle dissolution and clearance of AgNPs on the doses associated with the  
20 adverse effects observed in rats (described in Section 6.4.2); and (3) the potential for  
21 chronic adverse effects not observed in the subchronic studies (discussed in Sections  
22 6.4.3 and 6.4.4). As new data become available and further validation of the PBPK  
23 model becomes feasible, the uncertainties in this risk assessment could be reduced,  
24 resulting in improved OEL estimates for AgNPs.

## 25 **6.5 Summary**

26 The two subchronic inhalation studies in rats exposed to AgNPs [Sung et al. 2009; Song  
27 et al. 2013] were used by NIOSH and others to evaluate the potential occupational  
28 health risk of exposure to AgNPs and to develop OELs for silver nanomaterials (Section

1 6.3). The airborne exposure concentrations in these rat studies ranged from 49 to 515  
2  $\mu\text{g}/\text{m}^3$ , which spans the 100  $\mu\text{g}/\text{m}^3$  OEL for inhalable silver (Table 1-2). These rat study  
3 exposure concentrations are considered to be below the MTD dose because no  
4 significant dose-related changes in body weight or organ weight were observed, and no  
5 toxicity that interfered with the study interpretation was reported [Sung et al. 2009; Song  
6 et al. 2013]. The pulmonary clearance rates of silver were similar to normal rates for  
7 alveolar macrophage-mediated clearance of poorly-soluble particles (i.e., no evidence  
8 of overloading) (Section 6.2.1).

9 The observed lung and liver effects in rats associated with subchronic inhalation of  
10 silver nanoparticles are considered to be relevant to humans (Section 6.4.1), although  
11 the clinical significance of these early-stage effects is uncertain (Section 6.4.5). The rat  
12 pulmonary inflammation response at the LOAEL resolved by 12 weeks post-exposure  
13 [Song et al. 2013]; and pulmonary fibrosis was not reported as having been observed,  
14 suggesting that the pulmonary effects of AgNP exposure in the rat studies were early-  
15 stage and were not persistent (Section 6.4.1). Liver effects included hyperplasia at  
16 lower doses and necrosis at higher doses in the one subchronic inhalation study that  
17 reported liver effects [Sung et al. 2009]; however no information on the persistence of  
18 these rat liver effects was available.

19 As described in the sensitivity analysis (Section 6.4.6), the HEC estimates to the rat  
20 effect levels vary according to the rodent data selected and the dosimetric methods  
21 applied (Table A-9). The lowest HEC estimates are from PBPK model estimates of the  
22 total silver tissue dose after a 45-year working lifetime exposure (Table A-10). Studies  
23 in rodents suggest that the soluble/active form may be the most biologically-relevant  
24 dose metric for the observed acute inflammation responses [Roberts et al. 2013;  
25 Braakhuis et al. 2014] (Section 6.1.3); however, the role of the the different forms of  
26 silver on long-term effects is not well understood and may involve both ionic and  
27 particulate forms of silver as suggested from shorter-term studies both in vitro and in  
28 vivo (Sections 4.5 and 5.2.5).

1 In the external review draft (January 7, 2016) of this CIB, NIOSH considered the  
2 evidence to be insufficient to derive an OEL that is specific to particle size. Since that  
3 draft, a new risk assessment on silver nanoparticles was published [Weldon et al. 2016],  
4 and comments received from peer and public reviewers prompted NIOSH to reevaluate  
5 the available data and risk assessment methods. Although no new evidence was  
6 available in animals or humans that could be used in quantitative risk assessment, the  
7 current document provides a more comprehensive risk assessment with additional  
8 evaluations and comparisons of the available data and methods. An updated literature  
9 search provides further evidence of increased toxicity of nanoscale silver relative to  
10 microscale silver from in vivo and in vitro studies, as well as additional information on  
11 the biological modes of action and dose metrics. Uncertainties are discussed with  
12 regard to the estimated worker-equivalent concentrations that are based on the rodent  
13 subchronic effect levels. The OEL estimates depend on the data and methods used and  
14 the uncertainty factors applied (Section 6.4.6).

15 The OELs for silver nanoparticles derived in the risk assessment by NIOSH (Section 6.3)  
16 and others [Christensen et al. 2010; Weldon et al. 2013] vary by approximately an order  
17 of magnitude (Table 6-8). However, these OEL estimates for silver nanoparticles are all  
18 lower than the NIOSH REL of 10  $\mu\text{g}/\text{m}^3$  for total airborne silver (Section 6.4.6) (Table 1-  
19 2).

20 The overall findings from the quantitative risk assessment indicate that a REL of 0.9  
21  $\mu\text{g}/\text{m}^3$  would protect workers from developing adverse lung and liver effects, as  
22 observed in rodents exposed to silver nanoparticles. These findings are consistent with  
23 general guidance on the application of an OEL for the “bulk material” to a nanoscale  
24 form of the material when data are insufficient to develop a nanomaterial-specific OEL  
25 [ISO 2014, 2016], i.e., the NIOSH REL of 10  $\mu\text{g}/\text{m}^3$  for silver would be reduced by a  
26 factor of ~10 in applying those nanomaterial control-banding strategies. Workplace  
27 airborne exposure concentrations to silver nanomaterials were reported to be as low as  
28 0.02  $\mu\text{g}/\text{m}^3$  (as silver metal) [Lee et al. 2011b]; these findings provide evidence that

*This information is distributed solely for the purpose of pre-dissemination peer review under applicable information quality guidelines. It has not been formally disseminated by the National Institute for Occupational Safety and Health. It does not represent and should not be construed to represent any agency determination or policy.*

- 1 silver can be measured at and controlled to airborne concentrations below the NIOSH
- 2 REL of 0.9 µg/m<sup>3</sup>.
  
- 3 On the basis of the hazard review and quantitative risk assessment of AgNPs provided
- 4 in this CIB, and on prudent occupational health practice, NIOSH recommends that
- 5 worker airborne exposures be controlled below the REL of 0.9 µg/m<sup>3</sup> for silver
- 6 nanomaterials, as an 8-hour TWA concentration.
  
- 7

*This information is distributed solely for the purpose of pre-dissemination peer review under applicable information quality guidelines. It has not been formally disseminated by the National Institute for Occupational Safety and Health. It does not represent and should not be construed to represent any agency determination or policy.*

1 **TABLES AND FIGURE FOR CHAPTER 6**

2 **Table 6-1. Rat subchronic inhalation study data for silver nanoparticles –**  
 3 **response proportion for pulmonary inflammation (chronic, alveolar, minimal).<sup>a</sup>**

Rat Study and Sex	Response Proportion at Indicated Concentration ( $\mu\text{g}/\text{m}^3$ ) <sup>b</sup>			
	0 $\mu\text{g}/\text{m}^3$	49 $\mu\text{g}/\text{m}^3$	133 $\mu\text{g}/\text{m}^3$	515 $\mu\text{g}/\text{m}^3$
Sung et al. [2009], Male	2/10	3/10	2/10	8/9
Sung et al. [2009], Female	3/10	2/10	0/10	8/10
	0 $\mu\text{g}/\text{m}^3$	49 $\mu\text{g}/\text{m}^3$	117 $\mu\text{g}/\text{m}^3$	381 $\mu\text{g}/\text{m}^3$
Song et al. [2013], Male	0/5	0/5	3/5	5/5
Song et al. [2013], Female	0/4	0/4	0/4	4/4

4 <sup>a</sup> Histopathology results from Tables 9 and 10 of Sung et al. [2009] and from Table XII in Song et al.  
 5 [2013]; data at end of 13-week exposure in Sung et al. [2009] or at end of 12-week exposure in Song et  
 6 al. [2013].

7 <sup>b</sup> Pooled response proportion (responders/total rats) by exposure concentration,  $\mu\text{g}/\text{m}^3$ : 0 (5/29), 49  
 8 (5/29), 117 (3/9), 133 (2/20), 381 (9/9), 515 (16/19). BMDL<sub>10</sub> estimate is 62.8  $\mu\text{g}/\text{m}^3$  (Table B-11).

9

10 **Table 6-2. Rat subchronic inhalation study data for silver nanoparticles –**  
 11 **response proportion for liver bile duct hyperplasia (minimum or moderate).\***

Rat Study and Sex	Response Proportion at Indicated Exposure Concentration**			
	0 $\mu\text{g}/\text{m}^3$	49 $\mu\text{g}/\text{m}^3$	133 $\mu\text{g}/\text{m}^3$	515 $\mu\text{g}/\text{m}^3$
Sung et al. [2009], Male	0/10	0/10	1/10	4/9
Sung et al. [2009], Female	3/10	2/10	4/10	9/10

12 \* Histopathology results from Tables 9 and 10 of Sung et al. [2009]; data at end of 13-wk exposure.  
 13 These data could not be pooled, because of heterogeneity in the male and female exposure-response  
 14 data (Appendix B).

15 \*\* BMDL<sub>10</sub> estimates are 92.5 and 50.5  $\mu\text{g}/\text{m}^3$  in male and female rats, respectively (Table B-5).

16

This information is distributed solely for the purpose of pre-dissemination peer review under applicable information quality guidelines. It has not been formally disseminated by the National Institute for Occupational Safety and Health. It does not represent and should not be construed to represent any agency determination or policy.

1 **Table 6-3. Dosimetric adjustment factors (DAFs) proposed by NIOSH – applicable**  
 2 **to liver bile duct hyperplasia response in female Sprague-Dawley rats after**  
 3 **subchronic inhalation of silver nanoparticles [Sung et al. 2009].**

Adjustment Factor: Human (H) or Animal (A) <sup>a</sup>	Human DAF	Rat DAF	Basis
1. Ventilation per exposure day (m <sup>3</sup> /d) (VE) (H/A) <sup>b</sup>	9.6	0.053	Human: male reference worker, 70 kg BW [ICRP 1994] Rat: 196 g average female BW [Sung et al. 2009]; 0.15 L/min [U.S. EPA 1994]
2. Deposition fraction, by respiratory tract region (DF) (H/A)	0.6634	0.949	Total respiratory tract, both species <sup>c</sup>
3. Lung retention rate, long-term (RT) (H/A)	NA	NA	Clearance adjustment for subchronic to chronic differences in rat and humans addressed in uncertainty factors [Jarabek et al. 2005] given uncertain dissolution kinetics.
4. Normalization of dose (A/H), surface area (m <sup>2</sup> )	63.8979	0.24647	Total respiratory tract surface area [Miller et al. 2011; U.S. EPA 1994]
<b>Total DAF</b>	0.488 <sup>d</sup>		Less than 1
<b>Default DAF</b>	1		Assume HEC is not greater than PoD <sub>animal</sub>

4 Abbreviations: HEC: Human-equivalent concentration; PoD<sub>animal</sub>: Point of departure in animals (Section  
 5 6.2.3); NA: not applicable or not applied; BW: body weight.

6 <sup>a</sup> Indicates order of factors in ratio in Equation 6-2.

7 <sup>b</sup> Air intake per exposure day (m<sup>3</sup>/8-hour d) in humans is the reference worker average value [ICRP  
 8 1994]; in rats, this value calculation was based on average body weight, as shown in Section F.2.

9 <sup>c</sup> MPPD v. 3.04 [ARA 2015] input parameters:

10 *Particle characteristics:* 0.018 um diameter (CMD); 1.5 GSD; density 10.5 g/cm<sup>2</sup> [Sung et al. 2009].

11 *Human:* Yeh/Schum symmetric mode in MPPD 3.04; oronasal normal augmenter; no inhalability  
 12 adjustment; 1143 ml tidal vol; 17.5 breaths/min (equals 20 L/min [ICRP 1994]).

13 *Rat:* Sprague-Dawley, symmetric model MPPD v. 3.04; BW 196 g; and associated MPPD parameters:  
 14 1.37 ml tidal vol; 131 breaths/min; inhalability adjustment.

15 <sup>d</sup> From Equation 6-2: 0.488 = (9.6 m<sup>3</sup>/d / 0.053 m<sup>3</sup>/d) x (0.6634/0.949) x (0.24647 m<sup>2</sup> / 63.8979 m<sup>2</sup>)

16  
 17

This information is distributed solely for the purpose of pre-dissemination peer review under applicable information quality guidelines. It has not been formally disseminated by the National Institute for Occupational Safety and Health. It does not represent and should not be construed to represent any agency determination or policy.

1 **Table 6-4. Dosimetric adjustment factors (DAFs) proposed by NIOSH – applicable**  
 2 **to pulmonary inflammation response in male and female Sprague-Dawley rats**  
 3 **after subchronic inhalation of silver nanoparticles [Sung et al. 2009; Song et al.**  
 4 **2013].**

Adjustment Factor: Human (H) or Animal (A) <sup>a</sup>	Human DAF	Rat DAF	Basis
1. Ventilation per exposure day (m <sup>3</sup> /d) <sup>b</sup> (VE) (H/A)	9.6	0.0084	Human: male reference worker, 70 kg BW [ICRP 1994] Rat: 345 g average BW male [Sung et al. 2009]; 0.23 L/min [U.S. EPA 1994]
2. Deposition fraction, by respiratory tract region (DF) (H/A)	0.386	0.0635	Alveolar (pulmonary) region, both species <sup>c</sup>
3. Lung retention rate, long-term (RT) (H/A)	NA	NA	Clearance adjustment for subchronic to chronic differences in rat and humans addressed in uncertainty factors [Jarabek et al. 2005] given uncertain dissolution kinetics.
4. Normalization of dose (A/H), surface area (m <sup>2</sup> )	102	0.4	Alveolar surface area surface area [Stone et al. 1992; NIOSH 2011, 2013]
<b>Total DAF</b>	2.72 <sup>d</sup>		

5 Abbreviations: NA: not applicable or not applied; BW: body weight.

6 <sup>a</sup> Indicates order of factors in ratio in Equation 6-2.

7 <sup>b</sup> Air intake per exposure day (m<sup>3</sup>/8-hour d) in humans is the reference worker average value [ICRP  
 8 1994]; in rats, this value was calculated based on average body weight as shown in Section F-2.

9 <sup>c</sup> MPPD v. 3.04 [ARA 2015] input parameters:

10 *Particle characteristics:* 0.018 um diameter (CMD); 1.5 GSD; density 10.5 g/cm<sup>2</sup> [Sung et al. 2009].  
 11 {Note: the deposition fraction could be replaced with that for the 14 nm particle in Song et al. 2013}.

12 *Human:* Yeh/Schum symmetric mode in MPPD 3.04; oronasal normal augmenter; no inhalability  
 13 adjustment; 1143 ml tidal vol; 17.5 breaths/min (equals 20 L/min [ICRP 1994])

14 *Rat:* Sprague-Dawley, symmetric model MPPD v. 3.04; BW 345 g and associated MPPD parameters:  
 15 2.42 ml tidal volume; 111 breaths/min; inhalability adjustment.

16 <sup>d</sup> From Equation 6-2: 2.72 = (9.6 m<sup>3</sup>/d / 0.084 m<sup>3</sup>/d) x (0.386/0.0635) x (0.4 m<sup>2</sup> / 102 m<sup>2</sup>)

17  
 18

*This information is distributed solely for the purpose of pre-dissemination peer review under applicable information quality guidelines. It has not been formally disseminated by the National Institute for Occupational Safety and Health. It does not represent and should not be construed to represent any agency determination or policy.*

1 **Table 6-5. Dose normalization factors in humans and rats.**

Reference	Normalization Factor (unit)	Human	Rat	Ratio (Human/Rat)*
Stone et al. [1992]	Alveolar surface area (m <sup>2</sup> )	102	0.4	255
Miller et al. [2011]		63.462	0.2422	262
U.S. EPA [1994]		54	0.32	169
Miller et al. [2011]	Total respiratory tract surface area (m <sup>2</sup> )	63.8969	0.2464	259
U.S. EPA [1994]		54.34	0.34375	158
ICRP [1994] (human); Sung et al. [2009] (rat)	Body weight (kg)	70	0.345 (male)	203
		70	0.196 (female)	357
		70	0.270 (both)	259

2 Miller et al. [2011, Tables 4 and 5, except <sup>a</sup>(shown below) from U.S. EPA 1994)] for the following  
 3 respiratory tract regions: head, tracheobronchial, and alveolar surface area (cm<sup>2</sup>), respectively: Rat:  
 4 18.5+24.2+2422 = 2464.5 cm<sup>2</sup> total; Human: 200<sup>a</sup>+4,149+634,620 = 638,969 cm<sup>2</sup> total.

5 U.S. EPA [1994; Table 4-4] respiratory tract regions: head, tracheobronchial, and alveolar surface area  
 6 (cm<sup>2</sup>), respectively: Rat: 15+22.5+3,400 = 3,437.5 cm<sup>2</sup> total; Human: 200+3,200+540,000 = 543,400.

7 \*Note that the normalization factor ratio is expressed as Rat/Human in the dosimetric adjustment factor  
 8 approach shown in Equations 6.1 and 6.2.

9

*This information is distributed solely for the purpose of pre-dissemination peer review under applicable information quality guidelines. It has not been formally disseminated by the National Institute for Occupational Safety and Health. It does not represent and should not be construed to represent any agency determination or policy.*

1 **Table 6-6. Uncertainty factors in occupational risk assessment.** <sup>a</sup>

<b>Factor</b>	<b>Source of Uncertainty or Variability</b>	<b>Default Values in Workers</b>
UF <sub>A</sub>	Animal to human - Toxicokinetics (TK) Toxicodynamics (TD)	Allometric scaling (TK) 2.5–3 (TD)
UF <sub>H</sub>	Human inter-individual variability in TK and TD: workers	3–5
UF <sub>L</sub>	LOAEL to NOAEL adjustment	1–10
UF <sub>S</sub>	Subchronic to chronic exposure and effects	2–100
UF <sub>D</sub>	Modifying factor for database insufficiency or severity of endpoint	Not specified

2 <sup>a</sup> From Table II of Dankovic et al. [2015], who cite ECHA [2008].

3

*This information is distributed solely for the purpose of pre-dissemination peer review under applicable information quality guidelines. It has not been formally disseminated by the National Institute for Occupational Safety and Health. It does not represent and should not be construed to represent any agency determination or policy.*

1 **Table 6-7. UFs to apply to the HECs to the Rat Subchronic PoDs<sup>a</sup> – Estimated**  
 2 **with a DAF Method.<sup>b</sup>**

3

Factor <sup>c</sup>	Proposed Value	Rationale
Animal to human (UF <sub>A</sub> )	1 (TK) 2.5 (TD)	TK: Animal to human dose adjusted by the total respiratory tract deposition fractions and body weights (liver bile duct hyperplasia) or pulmonary deposition fractions and alveolar epithelial cell surface area (pulmonary inflammation). No adjustment for possible clearance rate differences. TD: No chemical-specific information on animal to human sensitivity. Default TD estimate of 2.5 from WHO/ICPS [2005a].
Human inter-individual variability (UF <sub>H</sub> )	$\sqrt{10}$ (3.16)	No chemical-specific information on which to base this factor, which includes both TK and TD considerations. Worker population factors typically less than 10 [Dankovic et al. 2015]; ECHA [2008] uses a factor of 5.
LOAEL used as PoD (UF <sub>L</sub> )	1	Not applicable because rat BMCL <sub>10</sub> estimates were used as the PoDs.
Subchronic to (UF <sub>S</sub> )	$\sqrt{10}$ (3.16)	Rat tissue concentrations of silver appear not to have reached steady-state in these subchronic studies (based on clearance half-time estimates) [Song et al. 2013], suggesting higher dose accumulation with chronic exposure, possibly causing increased incidence or severity of response. Default estimate of ~3 used [Naumann and Weideman 1995; Kalberlah et al. 2002].
<b>Total UF</b>	25	

4 <sup>a</sup> The rat PoDs were benchmark concentrations, lower 95% confidence interval (BMCL<sub>10</sub>), estimates of  
 5 bile duct hyperplasia or lung inflammation of minimal severity observed by histopathology examination  
 6 in Sung et al. [2009] and Song et al. [2013].

7 <sup>b</sup> DAF method used by NIOSH described in Section 6.2.3.

8 <sup>c</sup> An additional factor for database insufficiency or severity of effects (Table 6-6) was considered not  
 9 applicable to these analyses.

10 Abbreviations: Uncertainty factor (UF); Human-equivalent concentration (HEC); Point of departure  
 11 (PoD); Dosimetric adjustment factor (DAF); Lowest observed adverse effect level (LOAEL).

12

This information is distributed solely for the purpose of pre-dissemination peer review under applicable information quality guidelines. It has not been formally disseminated by the National Institute for Occupational Safety and Health. It does not represent and should not be construed to represent any agency determination or policy.

1 **Table 6-8. Derived occupational exposure limits (OELs) for silver nanomaterials,**  
 2 **determined by dosimetric adjustment factor (DAF) and uncertainty factor (UF)**  
 3 **methods.**

Rat Effect Endpoint and Sex [Study Reference]	Rat PoD ( $\mu\text{g}/\text{m}^3$ )	Total DAF	Human Equivalent Concentration (HEC) ( $\mu\text{g}/\text{m}^3$ )	Total UF	OEL Estimate ( $\mu\text{g}/\text{m}^3$ )
<b>Christensen et al. [2010] (Section G-1)</b>					
Lung function decrement, LOAEL, female [Sung et al. 2008]	49	2 <sup>a</sup>	25	75 <sup>b</sup> 250 <sup>b</sup>	0.33 0.1
Lung and liver effects, NOAEL, male and female [Sung et al. 2009]	133	2 <sup>a</sup>	67	100	0.67
<b>Weldon et al. [2016] (Section G-2)</b>					
Liver bile duct hyperplasia, BMCL <sub>10</sub> , female [Sung et al. 2009]	25.5	4.51	5.66	30	0.19
<b>NIOSH (Section 6.2.3)</b>					
Liver bile duct hyperplasia, BMCL <sub>10</sub> , female [Sung et al. 2009]	50.5	1 <sup>c</sup>	50.5	25	2.0
Pulmonary inflammation, BMCL <sub>10</sub> , pooled data in male and female rats [Sung et al. 2009; Song et al. 2013]	62.8	2.72	23.1	25	0.92

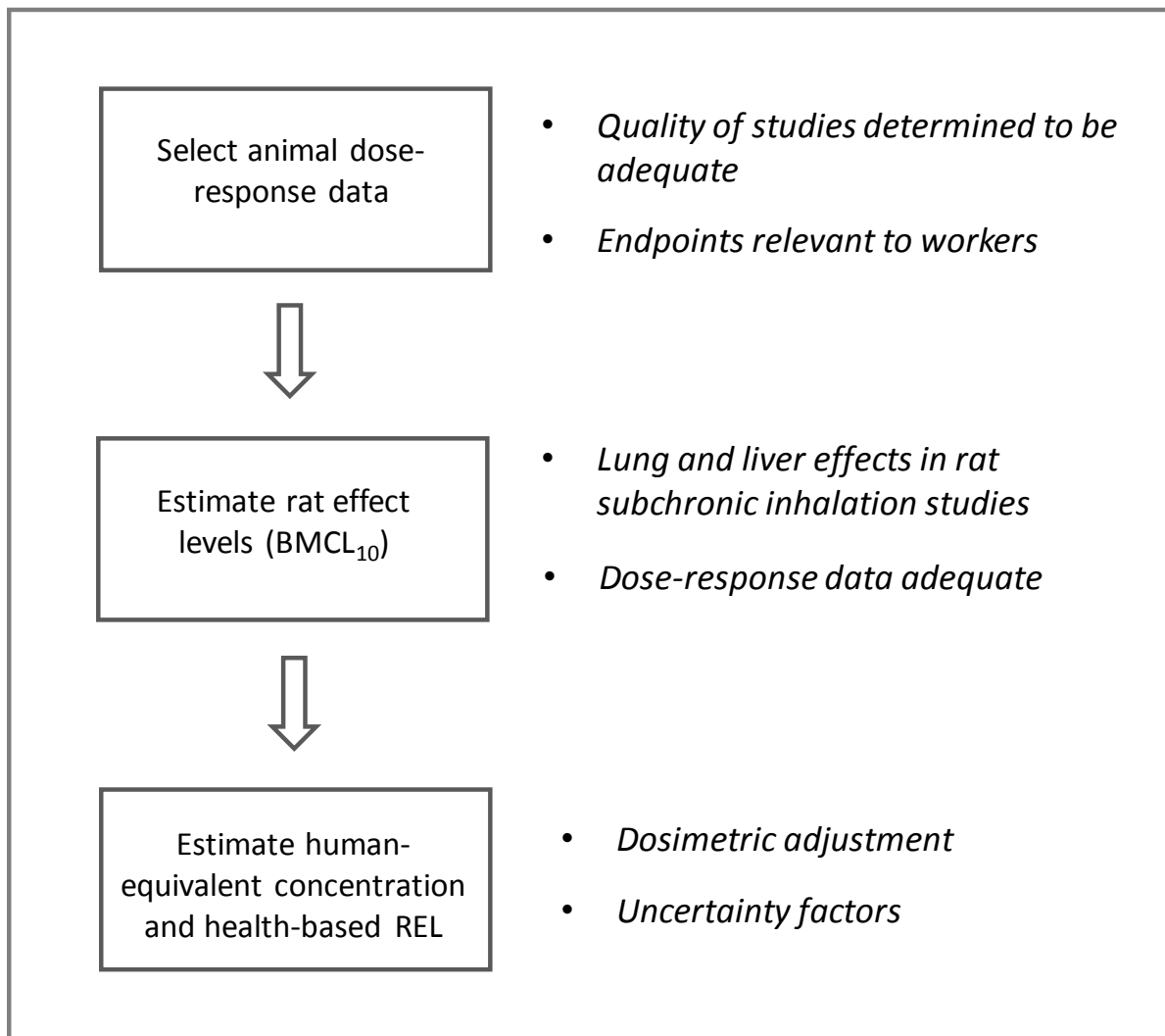
4 <sup>a</sup> Note that this is the inverse of the factor used in Christensen et al. [2010], who multiplied the rat effect level  
 5 (NOAEL or LOAEL) by the DAF to obtain the HEC (vs. dividing as shown in these analyses); also note that the term  
 6 adjustment factor, not DAF, was used by Christensen et al. [2010].

7 <sup>b</sup> Two different exposure scenarios in Christensen et al. [2010].

8 <sup>c</sup> Default DAF (Table 6-3).

9

1



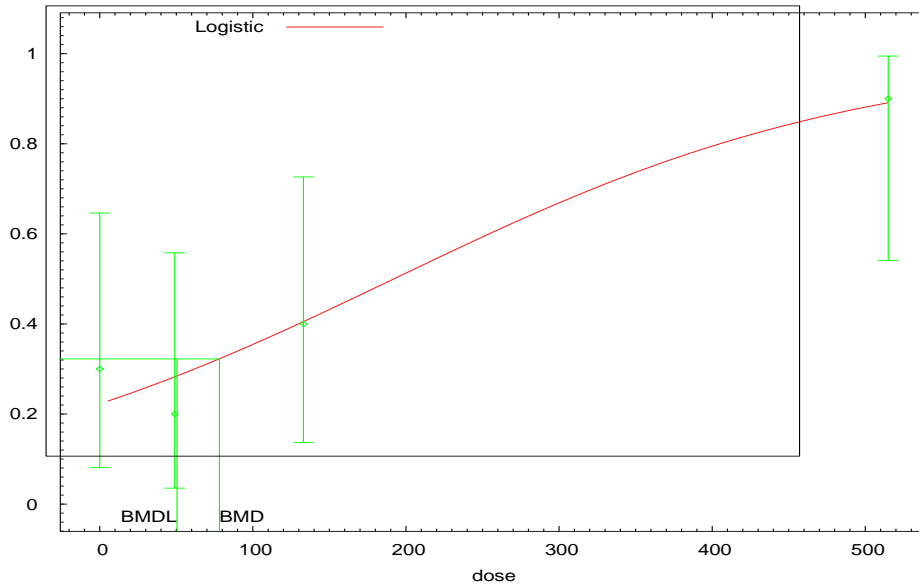
2

3 **Figure 6-1. Summary of main steps in quantitative risk assessment and derivation**  
4 **of a recommended exposure limit (REL) for silver nanomaterials. The dose**  
5 **response-data used are from two rat subchronic inhalation studies [Sung et al.**  
6 **2008, 2009; and Song et al. 2013]. Estimated BMCL10: benchmark concentration,**  
7 **95% lower confidence limit, is associated with 10% added risk of early-stage lung**  
8 **or liver effects (minimal or higher severity at histopathological examination) in**  
9 **rats. Risk assessment methods and data used are described in Sections 6.2.**

10

This information is distributed solely for the purpose of pre-dissemination peer review under applicable information quality guidelines. It has not been formally disseminated by the National Institute for Occupational Safety and Health. It does not represent and should not be construed to represent any agency determination or policy.

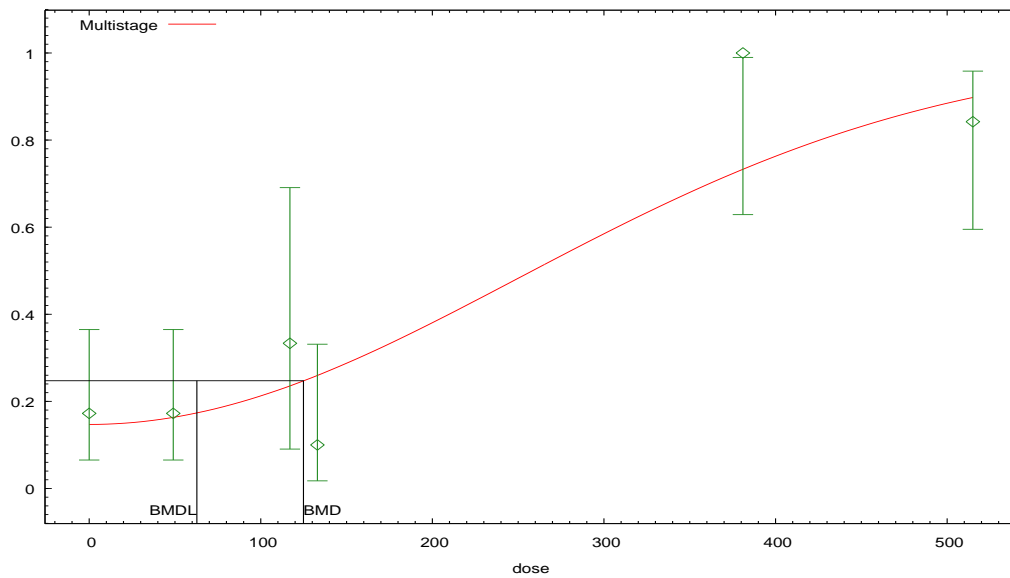
Logistic Model, with BMR of 10% Added Risk for the BMD and 0.95 Lower Confidence Limit for the BMDL



1

2 **Figure 6-2. Exposure-response model (logistic) fit to the airborne concentration of silver**  
3 **nanoparticles ( $\mu\text{g}/\text{m}^3$ ) and bile duct hyperplasia proportion in female rats [Sung et al.**  
4 **2009]. (Data and model results in Tables B-1 and B-5; same as Figure B-2.)**

Multistage Model, with BMR of 10% Added Risk for the BMD and 0.95 Lower Confidence Limit for the BMDL



5

12:09 02/02 2017

6 **Figure 6-3. Exposure-response model (multistage polynomial degree 3) fit to the pooled**  
7 **data on airborne concentration of silver nanoparticles ( $\mu\text{g}/\text{m}^3$ ) and chronic alveolar**  
8 **inflammation in male and female rats [Sung et al. 2009; Song et al. 2013]. (Data and**  
9 **model results in Table B-11; same as Figure B-9.)**

## 1 **7 Recommendations**

2  
3 NIOSH recommends that risk management control practices be implemented so that  
4 worker exposures to silver nanomaterials (primary particle size  $\leq 100$  nm; metal dust,  
5 fume, and soluble compounds, as Ag) do not exceed the NIOSH REL of  $0.9 \mu\text{g}/\text{m}^3$  (8-  
6 hour TWA), measured as a respirable airborne mass concentration. A nanoparticle is  
7 defined as having a primary particle size of  $\leq 100$  nm. A primary particle is the smallest  
8 identifiable subdivision of a particulate system [BSI 2005]. Additional methods are  
9 needed to determine if an airborne respirable particle sample includes silver  
10 nanomaterials (Chapter 7). NIOSH based the REL for silver nanomaterials on the lung  
11 and liver effects associated with exposure to silver nanomaterials in the rat subchronic  
12 inhalation studies, on estimates of human-equivalent concentrations in workers, and in  
13 consideration of the uncertainties in those estimates (Chapter 6).

14 In addition, the NIOSH REL of  $10 \mu\text{g}/\text{m}^3$  for total silver (metal dust, fume, and soluble  
15 compounds, as Ag) [NIOSH 1988, 2003, 2007] continues to apply. Worker exposures to  
16 silver should not exceed the NIOSH REL for silver nanomaterials or the NIOSH REL for  
17 total silver.

18 Development of a risk management program should include management and  
19 employee involvement. Elements of a good risk management program include:

20 (1) Identification of processes and job tasks where there is potential for exposure to  
21 silver nanomaterials. Comprehensive assessment of exposures (including  
22 exposures to other potential hazards) should be performed as part of job hazard  
23 analysis, and a hazard communication program should be developed following  
24 the OSHA Hazard Communication Standard [29 CFR 1910.1200(h)].

25 (2) Development of criteria and guidelines for selecting, installing, and evaluating  
26 engineering controls (such as LEV, dust collection systems), with the objective of

- 1           controlling worker airborne exposure to silver nanomaterials (metal dust, fume,  
2           and soluble compounds, as Ag) below the NIOSH REL of 0.9  $\mu\text{g}/\text{m}^3$  (respirable  
3           mass, 8-hour TWA), and to total airborne silver (metal dust, fume, and soluble  
4           compounds, as Ag) below the NIOSH REL of 10  $\mu\text{g}/\text{m}^3$  (total mass, 8-hour TWA).
- 5           (3) Routine systematic and comprehensive evaluation of worker exposures by all  
6           routes to silver nanomaterials at least annually, and/or whenever there is a  
7           change in a process or task associated with potential exposure to silver  
8           nanomaterials. Changes could include frequency, volume, duration, equipment,  
9           and procedures/processes.
- 10          (4) An education and training program for workers on how to recognize and prevent  
11          potential exposures
- 12          (5) Establishing and using good work practices to prevent exposure to silver,  
13          including the safe handling of silver nanomaterials.
- 14          (6) Development of procedures for selecting and using personal protective  
15          equipment (PPE; clothing, gloves, respirators). Development of a respiratory  
16          protection program following the OSHA respiratory protection standard (29 CFR  
17          1910.134) if respiratory protection is used.
- 18          (7) Development of spill control plans and routine cleaning procedures for work  
19          areas using a HEPA-filtered vacuum or wet-wipes. Do not use dry sweeping or  
20          air hoses. Avoid using or handling silver nanomaterials in powder form, where  
21          possible, and ensure silver nanomaterials are stored in tightly sealed containers  
22          and appropriately labeled.
- 23          (8) Provision of facilities for hand washing to reduce the potential for dermal and oral  
24          exposures, and encouragement of workers to use these facilities before eating or  
25          leaving the worksite.

- 1 (9) Use of established medical surveillance approaches for workers potentially  
2 exposed to silver including silver nanomaterials.

### 3 **7.1 Exposure Assessment for Silver Nanomaterials**

4 NIOSH continues to recommend the REL of 10  $\mu\text{g}/\text{m}^3$  (8-hr TWA) for total silver (metal  
5 dust, fume, and soluble compounds, as Ag) [NIOSH 1988, 2003, 2007]. Sampling and  
6 analysis methods for total silver are described in the NIOSH Manual of Analytical  
7 Methods (NIOSH Methods 7300, 7301, and 7306) [NIOSH 2017]. In addition, NIOSH is  
8 recommending an airborne respirable mass concentration of 0.9  $\mu\text{g}/\text{m}^3$  as an 8-hour  
9 time-weighted average (TWA) concentration to evaluate and monitor worker exposure  
10 to silver nanomaterials (primary particle size  $\leq 100$  nm). The REL for silver  
11 nanomaterials applies to the airborne mass fraction of particles with a primary particle  
12 size of 100 nm or less in any single dimension, including agglomerates comprising  
13 these primary particles. Although there are currently no personal sampling devices  
14 available to specifically measure the mass concentration of these ultrafine particles,  
15 there are several valid aerosol methods that will collect these ultrafine particles as part  
16 of a larger sample. Note that a combination of methods may be necessary to properly  
17 characterize exposure (Figure 7-1).

18 In recognition of this, NIOSH recommends the following for conducting exposure  
19 assessments of silver nanomaterials:

- 20
- 21 1) When the work environment may have multiple particulate sources, or the  
22 primary particle size is not well characterized, use of NIOSH Method 0600 with a  
23 size-selective sampler (such as a standard respirable cyclone) will collect most  
24 airborne ultrafine particles and fume (which rapidly condenses into ultrafine  
25 particulate). A duplicate sample (see recommendation 4, below) should be  
26 collected with a mixed cellulose ester filter in case further characterization by  
27 microscopy becomes necessary. NIOSH Method 7300 [NIOSH 2003] can  
28 determine the mass of silver present in the sample. Results below 0.9  $\mu\text{g}/\text{m}^3$  will

1           affirm that exposures are below the REL for silver nanomaterials, and thus the  
2           duplicate sample may be discarded.

3  
4           2) If the particle size has been well characterized, use of an established size-  
5           selective sampler with a low particle-size cut point (agglomerates should be  
6           considered when selecting an established size selective sampler) will provide a  
7           result more representative of the ultrafine particulate portion of the exposure.  
8           Again, a duplicate sample (see recommendation 4, below) should be collected  
9           with a mixed cellulose ester filter in case further characterization by microscopy  
10           becomes necessary. Results below  $0.9 \mu\text{g}/\text{m}^3$  will affirm that exposures are  
11           below the REL for silver nanomaterials, and thus the duplicate sample may be  
12           discarded.

13  
14           3) If the result from either method above is above  $0.9 \mu\text{g}/\text{m}^3$ , then further  
15           characterization with an electron microscope equipped with X-ray energy  
16           dispersive spectroscopy (EDS) is required, to be more specific to ultrafine  
17           particles.

18  
19           4) Duplicate samples: Because NIOSH method 7300 is a destructive analysis (the  
20           entire sample is consumed in analysis), a duplicate sample must be collected  
21           with the same type of size-selective sampler and a mixed cellulose ester filter for  
22           analysis by transmission electron microscopy. Electron microscopy equipped  
23           with X-ray energy dispersive spectroscopy (EDS) can identify particles and  
24           agglomerates of primary particles of 100 nm or less to determine the fraction to  
25           which the silver nanomaterial REL of  $0.9 \mu\text{g}/\text{m}^3$  is applicable.

26  
27           5) Once the exposure is well characterized and controlled below the REL, samples  
28           collected with the chosen size-selective sampler and analyzed with NIOSH 7300  
29           may be used to monitor exposure, without the need for microscopy samples.  
30

1 An important first step in applying any risk management program is to develop a job  
2 hazard analysis of the processes and job activities that place workers at risk of  
3 exposure (such as the handling of large volumes of silver nanomaterials, silver  
4 brazing/soldering operations, and other high-temperature processes involving silver) [as  
5 described in: <https://www.osha.gov/Publications/osha3071.pdf>]. When applicable, the  
6 job hazard analysis should include an initial assessment of a bulk sample of the material  
7 and/or documentation from the manufacturer to determine the presence of silver  
8 nanomaterials. The job hazard analysis can be used to determine the number of  
9 workers potentially exposed and to qualitatively determine which workers and  
10 processes are likely to have the greatest potential for exposure.

11  
12 Several exposure assessment strategies can be used to determine workplace  
13 exposures [NIOSH 1977; Corn and Esmen 1979; Leidel and Busch 1994; Rappaport et  
14 al. 1995; Lyles et al. 1997; Bullock and Ignacio 2006; Ramachandran et al. 2011;  
15 McNally et al. 2014]. These strategies can be tailored to a specific workplace,  
16 depending on available resources, the number of workers, and the complexity of the  
17 work environment (such as process type and rate of operation, exposure control  
18 methods, and physical state and properties of material). One approach for determining  
19 worker exposures to airborne silver concentrations would be to initially target similarly  
20 exposed groups (SEGs) of workers [Corn and Esmen 1979; Leidel and Busch 1994].  
21 This initial sampling effort may be more time efficient and require fewer resources for  
22 identifying workers with exposures to silver above the REL. However, this measurement  
23 strategy may produce incomplete and upwardly biased exposure estimates if the  
24 exposures are highly variable [Kromhout 2009]. Therefore, repeated measurements on  
25 randomly selected workers may be required to account for between- and within-worker  
26 variations in exposure concentrations [Rappaport et al. 1995; Lyles et al. 1997]. If  
27 workplace exposure measurement data for silver are available, as well as information  
28 on exposure variability, it may be possible to use a Bayesian model that combines  
29 expert knowledge with existing exposure measurement data to estimate workers'  
30 exposures [McNally et al. 2014]. Because there is no "best" exposure measurement  
31 strategy that can be applied to all workplaces, multi-day random sampling of workers

*This information is distributed solely for the purpose of pre-dissemination peer review under applicable information quality guidelines. It has not been formally disseminated by the National Institute for Occupational Safety and Health. It does not represent and should not be construed to represent any agency determination or policy.*

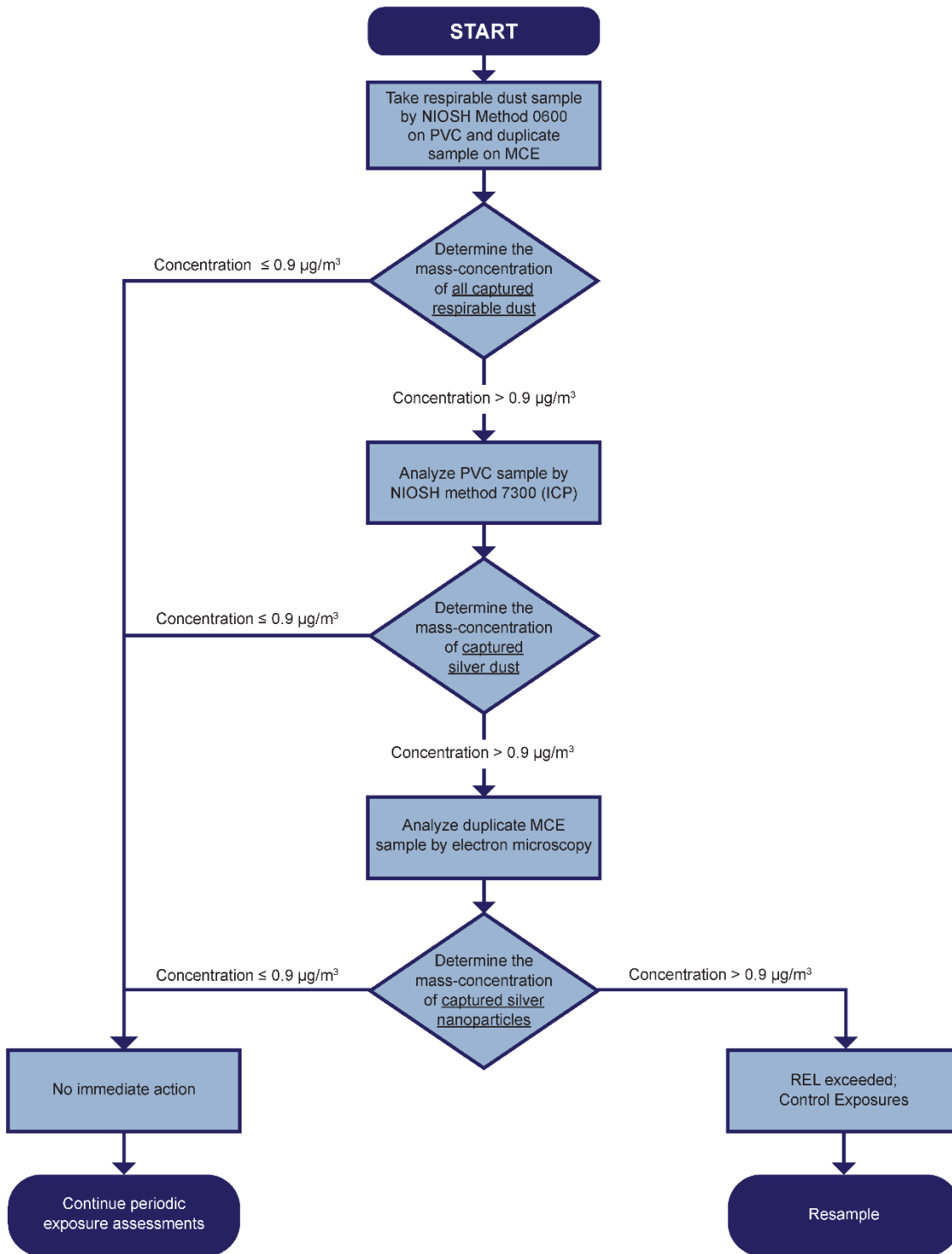
1 (all workers, if the exposed workforce is small) may be needed to accurately assess the  
2 airborne concentrations of silver to which workers are exposed. Additionally, the  
3 concentration mapping and job task–related measurement tools described by  
4 Ramachandran et al. would further complement the randomly selected worker method  
5 [2011]. In cases where resources and/or health and safety expertise are limited,  
6 consultation with an expert may be required.

7 Although the REL is not applicable to surface sampling, the potential adverse health  
8 effects of dermal exposure to silver reported in animal studies (Section E.3.1) suggest  
9 that dermal exposure should be minimized. Additionally, minimizing surface  
10 concentrations of silver nanomaterials reduces the likelihood of transferring silver  
11 nanomaterials out of the process areas. NIOSH recommends periodic surface-wipe  
12 sampling in process areas as well as office and common areas, using NIOSH NMAM  
13 9100 and analysis by NMAM 7300 or 7301 to validate containment of contaminants and  
14 the effectiveness of housekeeping procedures.

15 Brookhaven National Laboratory has published internal surface-wipe sampling criteria  
16 for metals [2014]. These criteria include acceptable surface levels for two categories:  
17 equipment release and housekeeping. The equipment release level, or the acceptable  
18 surface level of silver for transfer of equipment to non-operational areas or the public, is  
19  $1 \mu\text{g}/100 \text{ cm}^2$ . To meet the housekeeping criteria, surface levels should be below  $15$   
20  $\mu\text{g}/100 \text{ cm}^2$  during operational periods [Brookhaven National Laboratory 2014]. Surface  
21 contamination of silver should be maintained below  $15 \mu\text{g}/100 \text{ cm}^2$  for process areas  
22 and below  $1 \mu\text{g}/100 \text{ cm}^2$  for non-process areas.

23

This information is distributed solely for the purpose of pre-dissemination peer review under applicable information quality guidelines. It has not been formally disseminated by the National Institute for Occupational Safety and Health. It does not represent and should not be construed to represent any agency determination or policy.



1  
2 **Figure 7-1. Exposure assessment protocol for silver nanoparticles in an aerosol**  
3 **of unknown particle size distribution containing Ag and other particulates. For**  
4 **exposure assessment of total silver, see NIOSH Methods 7300, 7301, and 7306**  
5 **[NIOSH 2017].**

## 1 **7.2 Engineering Controls**

2 One of the best ways to prevent adverse health effects from exposure to a hazardous  
3 material is to eliminate exposure and minimize risks early in the design or redesign of  
4 manufacturing and downstream-user processes (see NIOSH Prevention through Design  
5 [PtD], at [www.cdc.gov/niosh/topics/PtD/](http://www.cdc.gov/niosh/topics/PtD/)). The concept of PtD is to design out or  
6 minimize hazards, preferably early in the design process. This can be accomplished  
7 through the establishment of a process safety management (PSM) program that is  
8 consistent with the requirements of the OSHA Process Safety Management Standard  
9 [29 CFR 1910.119]. PSM entails the development and implementation of programs or  
10 systems to ensure that the practices and equipment used in potentially hazardous  
11 processes are adequate and appropriately maintained. An integral part of the PSM  
12 program is a process hazard analysis prior to the initiation of work, to identify where  
13 sources of exposure to silver and other hazardous materials may occur so that process  
14 equipment can be designed or redesigned to minimize the risk of exposure. As part of  
15 the assessment, the health and safety professional should evaluate the potential  
16 magnitude and extent of emissions to determine the risk of exposure to workers. This  
17 initial assessment is an important first step toward identifying possible exposure control  
18 strategies.

19 Controlling exposures to occupational hazards is the fundamental method of protecting  
20 workers. Traditionally, a hierarchy of controls has been used as a means of determining  
21 how to implement feasible and effective control measures. Following the hierarchy  
22 normally leads to implementation of inherently safer systems, where the risk of illness or  
23 injury has been substantially reduced. Elimination and substitution are generally most  
24 effective if implemented when a process is in the design or development stage. If done  
25 early, implementation is simple, and in the long run it can result in substantial savings  
26 (such as in the cost of protective equipment and the initial and operation costs for the  
27 ventilation system) [NIOSH 2013b]. For an existing process, elimination or substitution  
28 of the material may require major changes in equipment and/or procedures in order to  
29 reduce the potential hazard. When elimination or substitution is not feasible, the use of  
30 engineering controls can be an effective control strategy for minimizing exposure to

*This information is distributed solely for the purpose of pre-dissemination peer review under applicable information quality guidelines. It has not been formally disseminated by the National Institute for Occupational Safety and Health. It does not represent and should not be construed to represent any agency determination or policy.*

1 hazards associated with processes and job tasks. Well-designed engineering controls  
2 can be highly effective in protecting workers and will typically be independent of worker  
3 interactions. The use of engineering controls to reduce worker exposure to all forms and  
4 particle sizes of silver is an effective means of minimizing health concerns and works  
5 best when it is part of an overall risk management program that includes worker  
6 exposure evaluation, education/training, administrative controls, and use of PPE.

7 Different types of exposure control systems can be used, depending on the  
8 configuration of the process and the degree of exposure control required [ACGIH 2013;  
9 NIOSH 2013b]. For example, source enclosure (that is, isolating the generation source  
10 from the worker) and well-designed local exhaust ventilation (LEV), equipped with high-  
11 efficiency particulate air (HEPA) filters, can be effective for capturing airborne silver  
12 particles at the source of exposure [NIOSH 2013b]. The selection of an appropriate  
13 exposure control system should take into account the extent to which the airborne  
14 concentration of silver nanomaterials is to be reduced (such as below the NIOSH REL  
15 of  $0.9 \mu\text{g}/\text{m}^3$ ), the quantity and physical form of the material (such as dispersible silver  
16 powder, a liquid slurry, or contained in a matrix), the task duration, the frequency with  
17 which workers may come into contact with silver or silver-containing material, and the  
18 characteristics of the task itself (such as how much energy is imparted to the material  
19 during sonication or powered sanding/cutting). For instance, working with materials  
20 containing silver nanomaterials (such as encapsulated in a fabric or solid material) may  
21 require a different type of exposure control system than would working with large  
22 quantities of silver nanomaterials in a highly dispersed free (powder) form. Specific  
23 processes (such as high-temperature melting of silver) and job tasks (such as silver  
24 brazing/soldering) have the potential to generate an aerosol or fume containing silver  
25 and therefore should incorporate exposure controls at the exposure source. Likewise,  
26 the manufacturing/synthesis of engineered silver nanomaterials and the handling of dry  
27 powders should be performed in enclosed systems and, when warranted, HEPA-  
28 ventilated systems. HEPA filtration has been shown to be effective in capturing  
29 nanoparticles and should be considered in situations where emissions may be regular,  
30 where processes are repeated, and where higher quantities are used in a way that may

1 lead to emissions. Research quantities of silver nanomaterials in laboratories can be  
2 safely handled if appropriate exposure-containment systems are used, such as a  
3 constant-velocity (variable air-volume) laboratory fume hood or air-curtain hood [Tsai et  
4 al. 2010] or a glove box to minimize worker exposure [NIOSH 2012]. These exposure  
5 control systems should be properly designed, tested, and routinely maintained and  
6 evaluated to ensure maximum efficiency [ACGIH 2010].

7 NIOSH found that in two facilities conducting brazing and soldering operations, airborne  
8 concentrations of silver (including silver nanoparticles) were less than  $0.015 \mu\text{g}/\text{m}^3$ ,  
9 measured as personal breathing zone TWA concentrations. Engineering controls  
10 included “canopy-type” ventilation hoods equipped with local exhaust ventilation; this  
11 was discharged directly through the roof of the building at high velocity, both downwind  
12 and approximately 50 or more feet from air intakes [NIOSH 1998].

13 Lee et al. [2011b; 2012a,b] examined silver nanoparticle production processes in two  
14 facilities. The first facility used an inductively-coupled plasma torch to vaporize various  
15 silver feedstocks, which were then condensed into nanoparticles; effectively a type of  
16 vapor-condensation synthesis process. The first study recorded silver concentrations in  
17 area samples between  $0.02$  and  $0.34 \mu\text{g}/\text{m}^3$ , with personal samples of  $0.12$  and  $1.20$   
18  $\mu\text{g}/\text{m}^3$  [Lee et al 2011b], though a subsequent visit to the site showed increase ranges  
19 of  $0.01$  to  $288.73 \mu\text{g}/\text{m}^3$  for area samples and  $0.02$  to  $2.43 \mu\text{g}/\text{m}^3$  for personal samples  
20 [Lee 2012b]. The only engineering control discussed was natural ventilation, which  
21 combined with the closed system maintained airborne silver concentrations of  
22 approximately  $1 \mu\text{g}/\text{m}^3$ . The greatest exposures occurred during the process of workers  
23 introducing feedstock, which was controlled by half-mask respirators and limiting worker  
24 time on this task [Lee 2012b]. Exposures from vapor-condensation and other airborne  
25 synthesis processes can frequently be reduced by optimization of reactor design and  
26 processes; and using hoods or enclosures, and local exhaust ventilation [Virji and  
27 Stefanaik 2014].

1 The second facility studied by Lee et al. [2011b] used two processes for silver  
2 nanoparticle production: a wet-chemistry reaction of sodium citrate and silver nitrate,  
3 and attrition milling. Both processes occurred in the same space, and silver  
4 concentrations ranged from 0.03 to 1.18  $\mu\text{g}/\text{m}^3$  in area samples and from 0.38 to 0.43  
5  $\mu\text{g}/\text{m}^3$  in personal samples. It was indicated that the workplace was “equipped with a  
6 fume hood and well ventilated” [Lee et al. 2011b]. While exposures from liquid and solid  
7 processes have been less studied, it has been indicated that emissions from wet-  
8 chemistry processes are lower than vapor phase processes, but that milling represents  
9 a significant emission possibility; fume hoods and local exhaust ventilation have been  
10 applied effectively to these methods as well [Virji and Stefanaik 2014].

11 In one study of such wet-chemistry processes, Park et al. [2009] examined a facility  
12 which used nitric acid and silver nitrate to produce a colloidal suspension, which was  
13 then filtered, dried, and milled. A vent hood was installed above the reactor, and  
14 ventilation facilities were in place near the grinding location. It was observed that  
15 opening the grinder door increased airborne particle concentrations and irregularities in  
16 concentration; moreover it was shown that activating the ventilation system directly  
17 reduced this irregularity. Additionally, the authors noted that particles on the floor were  
18 readily disturbed by workers and represent an additional potential exposure. The  
19 authors suggest that it would be better if the grinding room were airtight (while  
20 maintaining ventilation facilities) to prevent exposures to other zones [Park et al. 2009].

21 Table 7-1 provides examples of the types of engineering and other exposure control  
22 measures that could be used at various processes and job tasks to help control worker  
23 exposures to silver nanomaterials. In some cases, a combination of approaches may be  
24 necessary to accomplish exposure control goals (such as installing a continuous liner  
25 system inside a ventilated booth).

26

This information is distributed solely for the purpose of pre-dissemination peer review under applicable information quality guidelines. It has not been formally disseminated by the National Institute for Occupational Safety and Health. It does not represent and should not be construed to represent any agency determination or policy.

1 **Table 7-1. Engineering controls to reduce silver exposures below the NIOSH**

2 **RELs.\***

<b>Process and/or Task Activity</b>	<b>Potential Sources of Exposure</b>	<b>Exposure Containment/Control Options</b>
<b>Pilot and Research &amp; Development Operations</b>	<p>Potential exposures are generally to <i>small quantities</i> of AgNPs/AgNWs (such as µg and mg) during</p> <ul style="list-style-type: none"> <li>▪ Synthesis of AgNPs/AgNWs, including chemical vapor deposition, solution phase synthesis, and dry powder dispersion</li> <li>▪ Harvesting of AgNPs after synthesis</li> <li>▪ Removal of silver nanomaterials from a substrate</li> <li>▪ Powder transfer (AgNPs/AgNWs)</li> <li>▪ Reactor cleaning</li> </ul>	<p><b>Exposure Controls</b></p> <ul style="list-style-type: none"> <li>▪ Constant-velocity fume hood or nanomaterial enclosure with HEPA-filtration exhaust when warranted</li> <li>▪ HEPA-filtration exhaust enclosure (such as glove box isolators)</li> <li>▪ Biologic safety cabinet</li> <li>▪ Note: local exhaust ventilation or some type of enclosure control (glove box) may be required at the reactor and during the harvesting of material.</li> </ul>
<b>Research Laboratories</b>	<p>Potential exposures are generally to <i>small quantities</i> of AgNPs/AgNWs (such as µg and mg) during</p> <ul style="list-style-type: none"> <li>▪ Handling (such as mixing, weighing, blending, transferring) of AgNPs/AgNWs in free powder form or sonication of AgNP or AgNW liquid suspension</li> </ul>	<p><b>Exposure Controls</b></p> <ul style="list-style-type: none"> <li>▪ Constant-velocity fume hood or nanomaterial-handling enclosure with HEPA-filtration exhaust when warranted</li> <li>▪ HEPA-filtration exhaust enclosure (such as glove box isolators)</li> <li>▪ Biologic safety cabinet</li> </ul>
<b>Manufacturing and Synthesis of AgNPs and AgNWs</b>	<p>Potential exposures are generally to <i>large quantities</i> of AgNPs/AgNWs (≥ kg amounts) during</p> <ul style="list-style-type: none"> <li>▪ Synthesis of AgNPs (chemical vapor deposition, solution phase synthesis, and dry powder dispersion)</li> <li>▪ Harvesting of AgNPs after synthesis</li> <li>▪ Removal of silver nanomaterials from a substrate</li> <li>▪ Powder transfer of silver nanomaterials</li> <li>▪ Drum and bag filling</li> <li>▪ Reactor cleaning</li> <li>▪ Coating of AgNPs/AgNWs</li> </ul>	<p><b>Exposure Controls</b></p> <ul style="list-style-type: none"> <li>▪ Dedicated ventilated room (such as a down-flow room) for reactor with HEPA-filtration exhaust, potentially in conjunction with localized controls listed below</li> <li>▪ LEV at source of potential exposure when isolation or total enclosure of the process is not possible</li> <li>▪ Ventilated bagging/weighing stations and/or unidirectional down-flow ventilation booth</li> <li>▪ Non-ventilation options, including a continuous liner off-loading system for bagging operations</li> <li>▪ Ventilated bag dumping stations for product transfer</li> </ul>

Process and/or Task Activity	Potential Sources of Exposure	Exposure Containment Options
<p><b>Use of AgNPs and AgNWs to produce enabled materials</b></p>	<ol style="list-style-type: none"> <li>1. Potential exposures are generally to <i>small quantities</i> of AgNP/AgNW powder or liquid suspensions during <ul style="list-style-type: none"> <li>▪ Mixing, weighing, and transferring of AgNPs/AgNWs</li> <li>▪ Incorporation of AgNPs/AgNWs into matrices and coatings</li> <li>▪ Spraying of AgNPs/AgNWs on surfaces</li> </ul> </li> <li>2. Potential exposures are generally to <i>large quantities</i> of AgNPs or AgNWs in powder or liquid suspensions during <ul style="list-style-type: none"> <li>▪ Blending or pouring into other matrices</li> <li>▪ Impregnating of textile materials and spray coating of surfaces</li> </ul> </li> <li>3. Potential exposures during handling of <i>small pieces</i> of AgNP- and AgNW-enabled textiles, fabrics, materials and composites: <ul style="list-style-type: none"> <li>▪ Grinding, sanding, cutting, drilling, or other mechanical energy applied to materials containing AgNPs or AgNWs</li> </ul> </li> </ol>	<ol style="list-style-type: none"> <li>1. <b>Exposure Controls</b> <ul style="list-style-type: none"> <li>▪ Transfer of AgNPs/AgNWs in sealed, unbreakable, labeled containers</li> <li>▪ Constant velocity fume hood or nanomaterial handling enclosure (with filtered exhaust when warranted)</li> <li>▪ HEPA-filtration exhaust enclosure (such as glove box isolators)</li> <li>▪ Biologic safety cabinet</li> </ul> </li> <li>2. <b>Exposure Controls</b> <ul style="list-style-type: none"> <li>▪ Isolation techniques such as a dedicated ventilated room or process enclosure with HEPA-filtration exhaust</li> <li>▪ Process-based controls such as ventilated bagging/weighing station and unidirectional down-flow booth</li> <li>▪ Non-ventilation options such as continuous liner off-loading systems for bagging operations</li> <li>▪ Ventilated bag dumping stations for product transfer</li> </ul> </li> <li>3. <b>Exposure Controls</b> <p><b><u>Small pieces of AgNP/AgNW-enabled textiles, fabrics, materials, and composites</u></b></p> <ul style="list-style-type: none"> <li>▪ Constant-velocity fume hood or nanomaterial handling enclosure with filtered exhaust when warranted</li> <li>▪ HEPA-filtration exhaust enclosure (such as glove box isolators)</li> <li>▪ Biologic safety cabinet</li> <li>▪ Localized dust-suppression techniques, including ventilation-based (power tool-type) or mist/water-based, where appropriate</li> </ul> <p><b><u>Large pieces of AgNP/AgNW-enabled materials/composites, where use of isolation techniques (such as large ventilated enclosures) are not feasible</u></b></p> <ul style="list-style-type: none"> <li>▪ Ventilated process enclosure or unidirectional down-flow booth with HEPA-filtered exhaust</li> <li>▪ LEV at exposure source with HEPA-filtered exhaust</li> </ul> </li> </ol>

*This information is distributed solely for the purpose of pre-dissemination peer review under applicable information quality guidelines. It has not been formally disseminated by the National Institute for Occupational Safety and Health. It does not represent and should not be construed to represent any agency determination or policy.*

		<ul style="list-style-type: none"> <li>▪ Localized dust-suppression techniques, including ventilation-based (power tool-type) or mist/water-based, where appropriate</li> </ul>
<p><b>Processes requiring the application of high temperatures to Ag metals and alloys</b></p>	<p>Potential exposure to fumes generated during brazing, soldering, welding, and melting of Ag and Ag alloys</p>	<p><b>Exposure Controls</b></p> <ul style="list-style-type: none"> <li>• LEV-based welding fume control approaches should be used, including ventilated enclosing hoods, fixed slot/plenum ventilated worktables, or moveable capture hoods (such as a welding fume extraction unit)</li> <li>• Process-based controls, such as ventilated production welding booths, may be required for large-scale applications where fumes may be generated</li> </ul>

1

2 \*Note: Factors that influence the selection of appropriate engineering controls and other  
 3 exposure control strategies include the physical form (such as dry dispersible powder, fume,  
 4 liquid slurry, or a matrix/composite), task duration, frequency, quantity of the Ag (including  
 5 AgNPs and AgNWs) handled, and task characteristics (how much energy is imparted to the  
 6 material). **The airborne concentration of silver at the potential source of emission should**  
 7 **be measured to confirm the effectiveness of the exposure control measures.** See NIOSH  
 8 documents *Current Strategies for Engineering Controls in Nanomaterial Production and*  
 9 *Downstream Handling Process* [NIOSH 2013b] and *General Safe Practices for Working with*  
 10 *Engineered Nanomaterials in Research Laboratories* [NIOSH 2012] for guidance on the  
 11 selection of appropriate exposure control strategies.

12

### 1 **7.3 Worker Education and Training**

2 Establishing a safety and health program that includes educating and training workers  
3 on the potential hazards of silver, including exposure to silver nanomaterials, is critical  
4 to preventing adverse health effects from exposure. Research has shown that  
5 immediate and long-term objectives can be attained with training when (1) workers are  
6 educated about the potential hazards of their job, (2) knowledge and work practices  
7 become improved, (3) workers are provided the necessary skills to perform their jobs  
8 safely, and (4) management shows commitment and support for workplace safety  
9 [NIOSH 2010]. Requirements for the education and training of workers, as specified in  
10 the OSHA Hazard Communication Standard (29 CFR 1910.1200) [OSHA 2012b], and  
11 as described by Kulinowski and Lippy [2011] for workers exposed to nanomaterials,  
12 provide a minimum set of guidelines that can be used for establishing an education and  
13 training program. Workers who should receive training include those who work directly  
14 with silver nanomaterials, those who are likely to come into contact with or work in close  
15 proximity to silver nanomaterials, and managers or supervisors who are responsible for  
16 assignment and oversight of those workers' tasks.

17 The establishment and oversight of the program should be described in one or more  
18 SOPs to (1) ensure management's commitment to control exposures; (2) identify and  
19 communicate potential hazards to workers; (3) evaluate workplace exposures to silver;  
20 (4) identify and implement engineering controls and effective work practices; (5)  
21 establish documentation; and (6) periodically review the adequacy of exposure controls  
22 and other preventive practices. Management should systematically review and update  
23 these procedures and convey to workers the actions taken to resolve and/or improve  
24 workplace conditions.

25 A program for educating workers should also include both instruction and "hands on"  
26 training that addresses the following:

- 27 • The potential health risks associated with exposure to silver
- 28 • Potential routes of exposure to silver

- 1       • Recognizing effects of exposure
- 2       • The safe handling of silver nanomaterials and silver nanomaterial–containing
- 3           materials to minimize the likelihood of inhalation exposure and skin contact,
- 4           including the proper use of engineering controls, PPE (such as respirators and
- 5           gloves), and good work practices
- 6       • Procedures and tools for avoiding handling silver nanomaterials in powder form
- 7           where possible; ensuring silver nanomaterials are stored in tightly sealed
- 8           containers; cleaning work areas with a HEPA-filtered vacuum or wet-wipes;
- 9           avoiding use of dry sweeping or air hoses; and using hand washing facilities
- 10          before eating, smoking, or leaving the worksite.
- 11       • Instructions for reporting health symptoms
- 12       • The availability and benefits of medical surveillance and screening programs.

#### 13   **7.4 Cleanup and Disposal**

14   Procedures should be developed to protect workers from exposure to silver, with special  
15   emphasis on the safe cleanup and removal of silver nanomaterials from contaminated  
16   surfaces. Inhalation and dermal exposures will likely present the greatest risks. The  
17   potential for inhalation exposure during cleanup will be influenced by the likelihood of  
18   silver nanomaterials becoming airborne, with bulk silver nanomaterials (powder form)  
19   presenting a greater inhalation potential than silver nanomaterials in solution (liquid  
20   form), and liquids in turn presenting a greater potential risk than silver nanomaterials in  
21   encapsulated materials.

22   It would be prudent to base strategies for dealing with spills and contaminated surfaces  
23   on the use of current good practices, together with available information on exposure  
24   risks. Standard approaches for cleaning powder spills can be used for cleaning surfaces  
25   contaminated with silver. These include using HEPA-filtered vacuum cleaners, wiping  
26   up silver (in powder form) with damp cloths, and wetting the powder before wiping.  
27   Liquid spills containing silver nanomaterials can typically be cleaned up with absorbent  
28   materials or liquid traps. If vacuum cleaning is employed, extreme caution should be  
29   taken that HEPA filters are installed properly and that bags and filters are changed

1 according to the manufacturer's recommendations. Dry sweeping or air hoses should  
2 not be used to clean work areas. Task-specific PPE (i.e., designated for spill control)  
3 may be needed, depending on the amount of the spill and its location. A plan should be  
4 in place describing the steps that should be taken to address the issue and the type of  
5 PPE that should be used.

6 Waste (including all cleaning materials) and other contaminated materials (such as  
7 gloves) should be collected in a separate waste stream and be disposed of in  
8 compliance with all applicable regulations (federal, state, and local).

## 9 **7.5 Dermal Protection**

10 Although there are no regulations or guidelines for the selection of clothing or other  
11 apparel protective against exposure specific to silver, OSHA requires employers to  
12 ensure that employees wear appropriate PPE for their work tasks [OSHA 29 CFR  
13 1910.132 (d)(1)].

14 When exposure to AgNPs can occur from the dermal route, PPE (such as protective  
15 clothing, including gloves) is recommended when

- 16 • all technical measures to eliminate or control exposure to Ag, including silver  
17 nanomaterials, have not been successful, or
- 18 • there is a potential for dermal exposure to damaged or abraded skin.

19 Several performance criteria should be considered when selecting the appropriate PPE  
20 [Gao et al. 2014]:

- 21 • Penetration potential
- 22 • Durability (resistance to wear, tear, abrasions, punctures, and chemical  
23 degradation)
- 24 • Dexterity/flexibility
- 25 • Decontamination ability (for multi-use PPE)

- 1 • Comfort
- 2 • Compatibility with other equipment and interface regions (such as the glove/coat
- 3 interface)

4 The limited experimental evidence suggests that airtight fabrics made of nonwoven  
5 textiles are more efficient in protecting workers against nanoparticles than fabrics made  
6 of woven cotton or polyester [Golanski et al. 2009; Golanski et al. 2010]. A study of the  
7 penetration of nanoparticles and submicron particles (30–500 nm) through various  
8 nonwoven fabrics showed penetration levels up to 90% for some of the fabrics tested  
9 [Gao et al. 2011]. Particle penetration was observed to increase as particle size  
10 increased, with some fabrics reaching maximum penetration at 300 nm, and others up  
11 to 500 nm.

12 The challenge when selecting appropriate protective clothing is to strike a balance  
13 between comfort and protection. Garments that provide the highest level of protection  
14 (such as an impermeable Level A suit) are also the least comfortable to wear for long  
15 periods, whereas garments that are probably the least protective (such as a thin cotton  
16 laboratory coat) are the most breathable and comfortable to wear. The efficiency of  
17 commercial gloves in preventing dermal exposure to nanoparticles varies, depending on  
18 the glove material, its thickness, and the manner in which it is used (such as long  
19 exposure times and other chemical exposures) [NanoSafe 2008; Golanski et al. 2009,  
20 2010]. The proper selection of gloves should take into account their resistance to  
21 chemical attack by the nanomaterial and, if it is suspended in liquids, by the liquid itself  
22 [USDOE 2008]. If protective gloves (such as powder-free nitrile, neoprene, and latex  
23 gloves) are used, consider all work activities such as working with sharp instruments,  
24 which may require additional cut proof gloves in addition to chemical protective gloves  
25 [<http://nioshsciencepolicy.cdc.gov/PDF/97-135.pdf>]. Special attention should also be  
26 given to the proper removal and disposal of contaminated gloves to prevent skin  
27 contamination. Gloves should also be visually inspected for tears and routinely  
28 replaced.

29

## 1 **7.6 Respiratory Protection**

2 The decision to use respiratory protection should be based upon hazard assessment  
3 and risk management practices to keep worker inhalation exposure below prescribed  
4 occupational exposure limits. When engineering controls and work practices cannot  
5 reduce worker airborne exposures below the NIOSH REL of 10 µg/m<sup>3</sup> (8-hour TWA) for  
6 total airborne silver (metal dust, fume, and soluble compounds, as Ag) [NIOSH 1988,  
7 2003, 2007] or the NIOSH REL of 0.9 µg/m<sup>3</sup> (respirable mass, 8-hour TWA) for silver  
8 nanomaterials (primary particle size ≤100 nm, workers should be provided respiratory  
9 protection. The use of respirators may also be advisable for certain tasks that place  
10 workers at risk of potentially high peak concentrations of silver, such as cleanup of silver  
11 nanomaterial spills or debris (free form); maintenance of equipment used to process  
12 silver nanomaterials; large processes involving the electro-refining of silver; and  
13 cleaning and/or disposal of filtration systems used to capture airborne silver  
14 nanomaterials.

15 When selecting the appropriate respirator, the respirator program manager should  
16 consider the presence of other potentially hazardous aerosols, such as chemicals  
17 [Rengasamy and Eimer 2011]. On the basis of this information, the respirator program  
18 manager may decide to choose a respirator with a higher assigned protection factor or  
19 one with a higher level of filtration performance (such as changing from an N95 to a  
20 P100). Studies on the filtration performance of N95 filtering facepiece respirators have  
21 found that the mean penetration levels for 40-nm particles range from 1.4% to 5.2%,  
22 indicating that N95 and higher-performing respirator filters would be effective at  
23 capturing airborne AgNPs [Bałazy et al. 2006; Rengasamy et al. 2007, 2008]. Recent  
24 studies show that nanoparticles <20 nm are also effectively captured by NIOSH-  
25 approved filtering facepiece respirators [Rengasamy et al. 2008, 2009]. Other classes of  
26 respirators also can provide a higher level of protection (Table 7-2). The publication  
27 *NIOSH Respirator Selection Logic 2004* provides guidance for selecting an appropriate  
28 respirator [NIOSH 2005].

*This information is distributed solely for the purpose of pre-dissemination peer review under applicable information quality guidelines. It has not been formally disseminated by the National Institute for Occupational Safety and Health. It does not represent and should not be construed to represent any agency determination or policy.*

1 The OSHA respiratory protection standard (29 CFR 1910.134) requires establishment of  
2 a respiratory program for both voluntary and required respirator use. Elements of the  
3 standard include (1) a medical evaluation of each worker's ability to perform the work  
4 while wearing a respirator; (2) regular training of personnel; (3) periodic workplace  
5 exposure monitoring; (4) respirator fit-testing; and (5) respirator maintenance,  
6 inspection, cleaning, and storage. The program should be evaluated regularly, and  
7 respirators should be selected by the person who is in charge of the program and  
8 knowledgeable about the workplace and the limitations associated with each type of  
9 respirator.

10

*This information is distributed solely for the purpose of pre-dissemination peer review under applicable information quality guidelines. It has not been formally disseminated by the National Institute for Occupational Safety and Health. It does not represent and should not be construed to represent any agency determination or policy.*

1 **Table 7-2. Respiratory protection for exposure to silver.**

Workplace Airborne Concentrations of Silver or Conditions of Use <sup>a</sup> Options	Minimum Respiratory Protection
0.9–9.0 µg/m <sup>3</sup> (up to 10 × REL)	Any filtering facepiece respirator or air-purifying, elastomeric half-facepiece respirator equipped with appropriate type of particulate filter <sup>b</sup> ; any negative-pressure (demand), supplied-air respirator equipped with a half-mask
≤22.5 µg/m <sup>3</sup> (up to 25 × REL)	Any powered, air-purifying respirator equipped with a hood or helmet and a HEPA filter; any continuous-flow supplied-air respirator equipped with a hood or helmet
≤45.0 µg/m <sup>3</sup> (up to 50 × REL)	Any air-purifying full-facepiece respirator equipped with N-100, R-100, or P-100 filter; any powered air-purifying respirator equipped with a tight-fitting half-facepiece and a HEPA filter; any negative-pressure (demand) supplied-air respirator equipped with a full facepiece; any continuous-flow supplied-air respirator with a tight-fitting half-facepiece; any negative-pressure (demand) self-contained respirator equipped with a full facepiece

(Continued)

2

*This information is distributed solely for the purpose of pre-dissemination peer review under applicable information quality guidelines. It has not been formally disseminated by the National Institute for Occupational Safety and Health. It does not represent and should not be construed to represent any agency determination or policy.*

1 **Table 7-2 (Continued)**

Workplace airborne concentrations of silver or conditions of use options	Minimum respiratory protection
≤900 µg/m <sup>3</sup> ( up to 1,000 × REL)	Any pressure-demand supplied-air respirator equipped with a full facepiece

2

3 <sup>a</sup>The protection offered by a given respirator is contingent upon (1) the respirator user adhering  
 4 to complete program requirements (such as those required by OSHA in 29 CFR 1910.134), (2)  
 5 the use of NIOSH-certified respirators in their approved configuration, and (3) individual fit  
 6 testing to rule out those respirators for which a good fit cannot be achieved.

7 <sup>b</sup>The appropriate type of particulate filter means any 95- or 100-series (N, R, or P) filter. Note:  
 8 N-95 or N-100 series filters should not be used in environments where there is potential for  
 9 exposure to oil mists.

10 Note: Complete information on the selection of respirators can be found at (1) OSHA 3352-02  
 11 2009, *Assigned Protection Factors for the Revised Respiratory Protection Standard*, at  
 12 <http://www.osha.gov/Publications/3352-APF-respirators.html>, and (2) NIOSH  
 13 [<http://www.cdc.gov/niosh/docs/2005-100/default.html>].

## 1 **7.7 Occupational Health Surveillance**

2 Occupational health surveillance involves the ongoing systematic collection, analysis,  
3 and dissemination of exposure and health data on groups of workers for the purpose of  
4 preventing illness and injury. Occupational health surveillance is an essential  
5 component of an effective occupational safety and health program [Harber et al. 2003;  
6 Baker and Matte 2005; NIOSH 2006; Wagner and Fine 2008; Trout and Schulte 2010],  
7 and NIOSH continues to recommend occupational health surveillance as an important  
8 part of an effective risk management program. Occupational health surveillance  
9 includes the elements of hazard and medical surveillance.

### 10 **7.7.1 Hazard surveillance**

11 Hazard surveillance includes hazard and exposure assessment (see Sections 7 and  
12 7.1). Development of the job hazard analysis (discussed in Section 7.1) includes  
13 identification of hazards in the workplace and review of the best available information  
14 concerning toxicity of materials; such information may come from databases, texts, and  
15 published literature or available regulations or recommendations (such as from NIOSH  
16 or OSHA). Human studies, such as epidemiologic investigations and case series or  
17 reports, and animal studies may also provide valuable information. Currently, there are  
18 limited toxicological data and a lack of epidemiologic data pertaining to silver  
19 nanomaterials with which to make a complete hazard assessment. Exposure  
20 assessment involves evaluating relevant exposure route(s) (inhalation, ingestion,  
21 dermal, and/or injection), amount, duration, and frequency, as well as whether exposure  
22 controls are in place and how protective they are. Hazard surveillance for AgNPs  
23 provides information that is used in evaluating and implementing workplace controls.

### 24 **7.7.2 Medical screening and surveillance**

25 Medical surveillance targets actual health events or a change in a biologic function of an  
26 exposed person or persons. Medical surveillance involves the ongoing evaluation of the  
27 health status of a group of workers through the collection and aggregate analysis of

*This information is distributed solely for the purpose of pre-dissemination peer review under applicable information quality guidelines. It has not been formally disseminated by the National Institute for Occupational Safety and Health. It does not represent and should not be construed to represent any agency determination or policy.*

1 health data, for the purpose of preventing disease and evaluating the effectiveness of  
2 intervention programs (primary prevention). NIOSH recommends medical surveillance  
3 of workers when they are exposed to hazardous materials and therefore are at risk of  
4 adverse health effects from such exposures. Medical screening is a form of medical  
5 surveillance used to detect early signs of work-related illness in individual workers. It  
6 involves administering tests to apparently healthy persons to detect those with early  
7 stages of disease or risk of disease.

8 Medical screening and surveillance provide a second line of defense, behind the  
9 implementation of engineering, administrative, and work practice controls (including  
10 personal protective equipment). Integration of hazard and medical surveillance is key to  
11 an effective occupational health surveillance program [Trout and Schulte 2010; Schulte  
12 and Trout 2011; Schulte et al. 2016].

13 Based on the evidence summarized in this document, NIOSH concludes that workers  
14 occupationally exposed to airborne concentrations of silver above the NIOSH REL for  
15 total silver (10  $\mu\text{g}/\text{m}^3$ , 8-hr TWA) or the NIOSH REL for silver nanomaterials (0.9  $\mu\text{g}/\text{m}^3$ ,  
16 8-hr TWA) may potentially be at risk of developing argyria. In addition, workers  
17 exposed above the REL for silver nanomaterials may potentially be at risk of developing  
18 early-stage adverse lung and liver effects.

19 Currently there is insufficient scientific and medical evidence to recommend the specific  
20 medical screening of workers potentially exposed to silver nanomaterials. If medical  
21 screening recommendations are currently used in the workplace for total silver, those  
22 same screening recommendations would be applicable for workers exposed to silver  
23 nanomaterials as well.

24 As research into the potential hazards of silver nanomaterials continues, periodic  
25 reassessment of available data is critical to determine whether specific medical  
26 screening may be warranted. In the interim, the following recommendations related to  
27 occupational health surveillance are provided for workplaces where workers may be  
28 exposed to silver nanomaterials in the course of their work [NIOSH2009a]:

*This information is distributed solely for the purpose of pre-dissemination peer review under applicable information quality guidelines. It has not been formally disseminated by the National Institute for Occupational Safety and Health. It does not represent and should not be construed to represent any agency determination or policy.*

- 1 - Take prudent measures to control exposures to silver nanomaterials;
- 2 - Conduct hazard surveillance as the basis for implementing controls; and
- 3 - Use established medical surveillance approaches [NIOSH 2009a].

## 1 **8 Research Needs**

2 Additional data and information are needed to ascertain the occupational safety and  
3 health concerns of working with all forms of silver. Data are particularly needed on  
4 sources of exposure to silver nanomaterials (such as AgNPs and AgNWs) and on  
5 factors that influence workers' exposure; exposure control measures (such as  
6 engineering controls) and work practices that are effective in reducing worker exposures  
7 to below the NIOSH REL; and appropriate measurement methods and exposure metrics  
8 for characterizing workplace exposures. In vitro and in vivo studies with silver of  
9 different physical-chemical properties are needed to better understand the role of  
10 particle size, shape, surface charge, chemical composition, dissolution rate, and surface  
11 treatment in causing toxicity. Chronic inhalation studies in animals may provide  
12 information about the long-term potential for adverse health effects in workers.

13 Information gathered from the following research is needed to determine the appropriate  
14 risk management practices for protecting workers occupationally exposed to silver,  
15 including silver nanomaterials:

- 16 (1) Identification of industries or occupations in which exposures to silver may  
17 occur, including trends in the production and use of silver nanomaterials
- 18 (2) Description of work tasks and scenarios with a potential for exposure to silver  
19 nanomaterials
- 20 (3) Information on measurement methods and exposure metrics to quantify  
21 worker exposure to silver nanomaterials, including information on the utility  
22 and limitations of those methods for quantifying exposures
- 23 (4) Workplace exposure measurement data from the industries, jobs, and tasks  
24 where silver nanomaterials are manufactured and used
- 25 (5) Studies on the design and effectiveness of control measures (such as  
26 engineering controls, work practices, PPE) being used in the workplace to  
27 minimize worker exposure to silver, including silver nanomaterials

- 1 (6) Case reports or other health information demonstrating potential health  
2 effects in workers exposed to silver nanomaterials
- 3 (7) Epidemiologic studies of workers including quantitative exposure estimates by  
4 silver type and particle size
- 5 (8) Complementary in vivo and in vitro studies with silver nanomaterials to  
6 ascertain the role of particle size and other physical-chemical properties on  
7 the toxicity of silver, including quantitative dose measures in vitro that are  
8 comparable to in vivo doses. Studies should examine a standard set of  
9 physicochemical properties including: particle size and size dispersion  
10 (monodispersity, polydispersity), shape, zeta potential, surface coating,  
11 agglomeration, age of the sample, ion-producing potential, and dissolution  
12 rate. Studies should include the use of an accepted Ag reference material  
13 (e.g., National Institute of Standards and  
14 Technology) as a control.
- 15 (9) Studies to further elucidate the biological mechanisms of the toxicity of silver  
16 nanomaterials, including the dissolution rate and interactions with cellular and  
17 subcellular structures and cellular bioprocessing.
- 18 (10) Studies to determine genotoxicity and potential effects in other target  
19 organs, including the nervous and reproductive systems, following longer  
20 exposure durations.
- 21 (11) Long-term animal inhalation studies with AgNPs and AgNWs of different  
22 compositions and dimensions to assess biodistribution/accumulation and  
23 chronic effects; studies should include the use of an accepted AgNP  
24 reference material (e.g., National Institute of Standards and Technology  
25 [NIST 2015]) as a control.
- 26 (12) Further validation of the PBPK models of silver nanomaterials (e.g.,  
27 Bachler et al. [2013] used in the NIOSH risk assessment) to estimate silver  
28 tissue doses in rodents and humans by particle size and solubility, including  
29 utilization of experimental data on the interactions between silver  
30 nanoparticles and biological compounds, and possible changes in particle  
31 properties that could influence the toxicokinetics.

*This information is distributed solely for the purpose of pre-dissemination peer review under applicable information quality guidelines. It has not been formally disseminated by the National Institute for Occupational Safety and Health. It does not represent and should not be construed to represent any agency determination or policy.*

- 1           (13)   Studies investigating the effects of AgNP modification on AgNP toxicity;
- 2                 these studies should focus on modifications driven by trends in industrial
- 3                 interest and may include AgNPs that are functionalized, coated, or made up
- 4                 of silver-containing polymer. Relevant data include how such modifications
- 5                 affect dissolution rate, partitioning in vivo, and the lifespan of the modification.
- 6           (14)   Studies of potential biomarkers of adverse lung or liver effects associated
- 7                 with exposure to silver nanoparticles.

## 9 References

- 1
- 2
- 3 ACGIH [2001]. Silver and compounds. In: Documentation of threshold limit values and  
4 biological exposure indices. 7th ed. Vol. 1. Cincinnati, OH: American Conference of  
5 Governmental Industrial Hygienists.
- 6 ACGIH [2010]. Industrial ventilation: a manual of recommended practice for operation  
7 and maintenance. Cincinnati, OH: American Conference of Governmental Industrial  
8 Hygienists.
- 9 ACGIH [2013]. Industrial ventilation: a manual of recommended practice for design.  
10 Cincinnati, OH: American Conference of Governmental Industrial Hygienists.
- 11 Ahamed M, Karns M, Goodson M, Rowe J, Hussain SM, Schlager JJ, Hong Y [2008].  
12 DNA damage response to different surface chemistry of silver nanoparticles in  
13 mammalian cells. *Toxicol Appl Pharmacol* 233(3):404–410.
- 14 Aktepe N, Kocyigit A, Yukselten Y, Taskin A, Keskin C, Celik H [2015]. Increased DNA  
15 damage and oxidative stress among silver jewelry workers. *Biol Trace Elem Res* 164(2):  
16 185–191.
- 17 Amato C, Hussain S, Hess K, Schlager J [2006]. Interaction of nanomaterials with  
18 mouse keratinocytes. *The Toxicologist* 90(1-S):168.
- 19 Anderson DS, Patchin ES, Silva RM, Uyeminami DL, Sharmah A, Guo T, Das GK,  
20 Brown JM, Shannahan J, Gordon T, Chen LC, Pinkerton KE, van Winkle LS [2015a].  
21 Influence of particle size on persistence and clearance of aerosolized silver  
22 nanoparticles in the rat lung. *Toxicol Sci* 144(2):366–381.
- 23

*This information is distributed solely for the purpose of pre-dissemination peer review under applicable information quality guidelines. It has not been formally disseminated by the National Institute for Occupational Safety and Health. It does not represent and should not be construed to represent any agency determination or policy.*

- 1 Anderson DS, Silva RM, Lee D, Edwards PC, Sharmah A, Guo T, Pinkerton KE, van  
2 Winkle LS [2015b]. Persistence of silver nanoparticles in the rat lung: influence of dose,  
3 size and chemical composition. *Nanotoxicology* 9(5):591–602.
- 4 ARA [2011]. Multiple-path particle deposition (MPPD 2.1): a model for human and rat  
5 airway particle dosimetry. Raleigh, NC: Applied Research Associates, Inc.
- 6 Arai Y, Miyayama T, Hirano S [2015]. Difference in the toxicity mechanism between ion  
7 and nanoparticle forms of silver in the mouse lung and in macrophages. *Toxicology* 328:  
8 84–92, <http://dx.doi.org/10.1016/j.tox.2014.12.014>.
- 9 Armitage SA, White MA, Wilson HK [1996]. The determination of silver in whole blood  
10 and its application to biological monitoring of occupationally exposed groups. *Ann*  
11 *Occup Hyg* 40(3):331–338.
- 12 Arora S, Jain J, Rajwade JM, Paknikar KM [2008]. Cellular responses induced by silver  
13 nanoparticles: in vitro studies. *Toxicol Lett* 179(2):93–100.
- 14 Arora S, Jain J, Rajwade JM, Paknikar KM [2009]. Interactions of silver nanoparticles  
15 with primary mouse fibroblasts and liver cells. *Toxicol Appl Pharmacol* 236(3):310–318.
- 16 AshaRani PV, Mun GLK, Hande MP, Valiyaveetil S [2009]. Cytotoxicity and  
17 genotoxicity of silver nanoparticles in human cells. *ACS Nano* 3(2):279–290.
- 18 Ashraf A, Sharif R, Ahmad M, Masood M, Shahid A, Anjum DH, Rafique MS, Ghani S  
19 [2015]. In vivo evaluation of the biodistribution of intravenously administered naked and  
20 functionalised silver nanoparticles in rabbit. *IET Nanobiotechnol* 9(6):368–374.
- 21 ATSDR [1990]. Toxicological profile for silver. TP-90-24. Atlanta, GA: Agency for Toxic  
22 Substances and Disease Registry.

*This information is distributed solely for the purpose of pre-dissemination peer review under applicable information quality guidelines. It has not been formally disseminated by the National Institute for Occupational Safety and Health. It does not represent and should not be construed to represent any agency determination or policy.*

- 1 Austin CA, Umbreit TH, Brown KM, Barber DS, Dair BJ, Francke-Carroll S, Feswick A,  
2 Saint-Louis MA, Hikawa H, Siebein KN, Goering PL [2012]. Distribution of silver  
3 nanoparticles in pregnant mice and developing embryos. *Nanotoxicology* 6(8):912–922.
- 4 Avalos A, Haza AI, Mateo D, Morales P [2015]. Effects of silver and gold nanoparticles  
5 of different sizes in human pulmonary fibroblasts. *Toxicol Mech Methods* 25(4): 287–  
6 295, <http://dx.doi.org/10.3109/15376516.2015.1025347>.
- 7 Avalos Funez A, Isabel Haza A, Mateo D, Morales P [2013]. In vitro evaluation of silver  
8 nanoparticles on human tumoral and normal cells. *Toxicol Mech Methods* 23(3):153–  
9 160, <http://dx.doi.org/10.3109/15376516.2012.762081>.
- 10 Bachler G, von Goetz N, Hungerbühler K [2013]. A physiologically based  
11 pharmacokinetic model for ionic silver and silver nanoparticles. *Intl J Nanomed* 8:3365–  
12 3382.
- 13 Baker EL, Matte TP [2005]. Occupational health surveillance. In: Rosenstock L, Cullen  
14 E, Brodtkin R, eds. *Textbook of clinical occupational and environmental medicine*.  
15 Philadelphia, PA: Elsevier Saunders,  
16 <http://www.osha.gov/SLTC/medicals-surveillance/surveillance.html>.
- 17 Bałazy A, Toivola M, Reponen T, Podgorski A, Zimmer A, Grinshpun SA [2006].  
18 Manikin-based performance evaluation of N95 filtering facepiece respirators challenged  
19 with nanoparticles. *Ann Occup Hyg* 50(3):259–269.
- 20 Beer C, Foldbjerg R, Hayashi Y, Sutherland DS, Autrup H [2012]. Toxicity of silver  
21 nanoparticles: nanoparticle of silver ion? *Toxicol Lett* 208:286–292.
- 22 Bell RA, Kramer JR [1999]. Structural chemistry and geochemistry of silver-sulfur  
23 compounds: critical review. *Environ Toxicol Chem* 18(1):9–22.

*This information is distributed solely for the purpose of pre-dissemination peer review under applicable information quality guidelines. It has not been formally disseminated by the National Institute for Occupational Safety and Health. It does not represent and should not be construed to represent any agency determination or policy.*

- 1 Bergin IL, Wilding LA, Morishita M, Walacavage K, Ault AP, Axson JL, Stark DI,  
2 Hashway SA, Capracotta SS, Leroueil PR, Matnard AD, Philbert MA [2016]. Effects of  
3 particle size and coating on toxicological parameters, fecal elimination kinetics, and  
4 tissue distribution of acutely ingested silver nanoparticles in a mouse model.  
5 *Nanotoxicology* 10(3):352–360.  
6
- 7 Botelho DJ, Leo BF, Massa CB, Sarkar S, Tetley TD, Chung KF, Chen S, Ryan MP,  
8 Porter AE, Zhang J, Schwander SK, Gow AJ [2016]. Low-dose AgNPs reduce lung  
9 mechanical function and innate immune defense in the absence of cellular toxicity.  
10 *Nanotoxicology* 10(1):118–127.  
11
- 12 Boudreau MD, Imam MS, Paredes AM, Bryant MS, Cunningham CK, Felton RP, Jones  
13 MY, Davis KJ, Olson GR [2016]. Differential effects of silver nanoparticles and silver  
14 ions on tissue accumulation, distribution, and toxicity in the Sprague Dawley rat  
15 following daily oral gavage administration for 13 weeks. *Toxicol Sci* 150:131–160.  
16
- 17 Braakhuis H, Gosens I, Krystek P, Boere J, Cassee F, Fokkens P, Post J, van Loveren  
18 H, Park M [2014]. Particle size dependent deposition and pulmonary inflammation after  
19 short-term inhalation of silver nanoparticles. *Particle Fibre Toxicol* 11:49.
- 20 Braakhuis HM, Giannakou C, Peijnenburg WJ, Vermeulen J, van Loveren H, Park MV  
21 [2016]. Simple in vitro models can predict pulmonary toxicity of silver nanoparticles.  
22 *Nanotoxicology* 10(6):770–779, <http://dx.doi.org/10.3109/17435390.2015.1127443>.
- 23 Braydich-Stolle LK, Lucas B, Schrand A, Murdock RC, Lee T, Schlager JJ, Hussain SM,  
24 Hofmann MC [2010]. Silver nanoparticles disrupt GDNF/Fyn kinase signaling in  
25 spermatogonial stem cells. *Toxicol Sci* 116(2):577–589.
- 26 Brookhaven National Laboratory [2014]. IH75190 surface wipe sampling procedure.  
27 Upton, NY: Brookhaven National Laboratory,  
28 [https://www.bnl.gov/esh/shsd/sop/pdf/IH\\_SOPS/IH75190.pdf](https://www.bnl.gov/esh/shsd/sop/pdf/IH_SOPS/IH75190.pdf).

*This information is distributed solely for the purpose of pre-dissemination peer review under applicable information quality guidelines. It has not been formally disseminated by the National Institute for Occupational Safety and Health. It does not represent and should not be construed to represent any agency determination or policy.*

- 1 Brouwer D, van Duuren-Stuurman B, Berges M, Jankowska E, Bard D, Mark D [2009].  
2 From workplace air measurement results toward estimates of exposure? Development  
3 of a strategy to assess exposure to manufactured nano-objects. *J Nanopart Res*  
4 *11(8):1867–1881.*
- 5 Brune D, Nordberg G, Wester PO [1980]. Distribution of 23 elements in the kidney, liver  
6 and lungs of workers from a smeltery and refinery in North Sweden exposed to a  
7 number of elements and of a control group. *Sci Total Environ* *16(1):13–35.*
- 8 Bucher JR, Portier CJ, Goodman JI, Faustman EM, Lucier GW [1996]. Workshop  
9 overview - National Toxicology Program studies: Principles of dose selection and  
10 applications to mechanistic based risk assessment. *Fundam Appl Toxicol* *31:1-8.*
- 11 Buckley WR [1963]. Localized argyria. *Arch Derm* *88:531–539.*
- 12 Bullock W, Ignacio JS, eds. [2006]. A strategy for assessing and managing occupational  
13 exposures. 3rd ed. Fairfax, VA: AIHA Press.
- 14 Campagnolo L, Massimiani M, Vecchione L, Piccirilli D, Toschi N, Magrini A, Bonanno  
15 E, Scimeca M, Castagnozzi L, Buonanno G, Stabile L, Cubadda F, Aureli F, Fokkens  
16 PH, Kreyling WG, Cassee FR, Pietroiusti A [2017]. Silver nanoparticles inhaled during  
17 pregnancy reach and affect the placenta and the foetus. *Nanotoxicology* *11(5):687-698.*
- 18 Carlson C, Hussain SM, Schrand AM, Braydich-Stolle LK, Hess KL, Jones RL, Schlager  
19 JJ [2008]. Unique cellular interaction of silver nanoparticles: size-dependent generation  
20 of reactive oxygen species. *J Phys Chem B* *112(43):13608–13619.*
- 21 Catsakis LH, Sulica VI [1978]. Allergy to silver amalgams. *Oral Surg* *46:371–375.*
- 22 Chairuankitti P, Lawanprasert S, Roytrakul S, Aueviriyavit S, Phummiratch D, Kulthong  
23 K, Chanvorachote P, Maniratanachote R [2013]. Silver nanoparticles induce toxicity in

- 1 a549 cells via ros-dependent and ros-independent pathways. *Toxicol In Vitro*  
2 27(1):330–338, <http://dx.doi.org/10.1016/j.tiv.2012.08.021>.
- 3 Chang AL, Khosravi V, Egbert B [2006]. A case of argyria after colloidal silver ingestion.  
4 *J Cutan Pathol* 33(12):809–811.
- 5 Chen R, Zhao L, Bai R, Liu Y, Han L, Xu Z, Chen F, Autrup H, Long D, Chen C [2016].  
6 Silver nanoparticles induced oxidative and endoplasmic reticulum stresses in mouse  
7 tissues: implications for the development of acute toxicity after intravenous  
8 administration. *Toxicol Res 01 March*(2):602–608.  
9
- 10 Chen X, Schluesener HJ [2008]. Nanosilver: a nanoparticle in medical application.  
11 *Toxicol Lett* 176(1):1–12.
- 12 Cheng KH, Cheng YS, Yeh HC, Guilmette RA, Simpson SQ, Yang YH, Swift DL [1996].  
13 In vivo measurements of nasal airway dimensions and ultrafine aerosol deposition in the  
14 human nasal and oral airways. *J Aerosol Sci* 27(5):785–801.
- 15 Cho EA, Lee WS, Kim KM, Kim S-Y [2008]. Occupational generalized argyria after  
16 exposure to aerosolized silver. *J Dermatol* 35:759–760.
- 17 Cho W-S, Duffin R, Donaldson K [2012]. Zeta potential and solubility to toxic ions as  
18 mechanisms of lung inflammation caused by metal/metal oxide nanoparticles. *Toxicol*  
19 *Sci* 126(2):469–477.
- 20 Chrastina A, Schnitzer JE [2010]. Iodine-125 radiolabeling of silver nanoparticles for in  
21 vivo SPECT imaging. *Int J Nanomed* 5:653–659.
- 22 Christensen FM, Johnston HJ, Stone V, Aitken RJ, Hankin S, Peters S, Aschberger K  
23 [2010]. Nano-silver - feasibility and challenges for human health risk assessment based  
24 on open literature. *Nanotoxicology* 4(3):284-295.

*This information is distributed solely for the purpose of pre-dissemination peer review under applicable information quality guidelines. It has not been formally disseminated by the National Institute for Occupational Safety and Health. It does not represent and should not be construed to represent any agency determination or policy.*

- 1 Chuang H-C, Hsiao T-C, Wu C-K, Chang H-H, Lee C-H, Chang C-C, Cheng T-J [2013].  
2 Allergenicity and toxicology of inhaled silver nanoparticles in allergen-provocation mice  
3 models. *Internat J Nanomed* 8:4495–4506.  
4
- 5 Coccini T, Manzo L, Bellotti V, De Simone U [2014]. Assessment of cellular responses  
6 after short- and long-term exposure to silver nanoparticles in human neuroblastoma (sh-  
7 sy5y) and astrocytoma (d384) cells. *Sci World J* 2014:Article ID 259765,  
8 <http://dx.doi.org/10.1155/2014/259765>.
- 9 Connolly M, Fernandez-Cruz ML, Quesada-Garcia A, Alte L, Segner H, Navas JM  
10 [2015]. Comparative cytotoxicity study of silver nanoparticles (agnps) in a variety of  
11 rainbow trout cell lines (rtl-w1, rth-149, rtg-2) and primary hepatocytes. *Int J Environ*  
12 *Res Public Health*, 12(5):5386–5405, <http://dx.doi.org/10.3390/ijerph120505386>.
- 13 Corn M, Esmen N [1979]. Workplace exposure zones for classification of employee  
14 exposure to physical and chemical agents. *Am Ind Hyg Assoc* 40:47–57.
- 15 Cotton CV, Spencer LG, New RP, Cooper RG [2017]. The utility of comprehensive  
16 autoantibody testing to differentiate connective tissue disease associated and idiopathic  
17 interstitial lung disease subgroup cases. *Rheumatology* 56:1264-1271.
- 18 Cronholm P, Karlsson HL, Hedberg J, Lowe TA, Winnberg L, Elihn K, Wallinder IO,  
19 Möller L [2013]. Intracellular uptake and toxicity of Ag and CuO nanoparticles: a  
20 comparison between nanoparticles and their corresponding metal ions. *Small* 9(7):970–  
21 982.
- 22 Crump KS [1984]. A new method for determining allowable daily intakes. *Fund Appl*  
23 *Toxicol* 4(5):854–871.

*This information is distributed solely for the purpose of pre-dissemination peer review under applicable information quality guidelines. It has not been formally disseminated by the National Institute for Occupational Safety and Health. It does not represent and should not be construed to represent any agency determination or policy.*

- 1 Dabrowska-Bouta B, Zieba M, Orzelska-Gorka J, Skalska J, Sulkowski G, Frontczak-  
2 Baniewicz M, Talarek S, Listos J, Struzynska L [2016]. Influence of a low dose of silver  
3 nanoparticles on cerebral myelin and behavior of adult rats. *Toxicology* 363:29–36.  
4
- 5 Davenport LL, Hsieh H, Eppert BL, Carreira VS, Krishan M, Ingle T, Howard PC,  
6 Williams MT, Vorhees CV, Genter MB [2015]. Systemic and behavioral effects of  
7 intranasal administration of silver nanoparticles. *Neurotoxicol Teratol* 51:68–76.  
8
- 9 De Jong WH, Van Der Ven LT, Sleijffers A, Park MV, Jansen EH, Van Loveren H,  
10 Vandebriel RJ [2013]. Systemic and immunotoxicity of silver nanoparticles in an  
11 intravenous 28 days repeated dose toxicity study in rats. *Biomaterials* 34:8333–8343.  
12
- 13 Deng F, Olesen P, Foldbjerg R, Dang DA, Guo X, Autrup H [2010]. Silver nanoparticles  
14 upregulate connexin43 expression and increase gap junctional intercellular  
15 communication in human lung adenocarcinoma cell line A549. *Nanotoxicol* 4:186–195.
- 16 DFG [2013]. Deutsche Forschungsgemeinschaft. List of MAK and BAT values 2013.  
17 Weinheim, Germany: Wiley-VCH Verlag GmbH & Co. KGaA. ISBN: 978-3-527-33616-6.
- 18 DiVincenzo GD, Giordano CJ, Schriever LS [1985]. Biologic monitoring of workers  
19 exposed to silver. *Int Arch Occup Environ Health* 56:207–215.
- 20 Dong MS, Choi JY, Sung JH, Kim JS, Song KS, Ryu HR, Lee JH, Bang IS, An K, Park  
21 HM, Song NW, Yu IJ [2013]. Gene expression profiling of kidneys from Sprague-Dawley  
22 rats following 12-week inhalation exposure to silver nanoparticles. *Toxicol Mech*  
23 *Methods* 23(6):437–448.
- 24 Drake PL, Hazelwood KJ [2005]. Exposure-related health effects of silver and silver  
25 compounds: a review. *Ann Occup Hyg* 49(7):575–585.

*This information is distributed solely for the purpose of pre-dissemination peer review under applicable information quality guidelines. It has not been formally disseminated by the National Institute for Occupational Safety and Health. It does not represent and should not be construed to represent any agency determination or policy.*

- 1 Duan N, Mage T [1997]. Combination of direct and indirect approaches for exposure  
2 assessment. *J Expo Anal Environ Epidemiol* 7(4):439–470.
- 3 Dziendzikowska K, Gromadzka-Ostrowska J, Lankoff A, Oczkowski M, Krawczynska A,  
4 Chwastowska J, Sadowska-Bratek M, Chajduk E, Wojewodzka M, Dusinska M,  
5 Kruszewski M [2012]. Time-dependent biodistribution and excretion of silver  
6 nanoparticles in male Wistar rats. *J Appl Toxicol* 32:920–928.
- 7 ECHA [2008]. REACH guidance on information requirements and chemicals safety  
8 assessment. Chapter R.8. European Chemicals Agency (ECHA),  
9 <http://guidance.echa.europa.eu/>.
- 10 Elle RE, Gaillet S, Vide J, Romain C, Lauret C, Rugani N, Cristol JP, Rouanet JM  
11 [2013]. Dietary exposure to silver nanoparticles in Sprague-Dawley rats: effects on  
12 oxidative stress and inflammation. *Food Chem Toxicol* 60:297–301.
- 13
- 14 Elzey S, Grassian VH [2010]. Agglomeration, isolation, and dissolution of commercially  
15 manufactured silver nanoparticles in aqueous environments. *J Nanoparticle Res*  
16 12:1945–1958.
- 17 Eustis SL, Boorman GA, Harada T, Popp JA [1990]. Liver. In: Boorman GA, Eustis SL,  
18 Elwell MR, Montgomery CA Jr, MacKenzie WF, eds. *Pathology of the Fischer rat:*  
19 *reference and atlas*. New York: Academic Press.
- 20 Evanoff DD, Chumanov G [2005]. Synthesis and optical properties of silver  
21 nanoparticles and arrays. *Chem Phys Chem* 6:1221–1231.
- 22 Fennell TR, Mortensen NP, Black SR, Snyder RW, Levine KE, Poitras E, Harrington  
23 JM, Wingard CJ, Holland NA, Pathmasiri W, Sumner SC [2017]. Disposition of  
24 intravenously or orally administered silver nanoparticles in pregnant rats and the effect  
25 on the biochemical profile in urine. *J Appl Toxicol* 37(5):530–544.

- 1
- 2 Foldbjerg R, Dang DA, Autrup H [2011]. Cytotoxicity and genotoxicity of silver  
3 nanoparticles in the human lung cancer cell line, A549. *Arch Toxicol* 85(7):743–750.
- 4 Foldbjerg R, Irving ES, Hayaski Y, Sutherland DS, Thorsen K, Autrup H, Beer C [2012].  
5 Global gene expression profiling of human lung epithelial cells after exposure to  
6 nanosilver. *Toxicol Sci* 130(1):145–157.
- 7 Foldbjerg R, Olesen P, Hougaard M, Dang DA, Hoffmann HJ, Autrup H [2009]. PVP-  
8 coated silver nanoparticles and silver ions induce reactive oxygen species, apoptosis  
9 and necrosis in THP-1 monocytes. *Toxicol Lett* 190(2):156–162.
- 10 Furchner JE, Richmond CR, Drake GA [1968]. Comparative metabolism of  
11 radionuclides in mammals-IV. Retention of silver 110m in the mouse, rat, monkey and  
12 dog. *Health Physics* 15:505–514.
- 13 Future Markets, Inc. [2013]. The global nanotechnology and nanomaterials industry.  
14 Technology Report No. 68, [www.futuremarketsinc.com](http://www.futuremarketsinc.com).
- 15 Gaiser BK, Hirn S, Kermanizadeh A, Kanase N, Fytianos K, Wenk A, Haberl N, Brunelli  
16 A, Kreyling WG, Stone V [2013]. Effects of silver nanoparticles on the liver and  
17 hepatocytes in vitro. *Toxicol Sci*, 131(2):537–547,  
18 <http://dx.doi.org/10.1093/toxsci/kfs306>.
- 19 Gao P, Behar JL, Shaffer R [2014]. Considerations for selection of PPE to protect  
20 against nanoparticle dermal exposure. In Daniel Anna, ed. *Chemical Protective*  
21 *Clothing*. 2<sup>nd</sup> printing of 2<sup>nd</sup> ed. Fairfax, VA: AIHA Press, pp. 511–555.
- 22 Gao P, Jaques PA, Hsiao T, Shepherd A, Eimer BC, Yang M, Miller A, Gupta B, Shaffer  
23 R [2011]. Evaluation of nano- and submicron particle penetration through ten nonwoven  
24 fabrics using a wind-driven approach. *J Occup Environ Hyg* 8(1):13–22.

*This information is distributed solely for the purpose of pre-dissemination peer review under applicable information quality guidelines. It has not been formally disseminated by the National Institute for Occupational Safety and Health. It does not represent and should not be construed to represent any agency determination or policy.*

- 1 Garcia T, Lafuente D, Blanco J, Sanchez DJ, Sirvent JJ, Domingo JL, Gomez M [2016].  
2 Oral subchronic exposure to silver nanoparticles in rats. *Food Chem Toxicol* 92:177–  
3 187.  
4
- 5 Garcia-Reyero N, Kennedy AJ, Escalon BL, Habib T, Laird JG, Rawat A, Wiseman S,  
6 Hecker M, Denslow N, Steevens JA, Perkins EJ [2014]. Differential effects and potential  
7 adverse outcomes of ionic silver and silver nanoparticles in vivo and in vitro. *Environ Sci*  
8 *Technol*, 48(8):4546-4555, <http://dx.doi.org/10.1021/es4042258>.
- 9 Genter MB, Newman NC, Shertzer HG, Ali SF, Bolon B [2012]. Distribution and  
10 systemic effects of intranasally administered 25 nm silver nanoparticles in adult mice.  
11 *Toxicol Pathol* 40(7):1004–1013.  
12
- 13 Gliga AR, Skoglund S, Wallinder IO, Fadeel B, Karisson HL [2014]. Size-dependent  
14 cytotoxicity of silver nanoparticles in human lung cells: the role of cellular uptake,  
15 agglomeration and Ag release. *Particle Fibre Toxicol*, doi:10.1186/1743-8977-11-11.
- 16 Golanski L, Guiot A, Rouillon F, Pocachard J, Tardif F [2009]. Experimental evaluation  
17 of personal protection devices against graphite nanoaerosols: fibrous filter media,  
18 masks, protective clothing, and gloves. *Hum Exp Toxicol* 28(6–7):353–359.
- 19 Golanski L, Guiot A, Tardif F [2010]. Experimental evaluation of individual protection  
20 devices against different types of nanoaerosols: graphite, TiO<sub>2</sub> and Pt. *J Nanopart Res*  
21 12(1):83–89.
- 22 Gopinath P, Gogoi SK, Sanpui P, Paul A, Chattopadhyay A, Ghosk SS [2010]. Signaling  
23 gene cascade in silver nanoparticle induced apoptosis. *Colloids and Surface B:*  
24 *Biointerfaces* 77:240–245.
- 25 Gosens I, Kermanizadeh A, Jacobsen NR, Lenz A-G, Bokkers B, de Jong, WH, Krystek  
26 P, Tran L, Stone V, Wallin H, Stoeger T, Cassee FR [2015]. Comparative hazard

- 1 identification by a single dose lung exposure of zinc oxide and silver nanomaterials in  
2 mice. PLOS ONE, doi:10.1371/journal.pone.0126934.
- 3 Gregoratto, D, Bailey, M.R, Marsh, J.W. [2010]. Modelling particle retention in the  
4 alveolar-interstitial region of the human lungs. J Radiol Prot 30(3):491–512.
- 5 Greulich C, Diendorf J, Simon T, Eggeler G, Epple M, Koller M [2011]. Uptake and  
6 intracellular distribution of silver nanoparticles in human mesenchymal stem cells. Acta  
7 Biomaterialia 7:347–354.
- 8 Greulich C, Kittler S, Epple M, Muhr G, Koller M [2009]. Studies on the biocompatibility  
9 and the interaction of silver nanoparticles with human mesenchymal stem cells  
10 (hMSCs). Arch Surg 394:495–502.
- 11 Gromadzka-Ostrowska J, Dziendzikowska K, Lankoff A, Dobrzynska M, Instanes C,  
12 Brunborg G, Gajowik A, Radzikowska J, Wojewodzka M, Kruszewski M [2012]. Silver  
13 nanoparticles effects on epididymal sperm in rats. Toxicol Lett 214:251–258.
- 14 Guo H, Zhang J, Boudreau M, Meng J, Yin JJ, Liu J, Xu H [2016]. Intravenous  
15 administration of silver nanoparticles causes organ toxicity through intracellular ROS-  
16 related loss of inter-endothelial junction. Part Fibre Toxicol 13:21,  
17 <http://dx.doi.org/10.1186/s12989-016-0133-9>.
- 18 Haberl N, Hirn S, Wenk A, Diendorf J, Epple M, Johnston BD, Krombach F, Kreyling  
19 WG, Schleh C [2013]. Cytotoxicity and proinflammatory effects of PVP-coated silver  
20 nanoparticles after intratracheal instillation in rats. Beilstein J Nanotechnol 4:933–940.  
21
- 22 Hackenberg S, Scherzed A, Kessler M, Hummel S, Technau A, Froelich K, Ginzkey C,  
23 Koehler C, Hagen R, Kleinsasser N [2011]. Silver nanoparticles: evaluation of DNA  
24 damage, toxicity and functional impairment in human mesenchymal stem cells. Toxicol  
25 Lett 201(1):27–33.

*This information is distributed solely for the purpose of pre-dissemination peer review under applicable information quality guidelines. It has not been formally disseminated by the National Institute for Occupational Safety and Health. It does not represent and should not be construed to represent any agency determination or policy.*

- 1 Hadrup N, Lam HR, Loeschner K, Mortensen A, Larsen EH, Frandsen H [2012b].  
2 Nanoparticulate silver increases uric acid and allantoin excretion in rats, as identified by  
3 metabolomics. *J Appl Toxicol* 32:929–933.  
4
- 5 Hadrup N, Loeschner K, Bergstrom A, Wilcks A, Gao X, Vogel U, Frandsen HL, Larsen  
6 EH, Lam HR, Mortensen A [2012a]. Subacute oral toxicity investigation of  
7 nanoparticulate and ionic silver in rats. *Arch Toxicol* 86:543–551.
- 8 Hadrup N, Loeschner K, Mortensen A, Sharma AK, Qvortrup K, Larsen EH, Lam HR  
9 [2012c]. The similar neurotoxic effects of nanoparticulate and ionic silver *in vivo* and *in*  
10 *vitro*. *Neurotoxicology* 33:416–423.
- 11 Hagens WI, Oomen AG, de Jong WH, Cassee FR, Sips A [2007]. What do we (need to)  
12 know about the kinetic properties of nanoparticles in the body? *Reg Tox Pharm* 49:217–  
13 229.
- 14 Hamilton RF, Buckingham S, Holian A [2014]. The effect of size on ag nanosphere  
15 toxicity in macrophage cell models and lung epithelial cell lines is dependent on particle  
16 dissolution. *Int J Mol Sci* 15(4):6815–6830, <http://dx.doi.org/10.3390/ijms15046815>.
- 17 Han JW, Gurunathan S, Jeong JK, Choi YJ, Kwon DN, Park JK, Kim JH [2014].  
18 Oxidative stress mediated cytotoxicity of biologically synthesized silver nanoparticles in  
19 human lung epithelial adenocarcinoma cell line. *Nanoscale Res Lett* 9(1):459,  
20 <http://dx.doi.org/10.1186/1556-276X-9-459>.
- 21 Hansen RE, Roth D, Winther JR [2009]. Quantifying the global cellular thiol-disulfide  
22 status. *Proc Natl Acad Sci USA* 106(2):422–427.
- 23 Harber P, Conlon C, McCunney RJ [2003]. Occupational medical surveillance. In:  
24 McCunney RJ, ed. *A practical approach to occupational and environmental medicine*.  
25 Philadelphia, PA: Lippincott, Williams, and Wilkins.

*This information is distributed solely for the purpose of pre-dissemination peer review under applicable information quality guidelines. It has not been formally disseminated by the National Institute for Occupational Safety and Health. It does not represent and should not be construed to represent any agency determination or policy.*

- 1 Harker JM, Hunter D [1935]. Occupational argyria. *Br J Dermatol Syphilis*  
2 *November*:441–455.
- 3 Hathaway GJ, Proctor NH [2004]. *Chemical Hazards of the Workplace*. 5<sup>th</sup> ed. Hoboken,  
4 NJ: John Wiley & Sons, 632–634.
- 5 He Y, Du Z, Ma S, Liu Y, Li D, Huang H, Jiang S, Cheng S, Wu W, Zhang K, Zheng X  
6 [2016]. Effects of green-synthesized silver nanoparticles on lung cancer cells in vitro  
7 and grown as xenograft tumors in vivo. *Int J Nanomed* 11:1879-1887,  
8 <http://dx.doi.org/10.2147/IJN.S103695>.
- 9 Hendren CQ, Mesnard X, Droge J, Wiesner MR [2011]. Estimating production data for  
10 five engineered nanomaterials as a basis for exposure assessment. *Environ Sci*  
11 *Technol* 45:2562–2569.
- 12 Hendrickson OD, Klochkov SG, Novikova OV, Bravova IM, Shevtsova EF, Safenkova  
13 IV, Zherdev AV, Bachurin SO, Dzantiev BB [2016]. Toxicity of nanosilver in intragastric  
14 studies: biodistribution and metabolic effects. *Toxicol Lett Jan* 22(241):184–192.  
15
- 16 Herzog F, Clift MJ, Piccapietra F, Behra R, Schmid O, Petri-Fink A, Rothen-Rutishauser  
17 B [2013]. Exposure of silver-nanoparticles and silver-ions to lung cells in vitro at the air-  
18 liquid interface. *Part Fibre Toxicol*, 10:11, <http://dx.doi.org/10.1186/1743-8977-10-11>.
- 19 Herzog F, Loza K, Balog S, Clift MJ, Epple M, Gehr P, Petri-Fink A, Rothen-Rutishauser  
20 B [2014]. Mimicking exposures to acute and lifetime concentrations of inhaled silver  
21 nanoparticles by two different in vitro approaches. *Beilstein J Nanotechnol*, 5:1357-  
22 1370, <http://dx.doi.org/10.3762/bjnano.5.149>.
- 23 Hill WR, Pillsbury DM [1939]. *Argyria: the pharmacology of silver*. Baltimore, MD: The  
24 Williams and Wilkins Company.

*This information is distributed solely for the purpose of pre-dissemination peer review under applicable information quality guidelines. It has not been formally disseminated by the National Institute for Occupational Safety and Health. It does not represent and should not be construed to represent any agency determination or policy.*

- 1 Holland NACM, Becak DP, Shannahan JH, Brown JM, Carratt SA, Van Winkle LS,  
2 Pinkerton KE, Wang CM, Munusamy P, Baer DR, Sumner SJ, Fennell TR, Lust RM,  
3 Wingard CJ [2015]. Cardiac ischemia reperfusion injury following instillation of 20 nm  
4 citrate-capped nanosilver. *J Nanomed Nanotechnol*, doi:10.4172/2157-7439.  
5
- 6 Hsin YH, Chen CF, Huang S, Shih TS, Lai PS, Chueh PJ [2008]. The apoptotic effect of  
7 nanosilver is mediated by a ROS- and JNK-dependent mechanism involving the  
8 mitochondrial pathway in NIH3T3 cells. *Toxicol Lett* 179(3):130–139.
- 9 Hubbs AF, Mercer RR, Benkovic SA, Harkema J, Sriram K, Schwegler-Berry D,  
10 Goravanahally MP, Nurkiewicz TR, Castranova V, Sargent LM [2011]. Nanotoxicology –  
11 a pathologist’s perspective. *Toxicologic Pathol* 39:301–324.
- 12 Huo L, Chen R, Zhao L, Shi X, Bai R, Long D, Chen F, Zhao Y, Chang YZ, Chen C  
13 [2015]. Silver nanoparticles activate endoplasmic reticulum stress signaling pathway in  
14 cell and mouse models: the role in toxicity evaluation. *Biomaterials*, 61:307–315,  
15 <http://dx.doi.org/10.1016/j.biomaterials.2015.05.029>.
- 16 Hussain S, Hess K, Gearhart JM, Geiss KT, Schlager JJ [2005b]. Toxicity assessment  
17 of silver nanoparticles (Ag 15, 100 nm) in alveolar macrophages. *Toxicol Sci* 84(1-  
18 S):350.
- 19 Hussain SM, Hess KL, Gearhart JM, Geiss KT, Schlager JJ [2005a]. In vitro toxicity of  
20 nanoparticles in BRL 3A rat liver cells. *Toxicol In Vitro* 19(7):975–983.
- 21 Hyun J-S, Lee BS, Ryu HY, Sung JH, Chung KH, Yu IJ [2008]. Effects of repeated silver  
22 nanoparticles exposure on the histological structure and mucins of nasal respiratory  
23 mucosa in rats. *Toxicol Lett* 182:24–28.
- 24 ICRP [1960]. Report of Committee II on permissible dose for internal radiation, 1959.  
25 *Annals of the ICRP/ICRP Publication* 2:1–40.

*This information is distributed solely for the purpose of pre-dissemination peer review under applicable information quality guidelines. It has not been formally disseminated by the National Institute for Occupational Safety and Health. It does not represent and should not be construed to represent any agency determination or policy.*

- 1 ICRP [1994]. Human respiratory tract model for radiological protection. In: Smith H, ed.  
2 Annals of the ICRP. Tarrytown, NY: International Commission on Radiological  
3 Protection, ICRP Publication No. 66.
  
- 4 ISO [2006]. Workplace atmospheres; ultrafine, nanoparticle and nano-structured  
5 aerosols, exposure characterization and assessment. Geneva, Switzerland:  
6 International Standards Organization. Document No. ISO/TC 146/SC2/WGI N324.
  
- 7 ISO/TS [2008]. Nanotechnologies: terminology and definitions for nano-object,  
8 nanoparticle, nanofibre and nanoplate. ISO/TS 27687:2008. Vienna, Austria:  
9 International Organization for Standardization.
  
- 10 Ito S [2011]. Pharmacokinetics 101. Paediatr Child Health 16(9):535–536.
  
- 11 Jang S, Park JW, Cha HR, Jung SY, Lee JE, Jung SS, Kim JO, Kim SY, Lee CS, Park  
12 HS [2012]. Silver nanoparticles modify VEGF signaling pathway and mucus  
13 hypersecretion in allergic airway inflammation. Internat J Nanomed 7:1329–1343.  
14
- 15 Jeannet N, Fierz M, Schneider S, Kunzi L, Baumlin N, Salathe M, Burtscher H, Geiser  
16 M [2016]. Acute toxicity of silver and carbon nanoaerosols to normal and cystic fibrosis  
17 human bronchial epithelial cells. Nanotoxicology 10(3):279–291,  
18 <http://dx.doi.org/10.3109/17435390.2015.1049233>.
  
- 19 Jeong GN, Jo UB, Ryu HY, Kim YS, Song KS, Yu IJ [2010]. Histochemical study of  
20 intestinal mucins after administration of silver nanoparticles in Sprague-Dawley rats.  
21 Arch Toxicol 84:63–69.
  
- 22 Jeschke MG [2009]. The hepatic response to thermal injury: is the liver important for  
23 postburn outcomes? Mol Med 15:337–351.

*This information is distributed solely for the purpose of pre-dissemination peer review under applicable information quality guidelines. It has not been formally disseminated by the National Institute for Occupational Safety and Health. It does not represent and should not be construed to represent any agency determination or policy.*

- 1 Jeschke MG, Gauglitz GG, Song J, Kulp GA, Finnerty CC, Cos RA, Barral JM, Herndon  
2 DN, Boehning D [2009]. Calcium and ER stress mediate hepatic apoptosis after burn  
3 injury. *J Cell Mol Med* 13:1857–1865.
- 4 Ji JH, Jung JH Kim SS, Yoon J-U, Park JD Choi BS, Chung YH, Kwon IH, Jeong J, Han  
5 BS, Shin JH, Sung JH, Song KS, Yu IJ [2007b]. Twenty-eight-day inhalation toxicity  
6 study of silver nanoparticles in Sprague-Dawley rats. *Inhalation Toxicol* 19:857–871.
- 7 Ji JH, Jung JH, Yu IJ, Kim SS [2007a]. Long-term stability characteristics of metal  
8 nanoparticle generator using small ceramic heater for inhalation toxicity studies. *Inhal*  
9 *Toxicol* 19(9):745–751.
- 10 Ji JH, Yu IJ [2012]. Estimation of human equivalent exposure from rat inhalation toxicity  
11 study of silver nanoparticles using multi-path particle dosimetry model. *Toxicology*  
12 *Research*, The Royal Society of Chemistry, DOI: 10.1039/c2tx20029e.
- 13 Johnston HJ, Hutchison G, Christensen FM, Peters S, Hankin S, Stone V [2010]. A  
14 review of the in vivo and in vitro toxicity of silver and gold particulates: particle attributes  
15 and biological mechanisms responsible for the observed toxicity. *Crit Rev Tox*  
16 *40(4):328–346.*
- 17 Jun E-AH, Lim K-M, Kim K, Bae ON, Noh JY, Chung KH, Chung JH [2011]. Silver  
18 nanoparticles enhance thrombus formation through increased platelet aggregation and  
19 procoagulant activity. *Nanotoxicology* 5(2):157–167.
- 20  
21 Kaewamatawong T, Banlunara W, Maneewattanapinyo P, Thammachareon C, Ekgasit  
22 S [2014]. Acute and subacute pulmonary toxicity caused by a single intratracheal  
23 instillation of colloidal silver nanoparticles in mice: pathobiological changes and  
24 metallothionein responses. *J Environ Pathol Toxicol Oncol* 33(1):59–68.
- 25

*This information is distributed solely for the purpose of pre-dissemination peer review under applicable information quality guidelines. It has not been formally disseminated by the National Institute for Occupational Safety and Health. It does not represent and should not be construed to represent any agency determination or policy.*

- 1 Kalberlah F, Fost U, Schneider K [2002]. Time extrapolation and interspecies  
2 extrapolation for locally acting substances in case of limited toxicological data. *Ann*  
3 *Occup Hyg* 46(2):175–185.
- 4 Kalishwaralal K, Banumathi E, Pandian SBRK, Deepak V, Muniyandi J, Eom SH,  
5 Gurunathan S [2009]. Silver nanoparticles inhibit VEGF induced cell proliferation and  
6 migration in bovine retinal endothelial cells. *Colloids Surf B Biointerfaces* 73(1):51–57.
- 7 Katnelson BA, Privalova LI, Gurvich VB, Makeyev OH, Shur VY, Beikin YB, Sutunkova  
8 MP, Kireyeva EP, Minigalieva IA, Loginova NV, Vasilyeva MS, Korotkov AV, Shuman  
9 EA, Vlasova LA, Shishkina EV, Tyurnina AE, Kozin RV, Valamina IE, Pichugova SV,  
10 Tulakina LG [2013]. Comparative in vivo assessment of some adverse bioeffects of  
11 equidimensional gold and silver nanoparticles and the attenuation of nanosilver's effects  
12 with a complex of innocuous bioprotectors. *Internat J Mol Sci* 14:2449–2483.  
13
- 14 Kawata K, Osawa M, Okabe S [2009]. In vitro toxicity of silver nanoparticles at  
15 noncytotoxic doses to HepG2 human hepatoma cells. *Environ Sci Technol* 43:6046–  
16 6051.
- 17 Kennedy DC, Orts-Gil G, Lai C-H, Miller L, Haase A, Luch A, Seeberger PH [2014].  
18 Carbohydrate functionalization of silver nanoparticles modulates cytotoxicity and cellular  
19 uptake. *J Nanobiotechnology* 20:59.
- 20 Kenyon A, Antonini JM, Mercer RR, Schwegler-Berry D, Schaeublin NM, Hussain SM,  
21 Oldenburg SJ, Roberts JR [2012]. Pulmonary toxicity associated with different aspect  
22 ratio silver nanowires after intratracheal instillation in rats. *Society of Toxicology Annual*  
23 *Meeting, San Francisco, CA, March 11–15, 2012. Toxicol Sci: The Toxicologist*  
24 126(1):A652, p. 141.
- 25 Kermanizadeh A, Gaiser BK, Hutchison GR, Stone V [2012]. An in vitro liver model:  
26 assessing oxidative stress and genotoxicity following exposure of hepatocytes to a

- 1 panel of engineered nanomaterials. Part Fibre Toxicol 9:28,  
2 <http://dx.doi.org/10.1186/1743-8977-9-28>.
- 3 Kermanizadeh A, Pojana G, Gaiser BK, Birkedal R, Bilanicova D, Wallin H, Jensen KA,  
4 Sellergren B, Hutchison GR, Marcomini A, Stone V [2013]. In vitro assessment of  
5 engineered nanomaterials using a hepatocyte cell line: Cytotoxicity, pro-inflammatory  
6 cytokines and functional markers. Nanotoxicology 7(3):301–313,  
7 <http://dx.doi.org/10.3109/17435390.2011.653416>.
- 8 Kim E, Chu YC, Han JY, Lee DH, Kim YJ, Kim H-C, Lee SG, Lee SJ, Jeong SW, Kim  
9 JM [2010b]. Proteomic analysis of silver nanoparticle toxicity in rat. Toxicol Environ  
10 Health Sci 2:251–262.
- 11 Kim E, Maeng J-H, Lee DH, Kim JM [2009b]. Correlation of biomarkers and histological  
12 responses in manufactured silver nanoparticle toxicity. Toxicol Environ Health Sci 1:8–  
13 16.
- 14 Kim E, Lee JH, Kim JK, Lee GH, Ahn K, Park JD, Yu IJ [2016]. Case study on risk  
15 evaluation of printed electronics using nanosilver ink. Nano Converg 3(1):2.
- 16 Kim HR, Park YJ, Shin DY, Oh SM, Chung KH [2013a]. Appropriate in vitro methods for  
17 genotoxicity testing of silver nanoparticles. Environ Health Toxicol 28:e2013003,  
18 <http://dx.doi.org/10.5620/eh.2013.28.e2013003>.
- 19 Kim J, Kuk E, Yu K, Kim J, Park S, Lee H, Kim S, Park Y, Park YH, Hwang C, Kim Y,  
20 Lee Y, Jeong D, Cho M [2007]. Antimicrobial effects of silver nanoparticles.  
21 Nanomedicine 3:95–101 (as cited in Hackenberg et al. [2011]).
- 22 Kim JS, Song KS, Sung JH, Ryu HR, Choi BG, Cho HS, Lee JK, Yu IJ [2013b].  
23 Genotoxicity, acute oral and dermal toxicity, eye and dermal irritation and corrosion and  
24 skin sensitization evaluation of silver nanoparticles. Nanotoxicology 7(5):953–960.

*This information is distributed solely for the purpose of pre-dissemination peer review under applicable information quality guidelines. It has not been formally disseminated by the National Institute for Occupational Safety and Health. It does not represent and should not be construed to represent any agency determination or policy.*

- 1 Kim JS, Sung JH, Ji JH, Song KS, Lee JH, Kang CS, Yu IJ [2011]. In vivo genotoxicity  
2 of silver nanoparticles after 90-day silver nanoparticle inhalation exposure. *Saf Health*  
3 *Work* 2(1):34–38.
- 4 Kim K-J, Sung WS, Suh BK, Moon SK, Choi J-S [2009d]. Antifungal activity and mode  
5 of action of silver nano-particles on *Candida albicans*. *Biometals* 22(2):235–242.  
6
- 7 Kim S, Choi JE, Choi J, Chung KH, Park K, Yi J, Ryu DY [2009c]. Oxidative stress-  
8 dependent toxicity of silver nanoparticles in human hepatoma cells. *Toxicol In Vitro*  
9 23(6):1076–1084.
- 10 Kim TH, Kim M, Park HS, Shin US, Gong MS, Kim HW [2012]. Size-dependent cellular  
11 toxicity of silver nanoparticles. *J Biomed Mater Res Part A* 100A:1033–1043.
- 12 Kim W-Y, Kim J, Park JD, Ryu HY, Yu IJ [2009a]. Histological study of gender  
13 differences in accumulation of silver nanoparticles in kidneys of Fischer 344 rats. *J*  
14 *Toxicol Environ Health Part A* 72:1279–1284.
- 15 Kim YS, Kim JS, Cho HS, Rha DS, Park JD, Choi BS, Lim R, Chang HK, Chung YH,  
16 Kwon IH, Jeong J, Han BS, Yu IJ [2008]. Twenty-eight day oral toxicity, genotoxicity,  
17 and gender-related tissue distribution of silver nanoparticles in Sprague-Dawley rats.  
18 *Inhal Toxicol* 20:575–583.
- 19 Kim YS, Song MY, Park JD, Song KS, Ryu HR, Chung YH, Chang HK, Lee JH, Oh KH,  
20 Kelman BJ, Hwang IK, Yu IJ [2010a]. Subchronic oral toxicity of silver nanoparticles.  
21 *Particle Fibre Toxicol* 7:20.
- 22 Kitter S, Greulich C, Diendorf J, Koller M, Epple M [2010]. Toxicity of silver  
23 nanoparticles increases during storage because of slow dissolution under release of  
24 silver ions. *Chem Mater* 22:4548–4554.

*This information is distributed solely for the purpose of pre-dissemination peer review under applicable information quality guidelines. It has not been formally disseminated by the National Institute for Occupational Safety and Health. It does not represent and should not be construed to represent any agency determination or policy.*

- 1 Klaassen CD [1979]. Biliary excretion of silver in the rat, rabbit, and dog. *Tox Applied*  
2 *Pharm* 5:49–55.
- 3 Korani M, Rezayat SM, Gilani K, Arbabi Bidgoli S, Adeli S [2011]. Acute and subchronic  
4 dermal toxicity of nanosilver in guinea pig. *Int J Nanomed* 6:855–862.
- 5 Korani M, Rezayat SM, Arbadi Bidgoli S [2103]. Sub-chronic dermal toxicity of silver  
6 nano particles in guinea pigs: special emphasis to heart, bone, and kidney toxicities.  
7 *Iranian J Pharmaceut Res* 12(3): 511-519.
- 8 Kovvuru P, Mancilla PE, Shirode AB, Murray TM, Begley TJ, Reliene R [2015]. Oral  
9 ingestion of silver nanoparticles induces genomic instability and DNA damage in  
10 multiple tissues. *Nanotoxicology* 9(2):162–171.  
11
- 12 Kreyling WG, Hirn S, Möller W, Schleh C, Wenk A, Celik G, Lipka J, Schäffler M, Haberl  
13 N, Johnston BD, Sperling R, Schmid G, Simon U, Parak WJ, Semmler-Behnke M  
14 [2014]. Air-blood barrier translocation of tracheally instilled gold nanoparticles inversely  
15 depends on particle size. *ACS Nano* 28;8(1):222–233.
- 16 Kromhout H [2009]. Design of measurement strategies for workplace exposures. *Occup*  
17 *Environ Med* 59(5):349–354.
- 18 Kuempel ED, Tran CL [2002]. Comparison of human lung dosimetry models:  
19 implications for risk assessment. *Ann Occup Hyg* 46(Suppl.1):337–341.
- 20 Kuhlbusch TA, Asbach C, Fissan H, Gohler D, Stintz M [2011]. Nanoparticle exposure  
21 at nanotechnology workplaces: a review. *Part Fibre Toxicol* 8:22.
- 22 Kulinowski K, Lippy B [2011]. Training workers on risks of nanotechnology. Washington,  
23 DC: National Clearinghouse for Worker Safety and Health Training, National Institute of

- 1 Environmental Health Sciences (NIEHS) Worker Education and Training Program  
2 (WETP), <http://tools.niehs.nih.gov/wetp/index.cfm?id=537>.
  
- 3 Kurashina M, Kozuka S, Nakasima N, Hirabayasi N, Masafumi I [2006]. Relationship of  
4 intrahepatic bile duct hyperplasia to cholangiocellular carcinoma. *Cancer* 61(12):2469–  
5 2474.
  
- 6 Kwan KH, Yeung KW, Liu X, Wong KK, Shum HC, Lam YW, Cheng SH, Cheung KM,  
7 To MK [2014]. Silver nanoparticles alter proteoglycan expression in the promotion of  
8 tendon repair. *Nanomedicine* 10(7):1375–1383,  
9 <http://dx.doi.org/10.1016/j.nano.2013.11.015>.
  
- 10 Kwon J-T, Minai-Tehrani A, Hwang S-K, Kim J-E, Shin J-Y, Yu K-N, Chang S-H, Kim D-  
11 S, Kwon Y-T, Choi I-J, Cheong Y-H, Kim JS, Cho M-H [2012]. Acute pulmonary toxicity  
12 and body distribution of inhaled metallic silver nanoparticles. *Toxicol Res* 28(1):25–31.  
13 Lafuente D, Garcia T, Blanco J, Sanchez DJ, Sirvent JJ, Domingo JL [2016]. Effects of  
14 oral exposure to silver nanoparticles on the sperm of rats. *Reprod Toxicol* 60:133–139.  
15
- 16 Landsiedel R, Fabian E, Ma-Hock L, et al. [2012]. Toxicology/biokinetics of nanomaterials.  
17 *Arch Toxicol* 86(7):1021–1060.
  
- 18 Lankveld DP, Oomen AG, Krystek P, Neigh A, Troost-de Jong A, Noorlander CW,  
19 Eijkeren JC, Geertsma RE, De Jong WH [2010]. The kinetics of the tissue distribution of  
20 silver nanoparticles of different sizes. *Biomaterials* 31:8350–8361.
  
- 21 Lansdown ABG [2012]. Silver and gold. In: Bingham and Cohrssen, eds. *Patty's*  
22 *toxicology*. 6<sup>th</sup> ed. Vol. 1. New York: John Wiley & Sons.
  
- 23 Larese FF, D'Agostin F, Crosera M, Adami G, Renzi N, Bovenzi M, Maina G [2009].  
24 Human skin penetration of silver nanoparticles through intact and damaged skin.  
25 *Toxicology* 255:33–37.

*This information is distributed solely for the purpose of pre-dissemination peer review under applicable information quality guidelines. It has not been formally disseminated by the National Institute for Occupational Safety and Health. It does not represent and should not be construed to represent any agency determination or policy.*

- 1 Lee H-Y, Choi Y-J, Jung E-J, Yin H-Q, Kwon J-T, Kim J-E, Im H-T, Cho M-H, Kim, J-H,  
2 Kim H-Y, Lee B-H [2010]. Genomics-based screening of differentially expressed genes  
3 in the brains of mice exposed to silver nanoparticles via inhalation. *J Nanopart Res*  
4 *12*:1567–1578.
- 5 Lee JH, Ahn K, Kim SM, Jeon KS, Lee JS, Yu IJ [2012b]. Continuous 3-day exposure  
6 assessment of workplace manufacturing silver nanoparticles. *J Nanopart Res* *14*:1134.
- 7 Lee JH, Kim YS, Song KS, Ryu HR, Sung JH, Park JD, Park HM, Song NW, Shin BS,  
8 Marshak D, Ahn K, Lee JE, Yu IJ [2013a]. Biopersistence of silver nanoparticles in  
9 tissues from Sprague-Dawley rats. *Particle Fibre Toxicol* *10*:36.
- 10 Lee JH, Kwon M, Ji JH, Kang CS, Ahn KH, Han JH, Yu IJ [2011b]. Exposure  
11 assessment of workplaces manufacturing nanosized TiO<sub>2</sub> and silver. *Inhalation Toxicol*  
12 *23*:226–236.
- 13 Lee JH, Mun J, Park JD, Yu IJ [2012a]. A health surveillance case study of workers who  
14 manufacture silver nanomaterials. *Nanotoxicology* *6*:667–669.
- 15 Lee JH, Sohn EK, Ahn JS, Ahn K, Kim KS, Lee JH, Lee TM, Yu IJ [2013b]. Exposure  
16 assessment of workers in printed electronics workplace. *Inhal Toxicol* *25*:8.
- 17 Lee TY, Liu MS, Huang LJ, Lue SI, Lin LC, Kwan AL, Yang RC [2013c]. Bioenergetic  
18 failure correlates with autophagy and apoptosis in rat liver following silver nanoparticle  
19 intraperitoneal administration. *Particle Fibre Toxicol* *10*:40.
- 20 Lee Y, Kim P, Yoon J, Lee B, Choi K, Kil K-H, Park K [2013d]. Serum kinetics,  
21 distribution and excretion of silver in rabbits following 28 days after a single intravenous  
22 injection of silver nanoparticles. *Nanotoxicology* *7*(6):1120–1130.

*This information is distributed solely for the purpose of pre-dissemination peer review under applicable information quality guidelines. It has not been formally disseminated by the National Institute for Occupational Safety and Health. It does not represent and should not be construed to represent any agency determination or policy.*

- 1 Lee YS, Kim DW, Lee YH, Oh JH, Yoon S, Choi MS, Lee SK, Kim JW, Lee K, Song CW  
2 [2011a]. Silver nanoparticles induce apoptosis and G2/M arrest via PKCzeta-dependent  
3 signaling in A549 lung cells. Arch Toxicol doi: 10.1007/s00204-011-0714-1.
- 4 Leidel NA, Busch KA [1994]. Statistical design and data analysis requirements. In:  
5 Harris RL, Cralley LJ, Cralley LV, eds. Patty's Industrial Hygiene and Toxicology, 3rd  
6 ed. Vol. 3, Part A. New York: John Wiley and Sons, pp. 453–582.
- 7 Levard C, Hotze EM, Lowry GV, Brown GE [2012]. Environmental transformations of  
8 silver nanoparticles: impact on stability and toxicity. Environ Sci Technol 46(13):6900–  
9 6914.
- 10 Levard C, Reinsch BC, Michel FM, Oumahi C, Lowry GV, Brown GE [2011]. Sulfidation  
11 processes of PVP-coated silver nanoparticles in aqueous solution: impact on dissolution  
12 rate. Environ Sci Technol 45(12):5260–5266.
- 13 Lewis RC, Gaffney SH, Le MH, Unice KM, Paustenbach DJ [2012]. Airborne  
14 concentrations of metals and total dust during solid catalyst loading and unloading  
15 operations at a petroleum refinery. Int J Hyg Envir Health 215:514–521.
- 16 Lewis TR, Morrow PE, McClellan RO, Raabe OG, Kennedy GL, Schwetz BA, Goehl TJ,  
17 Roycroft JH, Chhabra RS [1989]. Establishing aerosol exposure concentrations for  
18 inhalation toxicity studies. Toxicol Appl Pharmacol 99:377–383.
- 19 Li M, Panagi Z, Avgoustakis K, Reineke J [2012a]. Physiologically based  
20 pharmacokinetic modeling of PLGA nanoparticles with varied mPEG content. Int J  
21 Nanomed 7:1345–1356.
- 22 Li PW, Kuo TH, Chang JH, Yeh JM, Chan WH [2010]. Induction of cytotoxicity and  
23 apoptosis in mouse blastocysts by silver nanoparticles. Toxicol Lett 197(2):82–87.

*This information is distributed solely for the purpose of pre-dissemination peer review under applicable information quality guidelines. It has not been formally disseminated by the National Institute for Occupational Safety and Health. It does not represent and should not be construed to represent any agency determination or policy.*

- 1 Li S-D, Huang L [2008]. Pharmacokinetics and biodistribution of nanoparticles. *Mol*  
2 *Pharm* 5(4):496–504.
- 3 Li Y, Chen DH, Yan J, Chen Y, Mittelstaedt RA, Zhang Y, Biris AS, Heflich RH, Chen T  
4 [2012b]. Genotoxicity of silver nanoparticles evaluated using the Ames test and *in vitro*  
5 micronucleus assay. *Mutation Res* 745:4–10.
- 6 Ling MP, Lin WC, Liu CC, Huang YS, Chueh MJ, Shih TS [2012]. Risk management  
7 strategy to increase the safety of workers in the nanomaterials industry. *J Haz Mat*  
8 <http://dx.doi.org/10.1016/j.jhazmat.2012.05.073>.
- 9 Liu H, Yang D, Yang H, Zhang H, Zhang W, Fang Y, Lin Z, Tian L, Lin B, Yan J, Xi Z  
10 [2013a]. Comparative study of respiratory tract immune toxicity induced by three  
11 sterilization nanoparticles: silver, zinc oxide and titanium dioxide. *J Haz Mat Mar*  
12 15(248–249):478–486.
- 13
- 14 Liu J, Hurt RH [2010]. Ion release kinetics and particle persistence in aqueous nano-  
15 silver colloids. *Environ Sci Technol* 44(6):2169–2175.
- 16 Liu J, Sonshine DA, Shervani S, Hurt RH [2010b]. Controlled release of biologically  
17 active silver from nanosilver surfaces. *ACS Nano* 4:6903–6913.
- 18 Liu P, Huang Z, Gu N [2013b]. Exposure to silver nanoparticles does not affect cognitive  
19 outcome or hippocampal neurogenesis in adult mice. *Ecotoxicol Environ Safety* 87:124–  
20 130.
- 21 Liu W, Wu Y, Wang C, Li HC, Wang T, Liao CY, Cui L, Zhou QF, Yan B, Jiang GB  
22 [2010a]. Impact of silver nanoparticles on human cells: effect of particle size.  
23 *Nanotoxicology* 4(3):319–330.

*This information is distributed solely for the purpose of pre-dissemination peer review under applicable information quality guidelines. It has not been formally disseminated by the National Institute for Occupational Safety and Health. It does not represent and should not be construed to represent any agency determination or policy.*

- 1 Liu Y, Guan W, Ren G, Yang Z [2012]. The possible mechanism of silver nanoparticle  
2 impact on hippocampal synaptic plasticity and spatial recognition in rats. *Toxicol Lett*  
3 209:227–231.  
4
- 5 Loeschner K, Hadrup N, Qvortrup K, Larsen A, Gao X, Vogel U, Mortensen A, Lam HR,  
6 Larsen EH [2011]. Distribution of silver in rats following 28 days of repeated oral  
7 exposure to silver nanoparticles or silver acetate. *Particle Fibre Toxicol* 8:18.
- 8 Lok C-N, Ho C-M, Chen R, He Q-Y, Yu W-Y, Sun H, Tam PK-H, Chiu J-F, Che C-M  
9 [2006]. Proteomic analysis of the mode of antibacterial action of silver nanoparticles. *J*  
10 *Proteome Res* 5:916–924.
- 11 Lyles RH, Kupper LL, Rappaport SM [1997]. A lognormal distribution-based exposure  
12 assessment method for unbalanced data. *Ann Occup Hyg* 41(1):63–76.
- 13 Ma J, Lü X, Huang Y [2011]. Genomic analysis of cytotoxicity response to nanosilver in  
14 human dermal fibroblasts. *J Biomed Nanotechnol* 7:263–275.
- 15 Mahabady MK [2012]. The evaluation of teratogenicity of nanosilver on skeletal system  
16 and placenta of rat fetuses in prenatal period. *Afr J Pharmacy Pharmacol* 6(6):419–424.
- 17 Maneewattanapinyo P, Banlunara W, Thammacharoen C, Ekgasit S, Kaewamatawong  
18 T [2011]. An evaluation of acute toxicity of colloidal silver nanoparticles. *J Vet Med Sci*  
19 73(11):1417–1423. E-pub June 29.
- 20 Mathias FT, Romano RM, Kizys ML, Kasamatsu T, Giannocco G, Chiamolera MI, Dias-  
21 da-Silva MR, Romano MA [2014]. Daily exposure to silver nanoparticles during  
22 prepubertal development decreases adult sperm and reproductive parameters. *Informa*  
23 *Healthcare*, 17 February, doi:10.3109/17435390.2014.889237.

*This information is distributed solely for the purpose of pre-dissemination peer review under applicable information quality guidelines. It has not been formally disseminated by the National Institute for Occupational Safety and Health. It does not represent and should not be construed to represent any agency determination or policy.*

- 1 Maynard AD, Kuempel ED [2005]. Airborne nanostructured particles and occupational  
2 health. *J Nanopart Res* 7:587–614.
- 3 McNally K, Warren N, Fransman W, Entink RK, Schinkel J, van Tongeren M, Cherrie  
4 JW, Kromhout H, Schneider T, Tielemans E [2014]. Advanced REACH Tool: a Bayesian  
5 model for occupational exposure assessment. *Ann Occup Hyg* 55(5):551–565.
- 6 Mei N, Zhang Y, Chen Y, Guo X, Ding W, Ali SF, Biris AS, Rice P, Moore MM, Chen T  
7 [2012]. Silver nanoparticle-induced mutations and oxidative stress in mouse lymphoma  
8 cells. *Environ Mol Mutagen* 53:409–419.
- 9 Meyer KC [2017]. Pulmonary fibrosis, part I: epidemiology, pathogenesis, and  
10 diagnosis. *Expert Review of Respiratory Medicine* 11(5):343-359.
- 11 Miller A, Drake PL, Hintz P, Habjan M [2010]. Characterizing exposures to airborne  
12 metals and nanoparticle emissions in a refinery. *Ann Occup Hyg* 54(5):504–513.
- 13 Minchenko DO, Yavorovsky OP, Zinchenko TO, Komisarenko SV, Minchenko OH  
14 [2012]. Expression of circadian gens in different rat tissues is sensitive marker of in vivo  
15 silver nanoparticles. *Mat Sci Engin*, doi:10.1088/1757-899X/40/1/012016.
- 16
- 17 Miresmaeili SM, Halvaei I, Fesahar F, Fallah A, nikonahad N, Taherinejad M [2013].  
18 Evaluating the role of silver nanoparticles on acrosomal reaction and spermatogenic  
19 cells in rat. *Iran J Reprod Med* 11(5):423–430.
- 20
- 21 Miura N, Shinohara Y [2009]. Cytotoxic effect and apoptosis induction by silver  
22 nanoparticles in HeLa cells. *Biochem Biophys Res Commun* 390(3):733–737.
- 23 Moss AP, Sugar A, Hargett NA, Atkin A, Wolkstein M, Rosenman KD [1979]. The ocular  
24 manifestations and functional effects of occupational argyrosis. *Arch Ophthalmol*  
25 97:906–908.

*This information is distributed solely for the purpose of pre-dissemination peer review under applicable information quality guidelines. It has not been formally disseminated by the National Institute for Occupational Safety and Health. It does not represent and should not be construed to represent any agency determination or policy.*

- 1 Muir DC, Cena K [1987]. Deposition of ultrafine aerosols in the human respiratory tract.  
2 Aerosol Sci Technol 6:183–190.
- 3 Murdaca F, Feci L, Acciai S, Biagioli M, Fimiani M [2014]. Occupational argyria. G Ital  
4 Dermatol Venereol 149(5):629–630.
- 5 Nallathamby PD, Xu X-HN [2010]. Study of cytotoxic and therapeutic effects of stable  
6 and purified silver nanoparticles on tumor cells. Nanoscale 2(6):942–952.
- 7 NanoSafe [2008]. Are conventional protective devices such as fibrous filter media,  
8 respirator cartridges, protective clothing and gloves also efficient for nanoaerosols? DR-  
9 325/326-200801-1. Brussels, Belgium: European Commission (EC),  
10 [http://www.nanosafe.org/home/liblocal/docs/Dissemination%20report/DRI\\_s.pdf](http://www.nanosafe.org/home/liblocal/docs/Dissemination%20report/DRI_s.pdf).
- 11 Naumann BD, Sargent EV, Starkman BS, Fraser WJ, Becker GT, Kirk GD [1996].  
12 Performance-based exposure control limits for pharmaceutical active ingredients. Am  
13 Ind Hyg Assoc J 57:33–42.
- 14 Naumann BD, Weideman PA [1995]. Scientific basis for uncertainty factors used to  
15 establish occupational exposure limits for pharmaceutical active ingredients. Hum Ecol  
16 Risk Assess 1:590–613.
- 17 NIOSH [1973]. Health Hazard Evaluation (HHE) report: Dunham-Bush, Incorporated,  
18 West Hartford, Connecticut. By Vandervort R, Polakoff PL, Flesch JP, Lowry LK.  
19 Cincinnati, OH: U.S. Department of Health and Human Services, Public Health Service,  
20 Centers for Disease Control, National Institute for Occupational Safety and Health  
21 (NIOSH). NIOSH HHE Report No. 72-84-31, NTIS No. PB 229627.
- 22 NIOSH [1977]. Occupational exposure sampling strategy manual. Cincinnati, OH: U.S.  
23 Department of Health and Human Services, Public Health Service, Centers for Disease

*This information is distributed solely for the purpose of pre-dissemination peer review under applicable information quality guidelines. It has not been formally disseminated by the National Institute for Occupational Safety and Health. It does not represent and should not be construed to represent any agency determination or policy.*

- 1 Control, National institute for Occupational Safety and Health, DHHS (NIOSH)
- 2 Publication No. 77-173.
  
- 3 NIOSH [1981]. Health Hazard Evaluation (HHE) report: General Electric Company,
- 4 Lynn, Massachusetts. By McManus KP, Baker EL. Cincinnati, OH: U.S. Department of
- 5 Health and Human Services, Public Health Service, Centers for Disease Control,
- 6 National Institute for Occupational Safety and Health (NIOSH), NIOSH HHE Report No.
- 7 80-084-927.
  
- 8 NIOSH [1988]. Silver (metal dust and fume). CDC-NIOSH 1988 OSHA PEL Project
- 9 Documentation: List by Chemical Name: Silver, [http://www.cdc.gov/niosh/pel88/7440-](http://www.cdc.gov/niosh/pel88/7440-22.html)
- 10 [22](http://www.cdc.gov/niosh/pel88/7440-22.html).html.
  
- 11 NIOSH [1992]. Hazard Evaluation and Technical Assistance (HETA) report: Langers
- 12 Black Hills Silver Jewelry, Inc, Spearfish, South Dakota. By Kiefer M. Cincinnati, OH:
- 13 U.S. Department of Health and Human Services, Public Health Service, Centers for
- 14 Disease Control and Prevention, National Institute for Occupational Safety and Health
- 15 (NIOSH), NIOSH HETA Report No. 92-097-2238.
  
- 16 NIOSH [1998]. Hazard Evaluation and Technical Assistance (HETA) report: Caterpillar
- 17 Inc, York, Pennsylvania. By Tepper A, Blade LM. Cincinnati, OH: U.S. Department of
- 18 Health and Human Services, Public Health Service, Centers for Disease Control and
- 19 Prevention, National Institute for Occupational Safety and Health (NIOSH), NIOSH
- 20 HETA Report No. 95-0001-2679.
  
- 21 NIOSH [2000]. Hazard Evaluation and Technical Assistance (HETA) report:
- 22 OmniSource Corporation, Precious Metal Recycling Facility, Ft. Wayne, Indiana. By
- 23 Gwin KK, Nemhauser JB. Cincinnati, OH: U.S. Department of Health and Human
- 24 Services, Public Health Service, Centers for Disease Control and Prevention, National
- 25 Institute for Occupational Safety and Health (NIOSH), NIOSH HETA Report No. 2000-
- 26 0041-2796.

*This information is distributed solely for the purpose of pre-dissemination peer review under applicable information quality guidelines. It has not been formally disseminated by the National Institute for Occupational Safety and Health. It does not represent and should not be construed to represent any agency determination or policy.*

- 1 NIOSH [2003]. Method 7300 and 7301 Elements by ICP (supplement issued March 15,  
2 2003). In: NIOSH manual of analytical methods (NMAM®). Cincinnati, OH: U.S.  
3 Department of Health and Human Services, Public Health Service, Centers for Disease  
4 Control and Prevention, National Institute for Occupational Safety and Health, DHHS  
5 (NIOSH) Publication No. 94-113.
- 6 NIOSH [2005]. NIOSH respirator selection logic. Cincinnati, OH: U.S. Department of  
7 Health and Human Services, Public Health Service, Centers for Disease Control and  
8 Prevention, National Institute for Occupational Safety and Health, DHHS (NIOSH)  
9 Publication No. 2005-100.
- 10 NIOSH [2006]. Criteria for a recommended standard: occupational exposure to  
11 refractory ceramic fibers. Cincinnati, OH: U.S. Department of Health and Human  
12 Services, Public Health Service, Centers for Disease Control and Prevention, National  
13 Institute for Occupational Safety and Health, DHHS (NIOSH) Publication No. 2006-125.
- 14 NIOSH [2007]. NIOSH Pocket Guide to Chemical Hazards. Cincinnati, OH: U.S.  
15 Department of Health and Human Services, Public Health Service, Centers for Disease  
16 Control and Prevention, National Institute for Occupational Safety and Health, DHHS  
17 (NIOSH) Publication No. 2005-149, <http://www.cdc.gov/niosh/pel88/7440-22.html>.
- 18 NIOSH [2009]. Approaches to safe nanotechnology: managing the health and safety  
19 concerns with engineered nanomaterials. Cincinnati, OH: U.S. Department of Health  
20 and Human Services, Public Health Service, Centers for Disease Control and  
21 Prevention, National Institute for Occupational Safety and Health, DHHS (NIOSH)  
22 Publication No. 2009-125.
- 23 NIOSH [2010]. A systematic review of the effectiveness of training and education for the  
24 protection of workers. By Robson L, Stephenson C, Schulte P, Amick B, Chan S,  
25 Bielecky A, Wang A, Heidotting T, Irvin E, Eggerth D, Peters R, Clarke J, Cullen K,  
26 Boldt L, Rotunda C, Grubb P. Toronto: Institute for Work & Health; Cincinnati, OH: U.S.

*This information is distributed solely for the purpose of pre-dissemination peer review under applicable information quality guidelines. It has not been formally disseminated by the National Institute for Occupational Safety and Health. It does not represent and should not be construed to represent any agency determination or policy.*

1 Department of Health and Human Services, Public Health Service, Centers for Disease  
2 Control and Prevention, National Institute for Occupational Safety and Health, DHHS  
3 (NIOSH) Publication No. 2010-127.

4 NIOSH [2011]. Current Intelligence Bulletin 63: Occupational exposure to titanium  
5 dioxide. Cincinnati, OH: U.S. Department of Health and Human Services, Public Health  
6 Service, Centers for Disease Control and Prevention, National Institute for Occupational  
7 Safety and Health, DHHS (NIOSH) Publication No. 2011-160.

8 NIOSH [2012]. General safe practices for working with engineered nanomaterials in  
9 research laboratories. Cincinnati, OH: U.S. Department of Health and Human Services,  
10 Public Health Service, Centers for Disease Control and Prevention, National Institute for  
11 Occupational Safety and Health, DHHS (NIOSH) Publication No. 2012-147.

12 NIOSH [2013a]. Current Intelligence Bulletin 65: Occupational exposure to carbon  
13 nanotubes and nanofibers. By Zumwalde R, Kuempel E, Birch E, Trout D, Castranova  
14 V. Cincinnati, Ohio: U.S. Department of Health and Human Services, Public Health  
15 Service, Centers for Disease Control and Prevention, National Institute for Occupational  
16 Safety and Health. DHHS (NIOSH) Publication No. 2013-14.

17 NIOSH [2013b]. Current strategies for engineering controls in nanomaterial production  
18 and downstream handling processes. Cincinnati, OH: U.S. Department of Health and  
19 Human Services, Public Health Service, Centers for Disease Control and Prevention,  
20 National Institute for Occupational Safety and Health, DHHS (NIOSH) Publication No.  
21 2014-102.

22 NIOSH [2015]. Promoting health and preventing disease and injury through workplace  
23 tobacco policies. Cincinnati, OH: U.S. Department of Health and Human Services,  
24 Public Health Service, Centers for Disease Control and Prevention, National Institute for  
25 Occupational Safety and Health, DHHS (NIOSH) Publication No. 2015-113.

*This information is distributed solely for the purpose of pre-dissemination peer review under applicable information quality guidelines. It has not been formally disseminated by the National Institute for Occupational Safety and Health. It does not represent and should not be construed to represent any agency determination or policy.*

- 1 NIOSH [2017]. NIOSH Manual of Analytical Methods, 5th edition. Ashley K, O'Connor  
2 PF, eds. Cincinnati, OH: U.S. Department of Health and Human Services, Public Health  
3 Service, Centers for Disease Control and Prevention, National Institute for Occupational  
4 Safety and Health, DHHS (NIOSH) Publication No. 2014-151.
- 5 NIST [2015]. National Institute of Standards and Technology (NIST): silver nanoparticle  
6 test material, [https://www-s.nist.gov/srmors/view\\_report.cfm?srm=8017](https://www-s.nist.gov/srmors/view_report.cfm?srm=8017).
- 7 Nowack B, Kurg HF, Height M [2011]. 120 Years of nanosilver history: implications of  
8 policy makers. *Environ Sci Technol* 45:1177–1183.
- 9 NTP [2014]. National Toxicology Program: NTP nonneoplastic lesion atlas. Liver, bile  
10 duct-hyperplasia, by Maronpot RR.  
11 <http://ntp.niehs.nih.gov/nnl/hepatobiliary/liver/bdhyperp/index.htm>.
- 12 Nymark P, Catalan J, Suhonen S, Jarventaus H, Birkedal R, Clausen PA, Jensen KA,  
13 Vippola M, Savolainen K, Norppa H [2013]. Genotoxicity of polyvinylpyrrolidone-coated  
14 silver nanoparticles in BEAS 2b cells. *Toxicology*, 313(1):38–48,  
15 <http://dx.doi.org/10.1016/j.tox.2012.09.014>.
- 16 Oberdörster G, Ferin J, Lehnert BE [1994]. Correlation between particle size, in vivo  
17 particle persistence, and lung injury. *Environ Health Perspect* 102 (Suppl 5):173-179.
- 18 Oberdörster G [1995]. Lung particle overload: implications for occupational exposures to  
19 particles. *Regul Toxicol Pharmacol* 21(1):123-135.
- 20 Oberdörster G [1997]. Pulmonary carcinogenicity of inhaled particles and the maximum  
21 tolerated dose. *Environ Health Perspect* 105 (Suppl 5):1347-1355.
- 22 Oberdörster G, Oberdörster E, Oberdörster J [2005]. Nanotoxicology: an emerging  
23 discipline evolving from studies of ultrafine particles. *Environ Health Perspect*  
24 113(7):823-839. [Erratum in: *Environ Health Perspect*. 2010 Sep;118(9):A380].

*This information is distributed solely for the purpose of pre-dissemination peer review under applicable information quality guidelines. It has not been formally disseminated by the National Institute for Occupational Safety and Health. It does not represent and should not be construed to represent any agency determination or policy.*

- 1 OECD (Organisation for Economic Co-operation and Development) [2004]. OECD  
2 guideline for the testing of chemicals. Skin absorption: in vitro method, [http://www.oecd-  
ilibrary.org/docserver/download/9742801e.pdf?expires=1423779844&id=id&accname=g  
uest&checksum=EEEE10E26F1C4EFFC7A40DBF2F9E39F6](http://www.oecd-<br/>3 ilibrary.org/docserver/download/9742801e.pdf?expires=1423779844&id=id&accname=g<br/>4 uest&checksum=EEEE10E26F1C4EFFC7A40DBF2F9E39F6).
- 5 OSHA (Occupational Safety and Health Administration) [1988]. Silver (metal dust and  
6 fume). Federal Register 53(109):21215. Proposed rules: Air Contaminants. Federal  
7 Register 53:20960-21393.
- 8 OSHA (Occupational Safety and Health Administration) [2012b]. Safety Data Sheets.  
9 Hazard Communication Standard (HCS). Washington, DC: U.S. Department of Labor.  
10 <https://www.osha.gov/Publications/OSHA3514.html>.
- 11 OSHA (Occupational Safety and Health Administration) [2012a]. Silver, metal and  
12 soluble compounds (as Ag): chemical sampling information. Washington, DC: U.S.  
13 Department of Labor, [http://www.osha.gov/dts/chemicalsampling/data/CH\\_267300.html](http://www.osha.gov/dts/chemicalsampling/data/CH_267300.html).
- 14 OSHA [2013]. United States Code of Federal Regulations, 29CFR Part 1910.1000, Air  
15 Contaminants, final rule. Vol. 54. Washington, DC: Occupational Safety and Health  
16 Administration, p. 2702.
- 17 Paino IM, Zucolotto V [2015]. Poly(vinyl alcohol)-coated silver nanoparticles: activation  
18 of neutrophils and nanotoxicology effects in human hepatocarcinoma and mononuclear  
19 cells. Environ Toxicol Pharmacol 39(2):614–621,  
20 <http://dx.doi.org/10.1016/j.etap.2014.12.012>.
- 21 Pang C, Brunelli A, Zhu C, Hristozov D, Liu Y, Semenzin E, Wang W, Tao W, Liang J,  
22 Marcomini A, Chen C, Zhao B [2016]. Demonstrating approaches to chemically modify  
23 the surface of Ag nanoparticles in order to influence their cytotoxicity and biodistribution  
24 after single dose acute intravenous administration. Nanotoxicology 10(2):129–139.  
25

*This information is distributed solely for the purpose of pre-dissemination peer review under applicable information quality guidelines. It has not been formally disseminated by the National Institute for Occupational Safety and Health. It does not represent and should not be construed to represent any agency determination or policy.*

- 1 Parikh JM, Dhareshwar S, Sharma A, Karanth R, Ramkumar VS, Ramaiah I [2014].  
2 Acute respiratory distress in a silversmith. *Indian J Occup Environ Med* 18(1):27–28.
- 3 Park EJ, Bae E, Yi J, Kim Y, Choi K, Lee SH, Yoon J, Lee BC, Park K [2010a].  
4 Repeated-dose toxicity and inflammatory responses in mice by oral administration of  
5 silver nanoparticles. *Environ Toxicol Pharmacol* 30:162–168.  
6
- 7 Park E-J, Choi K, Park K [2011b]. Induction of inflammatory responses and gene  
8 expression by intratracheal instillation of silver nanoparticles in mice. *Arch Pharm Res*  
9 34(2):299–307.
- 10 Park EJ, Yi J, Kim Y, Choi K, Park K [2010b]. Silver nanoparticles induce cytotoxicity by  
11 a Trojan-horse type mechanism. *Toxicol In Vitro* 24(3):872–878.
- 12 Park J, Kwak BK, Bae E, Lee J, Kim Y, Choi K Yi J [2009]. Characterization of exposure  
13 to silver nanoparticles in a manufacturing facility. *J Nanopart Res* 11:1705–1712.
- 14 Park K [2013]. Toxicokinetic differences and toxicities of silver nanoparticles and silver  
15 ions in rats after single oral administration. *J Toxicol Environ Health, Part A*  
16 76(22):1246–1260.
- 17 Park K, Park E-J, Chun IK, Choi K, Lee SH, Yoon J, Lee BC [2011a]. Bioavailability and  
18 toxicokinetics of citrate-coated silver nanoparticles in rats. *Arch Pharm Res* 34:153–158.
- 19 Park M, Neigh AM, Vermeulen JP, de la Fonteyne L, Verharen HW, Briede JJ, van  
20 Loveren H, de Jong WH [2011c]. The effect of particle size on the cytotoxicity,  
21 inflammation, developmental toxicity and genotoxicity of silver. *Biomaterials* 32:9810-  
22 9817.
- 23 Patchin ES, Anderson DS, Silve RM, Uyeminami DL, Scott GM, Guo T, Van Winkle LS,  
24 Pinkerton KE [2016]. Size-dependent deposition, translocation, and microglial activation

*This information is distributed solely for the purpose of pre-dissemination peer review under applicable information quality guidelines. It has not been formally disseminated by the National Institute for Occupational Safety and Health. It does not represent and should not be construed to represent any agency determination or policy.*

- 1 of inhaled silver nanoparticles in the rodent nose and brain. *Environ Health Perspect*,  
2 doi:10.1289/EHP234.
- 3 Pauluhn J [2010]. Multi-walled carbon nanotubes (Baytubes): approach for derivation of  
4 occupational exposure limit. *Regul Toxicol Pharmacol* 57(1):78–89.
- 5 Pauluhn J [2014]. Derivation of occupational exposure levels (OELs) of low-toxicity  
6 isometric biopersistent particles: How can the kinetic lung overload paradigm be used  
7 for improved inhalation toxicity study design and OEL-derivation? *Part Fibre Toxicol*  
8 20;11:72.
- 9 Philbrook NA, Winn LM, Nabiul Afrooz ARM, Saleh NB, Walker VK [2011]. The effect of  
10 TiO<sub>2</sub> and Ag nanoparticles on reproduction and development of *Drosophila*  
11 *melanogaster* and CD-1 mice. *Toxicol Appl Pharm* 257:429–436.
- 12
- 13 Piao MJ, Kang KA, Lee IK, Kim HS, Kim S, Choi JY, Choi J, Hyun JW [2011]. Silver  
14 nanoparticles induce oxidative cell damage in human liver cells through inhibition of  
15 reduced glutathione and induction of mitochondria-involved apoptosis. *Toxicol Lett*  
16 201(1):92–100.
- 17 Pifer JW, Friedlander BR, Kintz RT, Stockdale DK [1989]. Absence of toxic effects in  
18 silver reclamation workers. *Scand J Work Environ Health* 15:210–221.
- 19 Piña RA, Martinez MM, Rizo VHT, Lopes MA, Almeida OP. Cutaneous amalgam tattoo  
20 in a dental professional: an unreported occupational argyria. *Br J Dermatol* 167:1184–  
21 1185.
- 22 Qin G, Tang S, Li S, Lu H, Wang Y, Zhao P, Lin B, Zhang J, Peng L [2016].  
23 Toxicological evaluation of silver nanoparticles and silver nitrate in rats following 28  
24 days of repeated oral exposure. *Environ Toxicol* doi:10.1002/tox.22263.
- 25

*This information is distributed solely for the purpose of pre-dissemination peer review under applicable information quality guidelines. It has not been formally disseminated by the National Institute for Occupational Safety and Health. It does not represent and should not be construed to represent any agency determination or policy.*

- 1 Quadros ME, Marr LC [2010]. Environmental and human health risks of aerosolized  
2 silver nanoparticles. *J Air Waste Mgmt* 60:770–781.
  
- 3 Rahman MF, Wang J, Patterson TA, Saini UT, Robinson BL, Newport GD, Murdock RC,  
4 Schlager JJ, Hussain SM, Ali SF [2009]. Expression of genes related to oxidative stress  
5 in the mouse brain after exposure to silver-25 nanoparticles. *Toxicol Lett* 187:15–21.
  
- 6 Ramachandran G, Ostraat M, Evans DE, Methner MM, O’Shaughnessy P, D’Arcy J,  
7 Geraci CL, Stevenson E, Maynard A, Rickabaugh K [2011]. A strategy for assessing  
8 workplace exposures to nanomaterials. *J Occup Environ Hyg* 8:673–685.
  
- 9 Rappaport SM, Lyles RH, Kupper LL [1995]. An exposure-assessment strategy  
10 accounting for within—and between—worker sources of variability. *Ann Occup Hyg*  
11 39(4):469–495.
  
- 12 Recordati C, De Maglie M, Bianchessi S, Argenti S, Cella C, Mattiello S, Cubadda F,  
13 Aureli F, D’Amato M, Raggi A, Lenardi C, Milani P, Scanziani E [2016]. Tissue  
14 distribution and acute toxicity of silver after single intravenous administration in mice:  
15 nano-specific and size-dependent effects. *Part Fibre Toxicol* 13:12.  
16
  
- 17 Reidy B, Haase A, Luch A, Dawson KA, Lynch I [2013]. Mechanisms of silver  
18 nanoparticle release, transformation and toxicity: a critical review of current knowledge  
19 and recommendations for future studies and applications. *Materials* 6:2295–2350.
  
- 20 Rengasamy S, Eimer BC [2011]. Total inward leakage of nanoparticles through filtering  
21 facepiece respirators. *Ann Occup Hyg* 55(3):253–263.
  
- 22 Rengasamy S, Eimer BC, Shaffer RE [2009]. Comparison of nanoparticle filtration  
23 performance of NIOSH-approved and CE-marked particulate filtering facepiece  
24 respirators. *Ann Occup Hyg* 53(2):117–128.

*This information is distributed solely for the purpose of pre-dissemination peer review under applicable information quality guidelines. It has not been formally disseminated by the National Institute for Occupational Safety and Health. It does not represent and should not be construed to represent any agency determination or policy.*

- 1 Rengasamy S, King WP, Eimer B, Shaffer RE [2008]. Filtration performance of NIOSH-  
2 approved N95 and P100 filtering-facepiece respirators against 4-30 nanometer size  
3 nanoparticles. *J Occup Environ Hyg* 5(9):556–564.
- 4 Rengasamy S, Verbofsky R, King WP, Shaffer RE [2007]. Nanoparticle penetration  
5 through NIOSH-approved N95 filtering-facepiece respirators. *J Int Soc Respir Protect*  
6 24:49–59.
- 7 Rizvi S, Gores GJ [2014]. Molecular pathogenesis of cholangiocarcinoma.  
8 *Hepatobiliary Tumors. Digestive Disorders* 32:564–569.
- 9 Rizvi S, Borad MJ, Patel T, Gores GJ [2014]. Cholangiocarcinoma: molecular pathways  
10 and therapeutic opportunities. *Seminars in Liver Disease* 34(4):456-464.
- 11 Roberts JR, Kenyon A, Young SH, Schwegler-Berry D, Hackley, VA, MacCusprie RI,  
12 Stefaniak AB, Kashon ML, Chen BT, Antonini JM [2012]. Pulmonary toxicity following  
13 repeated intratracheal instillation of dispersed silver nanoparticles in rats. *The*  
14 *Toxicologist* 126(Suppl 1):141.
- 15 Roberts JR, McKinney W, Kan H, Krajnak K, Frazer DG, Thomas TA, Waugh S, Kenyon  
16 A, MacCusprie RI, Hackley VA, Castranova V [2013]. Pulmonary and cardiovascular  
17 responses of rats to inhalation of silver nanoparticles. *J Toxicol Environ Health, Part A*  
18 76:651–668.
- 19 Rongioletti F, Buffa RE [1992]. Blue nevi-like dotted occupational argyria. *J Am Acad*  
20 *Dermatol* 27:1015–1016.
- 21 Rosenman KD, Moss A, Kon S [1979]. Argyria: clinical implication of exposure to silver  
22 nitrate and silver oxide. *J Occup Med* 21:430–435.
- 23 Rosenman KD, Seixas N, Jacobs I [1987]. Potential nephrotoxic effects of exposure to  
24 silver. *Br J Ind Med* 44:267–272.

- 1 Rouse JG, Yang J, Ryman-Rasmussen JP, Barron AR, Monteiro-Riviere NA [2007].  
2 Effects of mechanical flexion on the penetration of fullerene amino acid-derivatized  
3 peptide nanoparticles through skin. *Nano Lett* 7(1):155–160.
- 4 Ryman-Rasmussen JP, Riviere JE, Monteiro-Riviere NA [2006]. Penetration of intact  
5 skin by quantum dots with diverse physicochemical properties. *Toxicol Sci* 91(1):159–  
6 165.
- 7 Sahu SC, Njoroge J, Bryce SM, Yourick JJ, Sprando RL [2014a]. Comparative  
8 genotoxicity of nanosilver in human liver hepg2 and colon caco2 cells evaluated by a  
9 flow cytometric in vitro micronucleus assay. *J Appl Toxicol* 34(11):1226–1234,  
10 <http://dx.doi.org/10.1002/jat.3065>.
- 11 Sahu SC, Njoroge J, Bryce SM, Zheng J, Ihrle J [2016a]. Flow cytometric evaluation of  
12 the contribution of ionic silver to genotoxic potential of nanosilver in human liver hepg2  
13 and colon caco2 cells. *J Appl Toxicol* 36(4):521–531, <http://dx.doi.org/10.1002/jat.3276>.
- 14 Sahu SC, Roy S, Zheng J, Ihrle J [2016b]. Contribution of ionic silver to genotoxic  
15 potential of nanosilver in human liver hepg2 and colon caco2 cells evaluated by the  
16 cytokinesis-block micronucleus assay. *J Appl Toxicol* 36(4):532–542,  
17 <http://dx.doi.org/10.1002/jat.3279>.
- 18 Sahu SC, Roy S, Zheng J, Yourick JJ, Sprando RL [2014b]. Comparative genotoxicity  
19 of nanosilver in human liver hepg2 and colon caco2 cells evaluated by fluorescent  
20 microscopy of cytochalasin b-blocked micronucleus formation. *J Appl Toxicol*  
21 34(11):1200–1208, <http://dx.doi.org/10.1002/jat.3028>.
- 22 Sahu SC, Zheng J, Graham L, Chen L, Ihrle J, Yourick JJ, Sprando RL [2014c].  
23 Comparative cytotoxicity of nanosilver in human liver hepg2 and colon caco2 cells in  
24 culture. *J Appl Toxicol* 34(11):1155–1166, <http://dx.doi.org/10.1002/jat.2994>.

*This information is distributed solely for the purpose of pre-dissemination peer review under applicable information quality guidelines. It has not been formally disseminated by the National Institute for Occupational Safety and Health. It does not represent and should not be construed to represent any agency determination or policy.*

- 1 Saint S, Veenstra DL, Sullivan SD [2000]. The potential clinical and economic benefits  
2 of silver alloy urinary catheters in preventing urinary tract infection. *Arch Intern Med*  
3 *160*:2670–2675.
- 4 Samberg M, Oldenburg SJ, Monteiro-Riviere NA [2010]. Evaluation of silver  
5 nanoparticle toxicity in skin in vivo and keratinocytes in vitro. *Environ Health Perspect*  
6 *118*:407–413.
- 7 Samberg ME, Lobo EG, Oldenburg SJ, Monteiro-Riviere NA [2012]. Silver  
8 nanoparticles do not influence stem cell differentiation but cause minimal toxicity.  
9 *Nanomedicine* 7(8):1197–1209.
- 10 Sarkar S, Leo BF, Carranza C, Chen S, Rivas-Santiago C, Porter AE, Ryan MP, Gow A,  
11 Chung KF, Tetley TD, Zhang JJ, Georgopoulos PG, Ohman-Strickland PA, Schwander  
12 S [2015]. Modulation of human macrophage responses to mycobacterium tuberculosis  
13 by silver nanoparticles of different size and surface modification. *PLoS One*,  
14 *10*(11):e0143077, <http://dx.doi.org/10.1371/journal.pone.0143077>.
- 15 Sato S, Sueki H, Nishijima A [1999]. Two unusual cases of argyria: the application of an  
16 improved tissue processing method for X-ray microanalysis of selenium and sulphur in  
17 silver-laden granules. *Br J Dermatol* *140*:158–163.
- 18 Sayes CM, Fortner J, Guo W, Lyon D, Boyd AM, Ausman KD, Tao YJ, Sitharaman B,  
19 Wilson LJ, Hughes JB, West JL, Colvin VL [2004]. The differential cytotoxicity of water  
20 soluble fullerenes. *Nano Lett* *4*(10):1881–1887.
- 21 Schaeblin NM, Estep CA, Roberts JR, Hussain SM [2011]. Silver nanowires induced  
22 inflammation in an in vitro human alveolar lung model. Society of Toxicology Annual  
23 Meeting, Washington, DC, March 6–10, 2011. *Toxicol Sci: The Toxicologist* *120*(Suppl  
24 2):A2181, p. 468.

*This information is distributed solely for the purpose of pre-dissemination peer review under applicable information quality guidelines. It has not been formally disseminated by the National Institute for Occupational Safety and Health. It does not represent and should not be construed to represent any agency determination or policy.*

- 1 Schinwald A, Chernova T, Donaldson K [2012]. Use of silver nanowires to determine  
2 thresholds for fibre length-dependent pulmonary inflammation and inhibition of  
3 macrophage migration in vitro. *Particle Fibre Toxicol* 9:47.
- 4 Schinwald A, Donaldson K [2012]. Use of back-scatter electron signals to visualize  
5 cell/nanowire interactions in vitro and in vivo; frustrated phagocytosis of long fibres in  
6 macrophages and compartmentalization in mesothelial cells in vivo. *Particle Fibre*  
7 *Toxicol*, doi: 10.1186/1743-8977-9-34.
- 8
- 9 Schug TT, Nadadur SS, Johnson AF [2013]. Nano GO Consortium-a team science  
10 approach to assess engineered nanomaterials: reliable assays and methods. *Environ*  
11 *Health Perspect* 121:A176–A177, <http://dx.doi.org/10.1289/eph.1306866>.
- 12 Schulte PA, Iavicoli I, Rantanen JH, Dahmann D, Iavicoli S, Pipke R, Guseva Canu I,  
13 Boccuni F, Ricci M, Polci ML, Sabbioni E, Pietroiusti A, Mantovani E [2016]. Assessing  
14 the protection of the nanomaterial workforce. *Nanotoxicology* 10(7):1013-1019.
- 15 Schulte PA, Trout DB [2011]. Nanomaterials and worker health: medical surveillance,  
16 exposure registries, and epidemiologic research. *J Occup Environ Med.* 53(6 Suppl):S3-  
17 7.
- 18 Scott KG, Hamilton JG [1948]. The metabolism of silver. *J Clin Invest* 27:555–556.
- 19 Scott KG, Hamilton JG [1950]. The metabolism of silver in the rat with radiosilver used  
20 as an indicator. *Univ Calif (Berk) Publ Pharmacol* 2:241–262.
- 21 Scrogges MW, Lewis JS, Proia AD [1992]. Corneal argyrosis associated with silver  
22 soldering. *Cornea* 11(3):264–269.
- 23 Seiffert J, Buckley A, Leo B, Martin NG, Zhu J, Dai R, Hussain F, Guo C, Warren J,  
24 Hodgson A, Gong J, Ryan MP, Zhang J, Porter A, Tetley TD, Gow A, Smith R, Chung

- 1 KF [2016]. Pulmonary effects of spark-generated silver nanoparticles in Brown Norway  
2 and Sprague-Dawley rats. *Resp Res* 17:85.  
3
- 4 Seiffert J, Hussain F, Wiegman C, Li F, Bey L, Baker W, Porter A, Ryan MP, Chang Y,  
5 Gow A, Zhang J, Zhu J, Tetley TD, Chung KF [2015]. Pulmonary toxicity of instilled  
6 silver nanoparticles: influence of size, coating, and rat strain. *PLOS ONE*,  
7 doi:10.1371/journal.pone.0119726.  
8
- 9 Shahare B, Yashpal M, Singh G [2013]. Toxic effects of repeated oral exposure of silver  
10 nanoparticles on small intestine mucosa of mice. *Toxicol Mech Methods* 23(3):161–167.  
11
- 12 Shannahan JH, Podila R, Aldossari AA, Emerson H, Powell BA, Ke PC, Rao AM, Brown  
13 JM [2015]. Formation of a protein corona on silver nanoparticles mediates cellular  
14 toxicity via scavenger receptors. *Toxicol Sci* 143(1):136–146,  
15 <http://dx.doi.org/10.1093/toxsci/kfu217>.
- 16 Sharma HS, Hussain S, Schlager J, Ali SF, Sharma A [2010]. Influence of nanoparticles  
17 on blood–brain barrier permeability and brain edema formation in rats. *Acta Neurochir*  
18 *Suppl* 106:359–364.
- 19 Shrivastava R, Kushwaha P, Bhutia YC, Flora SJS [2016]. Oxidative stress following  
20 exposure to silver and gold nanoparticles in mice. *Toxicol Ind Health* 32(8):1391–1404.  
21
- 22 Silva RM, Anderson DS, Franzi LM, Peake JL, Edwards PC, van Winkle LS, Pinkerton  
23 KE [2015]. Pulmonary effects of silver nanoparticle size, coating, and dose over time  
24 upon intratracheal instillation. *Toxicol Sci* 144(1):151–162.  
25
- 26 Silva RM, Anderson DS, Peake J, Edwards PC, Patchin ES, Guo T, Gordon T, Chen  
27 LC, Sun X, van Winkle LS, Pinkerton KE [2016]. Aerosolized silver nanoparticles in the  
28 rat lung and pulmonary response over time. *Toxicologic Pathol* 44(5):673–686.  
29

*This information is distributed solely for the purpose of pre-dissemination peer review under applicable information quality guidelines. It has not been formally disseminated by the National Institute for Occupational Safety and Health. It does not represent and should not be construed to represent any agency determination or policy.*

- 1 Silva RM, Xu J, Saiki C, Donaldson DS, Franzi LM, Vulpe CD, Gilbert B, van Winkle LS,  
2 Pinkerton KE [2014]. Short versus long nanowires: a comparison of in vivo pulmonary  
3 effects post instillation. *Particle Fibre Toxicol*, doi:10.1186/s12989-014-0052-6.
- 4 Silver S [2003]. Bacterial silver resistance: molecular biology and uses and misuses of  
5 silver compounds. *FEMS Microbiol Rev* 27:341–353.
- 6 Sleiman HK, Romano RM, de Oliveira CA, Romano MA [2013]. Effects of prepubertal  
7 exposure to silver nanoparticles on reproductive parameters in adult male Wistar rats. *J*  
8 *Toxicol Environ Health Part A* 76:1023–1032.
- 9 Smijs TGM, Bouwstra JA [2010]. Focus on skin as a possible post of entry for solid  
10 nanoparticles and the toxicological impact. *J Biomed Nanotechnol* 6(5):469–484.
- 11 Smock KJ, Schmidt RL, Hadlock G, Stoddard G, Grainger DW, Munger MA [2014].  
12 Assessment of orally dosed commercial silver nanoparticles on human ex vivo platelet  
13 aggregation. *Nanotoxicology* 8(3):328–333.
- 14
- 15 Smulders S, Larue C, Sarret G, Castillo-Michel H, Vanoirbeek J, Hoet PHM [2015a].  
16 Lung distribution, quantification, co-localization and speciation of silver nanoparticles  
17 after lung exposure in mice. *Toxicol Lett* 238:1–6.
- 18
- 19 Smulders S, Luyts K, Brabants G, Golanski L, Martens J, Vanoirbeek J, Hoet PH  
20 [2015b]. Toxicity of nanoparticles embedded in paints compared to pristine  
21 nanoparticles, in vitro study. *Toxicol Lett* 232(2):333–339,  
22 <http://dx.doi.org/10.1016/j.toxlet.2014.11.030>.
- 23 Smulders S, Luyts K, Brabants G, Van Landuyt K, Kirschhock C, Smolders E, Golanski  
24 L, Vanoirbeek J, Hoet PHM [2014]. Toxicity of nanoparticles embedded in paints  
25 compared with pristine nanoparticles in mice. *Toxicol Sci* 141(1):132–140.
- 26

*This information is distributed solely for the purpose of pre-dissemination peer review under applicable information quality guidelines. It has not been formally disseminated by the National Institute for Occupational Safety and Health. It does not represent and should not be construed to represent any agency determination or policy.*

- 1 Song KS, Sung JH, Ji JH, Lee JH, Lee JS, Ryu HR, Lee JK, Chung YH, Park HM, Shin  
2 BS, Chang HK, Kelman B, Yu IJ [2013]. Recovery from silver-nanoparticle-exposure-  
3 induced inflammation and lung function changes in Sprague Dawley rats.  
4 *Nanotoxicology* 7(2):169–180.
  
- 5 Soto K, Garza KM, Murr LE [2007]. Cytotoxic effects of aggregated nanomaterials. *Acta*  
6 *Biomaterialia* 3:351–358.
  
- 7 Sriram MI, Kanth SBM, Kalishwaralal K, Gurunathan S [2010]. Antitumor activity of  
8 silver nanoparticles in Dalton’s lymphoma ascites tumor model. *Int J Nanomed* 5:753–  
9 762.
  
- 10 Srivastava M, Singh S, Self WT [2012]. Exposure to silver nanoparticles inhibits  
11 selenoprotein synthesis and the activity of thioredoxin reductase. *Environ Health*  
12 *Perspect* 120(1):56–61, <http://dx.doi.org/10.1289/ehp.1103928>.
  
- 13 Stebounova LV, Adamcakova-Dodd A, Kim JS, Park H, O’Shaughnessy PT, Grassian  
14 VH, Thorne PS [2011]. Nanosilver induces minimal lung toxicity or inflammation in a  
15 subacute murine inhalation model. *Particle Fibre Toxicol* 8:5.
  
- 16 Stoehr LC, Gonzalez E, Stampfl A, Casals E, Duschl A, Puentes V, Oostingh GJ [2011].  
17 *Particle Fibre Toxicol* 8:36, <http://www.particleandfibretoxicology.com/content/8/1/36>.
  
- 18 Stone KC, Mercer RR, Freeman BA, Chang LY, Crapo JD [1992]. Distribution of lung  
19 cell numbers and volumes between alveolar and nonalveolar tissue. *Am Rev Respir Dis*  
20 146(2):454–456.
  
- 21 Su CK, Hung CW, Sun YC [2014a]. In vivo measurement of extravasation of silver  
22 nanoparticles into liver extracellular space by push-pull-based continuous monitoring  
23 system. *Toxicol Lett* 227(2):84–90.
- 24

- 1 Su CK, Liu HT, Hsia SC, Sun YC [2014b]. Quantitatively profiling the dissolution and  
2 redistribution of silver nanoparticles in living rats using a knotted reactor-based  
3 differentiation scheme. *Anal Chem* 86(16):8267–8274.  
4
- 5 Su C-L, Chen T-T, Chang C-C, Chuang K-J, Wu C-K, Liu W-T, Ho KF, Lee K-Y, Ho S-  
6 C, Tseng H-E, Chuang H-C, Cheng T-J [2013]. Comparative proteomics of inhaled  
7 silver nanoparticles in healthy and allergen provoked mice. *Internat J Nanomed* 8:2783–  
8 2799.  
9
- 10 Sun X, Wang Z, Zhai S, Cheng Y, Liu J, Liu B [2013]. In vitro cytotoxicity of silver  
11 nanoparticles in primary rat hepatic stellate cells. *Mol Med Rep* 8(5):1365–1372,  
12 <http://dx.doi.org/10.3892/mmr.2013.1683>.
- 13 Sung JH, Ji HJ, Yoon JU, Kim DS, Song MY, Jeong J, Han BS, Han JH, Chung YH,  
14 Kim J, Kim TS, Chang HK, Lee EJ, Lee JH, Yu IJ [2008]. Lung function changes in  
15 Sprague-Dawley rats after prolonged inhalation exposure to silver nanoparticles.  
16 *Inhalation Toxicol* 20:567–574.
- 17 Sung JH, Ji JH, Park JD, Yoon JU, Kim DS, Jeon KS, Song MY, Jeong J, Han BS, Han  
18 JH, Chung YH, Chang HK, Lee JH, Cho MH, Kelman BJ, Yu IJ [2009]. Subchronic  
19 inhalation toxicity of silver nanoparticles. *Toxicol Sci* 108:452–461.  
20
- 21 Sung JH, Ji JH, Song KS, Lee JH, Choi KH, Lee SH, Yu IJ [2011]. Acute inhalation  
22 toxicity of silver nanoparticles. *Toxicol Ind Health* 27:149–154.
- 23 Swanner J, Mims J, Carroll DL, Akman SA, Furdui CM, Torti SV, Singh RN [2015].  
24 Differential cytotoxic and radiosensitizing effects of silver nanoparticles on triple-  
25 negative breast cancer and non-triple-negative breast cells. *Int J Nanomed* 10:3937–  
26 3953, <http://dx.doi.org/10.2147/IJN.S80349>.

*This information is distributed solely for the purpose of pre-dissemination peer review under applicable information quality guidelines. It has not been formally disseminated by the National Institute for Occupational Safety and Health. It does not represent and should not be construed to represent any agency determination or policy.*

- 1 Takenaka S, Karg E, Roth C, Schulz H, Ziesenis A, Heinzmann U, Schramel P, Heyder  
2 J [2001]. Pulmonary and systemic distribution of inhaled ultrafine silver particles in rats.  
3 Environ Health Perspect 109(Suppl 4):547–551.  
4
- 5 Tang J, Xiong L, Wang S, Wang J, Liu L, Li J, Wan Z, Xi T [2008]. Influence of silver  
6 nanoparticles on neurons and blood–brain barrier via subcutaneous injection in rats.  
7 Applied Surface Sci 255:502–504.
- 8 Tang J, Xiong L, Wang S, Wang J, Liu L, Li, J, Yuan F, Xi T [2009]. Distribution,  
9 translocation and accumulation of silver nanoparticles in rats. J Nanosci Nanotech  
10 9:4924–4932.
- 11 Tang J, Xiong L, Zhou G, Wang S, Wang J, Liu L, Li J, Yuan F, Lu S, Wan Z, Chou L, Xi  
12 T [2010]. Silver nanoparticles crossing through and distribution in the blood–brain  
13 barrier in vitro. J Nanosci Nanotechnol 10:6313–6317.
- 14 Tanita Y, Kato T, Hanada K, Tagami H [1985]. Blue macules of localized argyria caused  
15 by implanted acupuncture needles. Arch Dermatol 121:1550–1552.
- 16 Tejamaya M, Romer I, Merrifield RC, Lead JR [2012]. Stability of citrate, PVP, and PEG  
17 coated silver nanoparticles in ecotoxicology media. Environ Sci Technol,  
18 dx.doi.org/10.1021/es2038596.
- 19 Teodoro JS, Simoes AM, Duarte FV, Rolo AP, Murdoch RC, Hussain SM, Palmeira CM  
20 [2011]. Assessment of the toxicity of silver nanoparticles in vitro: a mitochondrial  
21 perspective. Toxicol In Vitro 25(3):664–670, <http://dx.doi.org/10.1016/j.tiv.2011.01.004>.
- 22 Thakur M, Gupta H, Singh D, Mohanty I, Maheswari U, Vanage G, Joshi DS [2014].  
23 Histopathological and ultrastructural effects of nanoparticles on rat testis following 90  
24 days (chronic study) of repeated oral administration. J Nanobiotech 12:42.  
25

*This information is distributed solely for the purpose of pre-dissemination peer review under applicable information quality guidelines. It has not been formally disseminated by the National Institute for Occupational Safety and Health. It does not represent and should not be construed to represent any agency determination or policy.*

- 1 Tiwari DK, Jin T, Behari J [2011]. Dose-dependent in-vivo toxicity assessment of silver  
2 nanoparticle in Wistar rats. *Toxicol Mech Methods* 21(1):13–24.
  
- 3 Trickler WJ, Lantz SM, Murdock RC, Schrand AM, Robinson BL, Newport GD, Schlager  
4 JJ, Oldenburg SJ, Paule MG, Slikker W Jr, Hussain SM, Ali SF [2010]. Silver  
5 nanoparticle induced blood–brain barrier inflammation and increased permeability in  
6 primary rat brain microvessel endothelial cells. *Toxicol Sci* 118:160–170.
  
- 7 Triebig G, Valentin H [1982]. Berufskrankheit Argyrose? – Aktuelle Aspekte  
8 [Occupational disease argyrosis? - Current aspects]. In German. *Verhandlungen der*  
9 *Deutschen Gesellschaft für Arbeitsmedizin* 22:239–243.
  
- 10 Trop M, Novak M, Rodl S, Hellbom B, Kroell W, Goessler W [2006]. Silver-coated  
11 dressing Acticoat caused raised liver enzymes and argyria-like symptoms in burn  
12 patient. *J Trauma* 60:648–652.
  
- 13 Trout DB, Schulte PA [2010]. Medical surveillance, exposure registries, and  
14 epidemiologic research for workers exposed to nanomaterials. *Toxicology* 269(2–  
15 3):128–135.
  
- 16 Tsai S, Huang RF, Ellenbecker MJ [2010]. Airborne nanoparticle exposures while using  
17 constant-flow, constant-velocity, and air-curtain isolated fume hoods. *Ann Occup Hyg*  
18 54(1):78–87.
  
- 19 U.S. DOE [2008]. Approach to nanomaterial ES & H. Washington, DC: U.S. Department  
20 of Energy, Nanoscale Science Research Centers,  
21 [http://science.energy.gov/~media/bes/pdf/doe\\_nsrc\\_approach\\_to\\_nanomaterial\\_esh.pdf](http://science.energy.gov/~media/bes/pdf/doe_nsrc_approach_to_nanomaterial_esh.pdf).
  
- 22 U.S. EPA [1994]. Methods for derivation of inhalation reference concentrations and  
23 application of inhalation dosimetry. Washington, DC: U.S. Environmental Protection  
24 Agency, Office of Research and Development. EPA/600/8-90/066F,  
25 <http://nepis.epa.gov/EPA/html/Pubs/pubtitleORD.html>.

*This information is distributed solely for the purpose of pre-dissemination peer review under applicable information quality guidelines. It has not been formally disseminated by the National Institute for Occupational Safety and Health. It does not represent and should not be construed to represent any agency determination or policy.*

- 1 U.S. EPA [2004]. Risk assessment guidance for superfund, Vol. I: Human Health  
2 Evaluation Manual, <http://www.epa.gov/oswer/riskassessment/ragse/index.htm>. U.S.  
3 [EPA/540/R/99/005](http://www.epa.gov/oswer/riskassessment/ragse/index.htm).
- 4 U.S. EPA [2012a]. Nanosilver: summary of human health data for registration review.  
5 Washington, DC: Office of Chemical Safety and Pollution Prevention. PC Code:  
6 072599, Case No. 5042.
- 7 U.S. EPA [2012b]. Benchmark dose technical guidance. Washington, DC: U.S.  
8 Environmental Protection Agency. EPA/100/R-12/001.
- 9 U.S. EPA [2014]. Benchmark Dose Software (BMDS) Version 2.5. Environmental  
10 Protection Agency, National Center for Environmental Assessment. Available from:  
11 <http://bmds.epa.gov>.
- 12 U.S. EPA [2015]. Benchmark Dose Software (BMDS) Version 2.6.0.1 (Build 88,  
13 6/25/2015). Environmental Protection Agency, National Center for Environmental  
14 Assessment. Available from: <http://bmds.epa.gov>.
- 15 USGS [2014]. U.S. Geological Survey, Mineral Commodity Summaries, January 2013,  
16 <http://minerals.usgs.gov/minerals/pubs/commodity/silver/index.html>.
- 17 Van der Zande M, Vandebriel RJ, Van Doren E, Kramer E, Rivera ZH, Serrano-Rojero  
18 CS, Gremmer ER, Mast J, Peters RJB, Hollman PCH, Hendriksen PJM, Marvin HJP,  
19 Peijnenburh ACM, Bouwmeester H [2012]. Distribution, elimination, and toxicity of silver  
20 nanoparticles and silver ions in rats after 28-day oral exposure. ACS Nano 6(8):7427–  
21 7442.
- 22 Vance ME, Kuiken T, Vejerano EP, McGinnis SP, Hochella MF, Rejeski D, Hull MS  
23 2015]. Nanotechnology in the real world: Redeveloping the nanomaterial consumer  
24 products inventory. Beilstein J Nanotechnol 6(1):1769–1780.

*This information is distributed solely for the purpose of pre-dissemination peer review under applicable information quality guidelines. It has not been formally disseminated by the National Institute for Occupational Safety and Health. It does not represent and should not be construed to represent any agency determination or policy.*

- 1 Virji MA, Stefaniak AB [2014]. A Review of Engineered Nanomaterial Manufacturing  
2 Processes and Associated Exposures. In: Comprehensive Materials Processing.  
3 Bassim N, Editor. Elsevier Ltd. Vol. 8, pp 103–125.
- 4 Vlachou E, Chipp E, Shale E, Wilson YT, Papini R, Moiemmen NS [2007]. The safety of  
5 nanocrystalline silver dressings on burns: a study of systemic silver absorption. Burns  
6 33:979–985.
- 7 Wadhera A, Fung M [2005]. Systemic argyria associated with ingestion of colloidal  
8 silver. Dermatol Online J 11(1):12.
- 9 Wagner GR, Fine LJ [2008]. Surveillance and health screening in occupational health.  
10 In: Wallace RB, ed. Maxcy-Rosenau-Last Public Health and Preventive Medicine. 15<sup>th</sup>  
11 ed. New York: McGraw-Hill Medical Publishing, pp. 759–793.
- 12 Wahlberg JE [1965]. Percutaneous toxicity of metal compounds. Arch Environ Health  
13 11:201–204.
- 14 Wan AT, Conyers RAJ, Coombs CJ, Masterton JP [1991]. Determination of silver in  
15 blood, urine and tissue of volunteers and burn patients. Clin Chem 37:1683–1687.
- 16 Wang XQ, Chang HE, Francis R, et al. [2005]. Silver deposits in cutaneous burn scar  
17 tissue is a common phenomenon following application of a silver dressing. J Cutan  
18 Pathol 36(7):788–792.
- 19 Wang Z, Qu G, Su L, Wang L, Yang Z, Jiang J, Liu S, Jiang G [2013]. Evaluation of the  
20 biological fate and the transport through biological barriers of nanosilver in mice. Curr  
21 Pharm Des 19(37):6691–6697.
- 22  
23 Wei L, Tang J, Zhang Z, Chen Y, Zhou G, Xi T [2010]. Investigation of the cytotoxicity  
24 mechanism of silver nanoparticles in vitro. Biomed Mater 5(4):044103.

*This information is distributed solely for the purpose of pre-dissemination peer review under applicable information quality guidelines. It has not been formally disseminated by the National Institute for Occupational Safety and Health. It does not represent and should not be construed to represent any agency determination or policy.*

- 1 Wen R, Yang X, Hu L, Sun C, Zhou Q, Jiang G [2016]. Brain-targeted distribution and  
2 high retention of silver by chronic intranasal instillation of silver nanoparticles and ions in  
3 Sprague-Dawley rats. *J Appl Toxicol* 36:445–453.  
4
- 5 Wheeler MW, Bailer AJ [2007]. Properties of model-averaged BMDLs: a study of model  
6 averaging in dichotomous response risk estimation. *Risk Anal* 27(3):659–670.
- 7 WHO (World Health Organization) [2010]. Draft environmental health criteria (EHC):  
8 dermal exposure, <http://www.who.int/ipcs/methods/dermal.exposure.pdf>.
- 9 WHO/IPCS (World Health Organization, International Programme on Chemical Safety)  
10 [2005a]. Chemical-specific adjustment factors for interspecies differences and human  
11 variability: guidance document for use of data in dose/concentration assessment.  
12 Geneva: World Health Organization, International Programme on Chemical Safety.
- 13 WHO/IPCS [2005b]. IPCS Harmonization Project document no. 2. Geneva: World  
14 Health Organization, International Programme on Chemical Safety. Available at:  
15 [http://whqlibdoc.who.int/publications/2005/9241546786\\_eng.pdf](http://whqlibdoc.who.int/publications/2005/9241546786_eng.pdf).
- 16 Wijnhoven S, Peijnenburg W, Herberts C, Hagens WI, Oomen A, Heugens EHW,  
17 Roszek B, Bisschops J, Gosens I, Van De Meent D, Dekkers S, De Jong WH, Van  
18 Zijverden, Sips AJAM, Geertsma RE [2009]. Nano-silver: a review of available data and  
19 knowledge gaps in human and environmental risk assessment. *Nanotoxicology*  
20 3(2):109–138.
- 21 Wilding LA, Bassis CM, Walacavage K, Hashway S, Leroueil PR, Morishita M, Maynard  
22 AD, Philbert MA, Bergin IL [2016]. Repeated dose (928-day) administration of silver  
23 nanoparticles of varied size and coating does not significantly alter the indigenous  
24 murine gut microbiome. *Nanotoxicology* 10(5):513–520.  
25

*This information is distributed solely for the purpose of pre-dissemination peer review under applicable information quality guidelines. It has not been formally disseminated by the National Institute for Occupational Safety and Health. It does not represent and should not be construed to represent any agency determination or policy.*

- 1 Williams K, Milner J, Boudreau MD, Gokulan K, Cerniglia CE, Khare S [2016]. Effects of  
2 subchronic exposure of silver nanoparticles on intestinal microbiota and gut-associated  
3 immune response in the ileum of Sprague-Dawley rats. *Nanotoxicology* 9(3):279–289.  
4
- 5 Williams N [1999]. Longitudinal medical surveillance showing lack of progression of  
6 argyrosis in a silver refiner. *Occup Med* 49(6):397–399.
- 7 Williams N, Gardner I [1995]. Absence of symptoms in silver refiners with raised blood  
8 silver levels. *Occup Med* 45(4):205–208.
- 9 Wölbling RH, Milbradt R, Schopenhauer-Germann E, Euler G, König KH [1988]. Argyria  
10 in employees in the silver processing industry: dermatological investigations and  
11 quantitative measurements using atomic absorption spectrometry. *Arbeitsmed*  
12 *Sozialmed Präventivmed* 23:293–297.
- 13 Xue Y, Zhang S, Huang Y, Zhang T, Liu X, Hu Y, Zhang Z, Tang M [2012]. Acute toxic  
14 effects and gender-related biokinetics of silver nanoparticles following an intravenous  
15 injection in mice. *J Appl Toxicol* 32:890–899.
- 16 Youssef HF, Hegazy WH, Abo-Elmaged HH, El-Bassyouni GT [2015]. Novel synthesis  
17 method of micronized ti-zeolite na-a and cytotoxic activity of its silver exchanged form.  
18 *Bioinorg Chem Appl*, 2015:428121, <http://dx.doi.org/10.1155/2015/428121>.
- 19 Yu W-J, Son J-M, Lee J, Kim S-H, Lee I-C, Baek H-S, Shin I-S, Moon C, Kim S-H, Kim  
20 J-C [2014]. Effects of silver nanoparticles on pregnant dams and embryo-fetal  
21 development in rats. *Nanotoxicology* 8(S1):85–91.  
22
- 23 Yun J-W, Kim S-H, You J-R, Kim WH, Jang J-J, Min S-K, Kim HC, Chung DH, Jeong J,  
24 Kang B-C, Che J-H [2015]. Comparative toxicity of silicon dioxide, silver, and iron  
25 nanoparticles after repeated oral administration to rats. *J Appl Toxicol* 35:681–693.  
26

*This information is distributed solely for the purpose of pre-dissemination peer review under applicable information quality guidelines. It has not been formally disseminated by the National Institute for Occupational Safety and Health. It does not represent and should not be construed to represent any agency determination or policy.*

- 1 Zook JM, Long SE, Cleveland D, Geronimo CL, MacCuspie RI [2011]. Measuring silver
- 2 nanoparticle dissolution in complex biological and environmental matrices using UV-
- 3 visible absorbance. *Anal Bioanal Chem* 401:1993–2002.

## APPENDIX A

# Physiologically Based Pharmacokinetic (PBPK) Modeling

### A.1 Background

Risk assessment with rodent bioassay data necessitate exposure-concentration estimates that indicate the human equivalent to the animal effect level (e.g., the NOAEL or BMDL<sub>10</sub>). In estimating the risk of adverse health effects over a working lifetime (e.g., up to 45 years), the dose rate is an additional source of uncertainty, especially when these estimates are based on short-term exposures in animal studies (e.g., 13 weeks). Factors that can influence the retained tissue dose over time include the clearance and retention processes for inhaled particles and the physical-chemical properties of the particles (e.g., size, shape, solubility) or changes to the particles (e.g., dissolution or chemical transformation such as to silver-sulfur nanocrystals) after deposition or uptake in the body [Bachler et al. 2013]. These processes can influence the internal dose of the soluble, more biologically active form of the particles.

Silver is processed in the body through various mechanisms, including sulfidation (binding with sulfur) or opsonization (binding with protein), which results in stabilization of the silver, although it is not known if these processes occur within or outside cells (e.g., macrophages). In human skin and eyes, precipitated granules (micrometer scale) can occur regardless of the form of silver taken/administered, including metallic, ionic, or colloidal silver/nanosilver ([Scroggs et al. 1992; Wang et al. 2009; Wadhwa and Fung 2005; Chang et al. 2006], respectively). In a 28-day oral administration study of silver nanoparticles or silver acetate in rats, Loeschner et al. 2011 measured sulfur and selenium in the precipitated granules of silver in cells (e.g., macrophages). In an *in vitro* study, silver reacted with sulfur, forming "bridges" between the nanoparticles – resulting in decreased dissolution rate and decreased toxicity [Levard et al. 2011, 2012].

1 Silver nanoparticles have been shown to undergo dissolution in the lungs and  
2 translocation to blood, liver, skin, and other organs. Human exposures to silver resulting  
3 in argyria (bluish coloration of skin) have been reported [Hill and Pillsbury 1939; ATSDR  
4 1990; Drake and Hazelwood 2005; Wijnhoven et al. 2009; Johnston et al. 2010;  
5 Lansdown 2012]. To better estimate the airborne exposures and tissue doses  
6 associated with argyria in humans, physiologically based pharmacokinetic (PBPK)  
7 modeling is needed to estimate the relationship between external (airborne) exposure  
8 and internal tissue dose of Ag nanoparticles after inhalation.

9 The Bachler et al. [2013] PBPK model was developed on the basis of rat data and  
10 extrapolated to humans. It consists of two sub-models, one for ionic silver and one for  
11 silver nanoparticles. Both sub-models were validated with independent data from the  
12 literature. Figure 1 of Bachler et al. [2013] shows the structures and inter-dependencies  
13 between these sub-models. The PBPK models in Bachler 2013 were designed as  
14 membrane-limited models (vs. flow limited), as also used by Li et al. [2012]. In this  
15 model, both silver ions and nanoparticles can translocate from the lungs to the blood  
16 (Figures 2A and 2B in Bachler et al. 2013). In the blood, both ionic and nanoparticle  
17 silver are predicted to translocate to other organs, including the liver, kidney, and spleen  
18 (Figures 7A and 7B in Bachler et al. [2013]). Soluble silver is considered to be the most  
19 active form, from which silver ions are released at a rate that depends on various  
20 factors such as the particle form and size and the tissue compartment. Some evidence  
21 indicates that silver ions readily react with sulfhydryl groups to form silver-sulfur  
22 complexes. Glutathione (GSH) is the most common mercaptan (source of sulfhydryl  
23 groups) in many cells and, therefore, plays a major role in the biodistribution of ionic  
24 silver [Bell and Kramer 1999; Hansen et al. 2009]. Since liver has by far the highest  
25 levels of GSH of any organs, most ionic silver is taken up by the liver. Bachler et al.  
26 [2013] defined organ silver uptake as being proportional to the relative organ GSH  
27 concentration, thus allowing for a reduction in the number of model parameters.

28 In the general population, less than 0.5 g of silver is estimated to be stored in the  
29 human body within a lifetime, although 100 g or more of silver was been reported to be

1 stored in extreme cases [ICRP 1960; East et al. 1980; Wadhera and Fung 2005]. Based  
2 on this information, Bachler et al. [2013] modeled the storage compartments for each  
3 organ (except blood) as sinks from which no silver is released and which have infinite  
4 capacity. The total storage of ionic silver in the rat's body was set to 0.5%, based on  
5 experimental results after intravenous injection of an ionic silver solution [Furchner et al.  
6 1968].

7 In the Bachler et al. [2013] PBPK model, two possible scenarios were considered for the  
8 metabolism of AgNPs (as shown in Figure 3 of that publication): (1) AgNPs dissolve and  
9 release soluble silver species, which are described in the ionic silver PBPK model, and  
10 (2) AgNPs are directly transformed to silver sulfide particles. Scenario 2 was found to  
11 result in the best model fit to the data. Bachler et al. [2013] attribute their model finding  
12 (of no significant dissolution of AgNPs to silver ions) to the stabilization of the  
13 nanoparticles by proteins adsorbed to the particle surface and/or to the transformation  
14 of silver to silver-sulfur nanocrystals (either of which would reduce the dissolution rate).  
15 Scenario 2 was considered to be supported by the evidence that silver readily reacts  
16 with mercaptans, that silver sulfide is detected in tissue samples after exposure to ionic  
17 silver, and that the silver tissue burdens predicted by that model scenario agree well  
18 with the tissue burden data from Kim et al. [2008] after oral exposure to AgNPs in rats  
19 [Bachler et al. 2013, including supplementary material]. Thus, a direct storage  
20 mechanism of silver to silver sulfide particles (i.e., bypassing ion formation) was used in  
21 the main model calculations [Bachler et al. 2013].

22 The rat silver nanoparticle and ionic models in Bachler et al. [2013] were calibrated with  
23 data from Lankveld et al. [2010] and Klaassen [1979], respectively, with some of the  
24 individual rate parameters from other studies, as noted in Bachler et al. [2013]. Lankveld  
25 et al. [2010] and Klaassen [1979] administered silver intravenously to rats and  
26 measured the silver excretion or tissue doses for up to 16 or 7 days post-exposure,  
27 respectively. Silver particles of 20, 80, or 110 nm diameter were used in Lankveld et al.  
28 [2010], and an ionic silver solution was administered in Klaassen [1979]. Bachler et al.  
29 [2013] reported that in the calibration and validation of their model, they utilized

1 experimental data of only easily soluble silver species (silver nitrate and silver acetate)  
2 or ionic silver solutions. [Note: the form and solubility of the silver in Lankveld et al.  
3 [2010] was not verified, as it was not found to be reported in their publication]. Data from  
4 four additional studies in rats were compared to the rat model predictions in Bachler et  
5 al [2013] (Figures 4 and 5 in that article), including two inhalation studies of AgNPs in  
6 rats [Takenaka et al. 2001; Ji et al. 2007]. Bachler et al. [2013] then extrapolated the rat  
7 model to humans by adjusting for species-specific differences in the respective  
8 physiological factors and body or organ weights [ICRP 2002]. This rat-extrapolated  
9 human PBPK model showed good correlation with the human biomonitoring data from  
10 three sources [DiVincenzo et al. 1985] (Figure 6C in Bachler et al. [2013]). Human  
11 model parameter values were based on those for the reference worker (adult male)  
12 [ICRP 2002]; possible kinetic differences by sex or age were not considered. The  
13 human model-predicted [Bachler et al. 2013] and measured values of silver in blood  
14 and feces (detailed in the report of a worker biomonitoring study) [DiVincenzo et al  
15 1985] were shown to be in good agreement [Bachler 2013, Figure 6C].

16 In addition to the Ag tissue estimates from PBPK modeling in rats based on short-term  
17 exposures, silver tissue doses have been measured in rats following subchronic (13- or  
18 12-week) inhalation of AgNPs (~19- or 15-nm diameter, respectively) [Sung et al. 2009;  
19 Song et al. 2013]. As described in this section, the rat tissue burden data were used to  
20 estimate the human-equivalent tissue doses and working lifetime exposures associated  
21 with the adverse effects observed in the rat subchronic inhalation studies. These  
22 adverse effects included pulmonary inflammation and bile duct hyperplasia (see Section  
23 5.1). Thus, the lung and liver tissue dose data in rats were used to estimate the human-  
24 equivalent lung and liver doses of silver, assuming occupational airborne exposure to  
25 silver nanoparticles for up to a 45-year working lifetime.

26 The objectives of this evaluation are to (1) examine the relationship between the  
27 exposure concentrations and the lung and liver tissue doses in rats after subchronic  
28 inhalation exposure; (2) estimate the rat effect levels based on lung and liver tissue  
29 doses, including the NOAELs, LOAELs, and benchmark dose (BMD) estimates; and (3)

1 estimate the human-equivalent working lifetime exposure concentrations (up to 45  
2 years) associated with the rat adverse effect levels, based on either the active/soluble  
3 (i.e., able to release ions and/or form complexes such as silver sulfide) or the total silver  
4 concentrations (i.e., both the active/soluble and the complexed silver) in tissues. The  
5 PBPK model of Bachler et al. [2013] was used to estimate the occupational exposures  
6 (as 8-hour time-weighted average [TWA] concentrations) of AgNPs for up to a 45-year  
7 working lifetime associated with the estimated equivalent tissue doses to those in rats  
8 with no or minimal adverse effects in the lungs or liver.

9 Before estimation of the human-equivalent concentrations to the rat subchronic effect  
10 levels, analyses were performed to compare the airborne exposure and tissue dose  
11 concentrations of silver in the two rat subchronic inhalation studies. Analyses were also  
12 performed to compare the Bachler et al. [2013] model predictions of the measured  
13 tissue doses of silver in both rat studies [Sung et al. 2009; Song et al. 2013].

## 14 **A.2 Silver Tissue Doses in Rats**

15 The relationships between the airborne cumulative exposure concentration of AgNPs  
16 (19- or 15-nm diameter) and the measured silver burden in lung or liver tissues in rats  
17 (male and female) following subchronic inhalation (13 or 12 weeks) [Sung et al. 2009;  
18 Song et al. 2013] were examined (Sections A.2.1 and A.2.2). The cumulative exposure  
19 metric was used to adjust for the exposure duration difference in these two studies (13  
20 vs. 12 weeks in Sung et al. [2009] and Song et al. [2013], respectively). In both lung and  
21 liver, the variability in the silver tissue burdens increased with exposure concentration.

22 The finding of non-constant (heterogeneous) variance in the tissue burdens given  
23 exposure may be due to the inter-individual rat differences in the clearance and  
24 retention of silver nanoparticles (toxicokinetics). Despite the increased variability in the  
25 silver tissue doses at the highest dose, the two lower doses – which are associated with  
26 no or minimal adverse effects – are most relevant to human health risk assessment.

## 1 A.2.1 Lungs

2 The rat lung tissue burdens of silver also varied by study [Sung et al. 2009; Song et al.  
3 2013] and by sex (Figure A-1). The measured burdens are higher in Sung et al. [2009]  
4 at all doses for both male and female rats, and a disproportionately higher Ag lung tissue  
5 dose is seen in rats at the highest exposure concentration (515  $\mu\text{g}/\text{m}^3$ ) [Sung et al.  
6 2009]. The higher burdens observed at all airborne exposure concentrations in Sung et  
7 al. [2009] could be due to higher deposition efficiencies of inhaled AgNPs in the lungs of  
8 rats in that study, although this is considered unlikely because rats in both studies were  
9 exposed to similar-sized particles (~19-nm diameter vs. ~15-nm median diameter in  
10 Sung et al. [2009] and Song et al. [2013], respectively). Particles of similar diameter  
11 would be expected to have similar deposition efficiencies. Other, unexplained  
12 differences in the animals and/or experimental conditions may have resulted in these  
13 between-study differences. The relatively low number of animals also needs to be taken  
14 into account when comparing tissue burdens across groups (i.e.,  $n = 3\text{--}5$  rats per lung  
15 or liver tissue group in male or female rats in Sung et al. [2009];  $n = 9$  male rats and  $n =$   
16 4 female rats per lung or liver tissue group in Song et al. [2013]).

17 The steeper increase in the lung tissue burdens at the higher exposure concentration in  
18 Sung et al. [2009] (Figure A-1) is consistent with the possibility that impairment of lung  
19 clearance resulted in a disproportionate increase in the lung retention of silver particles  
20 at the highest exposure concentration (515  $\mu\text{g}/\text{m}^3$ ). In general, the within-study lung  
21 tissue burdens (among males or females) were less variable than the between-study  
22 (Sung et al. [2009] or Song et al. [2013]) Ag lung tissue burdens, at the same (or similar  
23 interpolated) airborne exposure concentrations.

## 24 A.2.2 Liver

25 The rat silver tissue burdens in the liver are generally more consistent across study and  
26 sex (Figure A-2) than those in the lungs (Figure A-1). At the two lower concentrations,  
27 the rat liver tissue burdens are relatively similar between the two studies [Sung et al.  
28 2009; Song et al. 2013] and between males and females within each study. As was also

1 observed in the lungs, the liver silver burdens seem to increase disproportionately at the  
2 highest concentration (515  $\mu\text{g}/\text{m}^3$  [Song et al. 2013]), suggesting increased tissue  
3 retention of silver at that concentration, especially in female rats. Male and female rat  
4 liver tissue doses of silver were similar in the Sung et al. [2009] study at the lower  
5 exposure concentrations and varied by a factor of approximately three between the  
6 studies [Sung et al. 2009; Song et al. 2013] at the lowest exposure concentration (49  
7  $\mu\text{g}/\text{m}^3$ ) (Figure A-2).

### 8 **A.3 Effect Level Estimates in Rats and Humans**

9 The rat subchronic inhalation studies [Sung et al. 2008, 2009; Song et al. 2013] yielded  
10 NOAELs or LOAELs for minimal adverse lung or liver effects. The lung response of  
11 chronic pulmonary inflammation (minimal) and the liver response of bile duct  
12 hyperplasia (minimal) were selected as potentially adverse responses of relevance to  
13 humans. The silver tissue doses associated with either no significant increase (NOAEL)  
14 or a low (10%) increase (BDML<sub>10</sub>) in these responses were selected as the target doses  
15 for risk assessment based on PBPK modeling [Bachler et al. 2013]. This model was  
16 used to estimate the working lifetime exposure concentrations that would result in the  
17 equivalent lung or liver tissue concentrations. In addition, for endpoints with sufficient  
18 data (at least one intermediate dose group with a response between that of the controls  
19 and the highest response), BMDL<sub>10</sub> values were estimated with dose-response  
20 modeling (as discussed in Appendix B).

21 Table A-1 shows estimated doses of silver in lung and liver tissues in rats after  
22 subchronic inhalation (for 12 or 13 weeks), at the NOAEL and BMDL<sub>10</sub> estimates. Dose-  
23 response data were not sufficient for modeling the chronic alveolar inflammation  
24 response in male or female rats in Sung et al. [2009] or in female rats in Song et al.  
25 [2013]. In those cases, the NOAELs only are provided in Table A-1. Dose-response  
26 data for chronic alveolar inflammation in male rats in Song et al. [2013] were minimally  
27 acceptable for BMDL<sub>10</sub> estimation (Appendix B). The highlighted doses are selected as  
28 representative target tissue doses of silver associated with either no or low estimated  
29 risk of adverse effects in the lungs or liver. These doses were selected as being the

1 lowest estimates for a given study, response endpoint, or sex and were used as target  
2 doses in the PBPK modeling.

3 As shown in Table A-1, the NOAEL lung tissue doses of silver vary substantially  
4 between the two studies [Song et al. 2013; Sung et al. 2009] (up to an order of  
5 magnitude or more), although the exposure concentrations and durations were similar.  
6 This suggests that rats in the Sung et al. [2009] study retained considerably more silver  
7 in their lungs during the 13-week exposure than did the rats in the Song et al. [2013]  
8 study (to a greater extent than the one additional week would suggest) but did not  
9 develop adverse lung effects at those doses. The generation method and particle size  
10 of the silver were similar between the two studies, which were performed in the same  
11 laboratory. The reason for the large difference in silver lung tissue burdens in the two  
12 studies is not known, and it contributes to uncertainty in the lung tissue dose level for  
13 use in risk assessment. Sex differences in the mean lung tissue silver dose are also  
14 observed, although these sex differences are smaller than the between-study  
15 differences in silver lung tissue dose. It is also possible that there may have been an  
16 unknown difference in solubility of the AgNP used in the two studies [Sung et al. 2009,  
17 diameter ~19 nm; Song et al. 2013, diameter ~15 nm], which could have resulted in  
18 different rates of clearance of AgNP from the lungs, or that the analytical method used  
19 for quantifying silver in tissues gave varying results.

20 Unlike the results for the lungs, the liver tissue doses of silver at the NOAEL were quite  
21 similar in male and female rats in Sung et al. [2009] (Table A-1) and in rats at the lower  
22 doses in the Song et al. [2013] study (which did not report any findings on bile duct  
23 hyperplasia) (see Figure A-2).

## 24 **A.4 PBPK Model Estimates**

### 25 **A.4.1 Overview of PBPK modeling runs**

26 A recently developed PBPK model for silver uptake and disposition in the body [Bacher  
27 et al. 2013] was used to estimate the internal tissue doses of silver in workers after up

1 to 45 years of inhalation exposure to AgNPs [Bachler 2015, report to NIOSH]. Model  
2 simulations were performed to estimate the following:

- 3 • Occupational exposure concentration (8-hour TWA, time-weighted average)  
4 concentration of AgNP over a 45-year working lifetime (8 hr/d, 5 d/wk) associated  
5 with the retention of Ag in the skin at the target dose of 3.2  $\mu\text{g Ag/g skin}$ , which is  
6 reported to be the lowest dose associated with argyria in humans [Bachler et al.  
7 2013]; estimates are provided for AgNPs of different diameters and for ionic  
8 silver. The purpose of these estimates is to evaluate whether working lifetime  
9 exposures to AgNPs at the current NIOSH REL for silver (10  $\mu\text{g/m}^3$ , 8-hour TWA  
10 concentration) would be likely to result in argyria.
- 11 • Tissue dose levels of silver in humans, assuming inhalation exposure to AgNPs  
12 (either 15 or 100 nm in diameter) or ionic silver over a 45-year working lifetime at  
13 10  $\mu\text{g/m}^3$  (8-hour TWA) concentration. The purpose of these estimates is to  
14 evaluate whether working lifetime exposures to AgNPs would result in lung and  
15 liver tissue concentrations of silver above the rat adverse effect levels.
- 16 • Occupational exposure concentration (8-hour TWA) of AgNPs over a 45-year  
17 working lifetime that would result in the human-equivalent lung or liver tissue  
18 dose to that in the rat associated with adverse (early-stage) effects; estimates for  
19 either 15- or 100-nm-diameter AgNPs. No tissue dose data are available on  
20 humans exposed to AgNPs; thus, the rat subchronic inhalation data of AgNPs  
21 (median diameter, ~15–20 nm) are extrapolated to humans to estimate the target  
22 tissue doses associated with early-stage adverse lung or liver effects in rats.

23 All human model simulations are for an adult male, assuming light exercise (typically 1.2  
24  $\text{m}^3/\text{d}$  for 8 hours) and nasal breathing pattern, using the parameter values reported in  
25 Bachler et al. [2013]. Prior to these human model simulations, rat model simulations  
26 were performed of compare estimates from the rat model calibrated from other rat data  
27 on AgNP kinetics by inhalation and other routes of exposure [Bachler et al. 2013]. The  
28 parameters used in the rat model and the human model are reported in Tables A-2 and  
29 A-3, respectively.

1 Additional model runs (results not shown) included evaluations of rat models with  
2 increased lung clearance rate; human model estimates for mixed particle sizes of 1–100  
3 nm, assuming uniform particle size distribution (these estimates are shown for argyria  
4 estimates only); and human model estimates for other rat-based target tissue doses,  
5 including the rat NOAEL estimates of 100 or 117  $\mu\text{g}/\text{m}^3$  and human-equivalent tissue  
6 dose estimates of 47 or 23  $\mu\text{g}/\text{m}^3$  (adult male, light exercise, nose breathing) estimated  
7 in Song et al. [2013] [Bachler 2015, report to NIOSH].

#### 8 A.4.2 Comparison of model-predicted and measured lung and liver tissue 9 burdens in rats

10 The Bachler et al. [2013] PBPK model was calibrated and validated on the basis of data  
11 on silver nanoparticles in rat studies, including inhalation exposure studies by Ji et al.  
12 [2007] (same laboratory as the Sung et al. [2008, 2009] and Song et al. [2013] studies)  
13 and by Takenaka et al. [2001]. These studies reports described tissue burden/kinetics  
14 data only, not biological response. Reports of other rat studies [Sung et al. 2008, 2009;  
15 Song et al. 2013] presented both tissue burden and response data, which are used in  
16 this risk assessment. As discussed in this section, the lung and liver tissue burdens  
17 reported in those four rat studies [Takenaka et al. 2001; Ji et al. 2007; Sung et al. 2009;  
18 Song et al. 2013] are compared to each other, and the model-predicted tissue burdens  
19 are compared to the data in Sung et al. [2009] and Song et al. [2013], which had not  
20 been used in the calibration or validation of the Bachler et al. [2013] model.

21 Ji et al. [2007] performed a 28-day inhalation exposure study in rats (male and female, 6  
22 weeks of age, specific-pathogen-free [SPF] Sprague-Dawley) exposed to 0, 0.5, 3.5, or  
23 61  $\mu\text{g}/\text{m}^3$  AgNPs (6 h/day, 5 days/wk, for 4 weeks). The AgNP diameter was ~12-15 nm  
24 (GSD ~1.5) in the three exposure concentrations. The AgNPs were generated by  
25 evaporation/condensation using a small ceramic heater; this is the same particle  
26 generation method used in the subchronic inhalation studies [Sung et al. 2008, 2009;  
27 Song et al. 2013]. Takenaka et al. [2001] conducted a 1-day inhalation exposure study  
28 in rats (female Fischer 344 rats; body weight, 150–200 g) that were exposed for 6 hours

1 at 133  $\mu\text{g}/\text{m}^3$  to silver nanoparticles; rats were killed on days 0, 1, 4, and 7. The silver  
2 lung burden immediately after exposure was 1.7  $\mu\text{g Ag}$ , which decreased rapidly to 4%  
3 of the initial lung burden by day 7. The AgNP median diameter was  $17.1 \pm 1.2$  nm  
4 (GSD = 1.38). The AgNPs were generated by a spark discharging through an argon  
5 atmosphere [Takenaka et al. 2001]. In the two studies, the AgNP diameters were  
6 similar, although the particle generation methods were different. These different  
7 generation methods could have resulted in different surface properties of the AgNPs,  
8 which could potentially have affected their toxikinetiic properties.

9 *Lungs:* Figure A-3 show the end-of-exposure silver lung tissue burdens in these four rat  
10 studies by cumulative exposure ( $\mu\text{g}/\text{m}^3 \times \text{hours}$ ) (normalized) to account for the  
11 differences in exposure concentration and duration. These plots do not account for  
12 differences in the clearance of silver from the lungs during the exposure time, ranging  
13 from 1 day (6-hour exposure) in Takenaka et al. [2001], to 28 days in Ji et al. [2007], to  
14 12 weeks in Song et al. [2013], and 13 weeks in Sung et al. [2009]. The results show  
15 much higher lung silver burdens in Takenaka et al. [2001] and Ji et al. [2007] at a given  
16 cumulative exposure concentration. These higher lung burdens could have been due to  
17 higher deposition fractions (although median particle sizes were similar) or a lower  
18 proportion of the deposited dose was cleared; given the short duration of exposure (6-  
19 hr) in Takenaka et al. [2001], there would have been less time for alveolar macrophage-  
20 mediated clearance, although the silver lung burden cleared rapidly in the 1-7 days  
21 post-exposure [Takenaka et al. 2001, Table 1].

22 *Liver:* Figure A-4 shows the end-of-exposure silver liver tissue burdens in these four rat  
23 studies, also plotted by cumulative exposure ( $\mu\text{g}/\text{m}^3 \times \text{hours}$ ) (normalized) to account for  
24 the differences in exposure concentration and duration. Again, these plots do not  
25 account for differences in the amount of silver cleared from the liver during the exposure  
26 time (as mentioned above for the lungs). These results show similar liver silver burdens  
27 in the 4-, 12-, and 13-week exposure studies [Ji et al. 2007; Song et al. 2013; Sung et  
28 al. 2009, respectively], suggesting similar build-up rates of silver in liver over time. The  
29 highest liver silver burden is observed in the Takenaka et al. [2001] study, relative to

1 similar cumulative exposure concentrations in the other studies, which may reflect the  
2 rapid initial translocation to the liver in this acute exposure. These findings illustrate the  
3 importance of accounting for the clearance pathways in the estimation of tissue doses  
4 over time. Cumulative exposure may be a good surrogate for the total deposited lung  
5 dose, but a PBPK model is needed to account for particle dissolution and clearance  
6 from the lungs and translocation to other organs.

7 The PBPK model–predicted tissue burdens of silver, based on the Bachler et al. [2013]  
8 rat model, were higher than the measured rat burdens of silver in lung and liver tissues  
9 at the end of the subchronic (12- or 13-week) inhalation exposure [Sung et al. 2009;  
10 Song et al. 2013] (Figures A-5 and A-6). For example, at the middle exposure  
11 concentration ( $133 \mu\text{g}/\text{m}^3$  in Sung et al. [2009] or  $117 \mu\text{g}/\text{m}^3$  in Song et al. [2013]), the  
12 model-predicted rat lung burdens were higher by a factor of approximately 3 compared  
13 to the measured lung burdens in Sung et al. [2009] and by a factor of approximately 4–7  
14 compared to the lung burdens in Song et al. [2013], among male and female rats. The  
15 model-predicted rat liver burden of silver was approximately 1.5- to 3-fold higher than  
16 the measured rat liver burdens in male and female rats in both studies [Sung et al.  
17 2009; Song et al. 2013]. The number of rats per tissue-burden group were 3–5 males  
18 and  $n = 5$  females in Sung et al. [2009] and  $n = 9$  males and  $n = 4$  females in Song et al.  
19 [2013]. The sample sizes for the Monte Carlo simulations in the PBPK model estimates  
20 were assumed to be equal to those of the same observed groups [Note: Bachler et al.  
21 2013 used 1,000 model iterations in the Monte Carlo simulations. Background levels of  
22 silver were not considered, although these would typically be low compared to the levels  
23 of silver from the inhalation exposure].

24 The over-prediction of the lung and liver tissue burdens compared to the measured  
25 tissue burdens in the rat subchronic inhalation studies may be due to several factors.  
26 First, between-study variability and small numbers of animals could contribute to the  
27 apparent differences. Second, the PBPK model was calibrated and validated against rat  
28 data from shorter durations of exposure (1- or 28-day inhalation) at exposure  
29 concentrations of  $133 \mu\text{g}/\text{m}^3$  (1 d) or 0, 0.5, 3.5, or  $61 \mu\text{g}/\text{m}^3$  (28 days) in Takenaka et

1 al. [2001] or Ji et al. [2007]. By comparison, rats were exposed to generally higher  
2 concentrations (0, 49, 117, or 133, and 381 or 515  $\mu\text{g}/\text{m}^3$ ) over longer durations (12 or  
3 13 weeks) in Song et al. [2013] or Sung et al. [2009]. The higher tissue burdens in the  
4 shorter-term inhalation studies [Takenaka et al. 2001; Ji et al. 2007] used in the PBPK  
5 modeling, extrapolated to longer-term exposures, may have contributed to over-  
6 estimation of the tissue burdens in the subchronic inhalation studies, in which there was  
7 apparently a higher clearance rate of silver from the rat lungs and liver [Sung et al.  
8 2009; Song et al. 2013]. Another possibility is the AgNPs differed (e.g., in solubility)  
9 across the studies; however, the particle sizes were similar (~12-19 nm in median  
10 diameter). The Ji et al. [2007] study used the same AgNP generation method as used  
11 in the subchronic studies [Sung et al. 2009; Song et al. 2013]. As discussed above, a  
12 different AgNP generation method was used by Takenaka et al. [2010], and the different  
13 generation methods could have resulted in differences in the surface properties and  
14 toxicokinetics of the AgNPs in those studies.

15 An area of uncertainty is how this apparent model over-prediction of rat silver tissue  
16 doses would influence the estimates of human-equivalent exposure concentrations.  
17 Other model uncertainties suggest the silver tissue burdens could be underestimated,  
18 for example, by extrapolating the rat subchronic data to human working-lifetime  
19 exposures based on a long-term clearance model (ICRP 1994), as used in Bachler et  
20 al. [2013]. Human studies have shown that the ICRP [1994] model under-predicts the  
21 long-term retention of poorly soluble particles in the lungs of humans [Kuempel and  
22 Tran 2002; Gregoratto et al. 2010], although these models do not include particle  
23 dissolution pathways.

#### 24 **A.4.3 Human-equivalent working lifetime exposure concentrations**

25 Estimation of working lifetime exposure concentrations of silver depend on the  
26 occupational exposure concentration and duration. The occupational route of exposure  
27 for these simulations is assumed to be inhalation. The deposited dose in the respiratory  
28 tract depends on the airborne particles size. The retained dose in the lungs and in other

1 organs depends on the absorption rate of Ag from the lungs to the systemic circulation  
2 [Bachler et al. 2013].

#### 3 A.4.4 Worker body burden estimates of silver from diet and occupational 4 exposures

5 Apart from some workers' potential occupational exposure to silver, humans take in a  
6 certain amount of silver in the daily diet. The routes of exposure differ but are assumed  
7 to be primarily inhalation in the workplace and oral from diet. Studies of intravenous  
8 silver administration have also been reported [e.g., Park et al. 2011a]. Regardless of the  
9 route of exposure, silver nanoparticles can be absorbed into the adjacent tissue, enter  
10 the systemic circulation, and be taken into all organs in the body, including liver, kidney,  
11 spleen, bone marrow, and brain [Bachler et al. 2013; Song et al. 2013; Brune 1980].

12 A few studies have measured or estimated the tissue dose or body burdens of silver  
13 from diet [Snyder et al. 1975; Kehoe et al. 1940] or occupational exposures [DiVincenzo  
14 et al. 1985; Wölbling et al. 1988]. Table A-4 show findings from DiVincenzo et al. [1985]  
15 on Ag body burden in humans from diet and from occupational exposure, as well as  
16 retention estimates based on Ag biomonitoring results in workers at a U.S. facility that  
17 produced silver for photographic processes and products. The study included workers  
18 with airborne exposure to silver (n = 30) and control workers at the same facility without  
19 airborne exposures to silver (n = 35) (randomly selected) (sample sizes from Table 2 of  
20 DiVincenzo et al. 1985). Most of the workers with silver exposure had worked for 5 or  
21 more years in a production area with the highest potential exposure to airborne silver.  
22 Job descriptions included burner operators, maintenance workers, smelter operators,  
23 and mechanics, as well as other jobs. In both groups the mean duration of employment  
24 was approximately 20 years and the mean age was approximately 45 years.

25 The annual body burden of silver from the diet in unexposed workers (controls)  
26 estimated by DiVincenzo et al. [1985] (assuming 1% intestinal absorption) was 2 µg  
27 Ag/kg body weight (BW), or storage/retention of 1% silver (form of silver not reported)

*This information is distributed solely for the purpose of pre-dissemination peer review under applicable information quality guidelines. It has not been formally disseminated by the National Institute for Occupational Safety and Health. It does not represent and should not be construed to represent any agency determination or policy.*

1 (Table A-4). Based on the Bachler et al. [2013] PBPK model (assuming 4% intestinal  
2 absorption), the estimated annual body burden of silver nanoparticles is 1 µg Ag/kg BW,  
3 and that of ionic silver is 3 µg Ag/kg BW (corresponding to either 0.77% or 0.25%  
4 storage/retention after 45 years). These similar estimates reported in DiVincenzo et al.  
5 [1985] and calculated from the Bachler et al. [2013] model provide information relevant  
6 to validation of the PBPK model predictions.

7 Table A-4 (as well as Table 5 of DiVincenzo et al. 1985) provides information from  
8 which to estimate the average airborne concentration of the workers in that study. The  
9 estimated exposed worker daily Ag uptake (as reported in Table 5 of DiVincenzo et al.  
10 1985) is 0.054 µg Ag/kg BW (assuming 1% of the "silver intake" was retained in the  
11 body), or 3.78 µg Ag/d for a 70-kg adult male. Although not specifically stated in  
12 Divincenzo et al. [1985], it is implied that the "silver intake" is the inhaled dose and that  
13 the 1% silver retained in the the body includes the fraction of the the inhaled dose that is  
14 deposited in the respiratory tract and then absorbed and retained in the body.

15 Thus, the daily airborne exposure concentration can be estimated as follows, assuming  
16 a reference worker air intake of 9.6 m<sup>3</sup> in an 8-hour day:

17  $3.78 \mu\text{g/d uptake in Ag worker} = X \mu\text{g/m}^3 * 9.6 \text{ m}^3/\text{d} * 0.01 \text{ intake fraction}$

18 or

19  $X \mu\text{g/m}^3 = 3.78 \mu\text{g/d} / [9.6 \text{ m}^3/\text{d} * 0.01]$

20 where  $X = 39.4 \mu\text{g/m}^3$ .

21 This estimate is consistent with the airborne exposure concentrations of 1–100 µg/m<sup>3</sup>  
22 measured over a 2-month period, as reported by DiVincenzo et al. [1985]. DiVincenzo  
23 et al. [1985] reported an estimated occupational airborne average exposure  
24 concentration of approximately 30 µg/m<sup>3</sup> [Note that DiVincenzo et al. 1985 used 3.38  
25 µg/d (vs. 3.78 µg/d from the Table 5 value of 0.054 ug/kg x 70 kg). An airborne  
26 concentration of 33.8 µg/m<sup>3</sup> is calculated from 3.38 µg/d / (10 m<sup>3</sup>/d \* 0.01), which

1 supports the interpretation that DiVincenzo et al. [1985] considered the 1% “intake  
2 fraction” to include the deposited respiratory tract dose and the retention/storage dose.  
3 “Insoluble silver” was considered to be the primary form of silver to which workers were  
4 exposed in that study (DiVincenzo et al. 1985, p. 208). The worker annual body burden  
5 of silver was approximately 6-fold higher (12 µg Ag/kg BW) than that from diet (2 µg  
6 Ag/kg BW) (total of (14 µg Ag/kg BW in exposed workers), although the route of  
7 exposure and internal organs exposed differ.

8 No adverse health effects were reported in the DiVincenzo et al. [1985] study (among  
9 workers with ~20-year exposure, age ~45 years). However, the purpose of that study  
10 was to estimate Ag body burdens based on measurements in feces, urine, blood, and  
11 hair, and the report did not present any biomedical findings. Thus, there is uncertainty  
12 about whether any adverse health effects occurred in those workers, associated with  
13 their occupational exposure to silver.

14 Silver tissue burden estimates in humans, based on measurements or model  
15 predictions, are provided in Tables A-5 and A-6. Measured tissue burdens of silver in  
16 smelter workers and in workers without occupational exposure to silver (controls), as  
17 reported in Brune [1980], are reported in Table A-5. Estimates of silver tissue burdens  
18 from dietary intake are provided in Table A-6 and are based on PBPK model [Bachler et  
19 al. 2013] estimates of silver tissue burden that assume exposure up to 45 years and an  
20 average dietary intake of 80 µg/d (based on an upper estimate of 60–80 µg/d from  
21 Snyder et al. [1975] and Kehoe et al. [1940], as reported in DiVincenzo et al. [1985]).

#### 22 A.4.5 Estimated working lifetime exposure concentrations associated with 23 argyria

24 Argyria (bluish pigmentation of the skin) has been observed in humans with Ag burdens  
25 of 3.2 µg/g skin tissue; this skin tissue dose was measured in an individual that  
26 developed argyria at the lowest administered dose of 1.84 g (intravenous) of silver

1 arspenamine [Triebig and Valentin 1982; Wadhera et al. 2005; Gaul and Staud 1935,  
2 as reported in Bachler et al. 2013].

3 Table A-7 shows the working lifetime exposure concentrations (8 hr/d, 5 d/wk, and 52  
4 wk/yr, for up to 45 years) estimated to result in an Ag skin concentration that has been  
5 associated with argyria at the lowest dose in humans (3.2  $\mu\text{g/g}$ , as reported in Bachler  
6 et al. 2013). These estimated working-lifetime exposure concentrations associated with  
7 argyria depend on the particle diameter (1–100, 15, 100 nm) and physical-chemical  
8 form (ionic, nanoparticle). The estimated average airborne exposure concentrations to  
9 reach the minimum skin tissue dose associated with argyria over a 45-year working  
10 lifetime range from 47  $\mu\text{g}/\text{m}^3$  for exposure to ionic silver to 78  $\mu\text{g}/\text{m}^3$  for exposure to 15-  
11 nm-diameter Ag nanoparticles or 253  $\mu\text{g}/\text{m}^3$  for exposure to 100-nm-diameter Ag  
12 nanoparticles. These estimated concentrations are based on the skin tissue dose in a  
13 sensitive human, i.e., at the lowest administered dose reported to be associated with  
14 argyria.

15 All of these estimates of working lifetime exposure concentrations associated with  
16 argyria exceed the current NIOSH REL and OSHA PEL of 10  $\mu\text{g}/\text{m}^3$  (for any particle  
17 size; soluble or insoluble), by factors of approximately 5 to 25. These PBPK model-  
18 based estimates suggest that the current NIOSH REL and OSHA PEL of 10  $\mu\text{g}/\text{m}^3$  (8-  
19 hour TWA concentration, up to 45-year working lifetime) would be protective against the  
20 development of argyria in workers exposed to airborne AgNPs or ions. These estimates  
21 are consistent with the estimates of silver body burdens not expected to result in argyria  
22 that were used as the basis for the OSHA PEL and NIOSH REL (see Section 1.4).

#### 23 **A.4.6 Estimated silver tissue burdens in workers with inhalation exposure to** 24 **10 $\mu\text{g}/\text{m}^3$ of AgNP**

25 The estimated tissue doses of silver in workers with airborne exposures at the current  
26 NIOSH REL for silver (i.e., 10  $\mu\text{g}/\text{m}^3$ , as an 8-hour TWA concentration; total airborne  
27 particle size sampling; soluble or insoluble particles) are shown in Table A-8. The

1 soluble/active Ag tissue dose appears to reach an approximate steady-state tissue  
2 concentration in the lung, liver, and other tissues (due to first-order rate of  
3 transformation of active/soluble silver to insoluble silver in the PBPK model). The total  
4 silver tissue doses appear to continue increasing up to the 45-year working lifetime  
5 (because of the slow pulmonary clearance of insoluble particles). These Ag tissue  
6 doses (ng/g) in workers (up to a 45-year working lifetime) are compared to the rat Ag  
7 target tissue dose estimates (Ag ng/g) (NOAEL or BMDL10) associated with no or low  
8 adverse (early stage) lung or liver effects in the rat subchronic inhalation studies. It  
9 should be noted that no UFs were applied to the rat effect level estimates in these  
10 comparisons.

#### 11 **A.4.6.1 Lungs**

12 The PBPK model-based estimates of the human lung tissue dose after 45 years of  
13 exposure to silver at the NIOSH REL of  $10 \mu\text{g}/\text{m}^3$  (8-hour TWA, total silver) depended  
14 on particle size and form (i.e., 222, 690, or 1,640 ng/g for 100-nm, 15-nm, or ionic silver,  
15 respectively) (Table A-8). The female rat Ag lung-tissue doses at the NOAEL (no  
16 pulmonary inflammation) were 672 ng/g [Song et al. 2013] and 4,242 ng/g [Sung et al.  
17 2009], which are lower than the male rat Ag lung-tissue dose of 5,450 ng/g at the  
18 NOAEL (Table A-1). Thus, the estimated soluble/active Ag tissue dose from a working  
19 lifetime exposure to 15-nm AgNP (690 ng/g) or ionic silver (1,640 ng/g) at  $10 \mu\text{g}/\text{m}^3$  (8-  
20 hour TWA) was estimated to exceed the rat NOAEL for pulmonary inflammation from  
21 one of the subchronic inhalation studies (672 ng/g) [Song et al. 2013] but did not exceed  
22 the rat NOAEL lung Ag tissue dose (4,241 ng/g) from the other rat study [Sung et al.  
23 2009] (Table A-1).

24 Some of the lung tissue estimates of Ag (Table A-8) also exceeded those reported for  
25 smelter workers ( $0.28 \mu\text{g}$  Ag/g lung tissue) (Table A-5) by more than two orders of  
26 magnitude; however, silver exposures of smelter workers were not reported [Brune  
27 1980]. Comparison of the estimated cumulative exposures to  $10 \mu\text{g}/\text{m}^3$  silver for 45  
28 years (i.e.,  $450 \mu\text{g}\text{-yr}/\text{m}^3$ ) to the average cumulative exposures reported in DiVincenzo  
29 et al. [1985] (estimated in Section A.4.4 at  $39.4 \mu\text{g}/\text{m}^3$  for 20 years, i.e.,  $788 \mu\text{g}\text{-yr}/\text{m}^3$ )

1 suggests that workers studied by DiVincenzo et al. [1985] had nearly two-fold higher  
2 cumulative exposures, compared to those estimated at the REL. Medical results were  
3 not reported by DiVincenzo et al. [1985].

#### 4 **A.4.6.2 Liver**

5 The PBPK model-based estimates of the human liver tissue dose after 45 years of  
6 exposure to silver at the NIOSH REL of 10  $\mu\text{g}/\text{m}^3$  (8-hour TWA, total silver) also  
7 depended on particle size and form (i.e., 3, 10, or 40 ng/g for 100-nm, 15-nm, or ionic  
8 silver, respectively) (Table A-8). The rat liver-tissue doses of silver at the NOAEL (no  
9 bile duct hyperplasia) were 12 ng/g in females and 14 ng/g in males, as reported by  
10 Sung et al. [2009] (Table A-1). The rat BMDL<sub>10</sub> estimates for bile duct hyperplasia were  
11 similar (6.3 and 12 ng/g) (Table A-1). Thus, the estimated soluble/active Ag tissue dose  
12 from a working lifetime exposure to 100-nm AgNP (3 ng/g) did not exceed the NOAEL  
13 or BMDL<sub>10</sub> tissue dose estimates (6–14 ng/g), whereas those for the 15-nm AgNP (10  
14 ng/g) or ionic silver (40 ng/g) were similar to or higher than those rat effect level  
15 estimates.

16 These results suggest that the estimated risk for developing bile duct hyperplasia  
17 (minimal or higher severity) depend on whether the relevant dose metric is the total  
18 silver or the soluble/active silver, as well as on the particle size and type. The total  
19 tissue dose of silver in workers would include both the background exposure (e.g., from  
20 diet) and the workplace exposure (e.g., from inhalation). Average human background  
21 level of silver in liver tissue (e.g., from dietary sources) has been reported at 0.017  $\mu\text{g}/\text{g}$   
22 [ICRP 1960]. This measured background level of silver in liver tissue is similar to the  
23 PBPK model-predicted liver tissue dose of silver from the diet after a 45-year working  
24 lifetime (0.023  $\mu\text{g}/\text{g}$  total silver) (Table A-6). In smelter workers, the average silver  
25 concentration in liver tissue was 0.032  $\mu\text{g}/\text{g}$  [Brune 1980], although the workplace  
26 exposure was not reported.

*This information is distributed solely for the purpose of pre-dissemination peer review under applicable information quality guidelines. It has not been formally disseminated by the National Institute for Occupational Safety and Health. It does not represent and should not be construed to represent any agency determination or policy.*

1 These estimated human liver tissue concentrations of silver are higher than the rat liver  
2 tissue silver concentrations at the estimated NOAEL and BMDL<sub>10</sub> (0.006–0.014 µg/g).  
3 Thus, it is difficult to interpret the significance of the rat study findings to humans, given  
4 that the rat effect levels are similar to the background level in humans (and presumably  
5 not associated with adverse effects in the general population). Possible explanations  
6 may include the following: (1) the silver nanoparticles in the rat study may be more toxic  
7 than the silver to which humans were exposed historically; (2) the rat may be more  
8 sensitive to silver at tissue doses equivalent to the human background level; (3) the  
9 silver liver tissue doses may be underestimated (e.g., if silver were lost in the analysis);  
10 and/or (4) the minimal severity liver effects near the rat effect levels may be subclinical  
11 in humans and therefore not observed. No information is available to assess these  
12 possible explanations, and thus, these quantitative estimates from the rat data are  
13 uncertain.

#### 14 **A.4.7 Estimated 45-year working lifetime airborne exposure concentrations** 15 **equivalent to rat effect levels**

16 Estimated human-equivalent 45-year working lifetime exposures of AgNP (8-hour TWA)  
17 to the rat effect levels (BMDL<sub>10</sub> or NOAEL) are shown in Table A-9, by particle size and  
18 type. Assuming total AgNP (both soluble and insoluble) is the relevant tissue dose  
19 metric, the 45-year working lifetime exposure concentration estimates that result in  
20 human lung or liver tissue doses equivalent to the rat target tissue doses (NOAEL or  
21 BMDL<sub>10</sub> estimates in Table A-1) are all lower than 10 µg/m<sup>3</sup>. The airborne concentration  
22 estimates for the 15-nm Ag are lower than those for the 100-nm Ag (Table A-9).

23 Assuming that soluble/active AgNP is the relevant tissue dose metric, some of these  
24 working lifetime 8-hour TWA concentration estimates are less than the existing NIOSH  
25 REL of 10 µg/m<sup>3</sup> (i.e., those at the BMDL<sub>10</sub>, which are the most sensitive target tissue  
26 dose estimates). Other estimates for the soluble/active Ag tissue burden are greater  
27 than 10 µg/m<sup>3</sup> (Table A-9). The most sensitive (lowest) dose metric is total silver; the

*This information is distributed solely for the purpose of pre-dissemination peer review under applicable information quality guidelines. It has not been formally disseminated by the National Institute for Occupational Safety and Health. It does not represent and should not be construed to represent any agency determination or policy.*

1 45-year working lifetime estimated 8-hour TWA exposure concentration at the BMDL<sub>10</sub>  
2 or NOAEL was 0.19–1.5 µg/m<sup>3</sup>, which suggests a REL.

### 3 **A.5 Evaluation of PBPK Modeling Results**

#### 4 **A.5.1 Utility of PBPK modeling estimates**

5 PBPK modeling permits evaluation of the predicted lung and liver doses in workers  
6 versus those measured in rat subchronic inhalation studies of silver nanoparticles (15-  
7 to 19-nm diameter) and associated with no or low level of early-stage adverse effects in  
8 the lungs or liver. This PBPK model also permits evaluation of the skin tissue burden  
9 associated with argyria in humans and estimates of silver in workers based on  
10 occupational (inhalation) or dietary (oral) exposure.

11 The Bachler et al. [2013] PBPK model was calibrated from AgNP kinetics data in rats  
12 and extrapolated to humans on the basis of interspecies adjustment of physiological  
13 and morphological parameters that influence the deposition and disposition of silver  
14 particles following inhalation. The human model was shown to provide good prediction  
15 of the limited biomonitoring data in workers exposed to silver [Bachler et al. 2013].

16 Bachler et al. [2013] report certain limitations in their PBPK model that could bias an  
17 evaluation of the particle dissolution. For instance, model calibration with the  
18 experimental data could have incorporated some dissolution that was not accounted for  
19 in the model (i.e., that may have occurred during the 5 days of intravenous  
20 administration of silver or during the 16 days post-exposure until Lankveld et al. [2013]  
21 investigated the silver tissue burdens and kinetics). In addition, since the Bachler et al.  
22 [2013] ionic PBPK model was also calibrated with data after the intravenous injection (in  
23 this case of an ionic silver solution, with rats examined 7 days post-exposure [Klaassen  
24 1979]), the model accounts only for silver ions that are able to freely distribute within the  
25 body. That means those that dissolve and transform to silver sulfide within cells would  
26 be outside of the application domain of the model, according to Bachler et al. [2013].

1 The pulmonary or intestinal absorption fraction of Ag ions or nanoparticles is an area of  
2 uncertainty in the human PBPK model [Bachler et al. 2013]. Although no human data  
3 are known to be available for these parameters, the sensitivity of the model estimates to  
4 the assumed parameter values could be investigated. Another area of uncertainty is  
5 whether the smaller AgNPs (e.g., <15 nm) may translocate more efficiently from the  
6 lungs to the blood. If this occurs, as was shown recently for gold nanoparticles [Kreyling  
7 et al. 2014], then the silver burdens in the lungs and other organs may depend to a  
8 greater extent on the particle size. A key data gap in the evaluation of this PBPK model  
9 is the lack of chronic inhalation exposure data of AgNPs in rats on which to further test  
10 it.

#### 11 A.5.2 Comparison of human data to rat-based estimates

12 A useful evaluation of the rat-based OEL estimates for silver nanoparticles is to  
13 compare those estimates to the occupational exposure and health effects data in  
14 workers exposed to silver in various processes (Section 2). Reports of studies in  
15 humans typically did not give the airborne particle sizes (Section 2). However, exposure  
16 to AgNPs would be anticipated in some production [e.g., in DiVincenzo et al. 1985].  
17 Miller et al. [2010] did measure and report airborne exposures to AgNPs in workers'  
18 breathing zones, including airborne concentrations that exceed the NIOSH REL.

19 No researchers have reported adverse health effects other than argyria in workers with  
20 long-term inhalation exposures to silver (e.g., ~20 years at ~39  $\mu\text{g}/\text{m}^3$  [DiVincenzo et al.  
21 1985], which is greater than the NIOSH REL of 10  $\mu\text{g}/\text{m}^3$  for up to 45 years); however,  
22 few studies have performed medical evaluations of workers exposed to silver dust and  
23 fumes (e.g., Pifer et al. [1989]; Rosenman et al. [1979, 1987], discussed in Sections 2  
24 and 3). Researchers who have reported argyria in workers have not reported adverse  
25 lung or liver effects associated with exposure to silver (although their studies were  
26 relatively small, e.g., involving a few dozen workers). Adverse lung or liver effects are  
27 predicted from the rat studies to develop at similar or lower Ag tissue doses than those  
28 associated with argyria (Table A-7; Table A-10), and therefore adverse lung or liver

1 effects would be expected to be observed in workers with sufficient exposures to cause  
2 argyria. This absence of reported lung or liver effects in workers (including those with  
3 argyria) suggests that the lung and liver effects in rats could be early-stage, pre-clinical  
4 effects that are not associated with adverse function. On the other hand, the absence of  
5 reported adverse health effects in workers could be due to insufficient study, especially  
6 of workers exposed to silver nanoparticles.

7 An evaluation of the available evidence from the human and rat studies, and from PBPK  
8 modeling, is discussed in detail below. Comparisons are made between the tissue dose  
9 levels of silver reported in the rat studies and as estimated in humans exposed for up to  
10 a 45-year working lifetime, including at the current NIOSH REL for silver of  $10 \mu\text{g}/\text{m}^3$ .  
11 These findings are discussed for the measured and/or estimated silver tissue doses and  
12 responses in the skin, lungs, and liver of rats and humans.

### 13 A.5.3 Argyria risk

14 Comparison of the PBPK-model [Bachler et al. 2013] estimates of skin tissue burdens to  
15 those associated with argyria in humans suggests that workers exposed for up to a 45-  
16 year working lifetime at the current NIOSH REL for silver would not likely develop  
17 argyria (Table A-7). That is, the estimated working lifetime airborne exposure  
18 concentrations (8-hour TWA) resulting in the lowest skin tissue dose reported to be  
19 associated with argyria in humans ( $3.2 \mu\text{g}/\text{g}$  [Triebig et al. 1982]) were higher than the  
20 REL of  $10 \mu\text{g}/\text{m}^3$  for all particle sizes and types evaluated. These exposure estimates  
21 were 47, 78, or  $253 \mu\text{g}/\text{m}^3$ , respectively, for ionic silver, AgNPs of 15-nm diameter, and  
22 AgNPs of 100-nm diameter.

23 These PBPK model-based estimates suggest an approximately 5- to 25-fold margin of  
24 exposure (MOE) between the current REL and the lowest reported human skin tissue  
25 dose of silver associated with argyria. An MOE is the ratio between an effect level and  
26 an exposure [Kim E et al. 2016]. As discussed previously, no other adverse effects  
27 associated with silver exposure have been reported to occur in humans with argyria.

#### 1 A.5.4 Lung inflammation risk

2 The rat effect levels (NOAEL or BMDL<sub>10</sub>) based on the lung tissue dose of silver (Table  
3 A-1) can be compared to the predicted human tissue doses of silver, given workplace  
4 exposure at the NIOSH REL of 10 µg/m<sup>3</sup> (Table A-8). These predictions depend on  
5 particle size and solubility. According to the Bachler et al. [2013] model, the human total  
6 silver doses in lung tissue after a 45-year working lifetime at the REL are estimated to  
7 be 11, 36, or 85 µg/g for 100-nm-diameter AgNPs, 15-nm-diameter AgNPs, or ionic Ag,  
8 respectively. The estimated human soluble/active silver doses in lung tissue are lower,  
9 at 0.22, 0.69, or 1.6 µg/g for the same particle size and form. These human silver lung  
10 tissue dose estimates exceed the rat BMDL<sub>10</sub> estimate of 0.033 µg/g and the rat NOAEL  
11 of 0.081 µg/g in male rats in Song et al. [2013] (Table A-1). The estimated human  
12 soluble/active silver doses in lung tissue do not exceed the NOAELs of 0.672 or 4.2  
13 µg/g silver in lung tissue in female rats in Song et al. [2013] or Sung et al. [2009],  
14 respectively.

15 Available data show the human background lung tissue dose of silver in unexposed  
16 workers is 0.032 µg/g (Table A-5) [Brune 1980]. In smelter workers, the average lung  
17 tissue dose was 0.33 µg/g, although the no data were available on exposures to silver  
18 or on adverse lung effects associated with that dose.

19 These findings indicate that the risk estimates of developing adverse lung effects after a  
20 working lifetime exposure to silver nanomaterials at the current REL depend on the  
21 assumed dose metric (total or soluble/active) and the rat effect level estimate. The rat  
22 lung tissue silver dose estimates (BMDL<sub>10</sub> or NOAEL) for pulmonary inflammation vary  
23 widely, depending on the study and sex (Table A-1). These large differences in the  
24 quantitative estimates of the rat lung tissue dose of silver associated with adverse  
25 pulmonary effects contributes to the uncertainty in the estimated human equivalent lung  
26 tissue dose after a working lifetime exposure at the current silver REL.

1 The wide difference in the effect level estimates for pulmonary inflammation in the same  
2 rat sex across the two studies raises uncertainty about the doses associated with that  
3 response (e.g., female rat NOAEL of 0.67 or 4.2 ng/g, associated with 117 or 133  
4 mg/m<sup>3</sup> exposure concentration, in Song et al. [2013] or Sung et al. [2009]) (Table A-1).  
5 Thus, for similar airborne exposure concentrations, the associated silver lung tissue  
6 doses were nearly an order of magnitude different. This difference in tissue dose could  
7 be due to differences in the particles between the two studies (although these were  
8 generated by the same method and had similar characteristics) or to difficulties in  
9 obtaining consistent analytical results for quantifying the tissue burdens. The challenge  
10 of obtaining adequate recovery of the silver administered to rodent lungs was reported  
11 in the NIEHS NanoGo consortium [<http://ehp.niehs.nih.gov/1306866/>] at SOT 2015  
12 [<http://www.toxicology.org/AI/MEET/am2015/ss.asp>]. High variability in the recovery  
13 amounts were also reported in the NIEHS studies, and it was difficult to achieve mass  
14 balance in many cases. The Sung et al. [2009] and Song et al. [2013] studies did not  
15 report mass balance (nor did the study design permit that estimate, since the initial  
16 deposited dose was not reported).

#### 17 **A.5.5 Bile dust hyperplasia risk**

18 The rat liver effect levels (NOAEL or BMDL<sub>10</sub>) (Table A-1) can be also compared to the  
19 predicted dose of silver in human liver tissue at the NIOSH REL of 10 µg/m<sup>3</sup> (Table A-  
20 8). These predictions depend on particle size and solubility, as seen also for the lung  
21 tissue dose estimates. Based on the Bachler et al. [2013] model, the human total silver  
22 dose in liver tissue after a 45-year working lifetime at the REL is estimated to be 0.077,  
23 0.25, or 0.50 µg/g for 100-nm-diameter AgNPs, 15-nm-diameter AgNPs, or ionic Ag,  
24 respectively. The estimated soluble/active silver tissue doses are lower, at 0.003, 0.01,  
25 or 0.04 µg/g for the same particle size and form. The total silver doses exceed the rat  
26 effect levels (BMDL<sub>10</sub> estimates of 0.006 µg/g in females and 0.012 µg/g in males). The  
27 rat NOAELs for bile duct hyperplasia, 0.012 µg/g in females and 0.014 µg/g in males,  
28 are similar to the BMDL<sub>10</sub> estimates (Table A-1). The human estimated liver tissue  
29 doses of soluble/active silver are similar to the rat effect levels, with some estimates in

1 humans above or below those in rats. These results suggest that the estimated risk for  
2 developing bile duct hyperplasia (minimal or higher severity) depend on whether the  
3 relevant dose metric is the total silver or the soluble/active silver, as well as on the  
4 particle size and type.

5 Available data on human background liver dose of silver (from dietary sources) indicate  
6 background silver levels of approximately 0.017 µg/g [ICRP 1960] or 0.032 µg/g [Brune  
7 1980]. These human liver tissue concentrations of silver are similar to or higher than the  
8 rat liver tissue silver concentrations at the NOAEL and BMDL<sub>10</sub> (0.0063–0.014 µg/g)  
9 (Table A-1). This finding suggests that on a mass basis, humans are exposed to  
10 background levels of silver that exceed the no or low effect level in rats for liver bile duct  
11 hyperplasia. It also suggests uncertainty in the quantification of the silver tissue doses.  
12 The estimated equivalent 45-year working lifetime exposures to the rat BMDL<sub>10</sub> estimate  
13 range from 0.26 to 1.5 µg/m<sup>3</sup> based on a total silver dose metric, and 6 to 37 µg/m<sup>3</sup>  
14 based on soluble/active silver (8-hour TWA airborne concentrations) (Table A-9). The  
15 range reflects differences in estimates by particle size and by sex.

16 These findings indicate that the risk estimates at the NIOSH REL depend on the  
17 assumed dose metric (total or soluble/active) for silver. However, some evidence  
18 suggests that the rat may be more sensitive or the effect level may be underestimated.  
19 First, the human predicted liver doses after dietary exposure to silver (0.023 µg/g total  
20 silver after 45 years) (Table A-9) exceed the rat effect levels. Second, the background  
21 concentrations of silver in liver tissue (from dietary sources) reported in the general U.S.  
22 population (~0.017 µg/g) also exceed the rat effect levels of 0.006 or 0.012 µg Ag/g  
23 tissue. Thus, the quantitative estimates from the rat data are uncertain, possibly  
24 because of (1) erroneous measurement of silver in rat tissue, (2) higher sensitivity of the  
25 rat to silver tissue levels, and/or (3) these effects being subclinical.

## 1 A.5.6 Silver nanoparticle form

2 The form of the silver in the human or rat tissues is not known. It may be reasonable to  
3 assume that the proportion of active/soluble silver in the rat subchronic inhalation  
4 studies would be greater than that in the humans over a lifetime. This assumption is  
5 based on the hypothesis that opsonization (protein binding) of silver occurs essentially  
6 immediately in mammals, forming a “protein corona” that stabilizes the particles  
7 [Bachler et al. 2013; Landsiedel et al. 2011]. Thus, over time, the proportion of total  
8 silver that is in the soluble/active form would be smaller. If the soluble/active form of  
9 silver is more relevant to the toxicity, then it may be more relevant to use an equivalent  
10 active/soluble silver dose in the rat and human tissues, based on the PBPK model  
11 estimates. On the other hand, if the insoluble nanoparticle dose is related to the toxicity,  
12 then the total silver tissue dose should be used to estimate the airborne concentration.  
13 The role of the physical-chemical form of the silver on its toxicity remains an area of  
14 uncertainty, although the general findings from the literature suggest that the smaller  
15 particle size and greater solubility are more toxic (Section 5.6).

16

This information is distributed solely for the purpose of pre-dissemination peer review under applicable information quality guidelines. It has not been formally disseminated by the National Institute for Occupational Safety and Health. It does not represent and should not be construed to represent any agency determination or policy.

1 **TABLES AND FIGURES FOR APPENDIX A**

2 **Table A-1. Estimated target tissue doses of silver nanoparticles, based on rat**  
 3 **subchronic inhalation studies.**

Target organ	Adverse endpoint	Sex	Exposure concentration (µg/m <sup>3</sup> )	Tissue dose, measured or estimated (ng/g) <sup>a</sup>	Type of effect level
<b>Song et al. 2013</b>					
Lung	Chronic alveolar inflammation, minimal	M	49	33 <sup>b</sup>	BMDL <sub>10</sub>
				81	NOAEL
		F	117	<b>672</b>	<b>NOAEL</b>
<b>Sung et al. 2009</b>					
Lung	Chronic alveolar inflammation, minimal	M	133	5,450	<b>NOAEL</b>
		F		<b>4,241</b>	
Liver	Bile duct hyperplasia, minimal	M	133	<b>11.6</b>	<b>BMDL<sub>10</sub></b>
				14	NOAEL
		F		<b>6.3</b>	<b>BMDL<sub>10</sub></b>
				12	NOAEL

4  
 5 <sup>a</sup> Tissue doses of silver, as NOAEL or BMDL<sub>10</sub>.  
 6 <sup>b</sup> Estimate was excluded from evaluation because of limited data and modeling options (see Appendix B).  
 7 NOAEL: No observed adverse effect level. The NOAEL is the highest dose group above the control (unexposed)  
 8 group that did not have a significantly greater proportion of rats with an adverse lung or liver response.  
 9 NOAELs are as reported in: Sung et al. 2009 - Table 7 (M), Table 8 (F); Song et al. 2013 - Table II (M), Table III (F).  
 10 BMDL<sub>10</sub>: Benchmark dose (95% lower confidence limit) associated with a 10% response (BMDL<sub>10</sub>), derived from  
 11 benchmark dose modeling (U.S. EPA BMDS version 2.5) of the measured tissue dose and response data,  
 12 including: liver bile dust hyperplasia - Sung et al. Table 9 (M), Table 10 (F); lung inflammation - Song et al. Table  
 13 XII (M). (See Appendix B for the BMD modeling results.)  
 14 Notes: The human-equivalent tissue dose is assumed to be equal to the rat target tissue dose expressed as ng Ag/g  
 15 tissue. PBPK modeling was used to estimate the occupational airborne exposure to Ag (as 8-hour time-weighted  
 16 average concentration, 40 hr/wk, up to 45 years) that would result in the same target tissue burden in humans  
 17 (Section A.4). Human-equivalent estimates to those in bold type are shown in Table A-9.

18

*This information is distributed solely for the purpose of pre-dissemination peer review under applicable information quality guidelines. It has not been formally disseminated by the National Institute for Occupational Safety and Health. It does not represent and should not be construed to represent any agency determination or policy.*

1 **Table A-2. Physiological parameters for rat used in silver nanoparticle PBPK**  
 2 **model [Bachler et al. 2013].**

RAT	Organ weight		Blood Flow amount		GSH concentration	
	[% of total body weight]	SD	[% of total Blood Volume]	SD	[ $\mu\text{mol/g}$ ]	SD
Skin <sup>°</sup>	19.0	2.620	5.80	0.09	0.37	0.08
Liver	3.66	0.650	18.30	2.50	9.37	0.86
Kidneys	0.730	0.110	14.10	1.90	2.45	0.14
Muscles <sup>°</sup>	40.4	7.170	27.80	13.34	0.73	0.20
Spleen*	0.200	0.050	0.85	0.26 <sup>†</sup>	2.12	0.09
Heart	0.330	0.040	5.10	0.10	2.12	0.52
Brain	0.570	0.140	2.00	0.30	1.64	0.11
Lung	0.500	0.090	2.10	0.40	2.04	0.01
Testes <sup>°</sup>	1.03	0.060	0.79	0.16	3.41	0.20
Small Intestines <sup>°</sup>	1.40	0.390	10.14	2.43	1.78	0.24
Large Intestines <sup>°</sup>	0.840	0.040	1.64	0.44	2.10	0.22
Thymus <sup>^</sup>	0.102	0.057	0.42	0.21	1.90	0.15
Remainder	31.2	7.67	26.26	13.94	1.22	0.09
Cardiac Output [L/min]	0.095	0.013		<b>Average:</b>	1.22	0.09
Blood [L]	0.022	0.002				
Body Weight [kg]	0.300					

3 Reference values taken from Brown et al. [1997], blood flow: \*Davies et al 1993, °Stott et al 2006.

4 ^ Hatai et al 1914, Alhamdan & Grimble 2003, Jansky & Hart 1968.

5 † Estimate based on the distribution of other organs; no exact values available.

6 Note: these parameters are used in Monte Carlo runs based on a new (unpublished) version of Bachler  
 7 et al. [2013] model; the new version also includes a remainder compartment to account for the  
 8 discrepancies observed between administered doses of silver and recovered doses measured in the  
 9 tissues; the remainder compartment includes muscles and bone marrow.

10

*This information is distributed solely for the purpose of pre-dissemination peer review under applicable information quality guidelines. It has not been formally disseminated by the National Institute for Occupational Safety and Health. It does not represent and should not be construed to represent any agency determination or policy.*

1 **Table A-3. Physiological parameters for humans used in silver nanoparticle PBPK**  
 2 **model [Bachler et al. 2013].**

Human	Organ weight		Blood Flow amount		GSH concentration	
	[% of total body weight]	SD	[% of total Blood Volume]	SD	[ $\mu\text{mol/g}$ ]	SD
Skin	4.36	0	5.92	1.13	0.46	0.20
Liver	2.47	0	21.3	4.84	6.40	0.40
Kidneys	0.420	0	18.1	2.32	4.00	0.30
Muscles	39.7	0	14.2	5.10	1.80	0.08
Spleen	0.210	0	3.43	1.24	2.12 <sup>a</sup>	0.09 <sup>a</sup>
Heart	0.450	0	4.91	1.32	1.20	0.20
Brain	1.99	0	11.8	1.77	1.40	0.30
Lung	0.680	0	3.38	2.49	2.04 <sup>a</sup>	0.01 <sup>a</sup>
Testes	0.048	0	0.10	0.00	3.41 <sup>a</sup>	0.20 <sup>a</sup>
Small Intestines	1.40	0	9.10	2.20	1.78 <sup>a</sup>	0.24 <sup>a</sup>
Large Intestines	0.490	0	3.80	0.40	2.10 <sup>a</sup>	0.22 <sup>a</sup>
Thymus <sup>^</sup>	0.034	0	0.42 <sup>a</sup>	0.21 <sup>a</sup>	1.90 <sup>a</sup>	0.15 <sup>a</sup>
Remainder	47.7	0	18.3	8.59	1.87	0.06
Cardiac Output [L/min]	6.5	1.300	<b>Average:</b>		1.87	0.06
Blood [L]	5.6	0.810				
Body Weight [kg]	73					

3 Reference value sources: weight, ICRP 2002; blood flow, Williams and Legget 1989; GSH, various [see  
 4 Bachler et al. 2013].

5 <sup>^</sup> Hatai et al. 1914, Alhamdan & Grimble 2003, Jansky & Hart 1968.

6 <sup>a</sup> Values from the rat.

7 Note: these parameters are used in Monte Carlo runs based on a new (unpublished) version of Bachler  
 8 et al. [2013] model; the new version also includes a remainder compartment to account for the  
 9 discrepancies observed between administered doses of silver and recovered doses measured in the  
 10 tissues; the remainder compartment includes muscles and bone marrow.

11

*This information is distributed solely for the purpose of pre-dissemination peer review under applicable information quality guidelines. It has not been formally disseminated by the National Institute for Occupational Safety and Health. It does not represent and should not be construed to represent any agency determination or policy.*

1 **Table A-4. Estimated annual body burden of silver in humans – based on**  
 2 **biomonitoring measurements and estimates [DiVincenzo et al. 1985] or PBPK**  
 3 **model predictions [Bachler et al. 2013].**

Study	Ag Form	Annual body burden (µg Ag/kg body wt)	Retention (%)
DiVincenzo et al. [1985]* Workers (workplace + diet)	NR	14	1
	NR	2	1
Bachler et al. [2013] – Controls (diet)	Nanoparticle	3	0.77
	Ionic	1	0.25

4 NR: not reported.

5 \*As reported in Table 5 of DiVincenzo et al. [1985].

6

7 **Table A-5. Silver tissue doses in smelter workers who had exposures to silver**  
 8 **and in workers without silver exposures [Brune 1980].**

Organ	Ag-exposed workers: Organ dose (µg Ag/g tissue)	Unexposed workers: Organ dose (µg Ag/g tissue)
Lung	0.28	0.06
Liver	0.33	0.032
Kidney	0.18	0.045
Skin	NR	NR

9 NR: not reported.

10

This information is distributed solely for the purpose of pre-dissemination peer review under applicable information quality guidelines. It has not been formally disseminated by the National Institute for Occupational Safety and Health. It does not represent and should not be construed to represent any agency determination or policy.

1 **Table A-6. Estimated silver tissue burdens after *dietary intake* of 80 µg/day in**  
 2 **adult male (BW: 70 kg) for up to 45 years, by silver particle size and physical form**  
 3 **– based on Bachler et al. [2013] human model.**

Duration (yr)	LUNG (µg Ag/g tissue)		LIVER (µg Ag/g tissue)		KIDNEY (µg Ag/g tissue)		SKIN (µg Ag/g tissue)	
	Sol/Activ	Total	Sol/Activ	Total	Sol/Activ	Total	Sol/Activ	Total
<b>Nanoparticles (average diameter 15 nm)</b>								
15	0.000	0.000	0.001	0.008 <sup>b</sup>	0.002	0.020	0.000	0.008
30	0.000	0.001	0.001	0.015 <sup>b</sup>	0.002	0.038	0.000	0.016
45	0.000	0.001	0.001	0.023 <sup>b</sup>	0.002	0.056 <sup>a</sup>	0.000	0.024
<b>Ionic silver</b>								
15	0.002	0.014	0.010 <sup>d</sup>	0.048 <sup>a,b</sup>	0.003	0.027	0.000	0.036
30	0.002	0.026	0.010 <sup>d</sup>	0.086 <sup>a,b</sup>	0.003	0.050 <sup>a</sup>	0.000	0.071
45	0.002	0.038	0.010 <sup>d</sup>	0.124 <sup>a,b</sup>	0.003	0.074 <sup>a</sup>	0.000	0.107

4 Notes: Intestinal absorption of silver estimated to be 4% for silver nanoparticles, assuming that nanosilver is  
 5 formed after the oral intake of soluble silver salts [Bachler et al. 2013]; this may be an upper estimate, given that  
 6 the rat intestinal absorption closer to 1%. Ionic silver absorption also estimated to be 4%.

7 For either silver nanoparticles or ions, model-predictions include the following. Intake: 1,314 mg; uptake: 52.6 mg  
 8 (at 4% absorption). Predicted retained dose was 3.27 mg for ionic silver and 10.2 mg for silver nanoparticles over  
 9 45 years.

10 <sup>a</sup> Higher than the Ag tissue burdens in unexposed workers (liver: 0.32 µg Ag/g tissue; kidney: 0.045 µg Ag/g tissue)  
 11 [Brune 1980] (Table A-5).

12 <sup>b</sup> Higher than the rat liver tissue levels (0.006 or 0.012 µg/g) associated with lower 95% confidence interval  
 13 estimate of the benchmark dose (BMDL<sub>10</sub>) associated with 10% excess of bile duct hyperplasia, minimal severity  
 14 (Table A-1). Also exceeds the human reference level of silver in liver (~0.017 µg/g), based on a study in deceased  
 15 persons in the United States [ICRP 1960] (Bachler et al. [2013], Figure 6).

16

*This information is distributed solely for the purpose of pre-dissemination peer review under applicable information quality guidelines. It has not been formally disseminated by the National Institute for Occupational Safety and Health. It does not represent and should not be construed to represent any agency determination or policy.*

- 1 **Table A-7. Estimated working lifetime (45-year) exposure concentrations of silver**  
2 **nanoparticles associated with argyria (retained skin dose of 3.2 µg Ag/g skin,**  
3 **minimum dose) [Bachler et al. 2013, citing Triebig et al. 1982].**

Physical-chemical form	Particle diameter (nm)	Airborne concentration (8-hour TWA) (µg/m <sup>3</sup> )
Ionic	NA	46.8
Nanoparticle	15	77.6
Nanoparticle	100	253
Nanoparticle	1–100	204

- 4 Assumptions: adult male (8hr/d, 5 d/wk), 1.2 m<sup>3</sup>/hr breathing rate, nose breather.  
5 NA: not applicable

6

This information is distributed solely for the purpose of pre-dissemination peer review under applicable information quality guidelines. It has not been formally disseminated by the National Institute for Occupational Safety and Health. It does not represent and should not be construed to represent any agency determination or policy.

1 **Table A-8. Estimated silver tissue burdens for up to a 45-year working lifetime**  
 2 **inhalation exposure to 10 µg/m<sup>3</sup> (current NIOSH REL for silver particles, soluble**  
 3 **and insoluble), by particle size and physical form of Ag (assuming adult male, air**  
 4 **intake 1.2 m<sup>3</sup>/hr, 8 hr/d, 5 d/wk) – based on Bachler et al. [2013] human model.**

Duration (yr)	LUNG (µg Ag/g tissue)		LIVER (µg Ag/g tissue)		KIDNEY (µg Ag/g tissue)		SKIN† (µg Ag/g tissue)	
	Sol/Activ	Total	Sol/Activ	Total	Sol/Activ	Total	Sol/Activ	Total
<b>Particle average diameter: 15 nm</b>								
15	0.67 <sup>a,*</sup>	25 <sup>a,b,*</sup>	0.01 <sup>c</sup>	0.090 <sup>c,d</sup>	0.024	0.22*	0.0008	0.088
30	0.68 <sup>a,*</sup>	31 <sup>a,b,*</sup>	0.01 <sup>c</sup>	0.17 <sup>c,d</sup>	0.025	0.42*	0.0008	0.18
45	0.69 <sup>a,*</sup>	36 <sup>a,b,*</sup>	0.01 <sup>c</sup>	0.25 <sup>c,d</sup>	0.026	0.62*	0.0008	0.26
<b>Particle average diameter: 100 nm</b>								
15	0.21 <sup>a</sup>	7.8 <sup>a,b,*</sup>	0.003	0.028 <sup>c,d</sup>	0.007	0.068	0.002	0.027
30	0.21 <sup>a</sup>	9.8 <sup>a,b,*</sup>	0.003	0.052 <sup>c,d</sup>	0.008	0.13	0.002	0.054
45	0.22 <sup>a</sup>	11 <sup>a,b,*</sup>	0.003	0.077 <sup>c,d</sup>	0.008	0.19*	0.002	0.810
<b>Ionic silver</b>								
15	1.59 <sup>a,*</sup>	58.8 <sup>a,b,*</sup>	0.04 <sup>c,d</sup>	0.19 <sup>c,d</sup>	0.016	0.11	0.00	0.14
30	1.61 <sup>a,*</sup>	74.4 <sup>a,b,*</sup>	0.04 <sup>c,d</sup>	0.35 <sup>c,d,*</sup>	0.016	0.22*	0.00	0.29
45	1.64 <sup>a,*</sup>	84.8 <sup>a,b,*</sup>	0.04 <sup>c,d</sup>	0.50 <sup>c,d,*</sup>	0.016	0.32*	0.00	0.44

5 <sup>a</sup> Exceeds the lung tissue level of 0.081 µg Ag/g (male rats) associated with the estimated NOAEL for lung effects,  
 6 following subchronic inhalation of Ag nanoparticles [Song et al. 2013] (Table A-1).  
 7 <sup>b</sup> Exceeds the lung tissue level of Ag of 4.2 µg Ag/g lung tissue (female rats) associated with the NOAEL (no  
 8 observed adverse effect level), following subchronic inhalation of Ag nanoparticles [Sung et al. 2009] (Table A-1).  
 9 <sup>c</sup> Similar to or exceeds the liver tissue levels (0.006 µg/g females; 0.012 µg/g males) associated with lower 95%  
 10 confidence interval estimate of the benchmark dose (BMDL<sub>10</sub>) associated with 10% of bile duct hyperplasia,  
 11 minimal severity, in rats [Sung et al. 2009] (Table A-1) .  
 12 <sup>d</sup> Exceeds the liver tissue level of silver in the general population (0.017 µg/g) [ICRP 1960] and/or that reported in  
 13 unexposed workers (0.032 µg/g) [Brune 1980].  
 14 \* Exceeds tissue levels of Ag reported in smelter workers (Table A-5) by Brune [1980], for whom airborne exposure  
 15 concentrations of Ag were not reported.  
 16 † The estimated skin tissue doses are all less than 3.2 µg/g, which is the minimum estimated Ag dose in skin  
 17 associated with argyria (as reported in Bachler et al. 2013).  
 18 Note: An *in vitro* Ag dose of 1 µg/g was associated with adverse effects [as discussed in Bachler et al. 2013].  
 19

This information is distributed solely for the purpose of pre-dissemination peer review under applicable information quality guidelines. It has not been formally disseminated by the National Institute for Occupational Safety and Health. It does not represent and should not be construed to represent any agency determination or policy.

1 **Table A-9. Working lifetime (45-year) exposure concentration of silver (Ag)**  
 2 **nanoparticles (soluble/active or total; 15- or 100-nm diameter) associated with Ag**  
 3 **target tissue doses (NOAEL or BMDL) in the rat subchronic inhalation studies**  
 4 **[Sung et al. 2009; Song et al. 2013] (adult male; reference worker air intake, 1.2**  
 5 **m<sup>3</sup>/hr).<sup>a</sup>**

Rat Study, Sex	Type of Effect Level	Silver Tissue Dose (ng/g)	Particle Diameter (nm)	Airborne Exposure (8-hour TWA) (µg/m <sup>3</sup> )	
				Assuming Tissue Dose Metric of Soluble/Active Ag	Assuming Tissue Dose Metric of Total Ag
<b><i>Lung – Chronic alveolar inflammation, minimal<sup>b</sup></i></b>					
Song 2013, Female	NOAEL (117 µg/m <sup>3</sup> )	672	15	9.7	0.19
			100	31	0.60
Sung 2009, Female	NOAEL (133 µg/m <sup>3</sup> )	4,241	15	61	1.2
			100	195	3.8
<b><i>Liver–Bile duct hyperplasia, minimal</i></b>					
Sung 2009, Female	BMDL <sub>10</sub>	6.30	15	6.2	0.26
			100	20	0.83
Sung 2009, Male	BMDL <sub>10</sub>	11.6	15	11.4	0.47
			100	37	1.5

6 <sup>a</sup> Based on Ag absorption rate from lungs to systemic circulation in humans as determined from an *in vivo* animal  
 7 study [Takenaka et al. 2001], which is 7-fold higher than the Ag absorption rate from Ji et al. [2007] that was used  
 8 in simulations of Sung et al. 2009 and Song et al. 2013 studies. Further information on the absorption rates are  
 9 provided in the Supplementary material of Bachler et al. [2013].

10 <sup>b</sup> Dose-response data from male rat Song et al. [2013] were minimally acceptable for BMD estimation (Tables B-2  
 11 and B-8), but are not included here because of higher uncertainty. Subsequent analyses (not included in PBPK  
 12 modeling) utilized pooled data from male and female rats in Sung et al. [2009] and Song et al. [2013] (Table B-11).  
 13

This information is distributed solely for the purpose of pre-dissemination peer review under applicable information quality guidelines. It has not been formally disseminated by the National Institute for Occupational Safety and Health. It does not represent and should not be construed to represent any agency determination or policy.

1 **Table A-10. Human-Equivalent Concentrations for Silver Nanomaterials from**  
 2 **PBPK Modeling.**<sup>a</sup>

Rat Effect Endpoint and Sex [Study Reference]	Rat PoD as silver tissue dose (ng/g) <sup>b</sup>	Particle size	Human-equivalent concentration (HEC) (µg/m <sup>3</sup> ) <sup>c</sup>
<b>Total Silver Dose Metric</b>			
Liver bile duct hyperplasia, BMCL <sub>10</sub> , female [Sung et al. 2009]	6.3	15	0.26
		100	0.83
Pulmonary inflammation, NOAEL, female [Song et al. 2013]	672	15	0.19
		100	0.60
<b>Soluble/Active Silver Dose Metric</b>			
Liver bile duct hyperplasia, BMCL <sub>10</sub> , female [Sung et al. 2009]	6.3	15	6.2
		100	20
Pulmonary inflammation, NOAEL, female [Song et al. 2013]	672	15	9.7
		100	31

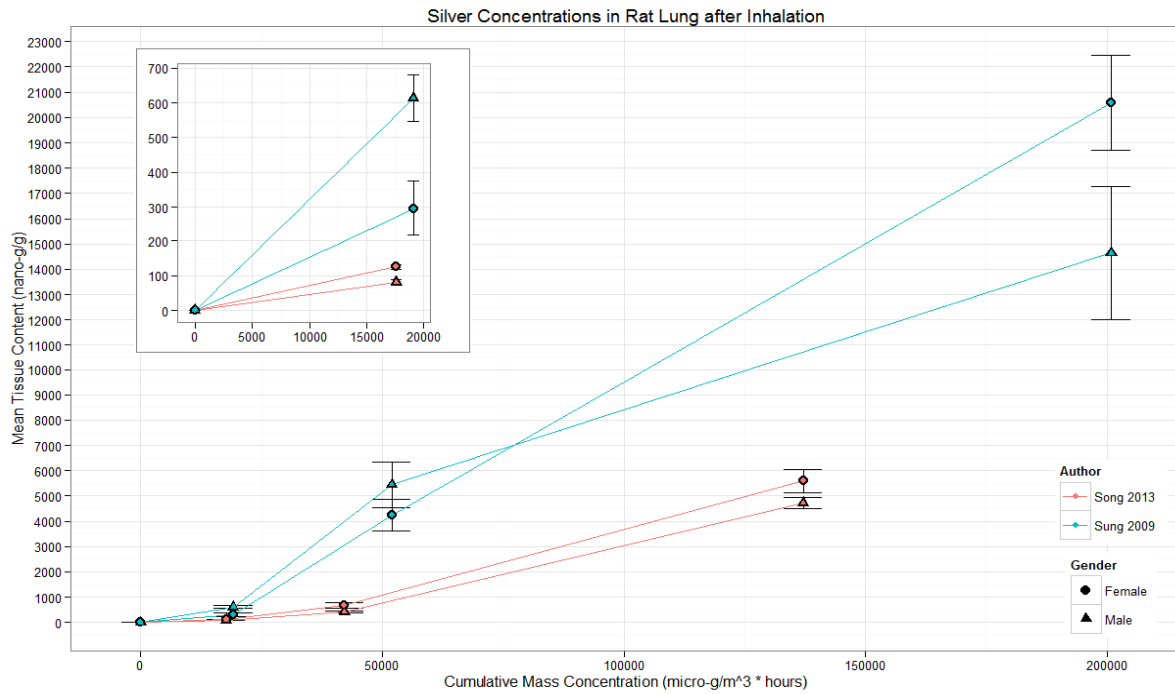
3 <sup>a</sup> This table is a subset of results shown in Table A-9, i.e., the results for the lowest silver tissue doses by  
 4 endpoint and particle size.

5 <sup>b</sup> From Table A-1. Rat PoD value for liver bile duct hyperplasia was selected as the lowest PoD among the  
 6 estimates for that endpoint. For pulmonary inflammation, the lowest PoD estimate (BMDL<sub>10</sub>) in male  
 7 rats from Song et al. [2013] was not selected because of the limited data and modeling options to  
 8 estimate that PoD. The female PoD (NOAEL) from Song et al. [2013] was selected as the next higher  
 9 estimate, which was ~6-8x lower than the NOAELs for the same response at similar exposure  
 10 concentrations (117 or 133 µg/m<sup>3</sup>) in male or female rats in Sung et al. [2009]. Alternatively, the male  
 11 rat NOAEL of 81 ng/g from Song et al. [2013] (which was ~70x lower than the NOAEL in male rats in  
 12 Sung et al. [2009]) could be used as the pulmonary inflammation PoD<sub>animal</sub>.

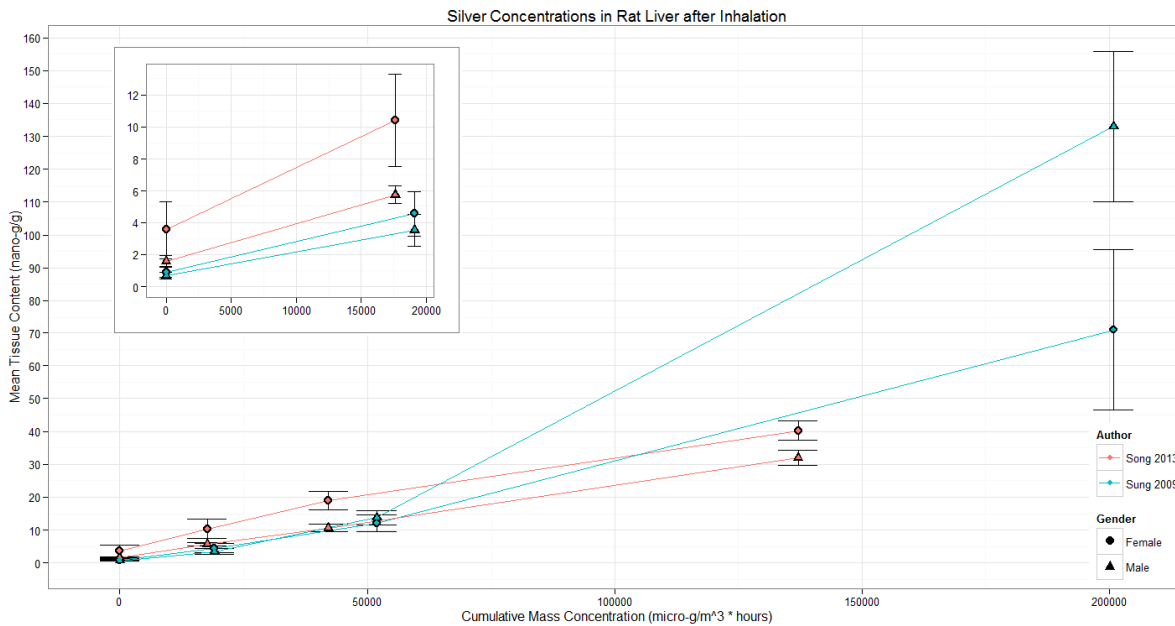
13 <sup>c</sup> Estimated from the Bachler et al. [2013] PBPK model for a 45-year working lifetime.

14

This information is distributed solely for the purpose of pre-dissemination peer review under applicable information quality guidelines. It has not been formally disseminated by the National Institute for Occupational Safety and Health. It does not represent and should not be construed to represent any agency determination or policy.

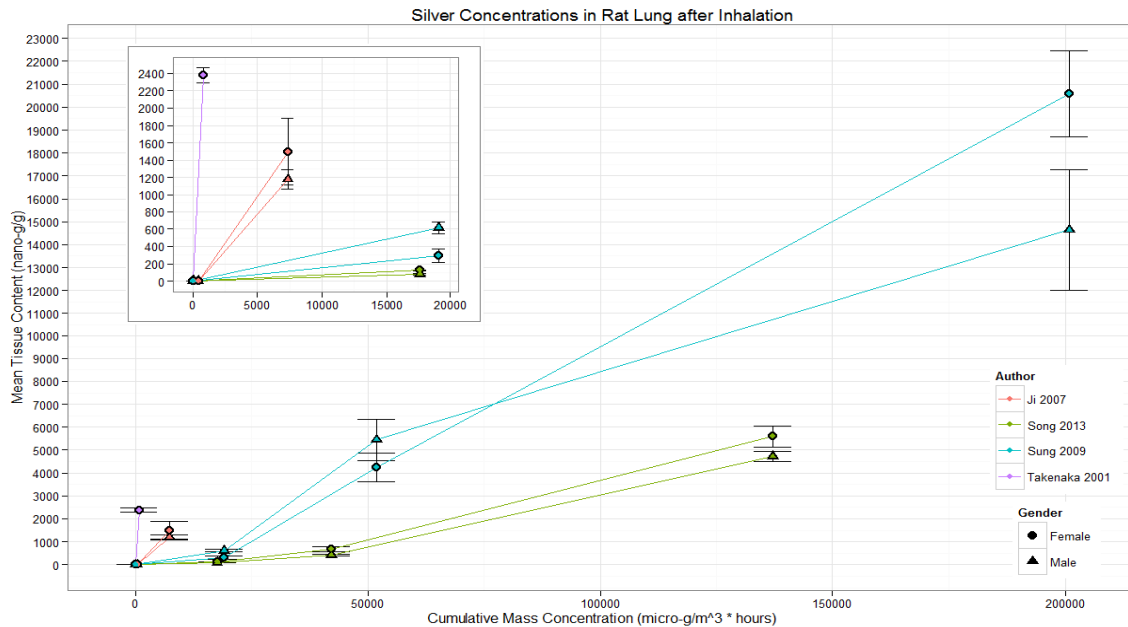


1  
 2 **Figure A-1. Lung silver burden ( $\mu\text{g Ag/g}$  wet tissue) by cumulative exposure ( $\mu\text{g}/\text{m}^3 \times \text{hours}$ ) in male and female**  
 3 **rats, measured at the end of the 13-week [Sung et al. 2009] or 12-week [Song et al. 2013] exposure. Tissue**  
 4 **concentrations are means  $\pm$  1 standard error. Lines fit to data, not modeled. Insert shows low exposure**  
 5 **concentration ( $49 \mu\text{g}/\text{m}^3$ ) and control (unexposed) data only.**

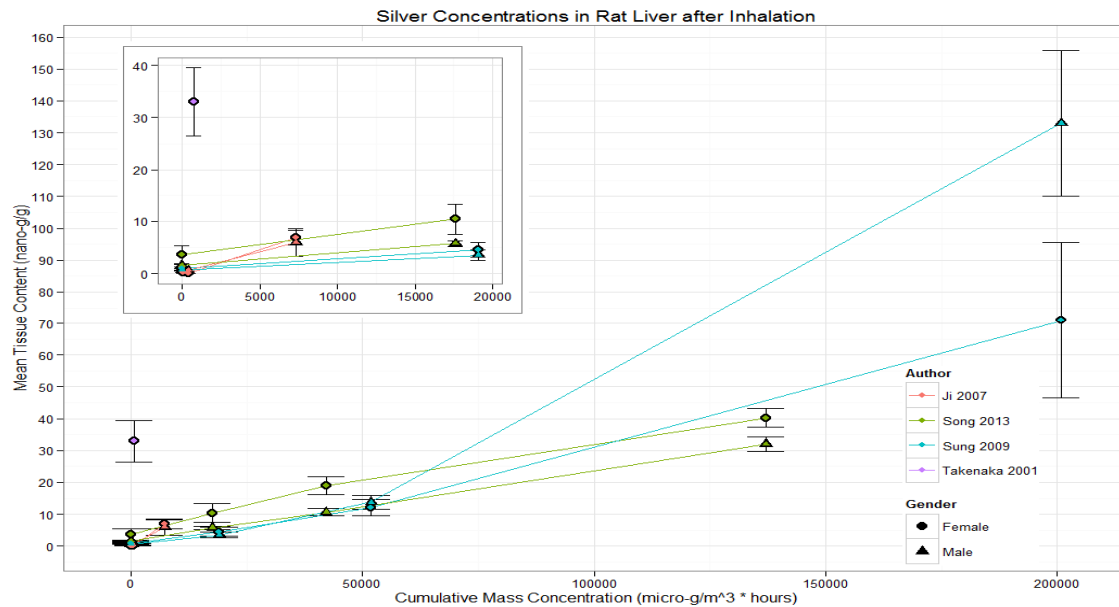


6  
 7 **Figure A-2. Liver silver burden ( $\mu\text{g Ag/g}$  wet tissue) by cumulative exposure ( $\mu\text{g}/\text{m}^3 \times \text{hours}$ ) in male and female**  
 8 **rats, measured at the end of the 13-week [Sung et al. 2009] or 12-week [Song et al. 2013] exposure. Tissue**  
 9 **concentrations are means  $\pm$  1 standard error. Lines fit to data, not modeled. Insert shows low exposure**  
 10 **concentration ( $49 \mu\text{g}/\text{m}^3$ ) and control (unexposed) data only.**

This information is distributed solely for the purpose of pre-dissemination peer review under applicable information quality guidelines. It has not been formally disseminated by the National Institute for Occupational Safety and Health. It does not represent and should not be construed to represent any agency determination or policy.

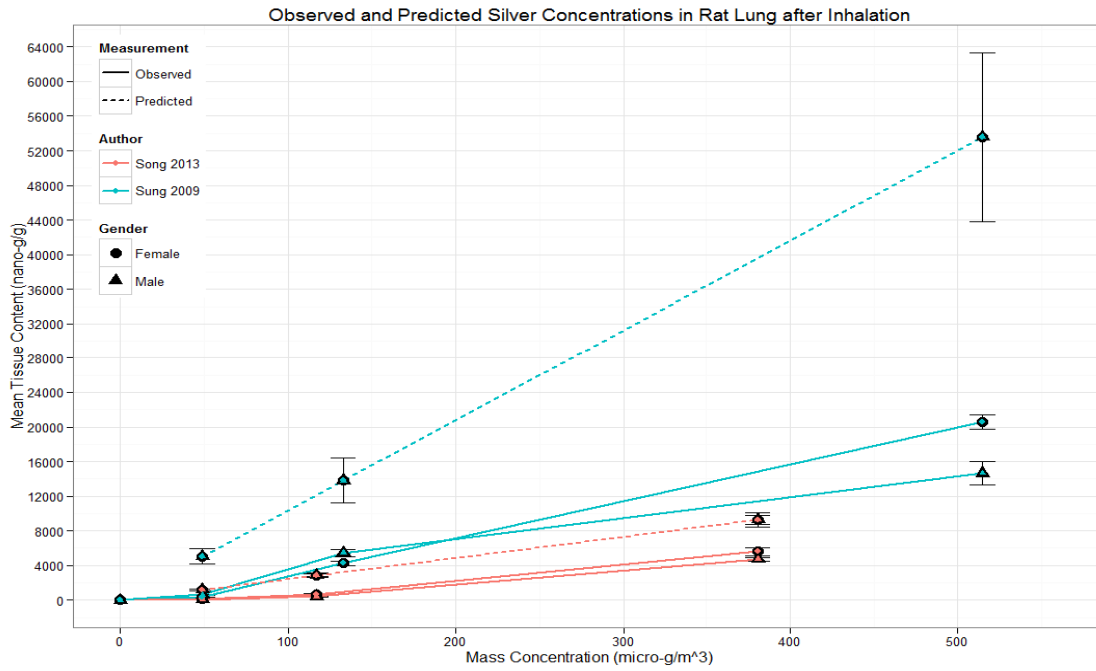


1  
2 **Figure A-3. Comparison of lung silver burden ( $\mu\text{g Ag/g}$  wet tissue) by cumulative exposure ( $\mu\text{g/m}^3 \times \text{hours}$ ) in**  
3 **male and female rats, measured at the end of inhalation exposure (day 0 “immediately” after 6 hours in**  
4 **Takenaka et al. [2001]; 4 weeks in Ji et al. [2007]; 13 weeks in Sung et al. [2009]; or 12 weeks in Song et al.**  
5 **[2013]. Tissue concentrations are means  $\pm$  1 standard error. Lines fit to data, not modeled. Insert shows data at**  
6 **lowest exposure concentration only (i.e., 133, 0.5, 49, 49  $\mu\text{g/m}^3$ , respectively, as cited above) and control**  
7 **(unexposed) data only.**

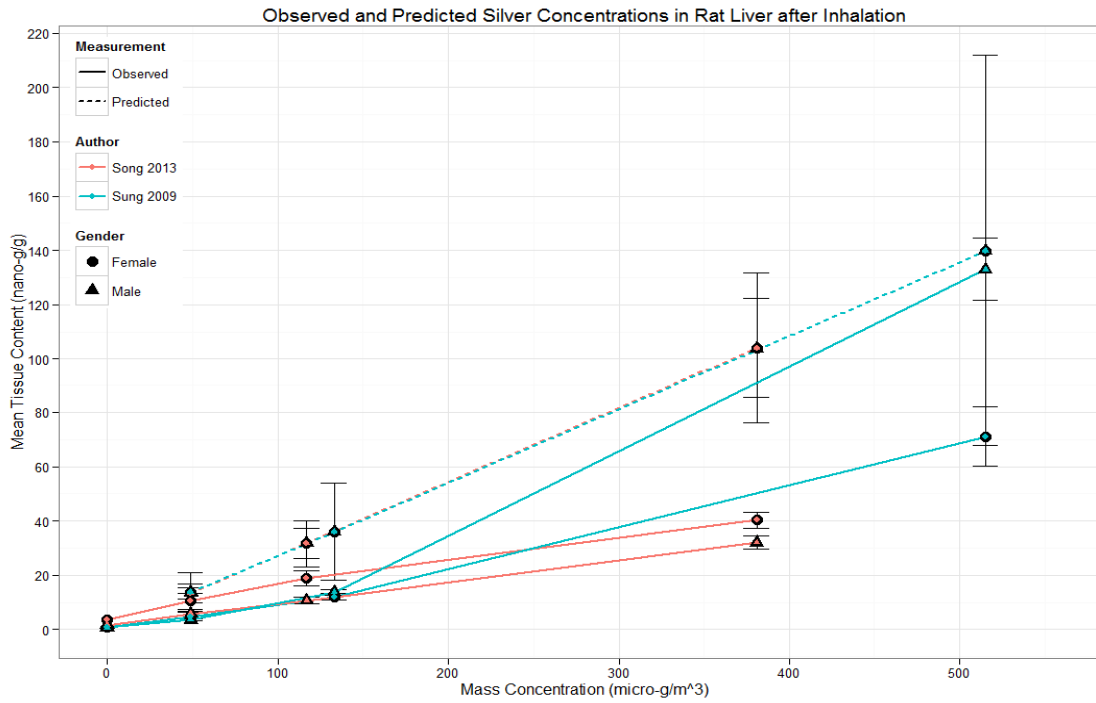


8  
9 **Figure A-4. Comparison of liver silver burden ( $\mu\text{g Ag/g}$  wet tissue) by cumulative exposure ( $\mu\text{g/m}^3 \times \text{hours}$ ) in**  
10 **male and female rats, measured at the end of inhalation exposure (day 0 “immediately” after 6 hours in**  
11 **Takenaka et al. [2001]; 4 weeks in Ji et al. [2007]; 13 weeks in Sung et al. [2009]; or 12 weeks in Song et al.**  
12 **[2013]. Tissue concentrations are means  $\pm$  1 standard error. Lines fit to data, not modeled. Insert shows data at**  
13 **lowest exposure concentration only (i.e., 133, 0.5, 49, 49  $\mu\text{g/m}^3$ , respectively, as cited above) and control**  
14 **(unexposed) data only; Takenaka et al. [2001] did not include a control group.**

This information is distributed solely for the purpose of pre-dissemination peer review under applicable information quality guidelines. It has not been formally disseminated by the National Institute for Occupational Safety and Health. It does not represent and should not be construed to represent any agency determination or policy.



1  
2 **Figure A-5: Observed and PBPK model–predicted lung burdens in male and female rats at the end of the 13-**  
3 **week [Sung et al. 2009] or 12-week [Song et al. 2013] inhalation exposure. [Note: the model predictions are the**  
4 **same for both sexes].**  
5



6  
7 **Figure A-6: Observed and PBPK-model predicted liver burdens in male and female rats at the end of the 13-week**  
8 **[Sung et al. 2009] or 12-week [Song et al. 2013] inhalation exposure. [Note: the model predictions are the same**  
9 **for both sexes].**

## APPENDIX B

### Statistical Analyses Supplement

#### **B.1 Benchmark Dose Modeling of Rat Subchronic Inhalation Studies**

A standard benchmark dose (BMD) modeling method [U.S. EPA 2012b] was used to model the dose-response relationships in the rat subchronic inhalation studies of silver nanoparticles [Sung et al. 2009; Song et al. 2013]. The in vivo toxicological studies on silver nanoparticles in experimental animals are summarized in Appendix E, Table E-5. More detailed accounts of the studies are also provided in the text of Appendix E. The studies considered to be the most applicable to the development of an OEL were subchronic inhalation studies in Sprague-Dawley rats reported by Sung et al. [2009] (90 days, or about 13 weeks) and Song et al. [2013] (12 weeks). These studies were evaluated for dose-response data that were sufficient for benchmark dose (BMD) modeling. Criteria include a monotonic dose-response relationship, dichotomous responses, and at least one dose group with response proportion between 0 and 1.

A BMD is a maximum likelihood estimate of the dose associated with a low response (e.g., 10%); a BMDL is the 95% lower confidence limit estimate of the BMD [Crump 1984]. BMDL estimates are often treated as NOAELs for use as PoDs to estimate exposure limits in humans [U.S. EPA 2012b]. The U.S. Environmental Protection Agency (EPA) benchmark dose software (BDMS) version 2.5 [U.S. EPA 2014] was used to model the data in Sung et al. [2009] and Song et al. [2013]. A pooled analysis of pulmonary inflammation data from both Sung et al. [2009] and Song et al. [2013] was performed with U.S. EPA BMDS version 2.6 [U.S. EPA 2015].

Both point-of-impact (lung) and systemic (liver) target organ endpoints were evaluated. These response endpoints include: (1) mixed cell perivascular infiltration in the lungs of males or females, accumulation of alveolar macrophages in males, and chronic alveolar inflammation in males; (2) bile duct hyperplasia in males or females; and (3) liver abnormality in males or females. The dose (as airborne exposure concentration) and

1 response data used in these BMD models are shown in Table B-1 [Sung et al. 2009]  
2 and Table B-2 [Song et al. 2013]. Tables B-3 and B-4 show dose as mean tissue  
3 concentration for the same responses and studies as Tables B-1 and B-2, respectively.

4 All of the available BMDS dichotomous response models were evaluated, which  
5 included gamma, logistic, log-logistic, probit, log-probit, multistage (polynomial degree 2  
6 and/or 3), Weibull, and quantal linear. Model averaging (MADR) per Wheeler and Bailer  
7 [2007], using the logistic, log-probit, multistage degree 2, and Weibull models, was also  
8 performed for comparison to the BMDS modeling results. All BMDS models were used  
9 to estimate a benchmark response (BMR) of 10% the excess (added) risk of early-stage  
10 adverse lung or liver effects in rats following subchronic inhalation of AgNP. The best-  
11 fitting model(s) were selected on the basis of optimal goodness-of-fit criteria, i.e., the  
12 models with the lowest Akaike Information Criteria (AIC) among the models with  
13 Goodness-of-Fit  $p$  values within the applicable range ( $> 0.1$ ). Care should be taken  
14 when selecting the model with the smallest AIC, as the EPA BMDS does not include  
15 parameters that are estimated to be at a boundary value (e.g., the background  
16 parameter) in the penalization of the log likelihood, which can misrepresent the best-  
17 fitting model for the given data.

18 For some models, such as the multistage, EPA BMDS did not report the standard errors  
19 for the parameter estimates, which can be used as an additional check for a statistically  
20 significant trend (i.e., the slope parameter). In those cases, the fitted model was  
21 compared to the null model by means of the likelihood ratio test for nested models.

22 The resulting benchmark concentration ( $BMC_{10}$ ) and lower 95% confidence interval  
23 ( $BMCL_{10}$ ) estimates associated with 10% response, along with the goodness-of-fit  
24 parameters for the best-fitting model(s), are shown in Tables B-5, B-7, and B-12 [Sung  
25 et al. 2009] and Tables B-6 and B-8 [Song et al. 2013]. These best-fitting models are  
26 shown in Figures B-1 through B-8.

1 The MADR-derived estimates of  $BMCL_{10}$  and  $BMDL_{10}$  for all endpoints and dose metrics  
2 are provided in Tables B-9 and B-10. The  $BMCL_{10}$  estimates based on BMDS and  
3 MADR were reasonably similar, but some differences (in part due to different criteria  
4 used for the model fit estimates) are observed. For example, for the Sung et al. [2009]  
5 endpoints, BMDS estimates of  $BMDL_{10}$  are smaller; and for the Song et al. [2013], the  
6 MADR estimates of  $BMDL_{10}$  are smaller.

7 All available alveolar lung inflammation data (male and female rats from Song et al.  
8 2013 & Sung et al. 2009) were combined (pooled) and modeled. The fact that a best-  
9 fitting model was able to be found for the combined data suggests that the data may be  
10 sufficiently homogenous to combine, that is, the exposure concentration adequately  
11 explains the variability in the alveolar lung inflammation response without explicitly  
12 accounting for lab and sex effects. The resulting benchmark concentration ( $BMC_{10}$ ) and  
13 lower 95% confidence interval ( $BMCL_{10}$ ) estimates associated with the added 10% risk  
14 of response, along with the goodness-of-fit estimates for the best-fitting model, are  
15 shown in Table B-11. The best-fitting model is shown in Figure B-9.

16 The liver bile duct hyperplasia and liver abnormality data [Sung et al. 2009] were  
17 analyzed separately by sex. For each histopathological endpoint, the observed  
18 responses were statistically significantly different for females and males, suggesting that  
19 the observed responses should be modeled while considering both concentration and  
20 sex; the interaction effect was not statistically significant ( $p > 0.05$ ) for both endpoints.  
21 The resulting benchmark concentrations ( $BMC_{10}$ ) and lower 95% confidence interval  
22 ( $BMCL_{10}$ ) estimates associated with the added 10% risk of response, along with the  
23 goodness-of-fit estimates for the best-fitting models, are shown in Table B-12. The best-  
24 fitting models are shown in Figures B-7 and B-8.

25 These  $BMCL_{10}$  and  $BMDL_{10}$  estimates are similar to or lower than the NOAELs (or  
26 LOAEL) reported in the animal studies (Table A-1). A  $BMCL_{10}$  or  $BMDL_{10}$  estimate may  
27 be considered equivalent to a NOAEL estimate [U.S. EPA 2012b], and equivalent  
28 uncertainty factors can be applied as described in Appendix A. The resulting OELs

*This information is distributed solely for the purpose of pre-dissemination peer review under applicable information quality guidelines. It has not been formally disseminated by the National Institute for Occupational Safety and Health. It does not represent and should not be construed to represent any agency determination or policy.*

1 would be similar to or lower than those estimated with use of the NOAELs (or LOAEL).  
 2 As discussed in Appendix A, the sources of uncertainty in the estimation of the BMCL<sub>10</sub>  
 3 or BMDL<sub>10</sub> estimates include the small number of rats per group (n = 5) for the  
 4 pulmonary inflammation endpoint and the large variability in the silver lung tissue doses  
 5 between the two subchronic studies [Sung et al. 2008; Song et al. 2013].

6 [TABLES AND FIGURES FOR SECTION B.1]

7 **Table B-1. Response proportions in Sprague-Dawley rats following subchronic**  
 8 **inhalation exposure to silver nanoparticles [Sung et al. 2009].**

Bile duct hyperplasia				
Group	Concentration (µg/m <sup>3</sup> )			
	0	49	133	515
Males	0/10	0/10	1/10	4/9
Females	3/10	2/10	4/10	9/10
Liver abnormality				
Group	Concentration (µg/m <sup>3</sup> )			
	0	49	133	515
Males	0/10	0/10	1/10	4/9
Females	3/10	5/10	5/10	9/10

9

10

11 **Table B-2. Response proportions in Sprague-Dawley rats following subchronic**  
 12 **inhalation exposure to silver nanoparticles [Song et al. 2013].**

Chronic alveolar inflammation (minimal)				
Group	Concentration (µg/m <sup>3</sup> )			
	0	49	117	381
Males <sup>a</sup>	0/5	0/5	3/5	5/5

13 <sup>a</sup> Female response proportions at same concentrations (0/4, 0/4, 0/4, 4/4) are inadequate for  
 14 BMD modeling.

15

This information is distributed solely for the purpose of pre-dissemination peer review under applicable information quality guidelines. It has not been formally disseminated by the National Institute for Occupational Safety and Health. It does not represent and should not be construed to represent any agency determination or policy.

1 **Table B-3. Response proportions in Sprague-Dawley rats following subchronic**  
 2 **inhalation exposure to silver nanoparticles [Sung et al. 2009].**

Bile duct hyperplasia <sup>a</sup>				
Group	Mean Liver Tissue Concentration (ng/g)			
	0.90	4.55	12.07	71.08
Females	3/10	2/10	4/10	9/10
	Mean Liver Tissue Concentration (ng/g)			
	0.70	3.52	13.75	132.97
Males	0/10	0/10	1/10	4/9

3 <sup>a</sup> Severity level in female rats: minimum (3/10, 2/10, 4/10, 8/10) and moderate (0/10, 0/10, 0/10,  
 4 1/10), respectively, in increasing dose groups; severity level in male rats: minimum in all dose  
 5 groups.

6  
 7 **Table B-4. Response proportions in Sprague-Dawley rats following subchronic**  
 8 **inhalation exposure to silver nanoparticles [Song et al. 2013].**

Chronic alveolar inflammation (minimal)				
Group	Mean Lung Tissue Concentration (ng/g)			
	0.82	80.65	417.40	4715.28
Males <sup>a</sup>	0/5	0/5	3/5	5/5

9 <sup>a</sup> Female response proportions at same concentrations (0/4, 0/4, 0/4, 4/4) are inadequate for  
 10 BMD modeling.

11  
 12

13 **Table B-5. Best-fitting Benchmark Concentration (BMC) models of subchronic**  
 14 **inhalation responses to silver nanoparticles in Sprague-Dawley rats [Sung et al.**  
 15 **2009].**

Model	AIC	p	BMC (µg/m <sup>3</sup> )	BMCL <sub>10</sub> (µg/m <sup>3</sup> )
<b>Male: Bile duct hyperplasia</b>				
Log-probit	21.1114	0.9806	155.8	92.5
<b>Female: Bile duct hyperplasia</b>				
Logistic	46.8796	0.7073	78.2	50.5

16 AIC = Akaike Information Criterion.

17  
 18

This information is distributed solely for the purpose of pre-dissemination peer review under applicable information quality guidelines. It has not been formally disseminated by the National Institute for Occupational Safety and Health. It does not represent and should not be construed to represent any agency determination or policy.

1 **Table B-6. Best-fitting Benchmark Concentration (BMC) models of subchronic**  
 2 **inhalation responses to silver nanoparticles in Sprague-Dawley rats [Song et al.**  
 3 **2013].**

Model	AIC	P	BMC (µg/m <sup>3</sup> )	BMCL <sub>10</sub> (µg/m <sup>3</sup> )
<i>Male: Alveolar inflammation (minimal)</i>				
Multistage (Degree = 2) <sup>a</sup>	10.1497	0.843	44.8	13.6

4 AIC = Akaike Information Criterion.

5 <sup>a</sup> Multistage model only fit to these data, following the methodology described in Appendix A of  
 6 NIOSH [2013].

7

8 **Table B-7. Best-fitting Benchmark Dose (BMD) models of subchronic inhalation**  
 9 **responses to silver nanoparticles in Sprague-Dawley rats [Sung et al. 2009].**

Model	AIC	P	BMD (ng/g)	BMDL <sub>10</sub> (ng/g)
<i>Male: Bile duct hyperplasia</i>				
Gamma, MS2, MS3, QL, and Weibull <sup>a</sup>	21.4821	0.9281	22.7	11.6
<i>Female: Bile duct hyperplasia</i>				
Logistic	46.7501	0.7624	10.3	6.3

10 AIC = Akaike Information Criterion.

11 <sup>a</sup> Identical model fits (AIC and *p* values) and BMD and BMDL<sub>10</sub> estimates for these five BMDs  
 12 models: Gamma, Multistage polynomial degree 2 or degree 3 (MS2 or MS3), quantal linear  
 13 (QL), and Weibull.

14

15 **Table B-8. Best-fitting Benchmark Dose (BMD) models of subchronic inhalation**  
 16 **responses to silver nanoparticles in Sprague-Dawley rats [Song et al. 2013].**

Model	AIC	p	BMD (ng/g)	BMDL <sub>10</sub> (ng/g)
<i>Male: Alveolar inflammation (minimal)</i>				
Multistage (Degree = 2) <sup>a</sup>	9.0622	0.9818	145.8	33.0

17 AIC = Akaike Information Criterion.

18 <sup>a</sup> Multistage model only fit to these data, following the methodology described in Appendix A of  
 19 NIOSH [2013].

20

21

*This information is distributed solely for the purpose of pre-dissemination peer review under applicable information quality guidelines. It has not been formally disseminated by the National Institute for Occupational Safety and Health. It does not represent and should not be construed to represent any agency determination or policy.*

1 **Table B-9. Model-Average BMCL<sub>10</sub> estimates from subchronic inhalation studies**  
 2 **in Sprague-Dawley rats for all endpoints modeled.**

Rat study	Endpoint	BMCL <sub>10</sub> estimate in rats (µg/m <sup>3</sup> ) - BCa	BMCL <sub>10</sub> estimate in rats (µg/m <sup>3</sup> ) – Percentile
Sung et al. [2009]	Bile duct hyperplasia in males	30.20	112.49
	Bile duct hyperplasia in females	32.87	24.52
Song et al. [2013]	Chronic alveolar inflammation in males	48.17	36.86

3  
 4 **Table B-10. Model-Average BMDL<sub>10</sub> estimates from subchronic inhalation studies**  
 5 **in Sprague-Dawley rats for all endpoints modeled.**

Rat study	Endpoint	BMDL <sub>10</sub> estimate in rats (ng/g) - BCa	BMDL <sub>10</sub> estimate in rats (ng/g) – Percentile
Sung et al. [2009]	Bile duct hyperplasia in males	2.61	14.55
	Bile duct hyperplasia in females	2.09	2.03
Song et al. [2013]	Chronic alveolar inflammation in males	57.18	43.50

6  
 7 **Table B-11. Pooled data and best-fitting Benchmark Concentration (BMC) models**  
 8 **for the subchronic inhalation responses to silver nanoparticles in male and**  
 9 **female Sprague-Dawley rats [Sung et al. 2009 & Song et al. 2013].**

Chronic alveolar inflammation (minimal)						
Group	Concentration (µg/m <sup>3</sup> )					
	0	49	117	133	381	515
Pooled	5/29	5/29	3/9	2/20	9/9	16/19
Model	AIC	P	BMC (µg/m <sup>3</sup> )		BMCL <sub>10</sub> (µg/m <sup>3</sup> )	
Multistage (Degree = 3)	108.324	0.125	124.9		62.8	

10 AIC = Akaike Information Criterion.

This information is distributed solely for the purpose of pre-dissemination peer review under applicable information quality guidelines. It has not been formally disseminated by the National Institute for Occupational Safety and Health. It does not represent and should not be construed to represent any agency determination or policy.

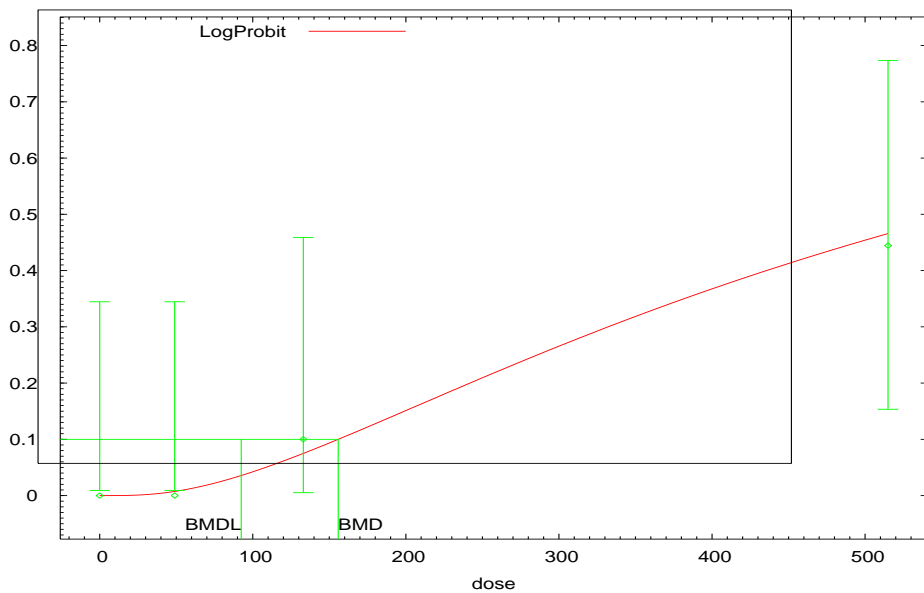
1 **Table B-12. Best-fitting Benchmark Concentration (BMC) models of subchronic**  
 2 **inhalation responses to silver nanoparticles in Sprague-Dawley rats [Sung et al.**  
 3 **2009].**

Model	AIC	$p$	BMC ( $\mu\text{g}/\text{m}^3$ )	BMCL <sub>10</sub> ( $\mu\text{g}/\text{m}^3$ )
<b>Male: Liver Abnormality</b>				
Quantal Linear	21.9566	0.888	111.1	57.3
<b>Female: Liver Abnormality</b>				
Logistic	50.892	0.7993	76.6	44.5

4 AIC = Akaike Information Criterion.

5  
6  
7

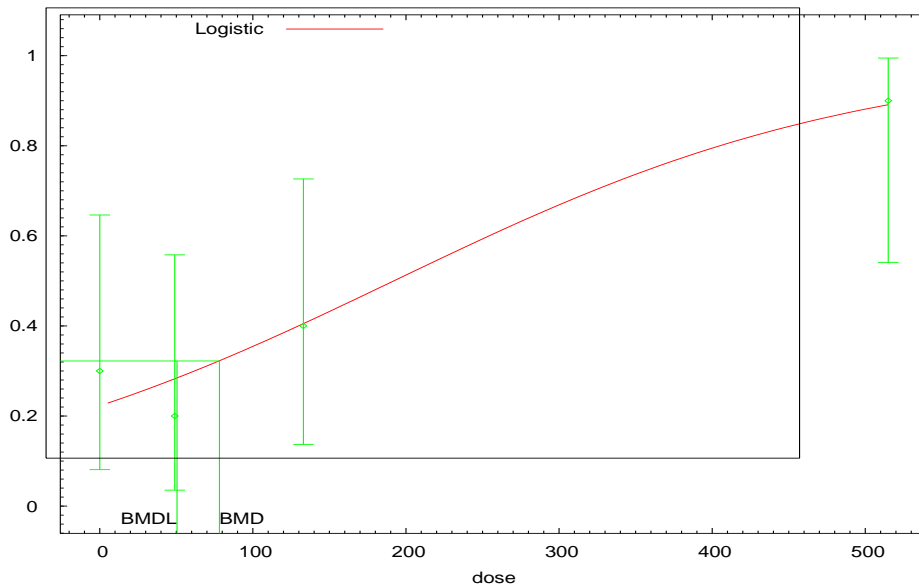
LogProbit Model, with BMR of 10% Added Risk for the BMD and 0.95 Lower Confidence Limit for the BMDL



8  
9 Figure B-1. Exposure-response model (log-probit) fit to the airborne concentration of silver  
 10 nanoparticles ( $\mu\text{g}/\text{m}^3$ ) and bile duct hyperplasia proportion in male rats [Sung et al. 2009]. (Data  
 11 and model results in Tables B-1 and B-5.)  
 12  
 13

This information is distributed solely for the purpose of pre-dissemination peer review under applicable information quality guidelines. It has not been formally disseminated by the National Institute for Occupational Safety and Health. It does not represent and should not be construed to represent any agency determination or policy.

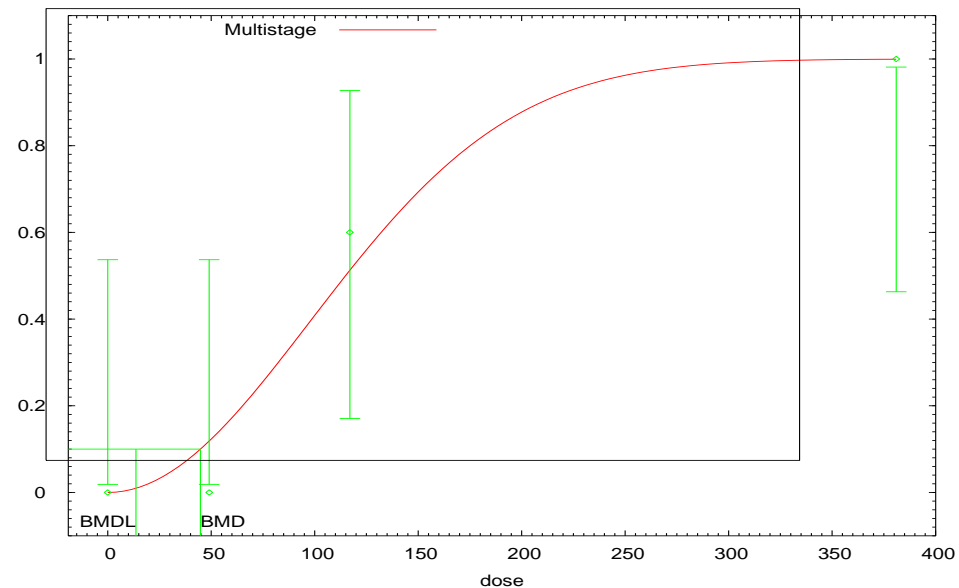
Logistic Model, with BMR of 10% Added Risk for the BMD and 0.95 Lower Confidence Limit for the BMDL



1  
2  
3  
4  
5  
6

Figure B-2. Exposure-response model (logistic) fit to the airborne concentration of silver nanoparticles ( $\mu\text{g}/\text{m}^3$ ) and bile duct hyperplasia proportion in female rats. [Sung et al. 2009]. (Data and model results in Tables B-1 and B-5.)

Multistage Model, with BMR of 10% Added Risk for the BMD and 0.95 Lower Confidence Limit for the BMDL



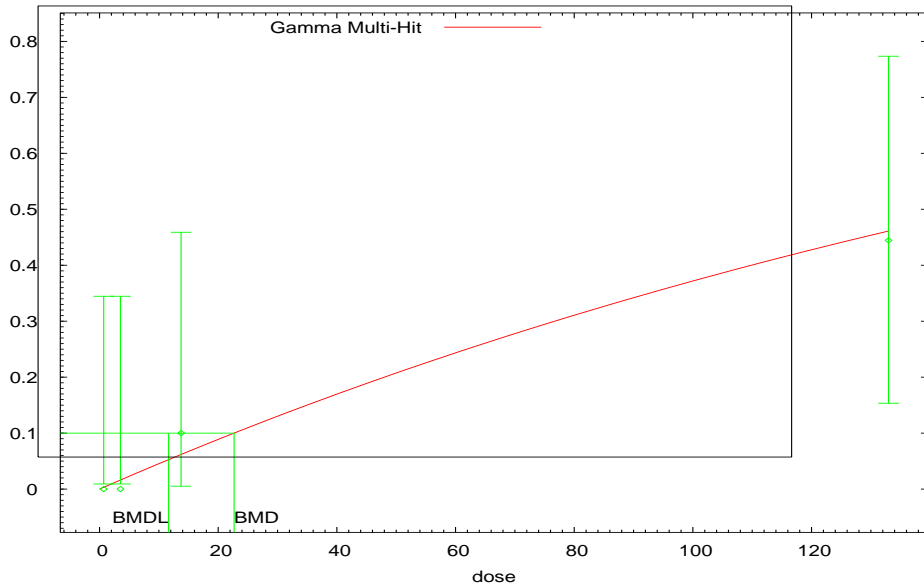
7  
8  
9  
10  
11  
12

15:16 02/02 2015

Figure B-3. Exposure-response model (multistage polynomial degree 2) fit to the airborne concentration of silver nanoparticles ( $\mu\text{g}/\text{m}^3$ ) and chronic alveolar inflammation proportion in male rats [Song et al. 2013]. (Data and model results in Tables B-2 and B-6.)

This information is distributed solely for the purpose of pre-dissemination peer review under applicable information quality guidelines. It has not been formally disseminated by the National Institute for Occupational Safety and Health. It does not represent and should not be construed to represent any agency determination or policy.

Gamma Multi-Hit Model, with BMR of 10% Added Risk for the BMD and 0.95 Lower Confidence Limit for the BMI

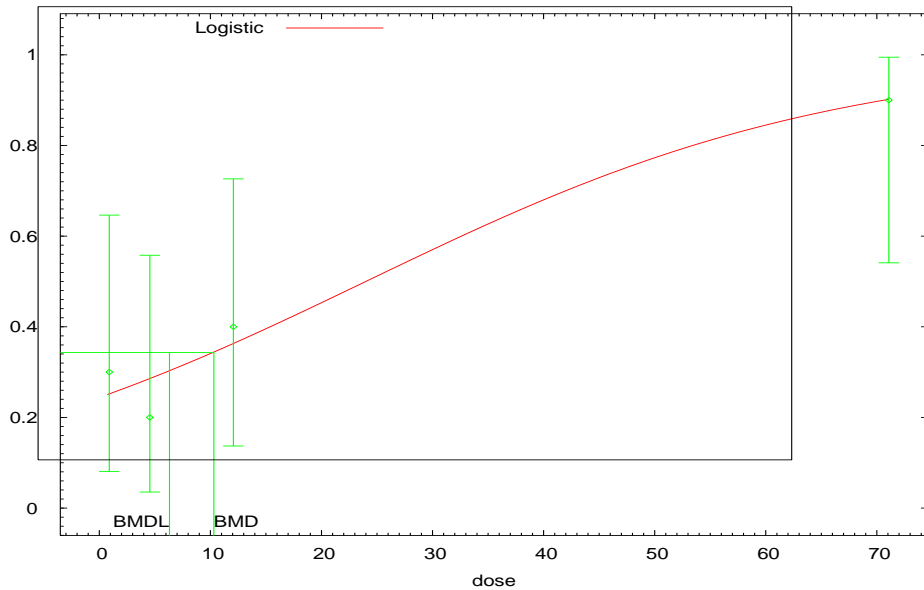


1 14:45 02/02 2015

2 Figure B-4. Dose-response model (gamma) fit to the silver tissue dose in liver (ng/g) and bile  
3 duct hyperplasia proportion in male rats [Sung et al. 2009]. (Data and model results in Tables B-  
4 3 and B-7; see Table B-7 for other models with equivalent fit as gamma model to these data.)

5  
6

Logistic Model, with BMR of 10% Added Risk for the BMD and 0.95 Lower Confidence Limit for the BMDL

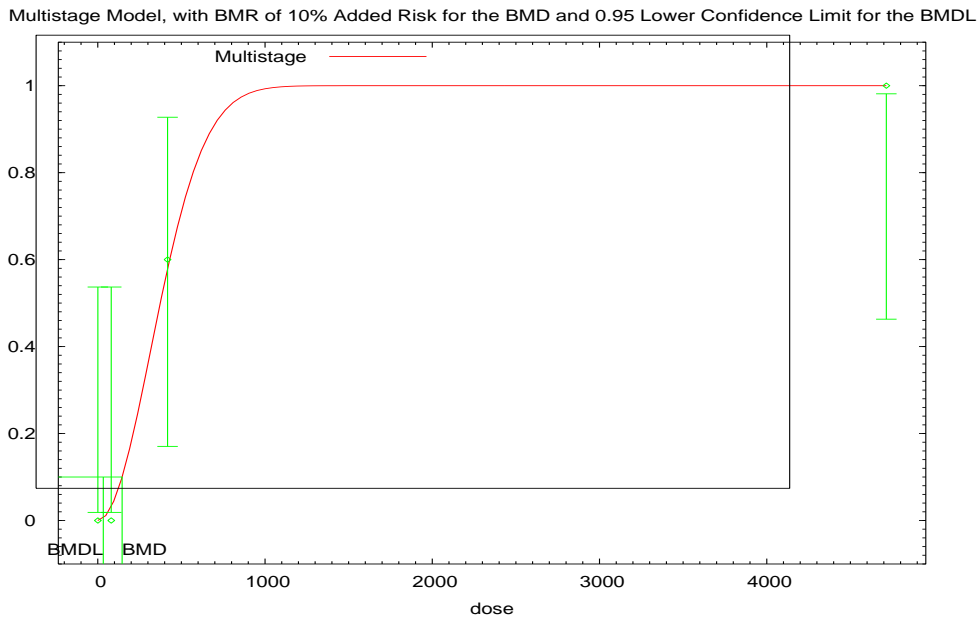


7 13:40 02/02 2015

8 Figure B-5. Dose-response model (logistic) fit to the silver tissue dose in liver (ng/g) and bile  
9 duct hyperplasia proportion in female rats [Sung et al. 2009]. (Data and model results in Tables  
10 B-3 and B-7.)

11  
12

*This information is distributed solely for the purpose of pre-dissemination peer review under applicable information quality guidelines. It has not been formally disseminated by the National Institute for Occupational Safety and Health. It does not represent and should not be construed to represent any agency determination or policy.*

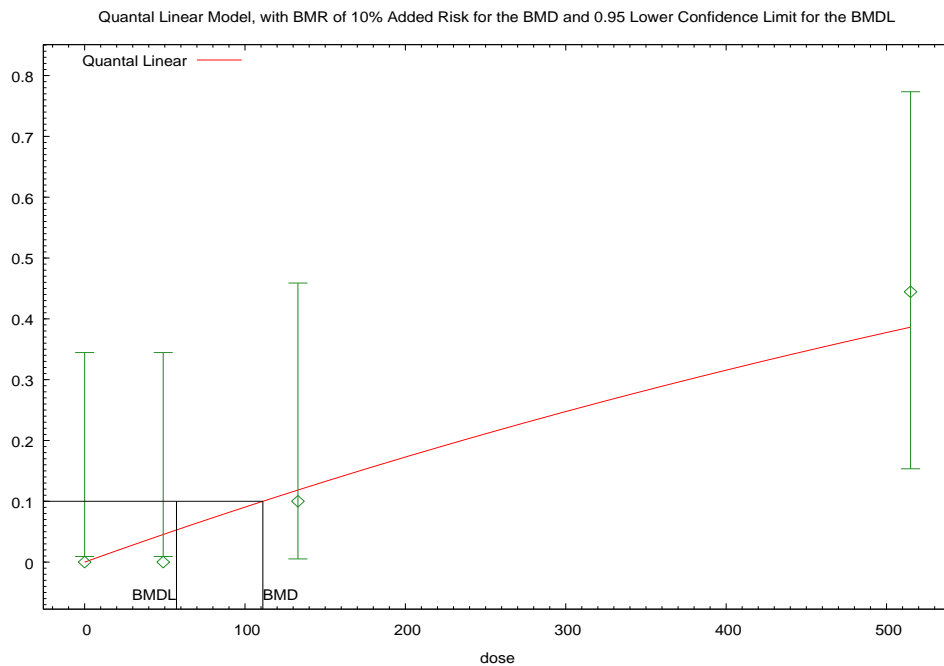


1

2 Figure B-6. Dose-response model (multistage polynomial degree 2) fit to the silver tissue dose  
3 in lung (ng/g) and chronic alveolar inflammation proportion in male rats [Song et al. 2013]. (Data  
4 and model results in Tables B-4 and B-8.)

5

6



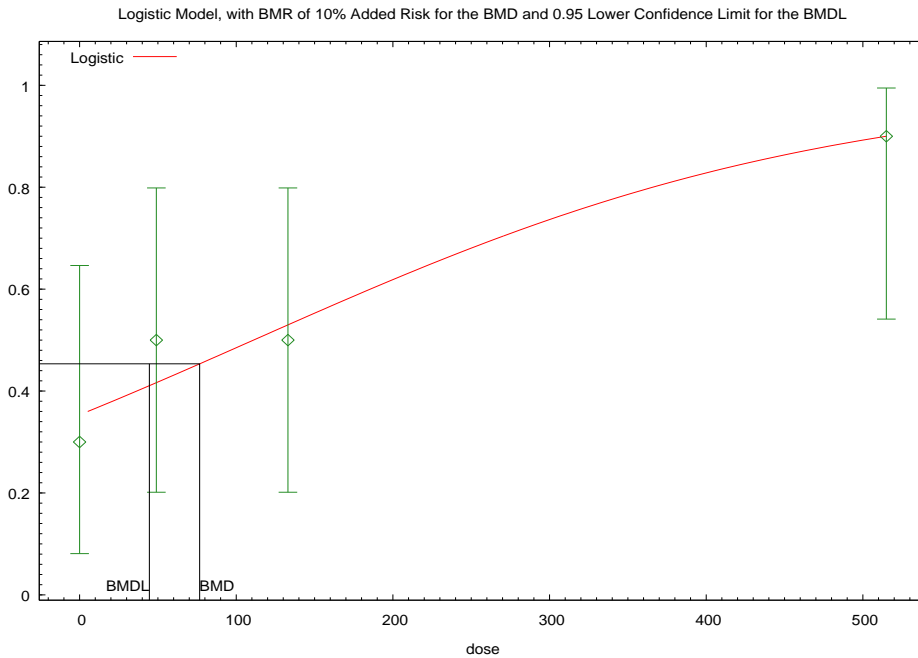
13:40 06/23 2017

7

8 Figure B-7. Exposure-response model (quantal linear) fit to the airborne concentration of silver  
9 nanoparticles (µg/m<sup>3</sup>) and liver abnormality proportion in male rats [Sung et al. 2009]. (Data and  
10 model results in Tables B-1 and B-12.)

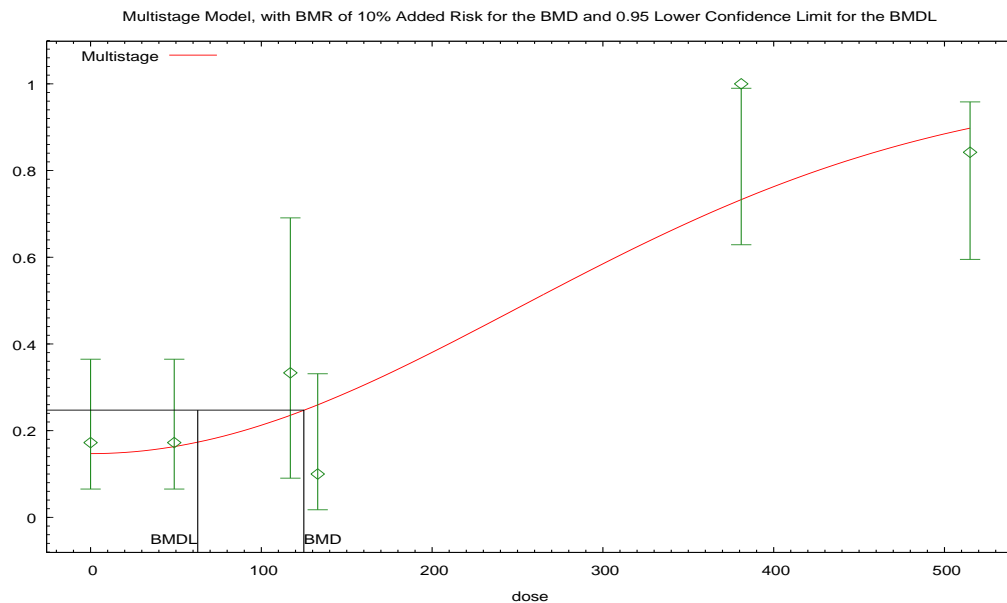
11

This information is distributed solely for the purpose of pre-dissemination peer review under applicable information quality guidelines. It has not been formally disseminated by the National Institute for Occupational Safety and Health. It does not represent and should not be construed to represent any agency determination or policy.



13:43 06/23 2017

1 Figure B-8. Exposure-response model (logistic) fit to the airborne concentration of silver  
2 nanoparticles ( $\mu\text{g}/\text{m}^3$ ) and liver abnormality proportion in female rats [Sung et al. 2009]. (Data  
3 and model results in Tables B-1 and B-12.)  
4  
5  
6



12:09 02/02 2017

7 Figure B-9. Exposure-response model (multistage polynomial degree 3) fit to the pooled data on  
8 airborne concentration of silver nanoparticles ( $\mu\text{g}/\text{m}^3$ ) and chronic alveolar inflammation  
9 proportion in male and female rats [Sung et al. 2009 & Song et al. 2013]. (Data and model  
10 results in Table B-11.)  
11

## 1 **B.2 No Observed Adverse Effect Level (NOAEL) Estimation of Rat** 2 **Liver Bile Duct Hyperplasia**

### 3 **B.2.1 Background**

4 A statistical examination of the rat dose and response data was performed to estimate  
5 the no observed adverse effect levels (NOAEL) in male and female rats with respect to  
6 liver bile duct hyperplasia in the subchronic inhalation study by Sung et al. [2009]. This  
7 analysis was performed to verify the NOAEL, which is defined as the highest dose  
8 group that was not significantly different from the controls.

9 An omnibus test first identified whether an association exists between subchronic  
10 inhalation exposure to silver nanoparticles and liver bile duct hyperplasia. This test was  
11 followed by multiple comparisons to identify the levels of exposure that result in a  
12 response statistically significantly different from background.

### 13 **B.2.2 Data**

14 The following data are taken from Sung et al. 2009, Tables 9 and 10. All hyperplasia  
15 responses (minimum and moderate) are combined for the female rats.

#### 16 *Male Rat Liver Bile Duct Hyperplasia (Only Minimum Reported)*

<b>Dose</b>	<b>Response</b>
Control (0 µg/m <sup>3</sup> )	0/10
Low (49 µg/m <sup>3</sup> )	0/10
Middle (133 µg/m <sup>3</sup> )	1/10
High (515 µg/m <sup>3</sup> )	4/9

#### 17 *Female Rat Liver Bile Duct Hyperplasia (Minimum and Moderate Hyperplasia* 18 *Combined)*

<b>Dose</b>	<b>Response</b>
Control (0 µg/m <sup>3</sup> )	3/10
Low (49 µg/m <sup>3</sup> )	2/10
Middle (133 µg/m <sup>3</sup> )	4/10
High (515 µg/m <sup>3</sup> )	9/10

## 1 B.2.3 Analysis

### 2 B.2.3.1 Male rats

3 Since these rodent data do not have large samples, and response proportions are near  
4 0, the traditional tests relying on asymptotic normal or chi-square distributions are not  
5 applicable. Instead, an exact inferential method, Fisher's exact test, can be used. A  
6 level of significance of 5% was used for decision-making. Statistical analysis was  
7 completed with SAS 9.4.

8 The following hypothesis was tested:

9  $H_0$ : Male Rat Hyperplasia is not associated with Dose

10  $H_A$ : Male Rat Hyperplasia is associated with Dose

11 The  $p$  value is 0.0081, thus suggesting an association between liver bile duct  
12 hyperplasia and subchronic inhalation exposure to silver nanoparticles in male rats.  
13 However, this test does not indicate which dose group(s) have statistically significantly  
14 different proportions of male rats with hyperplasia. To obtain this information (which is  
15 required to determine the NOAEL), pairwise exact tests were used to compare each  
16 exposure group (low, middle, and high) to the control group (Table 1). Results are not  
17 shown for the low ( $49 \mu\text{g}/\text{m}^3$ ) vs. control comparison, as both have responses of 0/10.

18 *Table 1: Comparisons of Hyperplasia Proportions, Male Rats*

Comparison	$P$ value (two-sided)
133 $\mu\text{g}/\text{m}^3$ vs. Control	1.0000
515 $\mu\text{g}/\text{m}^3$ vs. Control	0.0325

19  
20 Thus, the high-dose group is statistically significantly different from the control group,  
21 whereas the low and middle groups are not. Therefore, 133  $\mu\text{g}/\text{m}^3$  is the NOAEL.  
22 Adjustments for multiple comparisons (e.g., Bonferroni) were not made.

### 1 **B.2.3.2 Female rats**

2 The process above was also used for female rats.

3  $H_0$ : Female Rat Hyperplasia is not associated with Dose

4  $H_A$ : Female Rat Hyperplasia is associated with Dose

5 The  $p$  value is 0.0104; thus, these data do support an association between liver bile  
6 duct hyperplasia and subchronic inhalation exposure to silver nanoparticles in female  
7 rats.

8 Pairwise exact tests are used to compare each exposure group (low, middle, and high)  
9 to the control group (Table 2).

10

11 *Table 2: Comparisons of Hyperplasia Proportions, Female Rats*

<b>Comparison</b>	<b><i>P</i> value (two-sided)</b>
49 $\mu\text{g}/\text{m}^3$ vs. Control	1.0000
133 $\mu\text{g}/\text{m}^3$ vs. Control	1.0000
515 $\mu\text{g}/\text{m}^3$ vs. Control	0.0198

12

13 Thus, the high dose group is statistically significantly different from the control group,  
14 whereas the low and middle groups are not. Therefore, 133  $\mu\text{g}/\text{m}^3$  is the NOAEL.

15 Adjustments for multiple comparisons (e.g., Bonferroni) were not made.

### 16 **B.2.4 Conclusion**

17 Using an exact statistical test, subchronic inhalation exposure to silver nanoparticles is  
18 associated with liver duct hyperplasia in both male and female rats. In exact pairwise  
19 comparisons, the NOAEL is 133  $\mu\text{g}/\text{m}^3$  for both male and female rats.

20

## 1 **B.3 Pooled Data Analysis of Rat Subchronic Pulmonary Inflammation**

### 2 **B.3.1 Background**

3 In investigating the potency of silver nanomaterials, data from two studies [Sung et al.  
4 2009; Song et al. 2013] on pulmonary inflammation in rodents was analyzed separately  
5 by dose-response modeling. An exploratory plot illustrated variability in response due to  
6 lab effect.

7 This analysis investigates whether the information from these two studies can be  
8 combined in five phases:

- 9 1. Pool all data (both labs, both sexes)
- 10 2. Pool all male data (both labs, only males)
- 11 3. Pool all female data (both labs, only females)
- 12 4. Pool all Sung 2009 data (one lab, both sexes)
- 13 5. Pool all Song 2013 data (one lab, both sexes)

14 The traditional method to investigate pooled data would be to model the following  
15 multiple non-linear relationship:

$$16 \quad \text{Pulmonary Inflammation} = \text{Function}(\text{Dose}, \text{Lab}, \text{Sex}) + \varepsilon$$

17 EPA BMDS 2.6 cannot handle a relationship with more than one covariate (i.e., dose).  
18 As a result, the model above will be investigated in the five phases, where each phase  
19 is making an assumption of whether or not a covariate is statistically significant. For  
20 example, the model in phase 1, where all data are pooled, is assuming that Lab and  
21 Sex do not contribute statistically significantly to the variance in the response. Each of  
22 the five models can be evaluated separately in EPA BMDS.

23 Models will be fit to estimate the dose (concentration in  $\mu\text{g}/\text{m}^3$ ) associated with an  
24 added 10% risk. The best-fitting model is that which (1) has a goodness-of-fit  $p$  value  
25 greater than 0.1 and (2) has the smallest AIC.

*This information is distributed solely for the purpose of pre-dissemination peer review under applicable information quality guidelines. It has not been formally disseminated by the National Institute for Occupational Safety and Health. It does not represent and should not be construed to represent any agency determination or policy.*

1 As previously investigated, EPA BMDS does not include model parameters that are  
2 estimated to be a boundary value (e.g., zero) in the AIC calculation, which is -2 times  
3 the log likelihood plus 2 times the number of parameters in the model. The result is that  
4 of the best-fitting models, the “best” may have a smaller AIC value than it should by  
5 constant factor of 2. If the best model does have non-estimable parameters, the  
6 adjusted AIC will be computed. If this model still has the smallest AIC, then the process  
7 ends. If another model now has a smaller AIC, it will be checked for non-estimable  
8 parameters and the AIC will be adjusted. This process will be repeated until the best  
9 model is chosen.

## 10 **B.3.2 Analyses**

### 11 **B.3.2.1 Phase 1: Pool all data (both labs, both sexes)**

12 Binary data can be difficult to visualize, but there seems to be an association: below 200  
13  $\mu\text{g}/\text{m}^3$ , most rodents didn't exhibit pulmonary inflammation, whereas after 381  $\mu\text{g}/\text{m}^3$  a  
14 majority of rodents did exhibit pulmonary inflammation (Figure 1).

15

16

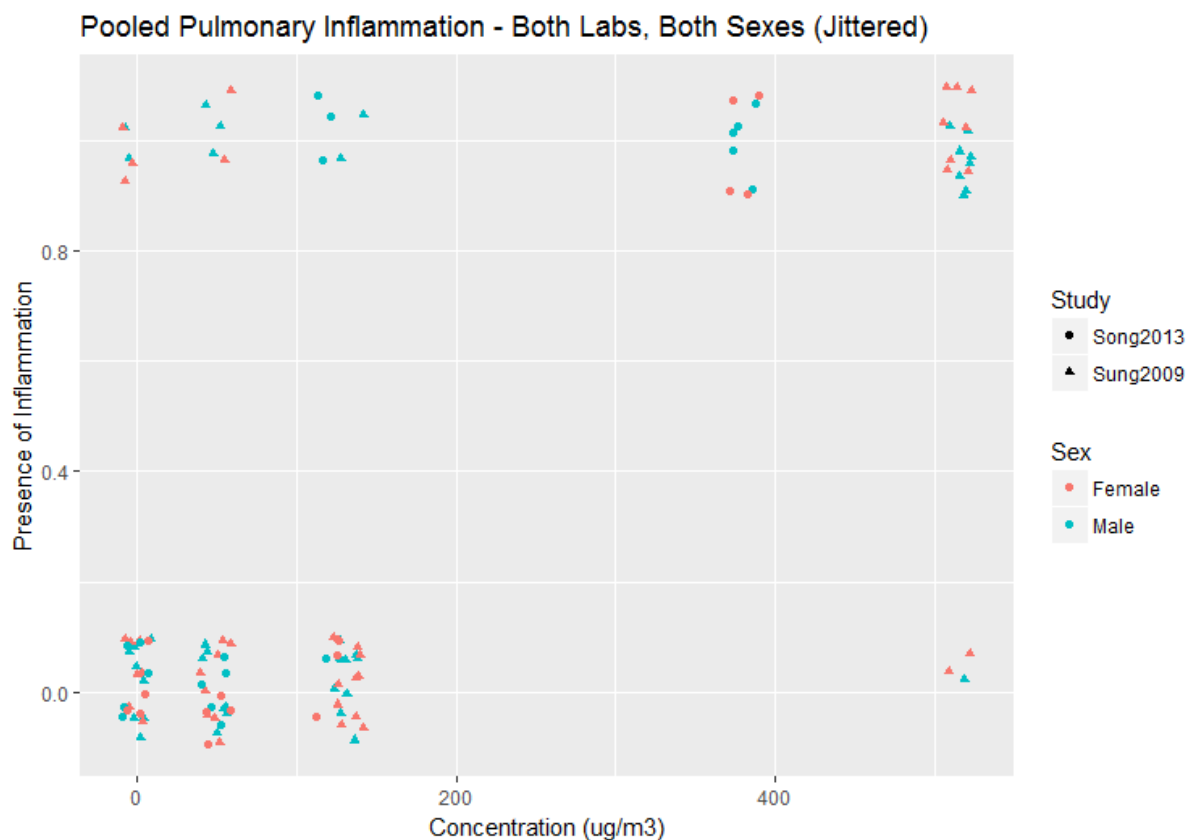
17

18

19

20

21



1

2 **Figure 1: All Data Pooled**

3 All models were fit with the default options, where BMR = Added 10%: Quantal Linear,  
4 Multistage 2, Multistage 3, Gamma, Logistic, Log Logistic, Log Probit, Probit, Weibull.  
5 The best-fitting model was the Multistage Degree 3 model, as it was the only one with  
6 adequate goodness-of-fit (Table 1). A visual inspection of the fit is also satisfactory  
7 (Figure 2). Note: the linear and cubic terms were estimated to be 0 (a boundary value)  
8 in the MS3 model (model parameter estimates not shown), but the MS2 model did not  
9 have the same quadratic and intercept parameter estimates and had a non-zero linear  
10 term. As previously identified, EPA BMDS does not include “boundary parameters”  
11 when computing AIC, which is  $-2*LL + 2*\#parameters$ . “Correcting” the MS3 AIC adds 4  
12 because there are 2 boundary parameters, but since MS3 is the only adequately fitting  
13 model, no conclusions change.

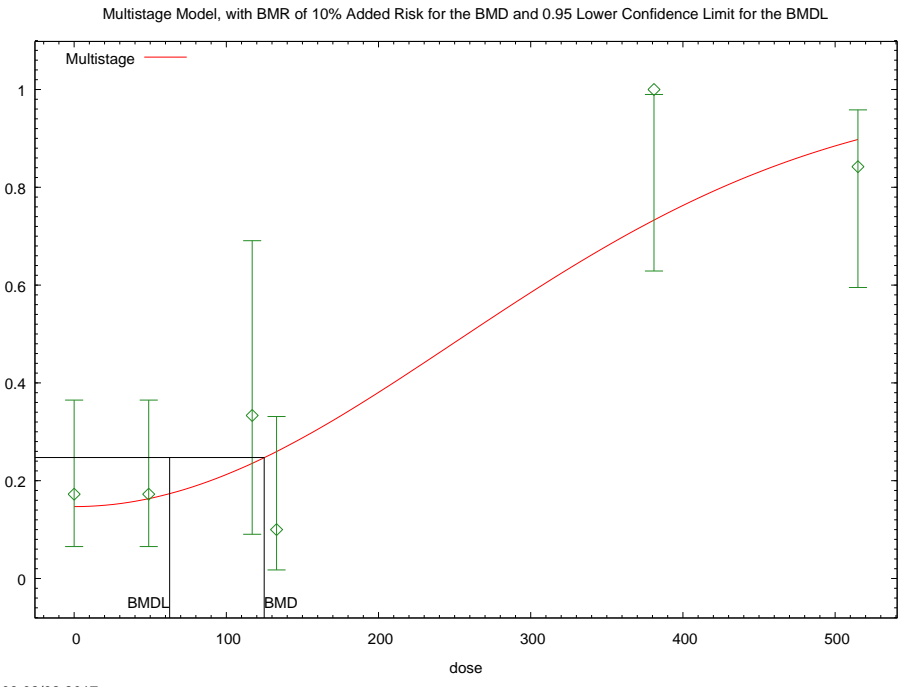
14

This information is distributed solely for the purpose of pre-dissemination peer review under applicable information quality guidelines. It has not been formally disseminated by the National Institute for Occupational Safety and Health. It does not represent and should not be construed to represent any agency determination or policy.

1 **Table 1: All Data Pooled; BMR = Added 10% Risk.**

Model Name	Goodness-of-Fit $p$ value	AIC	BMC ( $\mu\text{g}/\text{m}^3$ )	BMCL ( $\mu\text{g}/\text{m}^3$ )	AIC Adjustment	New AIC
<b>Multistage - 3</b>	0.125	108.324	124.879	62.7501	+4	112.324
<b>LogLogistic</b>	0.0948	108.494	160.708	91.9108		
<b>LogProbit</b>	0.0934	108.681	162.287	95.433		
<b>Logistic</b>	0.0929	109.166	91.0083	71.6765		
<b>Gamma</b>	0.0777	109.36	159.391	80.4167		
<b>Probit</b>	0.0821	109.658	86.5785	70.1134		
<b>Multistage - 2</b>	0.066	109.814	172.124	68.9935		
<b>Weibull</b>	0.0644	110.221	140.787	67.9829		
<b>Quantal-Linear</b>	0.0123	115.165	43.8085	30.1885		

2  
3

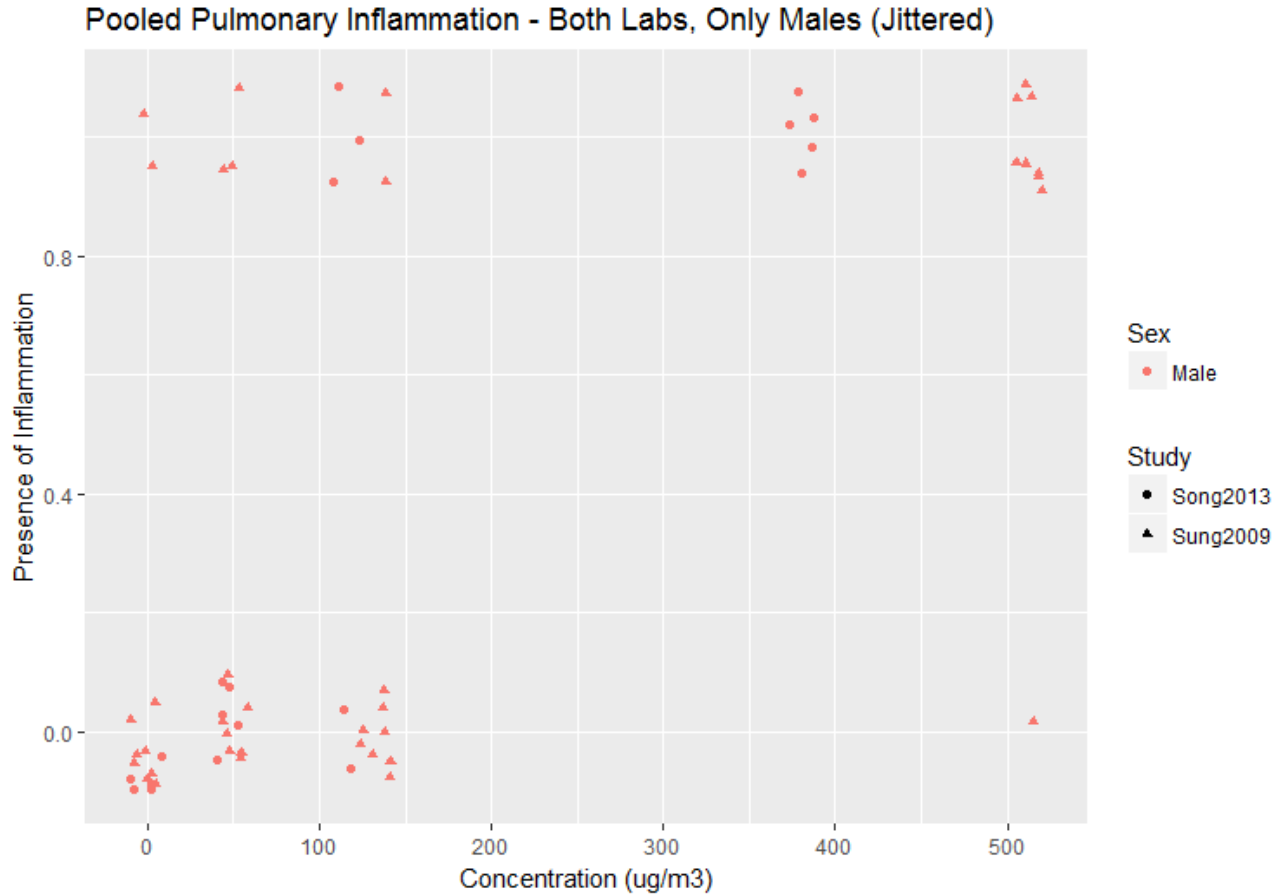


4  
5  
6  
7

**Figure 2: EPA BMDS Plot of Best Fitting Model – Multistage Degree 3.**

1 **B.3.2.2 Phase 2: Pool all male data (both labs, only males)**

2



3

4 **Figure 3: All Male Data Pooled.**

5 For Phase 2, the male pulmonary inflammation data from both labs was combined, and  
6 an association is visible (Figure 3). The best-fitting model was the Logistic model, as all  
7 models had adequate goodness-of-fit and the Logistic model had the smallest AIC  
8 (Table 2). All parameters were estimable. A visual inspection of the fit is also  
9 satisfactory (Figures 4).

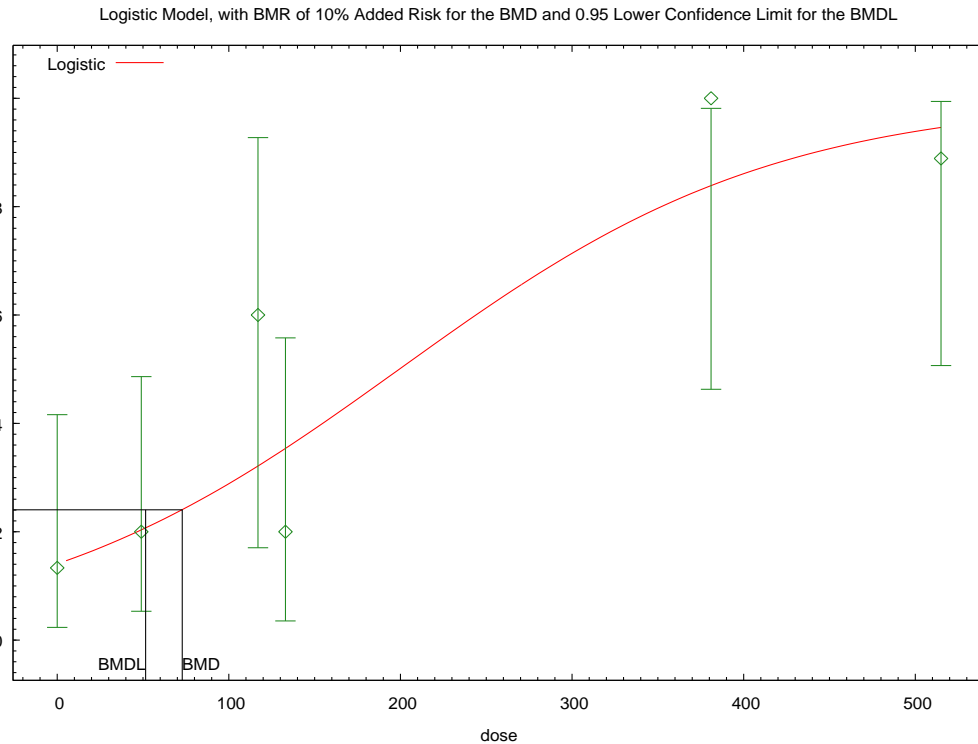
10

This information is distributed solely for the purpose of pre-dissemination peer review under applicable information quality guidelines. It has not been formally disseminated by the National Institute for Occupational Safety and Health. It does not represent and should not be construed to represent any agency determination or policy.

1 **Table 2: All Male Data Pooled, BMR = Added 10% Risk**

Model Name	Goodness-of-Fit $p$ value	AIC	BMC ( $\mu\text{g}/\text{m}^3$ )	BMCL ( $\mu\text{g}/\text{m}^3$ )	AIC Adjustment	New AIC
<b>Logistic</b>	0.3594	58.7911	72.8551	51.5364	0	
<b>Probit</b>	0.3464	59.0091	71.7603	53.3993		
<b>Quantal-Linear</b>	0.2822	60.1351	31.5999	19.588		
<b>LogLogistic</b>	0.2412	60.6002	93.1509	30.0721		
<b>Gamma</b>	0.2432	60.7511	76.9207	22.3897		
<b>LogProbit</b>	0.2324	60.7747	93.2812	30.508		
<b>Weibull</b>	0.2424	60.798	69.3448	22.2645		
<b>Multistage – 2</b>	0.2343	60.8748	64.0911	21.5788		
<b>Multistage – 3</b>	0.2343	60.8748	64.0907	22.0662		

2  
3

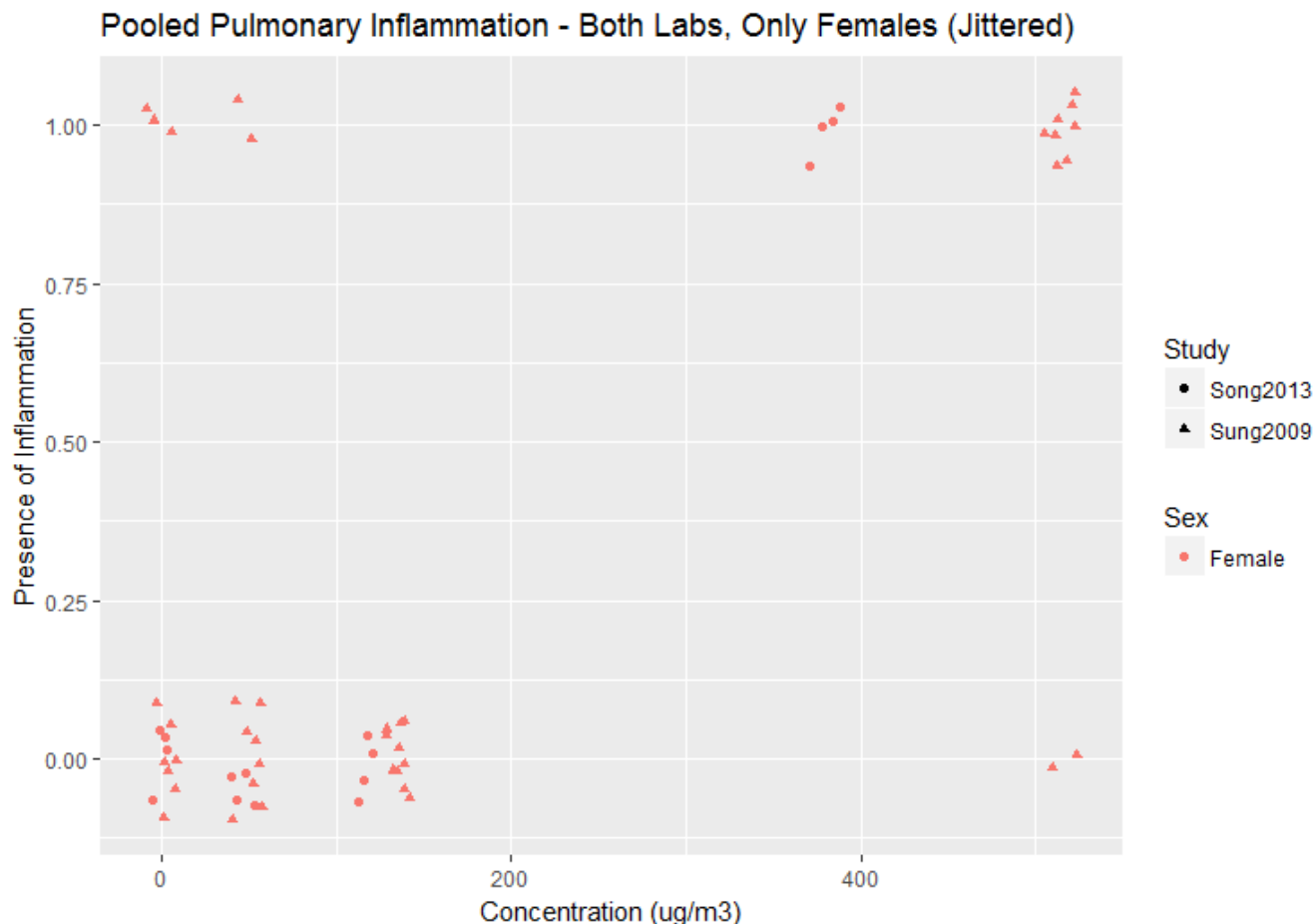


4  
5  
6

**Figure 4: EPA BMDS Plot of Best Fitting Model – Logistic**

1 **B.3.2.3 Phase 3: Pool all female data (both labs, only females)**

2



3

4 **Figure 5: All Female Data, Both Labs.**

5 The female pulmonary inflammation data from both labs was combined for Phase 3,  
6 and again an association is visible (Figure 5). The Multistage 2 model failed  
7 computationally, hence the goodness-of-fit  $p$  value of 0 and missing BMDL. The best-  
8 fitting model was the Multistage 3, which also visibly fits the data. However, two  
9 parameters were estimated to be the boundary value and aren't included in the AIC  
10 calculation, so the new AIC selection process begins (Table 3). The next best-fitting  
11 model is the Log Probit, which has no non-estimable parameters (Figure 6).

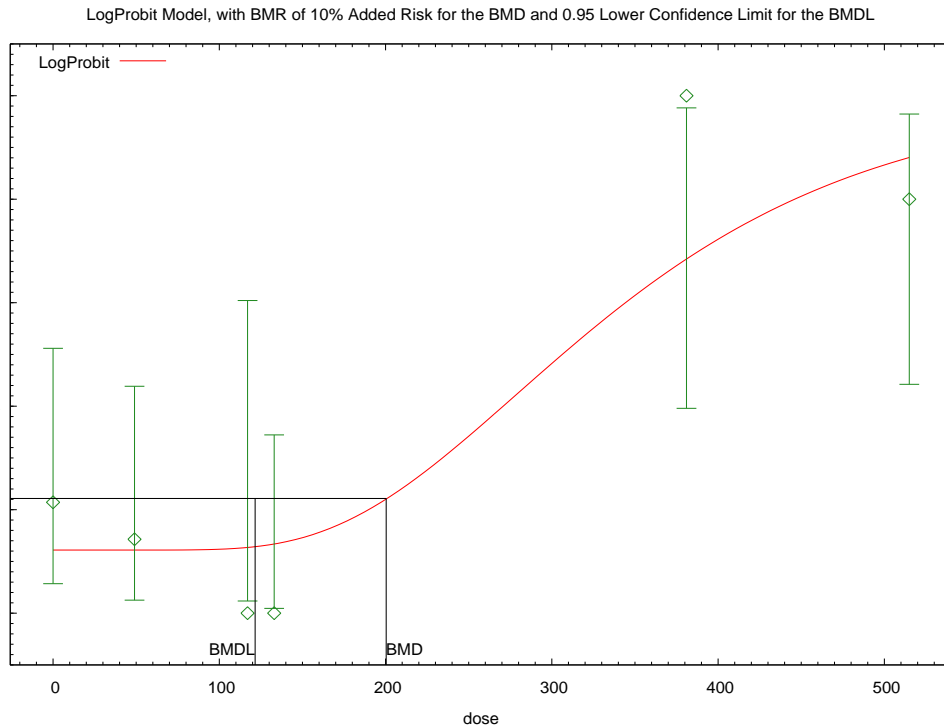
12

This information is distributed solely for the purpose of pre-dissemination peer review under applicable information quality guidelines. It has not been formally disseminated by the National Institute for Occupational Safety and Health. It does not represent and should not be construed to represent any agency determination or policy.

1 **Table 3: All Female Data Pooled, BMR = Added 10% Risk.**

Model Name	Goodness-of-Fit $p$ value	AIC	BMC ( $\mu\text{g}/\text{m}^3$ )	BMCL ( $\mu\text{g}/\text{m}^3$ )	AIC Adjustment	New AIC
<b>Multistage – 2</b>	0	41.7064	408.874		---	---
<b>Multistage – 3</b>	0.1508	50.0352	204.127	97.4488	+4	54.0352
<b>LogProbit</b>	0.1233	50.5459	200.377	121.54		
<b>LogLogistic</b>	0.1125	50.734	203.348	116.53		
<b>Gamma</b>	0.1051	51.0656	207.192	114.868		
<b>Weibull</b>	0.0819	52.0323	200.726	98.5956		
<b>Logistic</b>	0.0741	52.1996	112.311	80.2723		
<b>Probit</b>	0.0674	52.6595	103.843	76.7273		
<b>Quantal-Linear</b>	0.0207	56.9876	59.7879	34.8319		

2  
3



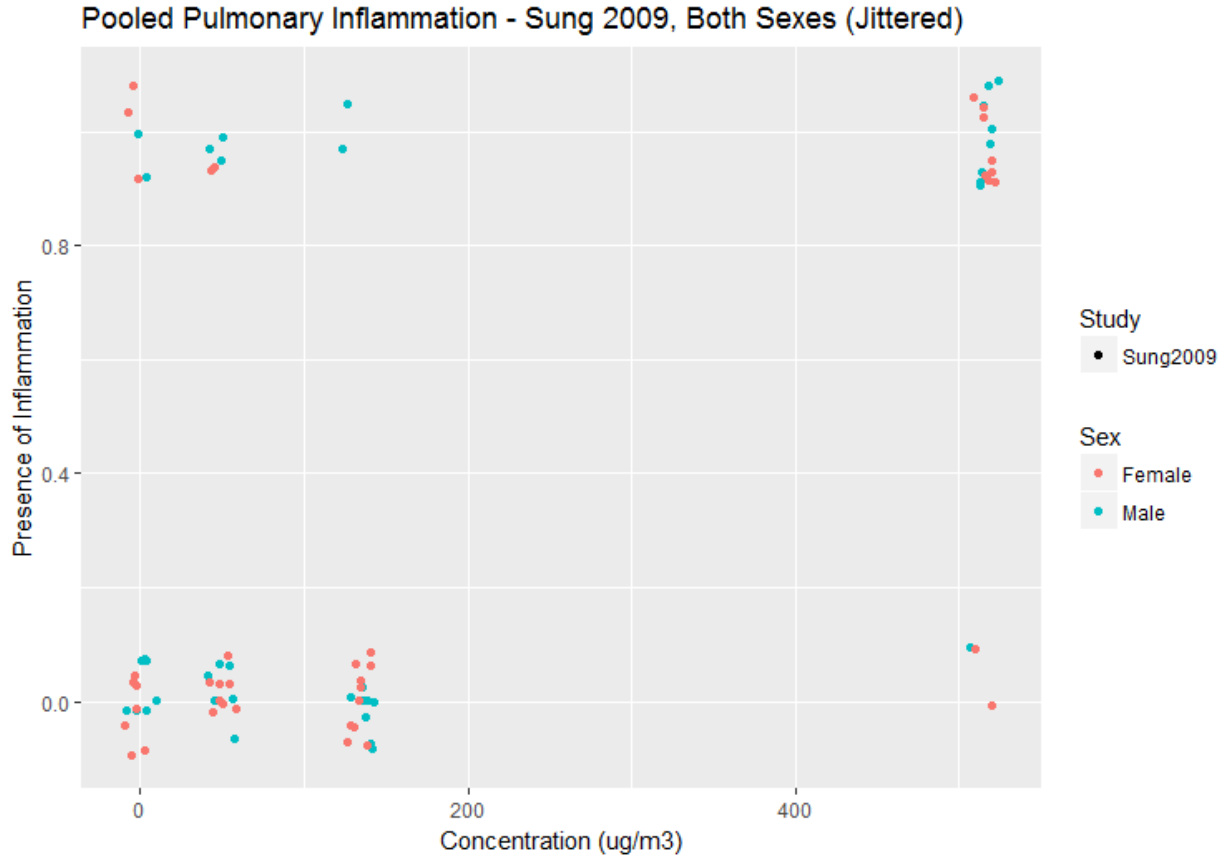
4 11:17 02/03 2017

5 **Figure 6: EPA BMDS Plot of Best-Fitting Model – Log Probit.**

6  
7

1 **B.3.2.4 Phase 4: Pool all Sung [2009] data (one lab, both sexes)**

2



3

4 **Figure 7: All Sung 2009 Data.**

5

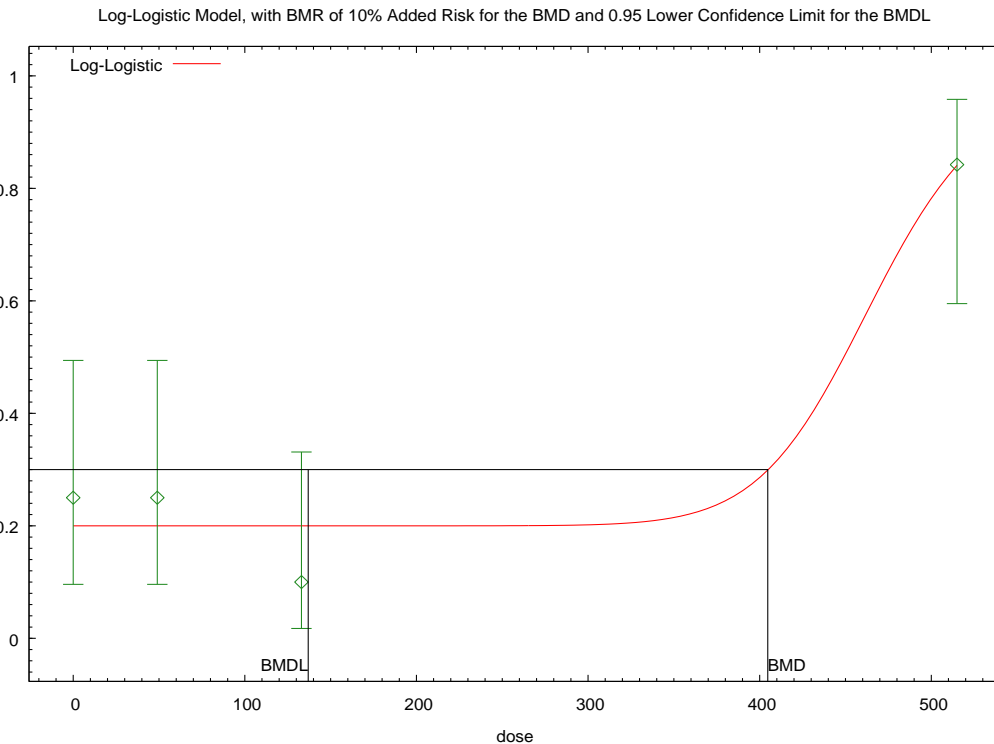
6 In Phase 4, the male and female pulmonary inflammation data was combined from the  
7 Sung et al. [2009] study (Figure 7). The initial best fitting model for these data is the  
8 Gamma, but one parameter was non-estimable. After adjusting AIC, the next best  
9 model was the MS2, but the visual fit is not monotonically increasing. The next best  
10 model is the MS3, which has two non-estimable parameters, so the AIC increases by 4.  
11 The Log Logistic now has the lowest AIC, just under that of the adjusted Gamma, with  
12 no adjustments needed for the AIC (Table 4). The visual fit of the Log Logistic model is  
13 also acceptable (Figure 8).

This information is distributed solely for the purpose of pre-dissemination peer review under applicable information quality guidelines. It has not been formally disseminated by the National Institute for Occupational Safety and Health. It does not represent and should not be construed to represent any agency determination or policy.

1 **Table 4: All Sung 2009 Data Pooled, BMR = Added 10% Risk.**

Model Name	Goodness-of-Fit $\rho$ value	AIC	BMC ( $\mu\text{g}/\text{m}^3$ )	BMCL ( $\mu\text{g}/\text{m}^3$ )	AIC Adjustment	New AIC
<b>Gamma</b>	0.3915	80.6229	318.101	136.966	+2	82.6229
<b>Multistage – 2</b>	0.4281	81.1782	318.297	179.964	---	---
<b>Multistage – 3</b>	0.3089	81.1835	225.822	111.115	+4	85.1835
<b>LogLogistic</b>	0.1709	82.6225	404.723	136.931		
<b>LogProbit</b>	0.1709	82.6225	334.777	137.979		
<b>Weibull</b>	0.1709	82.6225	425.373	135.438		
<b>Logistic</b>	0.0672	84.5596	104.932	78.6943		
<b>Probit</b>	0.0625	84.7756	99.4601	76.3518		
<b>Quantal-Linear</b>	0.0129	88.6681	63.1267	37.9974		

2  
3

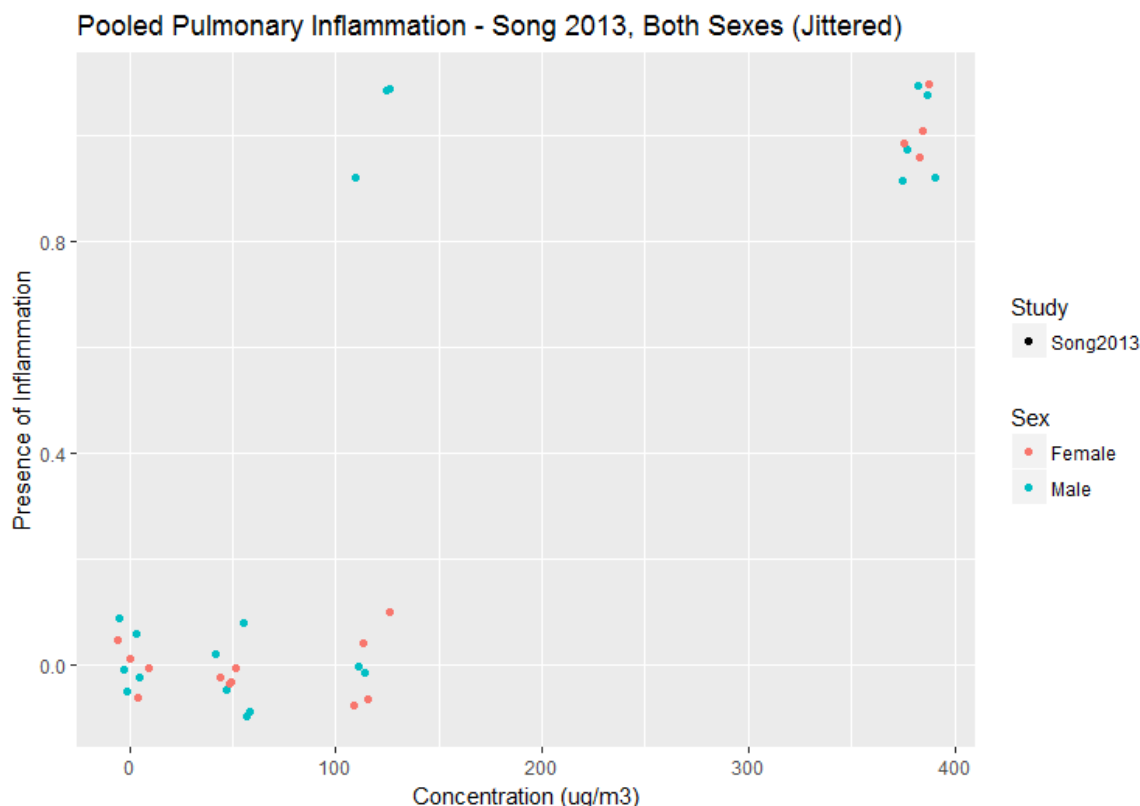


4 12:14 02/03 2017

5 **Figure 8: EPA BMDS Plot of Best Fitting Model – Log Logistic**

6

### 1 B.3.2.5 Phase 5: Pool all Song [2013] data (one lab, both sexes)



2

3 **Figure 9: All Song 2013 Data**

4 For the final phase of this analysis, the male and female pulmonary inflammation data  
5 from the Song et al. [2013] was combined (Figure 9). This is a “noisy” relationship, and  
6 as a result the parameter estimations across the models are affected. For the initial  
7 best-fitting model, the Log Logistic, the background estimate was not estimable as well  
8 as another parameter. Thus, the AIC was adjusted, and AICs had to be adjusted for the  
9 Gamma and MS3 models, as well. The Logistic, Log Probit, and Probit models all had  
10 identical goodness-of-fit  $p$  values and AICs. The smallest BMD estimate came from the  
11 Log Probit model, but this had a non-estimate parameter. The next smallest BMD  
12 estimate was from the Probit (Table 5). There was a large amount of variability around  
13 the background parameter estimate (95% CI: -3142.19, 3123.16), but all parameters  
14 were estimable. Thus, the best-fitting model was chosen to be the Probit model (Figure  
15 10).

16

*This information is distributed solely for the purpose of pre-dissemination peer review under applicable information quality guidelines. It has not been formally disseminated by the National Institute for Occupational Safety and Health. It does not represent and should not be construed to represent any agency determination or policy.*

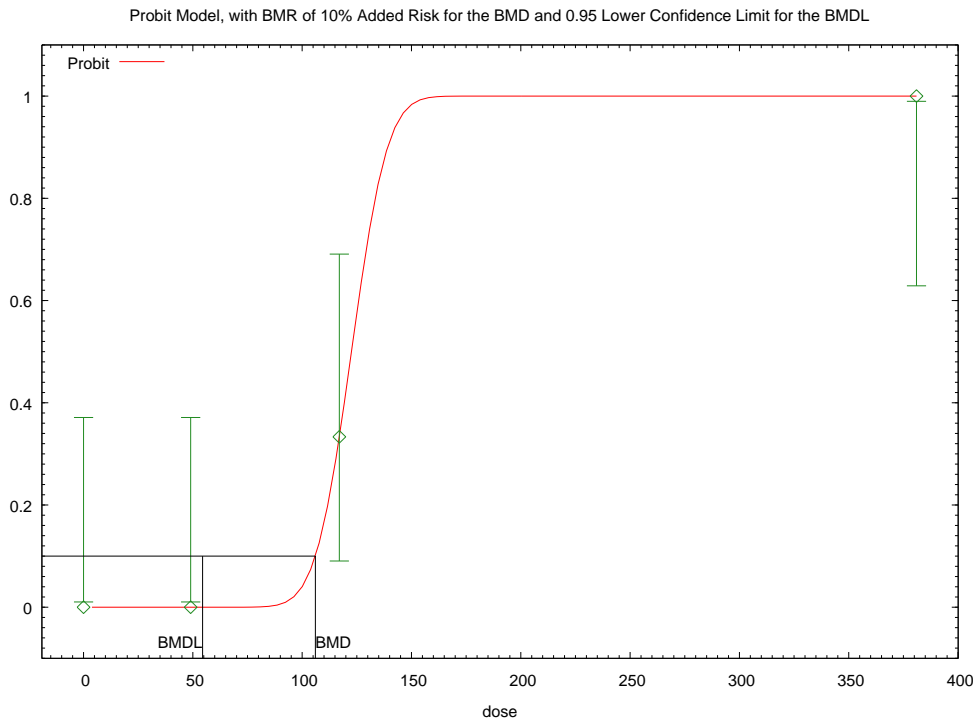
1 **Table 5: All Song 2013 Data Pooled, BMR = Added 10% Risk.**

Model Name	Goodness-of-Fit p value	AIC	BMC ( $\mu\text{g}/\text{m}^3$ )	BMCL ( $\mu\text{g}/\text{m}^3$ )	AIC Adjustment	New AIC
<b>LogLogistic</b>	1	13.4573	107.621	56.0969	+4	17.4573
<b>Gamma</b>	1	13.4609	94.2444	49.2345	+4	17.4609
<b>Multistage – 3</b>	0.9654	13.9705	76.8451	31.9106	+6	19.9705
<b>Logistic</b>	1	15.4573	111.425	58.8764	n/a, but massive SE on background	
<b>LogProbit</b>	1	15.4573	101.567	54.7316	+2	17.4573
<b>Probit</b>	1	15.4573	106.041	54.4632	n/a, but massive SE on background	
<b>Weibull</b>	0.9999	15.4576	103.883	45.4488		
<b>Quantal-Linear</b>	0.2178	21.1911	22.1765	13.4603		
<b>Multistage – 2</b>	0	1.95E+54	Computation failed. BMD is larger than three times maximum input doses.			

2

3

*This information is distributed solely for the purpose of pre-dissemination peer review under applicable information quality guidelines. It has not been formally disseminated by the National Institute for Occupational Safety and Health. It does not represent and should not be construed to represent any agency determination or policy.*



13:12 02/03 2017

1

2 **Figure 10: EPA BMDS Plot of Best Fitting Model – Probit**

3

4

### 5 **B.3.3 Conclusions**

6 In conclusion, a model could be fit to and a BMD/BMDL estimate found for each pooled  
7 data scenario (Table 6). The success of Phase 1, where all data were combined,  
8 suggests that accounting for Lab and Sex may not be necessary; that is, the Lab and  
9 Sex effects may not be statistically significant for explaining the variability in the  
10 response, and dose is sufficient. To better estimate the effects of Lab and Sex, a  
11 multiple non-linear regression model should be explored.

12

*This information is distributed solely for the purpose of pre-dissemination peer review under applicable information quality guidelines. It has not been formally disseminated by the National Institute for Occupational Safety and Health. It does not represent and should not be construed to represent any agency determination or policy.*

1 **Table 6: Summary of results.**

Phase	Best Model	Goodness-of-Fit $p$ value	AIC	BMC ( $\mu\text{g}/\text{m}^3$ )	BMCL ( $\mu\text{g}/\text{m}^3$ )
1: Pool all data (Both Labs, Both Sexes)	<b>Multistage - 3</b>	0.125	108.324	124.879	62.7501
2: Pool all Male data (Both Labs, Only Males)	<b>Logistic</b>	0.3594	58.7911	72.8551	51.5364
3: Pool all Female data (Both Labs, Only Females)	<b>LogProbit</b>	0.1233	50.5459	200.377	121.54
4: Pool all Sung 2009 (Sung lab, Both Sexes)	<b>LogLogistic</b>	0.1709	82.6225	404.723	136.931
5: Pool all Song 2013 (Song lab, Both Sexes)	<b>Probit</b>	1	15.4573	106.041	54.4632

2

3 For Phases 3–5, adjustments were made to AIC estimates because of the fact that EPA  
 4 BMDS does not penalize the likelihood for parameters estimated to be a boundary  
 5 value. BMD estimates did not tend to change by very much in these cases between the  
 6 “best” model by the as-shown AICs and the “best” model by the adjusted AICs.

7 The weighted average of the two pooled-sex BMD estimates is close to the overall  
 8 pooled BMD (134.9 vs. 124.9), but the weighted average of the two pooled-lab BMD  
 9 estimates is quite different from the overall pooled BMD (311.2 vs. 124.9), which  
 10 suggests that Lab may explain more of the response variability than Sex.

11

## 1 **B.4 Exploration of Pooling Rat Subchronic Liver Effects Data**

### 2 **B.4.1 Background**

3 A previous analysis explored the potential of grouping the alveolar inflammation data  
 4 from Sung et al. 2009 and Song et al. 2013. It was found that a simple concentration-  
 5 response model adequately fit the model without including covariates for Lab (Sung,  
 6 Song) or Sex (Female, Male).

7 This section explores whether the female and male data can be combined from the  
 8 Sung et al. [2009] report within two alternative endpoints: Liver Bile Duct Hyperplasia  
 9 and Liver Abnormality.

10 Hyperplasia was already analyzed separately by Sex. Abnormality is also of interest, so  
 11 points of departure (BMD and BMDL) will be estimated for those data.

### 12 **B.4.2 Analysis**

#### 13 **B.4.2.1 Liver Duct Hyperplasia**

14 The following pooled data (Table 1) were considered for modeling:

15 **Table 1: Rat Subchronic Inhalation Study Data for Silver Nanoparticles –**  
 16 **Response Proportion for Liver Bile Duct Hyperplasia (Minimum or Moderate).**

Rat Study and Sex	Response proportion			
	Exposure concentration ( $\mu\text{g}/\text{m}^3$ )			
	0	49	133	515
Sung et al. [2009] – Male	0/10	0/10	1/10	4/9
Sung et al. [2009] – Female	3/10	2/10	4/10	9/10
<i>Pooled</i>	<i>3/20</i>	<i>2/20</i>	<i>5/20</i>	<i>13/19</i>

17 \* Histopathology results from Tables 9 and 10 of Sung et al. [2009]; data at end of 13-week exposure.

1

2 To explore the significance of Sex, an exploratory Logistic model was fit to the pooled  
3 data in SAS 9.4.

$$4 \quad \pi_i = \frac{\exp\{\beta_0 + \beta_1 * Concentration_i + \beta_2 * Sex_i + \beta_3 * Concentration_i * Sex_i\}}{1 + \exp\{\beta_0 + \beta_1 * Concentration_i + \beta_2 * Sex_i + \beta_3 * Concentration_i * Sex_i\}}$$

5  $i = 1, \dots, 79$

6 Sex = 1 if female, 0 if male

7  $\pi_i$  is the expected probability of liver duct hyperplasia for rodent i

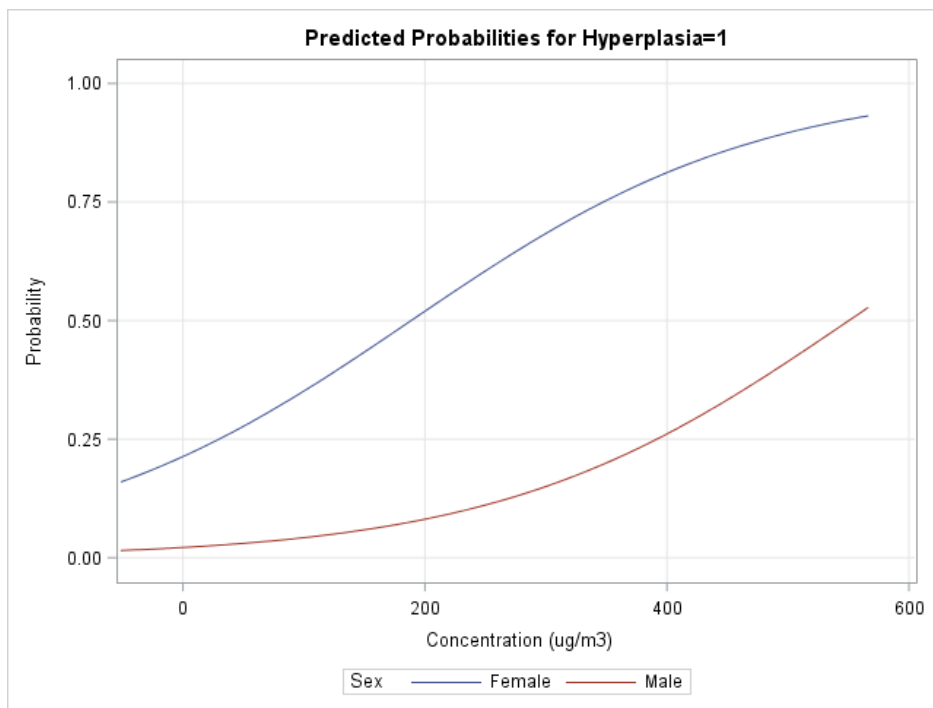
8 The interaction term was found to be not statistically significant ( $p = 0.7919$ ). In the  
9 resulting simpler logistic model, Sex was found to be statistically significant. Thus, the  
10 liver hyperplasia data for male and female rats should not be pooled, as the female rats  
11 were approximately 3.5 times more likely than males to develop liver bile duct  
12 hyperplasia (Table 2). Visually, the dose-response curves are distinct, further supporting  
13 the significant difference in liver hyperplasia development rates between male and  
14 female rats (Figure 1).

15 **Table 2: Logistic Model Fit Statistics**

Analysis of Maximum Likelihood Estimates							
Parameter		DF	Estimate	Standard Error	Wald Chi-Square	Pr > ChiSq	Exp(Est)
Intercept		1	-2.5560	0.5686	20.2054	<.0001	0.078
Conc		1	0.00692	0.00182	14.4495	0.0001	1.007
Sex	Female	1	1.2519	0.4096	9.3431	0.0022	3.497

16

This information is distributed solely for the purpose of pre-dissemination peer review under applicable information quality guidelines. It has not been formally disseminated by the National Institute for Occupational Safety and Health. It does not represent and should not be construed to represent any agency determination or policy.



1

2 **Figure 1: Logistic Model Fits to Male and Female Liver Hyperplasia Data**

3 **B.4.2.2 Liver Abnormality**

4 In addition to bile duct hyperplasia, Sung et al. [2009] also considered necrosis,  
 5 vacuolation, mineralization, granuloma, fibrosis, or pigment when histopathologically  
 6 analyzing the rodent livers. All of these endpoints were combined into a category called  
 7 Abnormality. The resulting data are below (Table 3).

8 **Table 3: Rat Subchronic Inhalation Study Data Used in NIOSH Risk Assessment –**  
 9 **Response Proportion for Liver Abnormalities**

Rat Study and Sex	Response proportion			
	Exposure concentration (µg/m <sup>3</sup> )			
	0	49	133	515
Sung et al. [2009] – Male	0/10	0/10	1/10	4/9
Sung et al. [2009] – Female	3/10	5/10	5/10	9/10
<i>Pooled</i>	<i>3/20</i>	<i>5/20</i>	<i>6/20</i>	<i>13/19</i>

10 \* Histopathology results from Tables 9 and 10 of Sung et al. [2009]; data at end of 13-week exposure.

1 In male rats, “Abnormality” consists of bile duct hyperplasia, necrosis, vacuolation, and  
 2 mineralization. In the female rats, “Abnormality” consists of bile duct hyperplasia,  
 3 necrosis, vacuolation, granuloma, fibrosis, and pigment. The combination of  
 4 histopathological responses observed in each rat is not clear because of the nature of  
 5 the reported summary data, that is, some rats may have had only bile duct hyperplasia  
 6 and others had some or all responses.

7 To explore the significance of Sex, an exploratory Logistic model was fit to the pooled  
 8 data in SAS 9.4.

$$\pi_i = \frac{\exp\{\beta_0 + \beta_1 * Concentration_i + \beta_2 * Sex_i + \beta_3 * Concentration_i * Sex_i\}}{1 + \exp\{\beta_0 + \beta_1 * Concentration_i + \beta_2 * Sex_i + \beta_3 * Concentration_i * Sex_i\}}$$

$$i = 1, \dots, 79$$

Sex = 1 if female, 0 if male

$\pi_i$  is the expected probability of liver abnormality for rodent i

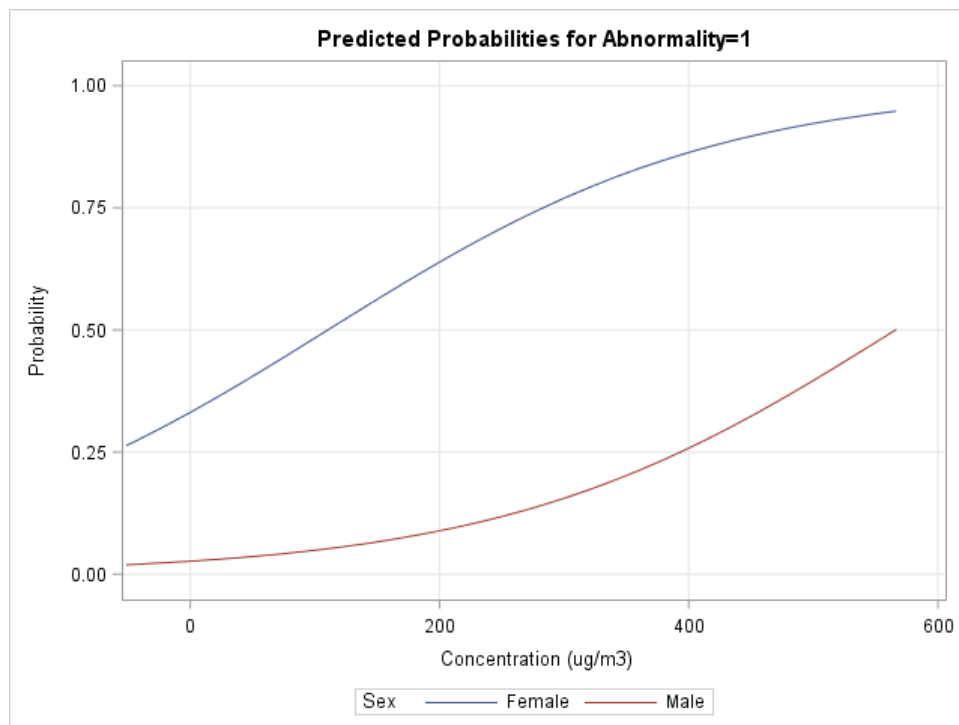
13 The interaction term was found to be not statistically significant ( $p = 0.5821$ ). In the  
 14 resulting simpler logistic model, Sex was found to be statistically significant. Thus, the  
 15 liver abnormality data for male and female rats should not be pooled, as the female rats  
 16 were approximately 4.3 times more likely than males to develop a liver abnormality  
 17 (Table 4). Visually, the dose-response curves are distinct, further supporting the  
 18 significant difference in liver abnormality development rates between male and female  
 19 rats (Figure 2).

20 **Table 4: Liver Abnormality Logistic Model Fit Statistics**

Analysis of Maximum Likelihood Estimates							
Parameter		DF	Estimate	Standard Error	Wald Chi-Square	Pr > ChiSq	Exp(Est)
<b>Intercept</b>		1	-2.1516	0.5393	15.9179	<.0001	0.116
<b>Conc</b>		1	0.00636	0.00185	11.8632	0.0006	1.006
<b>Sex</b>	<b>Female</b>	1	1.4493	0.4064	12.7205	0.0004	4.260

21

*This information is distributed solely for the purpose of pre-dissemination peer review under applicable information quality guidelines. It has not been formally disseminated by the National Institute for Occupational Safety and Health. It does not represent and should not be construed to represent any agency determination or policy.*



1

2 **Figure 2: Logistic Model Fits to Male and Female Liver Abnormality Data**

3

#### 4 **B.4.2.3 Point of Departure Estimation for Liver Abnormality**

5 The liver bile duct hyperplasia data were previously analyzed, and benchmark doses  
6 (the dose associated with 10% added risk of hyperplasia) were estimated for each sex  
7 separately.

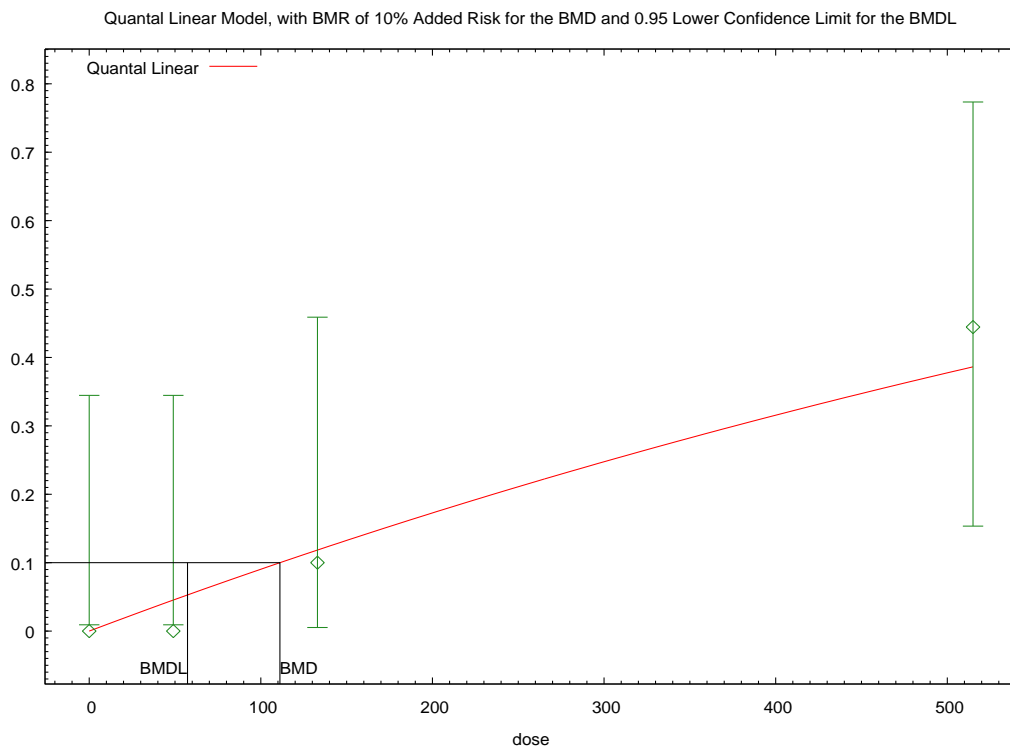
8 The liver abnormality data for each sex were modeled separately with use of EPA  
9 BMDS 2.6. All available models were considered (Gamma, Quantal Linear, Logistic,  
10 Log-Logistic, Log-Probit, Multistage Degree 2, Multistage Degree 3, Probit, Weibull).  
11 Default modeling options were used. The benchmark response was set at added 10%  
12 risk. The best model chosen is that having the smallest Akaike Information Criterion  
13 (AIC) where the Goodness-of-Fit p value is greater than 0.1.

14

This information is distributed solely for the purpose of pre-dissemination peer review under applicable information quality guidelines. It has not been formally disseminated by the National Institute for Occupational Safety and Health. It does not represent and should not be construed to represent any agency determination or policy.

1 **B.4.2.3.1 Male Liver Abnormality**

2 All models had adequate goodness-of-fit (Table 5), and the best-fitting model was the  
 3 Quantal Linear (Figure 3).



13:40 06/23 2017

4

5 **Figure 3: Quantal Linear Model Fit to Male Liver Abnormality Data**

6

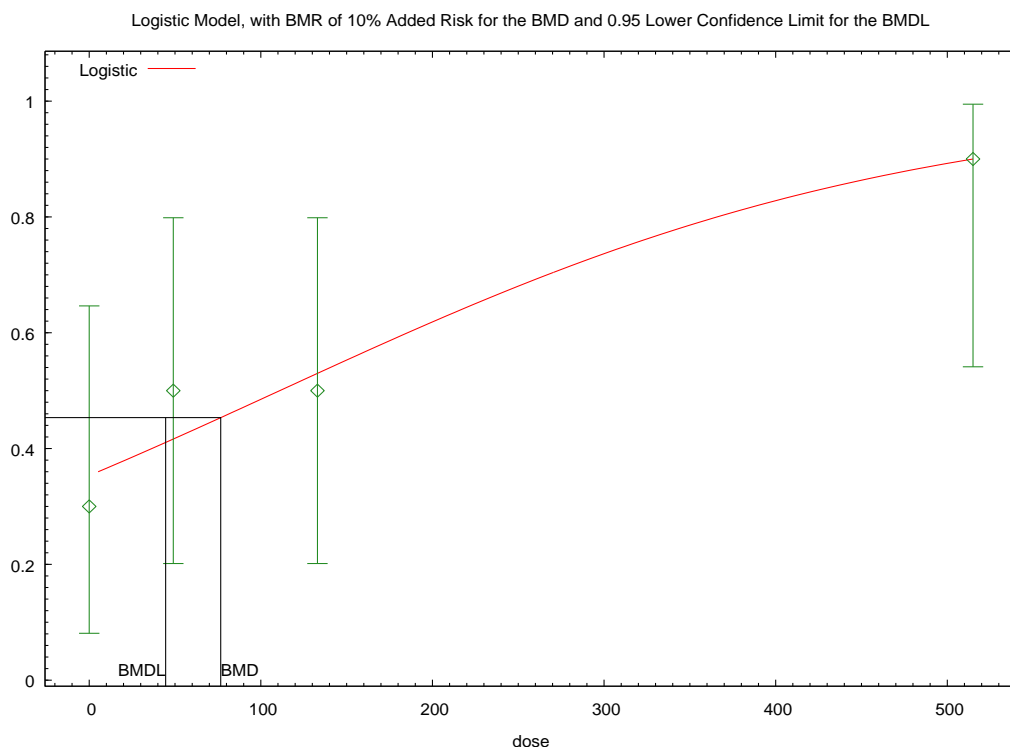
7 **Table 5: Summary of EPA BMDS Model Fits to Male Liver Abnormality Data**

Model	p Value	AIC	BMC	BMCL
Quantal-Linear	0.888	21.9566	111.126	57.2667
LogProbit	0.9257	23.1059	152.078	48.1568
LogLogistic	0.8873	23.2415	159.484	43.6585
Gamma	0.8797	23.2533	163.03	62.2946
Weibull	0.8704	23.2952	165.104	61.9547
Multistage – 3	0.8395	23.3923	173.845	61.1904
Multistage - 2	0.8395	23.3923	173.845	49.1907
Probit	0.6167	24.057	244.293	158.211
Logistic	0.5749	24.2378	268.699	173.98

8

1 **B.4.2.3.2 Female Liver Abnormality**

2 All models had adequate goodness-of-fit, and the best-fitting model was the Logistic  
 3 (Figure 4). The Probit and Logistic models had equal AIC estimates, but the Logistic  
 4 model had the smaller BMD estimate (Table 6).



13:43 06/23 2017

5

6 **Figure 4: Logistic Model Fit to Male Liver Abnormality Data**

7

8 **Table 6: Summary of EPA BMD5 Model Fits to Female Liver Abnormality Data**

Model	p Value	AIC	BMC	BMCL
Logistic	0.7993	50.892	76.629	44.541
Probit	0.7996	50.8919	80.359	50.3944
Quantal-Linear	0.7916	50.9086	45.9117	20.3863
Multistage – 3	0.5298	52.8376	61.5382	20.5724
Multistage - 2	0.5169	52.8622	59.9452	13.6063
Weibull	0.4966	52.9035	52.4935	20.3995
Gamma	0.4942	52.9086	46.0966	20.3863
LogLogistic	0.4144	53.1072	79.0148	0.136955
LogProbit	0.3922	53.171	67.6935	0.143749

9

This information is distributed solely for the purpose of pre-dissemination peer review under applicable information quality guidelines. It has not been formally disseminated by the National Institute for Occupational Safety and Health. It does not represent and should not be construed to represent any agency determination or policy.

### 1 B.4.3 Conclusion

2 There were statistically significant differences in the observed proportions of rats with  
 3 Liver Bile Duct Hyperplasia and Liver Abnormality between males and females in the  
 4 Sung et al. 2009 study; females were roughly four times more likely to have a response.  
 5 Therefore, the data for the two sexes should not be pooled.

6 Benchmark concentrations were estimated separately for male and female liver  
 7 abnormality. In the tables below, the data and results are summarized.

8

#### 9 Response proportions in Sprague-Dawley rats following subchronic inhalation 10 exposure to silver nanoparticles [Sung et al. 2009]

Liver Abnormality				
Group	Concentration ( $\mu\text{g}/\text{m}^3$ )			
	0	49	133	515
Males	0/10	0/10	1/10	4/9
Females	3/10	5/10	5/10	9/10

11

12

#### 13 Best-fitting Benchmark Concentration (BMC) models of subchronic inhalation 14 responses to silver nanoparticles in Sprague-Dawley rats [Sung et al. 2009].

Model	AIC	P	BMC ( $\mu\text{g}/\text{m}^3$ )	BMCL <sub>10</sub> ( $\mu\text{g}/\text{m}^3$ )
<b>Male: Liver Abnormality</b>				
Quantal Linear	21.9566	0.888	111.1	57.3
<b>Female: Liver Abnormality</b>				
Logistic	50.892	0.7993	76.6	44.5

15 AIC = Akaike Information Criterion.

16

## 1 **B.5 Evaluation of Biomarker Findings in Silver Jewelry Workers**

### 2 **B.5.1 Summary of findings**

3 The findings of increased DNA damage and oxidative stress among jewelry workers  
4 who were exposed to silver nanomaterials [Aktepe et al. 2015] were statistically  
5 evaluated in this analysis to determine if these findings could be verified on the basis of  
6 the information provided in the paper. The authors reported summary statistics which  
7 are sufficient for replication.

8 The authors measure differences in DNA damage and plasma parameters between a  
9 group of silver jewelry workers (n = 35) and a control group (n = 41) from a similar area  
10 in Mardin, Turkey. The authors state that the silver workers were exposed to silver  
11 particles via inhalation for at least 4 hours a day. The two groups were shown to have  
12 similar socioeconomic statuses, mean age, mean BMI, and proportions of smokers.  
13 Comparisons (group characteristics and biological effects) were evaluated by Student's  
14 *t*-test at a significance level of 0.001. The authors conclude that DNA damage and  
15 oxidative stress measurements were statistically significantly higher in the group of  
16 silver workers; therefore "exposure to silver particles among silver jewelry workers  
17 caused oxidative stress and accumulation of severe DNA damage."

18 Review of the statistical methods and results highlighted several concerns. First, the  
19 conclusion of causality is tenuous, given the experimental design. Second, the  
20 descriptions of the working environment and exposures are lacking. No information  
21 about silver levels in the blood was given. Third, the results of several of the statistical  
22 tests were unable to be replicated with the provided summary statistics. Fourth, the  
23 statistical test used (Student's *t*-test) is not appropriate in some cases, given the types  
24 of measurements (e.g., severity scores). Despite these concerns, it does appear that  
25 being a silver worker in Mardin, Turkey, is associated with differences in the measured  
26 biological effects.

## 1 B.5.2 Statistical evaluation of findings

2 This study reports a causal relationship between silver particle exposure and oxidative  
3 stress and severe DNA damage. This was not a completely randomized experiment, so  
4 establishing causality is not an automatic conclusion; other factors (i.e., lurking  
5 variables) could contribute to the effects seen but were not directly measured.

6 The authors state only that the silver jewelry workers were “working at least 4 h in a  
7 day.” There is no further information about length of employment or job tasks (e.g.,  
8 smelting would likely have a higher exposure than working with silver wires). There is no  
9 description of exposure controls or the working environment. There is no description  
10 about the form of the silver exposure other than “particle or nanoparticle,” e.g., dust or  
11 fume.

12 The “control” group (in quotes because it is more of a comparison group; the subjects  
13 were volunteers, as stated by the author) and the exposed group were compared on  
14 Socioeconomic Status (SES), Age, BMI, and Proportion of Smokers. To establish if  
15 silver exposure is associated with the biological effects of interest, the two groups must  
16 be highly similar, with the only difference being the exposure to silver particles. No data  
17 are provided about SES, but the authors claim they were similar between the two  
18 groups. Summary statistics (mean, standard deviation, sample size) are provided for the  
19 measurements of Age and BMI. Comparisons were made by the authors, using  
20 Student’s two-sample  $t$ -test (in SPSS 11.5), which assumes the following:

- 21 • The two groups are independent
- 22 • Measurements within each group are independently and identically  
23 approximately normally distributed

24 Student’s  $t$ -test has been shown to be robust to some deviation from these  
25 assumptions, and the assumptions are probably met for these data.

This information is distributed solely for the purpose of pre-dissemination peer review under applicable information quality guidelines. It has not been formally disseminated by the National Institute for Occupational Safety and Health. It does not represent and should not be construed to represent any agency determination or policy.

- 1 The authors state there is not a statistically significant difference in average age  
2 between the two groups ( $p$  value  $< 0.231$ ) nor in average BMI ( $p$  value  $< 0.234$ ).
- 3 These results were replicated in SAS 9.3 using Proc TTEST (Table 1). It was assumed  
4 that population variances were equal; this assumption was verified via the F-Test at the  
5 5% level of significance and  $p$  values were greater than 5% (not shown).

6 **Table 1: Replication Results for Age and BMI Comparisons**

Variable	Author's $p$ value	Replicated $p$ value
Age (years)	$<0.231$	0.2123
BMI (kg/m <sup>2</sup> )	$<0.234$	0.0226

7

8 The difference in average BMI was found to be more significant than stated by the  
9 authors; since the authors chose a 0.1% level of significance (presumably) *a priori*, their  
10 conclusions that the groups are similar with respect to Age and BMI remain the same in  
11 light of the replication differences.

12 It seems like there may have been a mistake by the authors when comparing the  
13 proportion of smokers between the two groups (41 control subjects, 35 silver workers).

14 The authors report the proportion as  $\frac{\# Yes}{\# No}$  rather than  $\frac{\# Yes}{n}$  and find a  $p$  value of  $<0.427$ . If  
15 one conducts the two-sided hypothesis test for two incorrect proportions,

16 
$$\text{Proportion of Smokers in Patients} = \frac{15}{20}$$

17 
$$\text{Number of Patients} = 20$$

18 
$$\text{Proportion of Smokers in Controls} = \frac{16}{25}$$

19 
$$\text{Number of Controls} = 25$$

20

21 then the resulting  $p$  value is 0.429, which is similar to that which was reported by the  
22 authors.

1 The comparison of the correct proportions was made with a chi-square test from Proc  
2 Freq. The resulting  $p$  value was 0.7347, indicating that there is not a statistically  
3 significant difference in proportion of smokers between the two groups. Again, the  
4 author's conclusion that there isn't a difference remains the same in light of the  
5 replication difference (and possible computational error).

6 Thus, it does appear that the comparison group is similar to the silver worker group in  
7 the dimensions of SES, Age, BMI, and Smoking Proportion.

8 This same process follows for the comparison of mean responses for six biological  
9 effects: TAS (total antioxidant status), TOS (total oxidant status), OSI (oxidative stress  
10 index, the sum of TAS and TOS), Ceruloplasmin, Total thiol, and Mononuclear  
11 leukocyte DNA damage. All of these appear to be continuous measurements and could  
12 reasonably be approximately normally distributed, except for the last measurement,  
13 DNA Damage, meaning a two sample  $t$ -test is sufficient for testing for differences in the  
14 average responses between the two groups.

15 DNA Damage is a total score of 100 slides, where each slide is rated 0, 1, 2, 3, or 4  
16 (undamaged to maximally damaged). Thus, for each subject, the total score could range  
17 from 0 to 400. This is a combination of ordinal measures, which may not be suitable for  
18 Student's  $t$ -test; a non-parametric test would typically be used. Without the individual  
19 scores, a proper replication cannot be done. Interpreting the results of this  $t$ -test as  
20 indicating there is a difference in average DNA damage score may be incorrect, given  
21 the improper use of the statistical test.

22 The six comparisons were replicated with use of Proc TTest in order to check the  
23 reported  $p$  value ranges (Table 2).

24

1 **Table 2: Replication Results for Biological Response Comparisons**

Variable	Author's <i>p</i> value	Replicated <i>p</i> value
TAS	<0.05	0.0041
TOS	<0.001	0.0005
OSI	<0.001	<0.0001
Ceruloplasmin	<0.01	0.0017
Total thiol	<0.001	<0.0001
DNA Damage	<0.001	<0.0001

2  
3 The replications tend to agree with the *p* value ranges of the authors, but there is a  
4 large difference in *p* values for TAS. It is unclear why the authors chose to indicate the  
5 range as <0.05, but it seems to indicate the *p* value was larger than 0.001 (the chosen  
6 level of significance) as well as 0.01.

## 7 **B.6 Conclusions**

8 Despite replication differences and having only summary statistics, it does appear that  
9 the silver workers are being affected by their silver exposure. The comparison group  
10 and silver worker group do appear to have similar characteristics, with the exception  
11 being silver exposure. Their average levels of TOS, OSI, and Total Thiol are statistically  
12 significantly different from the comparison group. Comparisons of TAS and  
13 Ceruloplasmin were not significant at the author's chosen level of significance. The  
14 statistical evaluation of DNA Damage completed by the authors is flawed because the  
15 nature of the measurements is not commensurate with the assumptions of a *t*-test.  
16 Therefore, a conclusion is unclear at this point.

17 For all of these comparisons, it would be helpful to see a discussion of the practical  
18 effects. For example, is a decrease of 0.11 millimoles/L in the average TAS biologically  
19 significant? As another example, for the DNA Damage metric, the control group had an  
20 average score (standard deviation of scores) of 7.48 (5.46) and the silver workers had  
21 an average score of 15.37 (6.07). The minimum score per worker is 0 and the maximum  
22 score is 400. Is a total score of 15 out of 400 indicative of severe DNA damage?

*This information is distributed solely for the purpose of pre-dissemination peer review under applicable information quality guidelines. It has not been formally disseminated by the National Institute for Occupational Safety and Health. It does not represent and should not be construed to represent any agency determination or policy.*

- 1 Across these biological effect comparisons, it does appear that the silver jewelry
- 2 workers have statistically significantly different measurements compared to a similar
- 3 non-exposed group, which suggests a potential need for occupational safety measures
- 4 for silver jewelry workers.

## 5 **B.7 References**

- 6 See References (Section 9) in main document.

## APPENDIX C

### Literature Search Strategy

An initial literature search, record retrieval, and evaluation of studies were conducted by the Oak Ridge Institute for Science and Education (ORISE). A report was submitted to NIOSH in June 2012 that provided an evaluation of the experimental in vivo and in vitro studies with silver nanoparticles. Studies cited in the report were identified from literature searches using PubMed, Toxline, Embase, and BIOSIS. Search terms included silver nanoparticles as well as the use of other relevant key words (e.g., toxicology, physical and chemical properties, dosimetry).

In January 2013, NIOSH conducted an updated and expanded literature search to identify studies with exposure to silver and/or silver nanoparticles. Search terms were selected to ensure that all in vivo and in vitro studies with silver and/or silver nanoparticles were identified, as well as studies describing workplace exposure. Literature searches were conducted in the online databases CINAHL, PubMed, Compendex, Embase, HSDB, NIOSHTIC-2, Risk Abstracts, Toxicology Abstracts, Toxline, and Web of Science. In June 2014 a follow-up literature search was conducted, using the same search terms to identify relevant studies published since January 2013.

In summer 2016, NIOSH conducted an updated and expanded literature search. Seven discrete subject areas were identified and a set of search terms was identified for each study area. These were assembled into the following search strings:

- human — (Occupational OR occupation OR occupations OR workplace OR worksite OR worker OR workers OR employee OR employees) AND (silver OR nanosilver OR nano-silver)),
- animal — ((Murine OR mouse OR mice OR rat OR rats OR rodent OR rodents OR hamster OR hamsters OR rabbit OR rabbits) AND (Inhalation OR inhaled OR inhale OR “intratracheal instillation” OR “pharyngeal aspiration”) AND (silver OR nanosilver OR nano-silver)),

- 1 • oral — ((Murine OR mouse OR mice OR rat OR rats OR rodent OR rodents OR  
2 hamster OR hamsters OR rabbit OR rabbits) AND (oral) AND (silver OR  
3 nanosilver OR nano-silver)),
- 4 • dermal — ((Porcine OR pig OR pigs) AND (dermal OR skin) AND (silver OR  
5 nanosilver OR nano-silver)),
- 6 • in vitro — ((In vitro) AND (lung OR liver OR pulmonary OR hepatic) AND (silver  
7 OR nanosilver OR nano-silver)),
- 8 • cell-free — (“Cell-free”) AND (silver OR nanosilver OR nano-silver)),
- 9 • and zebrafish — (Zebrafish AND (silver OR nanosilver OR nano-silver)).

10 The summer 2016 searches were bounded from January 1, 2011, and June 30, 2016,  
11 and were conducted using the online databases PubMed, Embase, and Toxline.  
12 Records were further curated to those which were topical (relating to silver toxicology,  
13 exposure, and epidemiology), with English-language full text available from accessible  
14 databases.

15 A final search was conducted in October 2016, updating the results through the end of  
16 the third quarter. These included the previously described subject areas, in addition to  
17 two new subject areas. The results of this search were curated just as the summer 2016  
18 searches. The new subject areas and their corresponding search strings were

- 19 • kinetics — ((Silver OR nanosilver OR nano-silver) AND (PBPK OR  
20 “physiologically-based pharmacokinetic model” OR biodistribution OR bio-  
21 distribution OR clearance OR fate OR kinetics) AND (worker OR workers OR  
22 occupation OR occupations OR occupational OR workplace OR workplaces OR  
23 worksite OR worksites OR murine OR mouse OR mice OR rat OR rats OR  
24 rodent OR rodents OR hamster OR hamsters OR rabbit OR rabbits)),
- 25 • and reproductive — ((Silver OR nanosilver OR nano-silver) AND (reproductive  
26 OR reproduction OR developmental)).

*This information is distributed solely for the purpose of pre-dissemination peer review under applicable information quality guidelines. It has not been formally disseminated by the National Institute for Occupational Safety and Health. It does not represent and should not be construed to represent any agency determination or policy.*

1 An additional literature search was conducted to evaluate further the biological  
2 significance of the rat biliary hyperplasia response to silver nanoparticles. The search  
3 terms were silver nanoparticles and liver and toxicity (date of search 1/24/17). Appendix  
4 E and Chapter 5 were reviewed and original references from those sections were  
5 evaluated for inclusion. This targeted review was designed to inform the evaluation of  
6 whether biliary hyperplasia seen in subchronic studies was or was not potentially related  
7 to general hepatobiliary damage.

8 Articles from the updated literature searches were retrieved if found to be relevant,  
9 following examination of titles and abstracts by the authors. The articles selected from  
10 the updated literature searches for full review included any in vivo studies on silver  
11 nanoscale or microscale particles and any in vitro studies that provided new information  
12 on the role of particle size and/or solubility on the toxicological effects. Studies cited in  
13 retrieved articles but not identified during the primary and follow-up database searches  
14 were retrieved for evaluation. For each article retrieved, the quality of the study design  
15 (including the risk of bias), relevance of the evidence to workers, and quality of the  
16 study methodology were assessed by the authors to determine their appropriateness for  
17 inclusion in the document.

## APPENDIX D

### In Vitro/Mechanistic Studies

A considerable number of research reports address the impacts of AgNPs on isolated cellular systems. These studies provide inferential evidence of the capacity of AgNPs to bring about cellular changes of potential toxicological consequence, and in many cases they contribute to our understanding of what biochemical and physiologic mechanisms might be triggered when AgNPs interact with cellular systems. In an extensive database of in vitro studies, the predominant topic areas for cellular and subcellular changes brought about by AgNPs are (1) development of oxidative stress and the induction of apoptosis and (2) DNA damage/genotoxicity. In the following paragraphs, results of in vitro and mechanistic studies of AgNPs are discussed within these general topic areas. Other relevant studies highlight possible impacts of AgNP exposure on gene expression and regulation, neurologic changes, effects on skin cells, and cytotoxicity.

#### D.1 Oxidative Stress/Induction of Apoptosis

A wide range of cellular isolates and cultures have been used to examine cellular uptake of AgNPs and the oxidative stress and apoptotic effects of AgNPs in vitro. These studies provide some evidence of the toxic potential of the particles and provide insight into the physiologic and biochemical mechanisms that may be responsible. Among the many cellular systems that have formed a platform for these investigations are liver/hepatoma cells [Piao et al. 2011; Liu et al. 2010a; Arora et al. 2009; Kim et al. 2009c; Hussain et al. 2005a; Avalos Funez et al. 2013; Gaiser et al. 2013; Garcia-Reyero et al. 2014; Kermanizadeh et al. 2012, 2013; Paino et al. 2015; Sahu et al. 2014a, 2014b, 2014c, 2016a, 2016b; Shannahan et al. 2015; Sun et al. 2013]; rat alveolar and mouse peritoneal macrophages [Park et al. 2010b; Carlson et al. 2008; Hussain et al. 2005b]; fibroblasts [Wei et al. 2010; Arora et al. 2009, 2009; Hsin et al. 2008; Avalos et al. 2015]; HeLa cells [Miura et al. 2009]; human acute monocytic leukemia cell lines (THP-1 monocytes) [Foldbjerg et al. 2009; Braakhuis et al. 2016]; tumoral leukemia cells (HL-60) [Avalos Funez et al. 2013]; rat vascular smooth muscle cells [Hsin et al. 2008]; bovine retinal endothelial cells [Kalishwaralal et al. 2009]; mouse

1 blastocysts [Li et al. 2010]; mouse MC3T3-E1 cells, rat adrenal PC12 cells, human  
2 HeLa cervical cancer cells, and hamster ovary CHO cells [Kim et al. 2012]; A549 human  
3 lung cells [Lee et al. 2011a; Liu et al. 2010a; Foldbjerg et al. 2011; Stoehr et al. 2011;  
4 Beer et al. 2012; Chairuangkitti et al. 2013; Han et al. 2014]; A431 human skin  
5 carcinoma cells [Arora et al. 2008]; SGC-7901 human stomach cancer cells [Liu et al.  
6 2010]; MCF-7 human breast adenocarcinoma cells [Liu et al. 2010a]; murine alveolar  
7 cell line and human macrophage and epithelial lung cell lines [Soto et al. 2007;  
8 Braakhuis et al. 2016; Jeanette et al. 2016]; human colon carcinoma (CaCo2) cells  
9 [Sahu et al. 2014a, 2014b, 2014c, 2016a, 2016b]; prostate cancer (VcAP), pancreas  
10 cancer (BxPC-3), and lung cancer (H1299) [He et al. 2016]; hamster kidney (BHK21)  
11 and human colon adenocarcinoma (HT29) cell lines [Gopinath et al. 2010]; human  
12 mesenchymal stem cells (hMSCs) [Greulich et al. 2009, 2011; Hackenberg et al. 2011];  
13 rat aortic endothelial cells [Shannahan et al. 2015]; human umbilical vein endothelial  
14 cells [Braakhuis et al. 2016; Guo et al. 2016]; peripheral blood and mononuclear cells  
15 [Paino et al. 2015; Sarkar et al. 2015]; and human adipose-derived stem cells (hASCs)  
16 [Samberg et al. 2012].

17 Examples of the general approach to in vitro experimentation with AgNPs may be found  
18 in studies conducted at Wright-Patterson Air Force Base in which rat alveolar  
19 macrophages were incubated with different sizes of AgNPs [Hussain et al. 2005b;  
20 Carlson et al. 2008]. The cells, at 80% confluence, were incubated for 24 hours with  
21 various concentrations of hydrocarbon-coated AgNPs in a physiologic medium. The  
22 particles were 15, 30, 55, or 100 nm in diameter. Parameters under investigation  
23 included cellular morphology and uptake of AgNPs, mitochondrial function, membrane  
24 integrity, generation of ROS, glutathione content, mitochondrial membrane potential,  
25 and the inflammatory response. Study results indicated that AgNPs with the smallest  
26 diameter were more effective than larger nanoparticles at bringing about physiologic  
27 and toxicological changes. For example, at silver concentrations up to 75 µg/mL, 15-nm  
28 AgNPs appeared to be more effective at releasing LDH from the cells, as a measure of  
29 lowered cell viability. Similarly, when the fluorescence intensity of dichlorofluorescein  
30 (DCF) in the presence of AgNPs was assessed for the various incubation products, 15-

1 nm silver nanoparticles appeared to induce a greater intensity of fluorescence, a  
2 response indicative of enhanced generation of ROS. Concomitant with the enhanced  
3 generation of ROS was a significant depletion of cellular reduced glutathione (GSH)  
4 levels, lowered mitochondrial function as indicated in the 3-(4,5-dimethylthiazol-2-yl)-  
5 2,5-diphenyltetrazolium bromide (MTT) viability assay, and the loss of mitochondrial  
6 membrane potential. Carlson et al. [2008] also demonstrated a treatment-related  
7 increase in TNF- $\alpha$ , macrophage inflammatory protein-2, and IL-1 $\beta$  but not IL-6 in the  
8 supernatant of macrophage/AgNP incubations. The authors suggested that the  
9 significant depletion of GSH levels may have created an imbalance between  
10 antioxidants and ROS, thereby resulting in oxidative stress and cellular damage.  
11 However, the degree to which this effect was related to the release of  
12 cytokines/chemokines remained unclear, since these responses did not appear to be  
13 influenced by particle size.

14 Arai et al. [2015] investigated differences between ionic silver and AgNP in murine  
15 macrophages (J774.1). Exposures to 20-, 60-, or 100-nm, or equal concentration of  
16 AgNO<sub>3</sub>, were conducted in medium with 1% albumin for 24 hours. It was observed that  
17 unfunctionalized AgNP grew 2.1 to 3.4 times larger in the presence of 1% albumin,  
18 while citrate-capped AgNPs retained their nominal size in solution. The cytotoxicity  
19 EC<sub>50</sub> values were 34.8, 27.9, 51.8, and 4.51  $\mu$ g Ag/mL, indicating that the 100-nm  
20 AgNP were less toxic than the 20- or 60-nm AgNP but that ions were more toxic than all  
21 the AgNPs. Inhibition of glutathione synthesis had no effect on AgNO<sub>3</sub> cytotoxicity,  
22 which may indicate dissolved ions are cytotoxic by a different, non-ROS-dependent  
23 pathway. Additionally, HPLC-ICP-MS was used to determine preferential silver binding.  
24 Ionic silver was eluted with the metallothioneins, while silver was detected in the AgNP  
25 sample with high-molecular-weight proteins. The authors identified AgNP in the  
26 lysozyme by microscopy and indicated an expectation that they would be present in  
27 other organelles but not free-floating in the cytoplasm. Finally, a parallel *in vivo*  
28 experiment demonstrated the dispersal of inhaled AgNP throughout ICR mice to  
29 secondary organs.

1 Sarkar et al. [2015] studied how differing AgNP size and surface modification might  
2 yield different effects on human monocyte–derived macrophage function. Four AgNP  
3 types were studied: each combination of 20- or 110-nm particles with citrate- or PVP-  
4 stabilization. Exposures were 5-, 10-, 20-, or 50- $\mu\text{g}/\text{mL}$ , for 3, 6, or 24 hours. Reduced  
5 viability was noted only for 24-hour exposures as measured by LDH leakage. Testing  
6 after 4-hour exposure showed an increase in mRNA coding for IL-1 $\beta$  only at 25- $\mu\text{g}/\text{mL}$ ,  
7 while a dose-dependent increase in IL-8 mRNA and a decrease in IL-10 were also  
8 noted, indicating an inflammatory response. Infection with *Mycobacterium tuberculosis*  
9 (M.tb) indicated AgNP exposure also suppressed the typical M.tb-induced expression of  
10 several NF- $\kappa\text{B}$ , which may inhibit immune responses. No significant differences were  
11 noted based on size or surface function, and comparison to both the stabilizers alone  
12 and carbon black NP indicated that AgNP was resulting in the toxicity.

13 Given the importance of the liver as an important target organ of toxicity associated with  
14 AgNPs, a number of research groups have used cultures of hepatocytes to investigate  
15 the possible toxic effects of AgNPs in vitro. For example, the Wright-Patterson Air Force  
16 Base group, using BRL 3A rat liver cells, studied a range of endpoints [Hussain et al.  
17 2005a] similar to those previously evaluated with use of rat alveolar macrophages  
18 [Hussain et al. 2005b; Carlson et al. 2008]. The two species of AgNPs employed were  
19 defined by diameters of either 15 or 100 nm, although little additional information was  
20 provided about the method of formation or their potential for aggregation. Using dose  
21 concentrations of 5 to 50  $\mu\text{g}/\text{mL}$  and incubation times of up to 24 hours, the authors  
22 measured cytotoxicity by leakage of LDH and deficits in mitochondrial function in the  
23 presence of MTT. Other parameters under investigation included changes in cellular  
24 morphology, formation of ROS, depletion of GSH levels, and changes to mitochondrial  
25 membrane potential. Both sets of AgNPs appeared to be effective at inducing a  
26 concentration-dependent depletion of mitochondrial function and the release of LDH to  
27 the culture medium. Under the microscope, the cells displayed a range of distortions in  
28 comparison with untreated cells, and by analogy to the same group's results with rat  
29 alveolar macrophages, they showed a concentration-dependent increase in ROS and

1 depletion of GSH. Hussain et al. [2005a] concluded that the cytotoxicity of AgNPs was  
2 likely to be mediated through oxidative stress.

3 Many of these same manifestations of oxidative stress and cell viability were evident  
4 when cultured HepG2 human hepatoma cells were incubated with commercially  
5 obtained 10-nm AgNPs dispersed in an aqueous medium [Kim et al. 2009c]. The  
6 researchers ensured that any deficits in these parameters could be unequivocally  
7 assigned to the effect of the AgNPs by using an ion exchange resin to remove any free  
8 silver ions that might have been associated with the nanoparticle preparations. Then, in  
9 parallel incubations, they compared the capacity of equivalent amounts of silver in  
10 AgNPs and solutions of silver nitrate to reduce cell viability and/or induce oxidative  
11 stress and DNA damage. Cytotoxicity was measured with MTT and AB reduction  
12 assays and by LDH leakage, and data were expressed as median inhibitory  
13 concentration (IC<sub>50</sub>) values. For each parameter under investigation, increasing  
14 concentrations of silver brought about a reduction in cell viability in a dose-dependent  
15 manner. However, for both dye-reduction assays, free silver ions reduced cell viability to  
16 a greater extent than did the silver nanoparticles. By contrast, release of LDH activity  
17 was brought about more completely and at a lower silver concentration by incubation  
18 with AgNPs as compared with free silver ions (with IC<sub>50</sub> of 0.53 ± 0.19 versus 0.78 ±  
19 0.10 µg/mL). This difference was not statistically significant. Pre-incubation of the cells  
20 with N-acetyl cysteine (NAC) abolished these manifestations of reduced cell viability by  
21 a presumed reduction in the oxidative stress that had become apparent whether the  
22 cells were incubated with either AgNPs or a silver solution. Moreover, further evidence  
23 of the importance of oxidative stress in relation to AgNP toxicity was obtained by  
24 including the antioxidant N-acetylcysteine in the incubation medium 2 hours prior to the  
25 addition of the AgNP or silver nitrate preparations. Deficits in mitochondrial function and  
26 cellular membrane integrity and the occurrence of oxidative stress were largely  
27 abolished by this pretreatment.

28 Kim et al. [2009c] used intracellular fluorescence as an indicator of the formation of  
29 ROS in the presence of either AgNP or silver anion preparations. In each case, ROS

1 formation was abolished by pretreatment with NAC. In an effort to understand the  
2 mechanism(s) whereby AgNPs caused intracellular oxidative stress, the authors used  
3 RT-PCR to study the expression of oxidative stress–related genes such as glutathione  
4 peroxidase 1 (GPx1), catalase, and superoxide dismutase 1 (SOD1). In contrast to the  
5 effect of aqueous silver nitrate, AgNPs did not induce messenger ribonucleic acid  
6 (mRNA) expression of GPx1. However, the mRNA levels of catalase and SOD1 were  
7 increased in response to 24-hour incubation with AgNPs. Detection of phosphorylation  
8 on the H2AX gene, indicative of DNA double-strand breaks, was also thought to be  
9 associated with oxidative stress, because this effect was abolished as well after pre-  
10 incubation with N-acetylcysteine. Kim et al. [2009c] concluded that silver in free solution  
11 or on nanoparticles induced cytotoxicity as a result of oxidative stress. However,  
12 because the expression of oxidative stress–related mRNA species appeared to be  
13 regulated differently by AgNPs than by silver cations, the precise mechanism of AgNP  
14 activity may be different from that of soluble silver.

15 HepG2 cells were also used as a platform for the study of AgNP toxicity by Liu et al.  
16 [2010]. The researchers used PVP-coated nanoparticles with defined sizes of 5, 20, and  
17 50 nm. All AgNP preparations were formed chemically by the reduction of silver nitrate  
18 by sodium hypophosphite in the presence of sodium hexametaphosphate and PVP,  
19 adjusted to a concentration of 1 g/L in deionized water, and dispersed by  
20 ultrasonication. In evaluating HepG2 responses to AgNPs, Liu et al. [2010a] observed  
21 changes to cell morphology, viability, membrane integrity, and induction of oxidative  
22 stress by experimental procedures that were closely similar to those previously  
23 described. Ultrastructural analysis using TEM revealed the presence of AgNPs inside  
24 the cells, with the smaller particles apparently more effective at penetrating the  
25 membrane and inducing the toxic effects. Liu et al. [2010a] attempted to distinguish  
26 between apoptotic and necrotic cell death as a result of AgNP treatment with the double  
27 staining technique, using annexin V-fluorescein isothiocyanate (FITC) for apoptosis and  
28 propidium iodide (PI) for necrosis. When HepG2 cells were incubated at 0.5 µg/mL for  
29 24 hours, the relative amounts of apoptotic cells were 4.64%, 8.28%, 6.53%, and 4.58%  
30 for silver nitrate and AgNPs (5 nm, 20 nm, and 50 nm), respectively, all compared to an

1 incidence in controls of 2.39%. The authors concluded that despite the increased  
2 fraction of apoptotic cells in the silver-exposed groups, there was no difference between  
3 the treated and control groups for necrosis. Therefore, the AgNP-induced cell death was  
4 caused mainly by apoptosis.

5 HepG2 cells, along with Caco2 human colon carcinoma cells, were the subject of  
6 several studies by Sahu et al. [2014a, 2014b, 2014c, 2016a, 2016b]. The initial studies  
7 used 20-nm AgNPs as well as AgNO<sub>3</sub> as a comparative source of Ag ions [Sahu et al.  
8 2014a, 2014b, 2014c], while the later studies included analogous exposures of the  
9 same cells to 50-nm AgNP under similar conditions [Sahu et al. 2016a, 2016b]. Cells  
10 were exposed at concentrations of up to 20.0 µg/mL. Generally, it was also found that  
11 HepG2 cells were affected at lower doses than Caco2 cells. Stronger genotoxic  
12 responses and pro-apoptotic markers were observed in AgNPs than Ag ions from 0.1 to  
13 1.0 µg/mL, but this trend reversed in the range of 10–20 µg/mL. Specifically, responses  
14 such as micronuclei formation were noted only in cases of AgNP exposure but not in  
15 cases of Ag ion exposure. Interestingly, the authors observed evidence of mitochondrial  
16 damage but did not directly detect a difference in oxidative stress.

17 Ávalos Fúnez et al. [2013] studied HepG2 cells and HL-60 tumoral human leukemia  
18 cells. After exposing cells to citrate-stabilized AgNP with a range of 30–123 nm for up to  
19 72 hours, both had significantly reduced viability (measured by MTT assay) and LDH  
20 release at concentrations as low as 0.84 µg/mL. However, this could be mitigated by the  
21 addition of the antioxidant N-acetyl-L-cystine to the medium, indicating toxicity through  
22 AgNP-induced oxidative stress.

23 Paino et al. [2015] studied the effects of polyvinyl-alcohol (PVA)-coated AgNP exposure  
24 on HepG2 cells and normal human peripheral blood mononuclear cells (PBMCs). Cells  
25 were exposed for 24 hours to PVA-AgNP (4.0-11.7 nm diameter) at concentrations of  
26 1.0 and 50.0 µM, resulting in decreased viability. Specifically, an increase in early  
27 apoptotic cells was noted for both concentrations and cell lines, as well as DNA damage  
28 (by Comet Assay). Likewise, an increase in necrotic cell population was present except

1 for the 1.0  $\mu\text{M}$  exposure in HepG2 cells. Isolated neutrophils also showed significantly  
2 increased oxidative stress following PCA-AgNP exposure (by DCFDA assay).

3 Kermanizadeh et al. [2012, 2013] also observed indicators of oxidative stress in two  
4 studies on the human hepatoblastoma cell line C3A after exposure AgNP. In these  
5 studies, AgNP (specifically 17-nm diameter NM-300) was found to result in upregulation  
6 of IL-8 and increased oxidative stress (assayed by glutathione and reduced GSH levels)  
7 after 24 hours of exposure. However, pretreatment with the antioxidant 6-hydroxy-  
8 2,5,6,7,8-tetramethylchroman-2-carboxylic acid mitigated these effects. Additionally,  
9 after 8 weeks of exposure, there was significant DNA damage (assayed by Comet). The  
10 response to AgNP occurred at higher concentrations relative to zinc oxide NP, titanium  
11 oxide NP, and multi-walled carbon nanotubes. [Kermanizadeh et al. 2012] A later study  
12 indicated that the LC50 of NM300 AgNPs was approximately 24 hr at 2  $\mu\text{g}/\text{mL}$ , but  
13 could not detect a significant change in IL-6, TNF- $\alpha$ , or C-reactive protein levels, nor did  
14 they affect albumin or urea concentrations. [Kermanizadeh et al. 2013]

15 Gaiser et al. [2013] conducted a study both *in vitro* and *in vivo* on AgNP toxicity to the  
16 liver. The *in vitro* portion of the study used the C3A cell line and NM300 AgNP.  
17 Following a 24-hour exposure to 0-625  $\mu\text{g}/\text{cm}^2$  AgNP, medium was removed for LDH  
18 analysis and cells were stained with Alamar Blue. Quantitation of LDH yielded an LC<sub>50</sub>  
19 of 2.5  $\mu\text{g}/\text{cm}^2$ . NP uptake by C3A cells into membrane-bound vesicles was observed  
20 with confocal microscopy. Reduced GSH was also examined following exposure to 1, 2,  
21 and 4  $\mu\text{g}/\text{cm}^2$  AgNP at 2, 6, and 24-hour timepoints, with no significant changes.  
22 Examination of IL-1 $\beta$ , IL-8, IL-10, TNF- $\alpha$ , MCP-1, and IL-1RI mRNA levels by RT-PCR  
23 was conducted following 0.1, 0.5, and 1  $\mu\text{g}/\text{cm}^2$  AgNP exposures at 4 and 24 hr  
24 timepoints; IL-8 increased relative to control except for the 24 hr timepoint of the 0.5  
25  $\mu\text{g}/\text{cm}^2$  AgNP exposure, TNF- $\alpha$  increased after exposure to 0.1  $\mu\text{g}/\text{cm}^2$  AgNP but  
26 decreased for 1  $\mu\text{g}/\text{cm}^2$  after 4 h, while IL-1RI only changed at 0.1  $\mu\text{g}/\text{cm}^2$  at the 24 hr  
27 timepoint. FACS analysis of medium of C3A cells after exposure to 1, 2, and 4  $\mu\text{g}/\text{cm}^2$   
28 AgNP indicated ICAM-1 and IL-8 release at 4 h following 40  $\mu\text{g}/\text{cm}^2$  exposure and at 24  
29 24 hr following 5  $\mu\text{g}/\text{cm}^2$  exposure.

1 Sun et al. [2013] investigated the effects of PVP-coated AgNPs of 10 or 30-50 nm  
2 diameter on primary rat hepatic stellate cells (HSCs). FITC-Annexin V and PI staining  
3 was used to identify apoptotic cells, and a dose-dependent increase in apoptotic rates  
4 was observed starting at 20 µg/mL, with 10 nm particles causing a higher apoptotic  
5 fraction than 30-50 nm particles. Cytokine analysis by ELISA indicated no significant  
6 differences in HGF, IL-6, TGF-β1, or TNF-α levels, however both MMP-2 and -9 were  
7 reduced after 48 hr exposure to 0.2 µg/mL AgNP (of either size).

8 Shannahan et al. [2015] studied the effect of protein corona on AgNP toxicity in rat liver  
9 epithelial (RLE) and rat aortic endothelial (RAEC) cells. Citrate-stabilized 20-nm AgNP  
10 were incubated with either human serum albumin (HAS), bovine serum albumin (BSA),  
11 or high-density lipoprotein (HDL) at 10°C for 8 hr. Their hydrodynamic sizes were  
12 69.99-, 30.60-, and 62.10-nm, respectively. HAS and BSA were found to reduce  
13 dissolution rate, while HDL increased it. Several changes in protein structure were  
14 observed. In both RLE and RAEC, a protein corona reduced uptake, though no strong  
15 correlation with hydrodynamic size could be established. Hyperspectral analysis  
16 indicated that 2 h after exposing RLE or RAEC to AgNP, those AgNP underwent a blue  
17 shift, indicating a loss of the protein corona. However, cytotoxicity of AgNP was reduced  
18 by the protein corona after a 3 or 6 hr exposure of 50 µg/mL, and adding a scavenger  
19 receptor B inhibitor (SR-BI) further reduced cytotoxicity. In RLE, AgNP-HDL was found  
20 to increase IL-6 expression, and SR-BI could prevent this. This was also true for all  
21 AgNP in RAEC.

22 Connolly et al. [2015] investigated the cytotoxicity of NM-300K AgNP in several rainbow  
23 trout cell types: RTH-149 and RTL-W1 liver cells, RTG-2 gonadal cells, and primary  
24 hepatocytes. AgNP concentrations from 0.73 to 93.5 µg/mL were tested, as well as Ag  
25 ion concentrations of 0.0345 to 345 µg/mL (AgNO<sub>3</sub>). Both relative cell sensitivities and  
26 absolute IC<sub>50</sub> values varied depending on whether Alamar Blue, CFDA-AM, or neutral  
27 red uptake assays were used. In general, each assay-cell type pair showed IC<sub>50</sub> for  
28 AgNP over tenfold greater than AgNO<sub>3</sub>, with AgNP IC<sub>50</sub> values ranging from 10.9 to

*This information is distributed solely for the purpose of pre-dissemination peer review under applicable information quality guidelines. It has not been formally disseminated by the National Institute for Occupational Safety and Health. It does not represent and should not be construed to represent any agency determination or policy.*

1 32.2 µg/mL in RTL-W1, 19.4-24.9 µg/mL in RTH-149, 37.2-43.1 µg/mL in RTG-1, and  
2 30.6-45.2 µg/mL in primary hepatocytes.

3 Piao et al. [2011] incubated human Chang liver cells with AgNPs prepared by the THF  
4 approach to demonstrate oxidative stress and to probe the biochemical and physiologic  
5 mechanisms that might be associated with this phenomenon. The authors reported that  
6 the nanoparticles had undergone a degree of aggregation in the incubation medium,  
7 with a size distribution of 28 to 35 nm in diameter, an increase from the original 5 to 10  
8 nm. Cellular morphology, viability, mitochondrial efficiency, intracellular formation of  
9 ROS, and GSH levels were measured by means of “standard techniques,” with and  
10 without N-acetylcysteine. A comparison of equivalent amounts of silver on nanoparticles  
11 or in solution in the MTT assay gave IC<sub>50</sub> that differed by a factor of two. This suggested  
12 that silver in nanoparticle form was more damaging to the cells than silver in free  
13 solution (IC<sub>50</sub> of 4 µg/mL for AgNPs, versus 8 µg/mL for silver nitrate). In mechanistic  
14 analysis, the spectrum of intracellular proteins was surveyed by Western blot analysis,  
15 and a comet assay was performed to determine the degree of oxidative DNA damage.  
16 Flow cytometry was used to determine the percentage of apoptotic sub-G1 hypodiploid  
17 cells, and the amount of cellular DNA fragmentation was assessed by cytoplasmic  
18 histone-associated DNA fragmentation. The expected picture of oxidative-stress-related  
19 cytotoxicity and partial blockade with N-acetylcysteine was obtained. The comet assay  
20 showed that incubating human Chang liver cells with silver nanoparticles increased the  
21 tail length and the percentage of DNA in the tails, as compared to control cells. Other  
22 markers of oxidative stress, such as the levels of lipid peroxidation and the degree of  
23 protein carbonyl formation, were increased in AgNP-treated cells compared to control  
24 cells. The authors of the study compiled an array of mechanistic data that pointed to  
25 AgNP-induced induction of apoptosis via a mitochondrial and caspase-dependent  
26 pathway. For example, after treatment with AgNPs, the AgNP-associated decrease in  
27 Bcl-2 expression and concomitant increase in Bax expression resulted in the following  
28 increases in Bax/Bcl-2 ratio with time: 1.0, 7.0, 9.5, 12.8, and 24.5 at 0, 6, 12, 24, and  
29 48 hours, respectively. A change in ratio at this level led to the release of cytochrome  
30 from the mitochondrion and the occurrence of active forms of caspases 9 and 3. The

1 authors interpreted their data as indicating that AgNP-induced apoptosis might be  
2 mediated through a caspase-dependent pathway with mitochondrial involvement.

3 The importance of c-Jun NH<sub>2</sub>-terminal kinase (JNK) in mediating the apoptotic effects in  
4 human Chang liver cells was demonstrated by its time-dependent phosphorylation in  
5 the presence of AgNPs. In parallel with the retention of cell viability, the effect was  
6 attenuated by pretreatment with the JNK-specific inhibitor SP600125 or by transfection  
7 with small, interfering RNA against JNK [Piao et al. 2011].

8 Many of the same responses that indicated induction of oxidative stress and apoptosis  
9 in macrophages and liver cells have also been observed in fibroblasts when incubated  
10 with AgNPs. For example, Arora et al. [2008] used a commercial preparation of AgNPs  
11 (7–20 nm in diameter) in an aqueous suspension to challenge HT-1080 human  
12 fibrosarcoma cells and A431 human skin carcinoma cells. Using a variant of the MTT  
13 assay for mitochondrial function with the compound sodium 3'-[1-  
14 (phenylaminocarbonyl)-3, 4-tetrazolium]-bis (4-methoxy-6-nitro) benzene sulfonic acid  
15 hydrate, a dose-dependent effect on cell viability was obtained in the concentration  
16 range of 6.25 to 50 µg/mL. Subsequent incubation of the cultures at one half the median  
17 inhibitory concentration (IC<sub>50</sub>) of approximately 11 µg/mL gave an array of responses  
18 indicative of oxidative stress, including a reduction in GSH content and SOD activity and  
19 an increase in lipid peroxidation. An increase in treatment-related DNA fragmentation  
20 and a biphasic response in caspase-3 activation (in which the enzyme was induced up  
21 to a AgNP concentration of 6.25 µg/mL but suppressed at higher concentrations)  
22 indicated that cell death occurred by apoptosis at AgNP concentrations up to 6.25  
23 µg/mL but by necrosis at higher concentrations. However, AgNP-induced oxidative  
24 stress and apoptosis were less evident when the same researchers carried out  
25 equivalent studies in primary mouse fibroblasts and liver cells [Arora et al. 2009].  
26 Respective IC<sub>50</sub> values were 61 and 449 µg/mL and little change was seen in  
27 intracellular GSH and lipid peroxidation at one half the IC<sub>50</sub>. The AgNPs in these studies  
28 were synthesized by an unspecified proprietary process. They were reported to be  
29 stable in culture media, with >90% of the particles with diameters between 7 and 20 nm.

1 Possible agglomeration of the particles in the culture media was not mentioned. The  
2 results suggest that the primary cell preparations contained sufficient antioxidant  
3 capacity to protect the cells from possible oxidative damage.

4 Similar to the results reported by Piao et al. [2011] from studies with human Chang liver  
5 cells, the study by Hsin et al. [2008] used NIH3T3 fibroblasts to investigate the link  
6 between the mitochondrial-related generation of ROS, the incidence of apoptosis, and  
7 the activation of JNK. Incubating mouse L929 fibroblasts with nanoparticles also  
8 resulted in an increased incidence of apoptosis and a greater percentage of cells  
9 arrested in the G2M phase of the cell cycle [Wei et al. 2010]. Larger-scale silver entities  
10 (silver microparticles with a range of shapes and diameters between 2 and 20  $\mu\text{m}$ ) did  
11 not bring about these changes and were not internalized by the cells to the same extent  
12 as AgNPs. Transmission electron micrographs appeared to provide direct evidence that  
13 AgNPs but not microparticles entered the cells via an endocytic pathway. The authors  
14 concluded that AgNPs were more cytotoxic to L929 cells than silver microparticles.  
15 Differences were characterized by the ability of nanoparticles to enter the cells, causing  
16 morphologic abnormalities and apoptosis, and the cell cycle being arrested in the G2M  
17 phase.

18 Avalos et al. [2015] investigated the effects of AgNP (4.7 and 42 nm) and gold NPs (30,  
19 50, 90 nm) on human pulmonary fibroblasts (HPF). Cytotoxicity was assayed 24, 48,  
20 and 72 hr after exposure to NP by both MTT and LDH assays. MTT assays detected  
21 viability loss at 0.84  $\mu\text{g}/\text{mL}$  at 24 and 72 hr timepoints for 4.7 nm AgNP, and at 1.68  
22  $\mu\text{g}/\text{mL}$  for 48 hr timepoint; LDH assays detected differences at all timepoints at 3.36  
23  $\mu\text{g}/\text{mL}$  or less. For the 42 nm particles, LDH assay detected differences at all timepoints  
24 at 13.45  $\mu\text{g}/\text{mL}$  or less, while MTT assay detected differences by 100  $\mu\text{g}/\text{mL}$ . Addition of  
25 NAC reduced the cytotoxic effect, suggesting an oxidative stress mechanism. ROS  
26 assay by DCF fluorescence demonstrated a 1.32-fold increase after exposure to 7.66  
27  $\mu\text{g}/\text{mL}$  4.7 nm AgNP, and a 1.55-fold increase after exposure to 1150  $\mu\text{g}/\text{mL}$  42 nm  
28 AgNP. AgNP exposure also depleted total glutathione content, though no significant  
29 change in superoxide dismutase (SOD) activity was detected by ELISA.

1 Foldbjerg et al. [2009] used a human acute monocytic leukemia cell line (THP-1 cells)  
2 as a platform for studying the relative capacity of AgNPs and ionic silver to induce ROS,  
3 apoptosis, and necrosis. As obtained from the supplier, the particles were 30 to 50 nm  
4 in diameter and coated with 0.2% PVP. When the AgNPs were prepared in a stock  
5 solution, a major peak size of 118 nm was obtained. This preparation, as well as an  
6 equimolar solution of silver cations, was used to incubate THP-1 at a dose range of 0 to  
7 7.5  $\mu\text{g}/\text{mL}$  (calculated as silver mass), with an incubation time of up to 24 hours. The  
8 fluorescent marker, DCF, was used to measure the intracellular generation of ROS, and  
9 the annexin V/PI double staining technique was used to discriminate between cells  
10 undergoing apoptosis or necrosis. The presence of apoptosis was confirmed with the  
11 terminal deoxynucleotidyl transferase dUTP nick end labeling (TUNEL) assay. As  
12 indicated by the results of the annexin V/PI assay, both AgNPs and silver cations  
13 brought about a significant reduction in the percentage of viable cells after 24 hours'  
14 exposure. The median effective concentrations ( $\text{EC}_{50}$ ) were 2.4 and 0.6  $\mu\text{g}/\text{mL}$ ,  
15 respectively, indicating that silver cations were approximately four times more toxic than  
16 AgNPs. Silver nanoparticles and silver cations likewise increased the production of  
17 ROS, as indicated by the differential formation of DCF. A 35% increase in cells positive  
18 for DNA breakage was observed when compared to controls when THP-1 cells were  
19 incubated with AgNPs for 6 hours at a concentration of 5  $\mu\text{g}/\text{mL}$ . In general, the findings  
20 of this study point to a strong correlation between the increase in intracellular ROS,  
21 DNA damage, and high levels of apoptosis and necrosis for both AgNPs and ionic  
22 silver. In a follow-up study, Beer et al. [2012] evaluated the degree to which the silver  
23 ion fraction of AgNP suspensions contribute to the toxicity of AgNPs, using A549 human  
24 lung carcinoma epithelial-like cell line. PVP-coated (0.2%) spherical AgNPs, with  
25 dimensions ranging in size from 30 to 50 nm, were exposed to  
26 suspensions/supernatants containing either 39% (0.2  $\mu\text{g}/\text{mL}$ ) or 69% (1.6  $\mu\text{g}/\text{mL}$ ) silver  
27 ions for 24 hours. At 1.6  $\mu\text{g}/\text{mL}$  total silver, A549 cells exposed to an AgNP suspension  
28 containing a 39% silver ion fraction showed a cell viability of 92%, whereas cells  
29 exposed to an AgNP suspension containing a 69% silver ion fraction had a cell viability  
30 of 54%, as measured by the MTT assay. At initial silver ion fractions of 5.5% and above,  
31 AgNP-free supernatant had the same toxicity as AgNP suspensions. Flow-cytometric

1 analyses of cell cycle and apoptosis confirmed that there was no significant difference  
2 between the treatments with AgNP suspension and AgNP supernatant, as measured by  
3 MTT assays. A clear association was observed between the amount of silver ions  
4 present in the solution and the toxicity of the AgNP suspensions. As found in the study  
5 of Foldbjerg et al. [2011], ionic and/or nanoparticulate silver induces ROS in A549 cells.

6 Braakhuis et al. [2016] used a co-culture model of human bronchial epithelial (16HBE),  
7 umbilical vein endothelial (HUVEC), and acute monocytic leukemia (THP-1) cells to  
8 assess the toxicity of AgNP. First, 16HBE cells were seeded and allowed to grow to  
9 confluence before adding differentiated THP-1 cells. Then, on the basal side of a  
10 transwell insert membrane with 0.4- $\mu$ m pores, HUVEC cells were seeded. AgNP  
11 solutions of 10, 20, 50, and 100 nm diameters in 2 nM citrate were used as stock for  
12 preparing exposure medium. Cell activity of 16HBE cells, as assayed by WST-1 cell  
13 proliferating agent absorbance, decreased after 24 hr of exposure to 30  $\mu$ g/mL AgNP,  
14 regardless of size. Electron spin resonance assay of ROS in buffer showed that 10 and  
15 20 nm AgNP were associated with additional H<sub>2</sub>O<sub>2</sub>-induced hydroxyl radical formation,  
16 but 50 and 100 nm AgNP were not. Intracellular ROS, as measured by DCFDA assay,  
17 doubled on exposure to AgNP, but did not show a significant dose-response  
18 relationship. AgNP exposure did create a dose-dependent decrease of MCP-1 and  
19 increase in IL-8 release, as measured by ELISA. The authors noted that dose-response  
20 correlations could be stronger for either AgNP mass or surface area, depending on the  
21 endpoint selected.

22 Liu et al. [2010a] examined the impact of different sizes of AgNPs on oxidative stress  
23 and incidence of apoptosis in HepG2 cells, also using cultures of SGC-7901 human  
24 stomach cancer cells, MCF-7 human breast adenocarcinoma cells, and A549 human  
25 lung adenocarcinoma cells to ensure the universality of the toxic effect. This study was  
26 followed-up by Lee et al. [2011a] to investigate the cytotoxic potential of AgNPs and the  
27 pathways by which they impact A549 cells. In addition to findings that AgNPs induce the  
28 reduction in cell viability, increase LDH release, alter cell cycle distribution, and change

1 the expression of Bax and Bcl-2 reflective of increased apoptosis, AgNPs were also  
2 found to alter mRNA levels of protein kinase C (PKC) isotypes.

3 Chairuangkitti et al. [2013] examined both ROS-dependent and ROS-independent  
4 pathways of AgNP toxicity in A549 cells. The AgNP were approximately 40-90 nm in  
5 diameter. Cytotoxicity was assayed by MTT assay at 24 and 48 hr post-exposure  
6 timepoints following exposure to 0, 25, 50, 100, or 200 µg/mL AgNP; a 35% and 50%  
7 loss of viability after 24 and 48 hr were respectively noted at 200 µg/mL. Cytotoxicity  
8 was assayed by DCFDA assay at 3 hr post-exposure following exposure to 0, 25, 50,  
9 100, or 200 µg/mL AgNP; at 200 µg/mL a 2-fold increase in ROS levels were noted.  
10 Mitochondrial membrane potential assayed by TMRE assay at 24, 48, and 72 hr post-  
11 exposure timepoints following exposure to 0, 100, or 200 µg/mL AgNP; the portion of  
12 TRME-positive cells decreased in a dose-dependent manner with AgNP exposure.

13 Pretreatment with 10 mM NAC could partially protect against the effects of AgNP  
14 exposure to viability and ROS levels, though the protective effect was greatest at time  
15 points of 24 hr or less. Cell cycle analysis by FACS with PI staining followed 24, 48, and  
16 72 hr post-exposure timepoints following exposure to 0, 100, or 200 µg/mL AgNP; both  
17 sub-G1 (including apoptotic) and in S phase cell populations increased while G1  
18 populations decreased. Pretreatment of NAC reduced the sub-G1 population, but did  
19 not affect the G1 or S populations, indicating cell cycle arrest not associated with ROS  
20 production. Western blot analysis of PCNA after 72 hr post-exposure to 0, 100, or 200  
21 µg/mL AgNP indicated that PCNA is downregulated by AgNP exposure, but is also no  
22 protected by NAC pretreatment. The combined results indicate both ROS- and non-  
23 ROS-mediated toxic pathways for AgNP exposure.

24 Han et al. [2014] investigated the oxidative stress response of A549 cells to two forms  
25 of 15 nm diameter AgNP: one synthesized by addition of AgNO<sub>3</sub> to an E. coli  
26 supernatant (bio-AgNP) and another by citrate-mediated synthesis (chem-AgNP).  
27 Comparing TEM and DLS showed that chem-AgNPs agglomerate more than bio-  
28 AgNPs. Viability was measured by MTT assay after 24 hr of AgNP exposure; the IC50

1 was indicated as about 25 µg/mL for bio-AgNP and about 70 µg/mL for chem-AgNP.  
2 This disparity was also present in membrane integrity measurements: LDH assays after  
3 24 hr of AgNP exposure showed greater leakage for chem-AgNP than bio-AgNP,  
4 especially over concentrations of 20 µg/mL. ROS measured by DCFDA assay was  
5 shown to both be concentration-dependent and increase over post-AgNP exposure  
6 incubation times (6, 12, 24 hr). Mitochondrial transmembrane potential by JC-1 assay  
7 indicated both AgNP, but particularly bio-AgNP, resulted in depolarization of the  
8 mitochondrial membrane (this is often linked to apoptotic pathways). Cellular uptake by  
9 TEM analysis also noted AgNP uptake into autophagosomes and autolysosomes which  
10 differed in structure from those of unexposed cells, leading the authors to speculate that  
11 AgNP exposure triggered autophagosome formation.

12 Soto et al. [2007] also used the results from a series of assays with A549 cells to  
13 compare the cytotoxicity potential of a wide range of nanoparticle material, including  
14 AgNPs, titanium dioxide (TiO<sub>2</sub>), multiwall carbon nanotubes, chrysotile asbestos, Al<sub>2</sub>O<sub>3</sub>,  
15 Fe<sub>2</sub>O<sub>3</sub>, and ZrO<sub>2</sub>, using both a murine lung macrophage cell line (RAW 264.7) and a  
16 human lung macrophage cell line (THB-1). Relative cell viabilities were measured at a  
17 constant nanoparticulate material concentration of 5 µg/mL for the different cell lines. All  
18 of the nanoparticulate materials, except for TiO<sub>2</sub>, showed a cytotoxic response, and  
19 AgNPs were particularly cytotoxic to the murine lung macrophage cell line. The  
20 nanoparticulate materials were observed to have a greater toxic effect in A549 cells,  
21 with the TiO<sub>2</sub> samples demonstrating a slight cytotoxic response. The A549 cells were  
22 found to be more sensitive than the murine and human macrophages. No correlation  
23 was found when particle surface area was used as an index for comparing cytotoxicity.  
24 Particle morphology or aggregate morphology was also not correlated with the  
25 cytotoxicity response for either the murine or the human cell line exposure, since a  
26 variety of morphologies within the nano-size range exhibited equivalent or similar  
27 cytotoxicity's.

28 The degree of cell viability after 24-hour incubation with AgNPs was assessed in HeLa  
29 cells with use of Alamar blue reagent as a probe for cell viability [Miura and Shinohara

1 2009]. An IC<sub>50</sub> of 92 µg/mL silver was obtained. The AgNPs were provided by the  
2 supplier with a specified diameter of 5 to 10 nm and were stabilized with a proprietary  
3 protectant. TEM analysis confirmed the particle size but showed the presence of some  
4 aggregates as well. To analyze for apoptosis, cells were incubated for 3 hours with  
5 various concentrations of AgNPs, double stained with Annexin V (FITC-conjugated) and  
6 PI, and then analyzed by flow cytometry. As charted by the authors, AgNPs appeared to  
7 induce apoptosis in a dose-dependent manner up to 120 µg/mL. In an effort to assess  
8 the expression level of genes potentially associated with apoptosis, Miura and  
9 Shinohara [2009] extracted total RNA from HeLa cells that had been incubated with  
10 silver nanoparticles for 4 hours and used RT-PCR to determine the expression of  
11 stress-related genes such as those for heme oxygenase-1, metallothionein-2A, and  
12 heat shock protein 70. Silver nanoparticles were effective in increasing the expression  
13 of heme oxygenase-1 and mettothionein-2A several-fold but not heat shock protein-70.  
14 This discrepancy was different from the pattern of gene expression obtained when cells  
15 were exposed to cadmium sulfate, in which all three stress-related genes were strongly  
16 expressed in response to treatment.

17 Guo et al. [2016] investigated the effects of 10, 75, and 110 nm AgNP or AgNO<sub>3</sub> in vitro  
18 and in vivo. HUVEC cultures which were used to further probe the results of the mouse  
19 injection study. Histopathology showed that treating HUVEC cultures with 1 µg/mL  
20 AgNP was sufficient to erode the dense VE-cadherin at the cell-junction and reduce  
21 cytoskeleton actin fiber length. It was noted that AgNO<sub>3</sub> had a more significant toxicity,  
22 followed by 110 nm AgNP, and finally by 10 and 75 nm AgNP. However, Hoersch/PI  
23 staining indicated that AgNO<sub>3</sub> promoted necrosis while AgNP promoted early apoptosis.  
24 The authors speculate that the cause is that AgNP are uptaken while AgNO<sub>3</sub> instead  
25 damages membranes directly. Additionally, DCFDA assay indicated that AgNP resulted  
26 in increased ROS, while AgNO<sub>3</sub> did not, indicating that silver ions have a different  
27 mechanism of action.

28 Jeanett et al. [2016] compared the effects of exposure to spark-generated 20-nm  
29 carbon black NP (CNP) or AgNP to human bronchial epithelials (HBE). In addition to the

1 BEAS-2B cell line, two additional HBE cultures were developed from organ donors: one  
2 normal, and one with cystic fibrosis (CF). Cell death was assessed by LDH assay after  
3 4 and 24 hr of exposure. In normal HBE and BEAS-2B cells, necrosis at 24 hr was low  
4 for both CNP and AgNP; however necrosis was increased in CF HBE relative to normal  
5 HBE by 12-18% for AgNP and 6-9% for CNP. Similarly, CF HBE caspase-3 activity was  
6 two- to four-fold greater than normal HBE caspase-3 activity in exposures. The authors  
7 conclude there are increased levels of IL-6 and IL-8 in all models after exposure to CNP  
8 or AgNP, and an increase in MCP-1 in BEAS-2B.

9 Gopinath et al. [2010] examined the effects of AgNPs on gene expression in an  
10 endeavor to assess the fundamental mechanisms that contribute to AgNP-induced cell  
11 death through mediated apoptosis. Hamster kidney (BHK21) and human colon  
12 adenocarcinoma (HT29) cells were treated with <20-nm-diameter AgNPs from 30  
13 minutes to 6 hours. In order to assess the mode of cell death induced by AgNPs,  
14 treated cells were stained with FITC Annexin V and PI for flow cytometric analysis. An  
15 increase in early apoptotic population was observed in treated BHK21 cells (9%) and  
16 HT29 cells (11%), compared to control cells. Expression profiles of apoptotic genes  
17 such as, bak, bax, bad, C-myc, and caspase-3 were analyzed, and an upregulation of  
18 p53 gene in the AgNP-treated cells was observed. On the basis of these gene  
19 expression profiles, the investigators proposed that AgNP treatment of both BHK21 and  
20 HT29 cells leads to programmed cell death (that is, apoptosis) as a result of a cascade  
21 reaction that activates caspase-3, which penetrates the nuclear membrane to induce  
22 DNA fragmentation. This extracellular cytotoxic stress on the cell membrane  
23 upregulates p53, which in turn acts on other apoptotic molecules and causes the  
24 mitochondria to induce apoptosis.

25 Schaeublin et al. [2011] evaluated the response to silver nanowires (4 or 20  $\mu\text{m}$  in  
26 length;  $\sim 90$  nm in diameter) in an in vitro co-culture assay with human alveolar lung  
27 cells [Schaeublin et al. 2011] 24 hours after exposure to 200 ng/mL. Neither AgNW  
28 length was toxic to the cells (on the basis of normal cell morphologic appearance) or  
29 decreased the cell viability (on the basis of MTS assay of mitochondrial function).

1 However, both AgNW lengths were associated with an increase in some inflammatory  
2 cytokines (IL-6, IL-8, and interferon gamma). These results showed that the AgNWs  
3 were not cytotoxic at the dose evaluated but did cause irritant and inflammatory  
4 responses.

## 5 **D.2 DNA Damage/Genotoxicity**

6 Ahamed et al. [2008] used mouse embryonic stem (MES) cells and mouse embryonic  
7 fibroblasts (MEF) to study the link between AgNP-induced apoptosis and DNA damage.  
8 Two types of AgNPs were used; uncoated plasma gas-synthesized particles and  
9 polysaccharide-coated particles, both approximately 25 nm in diameter. As visualized  
10 with a Cell Tracker Green fluorescent probe and observed under confocal microscopy,  
11 both types of AgNPs were taken up by the cell, although uncoated particles showed a  
12 greater tendency to aggregate and were excluded from certain organelles such as the  
13 nucleus and mitochondria. Coated particles were distributed throughout the cell. As  
14 determined by Western blot analysis, expression of annexin V protein was enhanced by  
15 both species of nanoparticles, confirming the role of AgNPs in the induction of apoptosis  
16 in these cell lines. This was accompanied by upregulation of the p53 tumor suppressor  
17 gene, increased induction of the Rad51 double strand break repair protein, and  
18 enhanced phosphorylation of the histone H2AX at the serine-139 residue. Because the  
19 latter effect is also thought to occur in response to a DNA double break, the authors  
20 interpreted their data as an indication that both types of AgNPs had induced increased  
21 p53 expression and double strand DNA breakage, with concomitant apoptosis in MES  
22 and MEF cells. Uncoated (and less agglomerated) particles appeared to be more  
23 effective in bringing about these responses.

24 Foldbjerg et al. [2011] detected perturbations in the genetic architecture of the human  
25 lung A549 cancer cell line in response to AgNPs and silver in solution. In the former  
26 case, the 30- to 50-nm particles were coated with 0.2% PVP. As before, the cytotoxicity  
27 of AgNPs and silver in solution was assessed by a decrease in mitochondrial activity  
28 with the MTT assay. Silver ions induced dose-dependent reductions in mitochondrial  
29 function to a greater extent than equivalent concentrations of silver in nanoparticle form.

1 In both cases, these effects were significantly reduced by pretreating the cells with  
2 NAC. However, AgNPs induced greater amounts of ROS, suggesting that these entities  
3 could not be solely due to the potential release of silver ions from the nanoparticles.  
4 AgNP-induced cytotoxicity and ROS formation were accompanied by the formation of  
5 bulky DNA adducts, as demonstrated by <sup>32</sup>P post-labeling. Although the chemical  
6 identity of adducts was not determined, the authors speculated that these endogenously  
7 formed “I-compounds” were similar to those found to accumulate in an age-dependent  
8 manner in the absence of exogenous carcinogens. The strongly correlated responses  
9 were both inhibited by pretreatment with the antioxidant N-acetyl-cysteine, suggesting  
10 the AgNPs had triggered ROS-induced genotoxicity.

11 The effect of particle shape and size of Ag particles on causing toxic and immunotoxic  
12 effects was investigated by Stoehr et al. [2011]. Silver nanowires (length, 1.5–25 μm;  
13 diameter, 100–160 nm), AgNPs (30 nm), and silver microparticles (<45 μm) were tested  
14 with alveolar epithelial cells (A549) for cell viability and cytotoxicity. AgNWs and AgNPs  
15 were synthesized by wet chemistry, while silver microparticles were synthesized by the  
16 reduction of silver salt with sodium citrate. AgNWs, AgNPs, and silver microparticles  
17 were all coated with PVP to make them biocompatible and to keep them dispersed in  
18 water. TEM analysis of sample preparations confirmed that AgNWs and AgNPs were  
19 mostly monodispersed with little agglomeration, while some sedimentation and minor  
20 agglomeration of the silver microparticles was observed. Eight different AgNW  
21 concentrations (range, 5.05–16.47 mg/mL) as well as single concentrations of AgNPs  
22 (0.33 mg/mL) and silver microparticles (13.5 mg/mL) were prepared that overlapped in  
23 mass concentration and surface area. Ion release by the tested silver materials was  
24 determined by means of inductively coupled plasma mass spectrometry (ICP-MS), and  
25 the effects of the released ions on cell viability and LDH generation were measured. To  
26 compare the effects on an activated and a resting immune system, the epithelial cells  
27 were stimulated with rhTNF-α or left untreated. Changes in intracellular free calcium  
28 levels were determined with calcium imaging. No effects were observed with AgNPs  
29 and silver microparticles on A549 cells, whereas AgNWs induced a strong cytotoxicity,  
30 loss in cell viability, and early calcium influx; however, the length of the AgNWs had

1 minimal effect on the observed level of toxicity. The investigators hypothesized that the  
2 increase in toxicity and the absence of specific immunotoxic responses to AgNWs may  
3 be a result of its needle-like structure, making it easier to penetrate the cell membrane.  
4 Also, because of the lengths of the AgNWs, entry into the cell may have been  
5 incomplete, causing cell membrane damage that resulted in impaired repair and  
6 eventually cell death.

7 Greulich et al. [2009] evaluated the biologic activity of AgNPs on human tissue cells by  
8 exposing hMSCs to PVP-coated AgNPs (~100 nm in diameter) and determining their  
9 effect on cell viability, cytokine release, and chemotaxis. AgNPs were prepared by the  
10 polyol process and hMSCs were exposed either to AgNP concentrations of 0.5, 1, 2.5,  
11 3, 3.5, 4, 5, and 50  $\mu\text{g}/\text{mL}$  or to silver ions (silver acetate) for up to 7 days. At AgNP  
12 concentrations of 3.5 to 50  $\mu\text{g}/\text{mL}$ , no viable cells were detected. When silver acetate  
13 was used, the cytotoxic effect of silver was observed at a silver concentration of 2.5  
14  $\mu\text{g}/\text{mL}$ , whereas no cytotoxic reactions of hMSC were observed with AgNPs at  
15 concentrations of  $\leq 3$   $\mu\text{g}/\text{mL}$  and with silver acetate at concentrations of  $\leq 1$   $\mu\text{g}/\text{mL}$ . There  
16 was also a significant decrease in the release of IL-6, IL-8, and VEGF (typical set of  
17 cytokines from hMSCs) in the presence of AgNPs as well as with silver acetate in the  
18 concentration range of 5 to 50  $\mu\text{g}/\text{mL}$ . Silver acetate concentrations below 2.5  $\mu\text{g}/\text{mL}$   
19 (for ions) and below 5  $\mu\text{g}/\text{mL}$  (for AgNPs) did not lead to a decrease in cytokine  
20 formation. The findings indicate that AgNPs exert cytotoxic effects on hMSCs at high  
21 concentrations but also induce cell activation (as analyzed by the release of IL-8) at  
22 high but nontoxic concentrations of nanosilver. The same investigators [Kittler et al.  
23 2010] also studied the effect of aging on the toxicity of PVP- and citrate-coated AgNPs  
24 (diameter of metallic core,  $50 \pm 20$  nm), using hMSCs at water-solution concentrations  
25 of 50, 25, 20, 15, 5, 2.5, and 1 mg/L. AgNPs were stored at these concentrations for 3  
26 days, 1 month, and 6 months and evaluated for cell viability and morphology. Aged  
27 AgNPs (at 50 mg/L) stored for 1 and 6 months caused complete cell death, whereas at  
28 3 days the reduction in viability was 70%. AgNPs that were stored in solution for 6  
29 months had a lethal concentration that was about 20 times smaller than that of freshly  
30 prepared AgNPs, indicating the release of silver ions during storage. However, the

1 released silver ions were probably bound by proteins and therefore rendered less toxic.  
2 Cell viability at 6 months increased as the concentration decreased. The dissolution  
3 rates for the PVP- and citrate-coated AgNPs were studied at different temperatures.  
4 Dissolution was only partial for each functionalized AgNP, and the degree of dissolution  
5 did not depend on the absolute concentration of silver nanoparticles but seemed to be  
6 an intrinsic (but temperature-dependent) property of the nanoparticles. The rate of  
7 dissolution and the final degree of dissolution were higher for the PVP-coated than for  
8 the citrate-functionalized AgNPs.

9 In a follow-up study by the same investigators [Greulich et al. 2011], the uptake of  
10 AgNPs into hMSC was examined to determine if more than one endocytotic pathway  
11 was involved. PVP-coated AgNPs with a metallic core of  $50 \pm 20$  nm in diameter were  
12 used. The uptake of AgNPs into hMSC was determined by exposing hMSC for 24 hours  
13 at concentrations of 2.5, 2.0, 1.5, 1.0, or 0.5  $\mu\text{g}/\text{mL}$  silver ions (silver acetate) or 50, 30,  
14 25, 20, or 15  $\mu\text{g}/\text{mL}$  AgNPs and quantitatively analyzing the intracellular side scatter  
15 signal by flow cytometry. AgNP uptake by hMSCs was observed to occur by clathrin-  
16 dependent endocytosis and by micropinocytosis, and the ingested nanoparticles  
17 subsequently occurred as agglomerates in the perinuclear region and not in the cell  
18 nucleus, endoplasmic reticulum, or Golgi complex. The inhibition of the clathrin-  
19 mediated pathway did not result in complete suppression of endocytosis, indicating that  
20 more than one endocytotic pathway might be involved.

21 The widespread use of AgNP-treated dressings to heal wounds and prevent infection  
22 led Hackenberg et al. [2011] to investigate the dosimetry for the agent's ability to induce  
23 toxicity in hMSCs. As supplied, the nanoparticles had a mean diameter of 46 nm,  
24 although aggregation to a mean diameter of 404 nm was observed when the particles  
25 were dispersed in physiologic medium or situated within the cells. Significant cytotoxicity  
26 was observed at a concentration of 10  $\mu\text{g}/\text{mL}$  and a degree of DNA damage was  
27 indicated in the comet assay and by a significant increase in chromosomal aberrations.  
28 Chromosomal aberrations consisting of chromatid deletions and exchanges were  
29 induced at concentrations of 0.1  $\mu\text{g}/\text{mL}$  and above. Hackenberg et al. [2011] compared

1 this concentration with published data on the growth inhibition of *Staphylococcus*  
2 *aureus*, for which AgNP concentrations of 3.5 µg/mL had been reported [Kim et al.  
3 2007]. This led Hackenberg et al. [2011] to conclude that the cytotoxic and genotoxic  
4 potential of AgNPs in hMSCs occurred at significantly higher doses than did their  
5 antimicrobial effects.

6 Similarly, Samberg et al. [2012] assessed the toxicity and cellular uptake of both  
7 undifferentiated and differentiated human adipose-derived stem cells (hASCs) exposed  
8 to AgNPs and evaluated their effect on hASC differentiation. The stem cells were  
9 exposed to 10- or 20-nm AgNPs (confirmed by TEM analysis) at concentrations of 0.1,  
10 1.0, 10.0, 50.0, and 100.0 µg/mL either before or after differentiation. Baseline-viable  
11 hASCs were first differentiated down the osteogenic and adipogenic pathways or  
12 maintained in their proliferative state for 14 days and then exposed for 24 hours at  
13 concentrations of 0.1 through 100.0 µg/mL. To evaluate potential cellular uptake of  
14 AgNPs into hASCs, undifferentiated hASCs were grown to 100% confluency in  
15 complete growth medium for 5 days, while the effects of AgNPs on hASC differentiation  
16 were determined also with use of undifferentiated hASCs grown to 100% confluency in  
17 complete growth medium for 5 days. Exposure to either 10- or 20-nm AgNPs resulted in  
18 no significant cytotoxicity to hASCs and minimal dose-dependent toxicity to adipogenic  
19 and osteogenic cells at 10 µg/mL. Adipogenic and osteogenic cells showed cellular  
20 uptake of both 10- and 20-nm AgNPs without significant morphologic changes to the  
21 cells, in comparison with controls. Exposure to 10- or 20-nm AgNPs did not influence  
22 the differentiation of the cells at any concentration and only resulted in a minimal  
23 decrease in viability at antimicrobial concentrations. Exposure to AgNPs also resulted in  
24 no significant cytotoxicity to undifferentiated hASCs, either prior to differentiation or  
25 following 14 days of differentiation.

26 The association of AgNP incubation of IMR-90 human lung fibroblast cells and U251  
27 human glioblastoma cells with genetic perturbations, as well as mitochondrial damage  
28 and ROS formation, was demonstrated by AshaRani et al. [2009]. The AgNPs  
29 employed in the study were administered at concentrations of 25, 50, or 100 µg/mL and

1 were to have been synthesized by the reduction of silver nitrate solution with sodium  
2 borohydride, followed by the addition of a filtered starch solution with constant stirring.  
3 The starch-coated particles were 6 to 20 nm in diameter and were stated to have good  
4 stability in water. Consistent with the work of others, the study demonstrated uptake of  
5 the particles into the cell cytoplasm and nucleus, causing an alteration in cell  
6 morphology and reduced viability, deficits in mitochondrial performance, and ROS  
7 production. Whereas annexin-V staining showed that only a small percentage of cells  
8 underwent apoptosis, cell cycle arrest in the G2M phase and data from the comet and  
9 cytokinesis-blocked MN assays gave an indication of treatment-associated DNA  
10 damage. For example, the comet assay of AgNP-treated cells showed a concentration-  
11 dependent increase in tail momentum, and chromosomal breaks were detected in the  
12 cytokinesis-blocked MN assay. This effect was especially noticeable in the U251 cell  
13 line.

14 Nallathamby and Xu [2010] used a novel approach to chart the changes in cellular  
15 growth and subcellular morphology when mouse fibroblast (L929) tumor cells were  
16 incubated with AgNPs. The particles were synthesized by chemical reduction of silver  
17 chlorate with sodium borohydride and sodium citrate. The product was stable in  
18 aqueous solution and inside single living cells with a median diameter of 12 nm. When  
19 the cells were incubated in flasks with AgNPs at 0, 11, or 22 µg/mL, the uptake of  
20 particles and inhibition of growth occurred as a function of concentration and duration of  
21 exposure. However, by culturing the cells on coverslips in Petri dishes, the impact of  
22 AgNPs on individual cells could be visualized by microscopy. The result was a dose-  
23 and exposure-related formation of cells with single giant nuclei or cells with two, three,  
24 or sometimes four nuclei per cell. After incubation for 72 hours, almost all of the L929  
25 fibroblast cells displayed one of these altered nuclear states. The authors interpreted  
26 their data as indicating that AgNPs induce malsegregation of the chromosomes rather  
27 than having a direct effect on replication.

28 Mei et al. [2012] evaluated the mutagenic potential of uncoated AgNPs (average size,  
29 ~5 nm; range, 4–12 nm), using a mouse lymphoma assay system. Modes of action

1 (MoA) were assessed by means of standard alkaline and enzyme-modified comet  
2 assays and gene expression analysis. The mouse lymphoma cells (L5178Y/TK<sup>+/-</sup>) were  
3 treated with AgNPs at a concentration of 5 µg/mL for 4 hours, at which time the AgNPs  
4 were observed to be in the cytoplasm of the lymphoma cells. AgNPs induced dose-  
5 dependent cytotoxicity and mutagenicity, with a marked increase in the mutation  
6 frequency at 4 and 5 µg/mL (<50% cell survival at ≥5 µg/mL), where nanosilver had a  
7 clastogenic MoA. In the standard Comet assay there was no significant induction of  
8 DNA damage, although the percentage of DNA in the tail increased slightly with  
9 increasing dose. However, in the oxidative DNA damage comet assays, addition of  
10 lesion-specific endonucleases resulted in significant induction of DNA breaks in a dose-  
11 dependent manner. Gene expression analysis with use of an oxidative stress and  
12 antioxidant defense polymerase chain reaction (PCR) array, showed that the  
13 expressions of 17 of the 59 genes on the arrays were altered in the cells treated with  
14 AgNPs. These genes are involved in the production of ROS, oxidative stress response,  
15 antioxidants, oxygen transporters, and DNA repair. The investigators concluded that the  
16 results from this study indicated that the mutagenicity of AgNPs used in this study  
17 resulted from a clastogenic MoA.

18 Several of the studies cited above have revealed significant toxic effects on cells that  
19 often occurred in a dose-dependent manner; however, only a few studies have  
20 evaluated AgNPs and the role of particle size on cellular toxicity [Park et al. 2011c; Kim  
21 et al. 2012; Gliga et al. 2014]. The effects of AgNPs of different sizes (20, 80, 113 nm)  
22 have been compared in in vitro assays for cytotoxicity, inflammation, genotoxicity, and  
23 developmental toxicity [Park et al. 2011c]. Cytotoxicity was investigated in L929 murine  
24 fibroblasts and RAW 264.7 murine macrophages, and effects of AgNPs were compared  
25 to those of silver in ionic form. The role of AgNP size on the generation of ROS and on  
26 parameters of inflammation were also evaluated, as well as the dependence of particle  
27 size on developmental toxicity and genotoxicity in mouse embryonic cells and  
28 embryonic fibroblasts, respectively. Metabolic activity of RAW 264.7 cells, embryonic  
29 stem cells, and L929 cells was evaluated with use of WST-1 cell proliferation reagent  
30 when the cells were exposed to AgNPs for 24 hours or for 10 days (embryonic stem

1 cells). In both L929 fibroblasts and RAW 264.7 macrophages, metabolic activity was  
2 decreased (concentration dependently) by AgNPs as well as by ionic silver. For ionic  
3 silver, the decrease in metabolic activity was similar between the two cell types. In  
4 contrast, for AgNPs, the metabolic activity was significantly more affected in 929  
5 fibroblasts than in RAW 264.7 macrophages. In both cell types the 20-nm AgNPs were  
6 the most potent in decreasing metabolic activity. In assessing cell membrane integrity  
7 (LDH), 20-nm AgNPs were more potent in reducing the cell membrane integrity of L929  
8 fibroblasts than was ionic silver, whereas ionic silver was more potent in RAW 264.7  
9 macrophages. In addition, the cellular generation of ROS was observed to increase for  
10 20-nm AgNPs but only marginally for the larger AgNPs when exposed to RAW 264.7  
11 macrophages. The generation of ROS in macrophages occurred only at concentrations  
12 above those decreasing the metabolic activity of macrophages, suggesting a secondary  
13 effect rather than causing the onset of cytotoxicity. The 20-nm AgNPs were also found  
14 to be the most potent for causing embryonic stem cell differentiation. However, 20-nm  
15 AgNPs did not induce an increase in gene mutation frequencies (genotoxicity  
16 evaluation) at concentrations up to 3  $\mu\text{g}/\text{mL}$ .

17 Kim et al. [2012] examined the size-dependent cellular toxicity of AgNPs, using three  
18 different sizes (~10, 50, and 100 nm in diameter). A series of cell lines, including  
19 osteoblastic MC3T3-E1 cells, rat adrenal PC12 cells, human cervical cancer HeLa cells,  
20 and hamster CHO cells, were exposed to AgNPs at doses of 10, 20, 40, 80, or 160  
21  $\mu\text{g}/\text{mL}$  to investigate the regulation of cell proliferation, ROS production, LDH release,  
22 apoptosis induction, and stress-related gene expression. Cell assays were conducted at  
23 24, 48, and 72 hours after treatment with AgNPs. Results from assays suggested that  
24 AgNPs exerted significant cytotoxic effects against all cell types, as indicated by  
25 decreased mitochondrial function, and that these effects occurred in a dose- and size-  
26 dependent manner. Both the MC3T3-E1 and PC12 cell lines were shown to be the most  
27 sensitive to toxic effects. In particular, the cytotoxic response to AgNPs was cell-  
28 dependent, with apoptosis occurring in MC3T3-E1 and necrosis in PC12 cell lines.  
29 Moreover, 10-nm-diameter AgNPs had a greater apoptotic effect against the MC3T3-E1  
30 cells than did AgNPs 50 and 100 nm in diameter.

1 Nymark et al. [2013] investigated the genotoxicity of PVP-coated AgNP in BEAS-2B  
2 cells. The AgNP had an average diameter of 42.5 nm, were coated in PVP,  
3 characterized, and suspended in cell medium. Cytotoxicity was assessed by Trypan  
4 Blue dye exclusion, after exposure to 1.9 to 182.4 µg/mL AgNP for 4, 24, or 48 hr.  
5 Approximately 50% viability was observed at 182.4 µg/mL after 4 hr or at doses  
6 exceeding 45.6 µg/mL at 48 hr, but with 34.2% cytotoxicity at the highest 24 hr dose.

7 Genotoxicity was assayed both by alkaline comet assay after 7.6 to 182.4 µg/mL AgNP  
8 for 4 or 24 hr, micronuclear analysis by fluorescent microscopy after exposure to 10 to  
9 240 µg/mL AgNP for 48 hr, and chromosomal aberration assay by microscopy after  
10 either 10-240 µg/mL AgNP exposure for 24 hr or 2.5 to 40 µg/mL for 48 hr. At 60.8  
11 µg/mL and higher doses, 4 and 24 hr treatments caused at least a 2-fold comet tail  
12 increase, though micronuclei induction or chromosomal aberrations were not noted.

13 Gliga et al. [2014] also investigated the size- and coating-dependent toxicity of AgNPs  
14 following exposure of human lung cells (BEAS-2B). BEAS-2B cells were exposed to  
15 citrate-coated AgNPs of different sizes (10-, 40-, and 75-nm diameters) as well as to 10-  
16 nm PVP-coated and 50-nm uncoated AgNPs, at doses of 5, 10, 20, and 50 µg/mL.  
17 Study parameters included evaluation of particle agglomeration, cell viability, ROS  
18 induction, genotoxicity, γH2AX foci formation (a marker for DNA damage and repair),  
19 and intracellular localization. To assess cytotoxicity, BEAS-2B cells were exposed to  
20 AgNPs for 4 and 24 hours in an AB assay. After 4 hours, no significant signs of toxicity  
21 of any of the AgNPs were observed, up to the highest dose tested. Significant cell  
22 toxicity was evident only for the 10-nm citrate-coated AgNPs ( $P \leq 0.05$ ) and 10-nm  
23 PVP-coated AgNPs ( $P \leq 0.01$ ) after 24 hours for the doses of 20 and 50 µg/mL. No  
24 significant alterations of the mitochondrial activity of the BEAS-2B cells were observed  
25 at doses of 5 and 10 µg/mL or for the other AgNPs. When the LDH assay was used for  
26 cytotoxicity determination, no significant toxicity was observed after 4 hours for any of  
27 the AgNPs. However, significant toxicity was observed after 24 hours for the 10-nm  
28 citrate-coated AgNPs ( $P \leq 0.05$ ) and the 10-nm PVP-coated AgNPs ( $P \leq 0.0001$ ) at the  
29 dose of 50 µg/mL. None of the larger AgNPs altered cell viability. In contrast, all AgNPs

1 tested caused an increase in overall DNA damage after 24 hours when assessed by the  
2 comet assay, suggesting an independent mechanism for cytotoxicity and DNA damage.  
3 No  $\gamma$ -H<sub>2</sub>AX formation was detected, and no increased production of intracellular ROS  
4 was observed. Despite different agglomeration patterns, there was no difference in the  
5 uptake or intracellular localization of the citrate- and PVP-coated AgNPs, and there was  
6 no coating-dependent difference in cytotoxicity. Furthermore, the 10-nm particles  
7 released significantly more Ag<sup>+</sup> than did all other AgNPs (approximately 24% by mass  
8 versus 4–7% by mass) following 24 hours in cell medium. The released fraction in cell  
9 medium did not induce any cytotoxicity, indicating that intracellular release of Ag could  
10 have been responsible for the toxicity.

11 The genotoxicity of AgNPs (range, 4–12 nm in diameter) was evaluated by Li et al.  
12 [2012], using a *Salmonella* reverse mutation assay (Ames) and an in vitro micronucleus  
13 test in TK6 human lymphoblastoid cells. The Ames assay was conducted according to  
14 OECD test guidelines, with use of *Salmonella typhimurium* tester strains TA98 and  
15 TA1537 for detection of frame-shift mutation and the use of tester strains TA100,  
16 TA1535, and TA102 for the measurement of base-pair substitution. For TA98 and  
17 TA100, frank toxicity (reduction of background revertant frequency and/or thinning of the  
18 background) was detected at 4.8  $\mu$ g/plate and higher doses; toxicity was observed for  
19 TA1535 and TA1537 at 9.6  $\mu$ g/plate and higher doses. At the highest dose of 76.8  
20  $\mu$ g/plate, all the bacteria from the five tester strains were killed. In general, AgNPs were  
21 found to be negative in the Ames test; this result may have been due to the  
22 agglomeration of the nanoparticles, making them too large to transport through the  
23 pores in the bacterial cell wall, or possibly due to the insensitivity of most tester strains  
24 to oxidative DNA damage. The cytotoxicity of AgNPs was evaluated with use of  
25 lymphoblast TK6 cells treated at concentrations of 10 to 30  $\mu$ g/mL, in accordance with  
26 OECD guidelines. Cytotoxicity was measured with relative population doubling, which  
27 reflects a combination of cell growth, death, and cytostasis. A dose-response increase  
28 in micronuclei was observed at a dose of 25  $\mu$ g/mL and was reported by the  
29 investigators as a weak positive, consistent with findings from other studies that tested  
30 various types of nanomaterials with mammalian cells.

1 To determine the mutagenic potential of colloidal AgNPs (average diameter, 10 nm),  
2 four histidine-requiring strains of *S. typhimurium* (TA98, TA100, TA1535, and TA1537)  
3 and one tryptophan-requiring strain of *Escherichia coli* (WP2uvrA) were used in the  
4 presence and absence of metabolic activation with S9 mix [Kim et al. 2013b]. In the  
5 absence of metabolic activation (that is, without S9 mix), cytotoxicity was found at ~62.5  
6 µg/plate (TA98, TA1535, TA1537, and WP2uvrA) and at ~31.25 µg/plate (TA100).  
7 Cytotoxicity was also exhibited at concentrations of ~125 µg/plate (TA98, TA100, and  
8 TA1537) and ~250 µg/plate (TA1535 and WP2uvrA) in the presence of metabolic  
9 activation. Precipitation and aggregation of the AgNPs were also observed at a dose  
10 level greater than 1.25 µg/plate with and without metabolic activation. No significant  
11 number of revertant colonies was observed for any of the bacterial strains, with or  
12 without metabolic activation, in comparison with the negative control. No dose-  
13 dependent increase of revertant colonies was observed for any of the bacterial strains.  
14 Kim et al. [2013] also conducted a chromosome aberration test to identify chromosomal  
15 abnormalities. A preliminary cytotoxicity test was carried out at a relative cell count  
16 (RCC) concentration of ~ 50%. At this RCC, AgNPs were found to induce cytotoxicity.  
17 For groups treated for 6 and 24 hours without the S9 mix, a cytotoxic effect was induced  
18 at about 15.625 µg/mL, whereas for the group treated for 6 hours with the S9 mix,  
19 cytotoxicity was induced above 31.25 µg/mL. On the basis of these results,  
20 chromosome slide samples were prepared at 3.906, 7.813, and 15.625 µg/mL, with  
21 50% of the RCC concentration as the highest concentration. AgNPs did not produce  
22 any statistically significant increase in the number of CHO-k1 cells with chromosome  
23 aberrations when compared to the negative controls with or without metabolic  
24 activation. AgNPs also did not cause a statistically significant increase in the number of  
25 cells with polyploidy or endoreduplication when compared with controls in the presence  
26 and absence of the S9 mix.

27 Induction of genotoxicity in CHO-K1 cells by AgNP was also studied by Kim et al.  
28 [2013a]. AgNP were a majority 40-59 nm based on SEM, TEM, and DLS, though  
29 aggregates up to 315 nm were observed. Comet assays demonstrated an AgNP dose-

1 dependent increase in DNA damage, with a 450% tail increase at 10 µg/mL exposure.  
2 Additionally, 10 µg/mL exposure was also sufficient to induce micronucleus formation.

3 However, bacterial mutagenicity was not detected in *Salmonella typhimurium* strains,  
4 TA98, TA100, TA1535, and TA 1537 by Ames test, regardless of the presence of S9  
5 mix, nor was AgNP exposure associated with changes in binucleated cells, cytokinesis-  
6 block proliferation index, or relative increase in cell counts in CHO-K1 cells.

### 7 **D.3 Changes in Gene Expression/Regulation**

8 A number of research groups have employed DNA microarray analysis in an attempt to  
9 understand the cellular responses to AgNPs at the molecular level. For example, using  
10 7- to 10-nm-diameter nanoparticles stabilized with PVP, Kawata et al. [2009] observed  
11 changes in cellular morphology, cell viability, and MN formation when HepG2 human  
12 hepatoma cells were incubated with AgNPs at noncytotoxic doses. However, MN  
13 formation was greatly reduced in cells incubated with either a polystyrene nanoparticle  
14 preparation or a silver carbonate solution, but it was only partially reduced in response  
15 to AgNPs where the cells had been pre-incubated with the antioxidant NAC.  
16 Accompanying these well-characterized responses was a significant induction of genes  
17 associated with cell cycle progression. Thus, AgNPs altered the expression levels of  
18 529 genes at least twofold, with 236 genes being induced and 293 repressed. Patterns  
19 of induction featured genes classified as “M phase” (31 genes), microtubule-based  
20 processes (19 genes), DNA repair (16 genes), DNA replication (24 genes), and  
21 intracellular transport (32 genes). Many of the genes were involved in chromosome  
22 segregation, cell division, and cell proliferation. Striking levels of induction were also  
23 observed for some stress-inducible gene, including three coding for metallothioneins  
24 and three for different heat-shock proteins. Overlapping patterns of gene expression in  
25 this cell line were observed in silver carbonate–altered gene profiles. For example, in  
26 comparisons of AgNPs and silver carbonate, 66 upregulated genes and 72  
27 downregulated genes were altered commonly in the same direction with both chemical  
28 treatments. Kawata et al. [2009] speculated that the upregulation of a number of genes

1 associated with DNA repair and the increase in MN in AgNP-exposed HepG2 cells  
2 might point to the DNA-damaging effects of silver in both nanoparticle and ionic form.

3 The A549 human lung adenocarcinoma cell line was used by Deng et al. [2010] as a  
4 platform for studying increased gap junction intercellular communication (GJIC) activity  
5 and increased expression of connexin43 (Cx43) mRNA in the presence of AgNPs. The  
6 particles were a proprietary formulation, 30 nm in diameter and coated with 0.2% PVP,  
7 although TEM and dynamic light scattering indicated that a degree of aggregation had  
8 occurred when the particles were dispersed in an aqueous medium. Assessment of  
9 GJIC was achieved by means of a scrape loading/dye transfer technique, and Cx43  
10 was detected by immunofluorescence. Furthermore, western blot assays were  
11 performed to determine the level of expression of Cx43 protein, and RT-PCR analysis  
12 showed that silver AgNPs upregulated the expression of Cx43 mRNA in a dose-  
13 dependent manner (1.2–1.8 times at concentrations ranging from 0.5 to 4.0 µg/mL after  
14 a 24-hour incubation). Deng et al. [2010] speculated that GJIC and Cx43 might mediate  
15 some of the biologic effects of AgNPs.

16 Ma et al. [2011] applied genomic analysis to responses to AgNPs (~20 nm in diameter)  
17 in human dermal fibroblasts. The particles employed had been prepared by reduction of  
18 a silver nitrate solution with sodium borohydride and were used at 200 micromolar (µM).  
19 However, TEM analysis showed a considerable degree of aggregation of the nearly  
20 spherical particles. For the microarray analysis, total RNA was isolated, amplified,  
21 labeled, and hybridized and cRNA probes were synthesized. A proprietary computer  
22 program (BeadStudio) used to survey changes in gene expression showed that 1,593  
23 genes were impacted by AgNPs after 1, 4, or 8 hours' incubation. Only 237 genes were  
24 affected after 1 hour, as compared to 1,149 after 4 hours and 684 after 8 hours. Biologic  
25 pathway analysis of the affected genes identified five functional clusters associated  
26 primarily with disturbance of energy metabolism, disruption of cytoskeleton and cell  
27 membrane, gene expression, and DNA damage/cell cycle arrest.

1 Foldbjerg et al. [2012] studied the effect of AgNPs (average particle diameter, 15.9 nm)  
2 on gene expression, using human lung epithelial cell line A549 exposed to 12.1 µg/mL  
3 AgNPs for 24 and 48 hours. Results were compared to control (unexposed) and silver  
4 ion (Ag<sup>+</sup>)–treated cells (1.3 µg/mL) with Affymetrix microarray analysis. AgNPs exposed  
5 for 24 hours altered the regulation of more than 1,000 genes (twofold regulation),  
6 compared to only 133 genes that responded to Ag<sup>+</sup> exposure. Nearly 80% of all genes  
7 induced by Ag<sup>+</sup> were also upregulated in AgNP-treated cells. Bioinformatic analysis of  
8 the upregulated genes in response to the 24-hour exposure with Ag<sup>+</sup> and AgNPs  
9 revealed similar functional gene groups that were significantly enriched. Exposure of  
10 epithelial cells to AgNP and Ag<sup>+</sup> resulted in intracellular production of ROS but did not  
11 induce apoptosis or necrosis at the concentrations used in the study. Exposure to AgNP  
12 influenced the cell cycle and led to an arrest in the G2/M phase, while exposure to Ag<sup>+</sup>  
13 caused a faster but less-persisting cellular response than did exposure to AgNPs. The  
14 investigators concluded that although the transcriptional response to exposure with Ag<sup>+</sup>  
15 is highly related to the responses caused by exposure to AgNPs, the particulate form  
16 and size of AgNPs “affect cells in a more complex way.”

17 Huo et al. [2015] investigated the effects of NM-300K 20-nm AgNP exposure in 16HBE,  
18 HUVEC, and HEPG2 cells. Cellular viability showed both time- and dose-dependent  
19 toxicity. Additionally, 16HBE cells were more sensitive than HEPG2 cells, and HUVEC  
20 was the least sensitive of the three. Notably, 2 µg/cm<sup>2</sup> AgNP exposure significantly  
21 upregulated both xbp-1s and chop mRNA levels in 16HBE cells, as well as chop mRNA  
22 levels in HEPG2. Other genes related to the ER stress signaling pathway were also  
23 upregulated in 16HBE by AgNP exposure. Western blot analysis showed upregulation  
24 of BIP and significantly Caspase-12 relative to Caspase-3 in AgNP exposed 16HBE  
25 cells, which indicates a pro-apoptotic response through the ER-targeted pathway (rather  
26 than mitochondrial-targeted pathway). Huo et al. [2015] also found that lung, liver, and  
27 kidney tissues showed significant increases in ER stress following intratracheal  
28 instillation of AgNP in vivo.

1 Srivastava et al. [2012] investigated selenoprotein synthesis in A549 and HaCat  
2 keratinocyte cells. MTT and LDH assays were used to examine the effects of up to 10  
3  $\mu\text{M}$  AgNP exposure on viability; little change was observed. However, AgNP exposure  
4 did result in a dose-dependent reduction of  $^{75}\text{Se}$  radioisotope incorporation into known  
5 selenoproteins. No changes were observed in incorporation of  $^{35}\text{S}$ -methionine/cysteine,  
6 indicating the change was specific to selenoproteins and not proteins overall. These  
7 changes also occurred with exposure to Ag ions (as  $\text{Ag}_2\text{SO}_4$ ). The authors indicated  
8 that the most likely mechanism was that leached Ag ion interfered with Se binding;  
9 additional experiments eliminated other possible mechanisms. Activity assays showed  
10 that both AgNP and Ag ions also decreased thioredoxin reductase (TrxR1) activity but  
11 not protein levels. This indicates the possibility that AgNP may interfere with  
12 selenoprotein synthesis.

#### 13 **D.4 Modeling the Perturbation of the Blood–Brain Barrier**

14 Tang et al. [2010] used co-cultures of rat brain microvessel vascular endothelial cells  
15 and astrocytes that were established on a polycarbonate membrane in a diffusion  
16 chamber to model the potential for AgNPs to cross the blood–brain barrier. The  
17 researchers used commercial preparations of AgNPs (diameter, 50–100 nm) and  
18 contrasted their passage with larger-scale silver microparticles (diameter, 2–20  $\mu\text{m}$ )  
19 incubated in the same system. The use of ICP-MS showed that AgNPs readily crossed  
20 the barrier, whereas silver microparticles did not. TEM analysis demonstrated the  
21 capacity of AgNPs to be taken up by the mixed culture. Some of the endothelial cells  
22 showed signs of morphologic disruption, with large vacuole formation and signs of  
23 necrosis of cellular organelles.

24 Primary brain microvessel endothelial cells isolated from Sprague-Dawley rats were  
25 employed by Trickler et al. [2010] to determine the capacity of AgNPs to potentiate the  
26 release of proinflammatory mediators, with possible impacts on blood–brain barrier  
27 permeability. Obtained from a commercial supplier, the PVP-coated AgNPs used in  
28 these experiments conformed to their size requirements of 25, 40, and 80 nm in  
29 diameter and were mostly spherical, as indicated by TEM and dynamic light-scattering

1 analysis. Cellular accumulation of silver was greater from the smaller nanoparticles, and  
2 cell viability was likewise more severely affected in those cultures exposed to the 25-  
3 nm-diameter particles. The cultures also showed a time-dependent preferential release  
4 of prostaglandin E<sub>2</sub> and the cytokines TNF- $\alpha$ , IL-1 $\beta$ , and IL-2, in relation to smaller  
5 AgNPs. According to the authors, these changes may be linked to ROS generation and  
6 an increase in microvascular permeability.

## 7 **D.5 Impact of Silver Nanoparticles on Keratinocytes**

8 Two research reports have examined the effects of AgNPs on keratinocytes, focusing in  
9 particular on the different results that were obtained when the toxicity of particles of  
10 different sizes and coatings were compared [Amato et al. 2006; Samberg et al. 2010].  
11 For example, Amato et al. [2006] reported in an abstract that hydrocarbon-coated  
12 AgNPs of 15, 25, or 55 nm in diameter induced greater degrees of toxicity than did  
13 uncoated forms of silver that were 80 or 130 nm in diameter. The use of a CytoViva 150  
14 Ultra Resolution Imaging system showed AgNP aggregates on the surface of the cells,  
15 along with some evidence of particle uptake into the HEL-30 mouse keratinocytes.  
16 Measuring caspase activity and using confocal fluorescent microscopy provided  
17 evidence of the onset of apoptosis at sublethal doses. These results differed from those  
18 of Samberg et al. [2010], who incubated human epidermal keratinocytes for 24 hours  
19 with eight different species of AgNPs. As supplied by nanoComposix, Inc. (San Diego,  
20 CA), these preparations included three unwashed colloids of 20-, 50-, and 80-nm-  
21 diameter AgNPs, three washed colloids of the same nominal size, and two carbon-  
22 coated powders that were 25 and 35 nm in diameter. In contrast to the findings of  
23 Amato et al. [2006], the loss of cell viability that was observed with unwashed AgNPs at  
24 silver concentrations of 0.34 or 1.7  $\mu\text{g}/\text{mL}$  was not seen when the cells were incubated  
25 with washed or carbon-coated particles, even though all silver nanoparticles were taken  
26 up into cytoplasmic vacuoles to roughly the same extent. The inflammatory potential of  
27 AgNPs was demonstrated by increases of IL-1 $\beta$ , IL-6, IL-8, and TNF- $\alpha$  in the media of  
28 cells exposed at 0.34  $\mu\text{g}/\text{mL}$ . The authors suggested that the toxicity of AgNPs to  
29 human epidermal keratinocytes might be influenced by residual contaminants in the  
30 AgNP preparations and not necessarily by the particles themselves.

## 1 **D.6 Effect of Silver Nanoparticles on Platelet Activation**

2 Jun et al. [2011] carried out a series of experiments to investigate the effect of AgNPs  
3 on platelet aggregation. The commercial AgNPs averaged slightly less than 100 nm in  
4 diameter and were maintained in solution in nonaggregated form by ultrasonication and  
5 vortexing. A colloidal dispersion of AgNPs (5,000–8,000 nm in diameter) was used in  
6 comparison. The measured parameters that were indicative of platelet activation  
7 included platelet aggregation per single-cell counts, TEM analysis, flow cytometric  
8 analysis of phosphatidylserine exposure (a measure of apoptosis), platelet pro-  
9 coagulant activity, serotonin secretion, detection of p-selectin expression, and  
10 determination of intracellular calcium levels. There was a dose-dependent increase in  
11 platelet aggregation with increased concentration of nanoparticle-borne but not  
12 microparticle-borne silver. Aggregation was further enhanced by the presence of  
13 thrombin. Other determinants of coagulation dose-dependently associated with the  
14 presence of AgNPs included the degree of phosphatidylserine exposure, pro-coagulant  
15 activity, expression of p-selectin, and secretion of serotonin. The presence of the  
16 calcium chelator ethylene glycol-bis ( $\beta$ -amino-ethyl ether) N,N,N',N'-tetra acetic acid in  
17 the incubation medium partially blocked the platelet aggregation activity of AgNPs,  
18 implicating a role for calcium ions in the induction of platelet aggregation. Overall, the  
19 results pointed to the capacity of AgNPs to enhance platelet aggregation and pro-  
20 coagulant activity, with a possible intermediary role for intracellular calcium and sub-  
21 threshold levels of thrombin.

## 22 **D.7 Antitumor and Antimicrobial Activity of Silver Nanoparticles**

23 The in vivo experiments of Sriram et al. [2010], in which intraperitoneal injected AgNPs  
24 appeared to enhance survival time and reduce the volume of ascites tumors in female  
25 Swiss albino mice, were supplemented by experiments in which Dalton's lymphoma cell  
26 lines were incubated for 24 hours with AgNPs in vitro. As described in Section 5.3.3, the  
27 researchers used 50-nm-diameter AgNPs that had been produced in *B. licheniformis*  
28 cultures incubated in the presence of silver nitrate. When the MTT assay was used as a  
29 measure of cell viability, a silver concentration of 500 nm was calculated for the IC<sub>50</sub>.

1 Measurement of caspase 3 in cell lysates showed a marked increase in activity  
2 compared to that in controls, and fragmentation of DNA indicated the presence of  
3 double strand breaks. The authors speculated that their data indicated a potential  
4 antitumor property of AgNPs and the relevance of apoptosis to this process.

5 In light of the extensive use of AgNP-bearing dressings to deter infection in wounds, Lok  
6 et al. [2006] used proteomic analysis to examine their mode of antibacterial action by  
7 incubating cultures of *E. coli* (wild-type K12 strain MG1655) with samples of spherical,  
8 9.3-nm-diameter bovine serum albumin-stabilized nanoparticles that had been produced  
9 by the borohydride reduction method. Two-dimensional electrophoresis was used to  
10 separate the spectrum of cellular proteins pre- and post-incubation; the resulting  
11 peptides were identified by MALDI-TOF MS and, in some cases, immunoblots. The  
12 initial concentrations of AgNPs and silver nitrate that inhibited bacterial proliferation  
13 were 0.4 nm and 6  $\mu$ m, respectively, suggesting that silver presented in the nanoparticle  
14 form was more efficient at deterring bacterial growth. With regard to changes in gene  
15 expression, induction of some cell envelope and heat-shock proteins appeared to be  
16 differentially enhanced, including outer membrane proteins A, C, and F (or their  
17 precursors), periplastic oligopeptide binding protein A, D-methionine binding protein  
18 (including body binding proteins A and B), and a 30S ribosomal subunit S6. However,  
19 the researchers reported that some of these stimulated proteins appeared to be in their  
20 precursor forms, which were said to generally contain a positively charged N-terminal  
21 signal sequence of about 2 kDa. In addressing the possible mode of action associated  
22 with the antimicrobial effect of AgNPs, the researchers found that short-term incubation  
23 of *E. coli* with AgNPs provided evidence of membrane destabilization, reduction in  
24 membrane potential, and depletion of intracellular potassium and ATP. These  
25 consequences were thought to be manifestations of the proteomic changes observed at  
26 the molecular level.

27 Swanner et al. [2015] investigated the cytotoxic and radiosensitizing effects of AgNP  
28 exposure on several triple-negative breast cancer (TNBC) and non-triple-negative  
29 breast cell lines. TNBC cell lines included MDA-MB-231, BT-549, and SUM-159 cells.

*This information is distributed solely for the purpose of pre-dissemination peer review under applicable information quality guidelines. It has not been formally disseminated by the National Institute for Occupational Safety and Health. It does not represent and should not be construed to represent any agency determination or policy.*

1 Non-TNBC cell lines included ER/PR positive, luminal A-like breast cancer cells (MCF-  
2 7); noncancerous, transformed breast cells (MCF-10A), immortalized human mammary  
3 epithelial cells (HMECs) (184B5), and post-stasis HMECs. TNBC cells showed greater  
4 cytotoxic sensitivity to AgNP exposure than non-TNBC cells as measured by MTT  
5 assay by approximately 10 µg/mL. Similarly, cytotoxicity assessed by clonogenic assay  
6 showed that 10 µg/mL was 100% inhibitive of TNBC cells, but not non-TNBC cells.  
7 However, all non-TNBC cells do uptake AgNP. Cystein thiols are more oxidized in  
8 TNBC cells than non-TNBC cells. Additionally, after exposure to AgNP and 4 Gy X-rays,  
9 DNA damage as quantified by γH2AX showed significantly increased damage in TNBC  
10 cells relative to non-TNBC cells.

**Table D-1. Summary of *in vitro* studies of silver nanoparticles (AgNPs) and nanowires (AgNWs)**

Cell Type	Particle Characteristics	Exposure Details		Major Outcomes	NOAEL/ LOAEL	Comments	Reference
		Concentrations/ Doses	Duration				
<b>Human Cells</b>							
HepG2 human hepatoma	AgNPs and Ag <sup>+</sup> ions: 5–10 nm particles dispersed in an aqueous medium; agglomerates 100–300 nm	0.2–1 µg/mL	24- to 28-hr incubation	Release of LDH activity; mRNA levels of catalase and SOD1 increased; detection of phosphorylation on the H2AX gene; ROS formation	NA	AgNPs exhibited cytotoxicity with a potency comparable to that of Ag <sup>+</sup> ions	Kim et al. [2009c]
HepG2 human hepatoma cells; SGC-7901 human stomach cancer cells; MCF-7 human breast adenocarcinoma cells; and A549 human lung adenocarcinoma cells	PVP coated; 5, 20, and 50 nm in diameter	Cell viability test: 0.01 – 100 µg/mL	6-, 12-, or 24-hr incubation	Apoptosis and necrosis test: 0.1, 0.5, 2.5 µg/mL; membrane damage and oxidative stress: 0.01–10 µg/mL	NA	Induced cell death caused by apoptosis; no difference between control group and exposed group for necrosis; smaller particles more effective at penetrating the membrane and inducing toxic effects	Liu et al. [2010a]
Human Chang liver cells	Particles started at 5–10 nm but aggregated to 28–38 nm after	4 µg/mL	0- to 24-hr incubation	Increased levels of lipid peroxidation and protein carbonyl formation;	NA	Apoptosis via a mitochondrial and caspase-dependent pathway; the	Piao et al. [2011]

*This information is distributed solely for the purpose of pre-dissemination peer review under applicable information quality guidelines. It has not been formally disseminated by the National Institute for Occupational Safety and Health. It does not represent and should not be construed to represent any agency determination or policy.*

Cell Type	Particle Characteristics	Exposure Details		Major Outcomes	NOAEL/ LOAEL	Comments	Reference
		Concentrations/ Doses	Duration				
	incubation in the medium			decrease in Bcl-2 expression; increase in Bax. ROS formation		importance of JNK in mediating the apoptotic effects was demonstrated by its time-dependent phosphorylation in the presence of AgNPs	
HT-1080 human fibrosarcoma cells; A431 human skin carcinoma cells	7–20-nm diameter in an aqueous suspension	6.25–50 µg/mL		Reduction in GSH content and SOD activity; increase in lipid peroxidation; increase in treatment-related DNA fragmentation	NA	Oxidative stress; cell death by apoptosis and necrosis	Arora et al. [2008]
Human acute monocytic leukemia cell line (THP-1 cells)	30–50 nm in diameter and coated with 0.2% PVP	0–7.5 µg/mL (calculated as silver mass)	Up to 24-hr incubation	Increase in intracellular ROS, DNA damage		Apoptosis; necrosis; significant reduction of viable cells after 24-hr exposure	Foldbjerg et al. [2009]
A549 human lung carcinoma epithelial-like cell line	30–50 nm, spherical, coated with 0.2% PVP	Suspensions/ supernatants containing 39% (0.2 µg/mL silver ions) or 69% (1.6 µg/mL silver ions)	24-hr incubation	Induced ROS	NA / 1.6 µg/mL total silver, suspension containing 39% silver	AgNP-free supernatant had the same toxicity as AgNP suspensions	Beer et al. [2012]
HeLa cells	5–10 nm in diameter, stabilized with a	IC <sub>50</sub> of 92 µg/mL silver	3- to 4-hr incubation	Increase in expression of heme oxygenase-		Apoptosis	Miura and Shinohara [2009]

This information is distributed solely for the purpose of pre-dissemination peer review under applicable information quality guidelines. It has not been formally disseminated by the National Institute for Occupational Safety and Health. It does not represent and should not be construed to represent any agency determination or policy.

Cell Type	Particle Characteristics	Exposure Details		Major Outcomes	NOAEL/ LOAEL	Comments	Reference
		Concentrations/ Doses	Duration				
	proprietary protectant			1 and metlothionein-2A			
A549 cells	~500 nm (agglomerated)	Morphology: 10, 50, 200 µg/mL Cytotoxicity: 5, 10, 50, 200 µg/mL Apoptosis: 50 and 100 µg/mL	Morphology: 24-hr incubation Cytotoxicity: 12, 24, 48, 72 hrs of incubation Apoptotic cell death: 24-hr incubation	Increased LGH release; altered cell cycle distribution; changes to expression of Bax and Bcl-2; altered mRNA levels of protein kinase C isotypes		Reduction in cell viability; increased apoptosis; cytotoxicity at 48 hrs	Lee et al. [2011a]
Human colon adenocarcinoma (HT29) cells	<20 nm in diameter	11 µg/mL	30-min to 6-hr incubation	Cascade reaction, which activates caspase-3, which penetrates nuclear membrane to induce DNA fragmentation		Programmed cell death (apoptosis)	Gopinath et al. [2010]
Human lung macrophage cell line (THB-1); human epithelial (A549) cells	Primary particle: 3-100 nm in diameter	5 µg/mL	52-hr incubation	Cytotoxic effect		Epithelial cells more sensitive to effects	Soto et al. [2007]
Human lung A549 cancer cell line	30–50 nm in diameter and coated with 0.2% PVP	AgNPs: 0–20 µg/mL Ag <sup>+</sup> : 0–10 µg/mL	24-hr incubation	Induced dose-dependent reductions in mitochondrial function to a greater extent than equivalent concentrations of silver in nano-form		Induced cytotoxicity and ROS formation was accompanied by formation of bulky DNA adducts; responses inhibited by	Foldbjerb et al. [2011]

*This information is distributed solely for the purpose of pre-dissemination peer review under applicable information quality guidelines. It has not been formally disseminated by the National Institute for Occupational Safety and Health. It does not represent and should not be construed to represent any agency determination or policy.*

Cell Type	Particle Characteristics	Exposure Details		Major Outcomes	NOAEL/ LOAEL	Comments	Reference
		Concentrations/ Doses	Duration				
						pretreatment with N-acetyl-cysteine	
Human mesenchymal stem cells (hMSCs)	Mean diameter of 46 nm; aggregation mean diameter of 404 nm when dispersed in medium	0.1, 1.0, and 10 µg/mL	1-, 3-, and 24-hr incubation	Chromosomal aberrations	NA / 0.1 µg/mL	Cytotoxic and genotoxic potential of AgNPs occurred at significantly higher doses than did their antimicrobial effects	Hackenberg et al. [2011]
Human mesenchymal stem cells (hMSCs)	PVP-coated, ~100 nm in diameter	Concentrations of 0.5, 1, 2.5, 3, 3.5, 4, 5 µg/mL or to silver ions (silver acetate)	Up to 7 days	Both types showed a decrease in release of IL-6, IL-8, and VEGF	Silver: 1 µg/mL; 2.5 µg/mL AgNP: 3 µg/mL; 3.5 µg/mL	AgNPs exert cytotoxic effects in hMSCs at high concentrations but also induce cell activation at high but nontoxic concentrations of nanosilver	Greulich et al. [2009]
Human mesenchymal stem cells (hMSCs)	PVP-coated, 50 nm ± 20 nm in diameter	Concentrations of 0.5, 1.0, 1.5, 2.0, or 2.5 µg/mL silver acetate (ions) or 15, 20, 25, 30, or 50 µg/mL AgNPs	24-hr incubation	80-nm AgNP agglomerates found in perinuclear region of hMSCs (clathrin-mediated endocytosis uptake)		Possibly more than one endocytotic pathway for cell uptake	Greulich et al. [2011]
Human adipose-derived stem cells (hASCs), undifferentiated and differentiated	10 or 20 nm in diameter	0.1, 1.0, 10.0, 50.0, 100.0 µg/mL, either before or after differentiation	Cells were differentiated down the osteogenic or adipogenic pathways or maintained in	No significant morphologic changes occurred in adipogenic and osteogenic cell uptake of both 10 & 20 nm; no	NA/ 10 µg/mL	No significant cytotoxicity to undifferentiated hASCs either prior to differentiation or following 14 days of differentiation	Samberg et al. [2012]

*This information is distributed solely for the purpose of pre-dissemination peer review under applicable information quality guidelines. It has not been formally disseminated by the National Institute for Occupational Safety and Health. It does not represent and should not be construed to represent any agency determination or policy.*

Cell Type	Particle Characteristics	Exposure Details		Major Outcomes	NOAEL/ LOAEL	Comments	Reference
		Concentrations/ Doses	Duration				
			their proliferative state for 14 days and then exposed for 24 hrs to evaluate potential cellular uptake of AgNPs the hASCs grew in a medium for 5 days	significant cytotoxicity to hASCs when exposed to 10- or 20-nm			
IMR-90 human lung fibroblasts; U251 human glioblastoma cells	6–20 nm in diameter; starch-coated	25, 50, or 100 µg/mL	2- to 48-hr incubation	Alteration in cell morphology; reduced viability; deficits in mitochondrial performance and ROS production		Small percentage of cells underwent apoptosis; indication of treatment-associated DNA damage	Asharani et al. [2009]
Human lung cells (BEAS-2B)	Citrate-coated: 10, 40, 75 nm in diameter PVP-coated: 10 nm in diameter Uncoated: 50 nm in diameter	5, 10, 20, 50 µg/mL	4- and 24-hr incubation	No cells showed significant signs of cell toxicity after 4 hrs; after 24 hrs, cell toxicity was significant in 10-nm citrate-coated and 10-nm PVP-coated from doses of 20 and 50 µg/mL; all cells showed overall DNA damage after 24 hrs		Independent mechanism for cytotoxicity and DNA damage	Gliga et al. [2014]

*This information is distributed solely for the purpose of pre-dissemination peer review under applicable information quality guidelines. It has not been formally disseminated by the National Institute for Occupational Safety and Health. It does not represent and should not be construed to represent any agency determination or policy.*

Cell Type	Particle Characteristics	Exposure Details		Major Outcomes	NOAEL/ LOAEL	Comments	Reference
		Concentrations/ Doses	Duration				
TK6 human lymphoblastoid cells	4–12 nm in diameter	10–30 µg/mL		Frank toxicity of TA98 and TA100; toxicity of TA1535 and TA1537; dose-response increase in micronuclei was observed at a dose of 25 µg/mL	Frank toxicity: 4.8 µg/plate; toxicity: 9.6 µg/plate	Results were weak-positive, consistent with results in similar studies	Li et al. [2012]
HepG2 human hepatoma cells	7–10 nm in diameter; stabilized by PVP	0, 0.1, 0.2, 0.5, 1.0, 1.5, 2.0, 2.5, 3.0 mg/L	24-hr incubation	Changes in cellular morphology; cell viability; MN formation; significant cytotoxicity at >1.0 mg/L		DNA-damaging effects; altered expression levels of 529 genes at least twofold	Kawata et al. [2009]
A549 human lung adenocarcinoma cell line	30 nm in diameter; coated with 0.2% PVP	0.5–4.0 µg/mL	24-hr incubation	Upregulated the expression of Cx43		GJIC and Cx43 might mediate some of the biologic effects of AgNPs	Deng et al. [2010]
Human dermal fibroblasts	~20 nm in diameter	Reduction of silver nitrate solution with sodium borohydride at 200 micromolar	1-, 4-, or 8-hr incubation	1,593 genes were impacted after 1-, 4-, and 8-hr incubations		Disturbance of energy metabolism; disruption of cytoskeleton, cell membrane, and gene expression; DNA damage/cell cycle arrest	Ma et al. [2011]
A549 human epithelial cell line	AgNPs: 30 nm in diameter; silver microparticles: <45 µm in	AgNPs: 0.33 mg/mL; silver nanoparticles: 13.5	24- and 48-hr incubation	Strong cytotoxicity, loss in cell viability, and early calcium		Cell damage and resulting cell death hypothesized by investigator as	Stoehr et al. [2011]

*This information is distributed solely for the purpose of pre-dissemination peer review under applicable information quality guidelines. It has not been formally disseminated by the National Institute for Occupational Safety and Health. It does not represent and should not be construed to represent any agency determination or policy.*

Cell Type	Particle Characteristics	Exposure Details		Major Outcomes	NOAEL/LOAEL	Comments	Reference
		Concentrations/Doses	Duration				
	diameter; AgNWs: 1.5–25 µm in length, 100–160 nm in diameter (all particles coated with PVP)	mg/mL; AgNWs: 5.05–16.47 mg/mL		influx with AgNWs; AgNPs and silver microparticles had minimal effect on A549 cells		being caused by the needle-like structure of the AgNWs	
Human epithelial cell line	15.9 nm average particle size	12.1 µg/mL	24- and 48-hr incubation	Altered the regulation of more than 1000 genes (twofold regulation); intracellular production of reactive oxygen species		Did not induce apoptosis or necrosis	Foldbjerg et al. [2012]
Human epidermal keratinocytes	Three unwashed colloids of 20, 50, and 80 nm in diameter; 3 washed colloids of 20, 50, and 80 nm in diameter; 2 carbon-coated powders 25 and 35 nm in diameter	0.000544–1.7 µg/mL	24-hr incubation	Loss of cell viability observed in unwashed AgNPs; increases in TNF-α, IL-1β, IL-6, and IL-8; decrease in cell viability for unwashed AgNPs <1.7 µg/mL	NA / 0.34 µg/mL (unwashed AgNPs)	Toxicity of AgNPs might be influenced by residual contaminants in the AgNP preparations and not necessarily by the particles themselves	Samberg et al. [2010]
Human platelets (washed)	100 nm in diameter; solution in nonaggregated form by ultrasonication and vortexing;	50, 100, and 250 µg/mL	5 min	Dose-dependent increase in platelet aggregation with increased concentration of nanoparticles but		Enhance platelet aggregation and pro-coagulant activity, with possible intermediary role for intracellular	Jun et al. [2011]

This information is distributed solely for the purpose of pre-dissemination peer review under applicable information quality guidelines. It has not been formally disseminated by the National Institute for Occupational Safety and Health. It does not represent and should not be construed to represent any agency determination or policy.

Cell Type	Particle Characteristics	Exposure Details		Major Outcomes	NOAEL/LOAEL	Comments	Reference
		Concentrations/Doses	Duration				
	colloidal dispersion (microparticles 5,000–8,000 nm in diameter) used for comparison			not microparticle-borne silver		calcium and sub-threshold levels of thrombin	
<b>Animal Cells</b>							
Rat alveolar macrophages	15, 30, 55, 100 nm in diameter	0, 5, 10, 25, 50, and 75 µg/mL	Cells at 80% confluence were incubated 24 hrs	Same as Hussain et al. [2005b]; treatment-related increase in TNF-α, macrophage inflammatory protein-2, IL-1β, in the supernatant of macrophage/AgNP incubations	NA	Oxidative stress; cellular damage.	Carlson et al. [2008]
Rat alveolar macrophages	15, 30, 55, 100 nm in diameter	5–50 µg/mL	Cells at 80% confluence incubated 24 hrs	Smaller-diameter AgNPs more effective than larger NPs at physiologic and toxicological changes	NA	Oxidative stress; cellular damage	Hussain et al. [2005b]
BRL 3A rat liver cells	15 or 100 nm in diameter	5–50 µg/mL	Incubation times up to 24 hrs	Both cell sizes induced a concentration-dependent depletion of mitochondrial function; release of LDH to culture medium	NA	Cytotoxicity through oxidative stress	Hussain et al. [2005a]

*This information is distributed solely for the purpose of pre-dissemination peer review under applicable information quality guidelines. It has not been formally disseminated by the National Institute for Occupational Safety and Health. It does not represent and should not be construed to represent any agency determination or policy.*

Cell Type	Particle Characteristics	Exposure Details		Major Outcomes	NOAEL/LOAEL	Comments	Reference
		Concentrations/Doses	Duration				
NIH3T3 fibroblasts	Ag 1–100 nm in diameter; non-nano Ag <250 µm in diameter	50 and 100 µg/mL	24 hrs for AgNPs; up to 72 hrs for non-nano Ag	Link between mitochondrial-related generations of ROS and incidence of apoptosis and activation of JNK; non-nano Ag not cytotoxic and no effect on apoptosis		Results similar to those for Piao et al. [2011]	Hsin et al. [2008]
Primary mouse fibroblasts and liver cells	>90% of particles 7–20 nm in diameter	IC50 values were 61–449 µg/mL	24-hr incubation	Primary cell preparations contained sufficient antioxidant capacity to protect cells from possible oxidative damage		Study similar to Arora et al. [2008], but oxidative stress and apoptosis were less evident	Arora et al. [2009]
L929 fibroblasts	AgNPs: 50–100 nm; Ag microparticles: 2–20 µm	10, 25, 50, 100 µg/mL	24-hr incubation	Greater percentage of cells arrested in G2M phase of cell cycle		Increased incidence of apoptosis; AgNPs caused greater level of apoptosis than did Ag microparticles at same dose	Wei et al. 2010
Murine lung macrophage (RAW 264.7)		5 µg/mL				Cytotoxic response	Soto et al. [2007]

*This information is distributed solely for the purpose of pre-dissemination peer review under applicable information quality guidelines. It has not been formally disseminated by the National Institute for Occupational Safety and Health. It does not represent and should not be construed to represent any agency determination or policy.*

Cell Type	Particle Characteristics	Exposure Details		Major Outcomes	NOAEL/LOAEL	Comments	Reference
		Concentrations/Doses	Duration				
Mouse embryonic stem cells, mouse embryonic fibroblasts	Uncoated plasma gas-synthesized AgNPs & polysaccharide-coated AgNPs, both approx. 25 nm in diameter	50 µg/mL	4-, 24-, 48-, and 72-hr incubation	Increased induction of the Rad51 double-strand break repair protein; enhanced phosphorylation of the histone H2AX at the serine-139 residue		Increased p53 expression and double DNA breakage, with concomitant apoptosis in both cells within 4 hrs after exposure	Ahamed et al. [2008]
Mouse fibroblast (L929) tumor cells	Median diameter of 12 nm; synthesized by chemical reduction of silver chlorate with sodium borohydride and sodium citrate	0, 11, 22 µg/mL	72-hr incubation	Formation of cells with single giant nuclei or cells with two, three, or sometimes four nuclei per cell		Induced malsegregation of the chromosomes rather than having direct effect on replication	Nallathamby and Xu [2010]
Mouse lymphoma assay system	4–12 nm in diameter; average size ~5 nm; uncoated	5 µg/mL	4-hr incubation	Observed in the cytoplasm of the lymphoma; DNA breaks; expressions of 17 of the 59 genes on the arrays were altered in the cells		Induced dose-dependent cytotoxicity and mutagenicity	Mei et al. [2012]
Rat brain microvessel vascular endothelial cells; astrocytes to model a blood-brain barrier	AgNPs: 50–100 nm in diameter; Ag microparticles: 2–20 µm in diameter	100 µg/mL	4-hr incubation	AgNPs readily crossed the barrier, whereas silver microparticles did not		Morphologic disruption, with large vacuole formation and signs of necrosis of cellular organelles	Tang et al. [2010]
Sprague-Dawley rat primary brain	25, 40, and 80 nm in diameter;	Cytotoxicity: 1.95–15.63 µg/cm <sup>2</sup> ;	24-hr incubation	ROS generation; increase in		Cell viability more severely affected	Trickler et al. [2010]

*This information is distributed solely for the purpose of pre-dissemination peer review under applicable information quality guidelines. It has not been formally disseminated by the National Institute for Occupational Safety and Health. It does not represent and should not be construed to represent any agency determination or policy.*

Cell Type	Particle Characteristics	Exposure Details		Major Outcomes	NOAEL/LOAEL	Comments	Reference
		Concentrations/Doses	Duration				
microvessel endothelial cells (rBMECs)	spherical; PVP-coated	prostaglandin E <sub>2</sub> and cytokine release in rBMECs: 10.4 µg/cm <sup>2</sup> ; cell morphology: 5.2 µg/cm <sup>2</sup>		microvascular permeability; release of prostaglandin E <sub>2</sub> and cytokines TNF-α, IL-1β, and IL-2		in cultures exposed to the 25- and 50-nm diameters; cerebral microvascular damage	
HEL-30 mouse keratinocytes	15-, 25-, or 55-nm diameter (coated with hydrocarbon); 80- or 130-nm diameter (not coated)	25, 40, 50, 65, and 100 µg/mL	24-hr incubation	Onset of apoptosis at 25 µg/mL	NA	The 15-, 25-, and 55-nm particles induced greater degrees of toxicity than the larger (uncoated) particles	Amato et al. [2006]
L929 mouse fibroblasts, RAW 264.7 and D3 embryonic stem cells	20-, 80-, 110-nm-diameter AgNPs, mostly spherical	0.1–100 µg/mL	24 hrs for RAW 264.7 and L929; 10 days for D3 cells	For L929 and RAW 264.7: metabolic activity highest with 20-nm AgNPs; RAW 264.7: increased ROS generation with 20-nm AgNPs; L929: compromised cell membrane integrity with all sizes	NA	Toxicity of AgNPs and silver ions dependent on particle size and cell type	Park et al. [2011c]
Cell lines: Osteoblastic MC3T3-E1, PC12, rat adrenal medulla, human cervical	10-, 50-, 100-nm-diameter AgNPs	10, 20, 40, 80, or 160 µg/mL: after 24-hr incubation, concentrations were 1,2,4, 8, and 16 µg	Additional incubation for 24, 48, or 72 hrs	Size- and dose-dependent cellular toxicity for all cell lines; ROS generation and cytotoxicity	NA	Toxicity of AgNPs dependent on particle size and cell type; effect may be related to cellular uptake	Kim et al. [2012]

This information is distributed solely for the purpose of pre-dissemination peer review under applicable information quality guidelines. It has not been formally disseminated by the National Institute for Occupational Safety and Health. It does not represent and should not be construed to represent any agency determination or policy.

Cell Type	Particle Characteristics	Exposure Details		Major Outcomes	NOAEL/LOAEL	Comments	Reference
		Concentrations/Doses	Duration				
cancer, HeLa, CHO				increased as size and concentration of AgNPs increased		processes from cell membrane to nuclear pores	
Dalton's lymphoma cell lines	50 nm in diameter; produced in <i>Bacillus licheniformis</i> cultures incubated in the presence of silver nitrate	Silver concentration of 500 nM was calculated for the IC <sub>50</sub>	24-hr incubation	Measurement of caspase 3 in cell lysates showed marked increase in activity in comparison with controls; fragmentation of DNA indicated presence of double-strand breaks	NA	Data indicated a potential antitumor property of AgNPs and the relevance of apoptosis to this process	Sriram et al. [2010]
J774.1 (murine macrophage)	AgNP, spherical, citrate-capped, 20-, 60-, 100-nm; AgNO <sub>3</sub> (as Ag ion source)	0, 5, 10, 50, 100 µg/mL	24-hr incubation (cytotoxicity), 3-hr (speciation, lysosome imaging)	20- and 60-nm more toxic than 100-nm. AgNO <sub>3</sub> more toxic than AgNP. AgNP bound to high MW proteins, while Ag ions bound to metallothioneins.	NA	Ag ions only adversely affected viability at greater than 2.5 µg/mL.	Arai et al. [2015]
HL-60 (tumoral human leukemia), HepG2 (hepatoma cells)	AgNP, citrate-stabilized, 30–123-nm	0.84, 1.68, 3.37, 6.72, 13.45 µg/mL	24-, 48-, 72-hr incubation	N-acetyl-L-cysteine rescues AgNP-exposed cells, indicating AgNP toxicity has an oxidative stress-related mechanism	NA		Avalos et al. [2013]

*This information is distributed solely for the purpose of pre-dissemination peer review under applicable information quality guidelines. It has not been formally disseminated by the National Institute for Occupational Safety and Health. It does not represent and should not be construed to represent any agency determination or policy.*

Cell Type	Particle Characteristics	Exposure Details		Major Outcomes	NOAEL/LOAEL	Comments	Reference
		Concentrations/Doses	Duration				
HPF (human pulmonary fibroblasts)	AgNP, spherical, 4.7-, 42-nm	0.84, 1.68, 3.37, 6.72, 13.45, 100, 500, 2000 µg/mL	24-, 48-, 72-hr incubation	4.7-nm AgNPs were more toxic than 42-nm. AgNP exposure depletes GSH, indicating oxidative stress.	NA		Avalos Funez et al. [2015]
16HBE (human bronchial epithelial), HUVEC (human umbilical vein endothelial), THP-1 (human acute monocytic leukemia) differentiated to macrophages	AgNP, spherical, 10-, 20-, 50-, 100-nm, in 2-mM Sodium Citrate	0.03–30 µg/cm <sup>2</sup>	24-hr incubation	AgNP exposure did not significantly affect transepithelial cell resistance. Dose response tended towards mass (rather than surface area) for co-culture models. Lower MCP-1 and IL-8 production in co-culture models.	NA	AgNP did not release ions in culture medium or artificial lysosomal fluid (ph 4.6). 10- and 20-nm (but not 50- or 100-nm) AgNP induced acellular ROS generation.	Braakhuis et al. [2016]
A549 (human lung epithelial)	AgNP, spherical, 40–90-nm	25, 50, 100, 200 µg/mL	24-, 48-, 72-hr incubation	AgNP causes ROS formation, cytotoxic effects, apoptosis, S phase cell cycle arrest and proliferating cell nuclear antigen. N-acetyl-L-cysteine rescues AgNP-exposed cells from cytotoxicity and apoptosis.	NA		Chairuangkitti et al. [2013]

*This information is distributed solely for the purpose of pre-dissemination peer review under applicable information quality guidelines. It has not been formally disseminated by the National Institute for Occupational Safety and Health. It does not represent and should not be construed to represent any agency determination or policy.*

Cell Type	Particle Characteristics	Exposure Details		Major Outcomes	NOAEL/LOAEL	Comments	Reference
		Concentrations/Doses	Duration				
SH-SY5Y (human blastoma), D384 (human astrocytoma), A549 (human lung epithelial)	AgNP, 20–100-nm, AgNO <sub>3</sub> (as Ag ion source)	1–100 µg/mL	4–48-hr (short-term), 10-day (long-term)	Cerebral cell lines were more sensitive than lung cell lines to AgNP toxicity. Ag ions had stronger effects than AgNP.	NA	AgNP doses less than 18 µg/mL were not cytotoxic.	Coccini et al. [2014]
RTH-149 (rainbow trout liver), RTL-W1 (rainbow trout liver), RTG-2 (rainbow trout gonadal)	NM-300K AgNP, 4- and 25-nm, AgNO <sub>3</sub> (as Ag ion source)	0.73–93.5 µg/mL (AgNP); 0.0345–345 µg/mL (Ag ion)	24-hr	AgNP is similarly toxic to Ag ion, but media conditions significantly impact toxicity. This is expected to be a function of protein effects on agglomeration.	NA	IC50 values ranged from 0.4 to 3.8 µg/mL for RTH-149 and RTL-W1, or 10.9 to 32.2 µg/mL for RTG-1. Authors postulated that AgNP acts on lysosome walls.	Connolly et al. [2015]
C3A (human hepatoblastoma)	NM-300 AgNP	0–625 µg/cm <sup>2</sup> (LDH), 1 µg/cm <sup>2</sup> (microscopy), 1, 2, 4 µg/cm <sup>2</sup> (GSH), 0-40 µg/cm <sup>2</sup> (cytokine release)	24-hr (LDH and microscopy), 2-, 6- 24-hr (GSH)	AgNPs are toxic to C3A cells (LD50 ~ 20 µg/cm <sup>2</sup> ). AgNP identified in cytoplasm and nucleus. Low dose does not affect C3A activity, but upregulates IL-8 and TNF-α expression.	NA	Study also included in-vivo component (not discussed here).	Gaiser et al. [2013]
HepG2 (hepatoma cells)	PVP-AgNP, 30-nm, AgNO <sub>3</sub> (as Ag ion source)	2–20 µg/L (PVP-AgNP), 5-211 µg/L (Ag ion)	24-hr	PVP-AgNP affected transcription-factor pathways that AgNO <sub>3</sub> did not.	NA	Study also included in-vivo component (not discussed here).	Garcia-Reyero et al. [2014]

*This information is distributed solely for the purpose of pre-dissemination peer review under applicable information quality guidelines. It has not been formally disseminated by the National Institute for Occupational Safety and Health. It does not represent and should not be construed to represent any agency determination or policy.*

Cell Type	Particle Characteristics	Exposure Details		Major Outcomes	NOAEL/LOAEL	Comments	Reference
		Concentrations/Doses	Duration				
HUVEC (human umbilical vein endothelial)	AgNP, 10-, 75-, 110-nm in 2 mM sodium citrate; AgNO <sub>3</sub> (as Ag ion source)	1–40 µg/mL	24-hr	Cytotoxicity occurred at lower dose for Ag ion than AgNP. Ag ions promoted necrosis; AgNP promoted apoptosis, cell detachment, ROS production, and shorted cytoskeleton actin fibers.	NA	Study also included in-vivo component (not discussed here).	Guo et al. [2016]
C1C10 (mouse Balb/C NAL-1A type II pneumocyte), MLE12 (FVN/N mouse SV40 transformed lung epithelial), LA-4 (A/He mouse adenoma lung epithelial)	AgNP, spherical, 20- and 100-nm, citrate- or PVP-stabilized	6.25, 12.5, 25, and 50 µg/mL	24-hr	Smaller AgNP were more cytotoxic and faster to dissolve in lysosome. Coating difference had no discernable effect.	NA	Cell lines varied significantly in response.	Hamilton et al. [2015]
A549 (human lung epithelial)	AgNP, 15-nm, two versions: one synthesized from an E. coli supernatant by addition of AgNO <sub>3</sub> (bio-AgNP); the other by citrate-mediated synthesis (chem-AgNP)	0–50 µg/mL (bio-AgNP) and 0–100 µg/mL (chem-AgNP)	24-hr	Both AgNPs cause cytotoxicity, increase intracellular ROS, and localize in autophagosomes and autolysosomes. AgNP promotes apoptosis.	NA	Bio-AgNP had a stronger effect than chem-AgNP in each case. No endotoxin assay reported.	Han et al. [2014]

This information is distributed solely for the purpose of pre-dissemination peer review under applicable information quality guidelines. It has not been formally disseminated by the National Institute for Occupational Safety and Health. It does not represent and should not be construed to represent any agency determination or policy.

Cell Type	Particle Characteristics	Exposure Details		Major Outcomes	NOAEL/LOAEL	Comments	Reference
		Concentrations/Doses	Duration				
VcAP (prostate cancer), BxPC-3 (pancreas cancer), H1299 (lung cancer)	AgNP, spherical, 8–22-nm	2, 5, 8, 10, 20, and 30 µg/mL (viability); 2, 5, 10, 15, and 20 µg/mL (NF-κB); 10 µg/mL (Western blot)	72-hr (viability), 24-hr (NF-κB), unknown (apoptosis, Western blot)	AgNP exposure reduced NF-κB activity, decreased BCL-2 expression and increased caspase-3 and survivin expression.	NA	Cell lines had differing sensitivity to AgNP (H1299 > BxPC-3 > VCaP). LC50 of H1299 between 5- and 8-µg/mL.	He et al. [2016]
A549 (human lung epithelial), MDM (monocyte-derived macrophage), MDDC (monocyte-derived dendritic cells)	AgNP, 33.4-nm, citrate-coated; AgNO <sub>3</sub> (as Ag ion source)	30–278 ng/cm <sup>2</sup>	4-h, 24-h	No significant toxicity at most AgNP and AgNO <sub>3</sub> concentrations.	NA		Herzog et al. [2013]
A549 (human lung epithelial), MDM (monocyte-derived macrophage), MDDC (monocyte-derived dendritic cells)	AgNP, PVP-coated.	10, 20 and 30 µg Ag/mL	4-, 24-hr	Cultures submerged expressed lower response than those at the air-liquid interface.	NA	All cell lines were co-cultured.	Herzog et al. [2014]
16HBE (human bronchial epithelial), HUVEC (human umbilical vein endothelial),	NM-300K AgNP, 20-nm; AgNO <sub>3</sub> (as Ag ion source)	1.5, 3, 6, 12, 24 µg/cm <sup>2</sup>	6-, 12-, 24-hr	AgNP exposure causes unfolded protein response in 16HBE cells, but not in HUVEC or HEPG2 cells. Ag ions were more	NA	Study also included in-vivo component (not discussed here).	Huo et al. [2015]

*This information is distributed solely for the purpose of pre-dissemination peer review under applicable information quality guidelines. It has not been formally disseminated by the National Institute for Occupational Safety and Health. It does not represent and should not be construed to represent any agency determination or policy.*

Cell Type	Particle Characteristics	Exposure Details		Major Outcomes	NOAEL/LOAEL	Comments	Reference
		Concentrations/Doses	Duration				
HEPG2 (human hepatoblastoma)				cytotoxic than AgNPs to all cell lines.			
BEAS-2B (human bronchial epithelial), organ-donor derived HBE (human bronchial epithelial)	spark-generated AgNP and CNP, 20-nm	4×10 <sup>7</sup> , 4×10 <sup>8</sup> , 4×10 <sup>9</sup> , AgNP/cm <sup>2</sup> ; 3.5×10 <sup>8</sup> , 3.5×10 <sup>9</sup> , 2×10 <sup>10</sup> , CNP/cm <sup>2</sup>	4-, 24-hr	AgNP exposure increased IL-6 and IL-8 secretion but reduced MCP-1 secretion. Cystic fibrotic cells were more sensitive.	NA		Jeanett et al. [2016]
C3A (human hepatoblastoma)	NM-300 AgNP 17-nm, ZnO, TiO <sub>2</sub> , MWCNT	1.25, 2.5, 5, 10, 20, 40, 80 µg/cm <sup>2</sup>	24-hr (antioxidants, GSH, DCFH-DA), 6-hr (Comet assay), 8 week (long term Comet assay)	AgNP had greater cytotoxicity than TiO <sub>2</sub> -NP, ZnO NP, or MWCNT. AgNP toxicity was prevented by pre-treatment with anti-oxidants. AgNP was less genotoxic than other selected exposures at LC 20, and no significant difference was found between the short- and long-term studies. IL-8 was upregulated for all NP exposures.	NA	AgNP LC50 was between 1.25 and 2.5 µg/cm <sup>2</sup> .	Kermanizadeh et al. [2012, 2013]

*This information is distributed solely for the purpose of pre-dissemination peer review under applicable information quality guidelines. It has not been formally disseminated by the National Institute for Occupational Safety and Health. It does not represent and should not be construed to represent any agency determination or policy.*

Cell Type	Particle Characteristics	Exposure Details		Major Outcomes	NOAEL/LOAEL	Comments	Reference
		Concentrations/Doses	Duration				
CHO-K1 (Chinese hamster ovary)	AgNP, 40–59-nm	0.01, 0.1, 1, 10 µg/mL	24-hr	AgNP exposure induced genotoxicity in CHO-K1 cells.	NA	Increase in DNA tail moment noted at 0.01-µg/mL Ag, MN formation at 0.1-µg/mL Ag.	Kim et al. [2013a]
Primary tenocytes from Sprague Dawley rats	AgNP, synthesized 5–10-nm	1, 10, 20 µM	42-days	AgNP exposure improved tendon healing and tensile modulus recovery.	NA	No AgNP toxicity shown at under 20 µM.	Kwan et al. [2014]
BEAS-2B (human bronchial epithelial),	PVP-coated AgNP, 42.5-nm	0.5, 1, 2, 4, 6, 8, 12, 24 and 48 µg/cm <sup>2</sup> (corresponding to 1.9, 3.8, 7.6, 15.2, 22.8, 30.4, 45.6, 91.2, and 182.4 µg/mL) (cytotoxicity); 2, 4, 8, 16, 24, 36 and 48 µg/cm <sup>2</sup> (corresponding to 7.6, 15.2, 30.4, 60.8, 91.2, 136.8, 182.4 µg/mL) (Comet, micronucleus, chromosomal aberration assays)	4-, 24-, 48-hr (cytotoxicity); 4-, 24-hr (Comet assay); 48-hr (micronucleus assay); 24-h (chromosomal aberration assay)	At 60.8-µg/mL, DNA damage (tail moment) increased. Micronuclei formation and chromosomal aberrations did not increase.	NA	Cytotoxicity assays needed to extrapolate from pre-apoptotic populations.	Nymark et al. [2013]
HepG2 (hepatoma cells), PBMC (peripheral blood and mononuclear cells)	PVA-coated AgNP, 4.0–11.7-nm	1.0 and 50.0 µM	24-hr	1 and 50 µM AgNP increased DNA damage, apoptosis, and necrosis (except for 1 µM in HepG2).	NA		Paino et al. [2015]

This information is distributed solely for the purpose of pre-dissemination peer review under applicable information quality guidelines. It has not been formally disseminated by the National Institute for Occupational Safety and Health. It does not represent and should not be construed to represent any agency determination or policy.

Cell Type	Particle Characteristics	Exposure Details		Major Outcomes	NOAEL/LOAEL	Comments	Reference
		Concentrations/Doses	Duration				
HEPG2 (human hepatoblastoma) , Caco2 (human colon carcinoma)	AgNP, 50-nm; AgC <sub>2</sub> H <sub>3</sub> O <sub>2</sub>	1.0, 2.5, 5.0, 10.0, 15.0 µg/mL	4-, 24-, 48-hr	AgNP cause micronuclei formation and potentially apoptosis. HepG2 cells are more sensitive than Caco2. AgNP also decreased mitochondria membrane potential. No AgNP-induced ROS detected. AgNP is more toxic from 0.1–1.0-µg/mL, Ag ions more toxic 10–20-µg/mL.	NA	Studies linked because of their similarity in materials, models, and endpoints, though specific methods varied.	Sahu et al. [2014a, 2014b, 2014c]
HEPG2 (human hepatoblastoma) , Caco2 (human colon carcinoma)	AgNP, 50-nm; AgC <sub>2</sub> H <sub>3</sub> O <sub>2</sub>	1, 3, 5, 10, 20 µg/mL	24-hr	Ag ion caused cytotoxicity at lower concentrations than AgNP. 50-nm AgNP induce micronuclei and are genotoxic to HEPG2 cells, but not Caco2 cells. Ag ion exposure does not cause micronuclei.	NA	Comparisons were made to the results of Sahu et al. [2014a, 2014b, 2014c]	Sahu et al. [2016a, 2016b]
Primary PBMC (peripheral blood and mononuclear	AgNP, spherical, 20- and 110-nm, citrate- or PVP-stabilized	5, 10, 20 and 50 µg/mL	3-, 6-, 24-hr	AgNP can reduce MDM viability, increase IL-8 expression, and	NA	Toxic effects were noted regardless of whether citrate	Sarkar et al. [2015]

This information is distributed solely for the purpose of pre-dissemination peer review under applicable information quality guidelines. It has not been formally disseminated by the National Institute for Occupational Safety and Health. It does not represent and should not be construed to represent any agency determination or policy.

Cell Type	Particle Characteristics	Exposure Details		Major Outcomes	NOAEL/LOAEL	Comments	Reference
		Concentrations/Doses	Duration				
cells) differentiated to MDM (macrophages)				suppress immune responses to M.tb (including IL-1B, IL-10, and TNF- $\alpha$ expression) and other NF- $\kappa$ B-related genes.		or PVP was used as a stabilizer.	
BMM (bone marrow-derived macrophages from 8-wk old wild-type C57/Bl6 mouse)	AgNW, 3-, 5-, 10-, 14-, 28- $\mu$ m length, 115 – 122-nm diameter	2.5 $\mu$ g/cm <sup>2</sup>	Up to 30-hr	AgNW over 5- $\mu$ m impair mobility in wound closure.	NA	Study also included in-vivo component (not discussed here).	Schinwald et al. [2012]
RLE (rat liver epithelial) RAEC (rat aortic endothelial)	AgNW, citrate coated	25 $\mu$ g/ml (uptake); 6.25, 12.5, 25, 50 $\mu$ g/ml (cytotoxicity); 50 $\mu$ g/ml (activation)	2-hr (uptake); 3-, 6-hr (cytotoxicity); 1-hr (activation)	Protein corona reduces AgNP uptake by cells; corona lost after uptake. SR-BI mediates AgNP uptake. AgNP induce IL-6 expression.	NA		Shannahan et al. [2015]
16HBE (human bronchial epithelial), THP-1 (human acute monocytic leukemia)	AgNP pristine (90-nm), aged paint (652-nm)	1, 3, 9, 27, 81 and 243 $\mu$ g/mL	24-hr	Aged paint NPs less toxic than pristine NPs.	NA	A co-culture was used in this study. NPs studied were not from the same paints prior to aging.	Smulders et al. [2015b]
A549 (human lung epithelial), HaCat (keratinocyte)	AgNP, synthesized; Ag <sub>2</sub> SO <sub>4</sub> (as Ag ion source)	1.0, 2.5, 5.0, 10 $\mu$ M AgNP; 100, 250, 500, 750 nM Ag <sub>2</sub> SO <sub>4</sub>	24-, 48hr	AgNP and/or Ag ions inhibit selenoprotein synthesis.	NA	Ag ions affected selenoprotein synthesis at lower concentrations.	Srivastava et al. [2012]
HSC (rat hepatic stellate cells)	PVP-coated AgNP, 10- and 30–50-nm	20, 100 and 250 $\mu$ g/ml (cytotoxicity); 20 and 100 $\mu$ g/ml	96-hr (cytotoxicity), 24-hr	PVP-AgNP have low acute (sub 4-hr) toxicity, but	NA		Sun et al. [2013]

*This information is distributed solely for the purpose of pre-dissemination peer review under applicable information quality guidelines. It has not been formally disseminated by the National Institute for Occupational Safety and Health. It does not represent and should not be construed to represent any agency determination or policy.*

Cell Type	Particle Characteristics	Exposure Details		Major Outcomes	NOAEL/LOAEL	Comments	Reference
		Concentrations/Doses	Duration				
		(Cell IQ), 20 µg/ml (Cytokine detection)	(apoptosis), 4-hr (LDH assay); 72-hr (Cell IQ); 2-days (Cytokine detection)	exposure causes apoptosis in a dose and inversely size-dependent manner. AgNP exposure inhibits MMP-2 and -9 production.			
184B5, MCF-7, MCF-10A, TNBC (triple-negative breast cancer) [MDA-MB-231 (human mammary epithelial cells), BT-549, SUM-159]	PVP-coated AgNP, 20–30-nm	0–100 µg/ml	24-hr	TNBCs were more sensitive to AgNPs than other models. Ag ions did not have same effects AgNP.	NA	Study also included in-vivo component (not discussed here).	Swanner et al. [2015]
isolated mitochondria from Wistar rat livers	AgNP, 40- or 80-nm	2, 5 µg AgNP/mg protein	Unknown	AgNP increase mitochondrial permeability, decrease function.	NA		Teodoro et al. [2011]
HEPG2 (human hepatoblastoma), HCT116 (human colon carcinoma), A549 (human lung epithelial), MCF-7 (human caucasian breast adenocarcinoma)	Ag-incorporating zeolites	0.78, 1.56, 3.125, 6.25, 12.5, 25, 50, 100 µg/mL	48-hr	Cell responses vary significantly between cell lines. All lines had LD50s under 15 µg/mL AgNP.	NA	Ag-incorporation into zeolites was part of experimental procedure.	Youssef et al. [2015]

This information is distributed solely for the purpose of pre-dissemination peer review under applicable information quality guidelines. It has not been formally disseminated by the National Institute for Occupational Safety and Health. It does not represent and should not be construed to represent any agency determination or policy.

<b>Bacteria/Viruses</b>							
Four histidine-requiring strains of <i>Salmonella typhimurium</i> (TA98, TA100, TA1535, TA1537); one tryptophan-requiring strain of <i>Escherichia coli</i> (WP2uvrA)	10 nm average particle size; colloidal; absence of metabolic activation; presence of metabolic activation	0, 7.8, 15.6, 31.2, 62.5, 125, 250, 500 and 1000 µg/mL	6- and 24-hr incubation	No significant number of revertant colonies observed in any strain, regardless of metabolic activation; no significant increase in cells with polyploidy or endoreduplication, regardless of metabolic activation	NA	Absence of metabolic activation: cytotoxic effect at 15.6 µg/mL; Presence of metabolic activation: cytotoxicity induced above 31.2 µg/mL	Kim et al. [2013]
<i>E. coli</i> (wild-type K12 strain MG1655) with bovine serum albumin	Spherical AgNPs: 9.3 nm in diameter	AgNPs: 0.4 and 0.8 nm; AgNO <sub>3</sub> : 6 and 12 nm	5–30 min	Short-term incubation of <i>E. coli</i> with AgNPs provided evidence of membrane destabilization; reduction in membrane potential; depletion of intracellular potassium and ATP	NA	Silver presented in the nanoparticle form was more efficient at deterring bacterial growth	Lok et al. [2006]

## **D.8 Dermal Absorption (in Vitro)**

A series of experiments by Larese et al. [2009] examined the capacity of AgNPs to penetrate human skin in vitro. The researchers used Franz diffusion cells to monitor the penetration of silver through either intact or abraded previously frozen, full-thickness skin preparations. The preparation was a 0.14-weight percent suspension of PVP--coated AgNPs in ethanol, with a mean diameter of  $25 \pm 7.1$  nm (range, 9.8–48.8 nm). The use of a PVP coat ensured structural stability of the particles and deterred aggregation. The particles were applied to the skin in a 1:10 dilution of synthetic sweat (pH, 4.5). After 24 hours, median silver concentrations of 0.46 and 2.32 nanograms per square centimeter ( $\text{ng}/\text{cm}^2$ ) were obtained in the receptor fluid for intact and damaged skin, respectively. Penetration of silver proceeded in a linear fashion between 4 and 24 hours through abraded skin but leveled off after approximately 8 hours in intact skin. The absorption rates of silver through abraded skin were about fivefold higher than for intact skin. Using TEM, the authors observed silver deposition in the stratum cornea and upper layers of the epidermis.

## APPENDIX E

### Toxicological and Toxicokinetic Effects of Silver Nanoparticles in Experimental Animal Studies

#### E.1 Inhalation Exposure

##### E.1.1 Toxicokinetics

The absorption and distribution of AgNPs via the inhalation route were studied in 16 female F344 rats that received a single 6-hour exposure to AgNPs at a concentration of 133  $\mu\text{g}/\text{m}^3$  and subsequently were killed (four animals per time point) at 0, 1, 4, or 7 days post-exposure [Takenaka et al. 2001]. The AgNPs, as generated by a spark discharging through an argon atmosphere, were compact and spherical, with a median diameter of  $17 \pm 1.2$  nm (GSD = 1.38) and minimal aggregation. Groups of four rats were killed on days 0, 1, 4, and 7 following exposure. Immediately after exposure, silver was detected at elevated concentrations in the lungs, nasal cavity, liver, and blood, but the concentrations declined over time. The researchers detected a total of 1.7  $\mu\text{g}$  of silver in the lungs immediately after exposure had ended, by using inductively coupled plasma mass spectroscopy (ICP-MS cannot differentiate elemental from ionic silver). However, this amount dropped quickly, and only about 4% of the initial pulmonary burden was present after 7 days. Evidence that absorption of the nanoparticles had occurred came from the detection of 8.9 nanograms per gram wet weight (ng/g) silver in the blood on the first day. This was lower in subsequent analyses, as silver was distributed to secondary target tissues such as the liver, kidney, heart, and tracheobronchial lymph nodes. Absorption data for inhaled AgNPs were compared with those obtained when 150 microliters ( $\mu\text{L}$ ) of an aqueous solution of silver nitrate was intratracheally instilled in 12 animals. Similarly, in another phase of the experiment, a 150- $\mu\text{L}$  aqueous suspension of AgNPs was intratracheal instilled in seven animals. A significant amount of aggregation of the AgNPs had occurred in the latter preparation, and in contrast to the findings with monodisperse AgNPs, up to 32% of the silver from the aggregated preparation was retained in the alveolar macrophages after 4 or 7 days.

1 The water-soluble silver was rapidly cleared from the lungs in a manner similar to that of  
2 the monodispersed AgNPs, suggesting that both entities can be readily absorbed via  
3 the lungs and undergo systemic distribution. Additional studies addressing  
4 toxicokinetics following inhalation are addressed in section E.1.2 in conjunction with  
5 toxicological findings in those studies.

## 6 E.1.2 Toxicological effects

7 Inhalation studies reported by Ji et al. [2007a,b], Sung et al. [2008, 2009, 2011], and  
8 Song et al. [2013] exposed Sprague-Dawley rats to AgNPs that were generated by  
9 using a small ceramic heater and an air supply to disperse defined amounts of AgNPs  
10 from an unspecified source material into the inhalation chambers. The particles were  
11 found to be composed of elemental silver, monodispersed and spherical, with diameters  
12 predominantly in the 15–20-nm range. In the acute study, five rats per sex per group  
13 received a single 4-hour exposure to 0 particles (fresh air controls);  $0.94 \times 10^6$   
14 particles/cm<sup>3</sup> (76 µg/m<sup>3</sup> silver; low concentration);  $1.64 \times 10^6$  particles/cm<sup>3</sup> (135 µg/m<sup>3</sup>  
15 silver; mid concentration); or  $3.08 \times 10^6$  particles/cm<sup>3</sup> (750 µg/m<sup>3</sup> silver; high  
16 concentration) [Sung et al. 2011]. Mortality, clinical signs, body weight changes, food  
17 consumption, and lung function were monitored over a 2-week period after exposure. At  
18 necropsy, weights of the major organs were compared to those of controls. Lung  
19 function parameters examined included tidal volume, minute volume, respiration rate,  
20 inspiration and expiration times, and peak inspiration and expiration flows. All animals  
21 survived exposure and the 2-week observation period, and there were no clinical signs  
22 of toxicity. Food consumption and body weights were closely similar to those of controls  
23 among the groups. Likewise, lung function tests showed no significant differences  
24 between the groups and controls. Sung et al. [2011] pointed to the difficulty of  
25 generating higher concentrations of monodispersed nanoparticles in their system.  
26 Nonetheless, the authors determined that the high concentration of 750 µg/m<sup>3</sup> was 7.5  
27 times higher than the ACGIH TLV (100 µg/m<sup>3</sup>) for silver dust and probably more than  
28 600 times the particle surface area for silver dust, assuming a 4-µm diameter for the  
29 latter and a nanoparticle surface area of  $8.69 \times 10^9$  nm<sup>2</sup>/cm<sup>3</sup>. However, no acute

1 toxicological effects of AgNPs at this exposure concentration were evident in these  
2 studies.

3 In a 28-day inhalation study, the same researchers exposed ten 8-week-old specific-  
4 pathogen-free (SPF) Sprague-Dawley rats per sex per group, 6 hours/day, 5  
5 days/week, for 4 weeks to 0 particles (fresh air controls);  $1.73 \times 10^4$  AgNPs/cm<sup>3</sup> (0.48  
6  $\mu\text{g}/\text{m}^3$  silver; low concentration);  $1.27 \times 10^5/\text{cm}^3$  (3.48  $\mu\text{g}/\text{m}^3$  silver; mid concentration);  
7 or  $1.32 \times 10^6/\text{cm}^3$  (61  $\mu\text{g}/\text{m}^3$  silver; high concentration), following OECD Test Guideline  
8 412 [Ji et al. 2007b]. Respective geometric mean particle diameters (and geometric  
9 standard deviations) were 11.93 nm (0.22), 12.40 nm (0.15), and 14.77 nm (0.11); the  
10 higher diameter at the high concentration was explained as being due to agglomeration  
11 of particles. Parameters monitored included clinical signs, body weight changes, and, at  
12 term, hematology and clinical chemistry values, organ weights, tissue silver, and  
13 histopathologic effects. The body weight changes among the groups did not differ  
14 significantly from those of controls, and there were no significant organ weight changes  
15 in either males or females after 28 days of exposure to AgNPs. Although isolated  
16 fluctuations in food consumption, hematology, or clinical chemistry parameters were not  
17 considered related to treatment, Ji et al. [2007b] observed instances of cytoplasmic  
18 vacuolization in the liver of exposed animals. This response was likely due to lipid  
19 accumulation and, as a common response to hepatic injury [Eustis et al. 1990], was  
20 probably treatment related. For males there was one such case among controls, and  
21 there were four cases in the low-concentration group and one each in the mid- and  
22 high-concentration groups. For females, the effects were more dose-related; there were  
23 two cases each in the control and low-concentration groups, six in the mid-  
24 concentration group, and seven in the high-concentration group. Other histopathologic  
25 effects on the liver included two cases of hepatic focal necrosis in high-concentration  
26 males and a single case among high-concentration females. No histopathologic effects  
27 of AgNPs were seen in the kidney, spleen, lungs, adrenals, heart, reproductive organs,  
28 brain, or nasal cavity. There was also a concentration-dependent increase in the  
29 concentration of silver deposited in the lungs. Likewise, silver was readily detected in  
30 the liver and brain of animals exposed at the high concentration but only marginally so

1 in the blood, suggesting rapid clearance from the bloodstream to the tissues after  
2 inhalation.

3 The South Korean group also examined the potential effects of inhaled AgNPs on the  
4 respiratory mucosa of Sprague-Dawley rats [Hyun et al. 2008], as studied and reported  
5 by Ji et al. [2007b]. Ten animals per sex per group were exposed 6 hours/day, 5  
6 days/week, for 28 days to 0 particles (fresh air controls);  $1.73 \times 10^4$  particles/cm<sup>3</sup> (0.5  
7  $\mu\text{g}/\text{m}^3$ ; low concentration);  $1.27 \times 10^5$  particles/cm<sup>3</sup> (3.5  $\mu\text{g}/\text{m}^3$ ; mid concentration); or  
8  $1.32 \times 10^6$  particles/cm<sup>3</sup> (61  $\mu\text{g}/\text{m}^3$ ; high concentration). Histochemical staining of the  
9 respiratory mucosa showed the number and size of neutral mucin-producing goblet cells  
10 to be increased, whereas those producing acid mucins were unchanged. No  
11 histopathologic changes were observed in the lungs or nasal cavity. Foamy alveolar  
12 macrophages were observed in rats exposed to 3.5 and 61  $\mu\text{g}/\text{m}^3$ . The toxicological  
13 significance of these changes was uncertain.

14 Sung et al. [2008, 2009] reported the toxicological effects of inhaled AgNPs from a  
15 single experiment (following OECD Test Guideline 413) in which 10 Sprague-Dawley  
16 rats per sex per group were exposed 6 hours/day, 5 days/week, for 90 days. The study  
17 was designed to identify possible adverse effects not detected in the 28-day study by Ji  
18 et al. [2007b] and Hyun et al. [2008]. AgNPs were generated and concentrations and  
19 size distributions were measured as described by Ji et al. [2007 a, b]. As reported by  
20 Sung et al. [2008], rats were exposed to 0 particles (fresh air controls);  $0.7 \times 10^6$   
21 particles/cm<sup>3</sup> (48.94  $\mu\text{g}/\text{m}^3$ );  $1.4 \times 10^6$  particles/cm<sup>3</sup> (133.19  $\mu\text{g}/\text{m}^3$ ); or  $2.9 \times 10^6$   
22 particles/cm<sup>3</sup> (514.78  $\mu\text{g}/\text{m}^3$ ). Lung function was tested weekly on four animals per  
23 dose group, 40 minutes after the end of exposure. Respective geometric mean  
24 diameters (and geometric standard deviations) were 18.30 nm (1.10), 18.71 nm (1.78),  
25 and 18.93 nm (1.59). As a mark of pulmonary inflammation, the appearance of albumin,  
26 lactate dehydrogenase, and total protein was monitored in bronchoalveolar fluid (BAL)  
27 obtained at term. Cell counts of macrophages, polymorphonuclear cells, and  
28 lymphocytes in BAL were obtained histologically. Excised pieces of lung were examined  
29 by histopathology.

*This information is distributed solely for the purpose of pre-dissemination peer review under applicable information quality guidelines. It has not been formally disseminated by the National Institute for Occupational Safety and Health. It does not represent and should not be construed to represent any agency determination or policy.*

1 Pulmonary function was evaluated weekly in four rats per sex per group by means of a  
 2 ventilated bias-flow whole-body plethysmograph to determine tidal volume, minute  
 3 volume, respiratory frequency, inspiration and expiration times, and peak inspiration and  
 4 expiration flow [Sung et al. 2008]. Among the lung function test results, tidal volume,  
 5 minute volume, and peak inspiration flow showed dose-related deficits in response to  
 6 AgNP inhalation. In addition, stained slides of lung sections indicated treatment-related  
 7 increases in the incidence of mixed cell infiltrate perivascular and chronic alveolar  
 8 inflammation, including alveolitis, granulomatous lesions, and alveolar wall thickening  
 9 and macrophage accumulation (Table E-1). In discussing their data, Sung et al. [2008]  
 10 compared the lung function deficits with those reported for subjects exposed to welding  
 11 fumes, drawing the conclusion that the cumulative lung dose of AgNPs at the high dose  
 12 ( $514.78 \mu\text{g Ag/m}^3$ ) was 10–15 times less than the welding fume exposure in terms of  
 13 mass dose for a similar level of response. Therefore, it was hypothesized that surface  
 14 area or particle number may be a more meaningful determinant of exposure than mass  
 15 when correlated with lung function deficits and associated histopathologic changes.

16 **Table E-1. Incidence and severity of silver nanoparticle–related histopathologic**  
 17 **changes in the lungs of Sprague-Dawley rats.**

Exposure Parameters	Males				Females			
	Control	Low	Mid	High	Control	Low	Mid	High
Number (particles/cm <sup>3</sup> ) × 10 <sup>5</sup>	0	6.64	14.3	28.5	0	6.64	14.3	28.5
Surface area (nm <sup>2</sup> /cm <sup>3</sup> ) × 10 <sup>9</sup>	0	1.08	2.37	6.61	0	1.08	2.37	6.61
Mass (μg/m <sup>3</sup> )	0	48.94	133.19	514.78	0	48.94	133.19	514.78
<b>Tissue deficits</b>								
Accumulation (macrophage, alveolar)	3/10	5/10	5/10	8/10	7/10	4/10	4/10	6/10
Inflammation (chronic, alveolar)	2/10	3/10	2/10	7/10	3/10	2/10	0/10	8/10
Infiltration (mixed-cell perivascular)	3/10	4/10	6/10	8/10	0/10	0/10	1/10	7/10

18 Source: Sung et al. [2008].

19

1 In the second report, data were presented on hematology and clinical chemistry  
 2 parameters, and excised pieces of the major organs and tissues were examined for  
 3 histopathology changes and silver deposition [Sung et al. 2009]. There were few, if any,  
 4 effects of AgNP administration during the in-life phase of the experiment, although one  
 5 high-concentration male died during an ophthalmologic examination. No treatment-  
 6 related effects for body weight change, food consumption or, at term, in organ weights,  
 7 hematology, or clinical chemistry parameters were observed in the remaining rats.  
 8 Tissue content of silver was dose-dependently increased in lung, liver, kidney, olfactory  
 9 bulb, brain, and whole blood, and some histopathologic lesions were noted in the liver  
 10 that appeared to be related to dose. For example, as shown in Table E-2, bile-duct  
 11 hyperplasia was noted with increased incidence in higher-concentration groups.  
 12 Furthermore, single-cell hepatocellular necrosis was seen in three of 10 high-  
 13 concentration female rats. The authors of the study suggested that their data were  
 14 indicative of a no observed adverse effect level (NOAEL) in the region of 100 µg/m<sup>3</sup> that  
 15 was consistent with the ACGIH TLV of 100 µg/m<sup>3</sup> for silver dust.

16 The finding of bile duct hyperplasia, in parallel with the lung function deficits plotted by  
 17 Sung et al. [2008], indicated statistically significant decrements. However, hepatic  
 18 effects can also be characteristic of aging rats as well as a common response to the  
 19 administration of some chemicals [Eustis et al. 1990], although the findings of dose-  
 20 dependent increases in lesions is most likely a result of AgNP exposure.

21 **Table E-2. Incidence and severity of silver nanoparticle–related histopathologic**  
 22 **changes in the livers of Sprague-Dawley rats.**

Exposure Parameters	Males				Females			
	Control	Low	Mid	High	Control	Low	Mid	High
Number (particles/cm <sup>3</sup> ) × 10 <sup>5</sup>	0	6.64	14.3	28.5	0	6.64	14.3	28.5
Surface area (nm <sup>2</sup> /cm <sup>3</sup> ) × 10 <sup>9</sup>	0	1.08	2.37	6.61	0	1.08	2.37	6.61
Mass (µg/m <sup>3</sup> )	0	48.94	133.19	514.78	0	48.94	133.19	514.78
<b>Tissue deficits</b>								

*This information is distributed solely for the purpose of pre-dissemination peer review under applicable information quality guidelines. It has not been formally disseminated by the National Institute for Occupational Safety and Health. It does not represent and should not be construed to represent any agency determination or policy.*

Bile duct hyperplasia	0/10	0/10	1/10	4/9	3/10	2/10	4/10	9/10
Hepatocellular necrosis (single cell)	0/10	0/10	0/10	0/9	0/10	0/10	0/10	3/10

1 Source: Sung et al. [2009].

2

3 Lee et al. [2010] screened for differentially expressed genes in the brains of C57Bl/6  
 4 mice exposed to AgNPs via inhalation. The nanoparticles were produced by the same  
 5 procedure described in the first paragraph of this section and had characteristics similar  
 6 to those used by other researchers [Sung et al. 2011, 2009, 2008; Hyun et al. 2008; Ji  
 7 et al. 2007a, b]. Two groups of seven male mice were exposed to silver nanoparticles  
 8 ( $1.91 \times 10^7$  particles/cm<sup>3</sup>; geometric mean diameter,  $22.18 \pm 1.72$  nm) 6 hours/day, 5  
 9 days/week, for 2 weeks. One of the exposure groups was observed for a 2-week  
 10 recovery period before being killed for necropsy. Two other groups of seven mice  
 11 served as untreated and sham-exposed controls. When total ribonucleic acid (RNA)  
 12 from the cerebrum and cerebellum was analyzed by gene microarray, the expression of  
 13 468 and 952 genes, respectively, showed some degree of response to AgNP exposure,  
 14 including several associated with motor neuron disorders, neurodegenerative disease,  
 15 and immune cell function. The use of real-time quantitative reverse-transcription  
 16 polymerase chain reaction (RT-PCR) to analyze the expression of selected genes in  
 17 whole blood identified five genes that were downregulated in response to AgNP  
 18 exposure. Expression of three of the five remained suppressed throughout the 2-week  
 19 recovery period, but expression of the other two returned to control levels during the  
 20 recovery phase. Lee et al. [2010] considered these genes to have potential as  
 21 biomarkers for recent exposure to AgNPs.

22 Kim et al. [2011a] reported on the evaluation of genotoxic potential of AgNPs that were  
 23 generated as described by Ji et al. [2007a] and Sung et al. [2008]. Male and female  
 24 Sprague-Dawley rats were exposed by inhalation for 90 days according to OECD Test  
 25 Guideline 413. Rats were exposed to AgNPs (18 nm in diameter) at concentrations of  
 26  $0.7 \times 10^6$  particles/cm<sup>3</sup> (low dose),  $1.4 \times 10^6$  particles/cm<sup>3</sup> (middle dose), and  $2.9 \times 10^6$   
 27 particles/cm<sup>3</sup> (high dose) for 6 hours per day and then killed 24 hours after the last

1 administration. The femurs were removed and bone marrow was collected and  
2 evaluated for micronucleus induction according to OECD Test Guideline 474. The in  
3 vivo micronucleus test was used for detection of cytogenetic damage. Although a dose-  
4 related increase was found in the number of micronucleated polychromatic erythrocytes  
5 (MNPCEs) in the male rats, no significant treatment-related increase in MNPCEs was  
6 found in the male and female rats in comparison with the negative controls. These  
7 findings were consistent with those reported by Kim et al. [2008], in which no  
8 genotoxicity (per in vivo micronucleus test) was found in rats following the oral  
9 administration of AgNPs for 28 days.

10 Song et al. [2013] reported the lung effects in male and female Sprague-Dawley rats (17  
11 males and 12 females per exposure group) following 12-week inhalation exposure to  
12 AgNPs (14–15 nm in diameter). Exposure concentrations were  $49 \mu\text{g}/\text{m}^3$  ( $0.66 \times 10^6$   
13  $\text{particles}/\text{cm}^3$ ; low dose);  $117 \mu\text{g}/\text{m}^3$  ( $1.41 \times 10^6$   $\text{particles}/\text{cm}^3$ ; middle dose); or  $381$   
14  $\mu\text{g}/\text{m}^3$  ( $3.24 \times 10^6$   $\text{particles}/\text{cm}^3$ ; high dose) for 6 hours per day. Lung function was  
15 measured every week during the exposure period and after cessation of exposure.  
16 Animals were killed after the 12-week exposure period and at 4 and 12 weeks after the  
17 exposure cessation. Lungs were analyzed for silver concentration with use of NIOSH  
18 Analytical Method 7300. Song et al. [2013] noted that histopathologic examination of rat  
19 lung tissue showed “a significant increase in the incidence of mixed cell infiltrate,  
20 perivascular and chronic alveolar inflammation, including alveolaritis, granulomatous  
21 lesions, and alveolar wall thickening and alveolar macrophage accumulation in both the  
22 male and female rats.” These effects were observed in the middle- and high-dose  
23 groups of male rats and in the high-dose group of female rats, at the end of the 12-week  
24 exposure. Gradual clearance of AgNPs and decreased inflammation of the lungs were  
25 observed in female rats but not in the high-dose males during the 12-week recovery  
26 period. The findings suggest a possible NOAEL of  $49 \mu\text{g}/\text{m}^3$  (low dose) and a lowest  
27 observed adverse effect level (LOAEL) of  $117 \mu\text{g}/\text{m}^3$  (middle dose), although the  
28 authors suggested that the effects at the middle dose could be considered a NOAEL on  
29 the basis of similar effects (minimal accumulation of macrophages and inflammation in  
30 the alveoli) to those observed in the control group of the study by Sung et al. [2009].

1 Some of the lung effects noted by Song et al. [2013] were reported to persist at the end  
2 of the 12-week exposure period, and male rats were observed to be more susceptible  
3 than the females to the lung effects of AgNP exposure. Lung function decreases  
4 (including tidal volume, minute volume, and peak expiratory flow) and lung inflammation  
5 were observed in male rats and persisted in the high-dose group at 12 weeks post-  
6 exposure. In female rats, no decrease in lung function was observed, and the lung  
7 inflammation showed gradual recovery after cessation of exposure [Song et al. 2013]. A  
8 dose-dependent statistically significant increase in silver concentration was observed in  
9 all tissues from the male and female rat groups exposed to AgNPs for 12 weeks, except  
10 for the female brain. Silver accumulation was still observed in some tissues at 4 weeks  
11 after the end of exposure (including the liver, kidneys, spleen, and blood, and in the  
12 ovaries in female rats). Silver concentrations remained significantly increased (in  
13 comparison with the unexposed control rats) in the liver and spleen at 12 weeks post-  
14 exposure. The silver concentrations in the kidneys also showed a sex difference, with  
15 the female kidneys containing five times more accumulated silver than the male  
16 kidneys. No histopathologic effects of silver were reported in organs other than the  
17 lungs [Song et al. 2013]. Exposure parameters and lung histopathology are summarized  
18 in Table E-3.

19

*This information is distributed solely for the purpose of pre-dissemination peer review under applicable information quality guidelines. It has not been formally disseminated by the National Institute for Occupational Safety and Health. It does not represent and should not be construed to represent any agency determination or policy.*

**Table E-3. Incidence and severity of silver nanoparticle-related histopathologic changes in the lungs of Sprague-Dawley rats.**

Exposure Parameters	Males				Females			
	Control	Low	Mid	High	Control	Low	Mid	High
Number (particles/cm <sup>3</sup> ) × 10 <sup>-5</sup>	0	6.6	14.1	32.4	0	6.6	14.1	32.4
Surface area (nm <sup>2</sup> /cm <sup>3</sup> ) × 10 <sup>-9</sup>	0	0.76	1.70	4.85	0	0.76	1.70	4.85
Mass (µg/m <sup>3</sup> )	0	48.76	117.14	381.43	0	48.76	117.14	381.43
<b>Tissue deficits – 12 weeks exposure</b>								
Accumulation (macrophage, alveolar)	0/5	1/5	3/5	5/5	0/4	0/4	0/4	4/4
Inflammation (chronic, alveolar)	0/5	0/5	3/5	5/5	0/4	0/4	0/4	4/4
Infiltration (mixed-cell perivascular)	1/5	1/5	3/5	5/5	0/4	0/4	0/4	4/4
<b>Tissue deficits – 4 week recovery</b>								
Accumulation (macrophage, alveolar)	0/4	0/4	1/4	2/4	0/4	0/4	1/4	2/4
Inflammation (chronic, alveolar)	0/4	0/4	0/4	0/4	0/4	0/4	0/4	0/4
Infiltration (mixed-cell perivascular)	2/4	0/4	0/4	0/4	0/4	1/4	0/4	0/4
<b>Tissue deficits – 12 week recovery</b>								
Accumulation (macrophage, alveolar)	1/5	0/4	2/4	3/4	0/4	0/4	1/4	0/4
Inflammation (chronic, alveolar)	0/5	0/4	0/4	1/4	0/4	0/4	0/4	0/4
Infiltration (mixed-cell perivascular)	0/5	0/4	1/4	0/4	0/4	0/4	1/4	0/4

Source: Song et al. [2013].

In a follow-up study, Dong et al. [2013] investigated the sex-dependent effect of AgNPs on the kidney gene level, based on toxicogenomic studies of kidneys from rats exposed to AgNPs via inhalation for 12 weeks. The exposure conditions were the same as those employed by Song et al. [2013], and the study included both male and female SPF Sprague-Dawley rats, divided into four groups. The male groups ( $n = 17$ ) consisted of 5 rats for 12-week exposure, 4 for 4-week recovery, 4 for 12-week recovery, and 4 for micronucleus testing after 12-week exposure. The female groups ( $n = 13$ ) consisted of 5 rats for 12-week exposure, 4 for 4-week recovery, and 4 for 12-week recovery. The air-control exposure group included four male and female rats. Exposure for the low-dose group was a target dose of  $0.6 \times 10^6$  particles/cm<sup>3</sup> ( $1.0 \times 10^9$  nm<sup>2</sup>/cm<sup>2</sup>,  $48.76 \mu\text{g}/\text{m}^3$ ); for the medium-dose group, a target dose of  $1.4 \times 10^6$  particles/cm<sup>3</sup> ( $2.5 \times 10^9$  nm<sup>2</sup>/cm<sup>2</sup>,  $117.14 \mu\text{g}/\text{m}^3$ ); and for the high-dose group, a target dose of  $3.0 \times 10^6$  particles/cm<sup>3</sup> ( $5.0 \times 10^9$  nm<sup>2</sup>/cm<sup>2</sup>,  $381.43 \mu\text{g}/\text{m}^3$ ). AgNPs were spherical, with diameters <47 nm (range, 4–47 nm; GSD, 1.71). After a 12-week exposure, silver concentrations in the kidneys confirmed a sex difference: in the low- and medium-dose groups there was a two-fold higher silver concentration in female versus male kidneys, and a fourfold higher silver concentration in the high-dose female kidneys was consistent with results previously reported [Kim et al. 2008; Sung et al. 2009; Song et al. 2013]. These sex differences have been suggested to be related to metabolism and hormonal regulation, because the kidneys are a target organ for several hormones such as thyroid hormones and testosterone [Kim et al. 2009a]. Gene expression changes were evaluated in the study by means of a deoxyribonucleic acid (DNA) microarray of the kidneys for the low- and high-dose groups of male and female rats. The genes that were upregulated or downregulated by more than 1.3-fold ( $p < 0.05$ ) were regarded as significant. As a result, 104 genes were found to have been upregulated or downregulated by more than 1.3-fold in male rats. Among the 104 genes changed by exposure, 24 genes were involved in the KEGG pathway and related to 49 biologic pathways. In the female kidneys, 72 genes were found to have been upregulated or downregulated by more than 1.3-fold. Among the 72 genes changed by exposure to either the low or high dose, 21 genes were involved in the KEGG pathway and related to 33 biologic pathways. The sex gene profiling in the study showed a predominant expression of metabolic enzyme–

*This information is distributed solely for the purpose of pre-dissemination peer review under applicable information quality guidelines. It has not been formally disseminated by the National Institute for Occupational Safety and Health. It does not represent and should not be construed to represent any agency determination or policy.*

related genes in the male rat kidneys, versus a predominant expression of extracellular signaling–related genes in the female rat kidneys. However, no significant gene alterations were observed in the redox system, inflammation, cell cycle, and apoptosis-related genes.

The capacity of AgNPs to bring about toxicological changes in the lung as a result of subacute inhalation was investigated in C57Bl/6 mice by Stebounova et al. [2011]. Twenty-six male C57Bl/6 mice underwent whole-body exposure to 3300  $\mu\text{g}/\text{m}^3$  AgNPs 4 hours/day, 5 days/week, for 2 weeks. Along with 13 sham-exposed controls, equal numbers of mice were necropsied within 1 hour or 3 weeks after exposure to determine BAL composition (5 per group), lung histopathology (3 per group), and silver deposition to the major organs (5 per group). The AgNPs were a commercial product with a stated particle size of 10 nm. The PVP--coated particles were ultrasonicated in water, nebulized to an aerosol, and then dried at 110°C prior to introduction into the exposure chamber. The AgNPs showed a bimodal particle size distribution, with peak maxima at 5 nm (85%–90% of the particle count) and 22 nm (<15%). However, in use, the aerosolized nanoparticles showed a degree of aggregation (with a geometric mean diameter of 79 nm). Stebounova et al. [2011] reported a median of 31  $\mu\text{g}$  silver per gram (g) dry weight in the lungs of mice necropsied immediately after exposure. Those necropsied after a 3-week recovery period had a median silver content of 10  $\mu\text{g}/\text{g}$ ; two of the five mice had none detected. Silver was also detected in the BAL of exposed animals, with mean concentrations of 13.9  $\mu\text{g}/\text{L}$  in animals necropsied at cessation of exposure and 1.7  $\mu\text{g}/\text{L}$  in those necropsied 3 weeks post-exposure. However, the silver content in the heart, liver, and brain was below the detection limit. In examining the cell content and presence of biomarkers in BAL from silver-exposed mice, the authors reported that the numbers of macrophages and neutrophils were approximately double those in the BAL of controls, although no biologic significance was assigned to this change. Furthermore, there were no treatment-related changes in total protein levels or lactate dehydrogenase (LDH) activity, and most cytokines assayed were below their limits of detection. Lung histopathology yielded unremarkable findings, allowing Stebounova et al. [2011] to conclude that overall, C57Bl/6 mice showed minimal

*This information is distributed solely for the purpose of pre-dissemination peer review under applicable information quality guidelines. It has not been formally disseminated by the National Institute for Occupational Safety and Health. It does not represent and should not be construed to represent any agency determination or policy.*

pulmonary inflammation or cytotoxicity when exposed to AgNPs under the prevailing exposure conditions.

An acute inhalation exposure study examining lung effects was conducted by Seiffert et al. [2016]. In this study, the investigators generated an AgNP aerosol using a spark generation method, yielding AgNP with a count mean diameter of 13 to 16 nm and geometric standard deviation of ~1.6. In this study, two different strains of rats, Sprague-Dawley (SD; outbred) and Brown Norway (BN; inbred), were exposed via nose-only inhalation to a  $3.68\text{--}4.55 \times 10^7$  particles/cm<sup>3</sup> (0.6--0.8 mg/m<sup>3</sup>) for 3 hours (low dose) or for 3 hours/day for 4 days (high dose). Lung and alveolar silver burden were estimated to be 8 and 6 µg for the low dose and 26--28 and 18--19 µg for the high dose, respectively, for both strains. Animals were euthanized 1 and 7 days following exposure, and AgNP lung distribution, lung mechanics (airway resistance and tissue elastance) and BAL parameters were evaluated (n = 8--12 per group per time point). Silver burden in the lung and in macrophages was higher for BN rats at day 1 compared to SD rats, although silver levels decreased with time in both strains. In SD rats, silver-staining showed particles localized in macrophages in the alveolar region and lung interstitium. In BN rats, silver-positive macrophages were located in alveolar septum, airway mucosa, and lamina propria of blood vessels, as well as in terminal bronchioles. No changes in airway mechanics were observed for SD rats, whereas increased airway resistance and tissue elastance were observed in BN rats 1 day post-exposure, which resolved by 7 days post-exposure. Inflammatory cells in the lung were increased at day 1, characterized by neutrophils in SD rats and neutrophils and eosinophils in BN rats, at the high dose, with resolution over time. Malonaldehyde levels in BAL, an index of oxidative stress, were elevated at day 1 along with phospholipid levels in both strains. Surfactant protein-D was lower overall in BN rats compared to SD rats and was increased at the low dose at day 1 in BN compared to air controls. It was reduced at the high dose in SD rats at day 7. The authors suggest that changes in phospholipid and protein may influence uptake and aggregation of particles in vivo. BAL cytokines related to immune and inflammatory responses (KC, IL-1β, MCP-1, MIP-2, IL-17a) were increased at day 1 in both strains in the high-dose rats and to a greater degree in the

*This information is distributed solely for the purpose of pre-dissemination peer review under applicable information quality guidelines. It has not been formally disseminated by the National Institute for Occupational Safety and Health. It does not represent and should not be construed to represent any agency determination or policy.*

BN rats. IL-6 was also increased in BN rats at day 1. At the low dose, there were greater elevations of cytokine in the BN rats. Cytokine responses resolved with time in both strains. Overall, AgNP exposure caused increased toxicity that showed some degree of resolution over time, and strain-related differences were attributed to the underlying inflammatory state of the lungs in BN rats.

An acute nose-only inhalation study was also conducted by Kwon et al. 2012, using a system similar to the studies by Jie et al. [2007a; b]. Male C57BL/6 mice were exposed to  $\sim 2.9 \text{ mg/m}^3$  ( $1.93 \times 10^7 \text{ particles/cm}^3$ ) AgNP with diameter of 20–30 nm for 6 hours. Silver biodistribution, lung pathology, and BAL parameters were analyzed at 0 and 24 hours following exposure ( $n = 5$  per group per time point). Lung burden decreased substantially between 0 and 24 hours post-exposure. Silver levels were increased in brain, heart, spleen, and tested at 0 hours. No silver was detected in the kidney, and silver in the liver was not above control levels. There was a trend for an increase in silver in liver and testis at 24 hours. Silver measured in the heart and spleen decreased over time. Changes in mitogen-activated protein kinase (MAPK) signaling were detected at the molecular level in lung tissue. Despite changes at the molecular level in tissue, no differences in neutrophil influx or LDH in BAL were observed; only an insignificant increase in BAL total protein was observed at 0 hours, and no histopathological changes were observed in the lungs.

Roberts et al. [2013] reported on the results of an inhalation study with rats exposed to silver nanoparticles to assess pulmonary and cardiovascular responses from acute exposure. Two sources of AgNPs were used in the study; the first was a commercial antimicrobial product that contained 20 mg/L total silver (75% colloidal silver and 25% silver ions), and the other was a synthesized AgNP sample from the National Institute of Standards and Technology (NIST), reported to be 1,000 mg/L stock silver in deionized water (100% colloidal silver). Male Sprague-Dawley rats were exposed by inhalation for 5 hours to a low concentration ( $100 \text{ }\mu\text{g/m}^3$ ) of the commercial antimicrobial product (20 mg/L total silver;  $\sim 33 \text{ nm}$  count median aerodynamic diameter [CMAD]) or to  $1000 \text{ }\mu\text{g/m}^3$  in a suspension from the NIST sample (200 mg/L total silver;  $\sim 39 \text{ nm}$  CMAD).

*This information is distributed solely for the purpose of pre-dissemination peer review under applicable information quality guidelines. It has not been formally disseminated by the National Institute for Occupational Safety and Health. It does not represent and should not be construed to represent any agency determination or policy.*

Estimated lung burdens determined from deposition models were 0 (control aerosol), 1.4  $\mu\text{g}$  Ag/rat (low dose), and 14  $\mu\text{g}$  Ag/rat (high dose). The low dose was selected to be equivalent to the TLV set by the ACGIH for particulate silver (100  $\mu\text{g}/\text{m}^3$ ). Two sets of exposures with paired controls were conducted for each dose. For each exposure set and each dose, 12 rats were exposed to air ( $n = 6$  for day 1 and  $n = 6$  for day 7) and 12 rats were exposed to AgNPs ( $n = 6$  for day 1 and  $n = 6$  for day 7). Rats from one set of exposures were killed on days 1 and 7 for evaluation of pulmonary response (inflammation, cell toxicity, alveolar air/blood barrier damage, macrophage activity, blood cell differentials) and for microvascular studies (responsiveness of tail artery to vasoconstrictor or vasodilatory agents, heart rate and blood pressure in response to isoproterenol or norepinephrine, respectively). Rats from the second set of exposures were killed on days 1 and 7 following measures for hemodynamic response. No significant changes in pulmonary or cardiovascular parameters were observed for either the commercial or NIST samples at days 1 and 7 post-exposure, although slight cardiovascular changes were observed in the 1.4- $\mu\text{g}$  exposure group, possibly because of the higher fraction of ionic silver in the commercial product than in the NIST sample.

A series of acute inhalation studies were conducted that compared effects of particle size on lung and tissue distribution [Anderson et al. 2015a; Braakhuis et al. 2014], pulmonary toxicity [Braakhuis et al. 2014; Silva et al. 2016], and translocation and effects in the olfactory bulb [Patchin et al. 2016]. Braakhuis et al [2014] compared tissue distribution and lung effects in male Fischer rats (F344/DuCrI) following nose-only exposure to 15 or 410 nm particles at concentrations of 179 and 169  $\mu\text{g}/\text{m}^3$ , respectively, for 6 hours per day for 4 consecutive days. Surface area and particle number were about 1 and 2 orders of magnitude greater for the 15-nm particles on a mass basis. Lung burden of silver measured by ICP-MS was determined at 1 day post-exposure to be about 5.5 and 8.5  $\mu\text{g}$  for 15- and 410-nm particles, respectively, with a degree of clearance for both particle sizes by day 7 post-exposure. Silver content was also measured in lung-associated lymph nodes, liver, kidney, spleen, testes, and brain. For all but the liver, silver levels were below the limit of detection. In the liver, silver was detected following exposure to the smaller particle only with clearance over time.

*This information is distributed solely for the purpose of pre-dissemination peer review under applicable information quality guidelines. It has not been formally disseminated by the National Institute for Occupational Safety and Health. It does not represent and should not be construed to represent any agency determination or policy.*

Pulmonary toxicity, measured as neutrophil influx, BAL cytokines, and glutathione level, and lung injury markers were significantly increased at 1 day post-exposure to the smaller particle when compared to the larger particle. Effects resolved by 7 days post-exposure. Effects were attributed in part to differences in internal dose and dissolution rate of the particles.

Exposure conditions for the Anderson et al. [2015a], Silva et al [2016], and Patchin et al. [2016] studies were identical. Male Sprague-Dawley rats underwent a 6 hour nose-only inhalation of 20 or 110 nm citrate-stabilized AgNP aerosolized at a concentration of 7.2 mg/m<sup>3</sup> or 5.3-5.4 mg/m<sup>3</sup>, respectively, or citrate buffer aerosol as a control. In these studies, agglomerate size following aerosolization was measured to be 81% and 82% less than 1.6 µm and the count mean diameter determined by SMPS was 77.4 and 78.2 for 20 and 110 nm particles, respectively. Anderson et al. [2015a] examined lung deposition and clearance at 0, 1, 7, 21, and 56 days post-exposure (n = 6 per group per time point). Investigators used ICP-MS to evaluate tissue silver burden, as well as hyperspectral analysis and autometallography of tissue and BAL macrophages to assess tissue distribution and clearance of silver. Thoracic deposition at day 0 was 321 and 357 ng for the 20- and 110-nm particles, respectively, and did not differ in distribution among lung lobes for the different particle sizes. One third of the initial load remained for both groups at day 56. Tissue clearance and distribution were comparable with particles localized to the terminal bronchiole/alveolar duct junction. Macrophage uptake and burden over time was greater with 20-nm AgNP in comparison to 110 AgNP. The authors attributed this difference in part to the particle number per mass being greater in the 20-nm exposure versus the 110-nm exposure. In a parallel study, Silva et al. 2016, examined pulmonary toxicity following the same exposure paradigm as Anderson et al. 2015. Histopathology and BAL were performed at 1, 7, 21, and 56 days post-exposure (n = 6 per group per time point). BAL LDH was equivalently elevated at 7 days post-exposure in both groups. BAL protein was significantly elevated in both the 20- and 110-nm AgNP groups at 1 and 7 days post-exposure; however, this occurred to a greater degree for the rats exposed to 20-nm particles. Neutrophil influx was significantly elevated at 7 and 21 days post-exposure in the 20-nm-exposed group

*This information is distributed solely for the purpose of pre-dissemination peer review under applicable information quality guidelines. It has not been formally disseminated by the National Institute for Occupational Safety and Health. It does not represent and should not be construed to represent any agency determination or policy.*

only. Histopathological changes included increased inflammatory cells and cellular exudate in airspaces, a degree of eosinophil influx, Type II cell hypertrophy, and sloughing of airway epithelium in the most severe instances. Responses for both groups peaked at day 7 and resolved by day 21 for the rats exposed to larger particles, and by day 56 for rats exposed to 20-nm particles. In agreement with Anderson et al. [2015a], macrophages from rats exposed to 20-nm particles had a greater particle load than those exposed to 110-nm particles. In this study, the 20-nm particles produced a greater and more persistent response than the 110-nm particles, with responses resolving toward the end of the time course.

In a related study, using the same exposure paradigm, Patchin et al. [2016], examined size-dependent silver particle transport to the brain following inhalation of 20- or 110-nm AgNP. In this study, the investigators examined deposition and clearance from the nasal cavity and the olfactory bulb (OB) using ICP-MS and autometallography of tissue, and assessed microglial activation as an index of toxicity in the OB at 0, 1, 7, 21, and 56 days post-exposure (n = 8 per group per time point). Silver deposition in the nasal cavity at day 0 was comparable for 20- and 110-nm particles; however, there was a significantly greater amount of silver in the OB following exposure to 20-nm particles. At days 1 to 56, silver content in OB after exposure to 20-nm particles remained relatively constant, whereas exposure to 110 nm resulted in a slight increase over time and a greater amount of silver in OB at day 56 when compared to animals exposed to 20-nm particles. Nasal cavity silver decreased dramatically by day 1 for both particle sizes. Microglia activation was assessed as Iba1- and/or TNF- $\alpha$ -positive staining of tissue. Activation increased at day 0 following exposure to both particle sizes, whereas activation was significantly increased following only the 20-nm particle exposure at 1 and 7 days. The results taken together show that size affects the temporal translocation to the OB.

In addition to evaluations of the direct effects of AgNP on toxicity following inhalation, studies have been conducted that assess the effects of AgNP inhalation on the course of the allergic response, using the ovalbumin (OVA) model of asthma in mice [Chuang

*This information is distributed solely for the purpose of pre-dissemination peer review under applicable information quality guidelines. It has not been formally disseminated by the National Institute for Occupational Safety and Health. It does not represent and should not be construed to represent any agency determination or policy.*

et al. 2013; Jang et al. 2012; Su et al. 2013]. The OVA model of asthma consists of an initial sensitization phase to OVA, followed by a pulmonary challenge with OVA in order to establish the elicitation phase of allergic response. Allergic (OVA sensitization and elicitation without AgNP exposure) and non-allergic controls (no OVA sensitization with or without AgNP exposure) were employed in all studies. In a pair of related studies by Chuang et al. [2013] and Su et al. [2013], the investigators delivered 33-nm AgNP to female BALB/c mice at a dose of 3.3 mg/m<sup>3</sup> for 7 consecutive days between the OVA sensitization and challenge phase of the model to assess the effect of AgNP exposure on the elicitation phase of allergic response (n = 5–6 per group). Chuang et al. [2013], found that AgNP alone in the absence of OVA sensitization caused did not enhance BAL IgE levels but did cause a nonsignificant increase in neutrophils and eosinophils in the lungs, and it increased airway reactivity versus non-allergic control animals. In the allergy model, AgNP exposure caused a significant increase in lung eosinophils, BAL IgE and IL-13 levels, and airway reactivity following the elicitation phase, compared to allergic and non-allergic controls, suggesting that the particle exposure exacerbated the allergic response. Su et al. [2013], used a proteomic evaluation of BAL fluid and plasma in the same animal model and found differentially altered protein levels in both allergic and nonallergic mice exposed to AgNP, with 18 proteins associated with systemic lupus erythematosus in both groups of mice. Jang et al. [2012] exposed female BALB/c mice to 6-nm AgNP by nebulization at 20 ppm (40 mg/kg) 1 x per day for 5 days immediately before OVA challenge in the elicitation phase of the allergy model. In addition, they investigated the role of the vascular endothelial growth factor (VEGF) pathway, using a VEGF receptor tyrosine kinase inhibitor in the model. They found AgNP to attenuate the allergic response, reducing mucus secretion, eosinophil influx, airway reactivity, and activity in the VEGF signaling pathway relative to allergic controls. It is unclear why the two groups have conflicting results, although it may be in part attributed to study design differences in particle size, dose, and timing of particle delivery.

## **E.2 Oral Exposure**

### **E.2.1 Toxicokinetics**

The absorption and distribution of AgNPs via the oral route were studied by Loeschner et al. [2011] in groups of seven or nine female Wistar rats. The AgNPs were made by reducing silver nitrate with hydrazine in the presence of polyvinylpyrrolidone (PVP). The resulting nanoparticles were sedimented by centrifugation and dialyzed against deionized water. Size analysis showed the existence of two populations. The first, comprising about 90% of the material, was spherical, with a mean diameter of  $14 \pm 2$  nm. Although the second population was larger (with a mean diameter of  $50 \pm 9$  nm), these particles were also shown to be distinct nanoparticles rather than agglomerates. Female Wistar rats ( $n = 9$ ) received 12.6 milligrams per kilogram body weight per day (mg/kg-day) of silver for 28 days via twice-daily gavage with the AgNP suspension, while seven rats underwent similar gavage with 9 mg/kg-day silver from an 11.5-mg/mL aqueous solution of silver acetate. Nine animals underwent gavage with an 11.5-mg/mL aqueous solution of PVP as vehicle controls. During the third week of the study, rats were kept for 24 hours in metabolic cages to obtain samples of urine and feces. At term, samples of blood, brain, stomach, liver, kidney, lung, and muscle were taken for silver analysis (by ICP-MS), histopathology, scanning electron microscopy (SEM), and TEM characterization, as well as auto-metallography (AMG) and EDS.

A substantial proportion of the oral load of silver appeared in the feces of animals exposed to AgNPs ( $63 \pm 23\%$ ) and the silver acetate solution ( $49 \pm 21\%$ ), indicating some absorption of silver in the stomach, small intestine, liver, kidney, muscle, and lungs. However, Loeschner et al. [2011] were unable to assess the contribution of hepatobiliary recirculation to these values. A greater proportion of the oral load of silver acetate was absorbed than of AgNPs, although the use of AMG to locate silver within target tissues did not reveal significant differences in the disposition of the element between the two administered forms. For example, silver was located in the lamina propria at the tips of the villae in the ileum but not in the epithelial cytoplasm. The use of

*This information is distributed solely for the purpose of pre-dissemination peer review under applicable information quality guidelines. It has not been formally disseminated by the National Institute for Occupational Safety and Health. It does not represent and should not be construed to represent any agency determination or policy.*

EDS confirmed that granules in the lysosomes of macrophages consisted of silver, and additional signals identified as selenium and sulfur were also detected. In the liver there was intense staining of the Kupffer cells and around the central veins and portal tracts. In both cases, staining the kidney for silver located it in the glomeruli and proximal tubules. The authors concluded that although silver concentrations in target organs were generally lower after administration of silver nanoparticles than with water-soluble forms of the element, there were few if any differences in the distribution pattern of silver from either source. Given the similarities in disposition within the tissues, Loeschner et al. [2011] were unable to determine whether AgNPs were absorbed as an entity or whether they had dissolved in the gastrointestinal tract, followed by re-deposition in the tissues.

An experiment by Park et al. [2011a] determined the bioavailability and toxicokinetics of citrate-coated AgNPs in male Sprague-Dawley rats. As obtained from a commercial vendor, the particles were  $7.9 \pm 0.95$  nm in diameter and coated with citrate; they were employed by the researchers from a 20% (w/v) aqueous solution. Other physical and chemical data included a mean particle volume of  $1.9 \times 10^3$  nm<sup>3</sup>, a mean surface area of  $7.53 \times 10^2$  nm<sup>2</sup>/particle, and a mean particle mass of  $2 \times 10^{-17}$  g. Animals received AgNPs at concentrations of 1 or 10 milligrams per kilogram body weight (mg/kg) orally or intravenously. After treatment, blood samples were taken at 10 minutes and then at 1, 2, 4, 8, 24, 48, and 96 hours. Feces and urine samples were collected for 24 hours after treatment, and excised pieces of liver, lung, and kidney were obtained at 24 and 96 hours post-dosing for silver analysis by ICP-MS.

With regard to absorption, a comparison of the ratio of the plasma areas under the curves for oral versus intravenous administration gave measures of the bioavailability for oral exposure to this species of nanoparticles. Values of 1.2% to 4.2% of the oral load were obtained, depending on the size of the applied dose. For distribution, no AgNPs were detected in lung or kidney after oral administration. However, there was a slight elevation of silver content in the liver of animals orally exposed to 10 mg/kg. In fact, most of the orally applied AgNPs were recovered in the feces, suggesting that only

*This information is distributed solely for the purpose of pre-dissemination peer review under applicable information quality guidelines. It has not been formally disseminated by the National Institute for Occupational Safety and Health. It does not represent and should not be construed to represent any agency determination or policy.*

a small proportion of the load had been absorbed. However, it is unclear how much of the fecal recovery of silver had been recycled through the hepatobiliary circulation after absorption. The fact that some silver was released to the feces after intravenous injection suggests that AgNPs could be voided after passage through the bile duct. Park et al. [2011a] speculated that gastrointestinal absorption of AgNPs might be low because of the citrated coat. It was thought that the presence of this hydrophilic center might render gastrointestinal absorption more difficult. However, the portion of the load that was absorbed was predominantly sequestered in the liver.

Although the citrate-coated AgNPs employed by Park et al. [2011a] appeared not to be readily absorbed via the oral route and showed no signs of tissue deposition other than in the liver, an earlier experiment by Kim et al. [2009a] detected silver deposition in the kidney, urinary bladder, and adrenal gland of F344 rats after oral administration of a proprietary preparation of 60 nm AgNPs dispersed in 0.5% carboxymethyl cellulose (CMC). The authors provided little physical and chemical information about the nanoparticles employed but stated that the preparation was at least 99.98% pure. As determined by specific staining of thin sections of excised tissue pieces, it appeared that silver deposition in these tissues was much more prevalent in female rather than male F344 rats. There was no obvious explanation for this disparity.

Hendrickson et al. [2016] measured tissue distribution of silver by atomic absorption spectroscopy, as well as hematological and biochemical parameters in blood, following an acute or subacute exposure of uncoated AgNPs in male Sprague-Dawley rats. AgNPs were spherical, with an average diameter of 12.3 nm, and were stabilized in a 1% starch solution with 0.1% Tween-80 prior to gavage. For the acute study, a dose of 2000 mg/kg was administered 1 time and measures were taken at 1 and 7 days post-exposure. In the repeated-dose study, AgNP were administered at a dose of 250 mg/kg once a day for 30 days. Distribution and blood parameters were measured on days 7, 14, and 30 of the exposure. For both dosing studies, the majority of the AgNPs were excreted (estimated at >99%), similar to Loeschner et al. [2011] and Park et al. [2011a]. Outside the gastrointestinal tract (stomach and small intestine), silver was detected in

*This information is distributed solely for the purpose of pre-dissemination peer review under applicable information quality guidelines. It has not been formally disseminated by the National Institute for Occupational Safety and Health. It does not represent and should not be construed to represent any agency determination or policy.*

liver, kidney, and spleen following both exposures. In the acute exposure, silver was measured in the liver  $\geq$  kidney  $>$  spleen at day 7. On day 7 of the repeated exposure, silver was detectable only in the spleen. On days 14 and 30 of exposure, silver was present in kidney  $>$  spleen  $\geq$  liver. Silver was not detected in blood, lung, brain, adrenal glands, testes, heart, thymus, skin, muscle, or adipose tissue following either exposure. Irrespective of the dosing regime, no changes in blood parameters were measured, a finding that is in contrast to some toxicology studies discussed in section E7.2.1.

Of relevance to absorption as well as the toxicological impacts of silver nanoparticles, Park et al. [2010b] orally administered repeated doses of 1 mg/kg AgNPs to ICR mice daily for 14 days. The AgNPs were initially suspended in tetrahydrofuran (THF) with sonication. Subsequently, the solvent was allowed to evaporate and was replaced with the same volume of de-ionized water. A critical feature of the experiment was the use of batches of AgNPs that had been screened by size. Thus, groups of five mice were orally administered AgNPs of 22, 42, or 71 nm, or silver particles that averaged 323 nm in diameter. The distribution of silver, the clinical chemistry fluctuations, the histopathologic findings, and the detection and measurement of cytokines were then described in relation to particle size. A critical finding was that silver from the smaller nanoparticles (up to and including 71 nm) was detected in brain, lung, liver, kidney, and brain, whereas the larger AgNPs (323 nm) were not detected in these tissues. Another response that was observed after administration of AgNPs, but not the larger silver microparticles, was increased serum concentrations of transforming growth factor-beta (TGF- $\beta$ ). Some differences in the subpopulations of whole-blood lymphocytes were also reported with varying particle size, but the data were less robust. However, the findings were consistent with the concept that small AgNPs are more active in exerting toxicological responses because of their expedient transport to susceptible sites.

A subacute oral AgNP exposure study with Sprague-Dawley rats was reported by Lee et al. [2013a], who focused on the clearance kinetics of tissue-accumulated silver. Rats were assigned to three groups, with 20 rats per group: control (no exposure), low dose (100 mg/kg body weight), and high dose (500 mg/kg body weight). The groups were

*This information is distributed solely for the purpose of pre-dissemination peer review under applicable information quality guidelines. It has not been formally disseminated by the National Institute for Occupational Safety and Health. It does not represent and should not be construed to represent any agency determination or policy.*

exposed to two different sizes of citrate-coated AgNPs (average diameter, 10 and 25 nm) over 28 days. Rats were observed during recovery for 4 months to identify the clearance of the tissue-accumulated silver. Regardless of the AgNP size, the silver content in most tissues gradually decreased during the 4-month recovery period. The exceptions were the silver concentrations in the brain and testes, which did not clear after the 4-month period, indicating an obstruction to the transporting of accumulated silver out of these tissues. Although the clearance half-times differed according to dose and sex, the tissues with no biologic barrier, such as the liver, kidneys, and spleen, showed a similar clearance trend. The silver concentration clearance was in this order:

blood > liver = kidneys > spleen > ovaries > testes = brain.

The different AgNP sizes used in the study had minimal effect on absorption, distribution, metabolism, and excretion, although the size difference was relatively narrow. The authors suggested that these findings support the hypothesis that silver toxicity originates mainly from silver ions, and in this study it was generated from the surface of the AgNPs. The findings also indicate that coated AgNPs and size differences may have minimal effect on absorption, distribution, metabolism, and excretion.

Effects of size, coating, and solubility were also investigated by Bergin et al. [2016]. The study was conducted in two parts: one examined biodistribution and the other evaluated organ weight and histopathological changes as indices of toxicity. For the toxicological evaluation male C57BL6/6NCrl mice (6 per group) were exposed to 20- or 110-nm colloidal AgNP coated with PVP or citrate at doses of 0.1, 1.0, or 10 mg/kg/day for 3 days in the presence or absence of an antibiotic. Additional exposure groups included controls for citrate and PVP buffers and a soluble form of silver, silver acetate. Body weight was monitored on days 1–3 and 1 week following the last exposure. On the last day of exposure and 1 week following the last exposure, the following organs were collected for toxicity assessment: brain, heart, lung, liver, spleen, thymus, gonads, GI tract (esophagus to rectum), left kidney and adrenal gland, right kidney and adrenal

*This information is distributed solely for the purpose of pre-dissemination peer review under applicable information quality guidelines. It has not been formally disseminated by the National Institute for Occupational Safety and Health. It does not represent and should not be construed to represent any agency determination or policy.*

gland, salivary glands, mammary glands, quadriceps muscle, bone marrow from sternum, bladder, skin, and mesenteric lymph nodes. No changes in body weight were observed and no significant changes in histopathology were found. In the second part of the study, mice were exposed to 10 mg/kg of AgNPs, buffer controls, or soluble Ag at time 0. Urine and feces were collected at 0, 3, 6, 9, 12, 18, 24, and 48 hours after exposure. Organ silver levels were measured by inductively coupled–optical emission spectroscopy at 48 hours post-exposure. The majority of administered silver (70.5% to 98.6%) was recovered in the feces regardless of size, coating, or solubility. Silver was detected in liver, kidney, spleen, gastrointestinal tract, and urine, and to a slightly greater degree for the soluble form of silver, although levels in these tissues totaled less than 0.5% the administered dose at the highest levels measured. The findings corroborate those of Lee et al. [2013a], indicating that size and coating had minimal effects on absorption, distribution, metabolism, and excretion following acute exposure.

### E.2.1 Toxicological effects

Experimental studies in humans are limited. Smock et al. [2014] examined effects of oral administration of 15 ml of 32 ppm silver nanocolloid (average particle size ranging from 25 to 40 nm) for 14 days on platelet aggregation (PA) as a risk factor for thrombosis in 18 healthy volunteers 18 to 60 years of age. The estimated daily dose equivalent was 480 µg/day. Sterile water was used as a placebo control. Blood was collected for testing prior to the first exposure following 8 hours of fasting to obtain a baseline measure of PA and following 8 hours of fasting after the last exposure. Unstimulated PA and PA in the presence of collagen or adenosine diphosphate were evaluated. Additionally, total concentration of silver in serum was assessed by ICP-MS. The peak serum silver concentration was reported to be  $6.8 \pm 4.5$  µg/L. Spontaneous PA in the absence of an agonist was not found. The collagen agonist at a dose of 0.5 µg/ml caused a significant decrease in PA, and a trend for a decrease was also noted at 1.0 µg/ml collagen. The authors note that these findings are in contrast to previous in vitro studies that showed increased PA [Jun et al. 2011; Kim et al. 2009d]; however, concentrations of silver were lower by an order of magnitude or greater in the human

*This information is distributed solely for the purpose of pre-dissemination peer review under applicable information quality guidelines. It has not been formally disseminated by the National Institute for Occupational Safety and Health. It does not represent and should not be construed to represent any agency determination or policy.*

study. The authors also note that the clinical significance of the findings are not clear but warrant further investigation.

In a survey of the acute toxicity of AgNPs, Maneewattanapinyo et al. [2011] attempted to determine a median lethal dose (LD<sub>50</sub>) for AgNPs in ICR mice. The AgNPs were produced by reducing a silver nitrate solution with sodium borohydride in the presence of soluble starch as a stabilizer. The particles were stated to be of high purity (99.96% silver), spherical, and with a narrow size range of 10–20 nm. Additionally, the content of free silver ions was very low (<0.04%). There were no deaths among mice observed for 14 days after a dose of 5,000 mg/kg, and there were no clinical signs of toxicity, reduced weight gain, hematologic or clinical chemistry changes, or gross and histopathologic findings. The oral LD<sub>50</sub> in ICR mice was thus designated as >5,000 mg/kg.

In a 28-day study by Kim et al. [2008] of the toxicological impacts of oral exposure to AgNPs, 4-week-old male and female SPF Sprague-Dawley rats (10 per dose group) underwent gavage with AgNPs (average diameter, 60 nm; range, 53–71 nm) in an aqueous solution of 0.5% carboxymethyl cellulose (CMC) as the vehicle. The authors provided little physical and chemical information about the nanoparticles employed but stated that the preparation was at least 99.98% pure. The experiment followed OECD Test Guideline 407, using doses of silver at 0, 30, 300, or 1,000 mg/kg that were given for 28 days. At the conclusion of the dosing phase, animals were unfed for 24 hours and then anesthetized to facilitate the withdrawal of blood for measuring hematologic and clinical chemistry parameters. Major organs and tissues were excised, weighed, and processed for silver determination and histopathologic examination. The rat bone marrow micronucleus (MN) test was carried out according to OECD Test Guideline 474 to assess genotoxicity. Clinical signs were unremarkable during the in-life phase of the experiment, and no compound-related changes in body weight gain or food consumption were observed. At term, there were no dose-dependent changes in organ weights, hematologic parameters, or bone marrow cytotoxicity. However, there were treatment-related increases in serum cholesterol concentration and alkaline

*This information is distributed solely for the purpose of pre-dissemination peer review under applicable information quality guidelines. It has not been formally disseminated by the National Institute for Occupational Safety and Health. It does not represent and should not be construed to represent any agency determination or policy.*

phosphatase (AP) activity that, at the highest dose, were significantly different from levels in controls (Table E-4).

**Table E-4. Serum cholesterol concentration and alkaline phosphatase activity in Sprague-Dawley rats that underwent gavage with AgNPs for 28 days.**

Dose Group (mg/kg)	Serum Cholesterol Concentration (mg/dL)		Alkaline Phosphatase Activity (IU/L)	
	Males	Females	Males	Females
0	69.0 ± 8.2	89.6 ± 9.1	427.2 ± 70.6	367.6 ± 125.7
30	73.1 ± 16	85.6 ± 12.2	475.4 ± 98.5	335.4 ± 79.0
300	82.1 ± 21.7	102.9 ± 17.7†	613.7 ± 128.6†	403.3 ± 75.9
1,000	87.5 ± 13.1*	117.5 ± 14.1†	837.7 ± 221.5†	499.0 ± 107.3†

\* $p < 0.05$ ; † $p < 0.01$  versus controls, as calculated by the authors.

IU/L = International units per liter.

Source: Kim et al. [2008].

As tabulated by the authors, dose-related increases in silver content were noted in the blood and tissues such as testis, kidney, liver, brain, lung, and stomach, with a two-fold higher accumulation in the kidneys of female rats versus males. Though difficult to explain mechanistically, this difference was consistent with that observed in F344 rats by Kim et al. [2009a]. Histopathologic examination of the liver showed an increased incidence of bile duct hyperplasia in AgNP--receiving rats. Other hepatic responses included infiltration of inflammatory cells in the hepatic lobe, portal tract, and dilated central veins. These changes are consistent with the clinical chemistry data, pointing collectively to a possible silver-related perturbation of the metabolism and structural architecture of the liver.

In a second oral study, scientists from the same research group carried out an exposure regimen identical to that used by Kim et al. [2008] but with the primary focus on silver deposition and changes to the structure of the ileum, colon, and rectum [Jeong et al. 2010]. The AgNPs were about 60 nm in diameter on average and were dispersed in an aqueous solution of 0.5% CMC at doses of 0 (vehicle control), 30, 300, or 1,000 mg/kg-

day for 28 consecutive days. The ileum, colon, and rectum were assessed for general histologic structure and amounts of mucins in the mucosa. Specific histochemical staining procedures were used to detect and distinguish between mucins, and the intensity of staining was subjectively scored to assess the amounts of mucins. In addition to the use of hematoxylin/eosin to stain mounted sections of these tissues, periodic acid-Schiff stain was used to detect neutral mucins, Alcian blue was used for acidic mucins, and high-iron diamine plus Alamar Blue (AB) was used to distinguish sulfated from nonsulfated mucins. There was a dose-dependent accumulation of AgNPs in the lamina propria of the small and large intestine, with higher numbers of goblet cells that had released their mucus, as compared to the number in controls. Given the detection of fluctuating amounts of differentially stained mucins among the groups, the researchers suggested that AgNPs might induce the discharge of mucus granules with abnormal compositions.

Sharare et al. [2013] also investigated effects of subacute silver exposure on the murine intestinal mucosa at lower doses than those used in the Kim et al. [2008] study. AgNPs, 3 to 220 nm, synthesized from silver nitrate in deionized water, were administered to male Swiss albino mice at doses of 0, 5, 10, 15, or 20 mg/kg/day for 21 days. Body weights were monitored once a week and animals were euthanized on the last day of treatment. Histopathology and TEM analysis were performed on the small intestine. A degree of weight loss was noted over the time course in mice treated with AgNPs (greatest at 10 mg/kg). In addition, histological findings included loss of microvilli, increased inflammatory cells in the villus, and increased mitotic figures in the intestinal glands (proliferation response to replace damaged epithelial cells). TEM confirmed damage to the microvilli. The authors hypothesize that the weight loss may be due to decreased intestinal absorption of nutrients because of AgNP--induced damage.

Further, related to responses in the ileum, a subchronic study was conducted on male and female Sprague-Dawley rats to examine effects of silver nanoparticles on gut-associated immune responses and on intestinal microbiota populations across phyla and genre, as well as within one family of gram-negative bacteria (Williams et al. 2015).

*This information is distributed solely for the purpose of pre-dissemination peer review under applicable information quality guidelines. It has not been formally disseminated by the National Institute for Occupational Safety and Health. It does not represent and should not be construed to represent any agency determination or policy.*

Rats (10/sex/group) were exposed to 9, 18, or 36 mg/kg AgNP that ranged in size (10, 75, or 110 nm), stabilized in 2 mM citrate divided into two doses a day for 13 weeks. An additional study examined effects of 100, 200, or 400 mg/kg silver acetate in the same dosing regimen. Bacteria populations and growth were assessed, and expression of *Enterobacteriaceae* family-specific genes in the ileum (*MUC2*, *MUC3*, *TLR2*, *TLR4*, *IL10*, *TGF- $\beta$* , *FOXP3*, *GPR43*, and *NOD2*) was measured following the final exposure. Findings showed that AgNP caused a size- and dose-dependent change in the populations of gut microbiota, with decreases in *Firmicutes* phyla and *Lactobacillus* genus and a shift toward gram-negative bacteria, whereby the smallest particles had the greatest effect. Sex differences were greatest in effects on gene expression in the ileum. In general, genes associated with family-specific bacterial immune response were decreased with decreasing particle size, particularly at the lower doses. TLR4 and MUC3 were downregulated to a greater degree in females, whereas TLR2 was downregulated to a greater degree in males. Less change in gene expression was observed at the higher dose (36 mg/kg), which followed a pattern similar to the 100-mg/kg soluble silver. The authors suggest that the higher dose was less effective possibly because of greater agglomeration of material and/or more efficient dissolution with decreasing particle size.

In addition to their experimental administration of differently sized AgNPs to ICR mice, as described in E.2, Park et al. [2010a] undertook a 28-day gavage study in which three mice per sex per group underwent gavage with 0 (vehicle control), 250, 500, or 1,000  $\mu\text{g}/\text{kg}$  AgNPs (average particle diameter, 42 nm) dispersed in an aqueous medium, doses that were significantly lower than those discussed above. Major organs and tissues were excised at term for silver analysis and histopathologic examination. Blood samples were measured for clinical chemistry parameters and the presence of cytokines. Although there were no histopathologic changes in the livers or small intestines of the treated groups, some liver-related clinical chemistry parameters changed in relation to dose, including the activities of AP and aspartate aminotransferase (AST) in high-dose mice (both sexes). Additionally, the activity of alanine aminotransferase (ALT) was increased in high-dose females but not males.

*This information is distributed solely for the purpose of pre-dissemination peer review under applicable information quality guidelines. It has not been formally disseminated by the National Institute for Occupational Safety and Health. It does not represent and should not be construed to represent any agency determination or policy.*

The only organ or tissue where histopathologic changes were observed was the kidney, where signs of slight cell infiltration were noted in the cortex of high-dose mice of either sex. Changes in the levels of cytokines and immunoglobulin (Ig)-E were also noted in high-dose mice, in comparison with the control group. These differences are listed in Table E-5. The authors noted that their doses were far lower than those that induced histopathologic responses in the liver of Sprague-Dawley rats after oral exposure [Kim et al. 2008]. Therefore, they concluded that doses of AgNPs at these low concentrations can induce inflammatory responses by repeated oral administration.

**Table E-5. Levels of cytokines in the serum of high-dose and control mice as a result of oral administration of AgNPs to ICR mice for 28 days**

Parameter	Controls (n = 3)	High-dose group (n =3)
<i>Pro-inflammatory cytokines (pg/mL)</i>		
Interleukin (IL)-1	ND	8.8 ± 0.7†
Tumor necrosis factor (TNF)-α	1.21	3.41 ± 0.06
IL-6	1.44	13.75 ± 0.57†
<i>Thyroid helper (Th)1–type cytokines (pg/mL)</i>		
IL-12	35.5	76.86 ± 5.2†
Interferon (IFN)-γ	ND	0.52 ± 0.04
<i>Th-2-type cytokines (pg/mL)</i>		
IL-4	ND	2.7 ± 0.07‡
IL-5	ND	1.34 ± 0.01
IL-10	ND	29.02 ± 1.7†
TGF-β (pg/mL)	ND	6.73 ± 0.52†
Ig E (ng/mL)	3.28	6.04 ± 0.74‡

ND = nondetectable.

†*P* < 0.01; ‡*P* < 0.05.

Source: Park et al. [2010a].

*This information is distributed solely for the purpose of pre-dissemination peer review under applicable information quality guidelines. It has not been formally disseminated by the National Institute for Occupational Safety and Health. It does not represent and should not be construed to represent any agency determination or policy.*

In a follow-up study to Park et al. [2010a], Kim et al. [2010a] treated 10 F344 rats per sex per group by gavage with AgNPs (average diameter, 56 nm; range, 25–125 nm) for 13 weeks at silver doses of 0, 30, 125, or 500 mg/kg-day. The monodisperse and nonaggregated AgNPs were dispersed in an aqueous solution of 0.5% CMC that also constituted the vehicle control. As before, clinical signs, body weights, and food consumption were monitored in the in-life phase of the experiment. At term, blood was withdrawn to measure hematologic and clinical chemistry parameters. Organ weights were recorded, and excised pieces of the major tissues and organs were processed for histopathologic examination and measurement of silver content.

Most major organs and tissues showed a dose-dependent increase in silver content. However, as observed in other studies of AgNPs in experimental animals [Kim et al. 2009a, 2008], there was an increased deposition of silver in female kidneys versus males' at equivalent doses. The authors of the study did not mention whether any of the exposed animals showed clinical signs of toxicity, but there were no significant changes in food consumption and water intake among the groups. Likewise, there were no dose-related changes in body weights of female rats, although high-dose males showed less body weight gain than controls after 4, 5, and 7 weeks of exposure. Body weight gain was also less in mid-dose males than in controls after 10 weeks. At term, there were few if any changes in organ weights associated with exposure to AgNPs. However, high-dose males showed an increase in the weight of the left testis and low- and mid-dose females showed decreases in weight of the right kidney. In a manner similar to the 28-day oral study in Sprague-Dawley rats [Kim et al. 2008], the most clear-cut treatment-related changes in clinical chemistry parameters were increases in AP activity in high-dose females (versus controls) that achieved statistical significance, as well as statistically significant increases in serum cholesterol concentration in high-dose rats of both sexes. Perhaps the most noteworthy toxicological responses to AgNPs in this study were histopathologic changes to the liver that showed a dose-related trend. Specifically, there were increased incidences in minimal to mild bile duct hyperplasia in both sexes of F344 rats. The proportions of males affected were 4/10 (controls), 7/10 (low dose), 9/10 (mid dose), and 6/10 (high dose); the respective proportions of affected

females were 3/10, 7/10, 8/10, and 7/10. These responses are similar to those in Sprague-Dawley rats described by Kim et al. [2008] following their 28-day oral exposure study and by Sung et al. [2009] following their 90-day inhalation study. However, related changes in such clinical chemistry parameters as serum cholesterol concentration or AP activity were not observed in the latter study. In summarizing their data, Kim et al. [2010a] concluded that a LOAEL of 125 mg/kg, with a NOAEL of 30 mg/kg, would be appropriate from their data. However, since the incidences of bile duct hyperplasia in the low-dose groups were elevated in comparison with controls and were clearly part of a dose-related trend, the point of departure for these responses could be lower than 30 mg/kg.

Taking together the data of Park et al. [2010a], where kidney damage was observed following oral exposure, and the data of Kim et al. [2010a], showing increased silver in the kidneys of females, Tiwari et al. [2017] performed a subchronic study that examined kidney-specific toxicity following a 60-day oral exposure to PVP--stabilized AgNPs in female Wistar rats. Rats were exposed to 50 or 200 ppm AgNPs (10–40 nm, average of ~27 nm diameter, <1% ionic) daily for 60 days. Accumulation of silver (ionic and non-ionic) was measured in kidneys immediately following the last exposure, and excretion was monitored at 1, 7, 28, and 60 days of exposure. There was a dose-dependent increase in silver accumulation in the kidneys, with approximately 70% to 75% of silver in the particulate form and 30% to 25% in the ionic form. After the first day of exposure, 62.5% of the low dose and 72.6% of the high dose were excreted, and excretion increased over time. Markers of nephrotoxicity in urine were observed to increase over time, starting at 7 days of exposure, and included an increase in total protein in urine, as well as clusterin, kidney injury molecule-1 (KIM-1), TIMP-1, and VEGF. Additionally, osteopontin was elevated at later times in the low-dose exposure group only. Following the 60-day exposure, serum levels of creatinine were elevated in both exposures. Kidney pathology was observed in the proximal and distal tubule as well as the glomerulus and Bowman's capsule. Structural changes included necrotic cells, damage to mitochondria, damage to villi in the brush border, and damage to organelles associated with the endocytic system. Proteins associated with immune response,

*This information is distributed solely for the purpose of pre-dissemination peer review under applicable information quality guidelines. It has not been formally disseminated by the National Institute for Occupational Safety and Health. It does not represent and should not be construed to represent any agency determination or policy.*

inflammation, and tissue injury were elevated in both serum and kidney tissue (erythropoietin, VEGF, RANTES, IL-7, IL-1 $\beta$ , and TNF- $\alpha$ ). Additionally, serum levels of IL-6, IL-12p70, IFN- $\gamma$ , GM-CSF, and MIP-2 were elevated, and IL-18 and IL-17A were also elevated in kidney tissue. mRNA expression of factors related to cell survival, proliferation, and autophagy were evaluated at the low dose in conjunction with immunohistochemistry. Markers of autophagy were not altered; however, markers for necrosis were increased and apoptotic markers were decreased. In addition, levels of ROS and 8-oxoG (oxidative DNA damage) were elevated in kidney tissue, while levels of anti-oxidants were found to decrease. The data implicates oxidative stress and inflammation in the promotion of kidney injury (necrosis) following subchronic exposure in female rats at a dose of 50 ppm.

Yun et al. [2015] also performed a 13-week exposure study in male and female Sprague-Dawley rats. This study was designed to compare toxicity of oral administration of three NPs that differed in composition (AgNP, SiO<sub>2</sub> NP, and Fe<sub>2</sub>O<sub>3</sub> NP). Parameters measured included body weight, organ weight, blood chemistry, urinalysis, and organ histopathology. In addition, silver distribution in blood, liver, kidney, spleen, lung, brain, urine, and feces was measured by ICP-MS. The dose was determined from a 14-day dose-response study (515, 1030, or 2060 mg/kg daily). In the subacute dose-response study, no significant effects were observed for the iron and silica NPs. AgNPs cause increased AP levels in males at the two higher doses and in females at all doses, suggesting greater effects in liver of females. The middle dose (~1000 mg/kg) was selected for subchronic study. No significant changes were observed in body weight across the course of the study. Silver was detectable in all organs, blood, urine and feces. The majority of silver was measured in the feces. No differences in distribution due to sex were observed. In both male and female rats, AP was significantly elevated following subchronic exposure, and lymphocyte infiltration into kidney and liver was noted for both sexes. Sex differences were observed in blood, with white blood cells elevated in females and platelets elevated in males. In addition, a significant elevation in serum calcium levels occurred in females, along with increased observation of calcification in the kidney. The study suggests liver and kidney as target

*This information is distributed solely for the purpose of pre-dissemination peer review under applicable information quality guidelines. It has not been formally disseminated by the National Institute for Occupational Safety and Health. It does not represent and should not be construed to represent any agency determination or policy.*

organs, with potential sex differences in response to oral exposure to AgNP, similar to other studies discussed above [Kim et al. 2009a; Park et al. 2010a; Kim et al. 2010a].

The potential mechanism of the effects of subchronic exposure to AgNP, particularly in relation to the effects in the liver, was investigated by Elle et al. [2013] with an emphasis on the role of oxidative stress in injury. AgNPs were delivered to Sprague-Dawley rats by gavage as collargol (70%--80% 20 nm AgNP and 20% protein gel) for 81 days at a dose of 500 mg/kg. One day following the last exposure, blood was collected for plasma analysis of lipids, liver enzymes, and antioxidant capacity. Liver and heart were harvested to evaluate biomarkers of oxidative stress and inflammation was measured in liver. Food intake and body weight were found to be significantly lower in exposed rats. In plasma, total cholesterol was significantly elevated along with an increased ratio of LDL to HDL cholesterol, triglycerides were significantly reduced, and ALT was significantly increased, indicating effects on the liver. Malondialdehyde (MDA) levels (lipid peroxidation) were increased and antioxidant capacity was decreased, along with decreased superoxide dismutase levels and paraoxonase activity. Superoxide anion as a biomarker of oxidative stress was increased in heart and liver of exposed rats; however, MDA and superoxide dismutase activity were not. In addition, IL-6 and TNF- $\alpha$  were elevated in the liver of exposed rats. Findings taken together support the concept that oxidative stress is at least in part a contributing mechanism to AgNP toxicity. An additional subacute exposure study also supports the involvement of oxidative stress in toxicity of AgNP in vivo [Shrivastava et al. 2016]. In this study, male Swiss albino mice were exposed to a dispersion of 20 nm AgNP or colloidal gold NP at a dose of 1 or 2  $\mu$ M by oral gavage for 14 days. Blood, brain, liver, kidney, and spleen were collected after the last exposure. A battery of assays were employed to assess blood and tissue reactive oxygen species and antioxidant capacity. Liver and kidney function were measured as AP and ALT, and urea and creatinine in serum, respectively. Systemic inflammatory potential was assessed as IL-6 and nitric oxide synthase in plasma, and DNA damage due to oxidative stress was measured as 8-hydroxy-2'-deoxyguanosine (8-OHdG) in urine. AgNP findings included significant elevations in IL-6 and nitric oxide synthase in plasma. ALT, AP, and urea were also elevated in plasma. Metallothionein

*This information is distributed solely for the purpose of pre-dissemination peer review under applicable information quality guidelines. It has not been formally disseminated by the National Institute for Occupational Safety and Health. It does not represent and should not be construed to represent any agency determination or policy.*

levels were increased in both liver and kidney and to a greater degree in kidney. In addition, reactive oxygen species in blood and all tissues collected were increased. Antioxidant capacity was decreased in plasma, whereas the various enzymes measured were altered in tissues differentially, depending on the enzyme and the tissue, and 8-OHdG increased in the urine following AgNP exposure. As with the subchronic study by Elle et al. [2013], the study by Shrivastava et al. [2016] supports the role of oxidative stress in AgNP toxicity.

In contrast to the subchronic studies discussed above [Kim et al. 2010a; Yun et al. 2015; Elle et al. 2013] that suggest liver and kidney as primary targets of AgNP toxicity following oral exposure, in addition to effects in other organ systems, a subchronic study by Garcia et al. [2016] did not find adverse effects in kidney or liver. In this study, male Sprague-Dawley rats were exposed to 20–30 nm PVP-coated AgNP by gavage at a dose of 0, 50, 100, or 200 mg/kg per day for 90 days. Silver accumulation in tissues (liver, kidney, spleen, thymus, brain, and ileum), subcellular distribution in those tissues, distribution of other metals in tissues, Ag excretion (urine and feces Ag levels), and plasma biochemical and hematological parameters were analyzed, and histopathology of tissues was performed. The majority of excreted Ag was found in feces (~10000–18000 µg/g, depending on dose), although there were low but detectable amounts in urine (< 0.1 µg/g). Ag was found in all tissues measured, with the greatest amount in the ileum. At the subcellular level, AgNPs could be found in liver and intestinal cells. No changes in blood cell differentials, blood chemistry (including BUN, creatinine, AST, ALT, AP), or histopathological parameters were found. The only significant difference in tissues was observed in the analysis of redistribution of Cu, Fe, Mg, and Zn. Differential elevations and decreases in Cu and Zn were found, depending on organ and dose. The lack of effects in kidney and liver, and in pathology in the ileum, in contrast to observations in other studies (Kim et al. 2010a; Yun et al. 2015; Elle et al. 2013; Jeong et al. 2010; Williams et al. 2015], could be due to a number of factors, such as dose (the highest dose was lower than in many of the studies, with the exception of Williams et al. [2015]). Another factor could be particle coating, which may affect absorption and/or

*This information is distributed solely for the purpose of pre-dissemination peer review under applicable information quality guidelines. It has not been formally disseminated by the National Institute for Occupational Safety and Health. It does not represent and should not be construed to represent any agency determination or policy.*

dissolution rate. Many of the discussed studies did not specifically examine dissolution or effect of the ion or coating of the materials.

However, several studies involved toxicological comparisons of one or more of the following parameters within a study: size, solubility, and coating or capping agent. Park [2013] investigated toxicokinetic differences and toxicities of AgNPs and silver ions in rats after a single oral administration of 2 mg/kg (low dose) or 20 mg/kg (high dose). Male Sprague-Dawley rats ( $n = 5$ ) were given a dose of either AgNPs (diameter,  $\sim 7.9$  nm) or silver ions ( $\text{Ag}^+$ ). The  $\text{AUC}_{24\text{hr}}$  of  $\text{Ag}^+$  was  $3.81 \pm 0.57$   $\mu\text{g}/\text{d}/\text{mL}$  when rats were treated with a dose of 20 mg/kg, whereas that of AgNPs was  $1.58 \pm 0.25$   $\mu\text{g}/\text{d}/\text{mL}$ . Blood levels, tissue distributions, and excretion of silver were measured up to 24 hours after oral administration. Tissue distribution of silver in liver, kidneys, and lungs was higher when  $\text{Ag}^+$  was administered than when AgNPs were administered. Silver concentrations in blood of rats treated with AgNPs were lower than those of rats treated with  $\text{Ag}^+$  at the same dose. Blood silver concentrations in rats treated with 20 mg/kg AgNPs were also found to be lower than those of rats administered 2 mg/kg  $\text{Ag}^+$ . Decreased red blood cell counts, hematocrit levels, and hemoglobin levels were found in  $\text{Ag}^+$ -treated groups, whereas increased platelet counts and mean platelet volume were noted in the AgNP-treated rats. The concentrations of silver in both the lung and liver were lower in rats treated with AgNPs than in rats treated with  $\text{Ag}^+$ , and the highest concentration of silver was found in the liver of rats treated with  $\text{Ag}^+$  (20-mg/kg dose). Orally administered AgNPs were not absorbed in the gastrointestinal tract but excreted via feces; however, excretion of silver through feces was negligible for rats treated with the same dose of  $\text{Ag}^+$ , a finding indicating that bioavailability of  $\text{Ag}^+$  may be greater than with AgNPs. Findings related to greater biodistribution of the soluble form of silver are in agreement with those of Bergin et al. [2016] previously discussed.

Qin et al. [2016] evaluated biodistribution and toxicity following a subacute exposure to AgNP (28–44 nm stabilized in PVP) or soluble silver ( $\text{AgNO}_3$ ). Male and female Sprague-Dawley rats (10 per group per sex) were orally dosed with 0.5 or 1.0 mg/kg AgNP or  $\text{AgNO}_3$  daily for 28 days. On day 28, blood was collected for hematology and

*This information is distributed solely for the purpose of pre-dissemination peer review under applicable information quality guidelines. It has not been formally disseminated by the National Institute for Occupational Safety and Health. It does not represent and should not be construed to represent any agency determination or policy.*

biochemical analysis, and liver, kidney, spleen, stomach, small intestine, and gonads underwent histopathological analysis. Additionally, silver was measured in liver, spleen, kidney, testes and plasma by atomic absorption spectroscopy. No significant differences in body weight, food consumption, or organ/body weight ratio were found for either exposure. In male and female rats, AgNP exposure led to increased red blood cells and decreased platelet counts. In addition, white blood cells were increased in female rats at the high dose of AgNP. In males, AgNP exposure led to an increase in AST in the plasma. The only change associated with soluble silver was an increase in red blood cells in females at the low dose. No histopathologic changes were observed in spleen, stomach, small intestine, or gonads for either sex following AgNP or soluble silver exposure. Minor pathological changes were noted in kidneys and livers of both sexes following exposure to AgNP and soluble silver, which did not differ significantly from each other. AgNP distribution was significantly lower compared to soluble silver for both sexes. In males both AgNP and AgNO<sub>3</sub> were greatest in liver and kidney, followed by testes and spleen, then plasma. AgNO<sub>3</sub> distribution in females followed a similar pattern, with liver having the highest burden (ovaries were not measured), followed by the kidneys and spleen. In females, organ burden of silver following AgNP exposure did not follow a similar distribution pattern, with equal amounts of silver detected across liver, kidney, spleen, and plasma. The results indicate that the soluble form is more readily absorbed, as had been indicated by others [Bergin et al. 2016; Lee et al. 2013a; Park et al. 2013]. The authors suggest that the biochemical and hematological changes that were greater for AgNP versus AgNO<sub>3</sub> indicate that the particle itself contributes in part to the overall toxicity.

In a study to examine the toxicokinetics and tissue distribution of two types of AgNPs, AgNO<sub>3</sub> (soluble silver), and two negative controls, five groups of Sprague-Dawley rats (five per group) were exposed by gavage daily for 28 days to <20-nm non-coated or <15-nm PVP-coated AgNPs and to AgNO<sub>3</sub> [van der Zande et al. 2012]. All groups of rats were followed for 8 weeks. Dissection was performed on day 29 and at 1 week and 8 weeks post-exposure. Silver was present in all examined organs (liver, spleen, kidney, testis, lungs, brain, heart), and the highest levels in all silver-treatment groups were in

*This information is distributed solely for the purpose of pre-dissemination peer review under applicable information quality guidelines. It has not been formally disseminated by the National Institute for Occupational Safety and Health. It does not represent and should not be construed to represent any agency determination or policy.*

the liver and spleen. Silver concentrations in the organs were highly correlated to the amount of  $\text{Ag}^+$  in the silver nanoparticle suspension, indicating that mainly  $\text{Ag}^+$  (and to a lesser extent, AgNPs) passed the intestines in the AgNP-exposed rats, a finding similar to Qin et al. [2016]. In all groups, silver was cleared from most organs at 8 weeks post-exposure, except for the brain and testis. By means of single-particle ICP-MS, AgNPs were detected in the AgNP-exposed rats but also in  $\text{AgNO}_3$ -exposed rats, demonstrating the in vivo formation (or precipitation) of nanoparticles from  $\text{Ag}^+$  that were probably composed of silver salts. Biochemical markers and antibody levels in blood, lymphocyte proliferation and cytokine release, and NK-cell activity did not reveal hepatotoxicity, unlike Qin et al. [2016], or immunotoxicity from the silver exposure. The authors noted that the consequences of in vivo formation of AgNPs and the long retention of silver in the brain and testis warrant further assessment of the potential health risk.

Subacute toxicity of 14-nm AgNPs stabilized with PVP and ionic silver in the form of silver acetate was investigated in 4-week-old male (6 per dose) and female (10 per dose) Wistar Hannover Galas rats for 28 days [Hadrup et al. 2012a]. Animals received by gavage a vehicle control and AgNP doses of 2.25 or 9 mg/kg BW/day or silver acetate doses of 9 mg silver/kg BW/day for 28 days. Clinical, hematologic, and biochemical parameters, organ weights, and macroscopic and microscopic pathologic changes were evaluated. No increase in AP or cholesterol was found for AgNPs at doses of up to 9 mg/kg/day. However, effects were observed for silver acetate (ionic form) at a dose of 14 mg/kg/day, including an increase in AP, decrease in plasma urea, and decrease in thymus weights.

Additionally, Hadrup et al. [2012a] found no observable effects in the microbiologic status of the rats' gastrointestinal tract caused by ingesting AgNPs. This finding is confirmed in a study by Wilding et al. [2016] that examined the role of size and surface coating on the murine microbiome following 28 days of exposure to 10 mg/kg/day of 20- or 110-nm AgNP stabilized in citrate of PVP. Silver acetate was employed as a control for effects of the ion (an antibiotic control group was also employed). At 1 day following

*This information is distributed solely for the purpose of pre-dissemination peer review under applicable information quality guidelines. It has not been formally disseminated by the National Institute for Occupational Safety and Health. It does not represent and should not be construed to represent any agency determination or policy.*

the last exposure, male C57BL/6CrI mice were euthanized and cecal tips were processed for microbial sequencing and molecular analysis. No differences in diversity, populations, or structures of the microbiome were found, regardless of size or coating following the subacute exposure. However, as previously mentioned, longer subchronic exposure to AgNP did result in effects on the microbiome with the smallest particles (10 nm) utilized in the study having the greatest effect [Williams et al. 2015]. The findings together suggest that effects may be related primarily to duration of silver exposure and particle size; however, further studies are needed for definitive conclusions to be made.

In a study related to Hadrup et al. [2012a], Hadrup et al. [2012b] exposed male and female Wistar rats to 0, 2.25, 4.5, or 9.0 mg/kg AgNP (14 nm, PVP-coated) or 9.0 mg/kg ionic silver (silver acetate) for 28 days. On day 18 of exposure, urine was collected for a 24-hour period for measures of metabolites. No effects on metabolites were found in male rats. However, in female rats, uric acid was significantly increased following exposure to the middle and high dose of particles, but not following exposure to silver acetate. Allantoin was significantly elevated following exposure to particle and to ionic silver. The findings suggest a greater sensitivity in females. In addition, the authors suggest that the increase in urine metabolism resulting in the increase in these metabolites is indicative of oxidative stress and cytotoxicity, resulting in DNA degradation, and that these are potential mechanisms for AgNP toxicity. The theory is supported by other studies discussed above that suggest oxidative stress is present following AgNP exposure [Elle et al. 2013; Shrivastava et al. 2016].

Hadrup et al. [2012c] also compared the neurotoxic effects, in vivo and in vitro, of PVP-stabilized AgNPs (average diameter, 14 nm) and silver acetate. Following 28 days of oral administration, AgNP (4.5 and 9 mg/kg/day) and silver acetate (9 mg/kg/day) significantly increased the concentration of dopamine in the brains of Wistar female rats, whereas the brain concentration of 5-hydroxytryptamine (5-HT) was increased only by AgNP at a dose of 9 mg/kg/day. However, in the 14-day range-finding study, the brain dopamine concentration decreased in rats treated with AgNP at doses of 2.25 and 4.5 mg/kg/day. Three solutions consisting of (1) AgNP, (2) an ionic silver solution obtained

*This information is distributed solely for the purpose of pre-dissemination peer review under applicable information quality guidelines. It has not been formally disseminated by the National Institute for Occupational Safety and Health. It does not represent and should not be construed to represent any agency determination or policy.*

by filtering a nanosilver suspension, and (3) silver acetate were found in neuronal-like PC12 cells in vitro. AgNPs were not observed to cause necrosis. However, cell viability was decreased, and apoptosis (involving both the mitochondrial and the death receptor pathways) was found for all three solutions, with silver acetate being most potent. The findings suggest that the ionic silver and 14-nm AgNP preparations have similar neurotoxic effects, possibly due to the release of ionic silver from the surface of AgNPs.

Dabrowska-Bouta et al. [2016] also examined neurological effects, specifically related to behavior and effects on cerebral myelin following low-dose subacute exposure to AgNP. Male Wistar rats were exposed to saline, 0.2 mg/kg AgNPs (10 nm, citrate stabilized), or 0.2 mg/kg silver citrate (ionic silver) for 14 days. Body weight and temperature were monitored on days 1, 8, and 14. On days 15 and 16 a battery of tests to evaluate behavioral effects were performed, including locomotor activity (distance traveled in 30 minutes), motor coordination (rotarod performance test), memory (novel object recognition test), anxiety performance (elevated plus-shaped maze apparatus), and nociceptive reaction (tail-immersion test). TEM was performed to assess myelin structure, and expression of myelin-specific proteins was quantified. AgNP and ionic silver caused an increase in body temperature on day 8, which persisted in the ionic silver group on day 14, and an increase in body weight on day 14 following AgNP exposure was observed. No differences in any groups were noted for tests assessing motor activity, motor coordination, or memory. Only exposure to ionic silver decreased sensitivity to noxious stimuli (nociceptive test) and increased behavioral anxiety. However, similar forms of damage to myelin were observed in brain of rats exposed to AgNP or ionic silver. Both forms of silver decreased expression of three myelin-related proteins. AgNP increased the mRNA expression of these three proteins, whereas ionic silver exposure increased only one of these proteins. The authors suggest that molecular and structural effects in myelin following low-dose exposure to AgNP indicate that the brain may be a target organ for silver and that more studies are required to better understand neurotoxicity outcomes.

*This information is distributed solely for the purpose of pre-dissemination peer review under applicable information quality guidelines. It has not been formally disseminated by the National Institute for Occupational Safety and Health. It does not represent and should not be construed to represent any agency determination or policy.*

In addition to the subacute oral exposure studies discussed above that try to establish the role of particle size and solubility in toxicity, there is one subchronic study that examined tissue distribution and toxicity following a 13-week exposure to ionic silver or citrate-coated AgNPs that vary in size [Boudreau et al. 2016]. In this study, which is related to Williams et al. [2015] discussed above, male and female Sprague-Dawley/CD-23 rats were orally exposed to 9, 13, or 36 mg/kg of 10, 75, or 110 nm AgNP, or 100, 200, or 400 mg/kg silver acetate daily for 13 weeks. Control groups included 2 mM citrate to control for the coating material, or water as a vehicle control. Following the last exposure, histopathology and tissue distribution of silver were evaluated in testes, uterine horn, mesenteric lymph nodes, femur bone marrow, eyes, proximal ileum, jejunum, proximal colon, kidney, liver, spleen, and heart. Localization of silver deposits in tissues was analyzed in TEM images. Additionally, micronuclei formation in blood was measured and reproductive toxicity was evaluated by vaginal cytology, sperm count, sperm mobility, and sperm morphology studies. It should be noted that direct comparison of soluble silver exposure to AgNP exposure in this study is difficult because the dose ranges were drastically different for the two materials; however, testing of both compounds provided information on distribution and toxicity in their own right.

The authors report that AgNP exposure did not result in any treatment-related pathology in tissues, nor did it cause and changes in blood chemistry or hematology values. Silver acetate exposure resulted in significant mortality at the high dose used in the study, with most animals removed before termination of the 13-week exposure. In those that survived the 400-mg/kg dose, there was an increased incidence and severity of lesions characterized by mucosal hyperplasia in small and large intestine and thymic atrophy/necrosis. Differences in hematological values were described as sporadic for animals exposed to the soluble silver (lower mean corpuscular volumes and higher red blood cell counts) and no differences in blood chemistry were noted. AgNP did not increase micronuclei formation, whereas the highest dose of soluble silver did result in increases at week 4 of the 13-week study. No differences in results of vaginal cytology or sperm analysis were detected. In the silver distribution portion of the study, light

*This information is distributed solely for the purpose of pre-dissemination peer review under applicable information quality guidelines. It has not been formally disseminated by the National Institute for Occupational Safety and Health. It does not represent and should not be construed to represent any agency determination or policy.*

microscopy revealed pigmentation in tissues following AgNP or silver acetate exposure that the authors deemed a product of silver translocation to these organs, and this was quantified. Pigmentation was greater in females compared to males following AgNP exposure, particularly in lymph nodes, large intestine, stomach, kidney, and spleen, but size differences could not be discerned. In males, a size difference could be detected whereby the smallest particle showed the greatest prevalence. Pigmentation was greatly increased in rats exposed to soluble silver. TEM examination further showed that the distribution of silver was different between AgNP and soluble silver at the cellular level, with AgNP found primarily within the cell, whereas the soluble silver localized to the extracellular membranes of the cells. Silver burden in tissues was measured by ICP-MS. Blood, bone marrow, and heart had the lowest measured values for silver content in both AgNP- and soluble silver-exposed groups. Blood and bone marrow levels were higher in the 10-nm AgNP group compared to the other sizes of AgNP, and levels in the soluble-silver group were higher than in the AgNP group, as would be anticipated because of dosing differences. In general, silver levels in the gastrointestinal tract were higher than in other tissues. Accumulation was greater in females in most portions of the gastrointestinal tract, with the exception of the ileum. The mesenteric lymph nodes had the highest concentration of silver. The AgNP and soluble-silver groups exhibited similar profiles of deposition in the gut. In the major organs outside the gastrointestinal tract, particle size and sex differences were observed, with the exposure to the smaller particle leading to greater deposition than larger particles. In female rats, levels in kidney and spleen were significantly higher than in male rats. Concentrations in organs were higher with the soluble silver exposure; however, the patterns of deposition were similar to those of the AgNP. To summarize, the major findings suggest that the smaller particle size led to increased tissue distribution relative to larger particles. At the organ level, patterns of distribution were similar between soluble and particle silver, with prominent sex differences, whereas distribution within cells differed depending on solubility.

In addition to studies of systemic toxicity in potential target organ systems such as liver, kidney, spleen, and brain, a number of studies have been performed that assess effects

of oral exposure to AgNP on reproduction and reproductive development in both males [Lafuente et al. 2016; Thakur et al. 2014; Miresmaeili et al. 2013; Mathiu et al. 2014; Sleiman et al. 2013] and females [Fennell et al. 2016; Philbrook et al. 2011; Yu et al. 2014]. Lafuente et al. [2016] conducted a subchronic exposure study in adult male Sprague-Dawley rats to assess effects on sperm count, motility, viability, and morphology, as well as epididymal and testicular pathology. Rats were orally administered 0, 50, 100, or 200 mg/kg of 20- to 30-nm AgNPs coated with PVP, for 90 days. Similar to the lower-dose study by Boudreau et al. [2016], no significant changes in sperm number or motility were found. However, an increase in changes in sperm morphology was found, including alterations in the shape of the tail (100 mg/kg) or the head (50 mg/kg) and in some instances detached head. Histopathological analysis of tissues showed no changes to testes or epididymis; however, a trend for an increment of desquamation into the tubular lumen following the highest dose was noted.

Another 90-day oral exposure study was conducted by Thakur et al. [2014] in adult male Wistar rats. Rats received 0 or 20 µg/kg/day of citrate-stabilized AgNPs (5–20 nm) for 90 days, a considerably lower dose than that used in the study by Lafuente et al. [2016]. Histopathology and TEM analysis of the testis were performed following exposure. Histopathological analysis indicated abnormalities in the testis related to atrophy of the seminiferous tubules, abnormalities in germinal epithelium, loss of spermatogenic cells, and exfoliation of germ cells. TEM analysis revealed thickened and fibrous seminiferous tubules, depletion and necrosis of germ cells, and abnormal structure among sertoli cells, spermatocytes, and spermatids. Reasons for difference in observations between Lafuente et al. [2016] and Thakur et al. [2014] could be attributable to the difference in AgNP coating or to the rat strain.

Three studies have been conducted on pre-pubertal male rats [Mathias et al. 2104; Sleiman et al. 2013; Miresmaeili et al. 2013]. Pre-pubertal male Wistar rats ( $n = 30$ ) were orally treated with 15 or 30 µg/kg/day AgNPs (~86 nm in diameter, citrate stabilized) from postnatal day 23 to postnatal day 58 (35 days, at a total dose of 131–263 µg Ag/rat) and killed on postnatal day 102 to evaluate the effects on sexual

*This information is distributed solely for the purpose of pre-dissemination peer review under applicable information quality guidelines. It has not been formally disseminated by the National Institute for Occupational Safety and Health. It does not represent and should not be construed to represent any agency determination or policy.*

behavior and reproduction [Mathias et al. 2014]. The acrosome integrity, plasma membrane integrity, mitochondrial activity, and morphologic alterations of the sperm were analyzed. Sexual partner preference, sexual behavior, and serum concentrations of follicle stimulating hormone (FSH), luteinizing hormone (LH), testosterone, and estradiol were also recorded. No measurements of blood silver were made. Exposure to AgNPs was found to reduce the acrosome and plasma membrane integrities, reduce mitochondrial activity ( $p < 0.05$ ), and increase the abnormalities of the sperm ( $<0.01$ ) in both the 15- and 30- $\mu\text{g}/\text{kg}$  groups versus controls. AgNP exposure also delayed the onset of puberty, although no changes in body growth were observed in either treatment group. The animals did not show changes in sexual behavior or serum hormone concentrations. The serum concentrations of FSH, LH, testosterone, and estradiol were not significantly different between the experimental groups. Because the hormone profiles of testosterone, estradiol, FSH, and LH were not altered by AgNP treatment, the investigators suggested that the defective sperm function and morphology observed in this study may have resulted from defective spermatogenesis due to direct effects of AgNPs on spermatogenic cells. Similar findings of increased sperm morphologic abnormalities were observed by Gromadzka-Ostrowska et al. [2012] following a single intravenous dosing of AgNPs in rats, and by Lafuente et al. [2016] and Thakur et al. [2014] following oral exposure, the latter having examined a similar dose in a longer subchronic study in adult rats as discussed above. Another commonality with the study by Thakur et al. [2014] was the citrate-coating or stabilizing agent, although the particle in Mathias et al. [2014] was larger, and the strain of rat used in the study was the same.

In a second oral study, scientists from the same research group [Sleiman et al. 2013] carried out a similar exposure regimen with male Wistar rats ( $n = 30$ ) exposed to AgNPs (~86 nm, citrate stabilized) during the pre-pubertal period and killed on postnatal days 53 and 90. Animals were treated orally with either 15  $\mu\text{g}/\text{kg}$  BW or 50  $\mu\text{g}/\text{kg}$  BW, from postnatal day 23 until postnatal day 53. Growth was assessed by daily weighing. The progress of puberty in the rats was measured by preputial separation, while spermatogenesis was assayed by measuring the sperm count in testes and epididymis and examining the morphologic and morphometric characteristics of seminiferous

*This information is distributed solely for the purpose of pre-dissemination peer review under applicable information quality guidelines. It has not been formally disseminated by the National Institute for Occupational Safety and Health. It does not represent and should not be construed to represent any agency determination or policy.*

epithelium by stereologic analysis. In addition, testosterone and estradiol levels were assayed by radioimmunoassay. The weight of animals during postnatal days 34 to 53 was lower in the 50- $\mu\text{g}/\text{kg}$  treatment group than in the control group and the 15- $\mu\text{g}/\text{kg}$  treatment group; however, at 90 days postnatal, the growth among groups was not markedly different. A numerical reduction in total and daily sperm production was observed in the 50- $\mu\text{g}/\text{kg}$  AgNP group on postnatal day 53. On postnatal day 90, both treatment groups had significantly lower total and daily sperm production ( $p < 0.05$ ) in comparison with the control group. Decreased sperm reserves in the epididymis and diminished sperm transit time were also observed on postnatal day 53. However, no alterations of testosterone and estradiol serum concentrations were found on postnatal days 53 and 90. On postnatal days 53 and 90, discontinuity and disorganization of seminiferous epithelium, cellular debris in the lumen, and sloughing of the germinal cells from the epithelium into the tubular lumen were found. The presence of cellular debris and germinal epithelial cells in the tubular lumen and vesicles was suggested as being a possible impairment to the spermatogenesis process.

In a separate study on pre-pubertal male Wistar rats, Maresmaeili et al [2013] administered 70-nm AgNPs (coating and stabilizing agent not characterized) to rats 45–50 days of age, twice a day for 48 days (equating to one spermatogenesis period), for a total dose per day of 0, 25, 50, 100, or 200 mg/kg. The epididymis was collected for spermatogenic cell counts and histology, and the acrosome reaction assay was performed and dead or viable sperm with and without acrosome reaction were measured. Significant differences for viable sperm with and without acrosomal reaction were noted at the two lower doses of AgNP. Thickening of connective tissue in seminiferous tubules was noted following AgNP exposure; however, tubule diameter did not increase. There was a significant reduction in the number of spermatocytes, spermatids, and spermatozoa in all groups. At the high dose, spermatogonia were also reduced. This study further substantiates the potential for the testis, and particularly the process of spermatogenesis, as a target following oral exposure to AgNP.

*This information is distributed solely for the purpose of pre-dissemination peer review under applicable information quality guidelines. It has not been formally disseminated by the National Institute for Occupational Safety and Health. It does not represent and should not be construed to represent any agency determination or policy.*

Studies have also been conducted on pregnant dams and embryo/fetal development (Fennel et al. 2016; Philbrook et al. 2011; Yu et al. 2014). Fennel et al. [2016] conducted a study that compared effects of AgNP size and solubility on tissue distribution, plasma biomarkers, and urine metabolites in pregnant Sprague-Dawley rats following oral gavage or intravenous administration. In this study, rats were dosed with 10 mg/kg of silver acetate stabilized in PVP or 20-nm or 110-nm PVP-coated AgNPs by oral gavage on gestation day 18. At 24 and 48 hours, tissues were collected for measurements of silver content by ICP-MS. Urine and feces were collected to measure excreted silver. Cardiovascular markers of injury were measured in plasma, and metabolites and 8-OH-dG (oxidative stress marker) were measured in urine. The same set of measurements were made in a separate group of rats administered 1 mg/kg of the different sample by intravenous exposure. Because of a limited number of animals per group per parameter evaluated ( $n = 1-3$ ), clear trends within a route of exposure were difficult to assess; however, following oral exposure, the majority of silver in the silver acetate group and the 110-nm group was recovered in the feces (total silver recovered in the 20 nm group was 28%, indicating a potential issue in measurement of that group). In all groups at 48 hours, outside of the GI tract tissue, silver content was highest in placenta and was also measureable in the fetus. In the liver, the highest levels were observed in the silver acetate group, potentially indicating a difference in distribution due to solubility. Following intravenous exposure, silver measurements in tissues, urine, and excretion indicated a recovery rate of 23% to 57% of the dose. Silver was detectable in most organs, including the placenta and the fetus, with the highest levels measured in the spleens for the particle-exposed groups and the lungs for the silver acetate-exposed groups at 48 hours, indicating again the differences in distribution related to solubility. No difference were observed in markers of toxicity in plasma or urine due to exposure or route of exposure; however, carbohydrate and amino acid metabolites were affected following silver exposure.

A size and particle comparison study was conducted by Philbrook et al. [2011] on female CD-1 mice. Mice were administered a single oral dose of 10, 100, or 1000 mg/kg of 20-nm AgNP, 3  $\mu\text{m}$  Ag microparticles, 50-nm  $\text{TiO}_2$  NP, or 1–2  $\mu\text{m}$   $\text{TiO}_2$  microparticles

*This information is distributed solely for the purpose of pre-dissemination peer review under applicable information quality guidelines. It has not been formally disseminated by the National Institute for Occupational Safety and Health. It does not represent and should not be construed to represent any agency determination or policy.*

on gestation day 9 or vehicle control (0.5 % tragacanth gum in deionized water). Effects of exposure on the fetus were assessed one day before spontaneous delivery. Skeletons were examined for defects in vertebrae and sternbrae, as well as cleft palate, and polydactyl, braincase abnormalities. TEM analysis of liver and kidney tissue was performed to evaluate translocation of silver to the fetus, and inflammation and cell death were assessed histologically in liver, kidney, and placenta. Additional studies were also performed on *Drosophila melanogaster* to assess effects on reproduction and egg and larval development. NP exposure did not alter weight gain in pregnant dams, litter size, fetal resorption, fetal length, or fetal weight. AgNP at 10 mg/kg and TiO<sub>2</sub> NP at 100- and 1000-mg/kg exposure did reduce the number of viable fetuses. In addition, TiO<sub>2</sub> NP at the two higher doses led to developmental abnormalities in fetuses (encephalopathy, open eye lids, and leg and tail defects). Neither NP caused cell death or inflammation in liver, kidney, or placenta; however, AgNP could be detected in kidney and liver. Similar to the mammalian toxicity study, TiO<sub>2</sub> NP had greater effects in the fruit fly than AgNP, although both NPs had greater effects than the micron-sized counterpart. Yu et al. [2014] conducted a subacute dose-response exposure in pregnant Sprague-Dawley rat dams. Rats were administered 100, 300, or 1000 mg/kg/day of 6.45-nm AgNP in 0.5% CMC on gestational days 6 to 19. Cesarean sections were performed on gestational day 20. Blood chemistry was performed on dams, and livers were homogenized to evaluate oxidative stress. Ovaries and uteruses of dams were also removed, and corpus lutea and implantation sites were evaluated. Fetuses were evaluated for viability, malformations, and morphological abnormalities. The only significant finding related to fetal effects in pregnancy was an increase at the highest dose in loss of pre-implanted embryos, and only one fetus in the high-dose group had skeletal malformation. Other skeletal variations existed among groups, but differences were not significant. No effects were observed regarding number of fetuses or litters. Weight gain and blood chemistry parameters in dams, including indices of kidney and liver function, were normal. Catalase and glutathione reductase were elevated in liver homogenates of dams in all dose groups, and glutathione content was elevated in the high-dose group, indicating the potential of AgNP to cause oxidative stress in

*This information is distributed solely for the purpose of pre-dissemination peer review under applicable information quality guidelines. It has not been formally disseminated by the National Institute for Occupational Safety and Health. It does not represent and should not be construed to represent any agency determination or policy.*

pregnancy. The authors concluded the NOEL to be <100 mg/kg/day for dams because of hepatic oxidative stress and 1000 mg/kg/day for fetal and embryo development.

In terms of genotoxic potential, Kovvuru et al. [2015] examined the potential for genotoxicity and DNA damage due to AgNP exposure in male and female mice, as well as offspring of pregnant mice, using a strain of knockout mice deficient in *Mhy* (*MutY* homologue), a DNA glycosylase involved in base excision repair to correct for promutagenic activity, whereby adenosine mispairs with 8-oxoguanine or where formation of 2-hydroxyladenine (2-OH-A) occurs. These mice would be more susceptible to genotoxic events involving DNA repair. The goal of the study was to determine whether genotoxicity following AgNP exposure is related to oxidative DNA damage. In this study, male and female C57BL/6J *p<sup>un</sup>/p<sup>un</sup>* background mice or *Mhy*<sup>-/-</sup> mice were exposed to 96.1-nm AgNP (determined by DLS) at a dose of 500 mg/kg/day for 5 days. Pregnant mice of each background were exposed to 500 mg/kg on gestational days 9.5 to 13.5. Wildtype and knockout mice were evaluated for micronuclei formation (chromosomal damage) and positive staining for  $\gamma$ -H2AX (double-strand breaks) in the blood and bone marrow, and positive staining for 8-oxoguanine (oxidative DNA damage) in the blood. Liver tissue was evaluated by PCR array profiling of genes involved in DNA repair. Offspring of dams were evaluated for DNA deletions, evidenced as eye spot formation visualized in the retinal epithelium at 20 days of age. AgNP exposure in wildtype mice increased micronuclei formation in blood and bone marrow, and this response was further increased in knockout mice. Induction of  $\gamma$ -H2AX foci and 8-oxoG was also increased in both groups of AgNP-exposed mice. Gene profiling showed that 36 or 84 DNA repair genes were modulated (24 downregulated, 12 upregulated) in AgNP-exposed mice, several of which were differentially up- or downregulated between the wildtype and knockout groups. In offspring of both wildtype and knockout mice, AgNP exposure led to increased eye spot formation on the retina epithelium, indicative of DNA deletion events in utero. Results taken together suggest that AgNP induces genotoxicity, which may be in part due to oxidative stress and damage to DNA. The role of oxidative stress in DNA damage is corroborated by oral exposure studies discussed previously [Shrivastava et al. 2016; Hadrup et al. 2012b].

## **E.3 Exposure via Other Routes**

### **E.3.1 Dermal**

Wahlberg [1965] reported on a series of percutaneous studies with guinea pigs in which various metal compounds were used to evaluate the rate of absorption. The rate of absorption for silver nitrate (2 mL applied to skin and observed 3 weeks post-exposure) was found to be small (<1% per 5-hour period) compared to the rate of absorption of the other metals. The rates of dermal absorption were compared to the toxicity of silver nitrate and the other metals following intraperitoneal administration at a dose of 2 mL. The relative toxicity (mortality) observed for the various metals following intraperitoneal administration was comparable to the rate of dermal absorption found with guinea pigs; the lowest mortality rate was among guinea pigs exposed to silver.

Recently published studies examined the dermal toxicity of AgNPs in female weanling pigs [Samberg et al. 2010] and guinea pigs [Maneewattanapinyo et al. 2011; Kim et al. 2013b; Korani et al. 2011]. In the study by Samberg et al. [2010], female pigs were topically exposed to washed and unwashed AgNPs (average diameters of 20 and 50 nm) that were suspended in deionized water solutions of 0.34, 3.4, or 34 µg/mL over a 14-day period. The site of application was then examined for irritation on the basis of the Draize scoring system, and excised pieces of skin were examined by light and electron microscopy. Other than a general graying of the skin, there were no direct signs of topical irritation, although some indications of focal inflammation and edema were seen when the skin was viewed under light microscopy. For example, the authors noted the occurrence of epidermal hyperplasia with an extension of rete pegs into the dermis. However, the AgNPs themselves appeared to be limited to the superficial layers of the stratum corneum. These findings were consistent with those reported by Maneewattanapinyo et al. [2011] and Kim et al. [2013]. Maneewattanapinyo et al. [2011] evaluated the dermal toxicity and irritation potential of 10–20-nm AgNP, following the OECD 434 guideline (acute dermal toxicity – fixed dose procedure). Male guinea pigs were exposed to 50 or 100,000 ppm AgNP, which remained in contact with the skin for

*This information is distributed solely for the purpose of pre-dissemination peer review under applicable information quality guidelines. It has not been formally disseminated by the National Institute for Occupational Safety and Health. It does not represent and should not be construed to represent any agency determination or policy.*

24 hours. Symptoms, along with weight and morbidity, were monitored at 1, 3, 7, and 14 days after exposure, and histopathological examination was done at day 14. No abnormal findings were reported. This study also examined eye irritation and found transient eye irritation at a dose of 5000 mg/kg at 24 hours after exposure, resolving by 72 hours. Kim et al. [2013] evaluated acute dermal toxicity in Sprague-Dawley rats (OECD 402 guideline), irritation potential in New Zealand White rabbits (OECD 404 guideline), and sensitization potential in SPF guinea pigs (OECD 406 guideline), using 10-nm AgNPs. No toxicity, change in body weight, or mortality was reported for doses of 2000 mg/kg following 24 hours of skin exposure, up to 2 weeks following exposure. During the study with rabbits, no significant clinical signs or deaths were observed. In the initial ocular test at a dose of 100 mg per animal, no signs of irritation to the cornea, iris, or conjunctiva were observed 1, 24, 48, and 72 hours after removal of the test substance. When AgNPs were applied to the skin of SPF guinea pigs in accordance with OECD Test Guideline 406, a sensitization protocol that involves an induction phase with adjuvant as well as a challenge phase, none of the tested animals died or showed any significant body weight change or abnormal clinical signs during the experimental period. Only 1 out of 20 animals had patchy erythema, yielding a 5% skin sensitization rate (classification of weak sensitizer).

However, these findings contrasted with those reported by Korani et al. [2011], in which an array of changes to the skin of Hartley guinea pigs were observed following dermal application of aqueous solutions of colloidal AgNPs (<100-nm diameters) at concentrations of 100 and 1,000 µg/mL in an acute study (6 animals/dose) using OECD Test Guideline 402 and three concentrations of 100, 1,000, and 10,000 µg/mL (6 animals/dose) in a subchronic study. In the acute study, 10% of the body surface was exposed and examined 1, 24, 48, and 72 hours post-exposure for presence of edema, erythema, or any type of dermal change. Observations continued for 14 days. In the subchronic study, a shaved skin area of 5 cm × 5 cm was applied 5 days/week with 100, 1000, or 10,000 µg/mL AgNPs for 13 weeks; skin of the positive controls was rubbed with 100 µg/mL of AgNO<sub>3</sub>. Korani et al. [2011] described an array of changes to the skin as a result of either dosing regimen, with increasing severity in such responses as

*This information is distributed solely for the purpose of pre-dissemination peer review under applicable information quality guidelines. It has not been formally disseminated by the National Institute for Occupational Safety and Health. It does not represent and should not be construed to represent any agency determination or policy.*

epidermal thickness, inflammation, presence of round and clear cells, and reduced papillary in relation to dose and exposure duration. Similar skin inflammatory responses were recorded in all treatment groups in the subchronic study. Increased incidence of histopathologic responses in the liver and spleen were also reported for the subchronic study, with signs of necrosis at the highest dose. The results indicate that dermal contact with AgNPs causes slight histopathologic abnormalities of the skin, liver, and spleen of animals that can occur at dermal concentrations  $>0.1$  mg/kg ( $>100$   $\mu$ g). In a follow-up study by Korani et al. [2013], the subchronic dermal exposure (5 days per week for 13 weeks to 0, 100, 1,000, or 10,000 ppm of colloidal AgNPs, or silver nitrate at 100  $\mu$ g/ml, as aqueous solutions applied to skin) was repeated with focus specifically on effects in kidneys, bone, and heart. Tissue distribution following dermal exposure was measured with an atomic absorption spectrophotometer, and degree of accumulation was reported as follows: kidney  $>$  muscle  $>$  bone  $>$  skin  $>$  liver  $>$  heart  $>$  spleen. Pathological studies were performed on heart, kidney, and bone. Bone was evaluated for inflammation, osteoclast formation, narrowing of marrow space, and line separating of lamellar bone. Abnormalities were observed with all doses, and dose-dependent increases in severity occurred for all parameters, with the exception of inflammation. Heart tissue was evaluated for inflammation, cardiocyte deformity, clear zone around nucleus, and congestion/hemorrhage, with dose-dependent increases found in all parameters. Toxicity in the kidney was evaluated as inflammation, proximal convoluted tubule (PCT) degeneration, adhesion of glomerular epithelial cells to Bowman's capsule (BC), capsular thickening, membranous thickening, and increased mesangial cells. Again, a dose-dependent increase was observed for most parameters, with the most severe affects including PCT degeneration, followed by effects in BC and capsular thickening. In all instances, the 100- $\mu$ g/ml silver nitrate control scored similarly in severity to the 100-ppm dose. Both studies together indicate the potential for silver to translocate to other organ systems following subchronic exposure; however, it is unclear whether this effect is related to dissolution rate and consequently delivery of ion or particle to tissue.

*This information is distributed solely for the purpose of pre-dissemination peer review under applicable information quality guidelines. It has not been formally disseminated by the National Institute for Occupational Safety and Health. It does not represent and should not be construed to represent any agency determination or policy.*

Ling et al. [2012] reported on the potential dermal exposure risk to workers for nanoscale zinc oxide powder, multiwall carbon nanotubes, and nanoscale silver (Ag-colloid, Ag-liquid) so that appropriate risk management practices could be incorporated in the workplace to protect workers. The assessment of workers' risk of exposure to nanoscale silver focused on the potential for dermal absorption of silver during the handling of nanoscale silver-colloid (average diameter, 9.87 nm) and silver-liquid (average diameter, 13.04 nm). Based on criteria by OECD [2004], WHO [2010], and U.S. EPA [2004], two skin exposure techniques were used (transdermal Franz diffusion cell drive and tape stripping) to evaluate dermal absorption of nanoscale silver. Excised porcine skin was used as a model for human skin in the transdermal Franz diffusion cell test. Nanoscale silver-colloid and silver-liquid samples flowed with specific rates through a portion of the skin for 18 hours. The sampled porcine skin and remaining fluids were analyzed for silver with use of flame atomic absorption spectrometry (FAAS); silver concentrations from the remaining skin and fluids were then added and compared with the original amounts. For the tape stripping technique, nanoscale silver-colloid and silver-liquid at concentrations of 20 µg/mL and 300 µg/mL, respectively, were applied evenly on human skin for 2 hours. After this, tapes with areas of 5 cm<sup>2</sup> were patched on the human skin and subjected to pressure, followed by immediate tape stripping. Stripping was repeated 5 times, with each taking up 6 to 8 layers of the stratum cornea, yielding about 30 to 40 cell layers of the stratum cornea being removed. The stripping tapes were analyzed by using inductively coupled plasma mass spectrometry (ICP/MS) to quantify silver contents. Results of the tape stripping analysis showed that the distribution of nanoscale silver colloid and silver liquid was predominantly on the first and second strippings of the stratum cornea. This occurred at both the 20-µg/mL and 300-µg/mL concentrations, indicating a low rate of skin penetration over a short period of exposure. In addition, the experiments showed that organic modifiers affected the infiltration of nanoscale silver. When a less-polar solvent such as isopropyl alcohol was used, the penetration rate was higher than for other polar solvents.

Although the dermal toxicity data from studies of animals and studies using porcine skin are limited, they suggest that AgNPs can penetrate the skin epidermis [Larese et al.

*This information is distributed solely for the purpose of pre-dissemination peer review under applicable information quality guidelines. It has not been formally disseminated by the National Institute for Occupational Safety and Health. It does not represent and should not be construed to represent any agency determination or policy.*

2009; Ling et al. 2012], can induce some systemic toxicity [Korani et al. 2011; 2013], and can cause topical irritation at the site of contact [Samberg et al. 2010; Korani et al. 2011], depending on dose and duration of exposure.

## E.3.2 Intratracheal instillation, oropharyngeal aspiration, or intranasal instillation

### E.3.2.1 Silver nanoparticles

Alternatives to inhalation exposure, including intratracheal (IT) instillation, oropharyngeal aspiration, or intranasal (IN) instillation, have been employed to study the in vivo responses to AgNPs in the lungs of experimental animals. All of the studies in Table E-5 examine various lung effects following exposure. A number of studies have focused on the pulmonary effects and/or lung distribution following exposure to a single form and size of AgNP alone or in comparison with other metal NPs [Arai et al. 2015; Haberl et al. 2013; Kaewamatawong et al. 2014; Katsnelson et al. 2013; Liu et al. 2013a; Park et al. 2011b; Roberts et al. 2012; Smulders et al. 2014, 2015a]. Other studies have focused on systemic effects in addition to lung responses following exposure to AgNPs [Davenport et al. 2015; Genter et al. 2012; Gosens et al. 2015; Holland et al. 2015; Huo et al. 2015; Liu et al. 2012; Minchenko et al. 2012; Wen et al. 2015]. Additionally, several studies have examined the effects of size and capping/coating agent on toxicity and biodistribution [Anderson et al. 2015b; Botelho et al. 2016; Silva et al. 2015; Seiffert et al. 2015].

Studies examined acute responses up to 1 day post-exposure to a single IT instillation of AgNP [Arai et al. 2015; Haberl et al. 2013; Katsnelson et al. 2013]. Haberl et al. [2013] examined lung injury and inflammation in BAL following a dose-response (0, 50, or 250 µg per rat) to AgNP ~70 nm in diameter with PVP coating in female Wistar-Kyoto rats. In this study, a trend for a dose-dependent increase in inflammation was measured as BAL neutrophil influx and increased BAL cytokines (IL-1β, IL-6, IL-12p70, MIP-1α, MIP-2, CINC-1, M-CSF); however, increases were significant only when compared to

*This information is distributed solely for the purpose of pre-dissemination peer review under applicable information quality guidelines. It has not been formally disseminated by the National Institute for Occupational Safety and Health. It does not represent and should not be construed to represent any agency determination or policy.*

control at the highest AgNP dose administered. The high dose also caused significant lung injury (increased BAL LDH and protein levels) 24 hours post-exposure.

Katsnelson et al. [2013] investigated pulmonary effects 24 hours after a single IT administration of 49-nm AgNP generated by laser ablation of a metal target, in comparison to gold NPs or micron-sized silver particles (1.1  $\mu\text{m}$  diameter) at a dose of 0.5 mg in 1 ml of vehicle in female rats. Inflammatory cell infiltration, phagocytosis, and cell distribution of particles were evaluated. AgNP exposure caused a greater degree of neutrophil influx into the lungs when compared to both the micron-size silver and gold NPs. A greater degree of phagocyte-uptake of AgNP occurred in comparison with micro-size silver particles, measured as pit number and size on the surface of alveolar macrophages by atomic force microscopy. TEM showed a difference in distribution of Ag NPs versus gold NPs, where Ag NPs did not penetrate cell nuclei but did have affinity for the mitochondria. The study demonstrated that cytotoxicity and distribution varied according to size and chemical composition of particles. Arai et al. [2015] examined lung effects and systemic distribution in male ICR mice at 4 and 24 hours post-exposure to 10  $\mu\text{g}$  of 20-nm citrate-coated AgNP or AgNO<sub>3</sub> solution as a control for effects of the ionic/soluble form of silver. Silver was measured by ICP-MS in lung, liver, kidney, spleen, and urine. Lung levels of silver were lower in mice administered the ionic form of silver, suggesting a faster rate of lung clearance versus AgNP. Both AgNP and the ionic form of silver were detected in the liver, and the increase was significantly greater for the ionic form as compared to AgNP, suggesting a faster rate of biodistribution for the ionic form. No significantly increased silver levels were detected for either form in kidney, spleen, or urine at these early time points post-exposure. Both forms of silver caused an increase in lung neutrophils. The increase was significant only for the ionic form at 24 hours. AgNP increased BAL IL-1 $\beta$  significantly at 4 hours post-exposure. In a parallel in vitro study in J774.1 cells, AgNPs were shown to distribute to metallothioneins and were found sequestered in the lysosome, with gradual dissolution over time. This study indicated that the soluble form of silver caused greater

*This information is distributed solely for the purpose of pre-dissemination peer review under applicable information quality guidelines. It has not been formally disseminated by the National Institute for Occupational Safety and Health. It does not represent and should not be construed to represent any agency determination or policy.*

inflammation at 24 hours post-exposure and was cleared faster from the lung (related to greater distribution to the liver), in comparison with AgNP.

Park et al. [2011b] and Kaewamatawong et al. [2014] examined lung responses up to 1 month following a single IT instillation of AgNP. Park et al. [2014] administered AgNPs at doses up to 500 µg/kg to ICR mice and evaluated the resulting inflammation by measuring the concentration of cytokines in BAL and in the blood. The commercially supplied AgNPs were originally suspended in THF with sonication. After all of the solvent had been allowed to evaporate, the particles were reconstituted in phosphate-buffered saline (PBS). A histopathologic analysis was also carried out on excised pieces of lung, and changes in gene expression were assessed by using a microarray method. The AgNPs were dispersed in an aqueous medium, and there was evidence of aggregation in that the average diameter of particles was 243.8 nm. A considerable number of dose-related changes were evident in the cytokine composition of BAL and blood as a result of exposure to AgNPs. In BAL, the most dramatic increases in cytokine levels were manifest in IL-1, IL-6, IL-10, and TGF-β. These agents appeared to reach a maximum concentration 28 days after exposure. In the blood, concentrations of IL-6, IL-12, IFN-γ, and IL-10 showed significant increases on the day after instillation. Histopathologic analysis indicated inflammatory responses, such as infiltration of alveolar macrophages, in lung tissue on day 1 but not on days 14 and 28. The responses were characterized by the presence of cell debris, dead neutrophils, and foreign bodies. A substantial number of changes in gene expression resulted from IT instillation of AgNPs, with 261 genes being upregulated and 103 genes downregulated. Changes in the functionality of induced genes appeared to be related to tissue damage. Kaewamatawong et al. [2014] measured parameters of lung injury, inflammation, and oxidative stress in male ICR mice at 1, 3, 7, 15, and 30 days post-exposure to colloidal AgNP (0 or 100 ppm, 10–20-nm diameter). Cytotoxicity in BAL cells was increased at days 1 and 3 post-exposure to AgNP. Neutrophil influx was significantly increased at 3 days post-exposure, and lymphocyte influx increased at 7 and 15 days post-exposure. Histopathological findings showed increased neutrophils and macrophages 1 and 3 days after instillation, mild-to-moderate multifocal alveolitis in areas with macrophages

*This information is distributed solely for the purpose of pre-dissemination peer review under applicable information quality guidelines. It has not been formally disseminated by the National Institute for Occupational Safety and Health. It does not represent and should not be construed to represent any agency determination or policy.*

that contained AgNP, and type II cell hypertrophy and hyperplasia. Histopathology responses peaked by 7–15 days post-exposure, with the additional findings of cellular necrosis, lymphocytic infiltration, and mild to moderate loss of structural architecture. Areas of lung injury in tissue corresponded to increased immunohistochemical staining of superoxide dismutase, suggesting AgNP exposure increased oxidative stress. Immunohistochemical staining of metallothionein in tissue also correlated to areas high in AgNP, further suggesting affinity of AgNP for these proteins.

Repeated-dose, subacute exposure studies using IT instillation [Liu et al. 2013a; Roberts et al. 2012] or oropharyngeal aspiration [Smulders et al. 2014, 2015a] have also been performed to assess lung toxicity and distribution of AgNP. Intratracheal instillation of AgNPs in male Sprague-Dawley rats was observed to cause an increase in the cellular and protein content of BAL fluid, as well as increased injury, as determined by histopathological analysis. Liu et al. [2013a] exposed Wistar rats by IT instillation to 3.5 or 17.5 mg/kg of 52-nm AgNP once every 2 days for 5 weeks (19-nm ZnO NP and 23-nm TiO<sub>2</sub> NP were also evaluated). Lung effects were observed 1 day following the last exposure. Inflammation (IL-1, IL-6, MIP-2, TNF- $\alpha$  levels) and oxidant damage (GSH, SOD, MDA, and NO levels) were measured in BAL fluid. Both doses of AgNP caused increases in all parameters of oxidant damage as well as increases in IL-6 and MIP-2. The high dose of AgNP also caused increased TNF- $\alpha$  levels in BAL. The study implicates oxidative stress as a pathway for increased immune and inflammatory responses following exposure to AgNP. In a study by Roberts et al. [2012], male Sprague-Dawley rats were exposed to AgNPs (20 nm in diameter) with a 0.3%-by-weight coating of PVP. Dispersion of AgNPs in a physiologic medium caused some degree of aggregation, as indicated by the average particle size of 180 nm. AgNPs were administered weekly for 8 weeks at a dose regimen lower than that of Liu et al. [2013a], at 0, 9.35, or 112  $\mu$ g per rat (~0, 0.03, or 0.3 mg/kg), with subsequent evaluation after 7, 28, or 84 days. The high dose of AgNPs was observed to induce acute pulmonary injury and inflammation that appeared to resolve to a degree over time. The low dose produced very little lung injury or inflammation.

*This information is distributed solely for the purpose of pre-dissemination peer review under applicable information quality guidelines. It has not been formally disseminated by the National Institute for Occupational Safety and Health. It does not represent and should not be construed to represent any agency determination or policy.*

Smulders et al. [2014] conducted a comparative toxicity study that examined the effects of a repeated aspiration exposure to AgNP (25–28-nm diameter, 90-nm-diameter aggregated) relative to other metal-based ENMs and paints containing ENMs. Oropharyngeal aspiration in male BALB/c mice was conducted once a week for 5 weeks at 20 µg per exposure, for a cumulative dose of 100 µg per mouse. At 2 and 28 days after the last exposure, BAL and blood cell and cytokine responses were measured, as well as silver levels in lung, kidney, liver, spleen, and heart. Regarding findings related to the AgNP, BAL neutrophil influx was increased at 2 days after the last exposure, along with BAL IL-1 $\beta$  and KC, indicating increased inflammation following AgNP exposure. Inflammatory responses resolved by 28 days post-exposure. Silver levels in the lung were lower at day 28 versus 2 days post-exposure, showing a slight degree of clearance over time. Silver was increased in liver, kidney, and spleen at 2 days post-exposure, but not in the heart, and was shown to be cleared by 28 days post-exposure in those organs. In a follow-up study [Smulders et al. 2015a], using a similar exposure regimen, the investigators examined distribution of AgNP (heterogeneous mixture, 20-nm spherical and 80–90-nm rods, with average agglomeration of ~ 500 nm) in the lung along with co-localization with other metals and speciation of silver at 2 days following the last exposure. A high percentage of macrophages in both the airways and alveolar regions contained AgNPs. A large portion of the AgNPs were dissolved and were determined to be complexed to thiol-containing proteins, likely metallothioneins.

Several studies have examined pulmonary and extrapulmonary toxicity following IT or IN instillation of AgNP. Holland et al. [2015] examined the effects of a single IT instillation of 0 or 1 mg/ml of 20-nm citrate-capped AgNP on pulmonary and cardiovascular responses in a model of cardiac ischemic reperfusion (I/R) injury in rats. Responses were evaluated at 1 and 7 days after exposure and were compared to a dose-response of silver acetate (AgAc) as a soluble/ionic form of silver. Histopathology of the lung revealed no effects 1 day post-exposure. By 7 days, only a thickening of the alveolar wall was noted in AgNP-exposed rats. AgNP exposure did not increase neutrophil influx or protein content in the lungs; however, increased neutrophils, lymphocytes, and total lung protein were measured in the AgAc group. Serum cytokine

*This information is distributed solely for the purpose of pre-dissemination peer review under applicable information quality guidelines. It has not been formally disseminated by the National Institute for Occupational Safety and Health. It does not represent and should not be construed to represent any agency determination or policy.*

analysis showed increased pro-inflammatory cytokines (IL-1 $\beta$ , IL-6, IL-18, and TNF- $\alpha$ ,) at 1 day, and IL-2, IL-13, and TNF- $\alpha$  were elevated at 7 days in AgNP-exposed mice. AgAc did not significantly elevate serum cytokines. AgNP also caused expansion of I/R injury and depression of coronary vessel reactivity. AgAc also produced vascular effects at the high dose, but this occurred in the absence of increased cytokines in BAL or serum. The differences lead the authors to conclude that the soluble form of silver is not entirely responsible for effects of AgNP on the cardiovascular system.

Pulmonary and systemic inflammation was assessed by Gosens et al. [2015] following a single IT instillation of AgNP (3–4 nm, capped with polyoxylethylene glycerol trioleate and Tween-20) in C57BL/6NT mice at doses ranging from 1 to 128  $\mu$ g per mouse. BAL parameters of injury and inflammation, blood cell profiles, and liver glutathione levels were measured 1 day after exposure, along with liver silver content. No increases in pulmonary neutrophil influx, cytokines, LDH, albumin, or AP levels were measured following AgNP exposure. In addition, no alterations in blood cell profiles were found. However, despite the lack of lung and systemic inflammatory parameters, silver content in liver was increased and glutathione levels were decreased, suggesting the sensitivity of the liver to effects following AgNP respiratory exposure, as suggested by inhalation studies discussed previously. Huo et al. [2015] also examined lung and systemic responses in mice following a single IT instillation of the same AgNP utilized by Gosens et al. [2015] at doses of 0.1 or 0.5 mg/kg. Lung, trachea, arterial tissue, liver, and kidney were analyzed for markers of stress to endoplasmic reticulum (ER) and apoptosis at 8 and 24 hours post-exposure. Silver content in tissues was also evaluated. Increased silver was detected in the liver at 8 hours after both doses and in the kidney at 24 hours following the high dose of AgNP. Rate of apoptosis was increased in the lung at the low and high doses and in the kidney at the high dose at 24 hours. mRNA levels of several ER markers were increased in the lung, liver, and kidney, but not in the trachea or arterial tissue, at different times following exposure. The findings also suggest liver sensitivity to AgNP exposure, as well as kidney sensitivity. A study by Minchenko et al. [2012] also detected changes in gene expression in different tissues following AgNP

*This information is distributed solely for the purpose of pre-dissemination peer review under applicable information quality guidelines. It has not been formally disseminated by the National Institute for Occupational Safety and Health. It does not represent and should not be construed to represent any agency determination or policy.*

exposure (single IT instillation in rats). Analysis of mRNA expression of genes related to circadian factors were measured at 1, 3, and 14 days post-exposure to 0.05 mg/kg AgNP (28–30-nm diameter, 30% in solution). Alterations in several genes, including PER1, PER2, and CLOCK, were observed at different times and to different degrees in lung, liver, kidney, brain, heart, and testes.

Genter et al. [2012] assessed organ distribution and systemic effects following a single IN instillation of AgNP (25-nm diameter) in mice. Whole blood, brain, kidney, liver, spleen, and nasal cavity specimens were collected at 1 and 7 days after exposure to 0, 100, or 500 mg/kg AgNP. In addition to deposition in the nasal cavity, AgNP were found to distribute to the lung, brain (olfactory bulb and lateral brain ventricles), spleen (localized in the red pulp to a greater degree than the white pulp), and the kidney. Pathology in the nasal cavity included mucosal erosion. Glutathione levels were found to be increased in the nasal cavity and blood, indicating a degree of oxidative stress in those tissues. No microglial cell activation or inflammation was noted in the brain. However, reduced cellularity in spleen was observed, localized to the red pulp, suggesting erythrocyte destruction in the spleen. In a related study, Davenport et al. [2015] examined systemic and behavioral responses following a single IN instillation (doses ranging from 10 to 500 mg/kg) or repeated IN instillation (50 mg/kg per day for 7 days). Silver content in tissues, spleen cellularity and glutathione levels, Hmox1 expression, and protein in brain were evaluated 7 days after the single IN exposure. Neurobehavioral response was measured with the Morris water maze in association with the 7-day exposure. Silver was detected in liver, gut-associated lymphoid tissue, choroid plexus, and lateral ventricles. Effects in the spleen included increased glutathione levels, increased monocyte and macrophage populations at 25 and 50 mg/kg, and a reduction in NK cells at doses of 25–500 mg/kg. Oxidative stress responses measured as Hmox1 were noted in the hippocampus but not in the cortex. Despite changes in oxidative stress in regions of the brain associated with learning and memory, no changes in learning behavior were observed, and only modest change in spatial reference memory was noted following AgNP exposure.

*This information is distributed solely for the purpose of pre-dissemination peer review under applicable information quality guidelines. It has not been formally disseminated by the National Institute for Occupational Safety and Health. It does not represent and should not be construed to represent any agency determination or policy.*

Two additional studies examined brain effects and distribution of silver to the brain following repeated IN instillation in rats [Liu et al. 2012; Wen et al. 2015]. Liu et al. [2012] administered 0, 3, or 30 mg/kg of 50–100-nm AgNPs (agglomerating to 33–380 nm) to male rats once every 2 days for 14 days. Histology and reactive oxygen species in hippocampus were measured, along with cognitive function as performance in the Morris water maze test and long-term potentiation tests. Dose-dependent impairment of cognitive function was found. Increased neuronal damage and reactive oxygen species in the hippocampus were observed, in the area involved in learning and memory. Wen et al. [2015] conducted a repeated IN exposure in neonatal male and female rats with 20-nm PVP-coated AgNP or soluble AgNO<sub>3</sub> at doses of 0.1 or 1.0 mg/kg once a day for 4 or 12 weeks, to assess organ distribution and retention. Silver was measured by ICP-MS in heart, liver, spleen, lung, kidney, pancreas, ovaries or testes, fat, and brain. In this study, no sex differences were observed. Exposure to ionic silver did cause 18% mortality at the highest dose, whereas no weight loss or mortality was observed following AgNP exposure, suggesting a greater degree of toxicity is associated with the ionic form of silver. For both forms of silver at a dose of 0.1 mg/kg per day, the highest levels at 4 weeks were detected in the liver, with significantly greater accumulation of ion versus particle in these organs. At 4 weeks, silver ion in the liver was measured at 424.8 ng/g of tissue, whereas AgNPs were measured at 35.5 ng/g of tissue. Silver ion was also detectable in the brain at 4 weeks. Dose-dependent increases were observed in liver and brain for both forms of silver at 4 weeks. After 12 weeks exposure to the lower dose, the brain contained the highest levels of silver for both ionic silver (58 ng/g) and AgNPs (9 ng/g). Silver ion also accumulated in kidney after 12 weeks of exposure (23 ng/g). Ionic silver was below 20 ng/g in all other tissues, and AgNP in all other organs was below 5 ng/g. These studies, taken together, suggest the brain may be a target for AgNP, particularly following intranasal exposure, and that there is a greater degree of translocation of the ionic form of silver than of the particle form.

The effects of the properties of size and particle coating/capping agent on AgNP distribution and toxicity were also evaluated in several studies [Anderson et al. 2015b; Botelho et al. 2016; Seiffert et al. 2015; Silva et al. 2015]. All four studies examined 20-

*This information is distributed solely for the purpose of pre-dissemination peer review under applicable information quality guidelines. It has not been formally disseminated by the National Institute for Occupational Safety and Health. It does not represent and should not be construed to represent any agency determination or policy.*

and 110-nm PVP- and citrate-coated AgNPs. In the study by Seiffert et al. [2015], strain-related differences were also investigated. BN or Sprague-Dawley (SD) rats were administered 0.1 mg/kg of the four different AgNPs by a single IT. Controls for the coating material were also examined, along with a soluble ion sample at a concentration ion in the form of silver nitrate, measured under in vitro conditions. Lung function, BAL cell and protein levels, histological analysis, and gene expression of proteins in lung tissue were measured at 1, 7, and 21 days post-exposure. The ion exposure at the concentration of 1 mg per rat did not produce any adverse effects in the lung. The greatest effects on lung function parameters were observed in BN rats, a strain that has a degree of pre-existing inflammation in the lung. In BN rats, airway resistance was increased following exposure to all AgNPs, regardless of size and coating, at 1 day post-exposure. At 7 days, only the citrate-capped particle caused an increase in resistance in the BN group, which resolved by day 21. At day 21, an increase was observed in resistance following exposure to the 20-nm PVP-coated particle. Compliance in BN rats was decreased on day 1 after exposure to all particles, with the exception of 110-nm citrate-capped AgNP; the decrease persisted for the 20-nm PVP-coated particle to day 7 and for the 20-nm citrate-coated particle to day 21. Airway resistance and hyperreactivity following acetylcholine challenge was increased following 20 nm PVP-coated particle exposure at day 1. At day 7, hyperresponsiveness was increased with both sizes of citrate-coated particles, and at day 21, both 20 nm particles increased hyperresponsiveness in BN rats. AgNP particle exposure did not alter baseline measure of resistance or resistance following acetylcholine challenge in SD rats. A decrease in compliance was observed at 1 day post-exposure to 20 nm citrate-capped particles, and airway hyperresponsiveness was increased on day 21 after exposure to 20 nm PVP-coated particles. BAL cell differentials showed increased neutrophils and eosinophils for BN rats 1 day following exposure regardless of particle type and size, with a significant increase for only citrate-coated particles at day 7. Neutrophil and lymphocyte numbers were increased in BAL of SD rats at 1 day post-exposure to the smaller particles for each coating with significant increase persisting to day 7 for only the 20-nm citrate-coated material. BAL protein levels, malondialdehyde (MDA) and cytokines (KC, CCL11, IL-13, eosinophil cationic protein), and IgE were

*This information is distributed solely for the purpose of pre-dissemination peer review under applicable information quality guidelines. It has not been formally disseminated by the National Institute for Occupational Safety and Health. It does not represent and should not be construed to represent any agency determination or policy.*

increased in BN rats at 1 day post-exposure to varying degrees with all particles. Increases in total protein and KC persisted following exposure to the 20-nm AGNPs at day 7, and MDA remained elevated following PVP-coated particle exposure at 7 days. In SD rats, MDA and eosinophil cationic protein were increased at day 1 following exposure to 20-nm particles, and KC was elevated following exposure to 20-nm PVP-coated particles. The authors concluded that the greatest differences could be attributed primarily to size, with differential and less significant differences due to particle coating. The greater degree of response in BN rats suggests there may be concern for responses related to immune effects such as those attributed to asthma.

Botelho et al. [2016] conducted a study to further examine size on innate immune defense and lung function following a single IT instillation of 0.05 mg/kg of 20- or 110-nm citrate- or PVP-coated particles in C57BL/6 mice. BAL cell counts, protein levels, phospholipid levels, and LDH were measured, and lung histology and tissue analysis of Cd11b (monocyte recruitment) were performed at 1 day post-exposure for all particles and at 7 and 21 days after exposure with PVP-coated particles. LDH, cell counts, and proteins levels were not significantly increased in BAL at 1 day following exposure to any of the particles. Surfactant protein D was decreased following PVP-coated particle exposure. The 110-nm PVP-coated particle had the greatest effect on lung mechanical function. Increased cell counts in BAL and reduced lung function were observed for the PVP-coated particles at 7 days post-exposure, with resolution by 21 days post-exposure. In this study, the PVP-coated particles and specifically the larger PVP-particle produced the greatest disruption in lung function. The authors attribute effects in part to particle solubility. It should be noted that citrate-coated materials were not investigated beyond 1 day post-exposure in this study.

Two related studies examined lung toxicity [Silva et al. 2015] and lung distribution [Anderson et al. 2015b] following a single IT instillation of 20- or 110-nm PVP- or citrate-coated AgNPs in rats. In the toxicity study, rats were exposed to 0, 0.1, 0.5, or 1.0 mg/kg of particles or buffers as controls. BAL and tissue analysis was performed at 1, 7, and 21 days post-exposure. All AgNPs caused increase polymorphonuclear cells in BAL

*This information is distributed solely for the purpose of pre-dissemination peer review under applicable information quality guidelines. It has not been formally disseminated by the National Institute for Occupational Safety and Health. It does not represent and should not be construed to represent any agency determination or policy.*

at 1 and 7 days post-exposure at the 0.5 and 1.0 mg/kg dose, and this increase remained significant following the larger PVP- and citrate-coated particle exposures at day 21. Lung injury measured at LDH was greatest on day 7 following all particle exposures at the 0.5 and 1.0 mg/kg dose. Lung tissue analysis showed the greatest difference at day 7 versus day 21 post-exposure for all particles examined. At day 1, AgNP exposure caused increased cellularity in the airspaces and centriacinar inflammation, which continued and increased to day 7, accompanied by cellular exudate and debris in airspaces. At day 21, inflammation continued, although not to the same degree as day 7, and a foaminess and irregular multi-nucleated appearance of macrophages were noted in all exposure groups but to the greatest degree in the 110-nm citrate- and PVP-coated groups. Results taken together showed the most persistent toxicity following exposure to the larger particles, regardless of coating.

In a related study, Anderson et al. [2015b] examined the lung distribution of these particles following 0.5 or 1.0 mg/kg administered by a single IT instillation, at 1, 7, and 21 days post-exposure. Findings indicated that citrate-coated AgNP persisted to a greater degree in the lung up to day 21 (90% retention at day 21) than did the PVP-coated particles (30% retention at day 21). Silver-positive macrophages in the lung decreased at a greater rate in the PVP-coated particle groups than in the citrate-coated groups. In terms of size, at 1 day post-exposure more 100-nm particles were located in the proximal airways than 20-nm particles. Larger particles were also more rapidly cleared from the lungs, while the 20-nm citrate-coated particles persisted to the greatest degree.

Some commonalities exist in the studies that utilize IT instillation, IN instillation, or oropharyngeal aspiration. Silver is observed to translocate to other organs systems, primarily to liver, kidney, and brain as targets (with temporal differences in tissue burden observed), as well as to spleen, testes, and heart in select studies. In most instances where study recovery points were carried out up to 1 month post-exposure, pulmonary responses appeared to resolve to varying degrees over time. In studies that examined ionic forms in comparison to particles at equal mass doses, the ionic form was usually

the more toxic form in the lung, and it was usually found to clear at a faster rate from the lung. There are discrepancies in responses related to size and coatings among studies that examined the same batteries of AgNPs, suggesting more research is needed in this area to understand the role of these properties as well as how the properties relate to ion release from particles, as well as potential subsequent toxicity over time in vivo.

### **E.3.2.2 Silver nanowires**

Kenyon et al. [2012] studied the lung toxicity of silver nanowires (AgNWs) of varying lengths in male Sprague-Dawley rats (by intratracheal instillation of long [20  $\mu\text{m}$ ] or short [4  $\mu\text{m}$ ] AgNWs, about 50 nm in diameter). Rats were administered AgNW doses of 10, 50, 125, or 500  $\mu\text{g}$ , alpha-quartz (positive control) at 500  $\mu\text{g}$ , or dispersion medium (vehicle control). Both wire samples caused a dose-dependent increase in lung injury (lactate dehydrogenase activity and albumin content in lavage fluid) and inflammation (increased lung neutrophils and phagocyte oxidant production). Neither the short nor the long wires at the 10- $\mu\text{g}$  dose had any effect on lung toxicity. The longer wires caused slightly more lung injury immediately following exposure, whereas the shorter wires induced greater toxicity over the time course. The authors suggested this finding may be due to greater wire number and surface area in the short wire sample when samples were compared on an equivalent mass basis.

Schinwald et al. [2012] studied the role of length of silver nanowires (AgNWs) on the acute lung responses in mice (C57BL/6, female, 9 weeks old). Mice (five per group) were exposed by pharyngeal aspiration to AgNWs of different lengths (3, 5, 10, or 14  $\mu\text{m}$ ) or to short or long fibers of amosite (SFA or LFA). The doses were selected to equalize the number of fibers per mouse, which resulted in mass doses of 10.7, 10.7, 17.9, 35.7, 50, and 50  $\mu\text{g}/\text{mouse}$  for SFA, AgNW3, AgNW5, AgNW10, AgNW14, and LFA, respectively. The 50- $\mu\text{g}$  dose was selected from an initial dose-response series as one that resulted in a persistent inflammatory response with AgNW14 and LFA. The acute inflammation response was evaluated 24 hours after aspiration exposure. A length-dependent trend in the pulmonary inflammatory response was observed for the

AgNWs, yet only the mice exposed to the longest (14  $\mu\text{m}$ ) AgNW showed a statistically significant increase in the granulocytes in BAL fluid. A nonlinear relationship was observed between exposure to AgNW by length and inflammation response, which suggested a length threshold based on a "discernible step-increase in granulocyte recruitment at a length between 10 and 14  $\mu\text{m}$ " [Schinwald et al. 2012; Schinwald and Donaldson 2012]. Frustrated phagocytosis (defined as incomplete uptake of fibers by cells) was observed in mice exposed to AgNW14 or LFA. Histopathology performed 24 hours after aspiration showed minor granulomas and lymphocyte infiltrates in mice exposed to AgNW5 or AgNW10. More extensive granuloma and lymphocyte infiltrates were observed in mice exposed to AgNW14 and LFA, which was consistent with the BAL inflammation findings. Although the AgNW14 produced more granulomatous areas compared to shorter fibers, that response was still relatively minor compared to the "extensive interstitial thickening and remodeling of the alveolar spaces after LFA treatment" [Schinwald et al. 2012]. The author's note that their results need to be confirmed in long-term inhalation studies using a range of different nanofibers at plausible exposure concentrations, before these thresholds can be used for risk assessment.

Silva et al. [2014] examined the effects of long and short AgNW in rats after a single IT instillation of 0, 0.1, 0.5, or 1.0 mg/kg AgNW per rat. Short wires were characterized to be 2  $\mu\text{m}$  in length and ~33 nm wide with an aspect ratio of 62.1, while long wires were 20  $\mu\text{m}$  in length and ~65 nm wide, with an aspect ratio of 321.4. BAL cell differentials and protein levels were assessed, along with pathological analysis of tissue, at 1, 7, and 21 days following exposure. At 1 day post-exposure, short and long AgNWs significantly increased neutrophils and eosinophils in the lung at the highest dose. Short AgNWs also increased neutrophils and eosinophils at the dose of 0.5 mg/kg. Both long and short AgNWs increased total protein in the lung at doses of 0.5 and 1.0 mg/kg. The increase persisted with the long wire at day 7 at the high dose. BAL parameters of injury and inflammation showed resolution by day 21. Microscopic examination of alveolar macrophages recovered by BAL indicated both long and short wires produced increased foreign body macrophages; however, only long wires produced a degree of

*This information is distributed solely for the purpose of pre-dissemination peer review under applicable information quality guidelines. It has not been formally disseminated by the National Institute for Occupational Safety and Health. It does not represent and should not be construed to represent any agency determination or policy.*

frustrated phagocytosis following exposure. Histopathology showed significant inflammation in tissue at doses of 0.5 and 1.0 mg/kg. Responses to the short wire appeared to increase with time, whereas responses following long wire exposure were worse at day 7 versus day 21. Despite trends for temporal differences in the pattern of injury, there were no significant differences between short and long wires in histopathological scores. Pathology was characterized by cellular exudate in the alveolar region and sloughing of cells in the terminal bronchioles, as well as tissue granulomas. By day 21, AgNWs were localized in granulomas and in terminal bronchiole/alveolar duct junctions with macrophage infiltrates. Immunohistochemistry showed TNF- $\alpha$ - and TGF- $\beta$ -positive cells at 1 and 7 days, respectively, following exposure to both long and short wires. The difference in BAL parameters at 1 and 7 days post-exposure in short versus long wires was attributed to a greater number of wires per mass instilled with the short wire sample compared to the long wire sample. The investigators suggest that further study by inhalation is necessary to determine if responses are related to delivery of a bolus dose from IT instillation.

### **E.3.3 Subcutaneous, intravenous, or intraperitoneal injection**

#### **E.3.3.1 Kinetics following subcutaneous injection**

Tang et al. [2008] investigated the potential of AgNPs (50–100 nm in diameter) and silver microparticles (2–20  $\mu$ m in diameter) to cross the blood–brain barrier. Wistar rats (90 females) were given a subcutaneous injection of either AgNPs or silver microparticles, and five rats from each group were killed at weeks 2, 4, 8, 12, 18, and 24 to obtain brain tissue to measure silver concentrations. Silver concentrations were higher for the AgNP group than for the silver microparticle and control groups and reached statistical significance at 4 weeks ( $p < 0.05$ ). In the AgNP group, silver concentrations reached a peak of  $0.41 \mu\text{g} \pm 0.16 \mu\text{g}$  at week 12 and did not change significantly by week 24. No significant difference in silver concentrations between the silver microparticle group and control group was detected ( $p > 0.05$ ). It could not be determined whether the silver concentrations in the brain were a result of AgNPs or Ag<sup>+</sup>.

*This information is distributed solely for the purpose of pre-dissemination peer review under applicable information quality guidelines. It has not been formally disseminated by the National Institute for Occupational Safety and Health. It does not represent and should not be construed to represent any agency determination or policy.*

However, in ultrastructural analysis, AgNPs were detected in vascular endothelial cells from the abnormal blood–brain barrier, which could have resulted from transcytosis of the endothelial cells of the brain–blood capillary. No abnormal substance was detected in the brains of rats from the control group and the silver microparticle group. However, many pyknotic, necrotic neurons were detected in the brain of the AgNP exposure group between 2 and 24 weeks.

Tang et al. [2009] also studied the distribution of AgNPs over a 24-month period after the subcutaneous injection of elemental AgNPs or silver microparticles in female Wistar rats at a single dose of 62.8 mg/kg. The preparation of nanoparticles (5 mg/mL in physiologic medium) was reported to be 50–100 nm in diameter, mostly spherical, and with a low degree of aggregation. The tissue and subcellular distribution of silver associated with this preparation was compared with that of a preparation of silver microparticles. These were said to be of various shapes and sizes, ranging from 2 to 20  $\mu\text{m}$ . Although most of the silver from both nanoparticles and microparticles accumulated at the site of administration, ICP-MS showed that about 0.15% of the nanoparticle load reached the bloodstream and was distributed to remote sites, including kidney, liver, spleen, brain, and lung. By contrast, silver microparticles did not pass to the general circulation to any great extent (no more than 0.02% of the injected load), and their distribution to the tissues was therefore markedly less than that of AgNPs. However, fecal excretion of silver from silver microparticles was greater than that from nanoparticles during early follow-up (2 weeks after injection). This pattern was reversed on later sampling dates (up to 24 weeks). For AgNPs, histopathologic examination of these target organs by TEM and EDS revealed localization of internalized silver. This showed silver-containing electron-dense droplets (as opposed to dissolute silver ions) in the renal tubular epithelial cells, at the margin of the renal capsule, and in hepatocytes, hepatic sinusoidal and perisinusoidal spaces, lymphocytes in the splenic cord, cerebral neurons, vascular endothelial cells of the blood-brain barrier, and alveolar epithelial cells.

### **E.3.3.2 Kinetics following intravenous injection**

Corroborative evidence of the distribution of internalized AgNPs to the liver has come from studies in which the deposition of intravenously injected <sup>125</sup>iodine-labeled AgNPs was monitored by single-photon emission computerized tomography (SPECT) imaging in Balb/c mice and Fischer CDF rats [Chrastina and Schnitzer 2010]. The PVP-coated AgNPs were spherical and largely monodispersed, with an average diameter of 12 nm. In addition to the SPECT imaging, the major organs were excised from the animals at term and counted for radioactivity. SPECT imaging gave a strong signal in the abdominal area that was thought to be associated with the liver and spleen. Less-intense signals were associated with the lung and bone. The level of activity in the blood after 24 hours was comparatively low, suggesting translocation from the blood via the mononuclear phagocyte system. Ashraf et al. [2015] also studied tissue distribution, using SPECT. A rabbit was administered dextran-coated AgNP (15.7 nm median size) or non-coated AgNP (53 nm median size) that had been labeled with technetium at a dose of ~200 µg/ml in a 1-mCi/ml solution. Following intravenous administration the animal was monitored up to 30 minutes. Similarly to Chrastina and Schnitzer [2010], the greatest accumulation of silver was observed in the liver/spleen region and the rate of uptake was faster for the un-coated AgNP. Silver was observed in the heart and lungs in the first 2 minutes and cleared rapidly. Silver was also observed in the stomach region, but not in the thyroid (a location where free technetium may be found). Silver was monitored in kidney and bladder for clearance studies, which indicated that un-coated AgNPs were cleared faster.

With respect to accumulation in liver following intravenous administration, Su et al. [2014a] utilized a push-pull probe-based system in male Sprague-Dawley rats to study translocation of silver to extracellular space in the liver. In this study, the probe was placed surgically into the center of the left lateral lobe of the liver; 30 µg/kg of AgNP (measuring 35 nm for primary particle size and ranging from 69 to 92 nm in agglomeration size) in vehicle (10% fetal bovine serum in DMEM) was administered intravenously. Accumulation in extracellular space was monitored every 10 minutes for

*This information is distributed solely for the purpose of pre-dissemination peer review under applicable information quality guidelines. It has not been formally disseminated by the National Institute for Occupational Safety and Health. It does not represent and should not be construed to represent any agency determination or policy.*

130 minutes. At the 180<sup>th</sup> minute, a second administration was given and animals were monitored similarly up to the 350<sup>th</sup> minute. Blood was collected at various time points, and five sections of liver were taken at the end of the study for measurement of silver content. Silver content in the blood increased rapidly up to 10 minutes post-administration and then declined rapidly over the subsequent 15–40 minutes. After the first administration, silver in the extracellular space of the liver increased to maximum by 10 minutes. Following the second administration, nearly twice as much entered the extracellular space. The authors suggest that the first administration may be blocking the reticuloendothelial system to a degree, a mechanism for cellular uptake of silver, leading to a greater rate of accumulation of silver in the extracellular space following the second administration.

The studies by Chrastina and Schnitzer [2010], Afshar et al. [2015], and Su et al. [2014a] followed the acute kinetics of silver distribution, from minutes up to 1 day following exposure. In a study to assess the distribution and excretion of silver, Klaassen [1979] intravenously administered silver nitrate, a soluble form of silver, in the femoral vein of rats (0.01, 0.03, 0.1, or 0.3 mg/kg Ag/kg), rabbits (0.1 mg/kg Ag/kg), and dogs (0.1 mg/kg Ag/kg), up to 4 days post-exposure. Within 4 days post-administration of silver to rats dosed at 0.1 mg/kg Ag/kg, 70% of the silver was excreted in the feces and <1% into the urine. The disappearance of silver from the plasma and its excretion into the bile were measured for 2 hours after the intravenous administration of 0.01, 0.03, 0.1, and 0.3 mg/kg of silver to rats. The concentration of silver in the bile was 16–20 times higher than that in the plasma. For the two lower doses, the overall plasma-to-bile gradient was due almost equally to the plasma-to-bile gradient and the liver-to-bile gradient, whereas for the doses at the two higher concentrations of silver, the liver-to-bile gradient became more important. Marked species variation in the biliary excretion of silver was observed. Rabbits and dogs excreted silver at rates about 1/10 and 1/100, respectively, of that observed in the rat. Although it is difficult to determine the excretion rate of silver in the bile of humans, the results indicate that biliary excretion is an important route for the elimination of silver.

*This information is distributed solely for the purpose of pre-dissemination peer review under applicable information quality guidelines. It has not been formally disseminated by the National Institute for Occupational Safety and Health. It does not represent and should not be construed to represent any agency determination or policy.*

Lee et al. [2013c] also found the serum kinetics, tissue distribution, and excretion of citrate-coated AgNPs in rabbits to be similar to those of the soluble form examined by Klaassen [1979] following intravenous injection. Citrate-coated AgNPs (~7.9-nm diameter) were intravenously injected into the ear vein of four SPF New Zealand White male rabbits at doses of 0.5 mg/kg and 5 mg/kg, based on a dose selection following the Organization for Economic Cooperation and Development (OECD) Test Guideline 417. Blood was sampled from the vein of the collateral ear before and after treatment, at 5, 10, and 30 minutes; at 1, 2, 6, and 12 hours; at the end of days 1 through 7; and at days 14, 21, and 28. Blood samples were also collected from the non-treated control group, at 1, 7, and 28 days. The concentration of AgNPs in the serum was at its highest 5 minutes following treatment, and 90% of the AgNPs were eliminated from the serum at 28 days. Tissue distribution of AgNPs was determined in the liver, lung, kidney, brain, spleen, testis, and thymus, revealing that the liver, spleen, and kidney were the main target organs. This finding was consistent with findings in other studies [Lankveld et al. 2010; Loeschner et al. 2011; Park et al. 2011]. Although the accumulated level of silver in the 5-mg/kg-dose group was higher than that in the 0.5-mg/kg-dose group, tissue accumulations of AgNPs observed in the high-dose group were not always 10-fold higher than in the low-dose group. The excretion of AgNPs through urine, in comparison with feces, was very low during the entire experimental period; more than 90% of AgNPs were still present in the body in the high-dose group at day 7, and 85% still remained in the low-dose group over the same period. Pigmentation in the liver was the main finding of histopathology at 7 and 28 days, whereas no pigmentation was observed in the non-treated control rabbits. Inflammatory cell infiltration was significantly increased in the liver, lung, and kidneys of the AgNP-treated rabbits. However, there were no significant histologic findings in the brain and thymus.

The distribution and biokinetics of AgNPs were also evaluated by Xue et al. [2012], following intravenous administration of AgNPs in the tail vein of ICR mice. Mice (three exposure groups and a control group, with six male and female mice per group) were exposed to doses of AgNPs at 7.5, 30, or 120 mg/kg. Average primary particle size of purchased AgNPs, as determined by TEM, was 21.8 nm (10–30 nm), but agglomeration

*This information is distributed solely for the purpose of pre-dissemination peer review under applicable information quality guidelines. It has not been formally disseminated by the National Institute for Occupational Safety and Health. It does not represent and should not be construed to represent any agency determination or policy.*

of particles (up to 117-nm diameter) was observed to occur at the time of intravenous administration. Toxic effects were assessed via general behavior, serum biochemical parameters, and histopathologic observation of the mice. Biokinetics and tissue distribution of AgNPs were evaluated at a dose of 120 mg/kg. Silver analysis using ICP-MS was used to quantify silver concentrations in blood and tissue samples at predetermined time intervals. After 2 weeks, AgNPs exerted no obvious acute toxicity in the mice; however, inflammatory reactions in lung and liver cells were induced in mice treated at the 120-mg/kg dose level. The distribution of silver was observed in all major organs, with the highest levels found in the spleen and liver, followed by the lungs and kidneys. Silver was retained in the spleen for the entire experiment, whereas the 120- $\mu\text{g/g}$  silver concentration found in the liver slowly decreased over 14 days. In the lungs, silver concentrations decreased from days 1 through 7 but increased slightly from days 7 through 14. The elimination half-lives and clearance rates of AgNPs were, respectively, 15.6 hours and 1.0 ml/hr for male mice, and 29.9 hours and 0.8 ml/hr for female mice. A sex-related difference in the biokinetic profiles of blood, as well as the distribution of silver to the lungs and kidneys, was observed, with significantly higher levels of silver found in the female mice than in male mice at 14 days post-injection. This sex difference in organ-specific silver concentration is consistent with findings reported by Kim et al. [2008] and Sung et al. [2008] in rats exposed to AgNPs. Mild histopathologic changes were also found in the lungs and liver of mice in the 120-mg/kg exposure group [Xue et al. 2012]. These findings are similar to those previously reported by Kim et al. [2008], in which liver damage was found in Sprague-Dawley rats exposed by oral administration to 300 mg AgNPs.

Dziendzikowska et al. [2012] evaluated the time-dependent biodistribution and excretion of AgNP of two different sizes by administering intravenously 20- and 200-nm AgNPs to male Wistar rats at a dose of 5 mg/kg body weight (bw) (2 exposure and 1 control group of 23 rats each). The study was designed to (1) analyze the effect of AgNP size on rat tissue distribution at different time points, (2) determine the accumulation of AgNPs in target organs, (3) analyze the intracellular distribution of AgNPs, and (4) examine the excretion of AgNPs by urine and feces. Biologic material was collected at 24 hours and

*This information is distributed solely for the purpose of pre-dissemination peer review under applicable information quality guidelines. It has not been formally disseminated by the National Institute for Occupational Safety and Health. It does not represent and should not be construed to represent any agency determination or policy.*

at 7 and 28 days after injection and analyzed by ICP-MS and TEM. AgNPs were found to translocate from the blood to the main organs (lungs, liver, spleen, kidneys, and brain), and the highest concentration of silver was in rats treated with 20-nm AgNPs, in comparison with 200-nm AgNPs. The highest concentration of silver was found in the liver after 24 hours, indicating that the liver may be the first line of defense as a consequence of intravenous administration and/or because of the activation of metallothioneins, involved in detoxication of heavy metals such as silver [Wijnhoven et al. 2009]. In addition, the high silver deposition in the liver (8  $\mu\text{g/g}$  wet weight) may have been associated with effective filtration and the presence of specific subpopulations of mononuclear phagocytic cells that can be involved in the sequestration of nanoscale particles. The concentration of silver in the liver decreased over time and reached the lowest concentration at 28 days post-administration. These findings possibly indicate a purification of the liver and redistribution of AgNPs to other organs or its excretion from the body in bile [Kim et al. 2010a; Park et al. 2011a]. Silver concentrations found in the lungs (that is, accumulated in alveolar macrophages) were similar to those observed in the spleen after 7 days, and the concentration of silver in the kidneys and brain increased with time and peaked at 28 days. Despite the high concentration of silver in the kidneys, the rate of silver excretion in the urine was low, which might be explained by the lack of renal glomerular filtration and tubular excretion of the kidneys if the particle size is larger than the distance of cell membranes, ranging from 5.5 to 10 nm. The size of AgNPs (20-nm particles) and their ability to accumulate in various organs were the highest. These findings are consistent with those of Lankveld et al. [2010], who showed a higher level of small (20-nm) AgNPs in the liver and a lower level in the kidneys, brain, and heart, whereas large AgNPs (80 and 100 nm) were concentrated mainly in the spleen and (in smaller amounts) in the liver and lungs. Repeated administration of AgNPs resulted in accumulation of silver in the liver, lung, and spleen, indicating a possible mechanism responsible for the distribution of different-sized nanoscale particles. These findings were consistent with those suggested by Li and Huang [2008], who found that particles smaller than the pores of liver fenestrae (about 100 nm) are captured more efficiently by the liver, whereas larger particles are absorbed with greater affinity in the spleen.

*This information is distributed solely for the purpose of pre-dissemination peer review under applicable information quality guidelines. It has not been formally disseminated by the National Institute for Occupational Safety and Health. It does not represent and should not be construed to represent any agency determination or policy.*

In addition to size, other physical-chemical properties, including dissolution rate and surface coatings, have been implicated in toxicological effects of AgNPs. Recordati et al. [2016] investigated both size and coating of AgNP in comparison to a soluble form of silver, silver acetate. Male CD-(ICR) mice (n = 3/group) were injected via the tail vein one time with a dose of 10 mg/kg of PVP- or citrate-coated AgNPs at sizes of 10, 40, or 100 nm, or 15.5 mg/kg silver acetate, equal to 10 mg/kg silver. Blood, liver, kidney, spleen, brain, and lung were collected for distribution analysis, as well as histopathological analysis. Irrespective of particle coating, the 10-nm particles had the greatest total tissue accumulation, a finding in agreement with Dziendzikowska et al. [2012]. All particles had the highest accumulation in liver and spleen but were also measurable in lung and kidney, with the exception of the 10-nm particle, which also had a high degree of accumulation in lung. Silver acetate accumulated to the highest degree in liver and to a lesser degree in kidney and spleen, where accumulation was comparable. In the kidney, silver acetate had the highest levels with respect to all treatments. The authors suggest a difference in target organs for soluble versus particle, with kidney being a greater target for soluble silver, and liver and spleen for particulate silver; however, it should be noted that soluble silver accumulated to the highest degree in the liver, and only one time point post-exposure was examined. Target organ toxicity may be highly dependent on the kinetic differences in clearance rate of the two forms of silver. In addition to tissue distribution, the authors investigated cellular localization of silver tissues, using autometallography. In the spleen, silver was found in the cytoplasm of macrophages in white and red pulp, as well as endothelial cells. In the liver, silver was found primarily in Kupffer cells along sinusoids, and occasionally in endothelial cells associated with sinusoids and portal endothelial cells. A size difference was noted, with the larger particles localizing primarily to the Kupffer cells and the smaller particles in both Kupffer and endothelial cells. The smallest particle was associated with uptake in gall bladder epithelial and endothelial cells as well. Silver was also detected in localized areas in kidney and lung following particle exposure, but not in brain.

*This information is distributed solely for the purpose of pre-dissemination peer review under applicable information quality guidelines. It has not been formally disseminated by the National Institute for Occupational Safety and Health. It does not represent and should not be construed to represent any agency determination or policy.*

Toxicity was also evaluated in this study. A single 10-mg/ kg intravascular injection of 10 nm citrate- or PVP-coated silver nanoparticles caused overt hepatotoxicity characterized by gall bladder hemorrhage, periportal hemorrhage, midzonal hepatic necrosis, portal vasculitis, and thrombosis. The same mass dose (10 mg/kg) of 40-nm nanoparticles caused similar gall bladder changes in one mouse which also had hepatocellular necrosis, while in the remaining five mice in that exposure group, liver changes were restricted to the gall bladder and were milder. Mice injected with 100-nm particles had only mild and occasional gall bladder edema or hyperemia, while mice receiving an equivalent silver ion exposure by silver acetate injection had kidney and not hepatobiliary changes, despite having the highest degree of silver accumulation in the liver for soluble silver. This corroborates the authors' hypothesis that kidney is the primary target for soluble versus particulate silver at this time point post-exposure. In this study, size appeared to be a more critical factor than the coatings of the materials for both distribution and toxicity, and differences were solubility-dependent as well.

To better understand kinetics-related dissolution and distribution or redistribution of AgNP, Su et al. [2014b] employed a knotted reactor-based differentiation scheme to monitor the ratio of ion to particle in tissues following intravenous administration of AgNP. In this study, male Sprague-Dawley rats were administered 125  $\mu\text{g}/50 \mu\text{l}$  vehicle (10% fetal bovine serum in DMEM) of AgNPs (35 nm primary particle size; 69 nm particle size agglomerated in vehicle), ~ 500  $\mu\text{g}/\text{kg}$  body weight AgNPs, or vehicle. Blood, liver, spleen, kidneys, lungs, and brains were collected at 1, 3, and 5 days post-exposure. Samples were processed for determination of the ion and particle fractions and silver was quantified by ICP-MS. Total silver was highest in the liver and spleen at all times. The ion to particle ratio was 100% for kidney, lung, brain, and blood. The ratio was <20% for liver, and it gradually decreased in spleen over time. This indicated that the silver was primarily in particle form in the liver and was in soluble form in the other tissues, suggesting AgNP degradation and redistribution. Histopathology was also performed on the tissues. The only organ with positive pathological findings was the liver, whereby inflammation and necrosis were noted at days 3 and 5 post-exposure.

*This information is distributed solely for the purpose of pre-dissemination peer review under applicable information quality guidelines. It has not been formally disseminated by the National Institute for Occupational Safety and Health. It does not represent and should not be construed to represent any agency determination or policy.*

The study demonstrates the kinetics of dissolution and the potential role of the particle in liver effects.

Pang et al. [2016] examined effects of various surface coating of AgNPs on biodistribution and pharmacokinetics in male Balb/c mice. The particles used in this study had a similar primary particle size of ~30 nm and were coated with one of the following compounds: citrate (negative charge), polyethylene glycol (PEG; negative charge), PVP (negative charge), or branched polyethylenimine (BPEI; positively charged). Silver nitrate was also tested as reference material for ionic silver. In solution, the hydrodynamic diameters of PVP and citrate AgNP were ~36 nm, PEG was ~55 nm, and BPEI was ~63 nm. BPEI had the lowest particle concentration per ml (~3 times lower than all other particles) and the highest Ag concentration per ml (~2 times higher than all other particles). Particles and silver nitrate were administered intravenously with 5 animals per group. Tissue burden was measured as  $\mu\text{g/g}$  tissues as well as total silver per tissue by ICP-MS at 24 hours post-exposure in liver, spleen, lung, kidneys, intestines, and brain. Blood concentration was measured at 2, 10, 30, and 60 minutes post-exposure and at 6, 12, 24, and 72 hours post-exposure. Ionic silver accumulated in liver to the greatest degree, followed by lower levels in all other organs. All particles had the greatest accumulation in liver and spleen, findings similar to that of Chen et al. [2016] (discussed below) and Xue et al. [2012]. PVP and citrate AgNP followed similar distribution patterns, with liver > spleen > lung = intestines > kidney = brain, a finding similar to that of Recordati et al. [2016]. PEG AgNP had the highest burden of all particles in the spleen, followed by BPEI AgNP, whereas BPEI had the greatest deposition in lung compared to all other particles. PEG AgNPs were distributed as follows: liver  $\geq$  spleen > intestines  $\geq$  lungs  $\geq$  kidney = brain. BPEI were distributed as follows: liver  $\geq$  spleen  $\geq$  lung > kidney = intestines = brain. In terms of total body silver burden as a sum of the data per tissue measured, PEG AgNPs were greatest, followed by BPEI AgNP. Ionic silver was lowest across tissues. This could be due to a faster clearance rate of the soluble form of the material or a greater accumulation in other organs not measured. Blood kinetic studies showed that PEG AgNPs remained in the circulation the longest in the first 60 minutes and had a longer elimination half-life than

*This information is distributed solely for the purpose of pre-dissemination peer review under applicable information quality guidelines. It has not been formally disseminated by the National Institute for Occupational Safety and Health. It does not represent and should not be construed to represent any agency determination or policy.*

all other particles. PEG AgNPs also had the lowest affinity for bovine serum albumin in an acellular test, indicating resistance to opsonization by protein in the blood. The authors suggest that a lower degree of protein-binding affinity may lead to slower uptake into tissues.

In the same study, authors examined toxicity of the particles and silver nitrate in a hepatoma cell line (Hepa1c1c7). A dose-response study was conducted to determine viability/cytotoxicity as EC50. BPEI had the lowest EC50 (10.38  $\mu\text{g/ml}$ ), followed closely by ionic silver, citrate AgNP, and PVP AgNP (12.39–14.28  $\mu\text{g/ml}$ ). PEG was the least toxic, with an EC50 of 63.14  $\mu\text{g/ml}$ . This finding correlated with particle uptake in cells, whereby PEG AgNP had the lowest levels of uptake in 24 hours. These findings correspond well with the biodistribution and elimination half-life data from the in vivo studies. Taken together, the data suggested that the BPEI AgNP may be slightly more cytotoxic due to surface charge or chemistry, whereas PEG AgNP, the more neutral of the negatively charged particles, was less toxic, had lower binding affinity for protein, and persisted to the greatest degree in vivo. The authors note that the study does not account for effects of coating on dissolution rate of particles, which may also affect the toxicity, kinetics, and distribution.

Additional studies that examine toxicity in conjunction with pharmacokinetics are discussed along with toxicological studies in section E.3.3.3.

### **E.3.3.3 Toxicological effects following intravenous or intraperitoneal injection**

Kim et al. [2009b] administered AgNPs intravenously to Sprague-Dawley rats (two per sex per group) to correlate clinical chemistry, histopathologic, and toxicogenomic responses, with the aim of identifying biomarkers for AgNP exposure. Animals were exposed to an unstated number of injections of AgNP preparations over a 4-week period. Exposure groups included a nonexposed control group, group I (receiving 100 mg/kg silver in 50- to 90-nm particles), and group II (receiving 1 mg/kg silver in 1- to 10-nm particles). The AgNPs were dispersed in an aqueous medium containing amino

acids. The only clinical chemistry changes observed were statistically significant increases in serum cholesterol concentrations in the two exposed groups and reductions in serum creatinine levels that also achieved statistical significance. Histopathologic examination of major tissues and organs showed silver particle deposition in the hepatic sinusoids and Kupffer cells. These effects were associated with moderate lymphocyte aggregation, destruction of hepatocytes, and lymphocytic infiltration of the hepatic perivenular area. Though not necessarily associated with histopathologic disorders, other sites of silver deposition were the lung alveolar septum, kidney glomerulus, and spleen white pulp. The most striking hematologic finding was a marked increase in the lymphocyte/granulocyte ratio in the AgNP exposure groups, compared to controls. Kim et al. [2009b] also observed alterations in gene expression in rats exposed to AgNPs when total RNA was extracted from the livers of control and exposed groups and used as a basis for microarray analysis. Using a threshold of 1.2 to assign genes into upregulated or downregulated categories, the researchers sorted 191 and 187 genes into these respective categories when the findings for groups I and II were considered together. Twenty genes were found to be commonly expressed in groups I and II, four of which (SLC7A13 [solute carrier family 7, member 13], PVR [poliovirus receptor], TBXAS1 [thromboxane A synthetase 1], and CKAP4 [cytoskeleton-associated protein 4]) were proposed as size-independent genomic biomarkers. Ten other genes were proposed as sentinels for the AgNP-induced histopathologic and clinical chemistry changes.

The same researchers also injected two male Sprague-Dawley rats per group with 50-nm AgNPs at doses of 0 (control), 1, or 100 mg/kg at 2- to 3-day intervals over a 4-week period, prior to performing a proteomic analysis of liver, lung, and kidney tissues [Kim et al. 2010b]. Protein extracts from liver, lung, and kidney were separated by means of two-dimensional gel electrophoresis. Protein spots selected as differentially expressed were cut from the gels, digested, and then identified with matrix-assisted laser desorption/ionization time-of-flight mass spectrometry (MALDI-TOF MS) and peptide mass fingerprinting. Functional analysis of the differentially expressed proteins, as related to exposure to AgNPs, demonstrated outcomes such as apoptosis, generation

*This information is distributed solely for the purpose of pre-dissemination peer review under applicable information quality guidelines. It has not been formally disseminated by the National Institute for Occupational Safety and Health. It does not represent and should not be construed to represent any agency determination or policy.*

of reactive oxygen species (ROS), thrombus formation, and inflammation. Differentially expressed proteins in the kidney also appeared to be associated with indicators of metabolic disorders such as diabetes.

Katsnelson et al. [2013] conducted a subacute intraperitoneal exposure study in outbred female white rats, using a similar-sized AgNP (50 nm) as Kim et al. [2009; 2010b]. The study was conducted in comparison with similar-sized gold NP (AuNP). Rats were injected times per week up to 20 injections (~3 weeks). Following exposure, the following were completed: blood hematology and biochemistry, urine analysis, CNS functional and behavioral tests (withdrawal reflex test and head dips into hole-boards for behavioral testing), genotoxicity tests in multiple organ tissues, histopathology, and metal content determinations (liver, kidney, and spleen). In a separate study, effects of administration of a bioprotective complex (mixture of dietary supplements and vitamins high in anti-oxidants and free radical scavengers as well as metals that act antagonistically to silver) given orally with AgNP exposure were measured. Both nanoparticles cause decreased red blood cells, succinate dehydrogenase activity in blood lymphocytes, and ceruloplasmin levels in serum, the later to a greater degree in AgNP-exposed rats. AuNP additionally caused an increase in blood monocytes, a decrease in hemoglobin, and a decrease in kidney mass. A similar trend was present for AgNP, although it was not significant. Both nanoparticles were detected in liver, kidney, and spleen. AuNP deposited to a greater extent in liver compared to AgNP, and AgNP to a greater extent in kidney compared to AuNP. Both particles increased the number of binucleate hepatocytes in liver (AuNP > AgNP) and Kupffer cells (AuNP = AgNP). A trend for an increase in particle load in Kupffer cells was present following AgNP exposure. Both particles caused equivalent decreased levels of white to red pulp ratio in spleen, and caused increased thickness to the glomerular basal membrane in kidneys. Overall, genotoxicity measured by the rapid amplification of polymorphic DNA (RAPD) test was greater for AgNP-exposed animals than AuNP-exposed animals, with both inducing genotoxicity. Increases were greatest in liver and spleen, followed by bone, kidney, and blood cells. Administration of the bioprotective complex attenuated the toxicity to a degree, possibly because of increased anti-oxidant activity. The authors

*This information is distributed solely for the purpose of pre-dissemination peer review under applicable information quality guidelines. It has not been formally disseminated by the National Institute for Occupational Safety and Health. It does not represent and should not be construed to represent any agency determination or policy.*

conclude that the primary difference in particles occurred in tissue distribution and genotoxicity, with AgNP causing a slightly greater toxicity than AuNP.

Increased oxidative and endoplasmic reticular stress have been implicated as mechanisms of toxicity following oral exposures to AgNP (Elle et al. 2013; Hadrup et al. 2012a; Kovvuru et al. 2015; Shrivastava et al. 2016; Yu et al. 2014) and pulmonary exposure to AgNP (Aria et al. 2015; Genter et al. 2012; Huo et al. 2015; Kaewamatawong et al. 2014; Liu et al. 2012; Liu et al. 2013a; Seiffert et al. 2016; Smulders et al. 2015a). Evidence of this mechanism of action is present in intravenous exposure studies also (Chen et al. 2015; Tiwari et al. 2011). Tiwari et al. [2011] reported an increase in ROS levels when Wistar rats were injected intravenously through the tail vein at doses of 4, 10, 20, and 40 mg/kg AgNPs (15–40 nm in diameter) at 5-day intervals over 32 days. Histopathologic examination revealed significant changes ( $p < 0.01$ ) in hematologic parameters (WBCs, platelets, hemoglobin, and RBCs) in the 20- and 40-mg/kg groups. In the 40-mg/kg group, statistically significant increases were also found in the liver function enzymes alanine aminotransferase (ALT), aspartate aminotransferase (AST), AP, gamma glutamyl transpeptidase, and bilirubin. AgNP deposition was reported to be found primarily in the liver and kidney of rats exposed at doses of 20 and 40 mg/kg. ROS was found to increase in all groups in a dose-related manner. The investigators suggested that the deposited AgNPs are endocytosed and interact with mitochondria to produce ROS. These increased levels of ROS (AgNP in doses  $>20$  mg/kg) enhance  $H_2O_2$  levels, which can cause damage in the DNA strand, chromosome aberration, and conformational changes in proteins. AgNP doses  $<10$  mg/kg were considered to be safe for biomedical application.

Chen et al. [2016] evaluated biodistribution, endoplasmic reticulum stress, and oxidative stress following intravenous exposure to AgNP. AgNP (NM-300K) had a primary particle size of 20 nm and a hydrodynamic diameter of  $\sim 38$  nm in dispersant, consisting of 4% Tween-20 and 4% polyoxyethylene (NM-300K-DIS). Balb/c mice were administered 0, 0.2, 2.0, or 5.0 mg/kg by the tail vein 1 time and were euthanized 8 hours after exposure. Tissue burden was measured by ICP-MS and was determined to deposit in

*This information is distributed solely for the purpose of pre-dissemination peer review under applicable information quality guidelines. It has not been formally disseminated by the National Institute for Occupational Safety and Health. It does not represent and should not be construed to represent any agency determination or policy.*

concentration from highest to lowest as spleen > liver > lung >> kidneys > heart > brain. IL-6 was found to be increased in serum only at the highest dose; however, there were no significant differences in serum TNF- $\alpha$ . Protein analysis by western blot for markers of endoplasmic reticulum stress and oxidative stress were measured in spleen and liver, and most were significantly elevated in a dose-dependent manner in both tissues when compared to control. Gene expression of endoplasmic reticulum stress markers, *xbp-1s* and *chop*, was elevated in liver at the high dose but not in spleen or other organs. Gene expression of *sod-1* and *ho-1* were also elevated in liver, indicating a greater degree of stress in this tissue. Kidney gene expression of *ho-1* was also elevated at the high dose. No histopathologic changes were observed in brain, heart, spleen, or kidneys. Lungs showed thickened alveolar walls and inflammation. Liver tissue showed necrosis in hepatic lobules, disorganized hepatic cords, and edema. The high dose of AgNP caused significant levels of apoptosis (DNA damage assessed by TUNNEL assay) in lung, liver, spleen, and kidneys, but not in heart or brain. In this study, toxicity appeared to be associated with target organs, mainly liver and spleen, followed by lung and kidney, and primarily occurred at the highest dose administered.

Lee et al. [2013b] intraperitoneally injected Sprague-Dawley rats (300–350 g/bw) with AgNPs (10–30 nm in diameter) at concentrations of 500 mg/kg to test the hypothesis that autophagy plays a role in mediating hepatotoxicity in animals. Autophagy is a homeostatic mechanism to promote cell survival by facilitating the removal of malformed or injured proteins or organelles [Lee et al. 2013c]. This study focused on the interrelationship between energy metabolism, autophagy, apoptosis, and hepatic dysfunction. All animals were killed on days 1, 4, 7, 10, or 30 post-exposure, and the concentration of silver in the liver was found to be 58–81  $\mu\text{g/g}$ . Uptake of AgNPs was observed to be rapid but not proportional to the blood Ag concentration. Declination of ATP (-64% in day 1) and autophagy (determined by LC3-II protein expression and morphologic evaluation) increased and peaked on the first day. ATP content remained at a low level even though the autophagy had been activated. Apoptosis began to rise sigmoidally at days 1 and 4, peaked at day 7, and remained constant during days 7–30 post-exposure. Meanwhile, autophagy exhibited a gradual decrease from days 1 to 10,

*This information is distributed solely for the purpose of pre-dissemination peer review under applicable information quality guidelines. It has not been formally disseminated by the National Institute for Occupational Safety and Health. It does not represent and should not be construed to represent any agency determination or policy.*

and the decrease at day 30 in comparison with the control group was statistically significant. The decline in autophagy, along with a high concentration of silver in the liver, was interpreted by the authors as causing insufficient self-protection, which contributed to the observed hepatotoxicity. An inflammatory response in the liver was observed by histopathologic evaluation on day 10 and was seen to progress to an advanced degree on day 30, when liver function was impaired.

Hepatotoxicity was also observed in a study by Wang et al. [2013]. To assess biodistribution and target organ toxicity, female Balb/c mice (5-10 per group) were exposed to 25-nm PVP-coated AgNP at a dose of 0, 22, or 108  $\mu\text{g}/\text{kg}$ , or silver nitrate at a dose of 108  $\mu\text{g}/\text{kg}$  intravenously or intraperitoneally every 2 days for weeks. Tissue distribution and histopathology were evaluated at 2 weeks after the last exposure. Following intraperitoneal exposure, silver, detected by ICP-MS, accumulated in a dose-dependent manner to the greatest degree in terms of ng/g tissue in liver and spleen, and to a greater degree for the high dose of particle versus ion, indicating ionic silver was cleared more rapidly. Silver could also be detected at much lower levels in kidney, heart, and spleen. Silver content in tissue was approximately 100-fold greater following intraperitoneal exposure versus intravenous exposure. At 2 weeks post-exposure, silver was detected in spleen > liver = kidney only for the high dose of AgNP. Because of particle persistence, histopathology was performed on liver, kidney, and spleen from the intraperitoneally exposed mice. Only liver showed pathological changes, including disorganized hepatic cords and enlarged central veins; this was more marked in the high-dose AgNP versus ionic silver. No pathology was observed in kidney or spleen, and no hematological changes were observed. The data again suggest that liver is a target organ following exposure. As part of the same study, an additional experiment using similar exposure durations was performed to determine pharmacokinetics across time following exposure. For the pharmacokinetic study, female mice were exposed only intravenously, with the same regimen as described for the previous study, at a dose of 1.3 mg/kg per dose (n = 3 per group). Liver, spleen, kidney, heart, lung, and serum were collected at 15, 39, and 78 days following the last exposure. The highest tissue burden of silver on day 15 was in liver, kidney, and spleen; silver content was less in lung and

*This information is distributed solely for the purpose of pre-dissemination peer review under applicable information quality guidelines. It has not been formally disseminated by the National Institute for Occupational Safety and Health. It does not represent and should not be construed to represent any agency determination or policy.*

heart. Burden decreased over time but was still measurable in liver, spleen, and kidney at day 78.

In the same study, Wang et al. [2013] also examined transport across the blood-testis barrier, as well as transport across placenta and effects on fetal liver. In the placental transport study, male and female mice were exposed by intraperitoneal injection to 0, 22, or 108  $\mu\text{g}/\text{kg}$  or 108  $\mu\text{g}/\text{kg}$  of silver nitrate, with the same exposure paradigm discussed above. After the 4 weeks of exposure, mice were mated. Placenta, fetal liver, and remaining fetus without liver were collected on gestational day 14.5 ( $n = 3\text{--}5/\text{group}$ ) and silver content was evaluated. Silver was detected in placenta, fetus without liver, and fetal liver for all groups. Silver in the placenta was highest for the high dose of AgNP, whereas in the fetus without liver and fetal liver, the low dose of AgNP was highest. The authors suggest this may be due to higher agglomeration in the high dose, resulting in a decreased ability to cross placenta because of agglomerate size. Soluble silver content was comparable to the low-dose AgNP in placenta and the high-dose AgNP in fetus and fetal liver, and this may be attributable to faster clearance for the males and females during exposure and prior to mating. To assess transport across the blood-testes barrier, male mice were exposed to 1.3 mg/kg intravenously, according to the same regimen described above. Silver burden was measured in liver, spleen, kidney, heart, lung, muscle, testis, and serum 4 months after the last exposure. Silver content was greatest and comparable in terms of ng/g tissue in liver, spleen, and testis. Silver was also detected in kidney, heart, lung, and muscle but not serum. These studies, taken together, indicate kidney and spleen as target organs, but particularly liver, and that AgNP exposure can lead to silver crossing biological barriers such as placenta and blood-testis barriers.

A number of other studies have examined effects on the reproductive system of males [Gromadzka-Ostrowska et al. 2012] and effects during pregnancy in females [Austin et al. 2012; Fennell et al. 2106; Mahabady 2012]. A study by Fennell et al. [2016] was discussed in a previous section. In this study, the investigators intravenously injected 1 mg/kg of 20-nm or 110-nm PVP-coated AgNP, silver acetate, or vehicle control on

*This information is distributed solely for the purpose of pre-dissemination peer review under applicable information quality guidelines. It has not been formally disseminated by the National Institute for Occupational Safety and Health. It does not represent and should not be construed to represent any agency determination or policy.*

gestation day 18 into pregnant Sprague-Dawley rats. At 1 and 2 days post-exposure, silver content was measured in tissues (blood, brain, heart, liver, kidneys, spleen, lung, gastrointestinal tract, skin, bone, carcass, fetus, and placenta). Urine and feces were collected to measure excreted silver. Cardiovascular markers of injury were measured in plasma, and metabolites and 8-OH-dG (oxidative stress marker) were measured in urine. The percent recovery of silver administered in animals was 56.7%, 22.6%, and 32.9% for silver acetate, 20-nm particles, and 110-nm particles, respectively. At 24 and 48 hours, the highest tissue concentration of silver was measured in the spleens for both sizes of particles. At 24 hours for the soluble silver, the highest tissue level was also in the spleen, and at 48 hours the highest level was detected in the lungs. In general, silver was detected in most tissues measured, including kidney and liver. Silver was detected in the placenta and fetus irrespective of the form or size of silver and was measured to a greater degree in the placenta than the fetus. There were no differences in plasma biomarkers or urinary 8-OH-dG. Urinary metabolic analysis indicated possible changes in carbohydrate and amino acid metabolism.

Austin et al. [2012] intravenously injected pregnant CD-1 mice with AgNPs (average diameter, 50 nm; range, 30–60 nm) on gestation days (GDs) 7, 8, and 9 at dose levels of 0 (citrate buffer), 35, or 66  $\mu\text{g}$  Ag/mouse (group sizes of 6–12) to evaluate the distribution of AgNPs in pregnant mice and their developing embryos. Additional groups of mice were treated with silver nitrate (dissolved in 0.25 M mannitol) at dose levels of 9 and 90  $\mu\text{g}$  Ag/mouse. Group sizes were nine and three mice for the 9- and 90- $\mu\text{g}$  dose levels, respectively. Mice were euthanized on GD 10, and tissue samples were collected and analyzed for silver content. A significant increase ( $p < 0.05$ ) in AgNP content, as compared to that in silver nitrate-treated animals, was observed in nearly all tissues; AgNP accumulation was significantly higher in liver, spleen, lung, tail (injection site), visceral yolk sac, and endometrium; the highest levels of silver were found in the liver, spleen, and visceral yolk sac. Concentrations of silver in embryos were about 25-fold less than those seen in the placenta or visceral yolk sac, suggesting that AgNPs become sequestered in visceral yolk sac vesicles and do not reach the fetal circulation in significant amounts; no adverse morphologic effects on the developing embryos were

*This information is distributed solely for the purpose of pre-dissemination peer review under applicable information quality guidelines. It has not been formally disseminated by the National Institute for Occupational Safety and Health. It does not represent and should not be construed to represent any agency determination or policy.*

observed. Austin et al. [2012] proposed that pinocytosis might be responsible for AgNP uptake by the visceral yolk sac.

The teratogenicity potential of AgNPs in pregnant 3- to 4-month-old Wistar rats was investigated by Mahabady [2012]. Pregnant rats ( $n = 30$ ) were randomly divided into five groups (24 pregnant rats in treatment group and six pregnant rats in saline control group). Two subgroups of six rats in one treatment group were given either 0.4 or 0.8 mg/kg nanosilver intraperitoneally on GD 8. The same doses of nanosilver were also administered to a second treatment group (two groups of six rats) on GD 9. All animals were killed on GD 20; the uterus was exteriorized and the number and location of fetuses and resorptions were noted. The mean of weight, volume, and width of fetuses' placenta decreased significantly ( $p < 0.05$ ) in both treatment groups in comparison with the saline control group; no observed skeletal abnormalities were observed in the fetuses. No information was provided on the size of the AgNPs or whether the AgNPs were coated.

Gromadzka-Ostrowska et al. [2012] described the results of a study in which male Wistar rats (four groups, 24/group) were intravenously injected (tail vein) with AgNPs to assess the effects on spermatogenesis and seminiferous tubule morphology. The described experimental study featured changes to the applied concentration and dimensions of the AgNPs. Thus, animals received either 5 or 10 mg/kg AgNPs that were roughly 20 nm in diameter, 5 mg/kg of AgNPs that measured 200 nm, or 0.9% NaCl for the control group. Rats were killed at 24 hours, 7 days, or 4 weeks after treatment. Additionally, sperm counts were taken and germ cells assessed for DNA damage by means of the comet assay. Silver nanoparticles at different doses and particle sizes appeared to be associated with increased comet tail moments after different durations. The frequency of abnormal spermatozoa in epididymal semen from experimental groups was not significantly different, as compared with the NaCl group at the given time points. However, in all treated groups, the number of abnormal spermatozoa found 1 or 4 weeks after treatment was higher ( $p < 0.05$ ). The comet assay showed that DNA damage (% DNA in tail) in the germ cells was significantly

*This information is distributed solely for the purpose of pre-dissemination peer review under applicable information quality guidelines. It has not been formally disseminated by the National Institute for Occupational Safety and Health. It does not represent and should not be construed to represent any agency determination or policy.*

increased at 24 hours in the 5- and 10-mg/kg (20-nm Ag) groups ( $p \leq 0.05$ ) but declined with time post-exposure. No difference in the DNA damage level was found between the control group and the 5-mg/kg group (200-nm Ag) at all post-exposure time points. The results were interpreted “as suggestive” that AgNP genotoxicity was more pronounced in mature sperm cells in the epididymis than in spermatozoa in seminiferous epithelium. Histologic examination of the testes showed change in the testes seminiferous tubule morphometry in the rats treated with 200-nm AgNPs.

In addition to examination of reproductive effects, studies have also focused on neurological effects [Liu et al. 2013b; Sharma et al. 2010]. A series of experiments by Sharma et al. [2010] in Sprague-Dawley rats examined the capacity of aqueous dispersions of manufactured AgNPs (50–60 nm in diameter) to disrupt the blood-brain barrier. Silver nanoparticles were administered intravenously (30 mg/kg), intraperitoneally (50 mg/kg), or as a cortical superfusion (20  $\mu$ g/10  $\mu$ L) in a 0.7% sodium chloride solution containing 0.05% Tween 80. The authors measured the permeability of the blood-brain barrier to a sterile solution of Evans blue albumin or a  $^{131}$ iodine tracer given intravenously and assessed the potential for edema formation in the brain by measuring tissue water content. AgNPs altered the blood-brain barrier to Evans blue albumin and radioiodine when administered intravenously or as a cortical superfusion but not by intraperitoneal administration. The leakage of Evans blue albumin was evident on the ventral surface of the brain and in the proximal frontal cortex. Cortical superfusion with nanoparticles gave moderate opening of the blood-brain barrier to protein tracers, with leakage of Evans blue albumin as well. A significant increase in brain water content was seen after administration of AgNPs intravenously or by cortical superfusion. As before, intraperitoneal administration was ineffective. In discussing their results, Sharma et al. [2010] stated that the increase in brain water content in areas where leakage of Evans blue albumin was observed was consistent with the capacity of systemically applied AgNPs to bring about edema formation and subsequent brain damage. A possible result of these changes could be AgNP-induced brain dysfunction, thereby raising the possibility of an association between acute exposure to AgNPs and neurodegenerative changes.

*This information is distributed solely for the purpose of pre-dissemination peer review under applicable information quality guidelines. It has not been formally disseminated by the National Institute for Occupational Safety and Health. It does not represent and should not be construed to represent any agency determination or policy.*

Although the intraperitoneal injection of AgNPs was ineffective in bringing about changes to the blood-brain barrier in Sprague-Dawley rats [Sharma et al. 2010], a study by Rahman et al. [2009] showed this route of application to be useful in bringing about changes in gene expression to regions of the brain in male C57BL/6N mice. They were intraperitoneally injected with 100, 500, or 1,000 mg/kg of 25-nm-diameter AgNPs and then killed after 24 hours. Total RNA was extracted from the caudate nucleus, frontal cortex, and hippocampus and analyzed by means of RT-PCR. Differential alterations in gene expression implicated AgNP-induced changes in apoptosis and free-radical-induced oxidative stress.

Liu et al. [2013b] reported that AgNPs do not affect spatial cognition or hippocampal neurogenesis in adult male ICR mice ( $n = 15$  per dose,  $n = 10$  for control). Mice were administered via intraperitoneal injection non-coated AgNPs with an average diameter of 36.3 nm at doses of 0 (control), 25, or 50 mg/kg, once a day in the morning for 7 consecutive days. Another group of mice received scopolamine (3 mg/kg) as a positive control for the behavioral studies. Spatial learning and memory ability were assessed with the Morris water maze test; after the behavioral test, mice were injected with bromodeoxyuridine and killed on days 1 and 28 post-exposure, and the brains were evaluated for proliferating cells. The test results showed that AgNP exposure did not alter either reference memory or working memory in the mice, in comparison with those in the non-exposed control group. Also, in the AgNP-treatment groups, no differences were revealed in hippocampal progenitor proliferation or in the survival and differentiation of newly generated cells.

This information is distributed solely for the purpose of pre-dissemination peer review under applicable information quality guidelines. It has not been formally disseminated by the National Institute for Occupational Safety and Health. It does not represent and should not be construed to represent any agency determination or policy.

**Table E-6. Summary of in vivo toxicological studies of silver nanoparticles (AgNPs) and nanowires (AgNWs)**

Species	Particle Characteristics	Exposure Details		Critical Effect(s)	NOAEL/LOAEL	Comments	Reference
		Concentration/ Dose	Duration				
<b><i>Inhalation Exposure – Acute or Subacute</i></b>							
Sprague-Dawley rats; 5 of each sex per group	Mostly spherical, 15–20 nm in diameter	0, 76, 135, or 750 $\mu\text{g}/\text{m}^3$	Single 4-hr exposure	Clinical signs and lung function parameters	–/–	No adverse effects observed	Sung et al. [2011]
Sprague-Dawley rats; 10 of each sex per group	Mostly spherical, diameter range 2–65 nm (median, 16 nm)	0, 0.48, 3.48, or 61 $\mu\text{g}/\text{m}^3$	6 hrs/day, 5 days/week for 4 weeks	Slight cytoplasmic vacuolization of the liver	0.48/3.48 $\mu\text{g}/\text{m}^3$	Dose-response effect in females only	Ji et al. [2007b]
Sprague-Dawley rats; 10 of each sex per group	Mostly spherical, diameter range 2–65 nm (median, 16 nm)	0, 0.48, 3.48, or 61 $\mu\text{g}/\text{m}^3$	6 hrs/day, 5 days/week for 4 weeks	Increase in number and size of the neutral mucin-producing goblet cells	0.48/3.48 $\mu\text{g}/\text{m}^3$		Hyun et al. [2008]
C57Bl/6 mice; 3×26 test animals, 13 controls	Spherical PVP-coated particles, >85% approx. 5 nm in diameter, but with 79-nm (GM) aggregates	0, 3,300 $\mu\text{g}/\text{m}^3$	4 hrs/day, 5 days/week for 2 weeks	Minimal pulmonary inflammation	3,300 $\mu\text{g}/\text{m}^3$	Single concentration tested	Stebounova et al. [2011]

*This information is distributed solely for the purpose of pre-dissemination peer review under applicable information quality guidelines. It has not been formally disseminated by the National Institute for Occupational Safety and Health. It does not represent and should not be construed to represent any agency determination or policy.*

**Table E-6. Summary of in vivo toxicological studies of silver nanoparticles (AgNPs) and nanowires (AgNWs)**

Species	Particle Characteristics	Exposure Details		Critical Effect(s)	NOAEL/LOAEL	Comments	Reference
		Concentration/Dose	Duration				
Sprague-Dawley male rats; 12 exposed and 12 controls	Two types of mostly spherical Ag [75% colloidal and 25% silver ions with 33-nm CMAD; and 100% colloidal with 39-nm CMAD]	0, 100 µg/m <sup>3</sup> (1.4 µg Ag/rat lung) or 1000 µg/m <sup>3</sup> (14 µg Ag/rat lung)	Single 5-hr exposure; evaluated 1 and 7 days post-exposure	No acute toxicity in pulmonary or cardiovascular parameters	-/-	No adverse effects observed	Roberts et al. [2013]
C57BL/6 male mice (2 groups of 7)	AgNPs geometric mean diameter, 22.18 ± 1.72 nm	AgNPs (1.91 × 10 <sup>7</sup> particles/cm <sup>3</sup> )	6 hrs/day, 5 days/week for 2 weeks; one of the groups was observed for 2 weeks of recovery before necropsy	RNA analysis of cerebrum and cerebellum showed several genes associated with motor neuron disorders, neurodegenerative disease, etc.; genes from whole blood modulated in parallel to those in the brain	NA	Investigators believe that these genes could serve as biomarkers for AgNP exposure	Lee et al. [2010]

This information is distributed solely for the purpose of pre-dissemination peer review under applicable information quality guidelines. It has not been formally disseminated by the National Institute for Occupational Safety and Health. It does not represent and should not be construed to represent any agency determination or policy.

**Table E-6. Summary of in vivo toxicological studies of silver nanoparticles (AgNPs) and nanowires (AgNWs)**

Species	Particle Characteristics	Exposure Details		Critical Effect(s)	NOAEL/LOAEL	Comments	Reference
		Concentration/Dose	Duration				
Fischer rats (F344/DuCrI); 12 males in each of 3 groups	15 nm and 410 nm (200-nm primary particles)	15-nm group: mass, 179 µg/m <sup>3</sup> ; particle number, 3.8 × 10 <sup>6</sup> . 410-nm group: mass, 167 µg/m <sup>3</sup> ; particle number, 2.0 × 10 <sup>4</sup> . Air-only group:	Nose only, 6 hrs per day, followed by 4 consecutive days to air only; 6 rats from each group killed 24 h after 4 days' exposure to air; remaining 6 rats killed 7 days after air exposure	No lung lesions observed; acute pulmonary inflammation response to 15-nm AgNPs post-exposure after 4 days of air exposure, but effects resolved after 7 days post-exposure	NA	AgNPs observed inside lung cells at 24 h post-exposure; average particle size reduced to <5 nm, attributed to dissolution; toxicity related to lung dose and particle number/surface area	Braakhuis et al. [2014]
Male C57BL/6 mice, 5 per group	20 nm AgNP	1.93 × 10 <sup>7</sup> particles/cm <sup>3</sup> (~2.9 mg/m <sup>3</sup> )	Nose only, 6 hours for 1 day, responses examined at 0 and 1 day after exposure	Distribution to brain, heart, liver, spleen, and testes with rapid clearance from lung. Activation of MAPK signal pathway, increased total protein in BAL with recovery by 1 day, no lung pathology.	ND		Kwon et al. [2012]

*This information is distributed solely for the purpose of pre-dissemination peer review under applicable information quality guidelines. It has not been formally disseminated by the National Institute for Occupational Safety and Health. It does not represent and should not be construed to represent any agency determination or policy.*

**Table E-6. Summary of in vivo toxicological studies of silver nanoparticles (AgNPs) and nanowires (AgNWs)**

Species	Particle Characteristics	Exposure Details		Critical Effect(s)	NOAEL/LOAEL	Comments	Reference
		Concentration/ Dose	Duration				
Sprague-Dawley rats and Brown Norway (BN) rats, 8-12 males per group	13-16 nm AgNP, spark-generated	3.68-4.55 x 10 <sup>7</sup> particles /cm <sup>3</sup> (~600-800 µg/m <sup>3</sup> )	Nose only, 3 hours for 1 day (low dose) or 3 hours/day for 4 days (high dose), responses measured at 1 and 7 days post-exposure	Increased inflammatory cells and proteins with high dose, increased lung phospholipids, transient effects on lung mechanics	ND	Strain-related differences were attributed to the pre-existing inflammatory state in BN rats.	Seiffert et al. [2016]
Male Sprague-Dawley rats, 6 per group per time point	Citrate capped 20 or 110 nm AgNP	Aerosolized citrate buffer (control), 7.2 mg/m <sup>3</sup> for 20 nm AgNP and 5.4 mg/m <sup>3</sup> for 110 nm AgNP; equivalent deposited dose in nasal epithelium of 4 and 1 µg/cm <sup>2</sup> , respectively.	Nose only, single 6-hour exposure, recovery time points of 0, 1, 7, 21 and 56 days	Increased deposition at terminal bronchiole/alveolar duct junction, 33 % persistence of particle in lung for both sizes, higher macrophage particle burden for smaller particle.	ND		Anderson et al. [2015a]

*This information is distributed solely for the purpose of pre-dissemination peer review under applicable information quality guidelines. It has not been formally disseminated by the National Institute for Occupational Safety and Health. It does not represent and should not be construed to represent any agency determination or policy.*

**Table E-6. Summary of in vivo toxicological studies of silver nanoparticles (AgNPs) and nanowires (AgNWs)**

Species	Particle Characteristics	Exposure Details		Critical Effect(s)	NOAEL/LOAEL	Comments	Reference
		Concentration/ Dose	Duration				
Male Sprague-Dawley rats, 6 per group per time point	Citrate capped 20 or 110 nm AgNP	Aerosolized citrate buffer (control), 7.2 mg/m <sup>3</sup> for 20 nm AgNP and 5.3 mg/m <sup>3</sup> for 110 nm AgNP; equivalent deposited dose in nasal epithelium of 4 and 1 µg/cm <sup>2</sup> , respectively.	Nose only, single 6-hour exposure, recovery time points of 1, 7, 21 and 56 days	Lung injury and inflammation peaked day 7; 20 nm AgNP caused slightly greater inflammation and persisted longer, responses resolved over time	ND		Silva et al. [2016]
Male Sprague-Dawley rats, 8 per group per time point	Citrate capped 20 or 110 nm AgNP	Aerosolized citrate buffer (control), 7.2 mg/m <sup>3</sup> for 20 nm AgNP and 5.4 mg/m <sup>3</sup> for 110 nm AgNP; equivalent deposited dose in nasal epithelium of 4 and 1 µg/cm <sup>2</sup> , respectively.	Nose only, single 6-hour exposure, recovery time points of 0, 1, 7, 21 and 56 days	Translocation to the olfactory bulb (OB); OB microglia activation was increased acutely up to 7 days post-exposure to 20 nm AgNP and at day 0 only for 110 nm AgNP	ND	Translocation greatest at day 0 for 20 nm AgNP whereas the greatest burden was at day 56 for the 110 AgNP; particles differed in temporal rate of translocation	Patchin et al. [2016]

*This information is distributed solely for the purpose of pre-dissemination peer review under applicable information quality guidelines. It has not been formally disseminated by the National Institute for Occupational Safety and Health. It does not represent and should not be construed to represent any agency determination or policy.*

**Table E-6. Summary of in vivo toxicological studies of silver nanoparticles (AgNPs) and nanowires (AgNWs)**

Species	Particle Characteristics	Exposure Details		Critical Effect(s)	NOAEL/LOAEL	Comments	Reference
		Concentration/ Dose	Duration				
BALB/c mice, 5-6 females per group	33 nm average diameter, spherical	0 or 3.3 mg/m <sup>3</sup>	6 hours/day for 7 days from day 16- day 22 (after OVA sensitization and before OVA challenge)	Exacerbated allergic response (lung eosinophils, BAL IgE and IL-13, airway reactivity); Silver distributed to heart, spleen, liver, kidneys, and brain.	ND	Histologic changes in capsule of liver and spleen, focal and mild inflammation in perirenal soft tissue AgNP exposed mice (allergic and non-allergic) and in allergic control mice.	Chuang et al. [2013]
BALB/c mice, 5-6 females per group	33 nm average diameter, spherical	0 or 3.3 mg/m <sup>3</sup>	6 hours/day for 7 days from day 16- day 22 (after OVA sensitization and before OVA challenge)	Increased OVA-Specific IgE; Altered protein levels in BAL fluid and plasma in both allergic and non-allergic AgNP treated mice; Altered 18 proteins related to systemic lupus erythematosus in allergic and non-allergic mice.	ND		Su et al. [2013]

*This information is distributed solely for the purpose of pre-dissemination peer review under applicable information quality guidelines. It has not been formally disseminated by the National Institute for Occupational Safety and Health. It does not represent and should not be construed to represent any agency determination or policy.*

**Table E-6. Summary of in vivo toxicological studies of silver nanoparticles (AgNPs) and nanowires (AgNWs)**

Species	Particle Characteristics	Exposure Details		Critical Effect(s)	NOAEL/LOAEL	Comments	Reference
		Concentration/Dose	Duration				
BALB/c mice, 8 females per group	6 nm, agglomerating to 24 nm, OVA control for allergy, control for VEGF activity (VEGF receptor tyrosine kinase inhibitor)	20 ppm (40 mg/kg) AgNP or control for VEGF pathway activation (VEGF receptor tyrosine kinase inhibitor)	Nebulization 1x /day for 5 days before each OVA challenge (days 20-24), VEGF control 3 times intraperitoneally at 24 hour intervals for 5 days (days 0-24).	Attenuated allergic response, including mucus secretion, airway reactivity, and allergic cytokines and suppressed the P13/HIF-1 $\alpha$ /VEGF signaling pathway	NA		Jang et al' [2012]

*This information is distributed solely for the purpose of pre-dissemination peer review under applicable information quality guidelines. It has not been formally disseminated by the National Institute for Occupational Safety and Health. It does not represent and should not be construed to represent any agency determination or policy.*

<b>Inhalation – Subchronic</b>							
Sprague-Dawley rats; 10 of each sex per group	Mostly spherical, diameter range 2–65 nm (median, 16 nm)	0, 49, 133, or 515 $\mu\text{g}/\text{m}^3$ .	6 hrs/day, 5 days/week for 90 days (whole body exposure)	Lung function deficits, alveolar inflammation, macrophage accumulation	133 (49) /515 $\mu\text{g}/\text{m}^3$	Lung function and histologic deficits at high dose	Sung et al. [2008]
Sprague-Dawley rats; 10 of each sex per group	Mostly spherical, diameter range 2–65 nm (median, 16 nm)	0, 49, 133, or 515 $\mu\text{g}/\text{m}^3$	6 hrs/day, 5 days/week for 90 days (whole body exposure)	Bile duct hyperplasia; hepatocellular necrosis	133/515 $\mu\text{g}/\text{m}^3$	Same experiment as Sung et al. [2008]	Sung et al. [2009]
Sprague-Dawley rats; 17 males and 12 females per group	Spherical, non-agglomerated; diameter range 4–45 nm (median, 14–15 nm)	0, 49, 117, or 381 $\mu\text{g}/\text{m}^3$	6 hrs/day, 5 days/week for 12 weeks (whole body exposure)	Lung function decrease, persistent lung inflammation in male rats; lung inflammation with gradual recovery in female rats	117 (49) /381 (117) $\mu\text{g}/\text{m}^3$	Silver nanoparticles generated as reported previously [Ji et al. 2007a]	Song et al. [2013]
Sprague-Dawley male and female rats; 4 groups of 10	AgNPs with 18-nm diameter	$0.7 \times 10^6$ particles/ $\text{cm}^3$ (low dose), $1.4 \times 10^6$ particles/ $\text{cm}^3$ (middle dose), $2.9 \times 10^6$ particles/ $\text{cm}^3$ (high dose)	6 hrs/day for 90 days; killed 24 hrs after last treatment	Bone marrow tested for toxicity with micronucleus assay; no treatment-related genetic toxicity observed	NA		Kim et al. [2011a]

This information is distributed solely for the purpose of pre-dissemination peer review under applicable information quality guidelines. It has not been formally disseminated by the National Institute for Occupational Safety and Health. It does not represent and should not be construed to represent any agency determination or policy.

Sprague-Dawley male and female rats; 17 male and 12 female per group	Spherical AgNPs with diameters <47 nm (range, 4–47 nm)	0.6 × 10 <sup>6</sup> particles/cm <sup>3</sup> (low dose), 1.4 × 10 <sup>6</sup> particles/cm <sup>3</sup> (middle dose), 3.0 × 10 <sup>6</sup> particles/cm <sup>3</sup> (high dose)	6 hrs/day, 5 days/week for 12 weeks; rats given micronucleus gene test at end of 12 weeks or after 4- or 12-week recovery	Genes found to be up- and downregulated for the kidney by more than 1.3-fold ( <i>P</i> < 0.05): 104 genes for males and 72 for females	NA	Female rats show a 2–4-fold higher Ag concentration in kidneys, possibly due to metabolism and hormonal regulation	Dong et al. [2013]
<b>Oral Exposure</b>							
Sprague-Dawley rats (male and female), 3 groups of 20	Citrate-coated (avg. diameters 10 and 25 nm)	Control (0.9% citrate), 100 mg/kg bw, 500 mg/kg bw)	Subacute; exposed once/day for 28 days; killed at 1, 2, and 4 months	AgNPs remained in brain and testes at 4 months	NA	Bio-persistence study; silver clearance concentration in blood > liver = kidneys > spleen > ovaries > testes = brain	Lee et al. [2013a]

*This information is distributed solely for the purpose of pre-dissemination peer review under applicable information quality guidelines. It has not been formally disseminated by the National Institute for Occupational Safety and Health. It does not represent and should not be construed to represent any agency determination or policy.*

Male Sprague-Dawley rats (n = 9/group/time point)	12.3 nm uncoated AgNP in 1% starch with 0.1% Tween-80	Acute exposure: 2000mg/kg Subacute exposure: 250 mg/kg	Acute: 1x administration with recovery points at 1, 7, and 14 days Subacute: 1x/day for 30 days; assessment at 7 <sup>th</sup> , 18 <sup>th</sup> , and 30 <sup>th</sup> day during exposure	No hematologic changes due to either exposure. >99% excreted for both acute and subacute exposure.	ND	Acute biodistribution beyond the GI tract at day 7 was liver ≥ kidney > spleen; repeated exposure distribution beyond GI tract was highest in spleen at day 7, and kidney > spleen ≥ liver at days 14 and 30.	Hendrickson et al. [2016]
C57BL/6NCrI mice; 6 males per group/ time point	20 or 110 nm AgNP with gold core, PVP and citrate coated, or silver acetate (ion control), with or without antibiotic treatment	0, 0.1, 1.0, or 10 mg/kg	3 days with recovery at 1 and 7 days post-exposure	No changes in weight or organ histopathology; 70.5-98.6 % of dose recovered in feces; ionic silver was more bioavailable to a degree	NA	Size and coating did not affect distribution; ionic silver was higher than AgNP in kidney, liver, and spleen	Bergin et al. [2016]
Human (18 healthy volunteers)	25-40 nm colloidal AgNP	480 µg/day (32 ppm in 15 ml water)	14 days	Decreased platelet aggregation in the presence of an agonist	NA	Peak silver concentration in blood was 6.8 ± 4.5 µg/L	Smock et al. [2014]
ICR mice (up-down procedure for oral lethality)	Spherical, starch-stabilized (colloidal) particles of 10–20-nm diameter	5,000 mg/kg	Single dose	No lethality or signs of toxicity	ND	The oral LD <sub>50</sub> was >5,000 mg/kg	Maneewattana-pinyo et al. [2011]

*This information is distributed solely for the purpose of pre-dissemination peer review under applicable information quality guidelines. It has not been formally disseminated by the National Institute for Occupational Safety and Health. It does not represent and should not be construed to represent any agency determination or policy.*

Sprague-Dawley rats; 10 of each sex per group	60-nm diameter in aqueous 0.5% carboxymethyl-cellulose (CMC), shape not specified*	0, 30, 300, or 1,000 mg/kg-day by gavage	28 days	Increases in serum cholesterol and alkaline phosphatase; liver histopathology	30/300 mg/kg-day	Silver deposited in major organs and tissues	Kim et al. [2008]
Sprague-Dawley rats, 4 males per group/time point	Citrate-coated 7.9-nm diameter in an aqueous medium, shape not specified	1 or 10 mg/kg	Single exposure	Silver deposition in plasma, feces, urine, and the major tissues and organs	-/1 mg/kg	Citrate-coating of the particles may have deterred absorption	Park et al. [2011a]
ICR mice; 5 of each sex per group	22-, 42-, 71-, and 323-nm-diameter particles in an aqueous medium, shape not specified	1 mg/kg-day	14 days	Silver deposition in a wide range of tissues; increased serum concentrations of TGF- $\beta$	NA	Smaller particles were more effective	Park et al. [2010b]
ICR mice; 3 of each sex per group	42-nm diameter in an aqueous medium, shape not specified	0, 250, 500, or 1,000 $\mu$ g/kg-day by gavage	28 days	Increases in serum AP, AST, ALT, and cytokines; kidney histopathology	500/1,000 $\mu$ g/kg-day		Park et al. [2010a]
F344 rats; 5 of each sex per group	60-nm diameter in aqueous 0.5% CMC, shape not specified*	0, 30, 125, or 500 mg/kg-day by gavage	90 days	Kidney histopathology and silver deposition	ND	Heavier silver deposition was observed in females	Kim et al. [2009a]
F344 rats; 10 of each sex per group	60-nm diameter in aqueous 0.5% CMC, spherical and monodisperse	0, 30, 125, or 500 mg/kg-day by gavage	90 days	Increases in serum cholesterol and AP; liver histopathology	30/125 mg/kg-day	NOAEL and LOAEL are as specified by the study authors	Kim et al. [2010a]

This information is distributed solely for the purpose of pre-dissemination peer review under applicable information quality guidelines. It has not been formally disseminated by the National Institute for Occupational Safety and Health. It does not represent and should not be construed to represent any agency determination or policy.

Sprague-Dawley rats; 10 of each sex per group	60-nm diameter in aqueous 0.5% CMC, shape not specified*	0, 30, 300, or 1,000 mg/kg-day by gavage	28 days	Intestinal silver deposition: Goblet cell activation	ND	Data are semi-quantitative	Jeong et al. [2010]
Male Swiss albino mice; 5 mice per group	3-20 nm AgNP (average diameter = 10.15 nm)	0, 5, 10, 15, or 20 mg/kg	21 days	Loss of microvilli, increased inflammatory cells in villus, increased mitotic figures in intestinal glands	ND		Shahare et al. [2013]
Male and female Sprague-Dawley rats; 10/sex/group	10, 75, or 110 nm citrate-stabilized AgNP in 1% CMC, or silver acetate (ion control)	0, 9, 18, or 36 mg/kg AgNP; 100, 200, or 400 mg/kg silver acetate	13 weeks	AgNP induces size and dose dependent changes in populations of gut microbiota; Sex differences found for AgNP effects on expression of <i>Enterobacteriaceae</i> -family genes	ND	Higher doses of silver acetate were selected to ensure a response rather than matching amounts present in AgNP	Williams et al. [2015]
Female Wistar rats; 5/group/parameter evaluated	10-40 nm PVP-stabilized AgNP; hydrodynamic diameter 87-230 nm	0, 50, or 200 ppm	Daily for 60 days	Increased necrosis and damage to organelles in kidney; increased marker of inflammation systemically and in kidney; increased indices of oxidative stress in kidney	ND	~60-70% of the dose was excreted on day 1 of exposure and increased over time; dose-dependent accumulation of AgNP in kidney at day 60 (70-75% non-ionic, 25-30% ionic)	Tiwari et al. [2017]

*This information is distributed solely for the purpose of pre-dissemination peer review under applicable information quality guidelines. It has not been formally disseminated by the National Institute for Occupational Safety and Health. It does not represent and should not be construed to represent any agency determination or policy.*

<p>Male and female Sprague-Dawley rats; 5/sex/group Male and female Sprague-Dawley rats; 12/sex/group</p>	<p>11 nm citrate-coated AgNP; 12 nm SiO<sub>2</sub> NP; 60 nm Fe<sub>2</sub>O<sub>3</sub> NP 11 nm citrate-coated AgNP; 12 nm SiO<sub>2</sub> NP; 60 nm Fe<sub>2</sub>O<sub>3</sub> NP</p>	<p>~0, 500, 1000, or 2000 mg/kg ~0, 250, 500, or 1000mg/kg</p>	<p>Subacute: 14 days Subchronic:13 weeks</p>	<p>AgNP resulted in increased serum AP in males at the middle and high dose and in females at all doses Ag detected in major organs; AP elevated in serum after high dose AgNP in males and females; Histological changes in liver of both sexes; platelets elevated in males at high dose; increased white blood cells, serum calcium, and kidney calcification in females</p>		<p>No toxicity associated with iron or silica NP No toxicity associated with iron and silica NP and no translocation of silica or iron NP to other organ systems</p>	<p>Yun et al. [2015]</p>
<p>Male Sprague-Dawley rats; 16 per group</p>	<p>70-80% 20 nm AgNP and 20% protein gel (Collargol)</p>	<p>820 mg/kg Collargol (500 mg/kg AgNP) daily</p>	<p>81 days</p>	<p>In plasma: increased cholesterol, increased ratio of LDL to HDL, decreased triglycerides; Increased oxidative stress markers in heart and liver; increased inflammatory markers in liver</p>	<p>ND</p>		<p>Elle et al. [2013]</p>

*This information is distributed solely for the purpose of pre-dissemination peer review under applicable information quality guidelines. It has not been formally disseminated by the National Institute for Occupational Safety and Health. It does not represent and should not be construed to represent any agency determination or policy.*

Male Swiss albino mice; 8 per group	20 nm colloidal AgNP or gold NP	1 or 2 $\mu$ M/day	14 days	Increased markers of systemic inflammation and kidney and liver injury; Increased marker of oxidative stress in blood, urine, kidney, and liver; Increased metallothionein greater in kidney than liver	ND		Shrivastava et al. [2013]
Male Sprague-Dawley rats; 12 per group	20-30 nm AgNP, PVP-coated	0, 50, 100, or 200 mg/kg/day	90 days	AgNP distributed to all major organs, also located in hepatic and ileum cells; no significant pathology in any tissues collected including liver and kidney	ND	Thymus and brain copper and zinc levels were altered following AgNP exposure	Garcia et al. [2016]
Male Sprague-Dawley rats ( $n = 5$ )	AgNPs (~7.9-nm diameter)	2 mg/kg or 20 mg/kg	Up to 24 hrs	Silver concentrations in blood, liver, and lungs higher with Ag <sup>+</sup> than with AgNPs at all doses	ND	Bioavailability of Ag <sup>+</sup> appears to be greater than with AgNPs	Park [2013]

*This information is distributed solely for the purpose of pre-dissemination peer review under applicable information quality guidelines. It has not been formally disseminated by the National Institute for Occupational Safety and Health. It does not represent and should not be construed to represent any agency determination or policy.*

Male and Female Sprague-Dawley rats; 10 group/sex	28-44 nm PVP-coated AgNP or silver nitrate (ionic silver)	0, 0.5 or 1.0 mg/kg	28 days	AgNP distribution lower than soluble silver distribution; distribution noted in liver, kidney, spleen and testes; minor pathological changes in kidney and liver of both sexes; sex differences noted in blood chemistry and distribution patterns		Sex differences: increased AST in males and increased white blood cells in females, male tissue distribution of AgNP was liver and kidney > testes and spleen while female distribution of AgNP was equal across liver, kidney and spleen	Qin et al. [2016]
Sprague-Dawley rats; 5 groups of 5	< 20-nm non-coated, <15-nm PVP and AgNO <sub>3</sub> particles	Ag = 90 mg/kg bw; AgNO <sub>3</sub> = 9 mg/kg bw, by gavage	28 days	Silver deposition; silver cleared from organs except for brain and testis	ND	AgNPs similar to exposure to silver salts	Van der Zande et al. [2012]

*This information is distributed solely for the purpose of pre-dissemination peer review under applicable information quality guidelines. It has not been formally disseminated by the National Institute for Occupational Safety and Health. It does not represent and should not be construed to represent any agency determination or policy.*

<p>Hannover Galas male rats; 3 groups of 6 Hannover Galas rats; 4 groups of females, 11 per group; 2 groups of males, 6 per group</p>	<p>14-nm AgNP (stabilized with PVP), or Ag acetate (ionic silver)</p>	<p>Control (PVP, 11.5 mg/mL), 4.5 mg Ag/kg bw/day once or twice daily, for total dose of 4.5 or 9 mg/kg bw Control (PVP, 11.5 mg/mL) administered to 10 females and 6 males twice/day; AgNPs at 2.25 mg Ag/kg bw/day (8 females), 4.5 mg Ag/kg bw/day (8 females), or 9.0 mg Ag/kg bw/day (10 females and 6 males twice/day at 4.5); or 14 mg Ag acetate/kg bw/day in 11 mg/mL PVP (8 females twice/day)</p>	<p>Killed on day 14 Killed on day 28</p>	<p>No evidence of toxicological effects in AgNP exposed groups; decreased body weights; increases in plasma alkaline phosphatase absolute and thymus weights in Ag acetate–exposed groups</p>	<p>ND</p>	<p>Some toxicity at 9 mg/kg bw/day ionic silver dose but not at an equimolar AgNP dose</p>	<p>Hadrup et al. [2012a]</p>
<p>Male C57BL/6NcrJ; 6 per group</p>	<p>Colloidal 20 or 110 nm over gold core, PVP- or citrate-coated, or silver acetate (AgAC ionic silver)</p>	<p>10 mg/kg/day with and without antibiotics</p>	<p>28 days</p>	<p>Study focused on murine gut microbiome: AgNP, regardless of size and coating, did not alter the gut microbiome</p>	<p>ND</p>	<p>Cecal tips were processed to evaluate microbiome</p>	<p>Wilding et al. [2016]</p>
<p>Male and female Wistar rats; 8-10 females per group, 6 males in the control and 9 mg/kg AGNP group</p>	<p>14 nm PVP-coated AgNP or AgAc (ionic silver)</p>	<p>0, 2.25, 4.5, or 9 mg/kg day AgNP, or 9.0 mg/kg/day ionic silver</p>	<p>28 days – urine collected on day 18 for 24 hours</p>	<p>Metabolomics on urine showed increased allantoin and uric acid in female urine only indicating oxidative stress</p>	<p>ND</p>	<p>AgAC only increased allantoin in female urine</p>	<p>Hadrup et al. [2012b]</p>

*This information is distributed solely for the purpose of pre-dissemination peer review under applicable information quality guidelines. It has not been formally disseminated by the National Institute for Occupational Safety and Health. It does not represent and should not be construed to represent any agency determination or policy.*

Female Wistar rats; 5 groups of 6	14-nm diameter AgNPs or AgAc (ionic silver)	Control (PVP, 11.5 mg/mL), 2.25, 4.5, or 9 mg AgNP/kg bw/day, or 14 mg ionic silver /kg bw/day	28 days	Decrease in dopamine concentration (5-HT) in brain at 14 days but increase at 28 days for AgNPs; increase in noradrenaline brain concentration at 28 days for AgAc but not AgNP	ND	Ionic silver and 14-nm AgNP have similar neurotoxic effects	Hadrup et al. [2012c]
Male Wistar rats; 12/group	10 nm citrate-coated AgNP or silver citrate (ionic silver)	0.2 mg/kg/day	14 days	No effect on memory, locomotor activity, or motor coordination; Ionic silver decreased sensitivity to noxious stimuli and increase behavioral anxiety; both forms cause myelin sheath damage and altered myelin-related protein expression	ND	Also noted increased body temperature which persisted longer after ionic silver exposure	Dabrowska-Bouta et al. [2016]

*This information is distributed solely for the purpose of pre-dissemination peer review under applicable information quality guidelines. It has not been formally disseminated by the National Institute for Occupational Safety and Health. It does not represent and should not be construed to represent any agency determination or policy.*

Male and female Sprague-Dawley/CD-23 rats; 10/group/sex	0 10, 75, or 110 nm citrate-coated AgNP or AgAc (ionic silver)	AgNP: 0, 9, 18, or 36 mg/kg/day AgAc: 0, 100, 200, or 400 mg/kg/day	13 weeks	AgNP appeared in cells whereas AgAc was localized to cell membranes; increased tissue deposition with decreased size and increased solubility; higher Ag levels in females in kidney, liver, and intestines; highest soluble dose led to significant mortality	ND	AgNP did not produce pathological results in major organs and no changes in blood chemistry or hematology	Boudreau et al. [2016]
Male Sprague-Dawley rats; 6 per group	20-30 nm PVP-coated AgNP	0, 50, 100, or 200 mg/kg/day	90 days	AgNP increased alteration in sperm morphology; trend for increased damage to tubular lumen	ND	No changes in sperm motility or number were noted; no significant pathological changes in testes or epididymus	Lafuente et al. [2016]
Male Wistar rats; 8 per group	5-20 nm AgNP synthesized in citrate	0 or 20 µg/kg/day	90 days	Pathological abnormalities in testes and semiferous tubules; abnormal structures in sertoli cells, spermatids and spermatocytes; necrosis/depletion of germ cells	ND		Thakur et al. [2014]

*This information is distributed solely for the purpose of pre-dissemination peer review under applicable information quality guidelines. It has not been formally disseminated by the National Institute for Occupational Safety and Health. It does not represent and should not be construed to represent any agency determination or policy.*

Pre-pubertal male Wistar rats ( <i>n</i> = 30)	AgNPs (~86-nm diameter)	15 or 50 µg/kg bw	Exposed from post-natal day 23 to day 53 and killed on days 53 and 90	Reduction in total and daily sperm production observed in 50-µg/kg group at day 53; at 90 days both exposure groups had lower sperm production ( <i>P</i> < 0.05)	ND	Presence of cellular debris and germinal epithelial cells in tubular lumen and vesicles suggestive of possible impairment to spermatogenesis process	Sleiman et al. [2013]
Pre-pubertal male Wistar rats ( <i>n</i> = 30)	AgNPs (~86-nm diameter)	15 or 30 µg/kg bw	Exposed from post-natal days 23 through 58 (35 days at a total dose of 131–263 µg Ag/rat) and killed on postnatal day 102	Reduction in acrosome and plasma membrane integrities, reduced mitochondrial activity, and abnormalities of sperm in both dose groups; no change in sexual behavior or serum hormone	ND	Possible direct effect of AgNPs on spermatogenic cells	Mathias et al. [2014]

*This information is distributed solely for the purpose of pre-dissemination peer review under applicable information quality guidelines. It has not been formally disseminated by the National Institute for Occupational Safety and Health. It does not represent and should not be construed to represent any agency determination or policy.*

Pre-pubertal male Wistar rats; 8 per group	70 nm AgNP	0, 25, 50, 100, or 200 mg/kg/day	48 days of exposure	Reduced spermatogonia at highest dose; reduction in spermatocytes, spermatozoa, and spermatids in all groups but the lowest dose; minor changes in connective tissue in seminiferous tubules	ND	No differences in Sertoli cell number or seminiferous tubule diameter noted	Miresmaeili et al. [2013]
Female Sprague-Dawley rats;	6.45 nm AgNP in 0.5% CMC	0, 100, 300, or 1000 mg/kg/day	14 days, on gestation days 6-19	Dams: Increased indices of oxidative stress in liver homogenates Fetuses: increased loss of pre-implanted embryos at highest dose	NOEL reported as < 100 mg/kg/day for dams and 1000 mg/kg/day for embryo-fetal development	No abnormal blood chemistry in dams; no pathology of liver or kidney	Yu et al. [2014]

*This information is distributed solely for the purpose of pre-dissemination peer review under applicable information quality guidelines. It has not been formally disseminated by the National Institute for Occupational Safety and Health. It does not represent and should not be construed to represent any agency determination or policy.*

<p>Female CD-1 mice; 3 pregnant dams per group with 10-18 litters per group</p>	<p>20 nm or 3 <math>\mu\text{m}</math> Ag particles, 50 nm or 1-2 <math>\mu\text{m}</math> <math>\text{TiO}_2</math> particles</p>	<p>0, 10, 100, or 1000 mg/kg/day</p>	<p>1 time on gestation day 9</p>	<p>AgNP at 10 mg/kg and <math>\text{TiO}_2</math> NP at 1 and 1000 mg/kg reduced number of viable fetuses; AgNP could be detected in kidney and liver; only <math>\text{TiO}_2</math> NP at high doses led to fetal developmental abnormalities; smaller particle had greater effect than larger particles</p>	<p>ND</p>	<p>No effects were observed in weight of dams or fetus, fetal resorption, or litter size; <math>\text{TiO}_2</math> NP had greater effect than AgNP; no adverse pathology of kidney or liver</p>	<p>Philbrook et al. [2011]</p>
<p>Female Sprague-Dawley rats; 1-3 per group per time point</p>	<p>20 nm or 110 nm PVP-coated AgNP, or silver acetate</p>	<p>10 mg/ml</p>	<p>1 time on gestation day 18; parameters assessed 1 and 2 days post-exposure</p>	<p>Silver was detectable in placenta and fetus at both times and to a greater degree in fetus. Markers of cardiovascular effects and oxidative stress were not altered.</p>	<p>ND</p>	<p>Silver was detectable in all major organs; to a greater degree in spleen, lung, liver, kidney, placenta, and cecum/large intestine. Urine analysis show changes in carbohydrate and amino acid metabolism.</p>	<p>Fennell et al. [2016]</p>

This information is distributed solely for the purpose of pre-dissemination peer review under applicable information quality guidelines. It has not been formally disseminated by the National Institute for Occupational Safety and Health. It does not represent and should not be construed to represent any agency determination or policy.

Male and female C57BL/6J $p^{un}/p^{un}$ background mice or $Mhy^{-/-}$ mice; 4-6 mice per group	96.1 nm AgNP (determined by DLS) with PVP coating	0 or 500 mg/kg/day	5 days, on gestation days 9.5–13.5	Dams: Increased micronuclei formation in blood and bone marrow in AgNP exposed mice, which was greater in knockout; Induction of oxidative stress markers in both groups of mice Fetuses: increased eye-spot formation indicative of DNA deletion events	ND	Differences in up and down regulation of gene expression of DNA repair genes between wildtype and knockout mice	Kovvuru et al [2015]
<b>Dermal Exposure</b>							
Pigs; strain, sex, and number not stated	Spherical, 20- and 50-nm washed and unwashed particles	Up to 34 $\mu\text{g}/\text{mL}$ applied to the shaved dorsal surface	14 days	No observed erythema or edema; slight epidermal hyperplasia was seen microscopically	ND		Samberg et al. [2010]
Male guinea pigs, 9 per group	Spherical, starch-stabilized (colloidal) particles of 10–20-nm diameter	0, 50, or 100,000 ppm applied to shaved surface	24-hour application, observation at 1, 3, 7, and 14 days; skin pathology at 14 days	No abnormalities reported in skin	ND	Ocular irritation and corrosion tests showed transient eye irritation with 5000 ppm at 24 hours – resolved by 72 hours	Maneewattanapinyo et al [2011]

*This information is distributed solely for the purpose of pre-dissemination peer review under applicable information quality guidelines. It has not been formally disseminated by the National Institute for Occupational Safety and Health. It does not represent and should not be construed to represent any agency determination or policy.*

Sprague-Dawley rats, 10 per group (5 male, 5 female)	10 nm, colloidal, stabilized in citric acid (1%)	0 or 2000 mg/kg applied to shaved surface	24-hour application, observed twice a day for 15 days	No irritation or toxicity observed	ND		Kim et al. [2013]
Male New Zealand White rabbits	10 nm, colloidal, stabilized in citric acid (1%)	0.5 ml test substance according to OECD guideline 404	Various duration from 3 min to 4 hours application, observed 1, 24, 48, and 72 hours post-exposure	No irritation or corrosion observed	ND	Ocular irritation/corrosion test resulted in conjunctival redness, edema, and discharge at 1 hour with resolution over time; no effects on cornea	Kim et al [2013]
Male SPF guinea pigs, 20 animals	10 nm, colloidal, stabilized in citric acid (1%)	102.4 mg in 0.5 ml	Applied for 48 hours on day 6 following induction period with a 24 hour challenge on day 21	1/20 animals showed discrete and patchy erythema 24 and 48 hours following challenge indicating 5% skin sensitization rate (weak sensitizer)	ND		Kim et al [2013]
Male Hartley guinea pigs; 6 per group F	<100-nm particles of various shapes and degrees of aggregation	0,100, or 1000 µg/mL	Single acute exposure with a 14-day observation period	No lethality: some histopathologic changes to skin	-/100 µg/mL		Korani et al. [2011]

*This information is distributed solely for the purpose of pre-dissemination peer review under applicable information quality guidelines. It has not been formally disseminated by the National Institute for Occupational Safety and Health. It does not represent and should not be construed to represent any agency determination or policy.*

Male Hartley guinea pigs; 6 per group	<100-nm particles of various shapes and degrees of aggregation	0, 100, 1000, or 10,000 µg/mL	Subchronic; once daily, 5 days/week for 13 weeks	Skin perturbation; liver and spleen histopathology	~100 µg/mL		Korani et al. [2011]
Male Hartley guinea pigs; 12 per treatment group	<100-nm particles of various shapes and degrees of aggregation	0, 100, 1000, 10,000 ppm AgNP or 100 µg/ml silver nitrate	Subchronic, 13 weeks	Dose-dependent increase of silver in kidney > muscle > bone > skin > liver > heart > spleen; middle and high dose induced kidney pathology; all doses resulted in degrees of bone pathology; high dose caused pathological effects in heart	ND	Kidney, heart, and bone were the focus for histopathology analysis; liver and spleen were previously analyzed.	Korani et al. [2013]

This information is distributed solely for the purpose of pre-dissemination peer review under applicable information quality guidelines. It has not been formally disseminated by the National Institute for Occupational Safety and Health. It does not represent and should not be construed to represent any agency determination or policy.

<b>Intratracheal Instillation and Pharyngeal Aspiration</b>							
Male ICR mice, 3-4 per group	20 nm citrate-coated AgNP, and AgNO <sub>3</sub> , (soluble control) (60 and 100 nm citrate-coated AgNP and PVP-coated particle were used additionally for in vitro studies)	10 µg of 20 nm citrate-stabilized AgNP or AgNO <sub>3</sub> per mouse	Single IT instillation, assessment at 4 and 24 hours	Increased IL-1β at 4 hr in AgNP versus soluble, greater neutrophil influx due to soluble form at 24 hours. Increased lung burden for AgNP versus soluble Ag indicating faster clearance for soluble Ag, and greater translocation to liver for soluble Ag, no detectable Ag in kidney, spleen or urine.		In vitro, Ag distributed to metallothioneins and macrophages sequester AgNP in the lysosome with gradual dissolution over time.	Arai et al. 2015
Female Wistar-Kyoto rats, 5 per group	70 nm PVP-coated AgNP	0, 50, or 250 µg per rat (~ 0, 0.2, or 1 mg/kg)	Single IT instillation with recovery time point of 24 hours	Increased BAL inflammatory cells, inflammatory cytokines, and lung injury at high dose.	ND		Haberl et al. 2013

*This information is distributed solely for the purpose of pre-dissemination peer review under applicable information quality guidelines. It has not been formally disseminated by the National Institute for Occupational Safety and Health. It does not represent and should not be construed to represent any agency determination or policy.*

Male imprinting control region mice; 7-9 per group for BAL parameters and 2-3 per group for histopathology	99.96 % colloidal, 10-20 nm, spherical	0 or 100 ppm/50 µl distilled water	Single IT instillation, recovery time points at 1, 3, 7, 15, and 30 days post-exposure	Cytotoxicity and neutrophil number in BAL increased acutely after exposure, lymphocyte influx occurred at 7 and 15 days post-exposure, lung injury was characterized by inflammatory nodules, necrotizing alveolitis, and type II cell hyperplasia	ND	Increased indices of oxidative stress correlated to particle laden areas and cells at acute time points post-exposure. Lung injury and inflammation resolved with time	Kaewamata-wong et al. 2014
Female rats (in-house breeding colony), 8-14 in control and exposed groups	49 nm AgNP, 50 nm AuNP, 1.1 µm Ag particles	0 (water) or 0.5 mg/ml	Single IT instillation, evaluation at 24 hours	Increased neutrophil influx in to lungs (AgNP> AuNP >micron Ag), Increased phagocytosis in macrophages and mitochondria affinity in macrophages and neutrophils with Ag versus Au, no nuclear penetration with AgNP			Katsnelson et al. 2013

*This information is distributed solely for the purpose of pre-dissemination peer review under applicable information quality guidelines. It has not been formally disseminated by the National Institute for Occupational Safety and Health. It does not represent and should not be construed to represent any agency determination or policy.*

Wistar rats (sex not specified), 6 rats per group	52 nm spherical AgNP, 19 nm hexagonal ZnO NPs, 23 nm spherical TiO <sub>2</sub> NPs	0, 3.5 and 17.5 mg/kg	IT instillation once every 2 days for 5 weeks with analysis 1 day post-exposure	Elevated indicators of oxidative stress, lung injury and inflammation in BAL; cytotoxicity was ZnO > Ag = TiO <sub>2</sub>	ND	Comparative analysis suggest particle composition and stability as factors for toxicity.	Liu et al. 2013a
Sprague-Dawley rats; number and sex not stated	20-nm PVP-coated particles that aggregated in a physiologic medium	0, 9.35, or 112 µg/rat	IT instillation once weekly for 8 weeks, with various recovery periods up to 84 days	Albumin, LDH, neutrophils, and lymphocytes increased in BAL in comparison with controls	9.35/112µg	Pulmonary injury and inflammation resolved with time	Roberts et al. [2012]
Male ICR mice (n = 48); 12 per group	AgNP at 243.8-nm average diameter	0, 125, 250, and 500 µg/kg	Single IT instillation; histopathologic analysis at different time points from treatment (1, 7, 14, and 28 days)	Dose-related change in cytokine composition of BAL and blood, with maximum concentration found at 28 days; changes in gene expression; marked inflammatory response from day 1 to 28	NA	Changes in functionality of induced genes appears to be related to tissue damage	Park et al. [2011b]

*This information is distributed solely for the purpose of pre-dissemination peer review under applicable information quality guidelines. It has not been formally disseminated by the National Institute for Occupational Safety and Health. It does not represent and should not be construed to represent any agency determination or policy.*

Male BALB/c OlaHsd mice, 4 per group	25-28 nm AgNP (90 nm aggregated), 15 nm TiO <sub>2</sub> NP (396 nm aggregated), 19 nm SiO <sub>2</sub> NP (192 nm aggregated), paints containing individual metal NP	0 or 20 µg per mouse per dose	Oropharyngeal aspiration once a week for 5 weeks with recovery at 2 and 28 days after last exposure	Increased silver in liver, spleen and kidney, but not heart, 2 days after last exposure, with clearance from all organs but lung at 28 day; increased lung inflammation with recovery over time.	ND	Ag NP distribution differed from TiO <sub>2</sub> which was only present in the lung and SiO <sub>2</sub> which was found in lung and liver only. AgNP were more toxic than TiO <sub>2</sub> and SiO <sub>2</sub>	Smulders et al. 2014
Male BALB/c OlaHsd mice, number per group not specified	Heterogenous, 20 nm spherical and 80-90 nm rod-shaped Ag NP, aggregating to ~ 500nm average.	0 or 20 µg per mouse per dose	Oropharyngeal aspiration once a week for 5 weeks with recovery at 2 days after last exposure	High degree of macrophage phagocytosis in airways and alveolar region, high degree of dissolution and conjugation to thiol-containing molecules	ND	Presence of Fe and Cu in Ag-rich areas indicate metallothionein conjugation	Smulders et al. 2015a
Male C57BL/6 mice, 2-4 per group	25 nm, noted to agglomerate in delivery vehicle	0, 100 or 500 mg/kg	Single IN instillation with recovery times of 1 and 7 days	AgNP measured in brain (OB and lateral brain ventricles), spleen (red pulp more than white pulp), kidney, lung, and nasal cavity.	ND	Elevated glutathione levels in nasal cavity and blood; nasal mucosal erosion and reduced cellularity in spleen; no alterations in cell infiltrates or microglial activation in the brain	Genter et al. 2012

*This information is distributed solely for the purpose of pre-dissemination peer review under applicable information quality guidelines. It has not been formally disseminated by the National Institute for Occupational Safety and Health. It does not represent and should not be construed to represent any agency determination or policy.*

Male C57BL/6 mice, 13-17 per group for repeated exposures, group number not stated for single exposures	25 nm, noted to agglomerate in delivery vehicle	Single dose of 10-500 mg/kg, repeated dose of 50 mg/kg	Single or repeated (1 time per day for 7 days) intranasal instillation, 1 week recovery following repeated exposure	Silver deposition in liver, gut associated lymphoid tissue, and brain; oxidative stress responses elevated in hippocampus but not cortex; no change in learning or memory related behaviors (Morris Maze Test)	ND		Davenport et al. 2015
Female C57BL/6NT mice, 3 per group for AgNP	8-47 nm AgNP (NM-300) capped with polyoxyethylene glycerol trioleate and Tween-20, 70-100 nm ZnO NP, 58-90 nm functionalized ZnO NP; aggregates ~ 200 nm	0, 1, 4, 8, 16, 32, 64, and 128 µg/mouse	Single IT instillation, responses evaluated 1 day post-exposure	AgNP decreased liver glutathione levels; no adverse pulmonary effects due to AgNP	ND	ZnO NP were more inflammatory in the lung than AgNP	Gosens et al. 2015
Male Sprague-Dawley rats, 4-5 per group	20 nm citrate-capped (AgNP), 26.2 nm hydrodynamic diameter; silver acetate (AgAc)	naïve, 2 mM citrate buffer vehicle, 1 mg/ml AgNP, or 0.01, 0.1, or 1 mg/ml AgAc	Single IT with recovery 1 and 7 days for AgNP and 1 day for AgAc	Both AgAc and AgNP caused a cardiac ischemic reperfusion injury but only AgNP resulted in changes in serum cytokines levels.	ND		Holland et al. 2015

*This information is distributed solely for the purpose of pre-dissemination peer review under applicable information quality guidelines. It has not been formally disseminated by the National Institute for Occupational Safety and Health. It does not represent and should not be construed to represent any agency determination or policy.*

Male Wistar rats, 3 groups of 8 for behavioral measures (half the group for histopathology and half for markers of oxidative stress in the brain and hippocampus.	50-100 nm AgNP primary size, 33-380 nm aggregated in deionized water (vehicle)	0, 3, or 30 mg/kg	IN administration (nose drops) once every 2 days for 14 days	Dose-dependent impairment in cognitive function, increased neuronal damage in hippocampus, and increased reactive oxygen species in hippocampus was observed		Morris water maze tests were the basis for cognitive function. Long term potentiation tests also showed impairment of synaptic connectivity in the AgNP groups.	Liu et al. 2012
Male ICR mice, 6 per group	20 nm AgNP (NM-300K) in polyoxyethylene glycerol trioleate and Tween-20 (NM-300K DIS), NM-300K DIS control	0, 0.1, and 0.5 mg/kg	Single IT instillation, assessment at 8 and 24 hours	Increased endoplasmic reticulum stress marker primarily in lung, liver and kidney, dose-dependent increased apoptosis in lung, apoptosis in kidney (high dose), increased Ag deposition in liver at 8 hours and kidney at 24 hours.	NA	In vitro studies showed ER stress response in human bronchial epithelial cells but not in umbilical vein endothelial cells or hepatocytes.	Huo et al. 2015

*This information is distributed solely for the purpose of pre-dissemination peer review under applicable information quality guidelines. It has not been formally disseminated by the National Institute for Occupational Safety and Health. It does not represent and should not be construed to represent any agency determination or policy.*

Male Wistar rats, 3 per group	28-30 nm, 30 % AgNP in NaCl matrix	0 or 0.05 mg/kg	Single IT instillation with recovery times of 1, 3, and 14 days.	Alterations in mRNA expression of circadian regulatory genes (including PER1, PER2, CLOCK) were observed in lung, liver, brain, heart, kidney, and testes at varying degrees and times across the study.			Minchenko et al. 2012
Neonatal male and female rats, animal number varied by group from 5 - 30	20 nm PVP-coated AgNP or AgNO <sub>3</sub> (ion control)	0, 0.1 or 1 mg/kg AgNP or silver ion	IN instillation 1x/day for 4 weeks or 12 weeks; organ samples taken immediately following 4 week exposure, and various times throughout the 12 week study up to 4 weeks.	Silver detected in all major organs and to a greater degree for ionic Ag compared to AgNP. For both forms of silver, the highest level of Ag was in liver at 4 weeks followed by brain, and highest in brain at 12 weeks. Dose-dependent differences were greater AgNP groups than in ionic silver groups.	ND	No sex-specific tissue accumulation observed. Increased mortality noted in the 1 mg/kg/d silver ion group.	Wen et al. 2015

*This information is distributed solely for the purpose of pre-dissemination peer review under applicable information quality guidelines. It has not been formally disseminated by the National Institute for Occupational Safety and Health. It does not represent and should not be construed to represent any agency determination or policy.*

Male C57BL/6, 4 per group	20 and 110 nm PVP-capped, and 20 and 110 nm citrate-capped AgNP	0.05 µg/g (0.05 mg/kg)	Single IT instillation with recovery at 1, 7, or 21 days	PVP-stabilized particles reduced surfactant protein D in BAL at 1 day and increased inflammation and reduced lung function (7 day). Larger particles had a greater effect. Responses resolved by 21 days.	ND	The subtoxic particle dose (0.05 µg/g) was determined by evaluating lung leakiness (injury) 1 day following a dose-response study, where no leakiness was observed.	Botelho et al. 2016
Male Sprague-Dawley (SD) rats and Male Brown Norway (BN) rats, 5-6 per group	20 and 110 nm PVP-capped, and 20 and 110 nm citrate-capped AgNP	0.1 mg/kg AgNP, or controls for coating material (1mM citrate, 33 or 62 µg/ml PVP for 20 and 110 nm PVP-coated AgNP, respectively)	Single IT instillation, responses measured at 1, 7, and 21 days post-exposure	Increased bronchial hyperresponsiveness (smaller particles > larger particles), increased inflammation, increased irritant response in BN rats	ND	Most cellular responses returned to baseline by day 21	Seiffert et al. [2015]
Male Sprague-Dawley rats, 72 rats per particle type with 6 rats per group	20 and 110 nm citrate stabilized AgNP, 20 and 110 nm PVP-stabilized Ag NP	0, 0.1, 0.5, and 1 mg/kg (buffer as control)	Single IT instillation, recovery evaluated at 1, 7, and 21 days	The larger particle produced more persistent effects in the lung based on mass; no differences in toxicity due to coating were noted.	ND	Increased alveolar neutrophils and airway cytotoxicity, variable degrees of resolution with time based on size and parameter examined	Silva et al. [2015]

*This information is distributed solely for the purpose of pre-dissemination peer review under applicable information quality guidelines. It has not been formally disseminated by the National Institute for Occupational Safety and Health. It does not represent and should not be construed to represent any agency determination or policy.*

Male Sprague-Dawley rats, 6 per group	20 and 110 nm citrate stabilized AgNP, 20 and 110 nm PVP-stabilized Ag NP	0, 0.5, and 1.0 mg/kg	Single IT instillation, recovery evaluated at 1, 7, and 21 days	Increased deposition in proximal airways for small vs large particles; faster airway clearance for larger particles, faster rate of lung clearance for 20 nm PVP AgNP vs 20 nm citrate AgNP	ND		Anderson et al. [2015]
Male Sprague-Dawley rats	Ag nanowires approx. 50-nm diameter; lengths 4 or 20 µm	10, 50, 125, or 500 µg; alpha-quartz positive control at 500 µg or dispersion medium vehicle control	Single IT instillation	Both samples showed dose-dependent lung injury and inflammation	NA	Shorter wires' greater toxicity over time possibly due to more wires/surface area per equivalent mass dose	Kenyon et al. [2012]
Female C57BL/6 mice; 5 per exposure group	Ag nanowires with lengths of 3, 5, 10, or 14 µm	Doses set to equalize number of wires/mouse: 10.7, 17.9, 35.7, and 50	Single pharyngeal aspiration; acute inflammation response evaluated 24 hrs post-exposure	Nanowire length-dependent trend in pulmonary inflammation; statistically significant increase in granulocytes in BAL only with 14-µm Ag wires	NA	Suggested Ag nanowire threshold between 10- and 14-µm lengths	Schinwald et al. [2012]

This information is distributed solely for the purpose of pre-dissemination peer review under applicable information quality guidelines. It has not been formally disseminated by the National Institute for Occupational Safety and Health. It does not represent and should not be construed to represent any agency determination or policy.

Male Sprague-Dawley rats, 63 rats per wire length	~2 µm x 33 nm and 20 µm x 64 nm (length x width) Ag NW	0, 35, 175, or 350 µg/rat (0, 0.1, 0.5 and 1 mg/kg, respectively)	Single IT instillation with recovery evaluated at 1, 7, and 21 days	Both sizes increased lung inflammation and injury at high dose; increased giant cell formation, terminal bronchiolar cell damage, and AgNW encapsulation in granulomas at day 21	ND	Only long wires induced a degree of frustrated phagocytosis by macrophages	Silva et al. 2014
<b>Intravenous Administration</b>							
Male Sprague-Dawley rats 9 n = 4/group/time point)	35 nm AgNP primary size; agglomerating to 69 nm in vehicle	125 µg/50 µl vehicle (~0.5 mg/kg); vehicle (10% fetal bovine serum in DMEM)	Single exposure with recovery points at 1, 3, and 5 days post-exposure	Inflammation and necrosis in liver only at days 3 and 5. Silver levels highest in liver and spleen at all times. Most of silver in liver was particulate. Ion/particle ration decreased in spleen over time. Silver in all other organs was primarily ionic.		No pathology noted in kidney, spleen, lung, or brain	Su et al. [2014b]

*This information is distributed solely for the purpose of pre-dissemination peer review under applicable information quality guidelines. It has not been formally disseminated by the National Institute for Occupational Safety and Health. It does not represent and should not be construed to represent any agency determination or policy.*

Male Balb/c mice; n= 5 for biodistribution studies and n= 3-5 for pharmacokinetic studies	PVP, citrate, PEG, or BPEI coated AgNPs ~30 nm; AgNO <sub>3</sub> soluble control	20 µg of silver per mouse in 200 µl volume	Single exposure; biodistribution assessed at 1 day; blood collected at 2, 10, 30, and 60 min, and at 6, 12, 24, and 72 hours	All particles distributed to the greatest degree to the liver and spleen; BPEI had the greatest biopersistence in tissues at 24 hours, PVP and citrate AgNP were similar in pharmacokinetics; PEG-coated particle also had a high biopersistence and remained in the circulation the longest in the first hour after exposure.	ND	Complementary in vitro studies showed DNA fragmentation and cytotoxicity with positively charged surface coating in liver cells	Pang et al. [2016]
Male CD-1 (ICR) mice (n = 3/group)	PVP- or citrate coated 10, 40, or 100 nm; or silver acetate	10 mg/kg of AgNO or 15.5 mg/kg silver acetate (10 mg/kg silver equivalent)	Single exposure with 24-hour recovery point	Coating did not influence distribution or toxicity; smaller particles accumulates to a greater degree in tissues than larger and were more hepato- and spleno-toxic.		Soluble silver accumulated in liver but also in a kidney to a greater degree than particulate silver and caused kidney toxicity	Recordati et al. [2016]
Male Wistar rats; 4 groups of 24	20- or 200-nm, almost spherical, agglomerated in solution	0, 5, or 10 mg/kg for the 20-nm particles, 0 and 5 mg/kg for the 200-nm particles	Single exposure (tail vein) with various recovery periods up to 4 weeks	Reduced sperm count, increased comet tail moments in germ cells	~5 mg/kg		Gromadzka-Ostrowska et al. [2012]

*This information is distributed solely for the purpose of pre-dissemination peer review under applicable information quality guidelines. It has not been formally disseminated by the National Institute for Occupational Safety and Health. It does not represent and should not be construed to represent any agency determination or policy.*

Sprague-Dawley rats; sex not stated; 5–8 per group	50–60-nm particles in 0.7% NaCl containing 0.05% Tween 80, shape not specified	30 mg/kg	Single exposure	Leakage of Evans blue dye into the brain, brain edema	–/30 mg/kg		Sharma et al. [2010]
Sprague-Dawley rats; 2 of each sex per group	Spherical 50–90 nm or 1–10 nm in diameter, but with aggregation in aqueous medium	100 mg/kg for the larger species, 1 mg/kg for the smaller	One injection in tail vein 3 days/week for 4 weeks	Silver deposition, changes to the lymphocyte/granulocyte ratio, changes in gene expression	NA	Dosing regimen insufficiently described	Kim et al. [2009b]
Sprague-Dawley rats; 2 males per group	Spherical 50-nm-diameter particles in an aqueous medium; some larger particles (up to 100 nm in length) were rod-shaped	0, 1, or 100 mg/kg	One injection in tail vein every 2–3 days for 4 weeks	Proteomic analysis of liver, kidney, and lung	NA	Functional analysis of proteomic changes implicated ROS formation and apoptosis in relation to silver nanoparticles treatment	Kim et al. [2010b]
Wistar rats; 4 dose groups and a control group; male and female rats; <i>n</i> per group not stated	Spherical 15–40-nm-diameter particles dispersed in ethylene glycol	4, 10, 20, or 40 mg/kg; phosphate buffer saline as control substance	One injection in tail vein at 5-day intervals over 32 days	Hematologic changes in WBC, platelet counts, hemoglobin, and RBC in 20- and 40-mg/kg groups; increase in liver function enzymes, ALT, AST, AP, GGTP in 40-mg/kg group	NOAEL at 10 mg/kg	ROS increased in all groups in a dose-related manner	Tiwari et al. [2011]

*This information is distributed solely for the purpose of pre-dissemination peer review under applicable information quality guidelines. It has not been formally disseminated by the National Institute for Occupational Safety and Health. It does not represent and should not be construed to represent any agency determination or policy.*

Balb/c mice (sex not specified); n = 3-6/group	20 nm AgNP (NM-300K) in medium 4 % Tween-20 + 4% polyoxyethylene (NM-300K-DIS)	0,0.2,2.0, or 5.0 mg/kg	Single dose, parameters assessed at 8 hours post-exposure	Highest dose caused lung and liver pathology; markers of oxidative and endoplasmic reticulum stress in liver and spleen; apoptosis in lung, liver, spleen, and kidney	ND	Tissue distribution spleen > liver > lungs >> kidneys > heart > brain	Chen et al. [2016]
Female Sprague-Dawley rats; 1-3 per group per time point	20 nm or 110 nm PVP-coated AgNP, or silver acetate	1 mg/ml	1 time on gestation day 18; parameters assessed 1 and 2 days post-exposure	Silver was detectable in placenta and fetus at both times and to a greater degree in fetus. Markers of cardiovascular effects and oxidative stress were not altered.	ND	Silver was detectable in all major organs; to a greater degree in spleen, lung, liver, kidney, placenta, and cecum/large intestine. Urine analysis show changes in carbohydrate and amino acid metabolism.	Fennell et al. [2016]

*This information is distributed solely for the purpose of pre-dissemination peer review under applicable information quality guidelines. It has not been formally disseminated by the National Institute for Occupational Safety and Health. It does not represent and should not be construed to represent any agency determination or policy.*

<p>Female Balb/c mice; n = 5-10/group Female Balb/c mice; n = 3/group Male Balb/c mice; n = 3-5/group</p>	<p>25 nm PVP-coated AgNP or silver nitrate 25 nm PVP-coated AgNP 25 nm PVP-coated AgNP</p>	<p>0, 22, or 108 µg/kg AgNP or 108 µg/kg silver nitrate 1.3mg/kg AgNP 1.3mg/kg AgNP</p>	<p>Every 2 days for 4 weeks, with recovery at 2 weeks after last exposure Every 2 days for 4 weeks with recovery at 15, 39, and 72 days after last exposure Every 2 days for 4 week with recovery at 4 months after last exposure</p>	<p>High dose of AgNP detected in Spleen &gt; liver = kidney Silver highest in liver, kidney and spleen at d 15, lower in heart and lung; clearance occurred over time for liver spleen and kidney, but was still measureable at day 78. Silver was highest in liver, spleen, and testis (ng/g tissue), followed by kidney, heart, lung, and muscle</p>	<p>ND</p>	<p>Comparative study: Intraperitoneal deposition and persistence was greater than intravenous exposure. Silver not detectable in serum Silver not detectable in serum</p>	<p>Wang et al. [2013]</p>
<p>CD-1 pregnant mice; groups of 6 to 12</p>	<p>Spherical 50-nm-diameter particles of AgNO<sub>3</sub></p>	<p>Doses of 0 (n = 11), 35 (n = 12), 66 (n = 6) µg AgNPs on the 7<sup>th</sup>, 8<sup>th</sup>, and 9<sup>th</sup> day of gestation; doses of 9 (n = 9) and 90 (n = 3) µg AgNO<sub>3</sub> on same days of gestation</p>	<p>One injection of each dose on the 7<sup>th</sup>, 8<sup>th</sup>, and 9<sup>th</sup> day of gestation; killed 24 hrs after 3<sup>rd</sup> injection</p>	<p>AgNPs identified in most maternal organs, extra-embryonic tissues, and embryos</p>	<p>NA</p>		<p>Austin et al. [2012]</p>
<p>Male Wistar rats; 2 exposure groups and 1 control group; 23 per group</p>	<p>20- and 200-nm-diameter AgNPs</p>	<p>Doses of 0 (control group) and 5 mg/kg (exposure groups)</p>	<p>One injection; killed at 24 hrs, 7 days, and 28 days</p>	<p>AgNPs identified in liver, lungs, spleen, kidneys, and brain; highest concentration of Ag in liver at 24 hrs</p>	<p>NA</p>	<p>Highest concentration of Ag found with 20-nm AgNPs</p>	<p>Dziedzikowska et al. [2012]</p>

*This information is distributed solely for the purpose of pre-dissemination peer review under applicable information quality guidelines. It has not been formally disseminated by the National Institute for Occupational Safety and Health. It does not represent and should not be construed to represent any agency determination or policy.*

ICR mice; 3 exposure groups and 1 control group; 6 male and female mice per group	21.8 nm average primary AgNP (range, 10–30 nm)	Doses of 0 (control group) and 7.5, 30, or 120 mg/kg	One injection; killed 10 min to 24 hrs post-injection for biokinetics; at 7 and 14 days post-injection for histopathology	No acute effects at 14 days; Ag found in all major organs, with highest concentration in liver and spleen	NA	Highest concentration of Ag found in lungs and kidneys of female mice	Xue et al. [2012]
Female Balb/c mice ( $n = 4$ ) and female Fisher CDF rats; $n$ not stated	PVP-coated AgNPs were spherical with 12-nm avg. diameter	Iodine-125-labeled AgNPs Mice: 4 $\mu$ Ci of the $^{125}$ I-AgNP Rats: 20 $\mu$ Ci of the $^{125}$ I-AgNP	One injection; Ag distribution evaluated at 30 min, 4 hrs, and 24 hrs with CT-SPECT imaging of organs	Prominent uptake of AgNPs in liver and spleen; level of AgNPs in blood relatively low at 24 hrs	NA		Chrastina and Schnitzed [2010]
Sprague-Dawley male rats; New Zealand white male rabbits; male dogs; $n$ not stated	Particle characterization not given	Ag nitrate mixed with $^{110}$ Ag given in femoral vein of rats (0.01, 0.03, 0.1, 0.3 mg/kg), rabbits (0.1 mg/kg), and dogs (0.1 mg/kg)	One injection; $^{110}$ Ag measured in urine and feces at 24-hr periods for 4 days	25%–45% of Ag excreted into bile during first 2 hrs; 70% excreted within 4 days; highest concentration of Ag occurred in liver at 2 hrs	NA	Ag concentration in bile 16–20 times higher than that found in plasma	Klaassen [1979]

*This information is distributed solely for the purpose of pre-dissemination peer review under applicable information quality guidelines. It has not been formally disseminated by the National Institute for Occupational Safety and Health. It does not represent and should not be construed to represent any agency determination or policy.*

SPF New Zealand white male rabbits ( <i>n</i> = 4)	Citrate-coated AgNPs (~7.9-nm diameter)	Injected into ear vein at doses of 0.5 mg/kg and 5 mg/kg	One injection; blood taken for Ag analysis from other ear at post-treatment times of 5, 10, and 30 min; 1, 2, 6, and 12 hrs; days 1 through 7; and days 14, 21, and 28	Concentration of AgNP in serum at highest concentration 5 min from treatment; 90% of AgNPs eliminated from serum at 28 days; tissue distribution of AgNPs highest in liver, spleen, and kidney	ND	Pigmentation found in liver at 7 and 28 days; inflammatory cell infiltration increased in livers, lungs, and kidneys	Lee et al. [2013c]
--	---	--	--	--	----	--	--------------------

*This information is distributed solely for the purpose of pre-dissemination peer review under applicable information quality guidelines. It has not been formally disseminated by the National Institute for Occupational Safety and Health. It does not represent and should not be construed to represent any agency determination or policy.*

<b>Intraperitoneal Injection</b>							
Outbred white female rats (n = 8-14 per group)	50 nm AgNP, 50 nm, AuNP, vehicle control (deionized water); 50 nm AgNP with bioprotective complex or bioprotective complex only as control	10 mg/kg	3 times/week for 20 injections (~3 weeks; bioprotective complex supplied orally	Pathological alteration in kidney, liver and spleen; genotoxicity AgNP > AuNP in liver, spleen, bone, kidney, and RBC; minor differences between particles in blood chemistry parameters with greater decrease in ceruloplasmin in AgNP exposure	ND	Particles deposited in liver, kidney, and spleen with greater AgNP in kidney and greater AuNP in liver; similar trends for decreased RBC, monocytes, and hemoglobin (AuNP > AgNP)	Katsnelson et al. [2013]
Female Balb/c mice; n = 5-10/group Female and Male Balb/c; exposed, then mated and fetuses collected; n = 3-5 per group	25 nm PVP-coated AgNP or silver nitrate 25 nm PVP-coated AgNP or silver nitrate	0, 22, or 108 µg/kg AgNP or 108 µg/kg silver nitrate 0, 22, or 108 µg/kg AgNP or 108 µg/kg silver nitrate	Every 2 days for 4 weeks, with recovery at 2 weeks after last exposure Males and females were exposed every 2 days for 4 weeks, then mated. Placenta, fetal liver, remaining fetus collected gestational day 14.5	Silver burden in tissue was dose-dependent and greatest in liver and spleen; burden was greater for high dose AgNP versus high dose of ionic silver All forms of silver detected in placenta, fetal liver and remaining fetus. High dose of AgNP greatest in placenta and low dose of AgNP greatest in fetal liver and remaining fetus		Tissue deposition was 100-fold greater following intraperitoneal exposure versus intravenous exposure Authors suggest particle agglomeration as a barrier to particles crossing placenta	Wang et al. [2013]

*This information is distributed solely for the purpose of pre-dissemination peer review under applicable information quality guidelines. It has not been formally disseminated by the National Institute for Occupational Safety and Health. It does not represent and should not be construed to represent any agency determination or policy.*

Male C57BL/6N mice	25-nm particles, shape not specified	0, 100, 500, or 1,000 mg/kg	Single exposure	Altered gene expression in extracted regions of the brain	ND	RT-PCR analysis used oxidative stress and antioxidant defense arrays	Rahman et al. [2009]
Female Wistar pregnant rats ( $n = 30$ ); 4 treatment groups and 1 control group	Nanosilver, size and type not specified	4 groups given either 0.4 and 0.8 mg/kg at 8 <sup>th</sup> day gestation or 0.4 and 0.8 mg/kg at 9 <sup>th</sup> day gestation	Single exposure; killed at 20 <sup>th</sup> day gestation	No evidence of teratogenicity; mean weights and lengths decreased in comparison with controls	NA		Mahabady [2012]
Sprague-Dawley rats; sex not stated; 5 to 8 per group	50–60-nm particles in 0.7% NaCl containing 0.05% Tween 80, shape not specified	50 mg/kg	Single exposure	No evidence of blood-brain barrier permeability or brain edema	NA		Sharma et al. [2010]
Sprague-Dawley rats; sex not stated; 6 to 8 per group	10–30-nm particles dispersed in deionized water	500 mg/kg <sup>-1</sup>	Single exposure	Decrease in autophagy; liver function impairment; hepatotoxicity	NA		Lee et al. [2013b]

*This information is distributed solely for the purpose of pre-dissemination peer review under applicable information quality guidelines. It has not been formally disseminated by the National Institute for Occupational Safety and Health. It does not represent and should not be construed to represent any agency determination or policy.*

<p>Male ICR mice; control group (<math>n = 10</math>); 3 experimental groups (<math>n = 15</math>) and 1 positive control group (<math>n = 10</math>)</p>	<p>Generally spherical with average diameter of 36.3 nm</p>	<p>Control group (<math>n = 10</math>) received 0.9% normal saline; 3 experimental groups (<math>n = 15</math>) received 10, 25, or 50 mg/kg bw AgNPs; 1 positive control group (<math>n = 10</math>) received scopolamine (3 mg/kg bw)</p>	<p>Daily for 7 days</p>	<p>No evidence of an effect on altering the reference memory or working memory</p>	<p>NA</p>	<p>Exposure to AgNPs did not affect neurocognitive outcome or hippocampal neurogenesis</p>	<p>Liu et al. [2013b]</p>
---	---	---	-------------------------	--	-----------	--	---------------------------

*This information is distributed solely for the purpose of pre-dissemination peer review under applicable information quality guidelines. It has not been formally disseminated by the National Institute for Occupational Safety and Health. It does not represent and should not be construed to represent any agency determination or policy.*

Subcutaneous Injection							
Wistar rats; 90 females	AgNPs: 50–100-nm diameter; Ag microparticles: 2–20- $\mu$ m diameter, control group	Single exposure: 62.8 mg/kg in a volume of 1 mL	Single exposures; 5 rats from each group killed at weeks 2, 4, 8, 12, 18, and 24 for analysis of Ag concentration in brain	Ag concentration higher for AgNPs than for Ag microparticles; Ag concentration peaked at 12 weeks and remained constant	NA	Could not determine whether Ag concentrations in brain were result of AgNPs or Ag+	Tang et al. [2008]
Wistar rats; 90 females	AgNPs: 50–100-nm diameter; Ag microparticles: 2–20- $\mu$ m diameter, control group	Single exposure: 62.8 mg/kg in a volume of 1 mL	Single exposure; 5 animals from each group killed at weeks 2, 4, 8, 12, 18, and 24 for analysis of Ag concentration in brains, liver, spleen, lung, and kidney	Concentrations of AgNPs in organs significantly higher than those of Ag microparticles	NA	Ag microparticles did not pass to the general circulation (~0.02% of the injected load)	Tang et al. [2009]

CMC = carboxymethyl cellulose; GGTP = gamma glutamyl transpeptidase; GM = geometric mean; 5-HT = 5-hydroxytryptamine; CMAD = count median aerodynamic diameter; NA = not applicable; ND = not determined; PVP = polyvinylpyrrolidone.

\*By analogy to the findings in Kim et al. [2010a], these particles are likely to have been spherical.

1  
2  
3  
4  
5  
6  
7  
8  
9  
10  
11  
12  
13  
14  
15  
16  
17  
18  
19  
20  
21  
22  
23  
24

## **APPENDIX F**

# **Rat Tissue Concentrations and Respiratory Parameters**

### **F.1 Estimating Lung Tissue Concentration of Silver Relative to Steady-State Tissue Concentration in Rats**

The objective of the analysis in this section is to investigate the question of whether silver had reached steady-state concentration in the rat tissues at the end of the subchronic inhalation exposure. Data to address this question are reported in Song et al. [2013]. This information is relevant to the extrapolation of subchronic to chronic responses in the rat, which is also relevant to estimating the dose associated with potential responses in humans over a working lifetime (e.g., dosimetric adjustment factor for subchronic to chronic exposure, DAF 3) (Section 6.2.3). To the extent that steady-state tissue concentration has not been achieved, the tissue dose with continued exposure at a given concentration would result in greater tissue doses and therefore a higher likelihood of adverse response.

The concentration of a substance in the body at any point in time depends on the rates of intake and elimination. Half-life is the time required for a property (such as concentration or activity) of a substance in the body to decrease by half. At steady-state, the intake of a substance is in approximate dynamic equilibrium with its elimination. The time required to reach a steady-state concentration is approximately four to five half-lives for a substance administered at a regular interval [ITO 2011]. Thus, for a 12-week (84-day) study, the half-life would need to be less than approximately 21 days in order to achieve steady-state concentrations in that subchronic study.

*This information is distributed solely for the purpose of pre-dissemination peer review under applicable information quality guidelines. It has not been formally disseminated by the National Institute for Occupational Safety and Health. It does not represent and should not be construed to represent any agency determination or policy.*

1 Lung tissue concentrations of silver after subchronic inhalation are shown in male and  
2 female rats in Figure 7 of Song et al. [2013]. The lung silver concentration declined by a  
3 factor of approximately three during the 12-wk post-exposure duration. Other tissue  
4 concentrations of silver cleared faster than those in lungs (shown in male and female  
5 rats separately in Tables IV, V, VII, and IX in Song et al. [2013]). However, the systemic  
6 tissue concentrations of silver depend on uptake from the lungs (portal of entry), such  
7 that steady state would not likely be achieved in the systemic tissues if not achieved in  
8 the lungs.

9 The proportion of steady-state concentration of a substance in the tissue at any time  
10 can be estimated from the following equation:

11 
$$\frac{C(t)}{C_{SS}} = 1 - e^{-kt} \quad \text{[Equation F-1]}$$

12 where C(t) is the concentration of a substance in tissue at time t, C<sub>SS</sub> is the steady-state  
13 tissue concentration, and k is the clearance rate constant; k is equal to ln(2)/half-life.

14 For example, in male rats exposed at the highest airborne exposure concentration (381  
15 µg/m<sup>3</sup>) of silver for 12 weeks (84 days), the retention half-life (t<sub>1/2</sub>) of silver in lung tissue  
16 was 42.3 days (as shown in Table X of Song et al. [2013]), and ln(2) is 0.693, as  
17 follows:

18 
$$\frac{C(t)}{C_{SS}} = 1 - e^{\left(\left(-\frac{0.693}{42.3}\right) \times 84\right)} = 0.75 \quad \text{[Equation F-2]}$$

19 That is, after 12 weeks of exposure, approximately 75% of the C<sub>SS</sub> lung concentration of  
20 silver had been achieved in those rats. Estimates for the other exposure groups in male  
21 rats and female rats are shown in Tables F-1 and F-2, respectively. These estimates  
22 suggest the steady-state concentration of silver in lung tissue had not been achieved.  
23 Thus, with chronic exposure at the same exposure concentrations, higher tissue  
24 burdens would be expected than those in the subchronic study. Higher tissue

1 concentrations of silver would be expected to increase the risk of adverse effects  
2 associated with that exposure.

### 3 **F.2 Rat Respiratory Parameters**

4 Some of the rat parameter values used in the dosimetric adjustment factors (DAF)  
5 (Section 6.2.3.2) are estimated from the average body weights. These include the DAFs  
6 for ventilation rate (DAF 1), deposition fraction of inhaled particles (DAF 2), and in some  
7 cases, dose normalization (DAF 4). Average body weight in female rats in Sung et al.  
8 [2009] was calculated as 196 g over the 13-week study, from the average body weights  
9 of 162 g at 8 weeks of age (start of study, all female rats) and 230.6 g at 21 weeks of  
10 age (end of study, control female rats). Average body weight in male rats in Sung et al.  
11 [2009] was calculated here as 345 g over the 13-week study, from the average body  
12 weights of 253 g at 8 weeks of age (start of study, all male rats) and 437 g at 21 weeks  
13 of age (end of study, control male rats).

14 Minute ventilation (L/min) was estimated with use of the average body weight in male or  
15 female rats, as shown in the following allometric [U.S. EPA 1994]:

$$16 \quad \ln(V_E) = b_0 + b_1 \ln(BW) \text{ [Equation F-3]}$$

17  
18 where  $V_E$  is the minute ventilation (L/min); BW is body weight (kg); and  $b_0 + b_1$  are the  
19 species-specific parameters, which for rat are -0.578 ( $b_0$ ) and 0.821 ( $b_1$ ) [Table 4-6 of  
20 U.S. EPA 1994].

21  
22 Thus, minute ventilation is calculated as

$$23 \quad V_E \text{ (L/min)} = \text{Exp}[b_0 + b_1 \times \ln(BW)] \text{ [Equation F-4]}$$

24  
25  
26 which results in  $V_E$  of 0.15 L/min for a 196-g female rat and 0.23 L/min for a 345-g male  
27 rat.

*This information is distributed solely for the purpose of pre-dissemination peer review under applicable information quality guidelines. It has not been formally disseminated by the National Institute for Occupational Safety and Health. It does not represent and should not be construed to represent any agency determination or policy.*

1 By comparison, for a 300-g rat, as used in the MPPD default Long Evans rat model,  $V_E$   
2 is 0.21 L/min. Tidal volume is 2.1 ml, assuming 102 breaths/min, calculated as follows:

3 
$$\text{Tidal volume (ml)} = V_E \text{ (L/min)} / [\text{breaths (min}^{-1}) \times 0.001 \text{ (L/ml)}] \text{ [Equation F-5]}$$

4 These values differ from those reported in Sung et al. [2008] and Song et al. [2013],  
5 which also differ from each other. Sung et al. [2008] reports minute ventilation (called  
6 minute volume) of ~25 ml/min (i.e., ~0.025 L/min) and tidal volume of ~0.25 ml; these  
7 values are approximately 10x lower than those for a standard (300-g) rat. Song et al.  
8 [2013] reports minute volume of ~800 ml/min (i.e., ~0.8 L/min) and tidal volume of ~8  
9 ml; these values are approximately 4x higher than those for a 300-g rat. Given these  
10 differences in the measured values reported in the two studies, and the resulting  
11 uncertainty, these values were estimated in this analysis from the allometric equation  
12 using body weight (Equations F-3 through F-5). It should be noted, however, that the  
13 estimation of these respiratory parameters can influence the estimates of the DAF and  
14 the HEC.

15 Air intake per exposure day ( $m^3$ ) was calculated as follows, based on a 6-hr exposure  
16 day in the rat studies:

17 
$$\text{Air intake (m}^3\text{)} = V_E \text{ (L/min)} \times (60 \text{ min/hr} \times 6 \text{ hr}) \times 0.001 \text{ m}^3\text{/L [Equation F-6]}$$

18 which results in 0.053  $m^3$  in female rats and 0.084  $m^3$  in male rats in Sung et al. [2009];  
19 these values are used in DAF1 (Section A.2.4).

### 20 **F.3 Rat Measured and MPPD Model–Predicted Lung Burdens**

21 DAF 2 is the ratio of the deposition fractions of particles in the target respiratory tract  
22 region in humans and rats. Thus, the measured and predicted rat lung burdens of silver  
23 are evaluated in this section to compare to those predicted from the multiple-path  
24 particle deposition (MPPD) model [ARA 2011]. The Long Evans rat model had been the  
25 only rat model in MPPD until the recent addition of a Sprague-Dawley rat model in

*This information is distributed solely for the purpose of pre-dissemination peer review under applicable information quality guidelines. It has not been formally disseminated by the National Institute for Occupational Safety and Health. It does not represent and should not be construed to represent any agency determination or policy.*

1 MPPD v. 3.04. The estimates from each of these models is compared to the measured  
2 lung doses of silver in male rats (Table F-3) and female rats (Table F-4) at the end of  
3 the 13-wk exposure in the Sung et al. [2009] study.

4 Each of these models over-predicted the measured lung burdens of silver, but the  
5 estimates from the Sprague-Dawley rat model were the closest to the reported values.  
6 Each model predicted that approximately half of the total deposited silver was retained  
7 at 13 weeks of exposure, based on clearance kinetics of poorly soluble particles. The  
8 lower retained doses may be due to dissolution in addition to alveolar macrophage-  
9 mediated clearance of silver particles.

10

*This information is distributed solely for the purpose of pre-dissemination peer review under applicable information quality guidelines. It has not been formally disseminated by the National Institute for Occupational Safety and Health. It does not represent and should not be construed to represent any agency determination or policy.*

1 **TABLES FOR Appendix F**

2 **Table F-1. Lung clearance kinetics and tissue concentration estimates in male**  
 3 **rats of Song et al. [2013].**

Exposure Group	Half-time ( $t_{1/2}$ , d)*	Clearance rate constant $k = \ln(2)/t_{1/2}$	Lung tissue concentration at end of exposure as proportion of estimated steady-state concentration $\frac{C(t)}{C_{SS}} = 1 - e^{-kt}$	Number of half-lives by end of 12-wk exposure ( $84 d / t_{1/2}$ )
low	28.5	0.0243	0.8704	2.95
med	84.9	0.0082	0.4963	0.99
high	42.3	0.0164	0.7475	1.99

4 \* From Table X in Song et al. [2013].

5  
6

7 **Table F-2. Lung clearance kinetics and tissue concentration estimates in female**  
 8 **rats of Song et al. [2013].**

Exposure Group	Half-time ( $t_{1/2}$ , d)*	Clearance rate constant $k = \ln(2)/t_{1/2}$	Lung tissue concentration at end of exposure as proportion of estimated steady-state concentration $\frac{C(t)}{C_{SS}} = 1 - e^{-kt}$	Number of half-lives by end of 12-wk exposure ( $84 d / t_{1/2}$ )
low	38.7	0.0179	0.7779	2.17
med	112.9	0.0061	0.4029	0.74
high	40.4	0.0172	0.7634	2.08

9 \* From Table XI in Song et al. [2013].

10

*This information is distributed solely for the purpose of pre-dissemination peer review under applicable information quality guidelines. It has not been formally disseminated by the National Institute for Occupational Safety and Health. It does not represent and should not be construed to represent any agency determination or policy.*

1 **Table F-3. Comparison of Measured and Predicted Rat Lung Burden of Silver after**  
 2 **Subchronic (13-week) Inhalation of Silver Nanoparticles in Male Sprague Dawley Rats**  
 3 **[Sung et al. 2009] and as Predicted by Multiple-path Particle Dosimetry (MPPD) Model, v. 3.04**  
 4 **[ARA 2015].**

Measured Exposure and Dose		Predicted Dose by MPPD Model and Rat Average Body Weight (BW)			
Airborne exposure concentration ( $\mu\text{g}/\text{m}^3$ )	Rat retained lung dose ( $\mu\text{g}$ ) after 13-wk exposure <sup>a</sup>	Retained Lung Dose ( $\mu\text{g}$ ), Estimated by Model <sup>b</sup>		Deposited Lung Dose ( $\mu\text{g}$ ), Estimated by Model & Equations <sup>c,d</sup>	
		Long Evans, Semi-symmetric (default), BW 300 g	Sprague Dawley rat, Symmetric, BW 345 g	Long Evans rat, Semi-symmetric (default), BW 300 g (DFalv: 0.28)	Sprague Dawley rat, Symmetric, BW 345 g (DFalv: 0.0635)
0	0.0011	0	0	0	0
49	0.88	30.1	7.5	75	17
133	7.96	93.2	22.5	205	46.3
515	21.82	445.2	104	790	179

5 <sup>a</sup> Calculated from data reported in Tables 1 and 7 of Sung et al. [2009], as follows:

6  $\text{Ag in whole organ } (\mu\text{g}) = \text{ng Ag/g tissue} \times \text{g tissue} \times 0.001 \mu\text{g Ag} / \text{ng tissue}$ , using female control rat  
 7 mean body weight at end of exposure (437.05 g).

8 <sup>b</sup> Symmetric or Semi-symmetric refers to the airway branching pattern in the MPPD model.

9 <sup>c</sup> Average deposited rat lung dose was calculated as follows:

10 Deposited lung dose (total) =  
 11 Exposure concentration ( $\mu\text{g}/\text{m}^3$ ) x Exposure duration (5 d/wk x 13 wk) x Alveolar deposition fraction  
 12 (DFalv) x Air intake per exposure day ( $\text{m}^3/6\text{-hr d}$ )

13 where exposure concentration and duration are as reported in the Sung et al. [2009]; DFalv was  
 14 estimated by the stated model; and air intake volume per exposure day was estimated on the basis of  
 15 the average rat body weight during the 13-wk study (Section F-2). For 345-g males, minute ventilation  
 16 was 0.23 L/min, and air intake volume was 0.084  $\text{m}^3/6\text{-hr d}$ .

17 <sup>d</sup> Deposition fraction in the alveolar region (DFalv) was estimated with use of the default respiratory  
 18 parameters in the stated MPPD model (including as adjusted by BW); note that minute ventilation is  
 19 similar, but not identical, to that calculated based on the allometric equation in Section F-2.

20

*This information is distributed solely for the purpose of pre-dissemination peer review under applicable information quality guidelines. It has not been formally disseminated by the National Institute for Occupational Safety and Health. It does not represent and should not be construed to represent any agency determination or policy.*

1 **Table F-4. Comparison of Measured and Predicted Rat Lung Burden of Silver after**  
 2 **Subchronic (13-week) Inhalation of Silver Nanoparticles in Female Sprague Dawley**  
 3 **Rats [Sung et al. 2009] and as Predicted by Multiple-path Particle Dosimetry (MPPD) Model, v. 3.04**  
 4 **[ARA 2015].**

Measured Exposure and Dose		Predicted Dose by MPPD Model and Rat Average Body Weight (BW)			
Airborne exposure concentration ( $\mu\text{g}/\text{m}^3$ )	Rat retained lung dose ( $\mu\text{g}$ ) after 13-wk exposure <sup>a</sup>	Retained Lung Dose ( $\mu\text{g}$ ), Estimated by Model <sup>b</sup>		Deposited Lung Dose ( $\mu\text{g}$ ), Estimated by Model & Equations <sup>c,d</sup>	
		Long Evans, Semi-symmetric (default), BW 300 g	Sprague Dawley rat, Symmetric, BW 196 g	Long Evans rat, Semi-symmetric, BW 196 g <sup>e</sup> (DFalv: 0.19)	Sprague Dawley rat, Symmetric, BW 196 g (DFalv: 0.0635)
0	0.001	0	0	0	0
49	0.31	30.1	3.08	32	7.04
133	4.31	93.2	9.08	87	19.1
515	23.55	445.2	40.8	337	74.0

5 <sup>a</sup> Calculated from data reported in Tables 2 and 8 of Sung et al. [2009], as follows:

6  $\text{Ag in whole organ } (\mu\text{g}) = \text{ng Ag/g tissue} \times \text{g tissue} \times 0.001 \mu\text{g Ag} / \text{ng tissue}$ , using female control rat  
 7 mean body weight at end of exposure (230.60 g).

8 <sup>b</sup> Symmetric or Semi-symmetric refers to the airway branching pattern in the MPPD model.

9 <sup>c</sup> Average deposited rat lung dose was calculated as follows:

10 Deposited lung dose (total) =  
 11 Exposure concentration ( $\mu\text{g}/\text{m}^3$ ) x Exposure duration (5 d/wk x 13 wk) x Alveolar deposition fraction  
 12 (DFalv) x Air intake per exposure day ( $\text{m}^3/6\text{-hr d}$ )

13 where exposure concentration and duration are as reported in the Sung et al. [2009]; DFalv was  
 14 estimated by the stated model; and air intake volume per exposure day was estimated on the basis of  
 15 the average rat body weight during the 13-wk study (Section A.2.5.2). For 196-g females, minute  
 16 ventilation was 0.15 L/min, and air intake volume was 0.053  $\text{m}^3/6\text{-hr d}$ .

17 <sup>d</sup> Deposition fraction in the alveolar region (DFalv) was estimated with use of the default respiratory  
 18 parameters in the stated MPPD model (including as adjusted by BW); note that minute ventilation is  
 19 similar, but identical, to that calculated based on the allometric equation in Section A.2.5.2. Tidal volume  
 20 of 1.47 ml for input to MPPD for female rat (196 g BW) was calculated as in Equation A-9.

## APPENDIX G

# Other Quantitative Risk Assessments for Silver Nanoparticles

### G.1 Christensen et al. [2010]

Christensen et al. [2010] calculated INELs (indicative no effect levels) for silver nanoparticles, following the EU European Chemicals Agency [ECHA 2010] guidelines. The data used were from one subchronic (90-day) inhalation study in rats (as reported in two publications [Sung et al. 2008, 2009]).

The lowest exposure concentration ( $49 \mu\text{g}/\text{m}^3$ ) [Sung et al. 2008, 2009] for decreased lung function in female rats [Sung et al. 2008] was used as a LOAEL by Christensen et al. [2010], although they noted that the severity of the effects at the LOAEL was unclear. A NOAEL of  $133 \mu\text{g}/\text{m}^3$  for lung and liver effects [Sung et al. 2009] was also used in the analysis by Christensen et al. [2010].

Following the ECHA [2008] guidelines, Christensen et al. [2010] adjusted the NOAEL or LOAEL for the difference in exposure duration in the rats (6 hours/day) and in humans (8 hours/day), as well as adjusting for resting (comparable to rat study) versus light work activity in workers (that is,  $6.7 \text{ m}^3$  vs.  $10 \text{ m}^3$ ) (Table G-1).

Thus, the human-equivalent concentration (HEC) corresponding to a LOAEL of  $49 \mu\text{g}/\text{m}^3$  was calculated as follows:

$$49 \mu\text{g}/\text{m}^3 \times 6 \text{ hrs}/8 \text{ hrs} \times 6.7 \text{ m}^3/10 \text{ m}^3 = 25 \mu\text{g}/\text{m}^3.$$

(The same adjustments result in  $67 \mu\text{g}/\text{m}^3$  as the human-equivalent concentration to  $133 \mu\text{g}/\text{m}^3$  in rats.)

*This information is distributed solely for the purpose of pre-dissemination peer review under applicable information quality guidelines. It has not been formally disseminated by the National Institute for Occupational Safety and Health. It does not represent and should not be construed to represent any agency determination or policy.*

1 Uncertainty factors of 3 and 10 (for two different exposure scenarios) were used for  
2 adjusting the rat subchronic LOAEL to estimate a NOAEL. Additional factors included  
3 2.5 for interspecies toxicodynamics and 1 for interspecies toxicokinetics (since the local  
4 effects were assumed to be independent of metabolic rate); a factor of 5 for interspecies  
5 extrapolation to workers; and a factor of 2 for subchronic to chronic uncertainty.

6 Thus, the human-equivalent concentration of  $25 \mu\text{g}/\text{m}^3$  was divided by these factors:

7 
$$3 \times 2.5 \times 5 \times 2 = 75; \text{ or } 10 \times 2.5 \times 5 \times 2 = 250$$

8 Thus, the derived INELs for the rat LOAEL of  $49 \mu\text{g}/\text{m}^3$  were calculated by dividing the  
9 human-equivalent LOAEL of  $25 \mu\text{g}/\text{m}^3$  by an overall adjustment factor of 75 or 250:

10 
$$25 \mu\text{g}/\text{m}^3 / 75 = 0.33 \mu\text{g}/\text{m}^3$$

11 
$$25 \mu\text{g}/\text{m}^3 / 250 = 0.1 \mu\text{g}/\text{m}^3$$

12 Similar calculations were applied to the NOAEL of  $133 \mu\text{g}/\text{m}^3$  for lung inflammation  
13 (male and female rats) from Sung et al. [2009] (Table G-1). In this case, the worker-  
14 equivalent concentration was  $67 \mu\text{g}/\text{m}^3$ . The assessment factors included 10 for  
15 interspecies (animal to human, TK and TD) systemic liver effects; 5 for intraspecies  
16 variability; and 2 for subchronic to chronic extrapolation:

17 
$$10 \times 5 \times 2 = 100$$

18 
$$67 \mu\text{g}/\text{m}^3 / 100 = 0.67 \mu\text{g}/\text{m}^3$$

19 These OEL estimates are summarized in Table G-1.

## 20 **G.2 Weldon et al. [2016]**

21 A dosimetric adjustment approach was recently applied by Weldon et al. [2016] in  
22 estimating an OEL for silver nanoparticles on the basis of data in one of the subchronic  
23 inhalation studies [Sung et al. 2008, 2009]. Weldon et al. [2016] reference NIOSH

1 [2013] for the version of the DAF method used in their HEC estimation. A separate  
2 evaluation of the individual factors used in the DAF method is provided in Section  
3 6.2.3.2.

4 In the Weldon et al. [2016] risk assessment, they evaluated the various effects observed  
5 in the rat lungs or liver shown in Table 9 of Sung et al. [2009], including pulmonary  
6 inflammation and liver bile duct hyperplasia. The specific endpoints were quantified as  
7 the proportion of rats examined in each group observed to have a given response and  
8 degree of severity, based on histopathological examination results in Table 9 of Sung et  
9 al. [2009].

10 BMDS modeling (EPA BMDS v. 2.6) was applied to the dose-response data [Weldon et  
11 al. 2016]. A multistage polynomial degree 2 model was selected as the best-fitting  
12 model, although the fit statistics for this and other BMDS models were not reported in  
13 Weldon et al. [2016]. The rat liver tissue burden ( $\mu\text{g Ag}$  in the liver) in female rats  
14 associated with a 10% added risk of bile duct hyperplasia, 95% lower confidence limit  
15 estimate ( $\text{BMDL}_{10}$ ), was selected as the critical effect level for use as the  $\text{PoD}_{\text{animal}}$ .  
16 Although not the lowest  $\text{BMDL}_{10}$  ( $\text{BMDL}_{10}$  for liver abnormalities was lower), bile duct  
17 hyperplasia was selected as “a specific, quantitative endpoint” to represent “the most  
18 sensitive level of biological effect.”

19 The rat tissue doses used in the BMDS dose-response modeling in Weldon et al. [2016]  
20 ( $\mu\text{g}$  per organ) were presumably estimated from the silver tissue dose ( $\text{ng Ag/g}$  tissue)  
21 reported in Tables 1 and 2 of Sung et al. [2009]. In those tables, the organ weights are  
22 reported as a percentage of body weight in male and female rats. Although not stated in  
23 Weldon et al. [2016], the total silver dose ( $\mu\text{g}$ ) in an organ could be estimated by  
24 multiplying the organ weight (g) (calculated from the percentage of body weight) by the  
25 silver tissue dose concentration ( $\text{ng/g}$ ) and adjusting units. The estimates by NIOSH of  
26 the lung and liver organ doses of silver (Tables G-2 and G-3) were very similar, but not  
27 identical, to the silver organ doses reported in Figures 2 and 3 of Weldon et al. [2016].

1 These slight differences in the dose data would only have a slight influence on the  
2 BMDL<sub>10</sub> estimates derived from the best-fitting model.

3 The rat BMDL<sub>10</sub> based on silver liver tissue dose ( $\mu\text{g}$ ) was converted to an equivalent  
4 airborne concentration ( $\mu\text{g}/\text{m}^3$ ) by fitting the tissue dose and airborne concentrations in  
5 the rat study with a linear regression model (shown in Supplementary Figure 1 of  
6 Weldon et al. [2016]) to identify the airborne concentration associated with a liver tissue  
7 dose equivalent to the BMDL<sub>10</sub> estimate. The  $R^2$  for the linear relationship between  
8 airborne exposure concentration ( $\mu\text{g}/\text{m}^3$ ) of silver and the lung tissue dose of silver ( $\mu\text{g}$ )  
9 was 0.87 in males and 0.96 in females. Although the specific BMDL<sub>10</sub> estimate is not  
10 reported, the values shown in Figure 4 and Supplementary Figure 1 of Weldon et al.  
11 [2010] are roughly consistent with the  $\sim 0.015 \mu\text{g}$  (i.e.,  $\sim 15 \text{ ng}$ ) estimate described  
12 above.

13 On the basis of the results of the linear regression (Supplemental Figure 1), Weldon et  
14 al. [2016] estimated a  $\text{PoD}_{\text{animal}}$  of  $25.5 \mu\text{g}/\text{m}^3$ , which is called a benchmark  
15 concentration (BMC) and is the 95% lower confidence limit estimate (BMCL<sub>10</sub>). Weldon  
16 et al. [2016] note that this estimated effect level (i.e.,  $\text{PoD}_{\text{animal}}$ ) is lower (more health  
17 protective) than the NOAEL of  $133 \mu\text{g}/\text{m}^3$  reported in Sung et al. [2009] for bile duct  
18 hyperplasia in male or female rats.

19 After estimating the  $\text{PoD}_{\text{animal}}$ , Weldon et al. [2016] derived the HEC\_PoD by dividing  
20 the  $\text{PoD}_{\text{animal}}$  by the total DAF (as shown in Equations 6-1 and 6-2 in Section 6.2.3.1).

21 Specifically, the Weldon et al. [2016] analysis included the following values:

22 
$$\text{HEC\_PoD } (5.66 \mu\text{g}/\text{m}^3) = 25.5 \mu\text{g}/\text{m}^3 /$$
  
23 
$$[(10 \text{ m}^3/\text{d} / 0.1015 \text{ m}^3/\text{d}) \times (0.348/0.29) \times (10/1) \times (2,422 \text{ cm}^2 / 634,620 \text{ cm}^2)]$$
  
24 [Equation G-1]

1           where the numerator is the  $PoD_{\text{animal}}$ , and the denominator is the total DAF,  
2           consisting of individual factors for ventilation rates, deposition fraction (pulmonary  
3           region), retention half-times, and interspecies dose normalization (pulmonary  
4           surface area).

5           On the basis of the dosimetric adjustment method and using the parameter values they  
6           describe, Weldon et al. [2016] proposed an OEL of  $0.19 \mu\text{g}/\text{m}^3$ . This value was derived  
7           by dividing the HEC\_PoD estimate of  $5.66 \mu\text{g}/\text{m}^3$  [Equation G-1] by a total uncertainty  
8           factor of 30. The individual uncertainty factors included 3 for toxicodynamic differences  
9           in animals and humans, 2 for extrapolation of subchronic to chronic effects, and 5 for  
10          inter-individual variability in workers (i.e.,  $2 \times 3 \times 5 = 30$ ), as described in Weldon et al.  
11          [2016].

12          Alternatively, NIOSH normalized the doses in rats and humans by using the total  
13          respiratory tract surface area (because soluble particles that deposit anywhere in the  
14          respiratory tract can potentially reach the liver) and the body weight (a common  
15          approach for systemically acting substances) (Section 6.2.3.2). These other dose  
16          normalization approaches may be more biologically plausible for soluble particles.

17          In an earlier study, Ji and Yu [2012] selected a rat PoD of  $100 \mu\text{g}/\text{m}^3$  for estimating an  
18          HEC. They estimated an HEC (worker-equivalent PoD) of  $59 \mu\text{g}/\text{m}^3$  by adjusting the  $100$   
19           $\mu\text{g}/\text{m}^3$  rat PoD by interspecies differences in the deposition fraction of silver  
20          nanoparticles (18 nm in diameter; GSD, 1.5) in the alveolar region ( $0.4 \text{ m}^2$  for rats;  $62.7$   
21           $\text{m}^2$  for humans) over a total of 13 weeks (5 days/week) of inhalation exposure and  
22          assuming light exercise in workers [Ji and Yu 2012]. The alveolar deposition fractions in  
23          rats and humans were estimated with the Multiple-Path Particle Dosimetry (MPPD) 2.0  
24          model [ARA 2009]. This worker-equivalent concentration estimate is similar to those  
25          estimated according to ECHA [2008] guidelines by Christensen et al. [2010] (Table G-  
26          1), and higher than that estimated in Weldon et al. [2016]. No OELs were proposed by  
27          Ji and Yu [2012].

### 1 **G.3 Acute Inhalation Exposure to Silver**

2 In an acute (5-hr) inhalation study of two types of silver (ionic and AgNP) in rats (male,  
3 Sprague-Dawley), no adverse pulmonary effects were observed 1 day or 7 days post-  
4 exposure [Roberts et al. 2013]. The ionic silver was a commercial antimicrobial spray,  
5 administered at an exposure concentration of 100  $\mu\text{g}/\text{m}^3$  (count median aerodynamic  
6 diameter [CMAD] of 33 nm). The AgNP sample was a NIST reference material of total  
7 silver nanoparticles with low ionic content, administered at 1,000  $\mu\text{g}/\text{m}^3$  (CMAD of 39  
8 nm). A transient significant increase in blood monocytes was observed 1 day after  
9 exposure to the high concentration (AgNP), but not in rats exposed to the low  
10 concentration (ionic Ag). Slight cardiovascular changes (significant reduction in vascular  
11 responsiveness to Ach-induced re-dilation) were observed at the low concentration  
12 (ionic Ag) at 1 day post-exposure, but not at the high concentration (AgNP). Both of  
13 these responses had resolved by 7 days post-exposure. Given the minimal, transient  
14 responses, each of these concentrations could be considered NOAELs for the  
15 respective types of silver.

16 In order to evaluate the short-term effects of exposure to silver nanoparticles, data from  
17 an acute (5-hr) inhalation study in rats was used to identify the rat NOAELs for airborne  
18 exposure to two types of silver (ionic and nanoparticles) [Roberts et al. 2013].  
19 Benchmark doses were not be estimated since there was only one exposure group for  
20 each type of silver. The human-equivalent concentrations to the rat acute NOAELs were  
21 calculated by normalizing of lung weights (i.e., 1.5 g assumed for 9-wk male Sprague-  
22 Dawley rats, approximately 300 g body weight; human lung weight of 1,200 g [ICRP  
23 2002]), and by using a human alveolar deposition fraction of 0.17 (33 nm) or 0.15 (39  
24 nm), based on the MPPD human deposition (Yeh and Schum) model [ARA 2011]. Lung  
25 dose estimates are shown for rats and humans in Table G-6. The estimated human-  
26 equivalent single-day (8-hr) exposure concentration is 620  $\mu\text{g}/\text{m}^3$  or 7.7  $\text{mg}/\text{m}^3$ ,  
27 respectively, for the commercial spray (ionic Ag) or NIST reference material (AgNP)  
28 (Table G-6). These human-equivalent concentrations (to the rat acute NOAEL for ionic  
29 or nanoparticle silver spray) are approximately 60 or 700 times higher than the NIOSH

*This information is distributed solely for the purpose of pre-dissemination peer review under applicable information quality guidelines. It has not been formally disseminated by the National Institute for Occupational Safety and Health. It does not represent and should not be construed to represent any agency determination or policy.*

1 REL for total silver ( $10 \mu\text{g}/\text{m}^3$ ). These factors provide information relevant to a margin of  
2 exposure (MOE) assessment [Kim E et al. 2016]. The MOE in this example is the ratio  
3 of the human-equivalent concentration (to the rat effect NOAEL) and the REL. These  
4 HEC NOAEL estimates of a single acute exposure are 62 to 770 times greater than the  
5 NIOSH REL for total silver of 10 micrograms per cubic meter ( $\mu\text{g}/\text{m}^3$ ), or 688 or 8,555  
6 times greater than the NIOSH proposed REL of  $0.9 \mu\text{g}/\text{m}^3$ . Thus, the MOE estimates  
7 would be these same factors. However, these estimates are based on only one acute  
8 study of two materials, and the possible effects of repeated exposures at these  
9 concentrations are not known.

10

*This information is distributed solely for the purpose of pre-dissemination peer review under applicable information quality guidelines. It has not been formally disseminated by the National Institute for Occupational Safety and Health. It does not represent and should not be construed to represent any agency determination or policy.*

1 **TABLES for Appendix G**

2

3 **Table G-1. Proposed OELs for silver nanoparticles, based on rat subchronic**  
4 **inhalation studies\* and European Chemicals Agency (ECHA) guidelines**  
5 **[Christensen et al. 2010].**

Rat PoD ( $\mu\text{g}/\text{m}^3$ )	PoD type	Worker- equivalent PoD ( $\mu\text{g}/\text{m}^3$ ) <sup>†</sup>	Total UF	Proposed OEL ( $\mu\text{g}/\text{m}^3$ )
49	LOAEL	25	250 or 75	0.1 or 0.33
133	NOAEL	67	100	0.67

6 PoD = point of departure; UF = uncertainty factor.

7 \*Sung et al. [2008, 2009] and Song et al. [2013] (respective diameters: 18 nm, GSD 1.5; 14 nm, GSD  
8 1.7).

9 <sup>†</sup>8-hour TWA concentration.

10

This information is distributed solely for the purpose of pre-dissemination peer review under applicable information quality guidelines. It has not been formally disseminated by the National Institute for Occupational Safety and Health. It does not represent and should not be construed to represent any agency determination or policy.

1 **Table G-2. Male rats – mean tissue doses of silver in Sung et al. [2009].**

Organ and Silver Tissue Concentration or Total Mass	Exposure Group			
	Control (0 µg/m <sup>3</sup> )	Low (49 µg/m <sup>3</sup> )	Med (133 µg/m <sup>3</sup> )	High (515 µg/m <sup>3</sup> )
Liver (ng Ag/g tissue) <sup>a</sup>	0.70	3.52	13.8	133
<b>Liver (µg) in organ<sup>b*</sup></b>	<b>0.0078</b>	<b>0.038</b>	<b>0.16</b>	<b>1.50</b>
Lung (ng Ag/g tissue) <sup>a</sup>	0.77	613	5,450	14,645
<b>Lung (µg) in organ<sup>b*</sup></b>	<b>0.0011</b>	<b>0.88</b>	<b>7.96</b>	<b>21.82</b>

2 <sup>a</sup> From Table 7 of Sung et al. [2009].

3 <sup>b</sup> Calculated as: Ag in whole organ (µg) = ng Ag/g tissue x g tissue x 0.001 µg Ag / ng tissue, using male control rat mean  
4 organ weights (Table G-4).

5 \* Should match doses used in Weldon et al. [2016].

6

7 **Table G-3. Female rats – mean tissue doses of silver in Sung et al. [2009].**

Organ and Silver Tissue Concentration or Total Mass	Exposure Group			
	Control (0 µg/m <sup>3</sup> )	Low (49 µg/m <sup>3</sup> )	Med (133 µg/m <sup>3</sup> )	High (515 µg/m <sup>3</sup> )
Liver (ng Ag/g tissue) <sup>a</sup>	0.90	4.55	12.07	71.08
<b>Liver (µg) in organ<sup>b*</sup></b>	<b>0.0055</b>	<b>0.026</b>	<b>0.07</b>	<b>0.46</b>
Lung (ng Ag/g tissue) <sup>a</sup>	1.01	296	4,241	20,586
<b>Lung (µg) in organ<sup>b*</sup></b>	<b>0.0010</b>	<b>0.31</b>	<b>4.31</b>	<b>23.55</b>

8 <sup>a</sup> From Table 8 of Sung et al. [2009].

9 <sup>b</sup> Calculated as: Ag in whole organ (µg) = ng Ag/g tissue x g tissue x 0.001 µg Ag / ng tissue, using female control rat  
10 mean organ weights (Table G-5).

11 \* Should match doses used in Weldon et al. [2016].

12

This information is distributed solely for the purpose of pre-dissemination peer review under applicable information quality guidelines. It has not been formally disseminated by the National Institute for Occupational Safety and Health. It does not represent and should not be construed to represent any agency determination or policy.

1 **Table G-4. Male rats – mean body and organ weights in Sung et al. [2009].**

Body or Organ (Weight or Percent) <sup>a</sup>	Exposure Group			
	Control (0 µg/m <sup>3</sup> )	Low (49 µg/m <sup>3</sup> )	Med (133 µg/m <sup>3</sup> )	High (515 µg/m <sup>3</sup> )
Body weight (BW) (g)	437.05	435.62	456.22	451.44
Liver (% of BW)	2.54	2.51	2.48	2.50
<b>Liver (g)<sup>b</sup></b>	<b>11.10</b>	<b>10.93</b>	<b>11.31</b>	<b>11.29</b>
Lung (left + right) (% of BW)	0.32	0.33	0.32	0.33
<b>Lungs (g)<sup>b</sup></b>	<b>1.40</b>	<b>1.44</b>	<b>1.46</b>	<b>1.49</b>

2 <sup>a</sup> From Table 1 of Sung et al. [2009].

3 <sup>b</sup> Calculated as percent of BW.

4

5 **Table G-5. Female rats – mean body and organ weights in Sung et al. [2009].**

Body or Organ (Weight or Percent) <sup>a</sup>	Exposure Group			
	Control (0 µg/m <sup>3</sup> )	Low (49 µg/m <sup>3</sup> )	Med (133 µg/m <sup>3</sup> )	High (515 µg/m <sup>3</sup> )
Body weight (BW) (g)	230.60	237.95	221.13	248.70
Liver (% of BW)	2.64	2.43	2.52	2.59
<b>Liver (g)<sup>b</sup></b>	<b>6.09</b>	<b>5.78</b>	<b>5.57</b>	<b>6.44</b>
Lung (left + right) (% of BW)	0.45	0.44	0.46	0.46
<b>Lung (g)<sup>b</sup></b>	<b>1.04</b>	<b>1.05</b>	<b>1.02</b>	<b>1.14</b>

6 <sup>a</sup> From Table 2 of Sung et al. [2009].

7 <sup>b</sup> Calculated as percent of BW.

8

9

*This information is distributed solely for the purpose of pre-dissemination peer review under applicable information quality guidelines. It has not been formally disseminated by the National Institute for Occupational Safety and Health. It does not represent and should not be construed to represent any agency determination or policy.*

1 **Table G-6. Acute (5-hr) inhalation exposure in rats – No observed adverse effect level (NOAEL)**  
 2 **[Roberts et al. 2013] and human-equivalent exposure concentration\***

Type of Ag	Count median aerodynamic diameter (nm)	Rat Ag lung dose (µg) [NOAEL]	Human-equivalent Ag lung dose (µg)	Airborne concentration (mg/m <sup>3</sup> ) in 1 d (8-hour TWA) resulting in human-equiv. lung dose
Commercial spray (ionic)	33	1.4	1,000	0.62
NIST reference (particulate)	39	14	11,000	7.7

3 \*Calculations based on the following: Rat (male rat Sprague-Dawley, 9-wk old) estimated body weight: 300 g; estimated lung weight:  
 4 1.5 g. Human lung weight 1,200 g [ICRP 2002]. Human alveolar deposition fraction (DFalv): 0.17 (33 nm) or 0.15 (39 nm), MPPD Yeh  
 5 and Schum model [ARA 2011]. Reference worker air inhaled (AI) of 9.6 m<sup>3</sup>/8-hour d [ICRP 1994]. The 8-hour time weighted average  
 6 (TWA) airborne concentration was calculated as  
 7  $X \text{ mg/m}^3 = \text{Lung dose (mg)} / [\text{DFalv} \times \text{AI}]$ .